Spontaneous Na^+ fluctuations in the neonatal mouse brain

Inaugural dissertation

Submitted for the degree of Doctor to

The Faculty of Mathematics and Natural Sciences

Heinrich-Heine-Universität Düsseldorf

by

Lisa Simona Felix

from Edinburgh

Düsseldorf, October 2020

Acknowledgements

Firstly, I'd like to thank Prof. Rose, who gave me the chance to do this work and who was a supportive supervisor, whilst also allowing me the freedom to develop and explore my own ideas. In addition, our technical assistants and senior post-doc, Claudia Roderigo and Simone Durry and Karl Kafitz, for keeping the lab up and running, and for offering many pieces of good advice over the years. Finally, I have to mention the other members of the institute, both past and present. It is rare to work in a team in which there is real comradery, wherein everyone will do everything they can to help each other. I will always be grateful to them for bringing fun to what can be such a stressful time.

Outside of the institute I was lucky enough to have found a real home and family in A-street, a bunch of weirdos who enriched my time in Düsseldorf beyond measure, and without whom I would not have met Boran, who was the recipient of the majority of my neurobiological frustrations. To all of them I would like to say thank you for believing in me, and for being there throughout good and bad.

Publications

1. Rose, C. R., **Felix, L**., Zeug, A., Dietrich, D., Reiner, A., Henneberger, C. (2018). Astroglial Glutamate Signaling and Uptake in the Hippocampus. *Frontiers in Molecular Neuroscience* 10 DOI: 10.3389/fnmol.2017.00451

2. **Felix, L.**, Ziemens, D., Seifert, G., and Rose, C. R. (2020). Spontaneous Ultraslow Na^+ Fluctuations in the Neonatal Mouse Brain. *Cells* 9, 102 DOI: 10.3390/cells9010102.

3. **Felix, L**., Delekate, A., Petzold, G. C., and Rose, C. R. (2020). Sodium Fluctuations in Astroglia and Their Potential Impact on Astrocyte Function. *Frontiers in Physiology* 11 DOI: 10.3389/fphys.2020.00871.

4. **Felix, L**., Stephan, J., and Rose, C. R. (2020). Astrocytes of the early postnatal brain. *Eur J Neurosci* DOI: 10.1111/ejn.14780.

5. Perez, C., **Felix, L**., Rose, C. R., Ullah, G. (2020) On the Origin of Ultraslow Spontaneous Na^+ Fluctuations in Neurons of the Neonatal Forebrain. *J Neurophysiology* (in revision)

6. Stopper, G., Caudall, L. C., **Felix, L**., Rose, C. R., Scheller, A., Kirchhoff, F. MSparkles – An open-source tool to visualize and analyze fluorescent microscopy image sequences (in preparation)

Abstract

Patterns of spontaneous activity are present across almost all structures within the neonatal brain, and are critical for the development of all cell types. In this environment, as in mature tissue, Na^+ drives a multitude of membrane mechanisms in both neurons and astrocytes, and has an impact on several intracellular processes. Here, high levels of synchronous activity in neonatal structures are coupled with underdeveloped transmitter uptake systems and low expression levels of the primary Na^+ extruder, the NKA. Taken together, these factors make it likely that cells undergo significant changes in their intracellular [Na^+] during this time.

Using the Na^+ specific fluorescent dye, SBFI, with *in situ* wide-field imaging in the mouse brain, I showed in this work for the first time, that a sub-set of both astrocytes and neurons undergo developmentally regulated spontaneous changes in $[Na^+]_i$ to similar degrees in the cortex and hippocampus. The fluctuations were long lasting (~8 min), irregular in form and a-synchronous between cells. Going forward the study focused on the hippocampus, and a broad pharmacological approach showed that the changes did not appear to be directly linked to spontaneous network oscillations in Ca^{2+}, which have been well described in neonatal neurons. The results indicate that hippocampal neuronal Na^+ fluctuations (seen in ~20% of measured cells) are based on the voltage-gated Na^+ channel dependent action potential firing, and consequent release of GABA from interneurons. This was confirmed by a model simulating neonatal interactions between interneurons and pyramidal cells, which was able to replicate the type of fluctuations seen in experimental measurements.

In addition to neurons, around 40% of measured astrocytes showed spontaneous fluctuations in their $[Na^+]_i$. These were reduced in amplitude via blocking of action potential firing, however, many of the classical transmitters were ruled out as providing the driving force behind the fluctuations generation. Due to the number of cellular processes linked to Na^+, and the extended nature of the elevation, we believe that the fluctuations are involved in regulating developmental processes such as migration and differentiation.

Abbreviations

ACSF	artificial cerebrospinal fluid
AMPA	α-amino-3-hydroxy-5-methyl-4-isoxazolepropionic acid
APV	(2R)-amino-5-phosphonopentanoate
BDNF	brain derived neurotrophic factor
BEST-1	bestrophin-1
CNQX	6-cyano-7-nitroquinoxaline-2,3-dione
CNS	central nervous system
Cx	connexin
ECS	extracellular space
ENO	early network oscillations
GABA	γ-aminobutyric acid
GAT	GABA transporter
GDP	giant depolarising potential
GIRK	G-coupled inwardly rectifying channels
IN	interneuron
KCC2	K^+/Cl^- co-transporter
K_{Na}	Na^+ activated K^+ channels
MGE	medial ganglionic eminence
NBC	Na^+/HCO_3^- cotransporter
NCX	Na^+/Ca^{2+} exchanger
NCLX	$Na^+/Ca^{2+}/Li^+$ exchanger
NHE	Na^+/H^+ exchanger
NKA	Na^+/K^+ ATPase
NKCC1	$Na^+/K^+/Cl^-$ co-transporter
NMDA	N-methyl-D-aspartate
PC	pyramidal cell
PSC	post-synaptic currents
PVBC	parvalbumin expressing basket cells
SBFI	sodium-binding benzofuran isophthalate
SOM IN	somatostatin positive interneurons
TTX	tetrodotoxin
VRAC	volume regulated anion channel

Table of Contents

Introduction

1. Cells within the Developing Brain

The early post-natal brain is an environment in constant flux, wherein cellular identity and function within the network is still being consolidated. The formation of cellular connections is underpinned by the Hebbian rule of 'cells that fire together, wire together', and therefore, interaction between cells is paramount during development. In addition to inter-neuronal communication, astrocytes, the most common form of glial cell in the central nervous system (CNS), modulate network formation by responding to signals and contributing their own. Therefore, both cell types are necessary to ensure normal development.

1.1 Neurons

While the majority of neurons are already in place shortly after birth, they are still in the process of forming synapses. At postnatal day 0 (P0), 80% of CA1 pyramidal cells show no post-synaptic currents (PSC), although they typically already express γ-aminobutyric acid (GABA) and glutamate receptors (Tyzio et al., 1999; Hennou et al., 2002). These young cells, consist of a small soma and axon, which later develop the apical dendrites required for GABAergic synapses, and finally establish basal dendrites. This developmental timeline has also been shown in *in utero* primates, and appears to be highly evolutionarily conserved (Khazipov et al., 2001). Young neurons first develop GABAergic synapses, a process which can be induced by repeated depolarisation of the cell (Gubellini et al., 2001). The glutamate releasing fibres are already in place before birth, and the deferred appearance of glutamatergic synapses is therefore due the delayed maturation of post synaptic targets (figure 1A) (Super and Soriano, 1994). Additionally, those synapses already present are often initially 'silent'- expressing N-methyl-D-aspartate (NMDA) but no α-amino-3-hydroxy-5-methyl-4-isoxazolepropionic acid (AMPA) receptors (Hsia et al., 1998; Gasparini et al., 2000). Therefore, much of the activity during this time period is driven by GABAergic transmission- which, (unlike in the mature brain) depolarises immature pyramidal cells (PC).

The Cl^- Switch

This depolarising effect is attributed to the well documented 'Cl^- switch'- which occurs due to the higher relative expression of the $Na^+/K^+/Cl^-$ cotransporter (NKCC1) during early development (Rohrbough and Spitzer, 1996; Rivera et al., 1999). The NKCC1 imports 2 Cl^-

into the cell along with 1 K^+ and 1 Na^+, thereby raising intracellular Cl^- concentrations ($[Cl^-]_i$) to between 20-40 mM in young neurons, depending on the region (Rohrbough and Spitzer, 1996; Yamada et al., 2004; Sipila et al., 2006b; Achilles et al., 2007). Later in postnatal development, expression of the Cl^- exporting K^+/Cl^- co-transporter (KCC2) increases, finally reaching adult levels at the end of the second week (Rivera et al., 1999; Yamada et al., 2004). The elevated $[Cl^-]_i$ in young neurons leads to an efflux of the anion upon opening of Cl^- channels such as $GABA_A$ receptors, thus rendering the transmitter excitatory in nature (figure 1B). This switch has been shown to be an integral part of post-natal development, as the premature upregulation of the KCC2 severely impairs dendritic development (Cancedda et al., 2007; Chen and Kriegstein, 2015). The upregulation itself seems to be mediated by activation of $GABA_A$ receptors, as the pharmacological inhibition of these prevents the switch from happening. However, the blocking of action potential firing via the application of the voltage gated Na^+ channel antagonist, tetrodotoxin (TTX) has no effect on KCC2 levels. Therefore, miniature PSCs triggered by quantal release of GABA must be sufficient to induce the upregulation (Ganguly et al., 2001; Ben-Ari, 2002). This high sensitivity is in part be due to the high input resistance of young neurons, which render currents from a single $GABA_A$ channel capable of depolarising neurons to their action potential threshold (Serafini et al., 1995). Interestingly, the relative expression of the NKCC1 and KCC2 remains plastic throughout development- and can be returned to the immature state by seizures, lesions, ischemic insults and other pathological conditions (Ben-Ari et al., 2012; Kaila et al., 2014).

Alternative mechanisms for GABAergic excitation in neonates

It should be noted that while the excitatory action of GABA has been broadly accepted since the 90's, more recent work has questioned the concept- as the phenomenon has not yet been proved *in vivo* (Valeeva et al., 2016). Zilberter (2016) have suggested that the switch from excitation to inhibition can rather be attributed to altered metabolism, as young animals have a reduced capacity to metabolise glucose (the substrate most commonly used in *in situ* artificial cerebrospinal fluid (ACSF)). As a functional metabolism is necessary to maintain $[Cl^-]_i$ (via HCO_3^- /Cl^- exchange and Cl^- ATPases) the authors suggest that the Cl^- switch is not developmentally regulated at all, but is instead an artefact of the preparation (Zilberter, 2016). However, several groups have demonstrated that the addition of physiological levels of lactate to neonatal preparations have no effect on the $[Cl^-]_i$ of the cells, although they do slightly alter the cell's pH (Kirmse et al., 2010; Ben-Ari et al., 2011; Tyzio et al., 2011). It has also been suggested that the excitatory action of GABA is an artefact, produced as a consequence of damage inflicted by slicing the tissue (Dzhala et al., 2012). While similar insults such as lesions have been shown to reproduce the

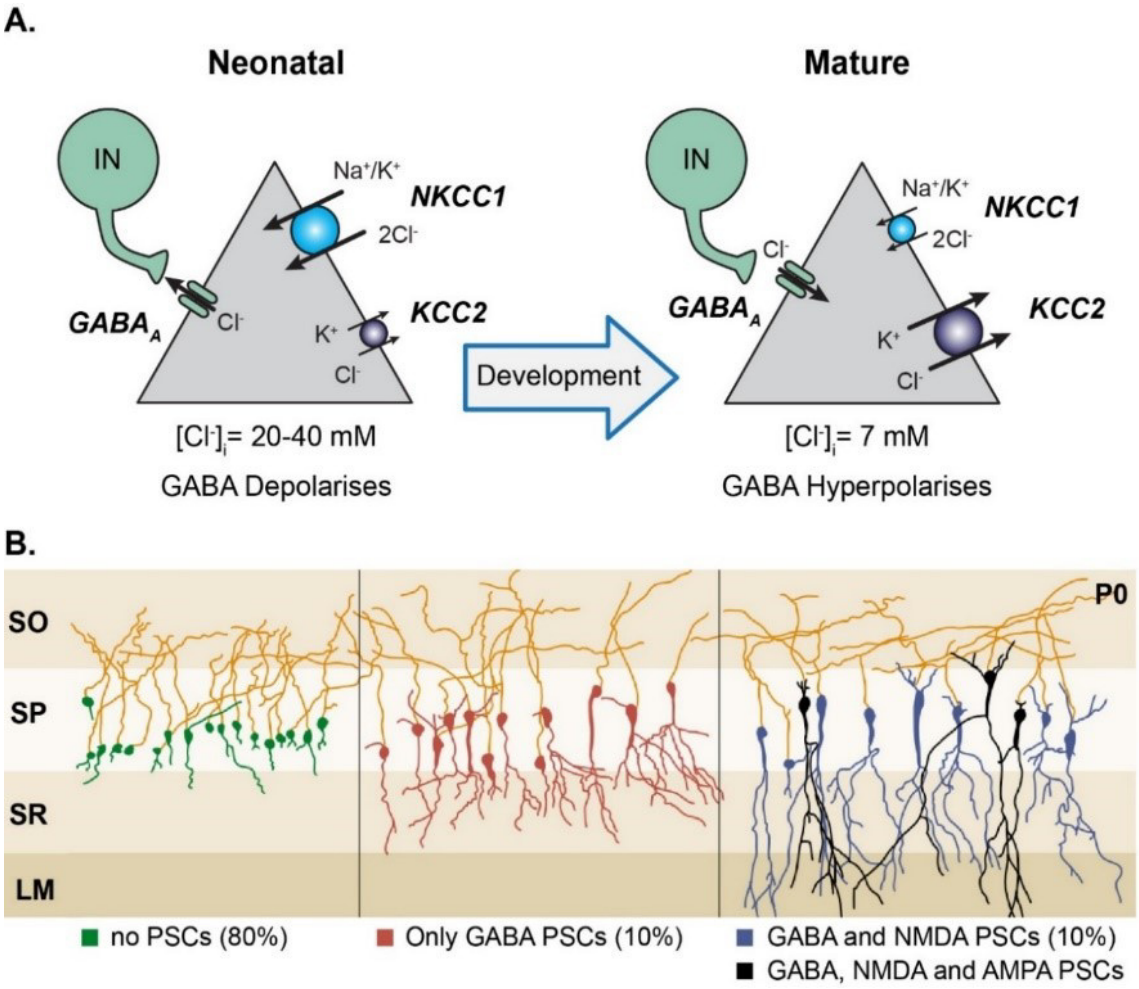

Figure 1. Characteristics of early post-natal pyramidal cells. A. Illustrating the 'chloride switch' wherein greater relative expression of the $Na^+/K^+/Cl^-$ co-transporter (NKCC1) compared to the K^+/Cl^- co-transporter (KCC2) raises intracellular Cl^- levels, thereby rendering the activation of $GABA_A$ receptors depolarising in developing cells. **B.** The various stages of pyramidal cell development present at P0 within the rat hippocampus and the associated PSCs for each stage. Small cells with only axons and small apical dendrites show no PSC- these represent 80% of neurons at P0. A further 10% are larger cells with developed apical dendrites which show GABAergic post synaptic currents (PSCs). The final 10% consist of cells which have both apical and basal dendrites, which show both GABA and glutamate-based PSCs. The majority of glutamate responses are α-amino-3-hydroxy-5-methyl-4-isoxazolepropionic acid (AMPA) only, with a minority of cells possessing both AMPA and N-methyl-D-aspartate (NMDA) currents. Data taken from: (B) Tyzio et al., 1999 modified

depolarising effect of GABA in mature tissue, the clear developmental sequence observed through developmental stages for *in situ* preparations speaks against this theory (Ben-Ari et al., 2012). In order to address the question directly, *in vivo* studies are required. However, the anaesthetics required to perform these experiments have been shown to interfere with GABAergic transmission, and the omission of such anaesthetics (aside from being ethically unacceptable) would be likely to disrupt physiological behaviour through the release of stress hormones (Ben-Ari et al., 2012). New techniques such as genetically expressed

voltage and Ca^{2+} sensors, along with the progression of optogenetic methods, may provide us with the tools needed to settle this debate.

Interneurons

In contrast to PCs, interneurons (IN) do not undergo the Cl^- switch as their expression of the NKCC1 during early development is very low and only reaches adult levels after P21 (Yan et al., 2001). Nevertheless, neonatal hippocampal IN reactions to GABA are often depolarising, although the extent of this excitatory action is diverse across different subtypes and is not yet fully explored (Leinekugel et al., 1995; Khazipov et al., 1997; Tyzio et al., 2008; Sauer and Bartos, 2010). However, there are also studies that show a shunting action of GABA in CA3 INs throughout all developmental stages, an effect which may act to prevent seizure activity during early network oscillations (see section 2) (Banke and McBain, 2006). Apart from spine development, INs undergo the same basic stages of synaptic development as PCs. However, they are typically post-mitotic at an earlier stage and therefore also mature before PCs (Hennou et al., 2002). For example, only 5% of measured INs lacked PSCs when measured at P0. Furthermore, as glutamatergic synapse formation is dependent on the maturation of the post-synaptic components, INs also receive glutamatergic input from PCs before the latter form connections within their own group (Ben-Ari, 2002; Hennou et al., 2002).

1.2 Astrocytes

Astrocytes differentiate and develop primarily postnatally (Freeman, 2010). Therefore, during the first week after birth, the astrocytes present across the brain are in an immature form and differ from their mature counterparts in morphology, expression patterns and signalling behaviour (for a full review of these differences see (Felix et al., 2020b)). These differences result in functional discrepancies which prevent astrocytes from fully fulfilling the tasks assigned to them in adult tissue- indicating that astrocytes may play different roles within the developing brain (figure 2A).

Regulation of the extracellular environment

For example, a prominent astrocytic function in the adult hippocampus is the Na^+ dependent uptake of excess glutamate from the extracellular space (ECS) and control of extracellular environment. However, young astrocytic processes are still in the process of extending out to reach synapses (figure 2C), and their transporter expression is heavily reduced. Therefore, their uptake capacity not fully established (Diamond, 2005; Hanson et al., 2015). Extracellular K^+ uptake is another important astrocytic function in the mature CNS, and is

paramount to preventing excitotoxicity (Larsen et al., 2016). This function is also diminished in the immature brain, partially due to a reduced expression of the α-subunits of the Na^+/K^+ ATPase (NKA). The NKA provides the primary pathway for astrocytic K^+ buffering by utilising the energy gained from the breakdown of 1 ATP, in order to extrude 3 Na^+ ions while bringing in 2 K^+ (Larsen et al., 2019). In addition, other K^+ uptake mechanisms such as inward rectifier potassium channels (especially Kir4.1) and the NKCC1 have a lower expression level in neonatal tissue compared to later in development (Yan et al., 2001; MacVicar et al., 2002; Seifert et al., 2009). A further factor exacerbating this effect is the limited gap junction coupling between young astrocytes (figure 2B). While the expansive, highly connected syncytium characteristic of the mature brain later provides with a route to shuttle K^+ away from uptake sites- the connexins (Cx) needed to build up gap junctions are expressed at low levels shortly after birth (Yamamoto et al., 1992; Schools et al., 2006; Houades et al., 2008). In addition to its impact on K^+ intake, the gap junction network also facilitates the trafficking of other ions, glucose and its metabolites to sites of high activity (Rouach et al., 2008; Clasadonte et al., 2017). This function was demonstrated to be

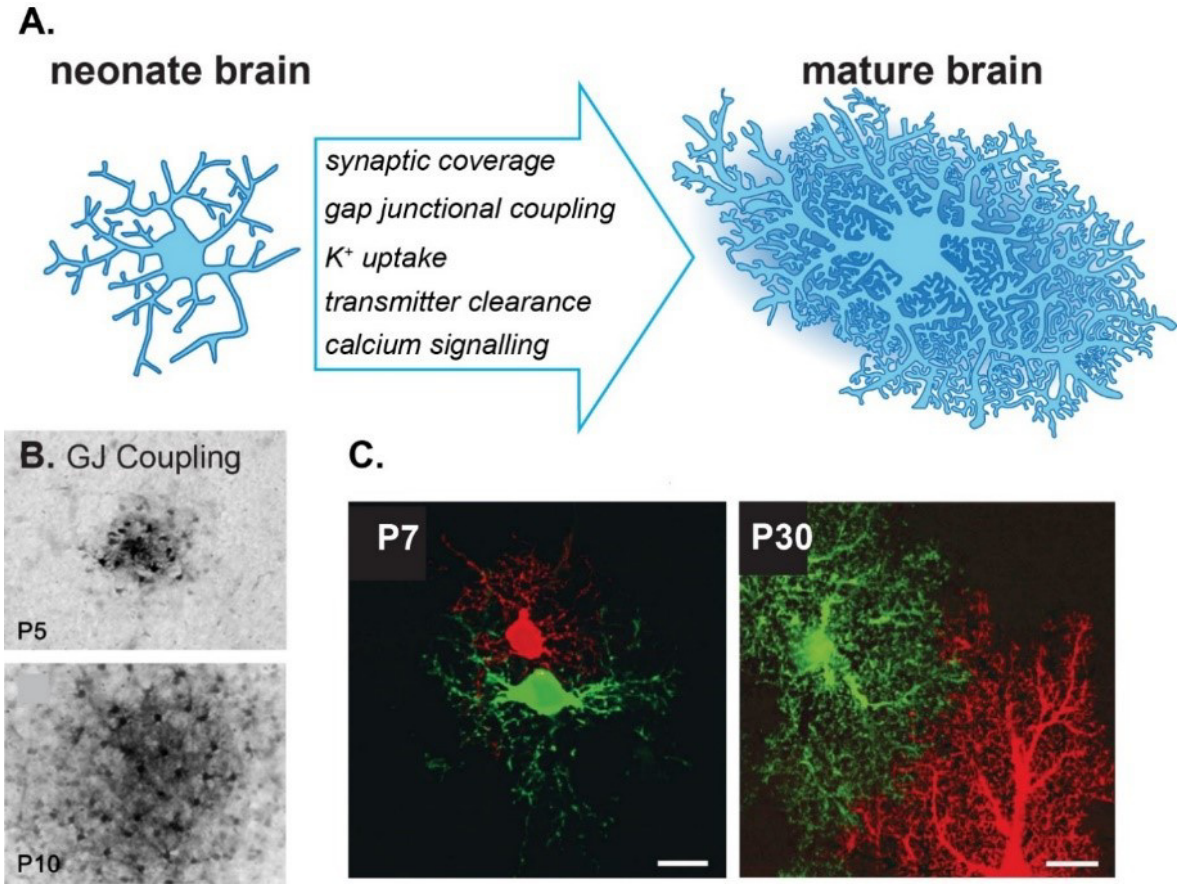

Figure 2. Early post-natal changes in astrocytes. A. Graphic describing the astrocytic functions which are upregulated during post-natal development. **B.** The development of gap junction coupling shown in the barrel cortex. Comparison of biotin spread between astrocytes in P5 (top) and P10 (bottom) mice. **C.** Domain establishment and process arborisation compared in P7 (left) and P30 (right) rats. Data taken from: (A) Felix et al., 2020b (B) Houades et al., 2008 (C) Bushong et al., 2004

diminished in the hippocampus of young animals- as Na^+ here was able to spread over significantly shorter distances compared to matured tissue (Langer et al., 2012).

Developmental roles

Multiple lines of evidence indicate that immature astrocytes fall short of fulfilling the roles classically assigned to them in the adult brain. However, glutamatergic signalling is still in the process of developing during early post-natal stages, and glutamatergic neurons may therefore have reduced need for active astrocytic support (Gasparini et al., 2000). In addition, compensatory mechanisms can fill in for some of the control of the ECS later carried out by astrocytes. For example, Larsen et al. (2019) showed that the increased volume of the ECS in young animals allows for greater diffusion, and thus limits the extent of extracellular K^+ build up even in the absence of fully functional glial uptake (Larsen et al., 2019).

One debate critical for determining astrocytes role during development is centred around Ca^{2+} dependent, vesicular release of transmitters. While many studies have shown that astrocytes are capable of releasing so termed 'glio-transmitters' such as glutamate, some groups have recently argued that this phenomenon is not physiological. The basis for this contention stems from the fact that 1) many studies performed in cultures, may not accurately reflect the behaviour of the cells *in vivo*, and 2) that manipulations performed *in vivo* are often not entirely specific. For example, many studies target astrocytes by using Glial fibrillary acidic protein (GFAP) promoters, and these have the capacity to 'leak', resulting in a minority expression in neurons. Furthermore, while astrocytes do produce vesicles, they do not express synaptotagmin and have no defined release zones (for a full list of arguments for both sides, the reader is referred to the dual perspectives reviews (Fiacco and McCarthy, 2018; Savtchouk and Volterra, 2018).

Nevertheless, developing astrocytes do express a number of receptors and transporters, rendering them capable of detecting and responding to changes in ion concentration and signals in the neonatal brain (for review see (Felix et al., 2020b)). While glio-transmission is under debate, it is clear that astrocytes can contribute to signalling via the reversal up transporters or mechano-channels such as VRACs (see sections 3.1 and 3.5 respectively). In fact, many studies have shown them to play a formative role in developmental processes such as synaptogenesis, via release of growth factors and other signalling molecules (Clarke and Barres, 2013). While this indicates that astrocytes are actively involved in driving development- the mechanisms at play and their consequences and not yet fully understood.

2. Spontaneous activity

In lieu of input from the still developing sensory system, interaction within this environment occurs mainly in the form of spontaneous activity, which has come to characterise the first post-natal weeks and has been demonstrated to be critical for development (Katz and Shatz, 1996). Spontaneously occurring, correlated activity patterns have been reported mainly in neurons. However, astrocytes too send out signals which influence surrounding cells to change their morphology, connectivity, expression profiles and behaviour. In shaping their environment, they alter the input coming back to them- which in turn pushes their own further development. This signalling cycle refines connections and consolidates the required physical complexity, and functional specificity within structures such as the hippocampus. The ability of cells to co-ordinate their activity seems to be innate, with synchronised patterns present even in cultured neurons as they form networks (Rolston et al., 2007; Sun et al., 2010). However, the mechanisms generating and regulating spontaneous activity are region-specific, as are the resulting cellular and network developments. While some of the pathways responsible for the production and regulation of these early patterns have been described, many questions about their generation, modulation and consequences remain unanswered.

Developmentally restricted, spontaneous activity has been measured *in vivo*, with similar electrical patterns found in mice, macaques and humans (reviewed in (Khazipov and Luhmann, 2006; Yang et al., 2009). However, most of our understanding of the mechanisms involved comes from recordings made *in situ*, wherein activity has been recorded both electrically, and as Ca^{2+} oscillations. These have been linked to several developmental processes including migration, establishment of connectivity, myelination, and cortical regionalisation (Spitzer, 2006; Ben-Ari and Spitzer, 2010; Griguoli and Cherubini, 2017; Kirischuk et al., 2017). Two of the best described patterns of spontaneous activity, giant depolarising potentials (GDPs) and early network oscillations (ENOs) will be described briefly below.

2.1 Giant depolarising potentials

The first form of early synchronised activity was described by Ben-Ari et al. (1989) in rat CA3 hippocampal neurons. The group measured regular, suprathreshold depolarisations which they termed ‘giant depolarising potentials’ or GDPs. These were most prominent during the first postnatal week, after which they reduced in frequency until they were no

longer detected at P13 (Ben-Ari et al., 1989). Similar patterns have since been reported *in vivo* (where they are termed sharp waves, (Sipila et al., 2006b), and in several different brain regions *in situ*. These include the developing cortex, thalamus and spinal cord, although the mechanisms of generation are distinct in each region (Pangratz-Fuehrer et al., 2007; Allene et al., 2008; Czarnecki et al., 2014).

The GDP itself is a recurrent depolarisation of up to 50 mV with superimposed action potentials, which lasts 300-500 ms (in contrast to action potentials, which typically have a duration of up to 2 ms (figure 3)) (Leinekugel et al., 2002). The extended depolarisation activates voltage gated Ca^{2+} channels, creating an associated Ca^{2+} signal with each GDP (Leinekugel et al., 1995). This effect is amplified as GABAergic depolarisation can be sufficient to release the Mg^{2+} block from NMDA channels, which then facilitate further Ca^{2+} influx (Leinekugel et al., 1997). Termination occurs when the membrane potential surpasses the reversal potential of $GABA_A$ receptor chloride conductance (E_{GABA}), at which point the transmitters effect switches to being inhibitory (Ben-Ari, 2001; Khalilov et al., 2015). In addition, repolarising K^+ currents are facilitated both via Ca^{2+} activated K^+ channels and through the activation of $GABA_B$ receptors (McLean et al., 1996; Sipila et al., 2006a; Khalilov et al., 2017). These mechanisms limit the duration of GDPs, and produce an inter-burst interval of 3-10 s (figure 3) (Leinekugel et al., 2002).

In the hippocampus, GDPs can stay confined to a relatively small group of several hundred neurons (Khazipov et al., 1997; Garaschuk et al., 1998). The majority of these hippocampal GDPs can be traced back to the CA3, which acts as a pacemaker due to a high level of spontaneous bursting in this region (Mendez de la Prida et al., 1998). However, 20% of GDPs originate in the CA1, which is also capable of generating oscillatory behaviour when surgically separated from the CA3- indicating that it too, has intrinsic hub cell capabilities (Ben-Ari et al., 2007). When propagating between regions in either direction, GDPs move at an average speed of around 25 mm/s (Mendez de la Prida et al., 1998). Across both regions, the blocking of NMDA receptors reduced the frequency, amplitude, synchronisation and duration of the GDPs, implicating glutamate as a modulator of the activity. However, the principle driving force has been shown to stem from the activation of $GABA_A$ receptors, and the reversal potential of GDPs lies close to that of GABA (Ben-Ari et al., 1989; Sipila et al., 2005).

Cortical neurons are also capable of producing GDPs with a similar pharmacology and electrophysiological profile (figure 3). These were synchronised across a subpopulation of around 13% of measured neurons, and were most prominent within deeper cortical layers (Allene et al., 2008). Here, as in the hippocampus, these suprathreshold bursts were also

accompanied by a series of fast Ca^{2+} events and occur at a frequency of around 0.1 Hz, and also triggered by the opening of voltage gated Ca^{2+} channels, and the removal of the Mg^{2+} block from NMDA receptors (Yuste and Katz, 1991; Leinekugel et al., 1995; Eilers et al., 2001).

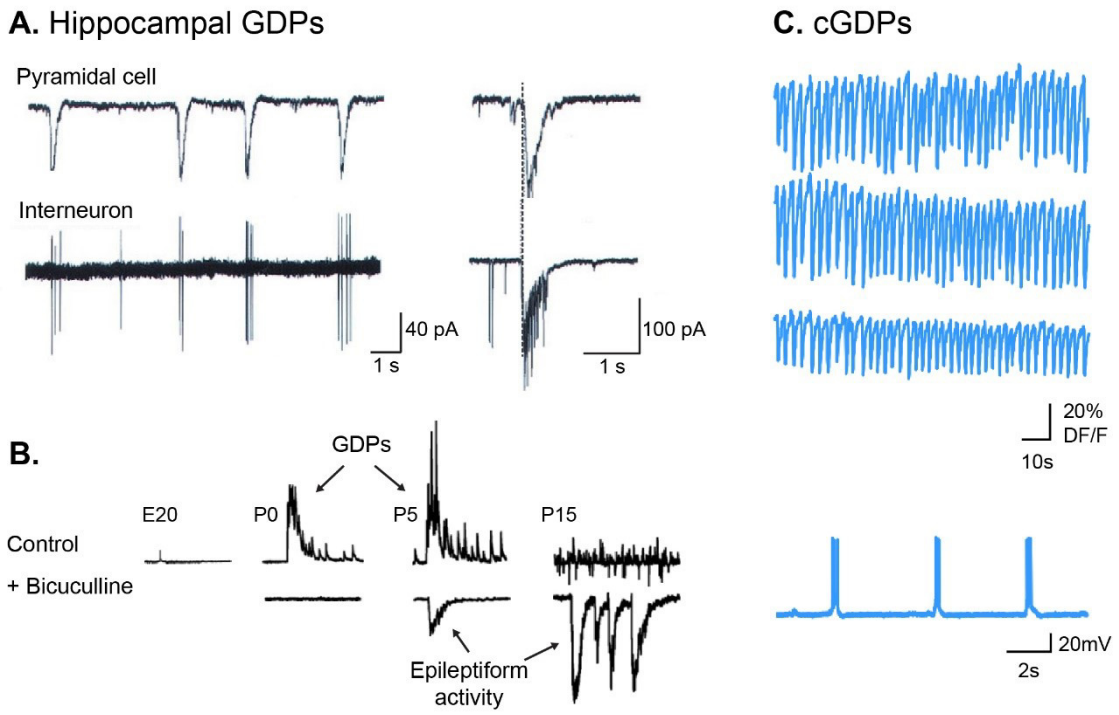

Figure 3. Giant depolarising potentials (GDPs). A. Synchronous bursts in pyramidal cells and interneurons within the hippocampus. Traces show simultaneous recordings of a CA3 pyramidal cell in whole cell voltage clamp configuration (left upper trace) and an interneuron in cell attached configuration (left lower trace). Magnified traces depict simultaneous whole cell recordings from a pyramidal cell (right upper trace) and interneuron (right lower trace). **B.** Changing effects of Bicuculline on giant depolarising potentials (GDPs) during development. As γ-aminobutyric acid (GABA) becomes inhibitory the effects of the antagonist move from blocking synchronised activity to eliciting an epileptiform response. **C.** examples of cortical GDPs with magnified section showing three individual bursts (below). Data taken from: (A) Khazipov et al., 1997 (B) Ben-Ari et al., 2001 (C) Allene et al., 2008

2.2 Neuronal early network oscillations

Early network oscillations in Ca^{2+} (or ENOs) were initially thought to be the cortical equivalent to GDPs (McCabe et al., 2007). However, ENOs precede the appearance of GDPs in the cortex, (having been measured from P0 while the latter first appears at P6) and go on to co-exist for a brief period (Allene et al., 2008). Ca^{2+} oscillations also have distinct characteristics which distinguish them from GDPs. They generally appear as slow waves which move through entire neuronal populations over a time frame of several

seconds (figure 4). While they have been recorded in many brain areas during the first few days after birth, their characteristics are regionally distinct.

For example- within the hippocampus, ENOs appear to be primarily GABAergic in origin, and are eradicated by applications of $GABA_A$ receptor blocker Bicuculline. However, they are also substantially reduced by the inhibition of AMPA and NMDA receptors via 6-cyano-7-nitroquinoxaline-2,3-dione (CNQX) and (2R)-amino-5-phosphonopentanoate (APV) respectively (figure 4B). In the CA1 region, ENOs start at P0 in the form of bursts, consisting of 2-14 individual Ca^{2+} transients with high amplitudes up to 1.5 μM, with a duration of 20 seconds, an inter-burst interval of 5 s and a frequency of 1 min^{-1} (Garaschuk et al., 1998). As development continues, the bursts are gradually replaced by regular, individual transients with decreasing amplitudes, higher frequencies and increased sensitivity to glutamatergic receptor blockers. This continues until the end of the second post-natal week, when ENOs are no longer detected (Garaschuk et al., 1998). This is contrast to the neighbouring CA3 region, where ENOs have been recorded either individually or in pairs, instead of clustering into bursts as is the case in the CA1 (Leinekugel et al., 1997). While they are also initially blocked by Bicuculline, this effect is only present up to P5 (Ben-Ari et al., 1989) (compared to effectiveness up to P13 in the CA1). Additionally, CNQX has been shown to completely block CA3 ENOs while it only partially removed those in the CA1 (Gaïarsa et al., 1990; Garaschuk et al., 1998). Interestingly, hippocampal bursts, although involving almost the entire neuronal population, are not correlated to changes in field potential (Garaschuk et al., 1998).

ENOs are also present across the neonatal cortex in the form of low frequency (~0.01 Hz), large-scale waves, which include around 90% of neurons and have also been measured *in vivo* (Adelsberger et al., 2005; Allene et al., 2008). These waves pass longitudinally along the cortex, primarily from posterior to anterior, travelling at around 2 mm/second (figure 4A/C) (Garaschuk et al., 2000). Cortical early network oscillations, or cENOs, have a distinct pharmacology, and can be blocked by application of NMDA and AMPA antagonists, as well as TTX. The waves thus appear to be propagated primarily by glutamatergic synaptic transmission- although most of the transmission in the cortex at this stage is still GABAergic in nature (Garaschuk et al., 2000; Corlew et al., 2004). However, GABA still appears to play an important role here, as its switch in action from excitatory to inhibitory coincides with the cessation of the cENOs at P6. At P1 the interval between waves is around 4 minutes, however, as development continues, the oscillations become regionally distinct. In the entorhinal cortex, the rate of activity increases from P1-P4 while the amplitudes of the spikes decrease. Furthermore, the activity begins to cluster into groups of 2-3, creating a burst like

pattern. In contrast, the oscillation amplitude in the anterior cortex remains consistent, while the frequency strongly decreases- until at P5, individual transients are only recorded every 20-50 minutes (Garaschuk et al., 2000).

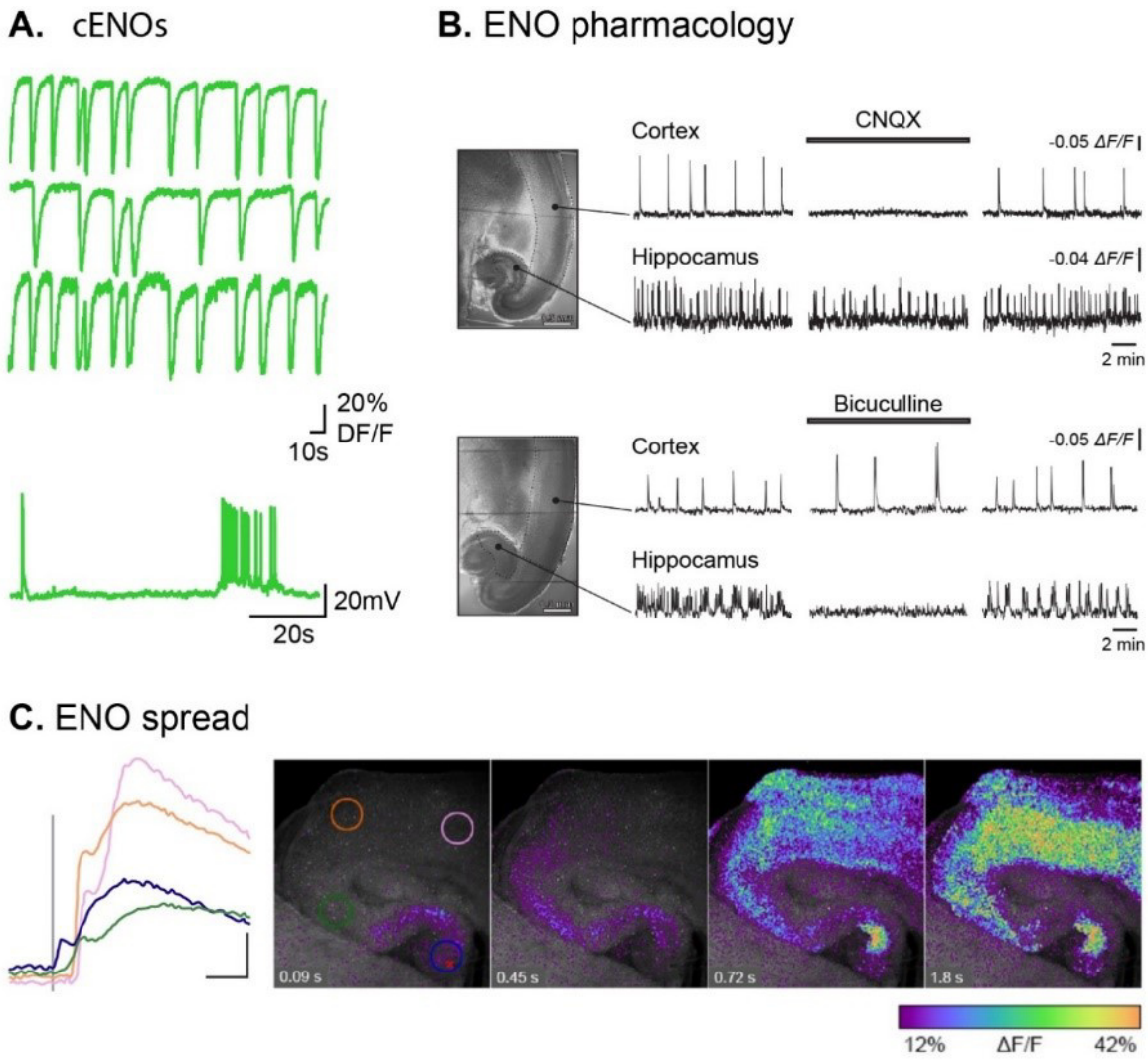

Figure 4. Early network oscillations (ENOs) in Ca^{2+}. A. ENOs measured in cortical pyramidal cells. One magnified trace showing a single ENO (bottom). **B.** Spatial heterogeneity of ENO pharmacology. Cortical ENOs are ablated in the presence of α-amino-3-hydroxy-5-methyl-4-isoxazolepropionic acid (AMPA) receptor blocker, 6-cyano-7-nitroquinoxaline-2,3-dione (CNQX) whereas hippocampal oscillations persist. In contrast, hippocampal ENOs are blocked by $GABA_A$ antagonist, Bicuculline, which does not affect cortical oscillations. **C.** Showing the spread of an ENO originating in the hippocampus and moving through the cortex, encompassing almost the entire population of neurons. Data taken from: (A) Allene et al., 2008 (B) Garaschuk et al., 2000 (C) Barger et al., 2016

Interestingly, these waves have also been shown to cross from the hippocampus into the cortex - a phenomenon which was reduced by antagonists for GABAergic transmission, and completely eradicate by blocking of glutamatergic transmission (figure 4C). However, the majority of cortical ENOs appear to stem from the piriform cortex (Easton et al., 2014; Barger et al., 2016). In addition, a subset of these ENOs was capable of recruiting astrocytes to take part in the Ca^{2+} wave- albeit with a slightly delayed spread (Barger et al., 2016).

2.3 Astrocytic Ca^{2+} oscillations

The involvement of astrocytes in spontaneous network activity is not limited to direct reactions to neuronal activity. Indeed, multiple studies have shown spontaneous oscillations in astrocytic $[Ca^{2+}]_i$ which occur independently from action potential firing. In fact, several lines of evidence point to the possibility that these signals may be a source for the generation of neuronal activity. For example, a study by Parri (2001) showed that around 20% of astrocytes in the ventrobasal thalamus display spontaneous Ca^{2+} oscillations which were directly tied to a slow, NMDA mediated current in nearby neurons. These oscillations propagated as waves through astrocytic populations, although synchrony was largely limited to direct neighbours (figure 5A). In addition to being insensitive to TTX, the activity was not dampened by the blocking of glutamatergic, GABAergic, or purinergic receptors and could only be reduced by antagonists for voltage gated Ca^{2+} channels, as well as preventing Ca^{2+} release from intracellular stores (figure 5C). While the trigger for this activity thus remains unclear, they do appear to be developmentally regulated, and are most prominent in the first post-natal week (Parri et al., 2001).

A further study by Aguado (2002) showed spontaneous Ca^{2+} activity in the neocortex, thalamus, striatum, cerebellum and hippocampus, although in these regions the signals appear to synchronise over larger populations composed of dozens of astrocytes. While the oscillations themselves are neither diminished by ionotropic receptor antagonists or TTX, the latter reduced the level of synchrony between astrocytes, and neurons therefore appear to play a role in co-ordinating the activity. Like in the thalamus, it appears that both intra, and extracellular sources of Ca^{2+} are required for the oscillation. The activity itself was highly irregular, consisting of a mixture of bursts and regular oscillations (figure 5B). This combination cumulated into extended events of 10-45 seconds, with variable amplitudes and frequencies within individual cells. Across all regions, activity first appeared around P2, and remained common within the first 2 postnatal weeks (Aguado et al., 2002).

Within the hippocampus, around 70% of astrocytes partake in oscillations between P5-9, with a reduction to less than half by the end of the third postnatal week and to around a quarter in adult cells. Like the astrocytic activity reported in other brain regions, the oscillations were unaffected by antagonists for purinergic, glutamatergic or GABAergic ionotropic receptors and also remained unaltered by the reduction of gap junction coupling or the blocking of vesicular release (Aguado et al., 2002; Nett et al., 2002). However, antagonists for metabotropic glutamate receptors have provided mixed results, with some evidence showing a reduction in oscillations while others show no effect (Nett et al., 2002; Zur Nieden and Deitmer, 2006). The events here were also irregular in shape and amplitude, with intervals of up to 2 minutes and little synchronicity between cells. Within single cells, the majority of events were confined in individual processes, as has been shown to be the case in mature astrocytes (Nett et al., 2002; Haustein et al., 2014; Rungta et al., 2016; Stobart et al., 2018). Interestingly, astrocytic spontaneous activity is only present in resting astrocytes, and is lost when they become reactive (Aguado et al., 2002). While the reason behind this remains unclear, it makes the use of systems with high levels of active astrocytes, such as organotypic slice cultures, potentially problematic for the study of spontaneous Ca^{2+} oscillations.

While spontaneous activity patterns such as those discussed are necessary for the long-term goal of normal development, they impose constant stress onto the participating cells in the form of short-term ionic imbalances. One ion in particular is critical for the cell to counteract these changes in intracellular concentrations and to retain a stable homeostasis. Na^+ provides, among many other functions, the driving force for the shuttling of other ions, as well as transmitters and metabolites across the membrane.

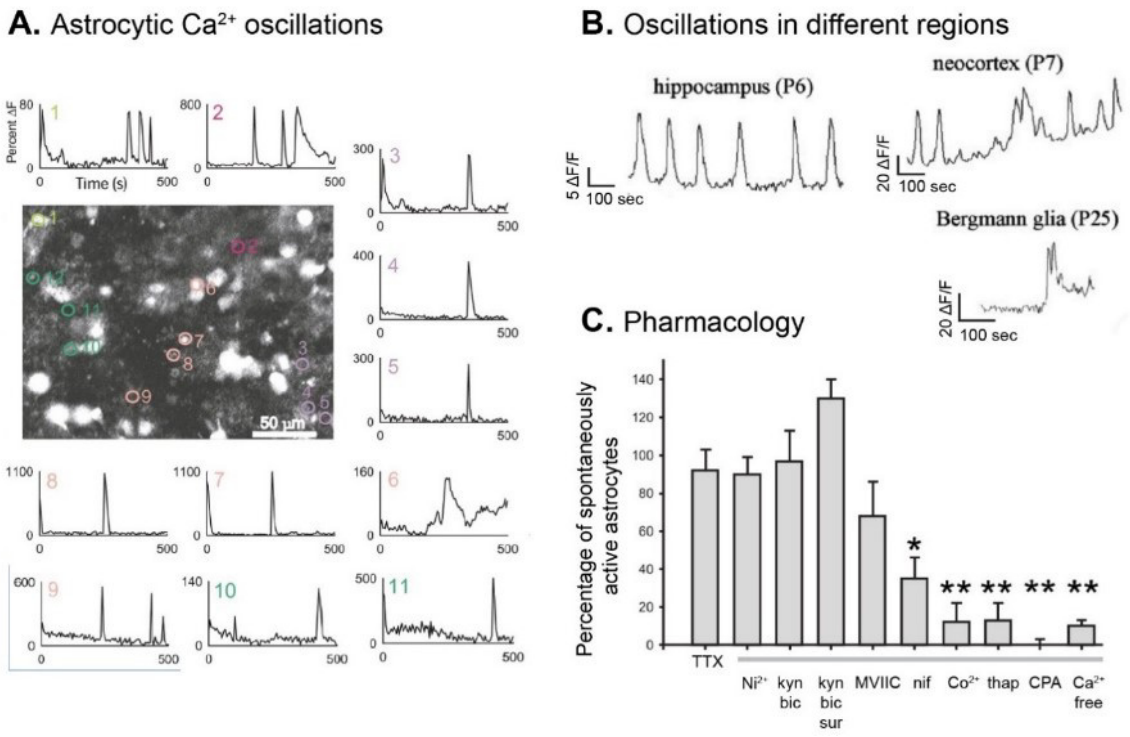

Figure 5. Spontaneous Ca^{2+} signals in astrocytes. A. Spontaneous Ca^{2+} signals in astrocytes of the ventrobasal thalamus. Cells are numbered in the image in the centre and their individual Ca^{2+} traces depicted around the edge (1-11). **B.** Example of oscillations recorded within astrocytes of different brain regions. Area and post-natal day at time of recording indicated. **C.** Percentage of astrocytes showing spontaneous Ca^{2+} activity in the presence of different pharmacological conditions. Voltage gated Na^+ channels, voltage gated Ca^{2+} channels, glutamate receptors, $GABA_A$ receptors, purinergic receptors, N, P and Q Ca^{2+} receptors were blocked by tetrodotoxin (TTX), nickel (Ni^{2+}), kynurenic acid (kyn), bicuculline (bic), suramin (sur) and MVIIC respectively without effect. However, nifedipine (nif), cobolt (Co^{2+}), thapsigarin (thap) and cyclopiazonic acid (CPA) which block L-type Ca^{2+} channels, non-specific Ca^{2+} channels and deplete intracellular Ca^{2+} stores respectively- all lowered the percentage. Data taken from: (A/C) Parri et al., 2001 (B) Aguado et al., 2002

3. Na^+ functions in the developing brain

Both neurons and astrocytes have low $[Na^+]_i$ of 10-17 mM, which does not significantly change throughout development (Kirischuk et al., 2012; Rose and Karus, 2013; Felix et al., 2020c). Coupled with an extracellular concentration ($[Na^+]_o$) of 140-150 mM (Rose and Karus, 2013), this creates a steep inwardly directed gradient, which provides the driving force for a number of membrane processes within all age groups. For electrically excitable neurons, the depolarisation induced influx Na^+ via voltage gated Na^+ channels is a principle component of action potential propagation. Interestingly, astrocytes have also been shown to express voltage gated Na^+ channels, although they are not classically excitable the expression is not sufficient to generate action potentials. These channels have been suggested to produce a persistent inward current of Na^+, which potentiates the activity of

the NKA and thereby controls $[K^+]_o$ levels and excitability (Sontheimer, 1994). In addition, astrocytes possess a number of Na^+ linked receptors, exchangers and transporters which allow them to sense and respond to surrounding activity (for a summary, see (Felix et al., 2020b)). Here, changes in $[Na^+]_i$ provides the cells with a form of excitability and which controls transmitter uptake rate and direction, metabolic support of neurons and K^+ buffering. Some of these mechanisms, and their relationship with the cells $[Na^+]_i$ are discussed below.

3.1 Na^+ dependent transporters

One of the main astrocytic Na^+ dependent functions is the uptake of excess transmitters. Transporters for ascorbic acid (SVCT2), adenosine (CNT), D-serine (ASCT2), glutamine (SNAT3/5), Glycine (GlyT), GABA (GAT) and glutamate (EAAT), are all able to take in their respective transmitter by using the energy gained from also importing Na^+ into the cell (for a summary of see (Felix et al., 2020a)). This allows astrocytes to effectively control the amount of transmitter present in the ECS, and prevent cell death via excitotoxicity. Furthermore, due to their individual reversal potentials, transient increases in $[Na^+]_i$ can trigger a reversal of glutamine, glycine and GABA transporters under physiological condition, thereby also providing a pathway for astrocytes to actively contribute to signalling (Danbolt, 2001; Huang and Bergles, 2004; Wu et al., 2006; Shibasaki et al., 2017).

3.2 pH homeostasis

In addition to transmitter transporters, increases in $[Na^+]_i$ can impact the transport rates and directions of other membrane transporters. This includes pH regulating proteins, namely the Na^+/H^+ exchanger (NHE) and the Na^+/HCO_3^- cotransporter (NBC) (figure 6). While the former of these has a very positive reversal potential which renders it a permanent Na^+ importer under physiological conditions, the NBC has a reversal potential of ~-80 mV, leaving it able to reverse after large Na^+ influx or alkalosis (Theparambil et al., 2015). In the adult brain, import of Na^+ and HCO_3^- by the NBC is activated by neuronal activity, due to the depolarisation caused by astrocytic take up of extracellular K^+ (Brookes and Turner, 1994). This simultaneously alkalises the astrocyte, while acidifying the ECS, which consequently decreases neuronal excitability, and impacts the regulation of blood flow to the area (Newman, 1991). However, while the NBC is expressed at P0, adult levels are not reached until the end of the second post-natal week, suggesting that neonatal animals might rely more heavily on other mechanisms to regulate pH (Giffard et al., 2000). The lack of NBC induced alkalisation may be partially responsible for the reduced sensitivity of neonatal astrocytes to pathological events such as ischemia, as acidification has been shown to have

protective effects under these conditions (Giffard et al., 1990). In contrast, dysfunction of the NHE has been linked to several neuro-developmental disorders.

3.3 Na^+ link to Ca^{2+} signalling

Another important example of Na^+ induced transport reversal is the Na^+/Ca^{2+} exchanger (NCX), which moves 3 Na^+ across the membrane in exchange for 1 Ca^{2+}, effectively coupling the two ions (figure 6). The reversal potential of the NCX lies very close to the resting membrane potential (between -90 and -60 mV), meaning that it can operate in either direction depending on the environment (Verkhratsky et al., 2018; Rose et al., 2020). During phases of high activity when Ca^{2+} is elevated, these transporters work to quickly shuttle Ca^{2+} back out of the cell, until the concomitant increase in Na^+ slows the exchangers activity, leaving the rest of the Ca^{2+} to be removed by the slower Ca^{2+}-ATPase (Regehr, 1997). Conversely, activity related Na^+ influxes (such as activation of NMDA receptors or influx via epithelial Na^+ channels (ENaCs) can be sufficient to reverse the exchanger, resulting in the influx of Ca^{2+} from the ECS and (reviewed in (Kirischuk et al., 2012; Petrik et al., 2018; Verkhratsky et al., 2019; Rose et al., 2020). Such a Na^+ induced rise in $[Ca^{2+}]_i$ has been implicated specifically in developmental functions, such as the migration of NG2 glia (Tong et al., 2009). Furthermore, the Ca^{2+} elevation caused by NCX reversal has been shown to induce ATP release from astrocytes in the hippocampus juvenile animals, which interacts with pre- and post-synaptic α1- receptors and inhibits network activity (Boddum et al., 2016; Matos et al., 2018).

In addition to the plasma membrane NCX, mitochondria possess a further Na+, Ca^{2+} exchanger, which (due to its capacity to also transport Li^+) is named the $Na^+/Ca^{2+}/Li^+$ exchanger (NCLX). These exchangers are highly sensitive the cytosolic changed in $[Na^+]$ and react to increases by pumping Na^+ into the mitochondria, thereby releasing Ca^{2+} into the cytosol (Parnis et al., 2013).

It is possible that the reversal of the NCX effect is exacerbated by the existence of spatial microdomains- a concept first put forward by Lederer (1990). In this model, it was speculated that the close proximity of the endoplasmic reticulum to the membrane would create confined areas, which could limit Na^+ diffusion and create spatially restricted $[Na^+]_i$ elevations (Lederer et al., 1990). In these regions, reversal of the NCX could be enhanced enough for the Ca^{2+} influx from the ECS to trigger further Ca^{2+} release from intracellular stores (Doengi et al., 2009). This is supported by immunohistochemical work, which showed a clustering of the NCX and NKA around areas where the ER lies close to the plasma membrane (Blaustein et al., 2002; Lee et al., 2006). Furthermore, the concept is supported

by modelling studies, which showed the creation of $[Na^+]_i$ microdomains by the restriction of cation diffusion within small peri-synaptic processes of astrocytes (Breslin et al., 2018; Wade et al., 2019). However, it should be noted that other studies have failed to find such Na^+ domains between the ER and PM and that the concept remains a topic of debate (Lu and Hilgemann, 2017; Sachse et al., 2017).

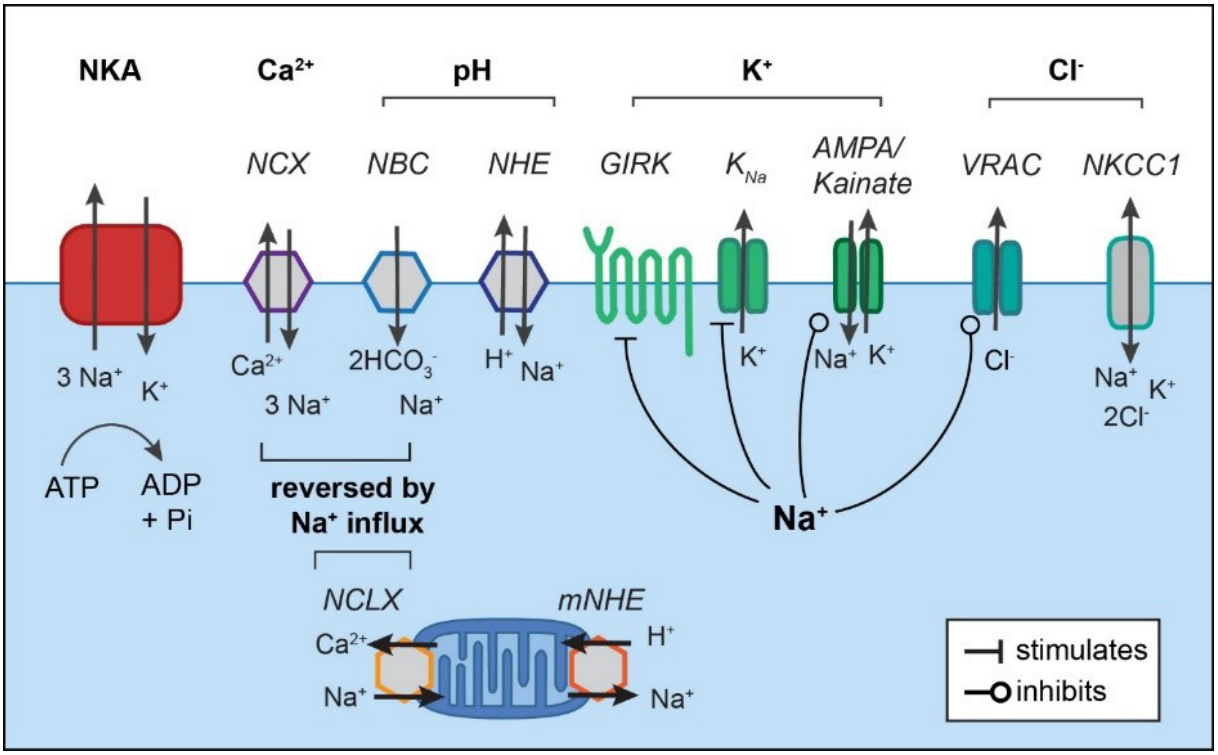

Figure 6. $[Na^+]_i$ linked ion homeostasis. Abbreviations: Na^+/K^+ ATP-ase (NKA), Na^+/Ca^{2+} exchanger (NCX), Na^+/HCO_3^- co-transporter (NBC), Na^+/H^+ exchanger, G protein-coupled inwardly-rectifying potassium channels (GIRK), Na^+ activated K^+ channels (K_{Na}), α-amino-3-hydroxy-5-methyl-4-isoxazolepropionic acid (AMPA), volume regulated anion channels (VRAC), $Na^+/K^+/Cl^-$ co-transporter 1 (NKCC1), $Na^+/Ca^{2+}/Li^+$ exchanger (NCLX), mitochondrial Na^+/H^+ exchanger (mNHE).

3.4 Na^+ responsive K^+ channels

A number of lines of evidence point to the fact that $[Na^+]_{i/o}$ can impact the K^+ currents of various channels (figure 6). These include G-coupled inwardly rectifying channels (GIRK or Kir3.1/3.2), the activation of which are facilitated by intracellular Na^+ elevations at physiological levels, and which regulate inhibition via modulation of $GABA_B$ channels (Sui et al., 1996; Ho and Murrell-Lagnado, 1999; Lujan and Aguado, 2015). GIRK channels are primarily expressed by neurons, although there is some *in vitro* evidence for their presence on astrocytes (Olsen and Sontheimer, 2004). However, expression is also temporally regulated, with low levels in the cortex or hippocampus of the neonatal brain, and gradual increases until adult levels are reached at P20 (Chen et al., 1997).

In addition, a subset of K^+ channels (so far only described in neurons) are directly activated by intracellular Na^+ during periods of high activity (Egan et al., 1992). These K_{Na} channels contribute to the after-hyperpolarisation and play a part in determining the firing rate of neurons (Bhattacharjee and Kaczmarek, 2005). Furthermore, it has been suggested that K_{Na} play a role in controlling basal neuronal excitability, as Na^+ influx via the persistent Na^+ current (I_{NaP}) is also sufficient to activate them (Hage and Salkoff, 2012).

In contrast, intracellular Na^+ elevations (up to around 30 mM) have been shown to have an inhibitory effect on voltage gated, outward delayed rectifying K^+ channels in both neurons and astrocytes (Van Damme et al., 2002). Furthermore, the high $[Na^+]_i$ was shown to lower the expression of K^+ channels expressed by oligodendrocyte precursor cells (Knutson et al., 1997). Elevations in Na^+ sufficient to induce this inhibitory response happen during AMPA/kainate channel activation *in vitro* (Borges and Kettenmann, 1995; Robert and Magistretti, 1997). The function of this mechanism remains unclear, as the consequence is a prolonged depolarisation, which hinders astrocytic K^+ transmitter uptake. However, several studies have tied the modulation to development in oligodendrocytes, where it has been shown to have an anti-proliferative role (Gallo et al., 1996; Knutson et al., 1997; Yuan et al., 1998).

3.5 Relationship between Na^+ and anions

As discussed above, the NKCC1 plays a critical part of PC development due to its involvement in the Cl^- switch (Rohrbough and Spitzer, 1996; Rivera et al., 1999). The transporter has a stoichiometry of $2Cl^-$: K^+: Na^+, with Na^+ intake providing the energy needed to transport the other ions (figure 6). Therefore, any changes in $[Na^+]_i$ are liable to impact the transport rate and consequently also effect intracellular Cl^- concentrations in young neurons. Interestingly, fluorescence lifetime imaging (FLIM) measurements have shown that neonatal Bergmann glia also have an increased $[Cl^-]_i$ compared to their adult counterparts (52 and 35 mM respectively), although their expression of the NKCC1 increases during development, peaking after the third post-natal week (Yan et al., 2001; Untiet et al., 2017). This developmental difference has instead been attributed to a transporter associated Cl^- conductance in Na^+ dependent glutamate transporters (GLT-1 and GLAST), which are upregulated during early development (Untiet et al., 2017).

Like in PCs, the high $[Cl^-]_i$ in neonatal astrocytes means that the reversal potential of Cl^- is more positive than the E_M of the cells, and therefore innervation of $GABA_A$ receptors has a depolarising effect (Kettenmann et al., 1984; Meier et al., 2008). Furthermore, the $[Cl^-]_i$ also shifts the reversal potential of GATs. In the neocortex, this shift, coupled with tonic uptake

of Na^+ via the action of EAATs was shown to be sufficient to keep GATs functioning primarily in the reverse (or outward) mode (Unichenko et al., 2013). The reversal results in elevated levels of ambient GABA in the ECS (~250 nM compared to 125 nM in older animals, (Kirmse and Kirischuk, 2006; Dvorzhak et al., 2010; Untiet et al., 2017).

Astrocytes are well known to adapt to the osmolarity of their surroundings with changes in their volume (Wilson and Mongin, 2018). Reduction or shrinkage of the cells has been in part attributed to the action of volume regulated anion channels (VRACs), which are also expressed by neurons (Kimelberg et al., 2006; Mongin, 2016). These channels are closed at rest, but open during swelling to permit efflux of both Cl^- and K^+. In addition to the ions, the channels have been shown to conduct transmitters including glutamate, D-aspartate, taurine, D-serine and GABA (figure 6) (Mothet et al., 2000; Lutter et al., 2017). This release has been shown to be triggered by G protein-coupled receptor activation, although there is *in vitro* evidence that these channels are also regulated by intracellular Na^+, as increases of 50 mM were shown to dampen their response (Takano et al., 2005; Minieri et al., 2014). Animals lacking the channel have high levels of lethality and serious defects after birth, suggesting an early developmental role for VRACs (Kumar et al., 2014).

3.6 Metabolism

The main mechanism allowing cell to extrude Na^+ against its gradient is the action of the NKA, the action of which requires the breakdown of ATP, thereby directly coupling Na^+ signals to cellular metabolism (figure 6) (Chatton et al., 2000; Langer et al., 2017; Lerchundi et al., 2019). However, to avoid energy exhaustion, the increase in energy consumption triggers mechanisms which compensate for the loss of ATP. For example, high NKA activity increases astrocytic uptake of glucose from vasculature, stimulates the breakdown of glycogen stores and enhances glycolysis and the action of the lactate shuttle (Brown and Ransom, 2007; Pellerin and Magistretti, 2012; Rose and Verkhratsky, 2016). This is critical as lactate is shuttled from the astrocytes to the neurons via the monocarboxylate transport protein (MCT), where it provides a primary energy source in lieu of neuronal glycogen stores (Chatton et al., 2016; Magistretti and Allaman, 2018).

As previously mentioned, Na^+ elevation can be sufficient to reverse the NCX, producing a Ca^{2+} influx which influences the mobility of mitochondria as a response to increased energy demand (Jackson and Robinson, 2018). Simultaneously, the increased $[Na^+]_i$ has direct consequences for ATP production via the mitochondrial NCLX, and mitochondrial NHE. These transporters pass on any changes in cystolic $[Na^+]$ directly to the organelle (Bernardinelli et al., 2006; Parnis et al., 2013). In doing so, they also alter mitochondrial

Ca^{2+} and H^+ concentrations, which in turn impacts the respiratory pathway and ATP production (Azarias and Chatton, 2011). These mechanisms also allow the mitochondria to store Na^+, and their internal $[Na^+]$ is often higher than that of their surroundings (Bernardinelli et al., 2006; Meyer et al., 2019).

3.7 Na^+ effect on receptors

Glutamatergic receptors are also in part modulated by levels of external Na^+. For instance, kainate receptors, which have been linked to spontaneous neonatal activity (see section on GDP mechanisms), are gated by extracellular Na^+ (Paternain et al., 2003). This positive relationship can also been seen in NMDA receptors, which- due to association with Src-kinase- have an increased open probability when $[Na^+]_i$ increases to ~30-40 mM (Yu and Salter, 1999). In hippocampal neurons, this effect has been linked to long term potentiation, while in the cortex, it was shown to enhance synaptogenesis and neurite outgrowth (Lu et al., 1998; George et al., 2012). Neocortical astrocytes also express functional NMDA receptors, the activation of which facilitates Na^+ influxes comparable to those in neurons (Schipke et al., 2001; Lalo et al., 2006; Ziemens et al., 2019). However, whether Na^+ based regulation of the receptor is also present here remains unclear.

In addition to ionotropic receptors, there is evidence that Na^+ can also modulate the activity of metabotropic, G protein-coupled receptors. Purinergic A_1/A_{2A}, dopaminergic, histaminergic and β-adrenergic receptors all contain an extracellular allosteric Na^+ binding site, which when occupied, reduces agonist binding and constitutive activity (Katritch et al., 2014; Strasser et al., 2015; Zarzycka et al., 2019). While it is possible that these are saturated at rest by the high $[Na^+]_o$, some (specifically the dopaminergic D4 and D2, and histaminergic H1 receptors) have a very low Na^+ affinity of K_B>100 mM. For these receptors, physiological changes in $[Na^+]_o$ may be sufficient to impact their function (Zarzycka et al., 2019).

3.8 Na^+ influence on intracellular processes

Up to this point the majority of roles discussed for Na^+ have been in its capacity as a driving force or regulator of membrane processes. However, there is increasing evidence that Na^+ is able to act as a second messenger within cells, and directly influence mechanisms such enzymic activity and transcription. For instance, in skeletal muscle, p94/calpin3 (which is also Ca^{2+} dependent) has been shown activated by physiologically relevant concentrations of Na^+ (Ono et al., 2010).

Muscle cells were also the model in which Na^+ was first implicated in the regulation of gene expression. Here, increases in $[Na^+]_i$ brought about by the inhibition of export by the NKA, and also increased both protein and RNA synthesis (Orlov et al., 2001). The suggested mechanism leading to this increase was the activation of Na^+ dependent response elements on the c-Fos and c-Jun genes (Taurin et al., 2002; Klimanova et al., 2019a). Since the initial discovery, a number of genes in several other cell types (including neurons) were also found to be either K^+ or Na^+ dependent (Koltsova et al., 2012; Klimanova et al., 2019b; Smolyaninova et al., 2019).

While no cases have been definitively shown in astrocytes, a possible example of the such an effect is the inhibition of glutamine synthase, which could be induced by several manipulations which elevated $[Na^+]_i$ (Benjamin, 1987). It remains unclear whether the Na^+ is directly responsible, or whether the upregulation of the ATPase after Na^+ increases simply depleted energy levels. However, the consequences for the cell are significant, as the enzyme is a critical factor both within the glutamate-glutamine cycle, and in the detoxification of ammonium (Danbolt, 2001; Albrecht et al., 2010).

Aim of the Study

It has long been established that developing networks in the CNS possess unique properties that cumulate in the appearance of spontaneous activity patterns. These patterns are present across almost all structures within the brain, and are critical in regulating and driving development of all cell types. In light of the multitude and variety of functions assigned to Na^+ in both neurons and astrocytes as outlined above, our aim in this study was to investigate whether this ion too, undergoes spontaneous changes within cells during neonatal development. To this end we used wide-field fluorescence imaging, primarily with the Na^+ sensitive dye, Sodium-binding benzofuran isophthalate (SBFI). In both astrocytes and neurons, we found spontaneous changes in $[Na^+]_i$ which strongly decreased over the first two postnatal weeks and therefore appeared to be developmentally regulated. To further explore the origin of these fluctuations, we used a broad pharmacological approach. In addition to this, possible connections between the Na^+ fluctuations and changes in other ions were investigated via the use of different ion sensitive fluorescent dyes. Finally, the neuronal signals were simulated within a model, wherein several structural factors were manipulated and their impact evaluated.

Results 1: Cells in the developing brain undergo spontaneous intracellular Na^+ fluctuations

The full methods and results of the initial part of this study can be found in the following paper:

Spontaneous Ultraslow Na^+ Fluctuations in the neonatal mouse brain.
***Felix L**, Ziemens D, Seifert G, Rose CR:* Cells 9 (102) 1-21 (2020a)

In short, we found that a sub-section of both astrocytes and neurons of the neonatal hippocampus and cortex, undergo fluctuations in their $[Na^+]_i$. These fluctuations bear little resemblance to other patterns of spontaneous activity in the neonatal brain, and were characterised as extremely long (average of ~8 minutes), irregular, unsynchronised fluctuations within the cell soma (figure 7). They appear to be developmentally regulated, and were strongly decreased in both cell types over the first two postnatal weeks.

Additional pharmacological investigation showed the amplitudes of neuronal signals to be significantly reduced in the presence of both TTX and the $GABA_A$ receptor blocker,

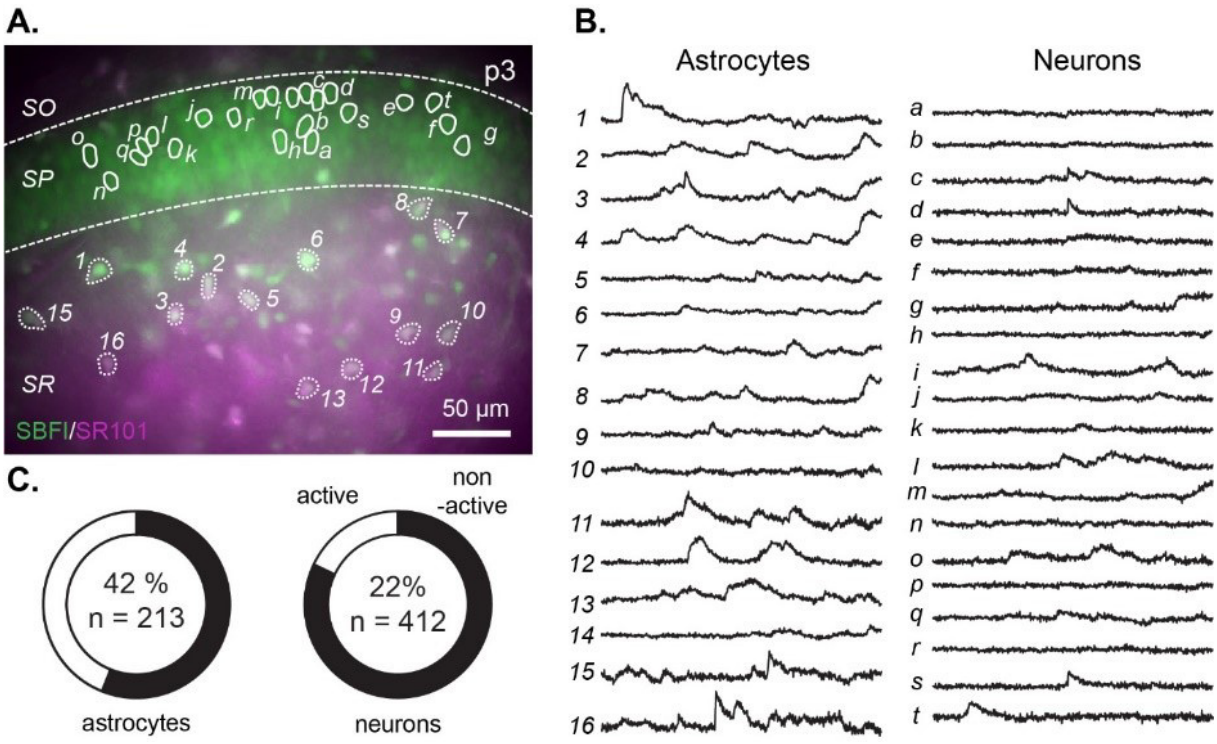

Figure 7. Spontaneous Na+ fluctuations in the developing brain. A. Bolus stained hippocampal slice from a P3 mouse. Na^+ sensitive dye sodium-binding benzofuran isophthalate (SBFI) is shown in green, and astrocyte specific satin SR101 in magenta, with cells containing both shown in white. **B.** example traces with numbers (for astrocytes) and letters (for neurons) corresponding to the cells indicated in A. **C.** Charts indicating the percentage of each cell type with spontaneous fluctuations. Data taken from: Felix et al., 2020a

Bicuculline (control amplitudes averaged around 2 mM). TTX also reduced the amplitude of astrocytic fluctuations, although these remained unaffected by antagonists for GABAergic, glutamatergic, glycinergic, cholinergic, purinergic or adrenergic signalling components (figure 8).

In addition, the possibility of hemi-channel or gap junction involvement was explored both pharmacologically, and via the use of Cx knock-out animals. Neither of these has a significant impact on the propensity or the characteristics of the fluctuations in either cell group.

The involvement of pH regulating mechanisms and Ca^{2+} signals were also tested. While the blocking of the NHE had no significant effect on the fluctuations, introduction of a CO_2/HCO_3^- free ACSF to the slices created a drop in Na^+, after which the fluctuations showed a higher amplitude. However, fluorescence recordings of neonatal cells using the pH sensitive dye 2′,7′-bis-(2-carboxyethyl)-5-(and-6)-carboxy-fluorescein (BCECF) showed no spontaneous changes during experiments. In contrast, Ca^{2+} measurements made using the Ca^{2+} dye Oregon Green 488 BAPTA-1 (OGB-1) showed high levels of spontaneous Ca^{2+} activity within cells. Elimination of these signals via the chelation of intra and extracellular Ca^{2+} substantially increased both the amplitude and duration of Na^+ fluctuations in astrocytes, while producing recurrent activity in neurons. However, neither antagonists for the NCX nor raising the experimental temperature had significant effects on the fluctuation properties for either cell types (figure 8).

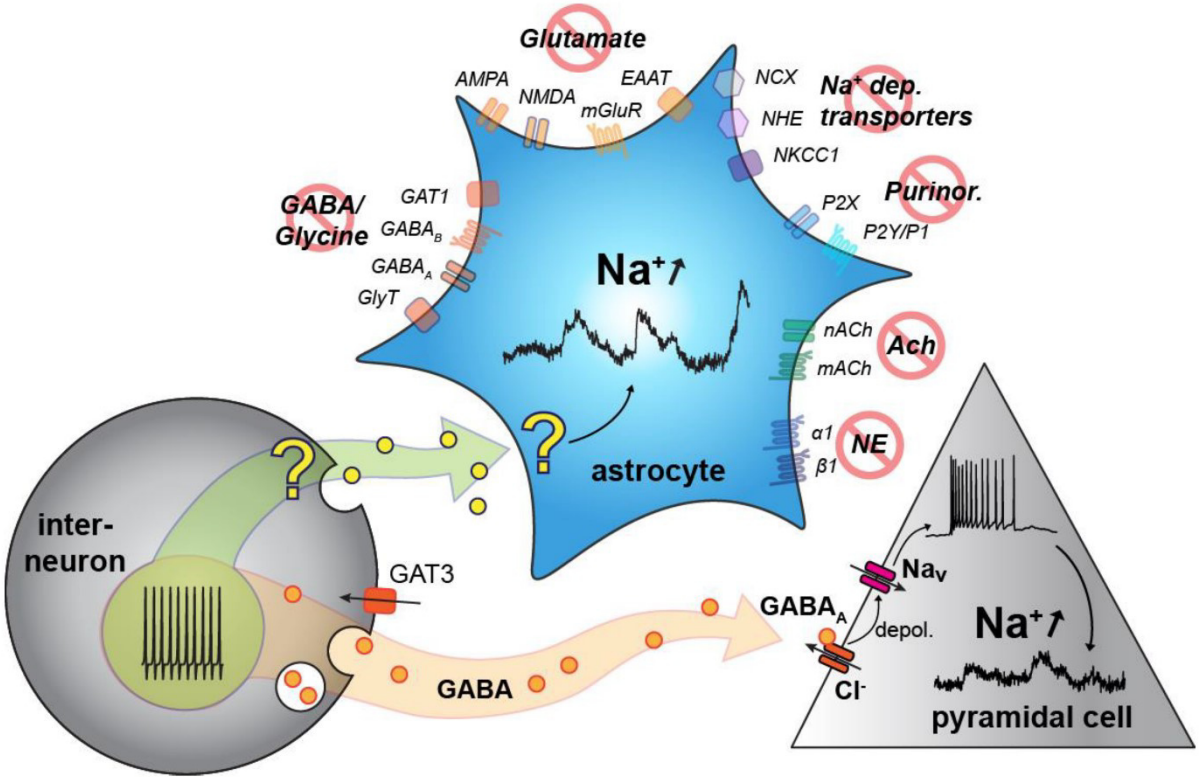

Figure 8: Summary of results. Interneuron firing (bottom left) stimulated release of GABA, which depolarises pyramidal cells (bottom right) via Cl^- efflux through $GABA_A$ receptors. This opens voltage gated Na^+ channels which produces neuronal Na^+ fluctuations. Interneuron activity also appears to be responsible for astrocytic fluctuations. These appear to have a separate trigger and mechanism, the source of which remains unclear at present. Abbreviations; Ach: acetylcholine, AMPA: α-amino-3-hydroxy-5-methyl-4-isoxazolepropionic acid, depol: depolarization, EAAT: excitatory amino acid transporter, GABA: γ-aminobutyric acid, GAT: GABA transporter, GlyT: Glycine transporters, Na_V: TTX-sensitive voltage-gated Na^+ channel, NCX: Na^+/Ca^{2+} exchanger, NE: nor-epinephrine, NHE: Na^+/H^+ exchanger, NKCC1: $Na^+/K^+/Cl^-$ co-transporter. Data taken from: Felix et al., 2020a

Discussion 1- open questions.

This initial portion of the study was able to establish, for the first time, that cells in the developing CNS undergo spontaneous fluctuations in their $[Na^+]_i$. In addition to characterising these fluctuations, fundamental questions as to the developmental timeline, regional heterogeneity and specific pathways involved were addressed within the scope of Felix (2020a). In continuing the investigation of Na^+ fluctuations, there remain a number of open questions, the answers to which could yield important information about the mechanisms and functions of fluctuations. In the following section, a number of these will be discussed as to their possible conclusions and the techniques with which these could best be investigated.

How do fluctuations behave intracellularly?

In this study the primary technique used was wide field imaging of bolus stained brain slices. This method has several advantages which suited it for the investigation of spontaneous fluctuations. Firstly, it allowed the imaging of almost the entire CA1 region of the hippocampus at once. As only a portion of cells showed spontaneous activity, and those that did had a low frequency rate average of 2 per hour, this type of imaging maximised the number of fluctuations that we could measure and analyse. In addition, simultaneous measurements of all the cells in the area allowed us to gauge the level of synchronisation, both between neurons in the pyramidal layer, and within the astrocytic population. However, the technique has limited spatial resolution, which, while sufficient to reveal fluctuations in the soma of cells, was not great enough to allow the separate analysis of sub-cellular compartments such as dendrites or astrocytic processes.

As mentioned above, the majority of astrocytic Ca^{2+} signals remain confined within the processes, with only the largest influxes spreading to the soma (Rungta et al., 2016; Stobart et al., 2018). This was also found to be true for neonatal astrocytes, even though they are still in the process of arborisation, and possess only a few, long processes rather than the dense fine web characteristic of mature cells (Nett et al., 2002). However, changes in Na^+ are more difficult to measure, as they have a much lower signal to noise ratio. This is because resting $[Na^+]_i$ stays at around 10 mM, intracellular Ca^{2+} is kept within the nM range. Furthermore, the latter is heavily buffered by endogenous systems within cells and its spread can therefore be restricted by immediate reaction with intracellular elements and uptake into intracellular stores. In contrast, outside of peri-synaptic processes (PAPs) which may create micro-domains by spatially restricting diffusion as discussed above, Na^+ is free

to diffuse rapidly, reaching over rates of up to 100 μm/s along large processes (Langer et al., 2012; Langer et al., 2017).

Single cell recordings

Within single cells, the higher resolution needed to image individual processes can be obtained by filling cells with dye via a patch pipette. This was performed for a series of astrocytes in neonatal slices, however, while the primary processes were clearly visible in these experiments, only a single signal was detected, which presented in all compartments of the cell simultaneously. The lack of spontaneous activity here can in part be explained as this technique only allows the measurement of one cell at a time, thereby reducing the chances that a fluctuation will be recorded. Furthermore, patched cells were recorded with the pipette still attached. As the inside of the patch pipette acts as an extension of the cytosol, it is possible that due to the rapid diffusion of Na^+, any influxes are immediately diluted to the point that they are no longer above the detection threshold. This may be addressed by repeating the experiments with the pipette first being removed from the membrane before recording. Alternatively, the development of reliable genetically encoded Na^+ markers could potentially enable high spatial resolution in multiple cells simultaneously, without the need for invasive techniques such as patch clamp, which have the potential to alter the physiological responses of the cell.

Culture experiments

A further way in which fluctuations in processes could be studied is through the use of astrocytes in primary culture, as the flattening of these astrocytes allows clear isolation of sub-compartments. Such cultures were also tested in the course of this investigation, however, no spontaneous changes in Na^+ were measured in these cells. This result speaks to the conclusion that spontaneous Na^+ fluctuations in neonatal astrocytes are reliant on activity of other cells in their developing environment, as was reflected in the reduction in amplitude upon TTX application. Furthermore, cultured cells are typically first used for experiments after several days *in vitro* to allow recover from preparation. Whether the cells undergo the same developmental changes during these days as they would *in vivo* remains unclear, and therefore this model is not certain to reflect cells of the neonatal brain from which they were isolated. This point should also be taken into consideration if using organotypic slice culture, although this preparation would have the benefit of retaining more of the cellular environment in which astrocytes and neurons develop. However, the slicing procedure acts as lesion-like insult to the tissue, rendering the many of the astrocytes reactive as part of a glial scar. Aguado (2002) showed reactive astrocytes to have no spontaneous Ca^{2+} oscillations, and while the glial scar can be removed to reveal more native

astrocytes in deeper layers, it is possible that the Na^+ fluctuations too would be altered in this experimental model. However, the high spatial resolution created by viral transfection of the slice with ion specific sensor dyes could make organotypic slices a useful tool in further investigation of neuronal fluctuations, as has been shown with ATP sensors (Lerchundi et al., 2019).

Temporal resolution

In addition to a higher spatial resolution, the fast spread rate of Na^+ through the cytosol of the cell would require a much higher temporal resolution to accurately assess the original influx point of Na^+. The scarcity of the fluctuations and their considerable duration meant that long measurements of an hour were necessary to ensure a sufficient quantity of analysable data. Therefore, we used a low imaging frequency (0.2 Hz) to limit phototoxic damage to the cells over the long experiment duration. However, tests were performed at 1 Hz to ensure that faster spikes were not being missed in the control measurements. To assess the spread of fluctuations within cells, an imaging frequency of several Hz would be required. This coupled with adequate spatial resolution, could offer clear answers to where the Na^+ first enters the cell. Such experiments help to determine if a specific sub-group if INs is responsible for the GABA driving the neuronal fluctuations, as different classes of IN preferentially form connection with different areas on PCs (Booker and Vida, 2018).

Do fluctuations pass between cells?

This spread of Na^+ is not limited to a single cell, and can pass across gap junctions into neighboring astrocytes or other glial cells (Langer et al., 2012; Griemsmann et al., 2015; Augustin et al., 2016; Moshrefi-Ravasdjani et al., 2018). The movement of Na^+ through the pan-glial network may provide a mechanism for maintaining the Na^+ gradient in adult tissue. In developing networks, the astrocytic syncytium is not fully connected, as the Cxs which form gap junctions are not expressed at adult levels until after the second postnatal week (Yamamoto et al., 1992; Nagy et al., 1999; Schools et al., 2006). Therefore, it is possible that the developmental drop in the spontaneous Na^+ fluctuations seen in our results is in part due to the increase in network size and therefore the greater capacity of astrocytes to spread their influx to other cells. However, the lack of synchrony between cells suggests that this kind of spread is not present to an extent that would significantly alter the measured properties of the fluctuations. In addition, if cells within reduced networks show larger Na^+ fluctuations, it would follow that cells completely isolated from a network, (as is the case for astrocytes in animals completely lacking Cxs) would have Na^+ fluctuations with even greater Na^+ amplitudes. The cells in Cx-/- animals showed no difference in signal frequency or

amplitude, suggesting that spread between astrocytes or other glia is a significant factor affecting the fluctuation properties.

Are the fluctuations physiological?

Although spontaneous activity is well documented *in vivo*, there are studies which question the suitability of *in situ* preparations to study their properties (for example, see section 1.1 on the action of GABA in neonatal tissue). Indeed, there are aspects of the model which may interfere with or alter the studied phenomena. For example, the introduction of anoxic conditions has been shown to have an inhibitory effect on GDPs, while augmenting ENOs (Dzhala et al., 2001). As the *in situ* preparation method prevents normal distribution of oxygen via blood flow, it is possible that spontaneous activity is more or less prominent in our experiments than they would be *in vivo*. Furthermore, the INs involved in neonatal pattern generation are characterised by a highly extended process morphology along the hippocampus and to other brain regions, and could thereby be severed during preparation (Bonifazi et al., 2009). Due to the possibility that fluctuations were influenced by extended exposure to experimental conditions or continuous stimulation by light, the properties and frequency of fluctuations measured during the first half or the experimental hour where compared to those occurring in the second. No significant differences were found between the two groups, suggesting that the prolonged nature of the experiments does not induce the fluctuation or influence their properties.

Ideally, the fluctuations should be confirmed by performing *in vivo* experiments. However, the most commonly used anaesthetic during these experiments- isofluorane- has been shown to ablate early Ca^{2+} oscillations (Stosiek et al., 2003). Therefore, it's potential impact on Na^{+} fluctuations should first be checked *in situ*.

Signal Analysis

In the studies mentioned in the course of this dissertation, analysis was carried out manually. This means that each fluctuation was identified visually, and that these were then filtered to only include those with amplitudes above three standard deviations of the baseline noise of the cell for further analysis. This method was chosen in lieu of programs capable of reliably identifying and analysing signals with irregular shapes and extended durations. The majority of such algorithms are targeted at Ca^{2+} signals, which (due to the very low intracellular concentration) tend to have much higher signal to noise ratio. As a part of this study, one such program (mSparkles) was adapted in order to be applicable for

Na^+ signals. The program is able to reliably identify and analyse Na^+ peaks during recurrent network activity, induced by chemical disinhibition as has been described in previous work (Karus, 2015). The further development of such software will offer a significant increase in analysis consistency, as well as allowing for analysis of a greater number of cells in a significantly shorter time.

Where is the GABA, driving neuronal fluctuations coming from?

The pharmacological investigation revealed that neuronal Na^+ fluctuations are significantly reduced after the application of $GABA_A$ antagonists, implicating these channels in their production. There are several different GABAergic signaling pathways that could contribute to this activation.

Tonic activation is mediated by primarily by extracellular $GABA_A$ receptors. These have a subunit composition which renders them highly sensitive, and they are therefore not saturated by ambient levels of GABA (Belelli et al., 2009). This means that small changes in external GABA concentrations can have significant effects on receptor response. Such tonic activation has been shown to have developmental consequences including the modulation of neuronal differentiation and migration (Song et al., 2013; Luhmann et al., 2015). The ambient GABA in the ECS responsible for tonic activation can be traced back to several sources. For example, in P0 mice, GABA was found to be released from growth cones in a Ca^{2+}, SNARE independent manor (Demarque et al., 2002). Additionally, GABA has been shown to be released by astrocytes, and levels of tonic inhibition have been shown to positively correlate with GABA immunoreactivity within astrocytes, which varies across brain regions and developmental stages (Yoon et al., 2011). That fact that astrocytic intracellular concentrations appear to be highest at early postnatal stages and gradually decrease over time, supports a developmental role for the transmitter in astrocytes (Yoon and Lee, 2014). While there is little evidence for vesicular GABA release from astrocytes, the reversal of GABA transporters (GATs) provides cells with an alternative pathway to release the transmitter. However, this reversal appears to limited to extracellular GATs, which function as exporters under resting conditions in neonatal tissue (see section 3.5, (Unichenko et al., 2015)). A further pathway for astrocytic GABA release is via Ca^{2+} activated Bestrophin 1 (BEST-1) channels- which are GABA permeable and have been shown to contribute to tonic release in the cerebellum (Lee et al., 2010). While the developmental consequences of BEST-1 channels in other brain regions remain unclear, there is immunohistochemical evidence for their early expression on both hippocampal and cortical astrocytes (Oh and Lee, 2017).

Tonic GABAergic activation may consistently hold neurons in the depolarised window in which spontaneous Na^+ fluctuations occur. However, the strong reduction of spontaneous Na^+ fluctuations by TTX suggests that the primary drive comes from neuronal synaptic GABA release. Synaptic GATs are unlikely to reverse due to the high concentrations of GABA in the cleft after synaptic release (Savtchenko et al., 2015). Instead, these transporters continuously take up excess GABA and limit the activation of post-synaptic $GABA_A$ receptors (Sipila et al., 2004). Therefore, synaptic GABA is primarily released from IN terminals, as has been shown to be the case for GDP generation. In order to speculate on the possible origins and purpose of spontaneous Na^+ fluctuations, it may be helpful to look at the mechanisms underlying GDPs in more detail.

GDP mechanisms

The GABA responsible for GDPs is primarily released from a group of 'hub' INs, which can release the transmitter in a Ca^{2+} and SNARE independent manner (Demarque et al., 2002; Bonifazi et al., 2009; Ben-Ari et al., 2012). While there are over 40 different groups of INs in the hippocampus, a genetic fate mapping study identified the hub cells to stem from a specific sub-population of early generated INs (Picardo et al., 2011). Although this group includes several types of cell, they were all shown to remain present into adulthood. In addition, they all have extensive widespread arborisation and a high connectivity index, even at early developmental stages (Picardo et al., 2011).

INs driving network activity

Many of these hub cells are somatostatin positive INs (SOM INs), which encompass a number cell types including oriens-lacuno-sum moleculare (OLM) cells and bistratified INs (Flossmann et al., 2019). SOM-IN synapses are primarily targeted to the dendrites of PCs, where they remain critical for rhythm generation into adulthood (Stark et al., 2014). The action of these cells is amplified by astrocytes, as the latter respond to GABA via $GABA_B$ receptors and GATs with an increase in $[Ca^{2+}]_i$. This triggers the release of astrocytic ATP, which is breaks down into adenosine in the ECS, and activates IN A_1 receptors- thereby upregulated SOM-IN activity (Matos et al., 2018).

Another IN group implicated as GDP hub cells are basket cells, which constitute around 14% of hippocampal INs, and can be further divided into fast spiking parvalbumin expressing basket cells (PVBC) and lower frequency cholecystokinin expressing basket cells (CCKBC) (Foldy et al., 2010; Pelkey et al., 2017). Of these subtypes, it is the PVBCs which have been connected to the generation of network activity. Morphologically, these

are a-spiny cells, with highly arborised axons which allow them to contact around 2500 PC somata each (with an average of 6 synapses per cell). In addition, they also form connections to other INs, although the percentage of synapses doing so is very low (1%) (Pelkey et al., 2017). The formation of their synapses temporally coincides with the appearance of GDPs within the developing hippocampus, indicating an involvement of PVBCs in their generation. Additionally, PVBCs are of medial ganglionic eminence (MGE) lineage, and the optogenetic blocking of MGE derived cells has been shown to prevent GDP generation (Wester and McBain, 2016). Unlike PCs, PVBCs and other INs have been shown to have AMPA currents from P1 onwards (Matta et al., 2013). This may contribute to their excitability, as is the case in immature CA3 hippocampal INs, which have a higher firing rate than in mature tissue due to the tonic activation of their kainate receptors by ambient glutamate, which acts to attenuate the K^+ based medium duration after-hyperpolarisations (Segerstrale et al., 2010).

Hub cell signalling

The true identity of the hub cells underpinning the production of GDPs remains unclear. It is possible that several IN sub-types are involved in their generation and modulation- either simultaneously, or transiently at distinct developmental stages. However, electrophysiological studies indicate that the hubs do not act as classical oscillating pacemakers, but are rather synaptically driven, with a high rate of excitatory PSCs compared to other GABAergic neurons (Hennou et al., 2002). By using electron microscopy, Takacs, (2008) showed that the synaptic contacts on hub cells were made almost exclusively by glutamatergic PCs (Takacs et al., 2008). These connections are central to a pathway put forward by Sipila, (2005), in which any depolarisation strong enough to trigger the intrinsic bursting behaviour of a small group of young CA3 PCs, would activate INs, which would then further the firing pattern by releasing GABA to further stimulate the PCs (Sipila et al., 2005). This is in contrast to earlier proposed mechanisms, wherein hub cells release GABA in a temporally synchronised manner, in order to produce time locked responses in PCs which trigger GDPs directly (Khazipov et al., 1997). Modelling work has suggested a middle ground, requiring a combination of the two mechanisms, where PCs and INs mutually drive each other to perpetuate the activity pattern (Flossmann et al., 2019). This is supported by the fact that electrophysiological recordings of INs in the CA3 region showed co-operative GABA and glutamatergic components to be required to depolarise the cells and produce GDPs (Khazipov et al., 1997). As the cellular environment is ever changing during the developmental GDP window, it is possible that the mechanism of generation is not static, and shifts from being entirely GABAergic to having a greater

glutamatergic portion due to the gradual development of glutamatergic synapses (Ben-Ari, 2001).

Intrinsic properties of CA3 primary neurons

At all stages, the intrinsic bursting capabilities of CA3 primary neurons appear to be integral for the triggering of GDPs, as GABAergic stimulation alone is not sufficient to induce the action potentials. Several factors contribute to the increased excitability which permits bursting activity upon GABA binding. Firstly, young cells are partially depolarised due to a persistent Na^+ current present (Sipila et al., 2006a; Valeeva et al., 2010). In addition, expression of Kv7.2/3 channels is very low. These channels facilitate I_M, a non-inactivating, low threshold current which is partially responsible for after-hyperpolarisations in mature tissue (Yue and Yaari, 2004). Furthermore, tonic activation of extrasynaptic $GABA_A$ receptors has been suggested to contribute to the depolarisation enabling GDPs, as these receptors are present even before GABAergic synapses are formed (Sipila et al., 2005). Several other factors have been put forward as potential modulators of GDPs. Antagonists against the I_h current and chemokine stromal cell derived factor 1- alpha (SDF-1), as well as gap junction uncoupling, have all been shown to effect GDP properties- however, the evidence remains incomplete and the extent and mechanism of their involvement is unclear (Griguoli and Cherubini, 2017). The culmination of these factors brings the membrane potential of PCs into a window which permits the generation of GDPs.

Connection to Na^+ fluctuations

As GDPs and Na^+ fluctuations are temporally correlated, and share pharmacological similarities, it is possible that these patterns are subject to the same underlying driver. Indeed, many of the pathways suggested to contribute to GDP generation are inherently linked to Na^+ homeostasis. However, the two patterns fundamentally differ in shape, and frequency. Furthermore, there is a large discrepancy in the propensity of GDPs and Na^+ fluctuations, with them involving ~85% and ~20% of the CA1 neuronal population respectively (Garaschuk et al., 1998; Felix et al., 2020c). These facts suggest that the two patterns could be the product of similar inputs, which produce different responses depending on the developmental stage of the individual cell.

Due to the prolonged duration, irregular form and lack of synchrony between cells showing Na^+ fluctuations, we hypothesised that they are the result from the summation of input from multiple INs. The extended increase in Na^+ may provide the PCs with the depolarisation required to develop mature Glu synapses, which in turn facilitate the cells inclusion in synchronised network activity such as GDPs. If this were the case, it is likely that the 20%

of neurons displaying Na^+ fluctuations would include primarily those cells not yet participating in GDPs.

In order to investigate this hypothesis of separate developmental groups further, we implemented a model simulating a series of PCs and basket cell INs, wherein we switched the action of GABA to being excitatory for PCs in order to replicate the developing brain. Furthermore, we conducted dual-staining experiments, where the groups of cells participating in each activity pattern could be compared.

Results 2: Neuronal spontaneous Na^+ fluctuations stem from GABAergic input from INs

The full methods and results of the initial part of this study can be found in the following paper:

On the Origin of Ultraslow Spontaneous Na^+ Fluctuations in Neurons of the Neonatal Forebrain. *Perez C, **Felix L**, Rose CR, Ullah, G:* (2020)

In summary, the model was able to recreate patterns within PCs, similar to those measured in neonatal brain slices (figure 9). Like the experimental results, simulated fluctuations were significantly diminished by removing GABAergic signaling, and were completely ablated when the model omitted voltage gated Na^+ receptors. However, they remained unaffected by the removal of glutamatergic signaling. Fluctuations were only present in modelled PCs in the presence of 'inverted inhibition', wherein the actions of GABA were set to be excitatory. Additionally, neither the model nor extracellular recordings showed large spontaneous changes in $[K^+]_o$ in accompaniment of intracellular Na^+ fluctuations.

By using a simulated network, we were also able to manipulate developmental factors which would be difficult to isolate and control experimentally. These results showed that a smaller neuronal soma size and lower levels of glial uptake both increased the amplitudes of Na^+ fluctuations, and may thereby contribute to the developmental regulation of the activity. Interestingly, increasing the ratio of inter- to ECS (as happens with ongoing development) also increased the amplitudes of intracellular fluctuations, suggesting that the larger relative ECS in young animals instead acts to suppress the fluctuations.

In addition, the modelled network was able to connect several properties of the developing brain to a higher incidence of seizures. This susceptibility was shown to be linked the reduced glial uptake capacities, decreased neuronal radius and most dramatically, the inversion of GABA to have excitatory effects on neurons.

Finally, a series of dual-staining experiments showed no discernable differences in Ca^{2+} activity levels, between the cells displaying Na^+ fluctuations and those for which these were absent. Therefore, Na^+ fluctuations do not sequentially precede GDPs. Instead, the two activity patterns appear to be separate manifestations of the same underlying signaling pathways.

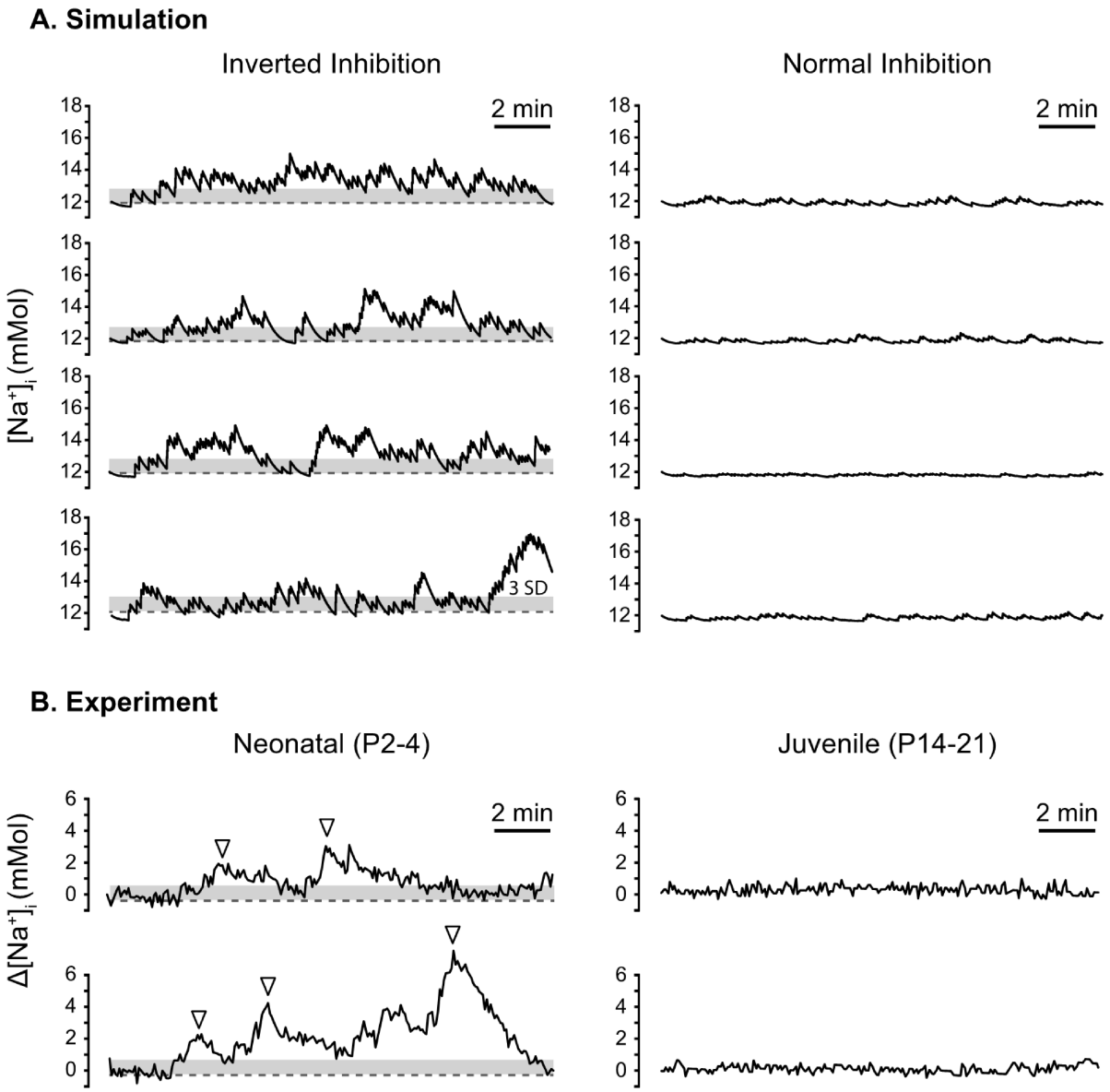

Figure 9: A comparison of fluctuations produced by the simulated cells in the presence of both inverted inhibition (A left) and mature inhibition (A right) with traces showing fluctuations taken from experiments using both neonatal (B left) and juvenile (B right) animals. Dashed lines indicate baseline $[Na^+]_i$ and light grey bars show 3 standard deviations of the baseline noise, which was the minimum amplitude required for fluctuation identification. Data taken from: Felix et al., 2020d

Discussion 2- Proposed mechanisms.

Proposed mechanism for neuronal fluctuations

This follow up study confirmed that the same GABAergic input from IN could summate to produce Na^+ fluctuations in PCs, such as those measured in our experiments. The depolarisation caused by continuous innervation of $GABA_A$ receptors leads to trains of action potentials, which are themselves driven by Na^+ influx through voltage gated channels. During such periods of high activity, this Na^+ builds up within the soma before being gradually extruded by the NKA. This summation of inputs from several different INs results in the irregularity and extended duration of fluctuations.

Interestingly, the system was initially modelled with uniform synaptic strengths across the network. This version of the model also produced extended, irregular Na^+ fluctuations. However, these were synchronised across the entire PC population- which did not reflect the experimental results. As discussed above (see section 1.1) synapses within developing network mature at different rates, depending on at which point individual cells became post-mitotic (Hennou et al., 2002). Therefore, the effect of IN transmission on PCs will vary, depending on the number of connections between them, as well as the maturity and expression profile of their synapses. When the synaptic strengths within the model were varied in order to reflect this, the fluctuations became a-synchronous and varied in shape and frequency between individual PCs, as was seen in the experimental results.

It should be noted, that the model simulates the basic phenomenon of Na^+ fluctuations, and that there are likely to be many contributing or modulatory factors, which influence the frequency and amplitude *in vivo*. For example, the model did not take into account the reduced efficiency of the NKA in developing neurons- which may act to enhance the fluctuations. Furthermore, our experimental results showed a decrease in fluctuation amplitude upon the blocking of α1-noradrenergic receptors, the activation of which has been linked to increased GABA output by INs in the hippocampus (Hillman et al., 2009).

Discussion of possible mechanism for astrocytic fluctuations

As is the case with spontaneous astrocytic Ca^{2+} signals reported previously (see section 2.3), the pharmacological results in this study were not able to give a clear answer as to the mechanism driving astrocytic Na^+ fluctuations. However, the reduction in amplitude after the application of TTX suggest that the fluctuations are at least in part reliant on neuronal activity. This is in contrast to early Ca^{2+} activity and suggests that the two phenomena are not directly linked. The absence of association with astrocytic ENOs is supported by the

apparent insensitivity of astrocytic Na^+ fluctuations to temperature, along with the lack of effect of NCX antagonists and the persistence of fluctuations during the chelation of intra and extracellular Ca^{2+}. The latter condition resulted in synchronised, regular Na^+ transients in neurons, and significantly increased the amplitude and frequency of fluctuations in astrocytes, providing more evidence for their connection to neuronal activity.

However, the nature of this connection remains unclear. As glutamatergic component antagonists had no effect on the fluctuations, it is unlikely that they are a response to PC activity. While there was also no effect on the fluctuations after blocking the components of the primary IN transmitter (GABA), these cells have been shown to co-release two transmitters simultaneously in developing tissue (Nusbaum et al., 2001; Tritsch et al., 2016). However, antagonists for several other signal receptors and transporters (glycinergic, cholinergic, purinergic, adrenergic) also failed to impact the activity. Another possibility is that afferents from other brain regions are responsible for the releasing the transmitter triggering astrocytic Na^+ changes. To investigate this further, transmitters which were not covered in the scope of this study could be examined (e.g. serotonin, dopamine and oxytocin). Indeed, oxytocin is capable of producing spontaneous patterns of Ca^{2+} in cortical neurons termed cortical synchronous plateau assemblies (SPAs) shortly after birth, which have a similar irregular shape and time course as the fluctuations measured here (Allene et al., 2008). However, studies have shown that astrocytes do not express oxytocin receptors, making their reaction to the transmitter unlikely (Ripamonti et al., 2017).

Aside from transmitters, neurons also release substances such as growth factors or neuropeptides, which influence astrocytic $[Na^+]_I$ and have been implicated in cellular physiology during development. For example, GABA induced Ca^{2+} influx (via voltage gated Ca^{2+} channels), has been shown to trigger the release of brain derived neurotrophic factor (BDNF) from PCs. BDNF goes on to target tyrosine kinase receptors on INs, reducing their internalisation of GAT1 and promoting differentiation (Marty et al., 1996; Scimemi, 2014). More recent studies showed that neuronally released BDNF is primarily taken up by astrocytes, due to their high expression of tyrosine receptor kinase B (TrkB) receptors (Stahlberg et al., 2018; Holt et al., 2019). Furthermore, this expression is developmentally regulated and appears to be directly required for astrocytic morphological maturation (Holt et al., 2019).

Alternatively, instead of releasing signals which can directly interact with astrocytes, the continuous firing of neurons could alter the extracellular environment, thereby triggering responsive changes in astrocyte physiology. For example, extracellular K^+ increases could induce swelling, thereby opening mechano-sensitive channels such as Piezo1 (He et al.,

2018). This type of mechanism could account for the extended duration and irregularity of fluctuations, and the a-synchronous responses in neighbouring cells could be a result of different expression patterns. However, extracellular recordings made using ion sensitive micro-pipettes showed no spontaneous changes in $[K^+]_o$ in the neonatal hippocampus (Perez et al., 2020).

A further possibility, is that the effect of TTX is not due to a connection to neuronal firing, but rather reflects the involvement of astrocytic voltage gated Na^+ channels. Like in neurons, these channels are activated by depolarisation, (such as that caused by GABAergic innervation of astrocytic $GABA_A$ receptors) and are sensitive to TTX. Although their function in non-excitable cells remains unclear, they have been shown to be upregulated in response to insult and injury (Pappalardo et al., 2016). The application of TTX after such injury was shown to attenuate the astrocytes ability to migrate and proliferate- a result that implicated astrocytic voltage gated Na^+ channels in these processes (Pappalardo et al., 2014).

Finally, it is possible the fluctuations arise as a consequence of the low expression of the NKA on neonatal astrocytes, which diminishes their ability to extrude Na^+. In this case the influx of Na^+ could stem from a multitude of sources (as many pathways use the Na^+ gradient as a driving force, see section 3), which summate into long, irregular fluctuations due to inefficient removal. This mechanism would explain the lack of synchronicity between cells, as they each have individual inputs and are at different stages of development in regards to their expression profile. In addition, the developmental upregulation of the NKA, along with the decrease in repetitive input patterns, compliments the time frame in which these fluctuations were measured (Larsen et al., 2019).

Conclusion

As outlined in section 3 of the introduction, changes in $[Na^+]_i$ are liable to effect almost all aspects of cellular homeostasis. Therefore, extended period of elevated Na^+ baseline such as those recorded here have to potential to impact cellular development of both neurons and astrocytes. The fluctuations had mean amplitudes of ~2 mM, which while unlikely to change the driving force of importers to a significant degree, could be sufficient to reverse transporters with E_{rev} close to the membrane potential. This extends to the NCX, the reversal of which could impact $[Ca^{2+}]_i$ which, along with being the triggering vesicular neurotransmitter release, is itself is a prolific and well described second messenger in developing cells (Uhlen et al., 2015). The fluctuations also have the potential to promote the outward direction of the NBC, which would alkalise cells and thereby increase neuronal activity (Rose, 1998). Furthermore, the extended elevations in $[Na^+]_i$ may also directly

contribute to signalling by reversing transporters such as those for glutamine, glycine and GABA (see section 3.1).

As discussed in section 1.1 and shown in figure 1, the majority of synapses form after birth. The formation of GABAergic synapses required for inclusion in GDPs can be induced via repeated depolarisation (Gubellini et al., 2001). It is possible that the extended periods of elevated Na^+ provide a portion of the depolarisation required for this synaptic maturation. However, the results in Perez (2020) show that cells showing Na^+ fluctuations are equally likely to participate in synchronised ENO-like activity as those which do not. This finding does not rule out that Na^+ fluctuation linked depolarisations are part of the mechanism driving the maturation of post-synapses, but does imply that the two activity patterns do not appear strictly sequentially. Therefore, it is also possible that they are simply two manifestations of the same underlying signal.

Much of the development of the CNS takes place before cues from the outside world reach the brain through the sensory system. During this time, complex structures such as the hippocampus are shaped by spontaneous activity. These patterns of activity drive changes in just a handful of ions, which are capable of determining the identity of each cell as an individual and within its network. In order to produce the enormous variety of cellular functions and connections needed within fully functioning network, inputs from many different sources may influence the cells in a gradient of degrees. Na^+ fluctuations appear to be the summation of a variety of these inputs, and may provide the cells with a way to integrate all of the information coming in from the environment. This work was the first to record such fluctuations- and many questions remain about their generation, modulation and function. However, the increasing evidence for Na^+ as an active signal within cells, along with the development of new biological tools available to study intracellular changes in $[Na^+]$ with a higher temporal and spatial resolution may soon afford greater insight into their origin and purpose.

References

Achilles, K., Okabe, A., Ikeda, M., Shimizu-Okabe, C., Yamada, J., Fukuda, A., Luhmann, H. J., and Kilb, W. (2007). Kinetic properties of Cl uptake mediated by Na^+-dependent K^+-2Cl cotransport in immature rat neocortical neurons. *J Neurosci* 27**,** 8616-8627 DOI: 10.1523/JNEUROSCI.5041-06.2007.

Adelsberger, H., Garaschuk, O., and Konnerth, A. (2005). Cortical calcium waves in resting newborn mice. *Nat Neurosci* 8**,** 988-990 DOI: 10.1038/nn1502.

Aguado, F., Espinosa-Parrilla, J. F., Carmona, M. A., and Soriano, E. (2002). Neuronal activity regulates correlated network properties of spontaneous calcium transients in astrocytes in situ. *J Neurosci* 22**,** 9430-9444 DOI: 10.1523/JNEUROSCI.22-21-09430.2002.

Albrecht, J., Zielinska, M., and Norenberg, M. D. (2010). Glutamine as a mediator of ammonia neurotoxicity: A critical appraisal. *Biochem Pharmacol* 80**,** 1303-1308 DOI: 10.1016/0006-8993(89)90741-5.

Allene, C., Cattani, A., Ackman, J. B., Bonifazi, P., Aniksztejn, L., Ben-Ari, Y., and Cossart, R. (2008). Sequential generation of two distinct synapse-driven network patterns in developing neocortex. *J Neurosci* 28**,** 12851-12863 DOI: 10.1523/JNEUROSCI.3733-08.2008.

Augustin, V., Bold, C., Wadle, S. L., Langer, J., Jabs, R., Philippot, C., Weingarten, D. J., Rose, C. R., Steinhäuser, C., and Stephan, J. (2016). Functional anisotropic panglial networks in the lateral superior olive. *Glia* 64**,** 1892-1911 DOI: 10.1002/glia.23031.

Azarias, G., and Chatton, J. Y. (2011). Selective ion changes during spontaneous mitochondrial transients in intact astrocytes. *PLoS One* 6**,** e28505 DOI: 10.1371/journal.pone.0028505.

Banke, T. G., and Mcbain, C. J. (2006). GABAergic input onto CA3 hippocampal interneurons remains shunting throughout development. *J Neurosci* 26**,** 11720-11725 DOI: 10.1523/JNEUROSCI.2887-06.2006.

Barger, Z., Easton, C. R., Neuzil, K. E., and Moody, W. J. (2016). Early network activity propagates bidirectionally between hippocampus and cortex. *Dev Neurobiol* 76**,** 661-672 DOI: 10.1002/dneu.22351.

Belelli, D., Harrison, N. L., Maguire, J., Macdonald, R. L., Walker, M. C., and Cope, D. W. (2009). Extrasynaptic GABAA receptors: form, pharmacology, and function. *J Neurosci* 29**,** 12757-12763 DOI: 10.1523/JNEUROSCI.3340-09.2009.

Ben-Ari, Y. (2001). Developing networks play a similar melody. *Trends Neurosci* 24**,** 353-360 DOI: 10.1016/s0166-2236(00)01813-0.

Ben-Ari, Y. (2002). Excitatory actions of gaba during development: the nature of the nurture. *Nat Rev Neurosci* 3**,** 728-739 DOI: 10.1038/nrn920.

Ben-Ari, Y., Cherubini, E., Corradetti, R., and Gaiarsa, J. L. (1989). Giant synaptic potentials in immature rat CA3 hippocampal neurones. *J Physiol* 416**,** 303-325 DOI: 10.1113/jphysiol.1989.sp017762.

Ben-Ari, Y., Gaiarsa, J. L., Tyzio, R., and Khazipov, R. (2007). GABA: a pioneer transmitter that excites immature neurons and generates primitive oscillations. *Physiol Rev* 87**,** 1215-1284 DOI: 10.1152/physrev.00017.2006.

Ben-Ari, Y., Khalilov, I., Kahle, K. T., and Cherubini, E. (2012). The GABA excitatory/inhibitory shift in brain maturation and neurological disorders. *Neuroscientist* 18**,** 467-486 DOI: 10.1177/1073858412438697.

Ben-Ari, Y., and Spitzer, N. C. (2010). Phenotypic checkpoints regulate neuronal development. *Trends Neurosci* 33**,** 485-492 DOI: 10.1016/j.tins.2010.08.005.

Ben-Ari, Y., Tyzio, R., and Nehlig, A. (2011). Excitatory action of GABA on immature neurons is not due to absence of ketone bodies metabolites or other energy substrates. *Epilepsia* 52**,** 1544-1558 DOI: 10.1111/j.1528-1167.2011.03132.x.

Benjamin, A. M. (1987). Influence of Na^+, K^+, and Ca^{2+} on glutamine synthesis and distribution in rat brain cortex slices: a possible linkage of glutamine synthetase with cerebral transport processes and energetics in the astrocytes. *J Neurochem* 48**,** 1157-1164 DOI: 10.1111/j.1471-4159.1987.tb05641.x.

Bernardinelli, Y., Azarias, G., and Chatton, J. Y. (2006). In situ fluorescence imaging of glutamate-evoked mitochondrial Na^+ responses in astrocytes. *Glia* 54**,** 460-470 DOI: 10.1002/glia.20387.

Bhattacharjee, A., and Kaczmarek, L. K. (2005). For K^+ channels, Na^+ is the new Ca^{2+}. *Trends Neurosci* 28**,** 422-428 DOI: 10.1016/j.tins.2005.06.003.

Blaustein, M. P., Juhaszova, M., Golovina, V. A., Church, P. J., and Stanley, E. F. (2002). Na/Ca Exchanger and PMCA Localization in Neurons and Astrocytes. *Ann N Y Acad Sci* 976**,** 356-366 DOI: 10.1111/j.1749-6632.2002.tb04762.x.

Boddum, K., Jensen, T. P., Magloire, V., Kristiansen, U., Rusakov, D. A., Pavlov, I., and Walker, M. C. (2016). Astrocytic GABA transporter activity modulates excitatory neurotransmission. *Nat Commun* 7**,** 13572 DOI: 10.1038/ncomms13572.

Bonifazi, P., Goldin, M., Picardo, M. A., Jorquera, I., Cattani, A., Bianconi, G., Represa, A., Ben-Ari, Y., and Cossart, R. (2009). GABAergic hub neurons orchestrate synchrony in developing hippocampal networks. *science* 326**,** 1419-1424 DOI: 10.1126/science.1175509

Booker, S. A., and Vida, I. (2018). Morphological diversity and connectivity of hippocampal interneurons. *Cell Tissue Res* 373**,** 619-641 DOI: 10.1007/s00441-018-2882-2.

Borges, K., and Kettenmann, H. (1995). Blockade of K^+ channels induced by AMPA/kainate receptor activation in mouse oligodendrocyte precursor cells is mediated by Na^+ entry. *J Neurosci Res* 42**,** 579-593 DOI: 10.1002/jnr.490420416.

Breslin, K., Wade, J. J., Kongfatt, W., Harkin, J., Flanagan, B., Zalinge, H. V., Hall, S., Walker, M., Verkhratsky, A., and Mcdaid, L. (2018). Potassium and sodium microdomains in thin astroglial processes: A computational model study. *PLOS Computational Biology***,** e1006151 DOI: 10.1371/journal.pcbi.1006151.

Brookes, N., and Turner, R. J. (1994). K^+-induced alkalinization in mouse cerebral astrocytes mediated by reversal of electrogenic Na^+-$HCO3^-$ cotransport. *Am J Physiol* 267**,** C1633-1640 DOI: 10.1152/ajpcell.1994.267.6.C1633.

Brown, A. M., and Ransom, B. R. (2007). Astrocyte glycogen and brain energy metabolism. *Glia* 55**,** 1263-1271 DOI: 10.1002/glia.20557.

Cancedda, L., Fiumelli, H., Chen, K., and Poo, M. M. (2007). Excitatory GABA action is essential for morphological maturation of cortical neurons in vivo. *J Neurosci* 27**,** 5224-5235 DOI: 10.1523/JNEUROSCI.5169-06.2007.

Chatton, J. Y., Magistretti, P. J., and Barros, L. F. (2016). Sodium signaling and astrocyte energy metabolism. *Glia* 64**,** 1667-1676 DOI: 10.1002/glia.22971.

Chatton, J. Y., Marquet, P., and Magistretti, P. J. (2000). A quantitative analysis of L-glutamate-regulated Na^+ dynamics in mouse cortical astrocytes: implications for cellular bioenergetics. *Eur J Neurosci* 12**,** 3843-3853 DOI: 10.1046/j.1460-9568.2000.00269.x.

Chen, J., and Kriegstein, A. R. (2015). A GABAergic projection from the zona incerta to cortex promotes cortical neuron development. *Science* 350**,** 554-558 DOI: 10.1126/science.aac6472.

Chen, S., Ehrhard, P., Goldowitz, D., and Smeyne, R. J. (1997). Developmental expression of the GIRK family of inward rectifying potassium channels: implications for abnormalities in the weaver mutant mouse. *Brain research* 778**,** 251-264 DOI: 10.1016/s0006-8993(97)00896-2.

Clarke, L. E., and Barres, B. A. (2013). Emerging roles of astrocytes in neural circuit development. *Nat Rev Neurosci* 14**,** 311-321 DOI: 10.1038/nrn3484.

Clasadonte, J., Scemes, E., Wang, Z., Boison, D., and Haydon, P. G. (2017). Connexin 43-Mediated Astroglial Metabolic Networks Contribute to the Regulation of the Sleep-Wake Cycle. *Neuron* 95**,** 1365-1380 DOI: 10.1016/j.neuron.2017.08.022.

Corlew, R., Bosma, M. M., and Moody, W. J. (2004). Spontaneous, synchronous electrical activity in neonatal mouse cortical neurones. *J Physiol* 560**,** 377-390 DOI: 10.1113/jphysiol.2004.071621.

Czarnecki, A., Le Corronc, H., Rigato, C., Le Bras, B., Couraud, F., Scain, A. L., Allain, A. E., Mouffle, C., Bullier, E., Mangin, J. M., Branchereau, P., and Legendre, P. (2014). Acetylcholine controls GABA-, glutamate-, and glycine-dependent giant depolarizing potentials that govern spontaneous motoneuron activity at the onset of synaptogenesis in the mouse embryonic spinal cord. *J Neurosci* 34**,** 6389-6404 DOI: 10.1523/JNEUROSCI.2664-13.2014.

Danbolt, N. C. (2001). Glutamate uptake. *Prog Neurobiol* 65**,** 1-105 DOI: 10.1016/s0301-0082(00)00067-8.

Demarque, M., Represa, A., Becq, H., Khalilov, I., Ben-Ari, Y., and Aniksztejn, L. (2002). Paracrine intercellular communication by a Ca^{2+}- and SNARE-independent release of GABA and glutamate prior to synapse formation. *Neuron* 36**,** 1051-1061 DOI: 10.1016/s0896-6273(02)01053-x.

Diamond, J. S. (2005). Deriving the glutamate clearance time course from transporter currents in CA1 hippocampal astrocytes: transmitter uptake gets faster during development. *J Neurosci* 25**,** 2906-2916 DOI: 10.1523/JNEUROSCI.5125-04.2005.

Doengi, M., Hirnet, D., Coulon, P., Pape, H. C., Deitmer, J. W., and Lohr, C. (2009). GABA uptake-dependent Ca^{2+} signaling in developing olfactory bulb astrocytes. *Proc Natl Acad Sci U S A* 106**,** 17570-17575 DOI: 10.1073/pnas.0809513106.

Dvorzhak, A., Myakhar, O., Unichenko, P., Kirmse, K., and Kirischuk, S. (2010). Estimation of ambient GABA levels in layer I of the mouse neonatal cortex in brain slices. *J Physiol* 588**,** 2351-2360 DOI: 10.1113/jphysiol.2010.187054.

Dzhala, V., Khalilov, I., Ben-Ari, Y., and Khazipov, R. (2001). Neuronal mechanisms of the anoxia-induced network oscillations in the rat hippocampus in vitro. *j Physiol* 536**,** 521-531 DOI: 10.1111/j.1469-7793.2001.0521c.xd

Dzhala, V., Valeeva, G., Glykys, J., Khazipov, R., and Staley, K. (2012). Traumatic alterations in GABA signaling disrupt hippocampal network activity in the developing brain. *J Neurosci* 32**,** 4017-4031 DOI: 10.1523/JNEUROSCI.5139-11.2012.

Easton, C. R., Weir, K., Scott, A., Moen, S. P., Barger, Z., Folch, A., Hevner, R. F., and Moody, W. J. (2014). Genetic elimination of GABAergic neurotransmission reveals two distinct pacemakers for spontaneous waves of activity in the developing mouse cortex. *J Neurosci* 34**,** 3854-3863 DOI: 10.1523/JNEUROSCI.3811-13.2014.

Egan, T. M., Dagan, D., Kupper, J., and Levitan, I. B. (1992). Na^+-activated K^+ channels are widely distributed in rat CNS and in Xenopus oocytes. *Brain Res* 584**,** 319-321 DOI: 10.1016/0006-8993(92)90913-t.

Eilers, J., Plant, T. D., Marandi, N., and Konnerth, A. (2001). GABA-mediated Ca^{2+} signalling in developing rat cerebellar Purkinje neurons *j Physiol* 536**,** 429-437 DOI: 10.1111/j.1469-7793.2001.0429c.xd

Felix, L., Delekate, A., Petzold, G. C., and Rose, C. R. (2020a). Sodium Fluctuations in Astroglia and Their Potential Impact on Astrocyte Function. *Frontiers in Physiology* 11 DOI: 10.3389/fphys.2020.00871.

Felix, L., Stephan, J., and Rose, C. R. (2020b). Astrocytes of the early postnatal brain. *Eur J Neurosci* DOI: 10.1111/ejn.14780.

Felix, L., Ziemens, D., Seifert, G., and Rose, C. R. (2020c). Spontaneous Ultraslow Na^+ Fluctuations in the Neonatal Mouse Brain. *Cells* 9**,** 102 DOI: 10.3390/cells9010102.

Fiacco, T. A., and Mccarthy, K. D. (2018). Multiple Lines of Evidence Indicate That Gliotransmission Does Not Occur under Physiological Conditions. *J Neurosci* 38**,** 3-13 DOI: 10.1523/JNEUROSCI.0016-17.2017.

Flossmann, T., Kaas, T., Rahmati, V., Kiebel, S. J., Witte, O. W., Holthoff, K., and Kirmse, K. (2019). Somatostatin Interneurons Promote Neuronal Synchrony in the Neonatal Hippocampus. *Cell Rep* 26**,** 3173-3182 e3175 DOI: 10.1016/j.celrep.2019.02.061.

Foldy, C., Lee, S. H., Morgan, R. J., and Soltesz, I. (2010). Regulation of fast-spiking basket cell synapses by the chloride channel ClC-2. *Nat Neurosci* 13**,** 1047-1049 DOI: 10.1038/nn.2609.

Freeman, M. R. (2010). Specification and morphogenesis of astrocytes. *Science* 330**,** 774-778 DOI: 10.1126/science.1190928.

Gaïarsa, J. L., Corradetti, R., Ben-Ari, Y., and Cherubini, E. (1990). "GABA Mediated Synaptic Events in Neonatal Rat CA3 Pyramidal Neurons in Vitro: Modulation by NMDA and Non-NMDA Receptors," in *Excitatory Amino Acids and Neuronal Plasticity,* ed. Y. Ben-Ari. (Boston, MA: Springer US), 151-159.

Gallo, V., Zhou, J. M., Mcbain, C. J., Wright, P., Knutson, P. L., and Armstrong, R. C. (1996). Oligodendrocyte progenitor cell proliferation and lineage progression are regulated by glutamate receptor-mediated K^+ channel block. *J Neurosci* 16**,** 2659-2670 DOI: 10.1523/JNEUROSCI.16-08-02659.1996.

Ganguly, Schinder, A. F., Wong, S. T., and Poo, M. M. (2001). GABA itself promotes the developmental switch of neuronal GABAergic responses from excitation to inhibition. *Cell* 105**,** 521-532 DOI: 10.1016/S0092-8674(01)00341-5

Garaschuk, O., Hanse, E., and Konnerth, A. (1998). Developmental profile and synaptic origin of early network oscillations in the CA1 region of rat neonatal hippocampus. *J Physiol* 507 (Pt 1)**,** 219-236 DOI: 10.1111/j.1469-7793.1998.219bu.x.

Garaschuk, O., Linn, J., Eilers, J., and Konnerth, A. (2000). Large-scale oscillatory calcium waves in the immature cortex. *Nat Neurosci* 3**,** 452-459 DOI: 10.1038/74823.

Gasparini, S., Saviane, C., Voronin, L. L., and Cherubini, E. (2000). Silent synapses in the developing hippocampus: lack of functional AMPA receptors or low probability of glutamate release? *Proc Natl Acad Sci U S A* 97**,** 9741-9746 DOI: 10.1073/pnas.170032297.

George, J., Baden, D. G., Gerwick, W. H., and Murray, T. F. (2012). Bidirectional influence of sodium channel activation on NMDA receptor-dependent cerebrocortical neuron structural plasticity. *Proc Natl Acad Sci U S A* 109**,** 19840-19845 DOI: 10.1073/pnas.1212584109.

Giffard, G., Monyer, H., Christine, A. W., and Choi, D. W. (1990). Acidosis reduces NMDA receptor activation, glutamate neurotoxicity, and oxygen-glucose deprivation neuronal injury in cortical cultures. *brain research* 506**,** 339-342 DOI: 10.1016/0006-8993(90)91276-m

Giffard, G., Papadopoulos, M. C., Van Hooft, J. A., Xu, L., Giuffrida, R., and Monyer, H. (2000). The Electrogenic Sodium Bicarbonate Cotransporter: Developmental Expression in Rat Brain and Possible Role in Acid Vulnerability. *j Neurosci* 20**,** 1001-1008 DOI: 10.1523/JNEUROSCI.20-03-01001.2000

Griemsmann, S., Hoft, S. P., Bedner, P., Zhang, J., Von Staden, E., Beinhauer, A., Degen, J., Dublin, P., Cope, D. W., Richter, N., Crunelli, V., Jabs, R., Willecke, K., Theis, M., Seifert, G., Kettenmann, H., and Steinhauser, C. (2015). Characterization of Panglial Gap Junction Networks in the Thalamus, Neocortex, and Hippocampus Reveals a Unique Population of Glial Cells. *Cereb Cortex* 25**,** 3420-3433 DOI: 10.1093/cercor/bhu157.

Griguoli, M., and Cherubini, E. (2017). Early Correlated Network Activity in the Hippocampus: Its Putative Role in Shaping Neuronal Circuits. *Front Cell Neurosci* 11**,** 1-11 DOI: 10.3389/fncel.2017.00255.

Gubellini, P., Ben-Ari, Y., and Gaiarsa, J. L. (2001). Activity and age dependent GABAergic synaptic plasticity in the developing rat hippocampus. *Eur J Neurosci* 14**,** 1937-1946 DOI: 10.1046/j.0953-816x.2001.01823.x

Hage, T. A., and Salkoff, L. (2012). Sodium-activated potassium channels are functionally coupled to persistent sodium currents. *J Neurosci* 32**,** 2714-2721 DOI: 10.1523/JNEUROSCI.5088-11.2012.

Hanson, E., Armbruster, M., Cantu, D., Andresen, L., Taylor, A., Danbolt, N. C., and Dulla, C. G. (2015). Astrocytic glutamate uptake is slow and does not limit neuronal NMDA receptor activation in the neonatal neocortex. *Glia* 63**,** 1784-1796 DOI: 10.1002/glia.22844.

Haustein, M. D., Kracun, S., Lu, X. H., Shih, T., Jackson-Weaver, O., Tong, X., Xu, J., Yang, X. W., O'dell, T. J., Marvin, J. S., Ellisman, M. H., Bushong, E. A., Looger, L. L., and Khakh, B. S. (2014). Conditions and constraints for astrocyte calcium signaling in the hippocampal mossy fiber pathway. *Neuron* 82**,** 413-429 DOI: 10.1016/j.neuron.2014.02.041.

He, L., Si, G., Huang, J., Samuel, A. D. T., and Perrimon, N. (2018). Mechanical regulation of stem-cell differentiation by the stretch-activated Piezo channel. *Nature* 555**,** 103-106 DOI: 10.1038/nature25744.

Hennou, S., Khalilov, I., Diabira, D., Ben-Ari, Y., and Gozlan, H. (2002). Early sequential formation of functional GABA(A) and glutamatergic synapses on CA1 interneurons of the rat foetal hippocampus. *Eur J Neurosci* 16**,** 197-208 DOI: 10.1046/j.1460-9568.2002.02073.x.

Hillman, K. L., Lei, S., Doze, V. A., and Porter, J. E. (2009). Alpha-1A adrenergic receptor activation increases inhibitory tone in CA1 hippocampus. *Epilepsy Res* 84**,** 97-109 DOI: 10.1016/j.eplepsyres.2008.12.007.

Ho, I. H., and Murrell-Lagnado, R. D. (1999). Molecular determinants for sodium-dependent activation of G protein-gated K^+ channels. *J Biol Chem* 274**,** 8639-8648 DOI: 10.1074/jbc.274.13.8639.

Holt, L. M., Hernandez, R. D., Pacheco, N. L., Torres Ceja, B., Hossain, M., and Olsen, M. L. (2019). Astrocyte morphogenesis is dependent on BDNF signaling via astrocytic TrkB.T1. *Elife* 8 DOI: 10.7554/eLife.44667.

Houades, V., Koulakoff, A., Ezan, P., Seif, I., and Giaume, C. (2008). Gap junction-mediated astrocytic networks in the mouse barrel cortex. *J Neurosci* 28**,** 5207-5217 DOI: 10.1523/JNEUROSCI.5100-07.2008.

Hsia, A. Y., Malenka, R. C., and Nicoll, R. A. (1998). Development of excitatory circuitry in the hippocampus. *J Neurophysiol* 79**,** 2013-2024 DOI: 10.1152/jn.1998.79.4.2013.

Huang, Y. H., and Bergles, D. E. (2004). Glutamate transporters bring competition to the synapse. *Curr Opin Neurobiol* 14**,** 346-352 DOI: 10.1016/j.conb.2004.05.007.

Jackson, J. G., and Robinson, M. B. (2018). Regulation of mitochondrial dynamics in astrocytes: Mechanisms, consequences, and unknowns. *Glia* 66**,** 1213-1234 DOI: 10.1002/glia.23252.

Kaila, K., Price, T. J., Payne, J. A., Puskarjov, M., and Voipio, J. (2014). Cation-chloride cotransporters in neuronal development, plasticity and disease. *Nat Rev Neurosci* 15**,** 637-654 DOI: 10.1038/nrn3819.

Karus, C.,Mondragao, M. A., Ziemens, D. Rose, C. R. (2015). Astrocytes restrict discharge duration and neuronal sodium loads during recurrent network activity. *Glia* 63, 936-957 DOI: 10.1002/glia.22793

Katritch, V., Fenalti, G., Abola, E. E., Roth, B. L., Cherezov, V., and Stevens, R. C. (2014). Allosteric sodium in class A GPCR signaling. *Trends Biochem Sci* 39**,** 233-244 DOI: 10.1016/j.tibs.2014.03.002.

Katz, L. C., and Shatz, C. J. (1996). Synaptic activity and the construction of cortical circuits. *Science* 274**,** 1133-1138 DOI: 10.1126/science.274.5290.1133

Kettenmann, H., Backus, K. H., and Schachner, M. (1984). Aspartate, glutamate and gamma-aminobutyric acid depolarize cultured astrocytes. *Neurosci Lett* 52**,** 25-29 DOI: 10.1016/0304-3940(84)90345-8.

Khalilov, I., Minlebaev, M., Mukhtarov, M., Juzekaeva, E., and Khazipov, R. (2017). Postsynaptic GABA(B) Receptors Contribute to the Termination of Giant Depolarizing Potentials in CA3 Neonatal Rat Hippocampus. *Front Cell Neurosci* 11**,** 179 DOI: 10.3389/fncel.2017.00179.

Khalilov, I., Minlebaev, M., Mukhtarov, M., and Khazipov, R. (2015). Dynamic Changes from Depolarizing to Hyperpolarizing GABAergic Actions during Giant Depolarizing Potentials in the Neonatal Rat Hippocampus. *J Neurosci* 35**,** 12635-12642 DOI: 10.1523/JNEUROSCI.1922-15.2015.

Khazipov, R., Esclapez, M., Caillard, O., Bernard, C., Khalilov, I., Tyzio, R., Hirsch, J., Dzhala, V. I., Berger, B., and Ben-Ari, Y. (2001). Early development of neuronal activity in the primate hippocampus in utero. *j neurosci* 21**,** 9770-9781 DOI: 10.1523/JNEUROSCI.21-24-09770.2001.

Khazipov, R., Leinekugel, X., Khalilov, I., Gaiarsa, J. L., and Ben-Ari, Y. (1997). Synchronization of GABAergic interneuronal network in CA3 subfield of neonatal rat hippocampal slices. *j Physiol* 498**,** 763-772 DOI 10.1113/jphysiol.1997.sp021900

Khazipov, R., and Luhmann, H. J. (2006). Early patterns of electrical activity in the developing cerebral cortex of humans and rodents. *Trends Neurosci* 29**,** 414-418 DOI: 10.1016/j.tins.2006.05.007.

Kimelberg, H. K., Macvicar, B. A., and Sontheimer, H. (2006). Anion channels in astrocytes: biophysics, pharmacology, and function. *Glia* 54**,** 747-757 DOI: 10.1002/glia.20423.

Kirischuk, S., Parpura, V., and Verkhratsky, A. (2012). Sodium dynamics: another key to astroglial excitability? *Trends Neurosci* 35**,** 497-506 DOI: 10.1016/j.tins.2012.04.003.

Kirischuk, S., Sinning, A., Blanquie, O., Yang, J. W., Luhmann, H. J., and Kilb, W. (2017). Modulation of Neocortical Development by Early Neuronal Activity: Physiology and Pathophysiology. *Front Cell Neurosci* 11**,** 379 DOI: 10.3389/fncel.2017.00379.

Kirmse, K., and Kirischuk, S. (2006). Ambient GABA constrains the strength of GABAergic synapses at Cajal-Retzius cells in the developing visual cortex. *J Neurosci* 26**,** 4216-4227 DOI: 10.1523/JNEUROSCI.0589-06.2006.

Kirmse, K., Witte, O. W., and Holthoff, K. (2010). GABA depolarizes immature neocortical neurons in the presence of the ketone body ss-hydroxybutyrate. *J Neurosci* 30**,** 16002-16007 DOI: 10.1523/JNEUROSCI.2534-10.2010.

Klimanova, E. A., Sidorenko, S. V., Smolyaninova, L. V., Kapilevich, L. V., Gusakova, S. V., Lopina, O. D., and Orlov, S. N. (2019a). Ubiquitous and cell type-specific transcriptomic changes triggered by dissipation of monovalent cation gradients in rodent cells: Physiological and pathophysiological implications. *Curr Top Membr* 83**,** 107-149 DOI: 10.1016/bs.ctm.2019.01.006.

Klimanova, E. A., Sidorenko, S. V., Tverskoi, A. M., Shiyan, A. A., Smolyaninova, L. V., Kapilevich, L. V., Gusakova, S. V., Maksimov, G. V., Lopina, O. D., and Orlov, S. N. (2019b). Search for Intracellular Sensors Involved in the Functioning of Monovalent Cations as Secondary Messengers. *Biochemistry (Mosc)* 84**,** 1280-1295 DOI: 10.1134/S0006297919110063.

Knutson, P., Ghiani, C. A., Zhou, J. M., Gallo, V., and Mcbain, C. J. (1997). K^+ channel expression and cell proliferation are regulated by intracellular sodium and membrane depolarization in oligodendrocyte progenitor cells. *J Neurosci* 17**,** 2669-2682 DOI: 10.1523/JNEUROSCI.17-08-02669.1997.

Koltsova, S. V., Trushina, Y., Haloui, M., Akimova, O. A., Tremblay, J., Hamet, P., and Orlov, S. N. (2012). Ubiquitous $[Na^+]_i/[K^+]_i$-sensitive transcriptome in mammalian cells: evidence for Ca^{2+i}-independent excitation-transcription coupling. *PLoS One* 7**,** e38032 DOI: 10.1371/journal.pone.0038032.

Kumar, L., Chou, J., Yee, C. S., Borzutzky, A., Vollmann, E. H., Von Andrian, U. H., Park, S. Y., Hollander, G., Manis, J. P., Poliani, P. L., and Geha, R. S. (2014). Leucine-rich repeat containing 8A (LRRC8A) is essential for T lymphocyte development and function. *J Exp Med* 211**,** 929-942 DOI: 10.1084/jem.20131379.

Lalo, U., Pankratov, Y., Kirchhoff, F., North, R. A., and Verkhratsky, A. (2006). NMDA receptors mediate neuron-to-glia signaling in mouse cortical astrocytes. *J Neurosci* 26**,** 2673-2683 DOI: 10.1523/JNEUROSCI.4689-05.2006.

Langer, J., Gerkau, N. J., Derouiche, A., Kleinhans, C., Moshrefi-Ravasdjani, B., Fredrich, M., Kafitz, K. W., Seifert, G., Steinhauser, C., and Rose, C. R. (2017). Rapid sodium signaling couples glutamate uptake to breakdown of ATP in perivascular astrocyte endfeet. *Glia* 65**,** 293-308 DOI: 10.1002/glia.23092.

Langer, J., Stephan, J., Theis, M., and Rose, C. R. (2012). Gap junctions mediate intercellular spread of sodium between hippocampal astrocytes in situ. *Glia* 60**,** 239-252 DOI: 10.1002/glia.21259.

Larsen, B. R., Holm, R., Vilsen, B., and Macaulay, N. (2016). Glutamate transporter activity promotes enhanced Na^+/K^+-ATPase mediated extracellular K^+ management during neuronal activity. *j Physiol***,** 1-15 DOI: 10.1113/JP272531

Larsen, B. R., Stoica, A., and Macaulay, N. (2019). Developmental maturation of activity-induced K^+ and pH transients and the associated extracellular space dynamics in the rat hippocampus. *J Physiol* 597**,** 583-597 DOI: 10.1113/JP276768.

Lederer, W. J., Niggli, E., and Hadley, R. W. (1990). Sodium-calcium exchange in excitable cells: fuzzy space. *Science* 248**,** 283-283 DOI: 10.1126/science.2326638.

Lee, M. Y., Song, H., Nakai, J., Ohkura, M., Kotlikoff, M. I., Kinsey, S. P., Golovina, V., and Blaustein, M. P. (2006). Local subplasma membrane Ca^{2+} signals detected by a tethered Ca^{2+} sensor. *PNAS* 103**,** 13232-13237 DOI: 10.1073/pnas.0605757103.

Lee, S., Yoon, B. E., Berglund, K., Oh, S., Park, H., Shin, H., Augustin, G. J., and Lee, C. J. (2010). Channel-mediated tonic GABA release from glia. *Science* 330**,** 790-796 DOI: 10.1126/science.1184334

Leinekugel, X., Khazipov, R., Cannon, R., Hirase, H., Ben-Ari, Y., and Buzsaki, G. (2002). Correlated bursts of activity in the neonatal hippocampus in vivo. *Science* 296**,** 2049-2052 DOI: 10.1126/science.1071111.

Leinekugel, X., Medina, I., Khalilov, I., Ben-Ari, Y., and Khazipov, R. (1997). Ca^{2+} Oscillations mediated by the synergistic excitatory actions of GABAa and NMDA receptors in the neonatal hippocampus. *neuron* 18**,** 243-255 DOI: 10.1016/s0896-6273(00)80265-2.

Leinekugel, X., Tseeb, V., Ben-Ari, Y., and Bregestovski, P. (1995). Synaptic $GABA_A$ activation induces Ca^{2+} rise in pyramidal cells and interneurons from rat neonatal hippocampal slices. *j Physiol* 487**,** 319-329 DOI: 10.1113/jphysiol.1995.sp020882.

Lerchundi, R., Kafitz, K. W., Winkler, U., Farfers, M., Hirrlinger, J., and Rose, C. R. (2019). FRET-based imaging of intracellular ATP in organotypic brain slices. *J Neurosci Res* 97**,** 933-945 DOI: 10.1002/jnr.24361.

Lu, F. M., and Hilgemann, D. W. (2017). Na/K pump inactivation, subsarcolemmal Na measurements, and cytoplasmic ion turnover kinetics contradict restricted Na spaces in murine cardiac myocytes. *J Gen Physiol* 149**,** 727-749 DOI: 10.1085/jgp.201711780.

Lu, Y. M., Roder, J. C., Davidow, J., and Salter, M. W. (1998). Src activation in the induction of long-term potentiation in CA1 hippocampal neurons. *Science* 279**,** 1363-1367 DOI: 10.1126/science.279.5355.1363.

Luhmann, H. J., Fukuda, A., and Kilb, W. (2015). Control of cortical neuronal migration by glutamate and GABA. *Front Cell Neurosci* 9**,** 4 DOI: 10.3389/fncel.2015.00004.

Lujan, R., and Aguado, C. (2015). Localization and Targeting of GIRK Channels in Mammalian Central Neurons. *Int Rev Neurobiol* 123**,** 161-200 DOI: 10.1016/bs.irn.2015.05.009.

Lutter, D., Ullrich, F., Lueck, J. C., Kempa, S., and Jentsch, T. J. (2017). Selective transport of neurotransmitters and modulators by distinct volume-regulated LRRC8 anion channels. *J Cell Sci* 130**,** 1122-1133 DOI: 10.1242/jcs.196253.

Macvicar, B. A., Feighan, D., Brown, A., and Ransom, B. (2002). Intrinsic optical signals in the rat optic nerve: role for K^+ uptake via NKCC1 and swelling of astrocytes. *Glia* 37**,** 114-123 DOI: 10.1002/glia.10023.

Magistretti, P. J., and Allaman, I. (2018). Lactate in the brain: from metabolic end-product to signalling molecule. *Nat Rev Neurosci* 19**,** 235-249 DOI: 10.1038/nrn.2018.19.

Marty, S., Berninger, B., Carroll, P., and Thoenen, H. (1996). GABAergic stimulation regulates the phenotype of hippocampal interneurons through the regulation of brain-derived neurotrophic factor. *Neuron* 16**,** 565-570 DOI: 10.1016/s0896-6273(00)80075-6

Matos, M., Bosson, A., Riebe, I., Reynell, C., Vallee, J., Laplante, I., Panatier, A., Robitaille, R., and Lacaille, J. C. (2018). Astrocytes detect and upregulate transmission at inhibitory synapses of somatostatin interneurons onto pyramidal cells. *Nat Commun* 9**,** 4254 DOI: 10.1038/s41467-018-06731-y.

Matta, J. A., Pelkey, K. A., Craig, M. T., Chittajallu, R., Jeffries, B. W., and Mcbain, C. J. (2013). Developmental origin dictates interneuron AMPA and NMDA receptor subunit composition and plasticity. *Nat Neurosci* 16**,** 1032-1041 DOI: 10.1038/nn.3459.

Mccabe, A. K., Easton, C. R., Lischalk, J. W., and Moody, W. J. (2007). Roles of glutamate and GABA receptors in setting the developmental timing of spontaneous synchronized activity in the developing mouse cortex. *Dev Neurobiol* 67**,** 1574-1588 DOI: 10.1002/dneu.20533.

Mclean, H. A., Caillard, O., Khazipov, R., Ben-Ari, Y., and Gaiarsa, J. L. (1996). Spontaneous release of GABA activates $GABA_B$ receptors and controls network activity in the neonatal rat hippocampus. *j Neurophysiol* 76**,** 1036-1046 DOI: 10.1152/jn.1996.76.2.1036

Meier, S. D., Kafitz, K. W., and Rose, C. R. (2008). Developmental profile and mechanisms of GABA-induced calcium signaling in hippocampal astrocytes. *Glia* 56**,** 1127-1137 DOI: 10.1002/glia.20684.

Mendez De La Prida, L., Bolea, S., and Sanchez-Andres, J. V. (1998). Origin of the synchronized network activity in the rabbit developing hippocampus. *Eur J Neurosci* 10**,** 899-906 DOI: 10.1046/j.1460-9568.1998.00097.x

Meyer, J., Untiet, V., Fahlke, C., Gensch, T., and Rose, C. R. (2019). Quantitative determination of cellular $[Na^+]$ by fluorescence lifetime imaging with CoroNaGreen. *J Gen Physiol* 151**,** 1319-1331 DOI: 10.1085/jgp.201912404.

Minieri, L., Pivonkova, H., Harantova, L., Anderova, M., and Ferroni, S. (2014). Intracellular Na^+ inhibits volume-regulated anion channel in rat cortical astrocytes. *J Neurochem* 132**,** 286-300 DOI: 10.1111/jnc.12962.

Mongin, A. A. (2016). Volume-regulated anion channel--a frenemy within the brain. *Pflugers Arch* 468**,** 421-441 DOI: 10.1007/s00424-015-1765-6.

Moshrefi-Ravasdjani, B., Ziemens, D., Pape, N., Färfers, M., and Rose, C. R. (2018). Action Potential Firing Induces Sodium Transients in Macroglial Cells of the Mouse Corpus Callosum. *Neuroglia* 1**,** 106-125 DOI: 10.3390/neuroglia1010009.

Mothet, J. P., Parent, A. T., Wolosker, H., Brady, J. R. O., Linden, D. J., Ferris, C. D., Rogawski, M. A., and Snyder, S. H. (2000). D-serine is an endogenous ligand for the glycine site of the N-methyl-D-aspartate receptor. *PNAS* 97**,** 4926-4931 DOI: 10.1073/pnas.97.9.4926

Nagy, J. I., Patel, D., Ochalski, P. a. Y., and Stelmack, G. L. (1999). Connexin30 in rodent, cat and human brain: selective expression in grey matter astrocytes, co-localization with connexin43 at gap junctions and late dvelopmental appearance. *Neuroscience* 88**,** 447-468 DOI: 10.1016/s0306-4522(98)00191-2.

Nett, W. J., Oloff, S. H., and Mccarthy, K. D. (2002). Hippocampal astrocytes in situ exhibit calcium oscillations that occur independent of neuronal activity. *j Neurophysiol* 87**,** 528-537 DOI: DOI 10.1152/jn.00268.2001.

Newman, E. A. (1991). Sodium-bicarbonate cotransport in retinal müller (glial) cells of the salamander. *j Neurosci* 11**,** 3972-3983 DOI: 10.1523/JNEUROSCI.11-12-03972.1991

Nusbaum, M. P., Blitz, D. M., Swensen, A. M., Wood, D., and Marder, E. (2001). The roles of co-transmission in neural network modulation. *Trends in neuroscience* 24**,** 146-154 DOI: 10.1016/s0166-2236(00)01723-9

Oh, S. J., and Lee, C. J. (2017). Distribution and Function of the Bestrophin-1 (Best1) Channel in the Brain. *Exp Neurobiol* 26**,** 113-121 DOI: 10.5607/en.2017.26.3.113.

Olsen, M. L., and Sontheimer, H. (2004). Mislocalization of Kir channels in malignant glia. *Glia* 46**,** 63-73 DOI: 10.1002/glia.10346.

Ono, Y., Ojima, K., Torii, F., Takaya, E., Doi, N., Nakagawa, K., Hata, S., Abe, K., and Sorimachi, H. (2010). Skeletal muscle-specific calpain is an intracellular Na^+-dependent protease. *J Biol Chem* 285**,** 22986-22998 DOI: 10.1074/jbc.M110.126946.

Orlov, S. N., Taurin, S., Tremblay, J., and Hamet, P. (2001). Inhibition of Na^+,K^+ pump affects nucleic acid synthesis and smooth muscle cell proliferation via elevation of the $[Na^+]_i/[K^+]_i$ ratio: possible implication in vascular remodelling. *J Hypertens* 19**,** 1559-1565 DOI: 10.1097/00004872-200109000-00007.

Pangratz-Fuehrer, S., Rudolph, U., and Huguenard, J. R. (2007). Giant spontaneous depolarizing potentials in the developing thalamic reticular nucleus. *J Neurophysiol* 97**,** 2364-2372 DOI: 10.1152/jn.00646.2006.

Pappalardo, L. W., Black, J. A., and Waxman, S. G. (2016). Sodium channels in astroglia and microglia. *Glia* 64**,** 1628-1645 DOI: 10.1002/glia.22967.

Pappalardo, L. W., Samad, O. A., Black, J. A., and Waxman, S. G. (2014). Voltage-gated sodium channel Nav 1.5 contributes to astrogliosis in an in vitro model of glial injury via reverse Na^+ /Ca^{2+} exchange. *Glia* 62**,** 1162-1175 DOI: 10.1002/glia.22671.

Parnis, J., Montana, V., Delgado-Martinez, I., Matyash, V., Parpura, V., Kettenmann, H., Sekler, I., and Nolte, C. (2013). Mitochondrial Exchanger NCLX Plays a Major Role in the Intracellular Ca^{2+} Signaling, Gliotransmission, and Proliferation of Astrocytes. *j Neurosci* 33**,** 7206-7219 DOI: 10.1523/JNEUROSCI.5721-12.2013.

Parri, H. R., Gould, T. M., and Crunelli, V. (2001). Spontaneous astrocytic Ca^{2+} oscillations in situ drive NMDAR-mediated neuronal excitation. *Nat Neurosci* 4**,** 803-812 DOI: 10.1038/90507.

Paternain, A. V., Cohen, A., Stern-Bach, Y., and Lerma, J. (2003). A role for extracellular Na^+ in the channel gating of native and recombinant kainate receptors. *J Neurosci* 23**,** 8641-8648 DOI: 10.1523/JNEUROSCI.23-25-08641.2003.

Pelkey, K. A., Chittajallu, R., Craig, M. T., Tricoire, L., Wester, J. C., and Mcbain, C. J. (2017). Hippocampal GABAergic Inhibitory Interneurons. *Physiol Rev* 97**,** 1619-1747 DOI: 10.1152/physrev.00007.2017.

Pellerin, L., and Magistretti, P. J. (2012). Sweet sixteen for ANLS. *J Cereb Blood Flow Metab* 32**,** 1152-1166 DOI: 10.1038/jcbfm.2011.149.

Perez, C., Felix, L., Rose, C. R., and Ullah, G. (2020). On the origin of ultraslow spontaneous Na^+ fluctuations in neurons of the neonatal forebrain. DOI: 10.1101/2020.05.29.123026.

Petrik, D., Myoga, M. H., Grade, S., Gerkau, N. J., Pusch, M., Rose, C. R., Grothe, B., and Gotz, M. (2018). Epithelial Sodium Channel Regulates Adult Neural Stem Cell Proliferation in a Flow-Dependent Manner. *Cell Stem Cell* 22**,** 865-878 e868 DOI: 10.1016/j.stem.2018.04.016.

Picardo, M. A., Guigue, P., Bonifazi, P., Batista-Brito, R., Allene, C., Ribas, A., Fishell, G., Baude, A., and Cossart, R. (2011). Pioneer GABA cells comprise a subpopulation of hub neurons in the developing hippocampus. *Neuron* 71**,** 695-709 DOI: 10.1016/j.neuron.2011.06.018.

Regehr, W. G. (1997). Interplay Between Sodium and Calcium Dynamics in Granule Cell Presynaptic Terminals. *Biophysical Journal* 73**,** 2476-2488 DOI: 10.1016/S0006-3495(97)78276-6

Ripamonti, S., Ambrozkiewicz, M. C., Guzzi, F., Gravati, M., Biella, G., Bormuth, I., Hammer, M., Tuffy, L. P., Sigler, A., Kawabe, H., Nishimori, K., Toselli, M., Brose, N., Parenti, M., and Rhee, J. (2017). Transient oxytocin signaling primes the development and function of excitatory hippocampal neurons. *Elife* 6 DOI: 10.7554/eLife.22466.

Rivera, C., Voipio, J., Payne, J. A., Ruusuvuori, E., Lahtinen, H., Lamsa, K., Pirvola, U., Saarma, M., and Kaila, K. (1999). The K^+/Cl^- co-transporter KCC2 renders GABA hyperpolarizing during neuronal maturation. *Nature* 397**,** 251-255 DOI: 10.1038/16697.

Robert, A., and Magistretti, P. J. (1997). AMPA/kainate receptor activation blocks K^+ currents via internal Na^+ increase in mouse cultured stellate astrocytes. *Glia* 20**,** 38-50 DOI: 10.1002/(SICI)1098-1136(199705)20:1<38::AID-GLIA4>3.0.CO;2-1.

Rohrbough, J., and Spitzer, N. C. (1996). Regulation of intracellular Cl^- levels by Na^+- dependent Cl^- cotransport distinguishes depolarizing from hyperpolarizing $GABA_A$ receptor-mediated responses in spinal neurons. *j Neurosci* 16**,** 82-91 DOI: 10.1523/JNEUROSCI.16-01-00082.1996

Rolston, J. D., Wagenaar, D. A., and Potter, S. M. (2007). Precisely timed spatiotemporal patterns of neural activity in dissociated cortical cultures. *Neuroscience* 148**,** 294-303 DOI: 10.1016/j.neuroscience.2007.05.025

Rose, C. R., and Karus, C. (2013). Two sides of the same coin: Sodium homeostasis and signaling in astrocytes under physiological and pathophysiological conditions. 61**,** 1191-1205 DOI: 10.1002/glia.22492.

Rose, C. R., Ransom, B. R. (1998) pH Regulation in Mammalian Glia; Wiley-Liss, Inc.: New York, NY, USA, pp. 253–275

Rose, C. R., and Verkhratsky, A. (2016). Principles of sodium homeostasis and sodium signalling in astroglia. *Glia* 64**,** 1611-1627 DOI: 10.1002/glia.22964.

Rose, C. R., Ziemens, D., and Verkhratsky, A. (2020). On the special role of NCX in astrocytes: Translating Na^+-transients into intracellular Ca^{2+} signals. *Cell Calcium* 86**,** 102154 DOI: 10.1016/j.ceca.2019.102154.

Rouach, N., Koulakoff, A., Abudara, V., Willecke, K., and Giaume, C. (2008). Astroglial metabolic networks sustain hippocampal synaptic transmission. *Science* 322**,** 1551-1555 DOI: 10.1126/science.1164022.

Rungta, R. L., Bernier, L. P., Dissing-Olesen, L., Groten, C. J., Ledue, J. M., Ko, R., Drissler, S., and Macvicar, B. A. (2016). Ca^{2+} transients in astrocyte fine processes occur via Ca^{2+} influx in the adult mouse hippocampus. *Glia* 64**,** 2093-2103 DOI: 10.1002/glia.23042.

Sachse, F. B., Clarke, R., and Giles, W. R. (2017). No fuzzy space for intracellular Na^+ in healthy ventricular myocytes. *j Gen Physiol* 149**,** 683-687 DOI: 10.1085/jgp.201711826.

Sauer, J. F., and Bartos, M. (2010). Recruitment of early postnatal parvalbumin-positive hippocampal interneurons by GABAergic excitation. *J Neurosci* 30**,** 110-115 DOI: 10.1523/JNEUROSCI.4125-09.2010.

Savtchenko, L., Megalogeni, M., Rusakov, D. A., Walker, M. C., and Pavlov, I. (2015). Synaptic GABA release prevents GABA transporter type-1 reversal during excessive network activity. *Nat Commun* 6**,** 6597 DOI: 10.1038/ncomms7597.

Savtchouk, I., and Volterra, A. (2018). Gliotransmission: Beyond Black-and-White. *J Neurosci* 38**,** 14-25 DOI: 10.1523/JNEUROSCI.0017-17.2017.

Schipke, C. G., Ohlemeyer, C., Matyash, M., Nolte, C., Kettenmann, H., and Kirchhoff, F. (2001). Astrocytes of the mouse neocortex express functional N-methyl-D-aspartate receptors. *FASEB journal* 15**,** 1270-1272 DOI: 10.1096/fj.00-0439fje.

Schools, G. P., Zhou, M., and Kimelberg, H. K. (2006). Development of gap junctions in hippocampal astrocytes: evidence that whole cell electrophysiological phenotype is an intrinsic property of the individual cell. *J Neurophysiol* 96**,** 1383-1392 DOI: 10.1152/jn.00449.2006.

Scimemi, A. (2014). Structure, function, and plasticity of GABA transporters. *Front Cell Neurosci* 8**,** 161 DOI: 10.3389/fncel.2014.00161.

Segerstrale, M., Juuri, J., Lanore, F., Piepponen, P., Lauri, S. E., Mulle, C., and Taira, T. (2010). High firing rate of neonatal hippocampal interneurons is caused by attenuation of afterhyperpolarizing potassium

currents by tonically active kainate receptors. *J Neurosci* 30**,** 6507-6514 DOI: 10.1523/JNEUROSCI.4856-09.2010.

Seifert, G., Huttmann, K., Binder, D. K., Hartmann, C., Wyczynski, A., Neusch, C., and Steinhauser, C. (2009). Analysis of astroglial K^+ channel expression in the developing hippocampus reveals a predominant role of the Kir4.1 subunit. *J Neurosci* 29**,** 7474-7488 DOI: 10.1523/JNEUROSCI.3790-08.2009.

Serafini, R., Valeyev, A. Y., Barker, J. L., and Poulter, M. O. (1995). Depolarizing GABA-activated Cl^- channels in embryonic rat spinal and olfactory bulb cells. *j Physiol* 488**,** 371-386 DOI: 10.1113/jphysiol.1995.sp020973

Shibasaki, K., Hosoi, N., Kaneko, R., Tominaga, M., and Yamada, K. (2017). Glycine release from astrocytes via functional reverse of GlyT1. *j Neurochem* 140**,** 395-403 DOI: 10.1111/jnc.13741.

Sipila, S., Huttu, K., Voipio, J., and Kaila, K. (2004). GABA uptake via GABA transporter-1 modulates GABAergic transmission in the immature hippocampus. *J Neurosci* 24**,** 5877-5880 DOI: 10.1523/JNEUROSCI.1287-04.2004.

Sipila, S. T., Huttu, K., Soltesz, I., Voipio, J., and Kaila, K. (2005). Depolarizing GABA acts on intrinsically bursting pyramidal neurons to drive giant depolarizing potentials in the immature hippocampus. *J Neurosci* 25**,** 5280-5289 DOI: 10.1523/JNEUROSCI.0378-05.2005.

Sipila, S. T., Huttu, K., Voipio, J., and Kaila, K. (2006a). Intrinsic bursting of immature CA3 pyramidal neurons and consequent giant depolarizing potentials are driven by a persistent Na^+ current and terminated by a slow Ca^{2+} -activated K^+ current. *Eur J Neurosci* 23**,** 2330-2338 DOI: 10.1111/j.1460-9568.2006.04757.x.

Sipila, S. T., Schuchmann, S., Voipio, J., Yamada, J., and Kaila, K. (2006b). The cation-chloride cotransporter NKCC1 promotes sharp waves in the neonatal rat hippocampus. *J Physiol* 573**,** 765-773 DOI: 10.1113/jphysiol.2006.107086.

Smolyaninova, L. V., Shiyan, A. A., Kapilevich, L. V., Lopachev, A. V., Fedorova, T. N., Klementieva, T. S., Moskovtsev, A. A., Kubatiev, A. A., and Orlov, S. N. (2019). Transcriptomic changes triggered by ouabain in rat cerebellum granule cells: Role of alpha3- and alpha1-Na^+,K^+-ATPase-mediated signaling. *PLoS One* 14**,** e0222767 DOI: 10.1371/journal.pone.0222767.

Song, I., Volynski, K., Brenner, T., Ushkaryov, Y., Walker, M., and Semyanov, A. (2013). Different transporter systems regulate extracellular GABA from vesicular and non-vesicular sources. *Front Cell Neurosci* 7**,** 23 DOI: 10.3389/fncel.2013.00023.

Sontheimer, H. (1994). Voltage-dependent ion channels in glial cells. *glia* 11**,** 156-172 DOI: 10.1002/glia.440110210

Spitzer, N. C. (2006). Electrical activity in early neuronal development. *Nature* 444**,** 707-712 DOI: 10.1038/nature05300.

Stahlberg, M. A., Kügler, S., and Dean, C. (2018). Visualizing BDNF cell-to-cell transfer reveals astrocytes are the primary recipient of neuronal BDNF. DOI: 10.1101/255935.

Stark, E., Roux, L., Eichler, R., Senzai, Y., Royer, S., and Buzsaki, G. (2014). Pyramidal cell-interneuron interactions underlie hippocampal ripple oscillations. *Neuron* 83**,** 467-480 DOI: 10.1016/j.neuron.2014.06.023.

Stobart, J. L., Ferrari, K. D., Barrett, M. J. P., Stobart, M. J., Looser, Z. J., Saab, A. S., and Weber, B. (2018). Long-term In Vivo Calcium Imaging of Astrocytes Reveals Distinct Cellular Compartment Responses to Sensory Stimulation. *Cereb Cortex* 28**,** 184-198 DOI: 10.1093/cercor/bhw366.

Stosiek, C., Garaschuk, O., Holthoff, K., and Konnerth, A. (2003). In vivo two-photon calcium imaging of neuronal networks. *PNAS* 100**,** 7319-7324 DOI: 10.1073/pnas.1232232100

Strasser, A., Wittmann, H. J., Schneider, E. H., and Seifert, R. (2015). Modulation of GPCRs by monovalent cations and anions. *Naunyn Schmiedebergs Arch Pharmacol* 388**,** 363-380 DOI: 10.1007/s00210-014-1073-2.

Sui, J. L., Chan, K. W., and Logothetis, D. E. (1996). Na^+ activation of the muscarinic K^+ channel by a G-protein-independent mechanism. *J Gen Physiol* 108**,** 381-391 DOI: 10.1085/jgp.108.5.381.

Sun, J. J., Kilb, W., and Luhmann, H. J. (2010). Self-organization of repetitive spike patterns in developing neuronal networks in vitro. *Eur J Neurosci* 32**,** 1289-1299 DOI: 10.1111/j.1460-9568.2010.07383.x.

Super, H., and Soriano, E. (1994). The organization of the embryonic and early postnatal murine hippocampus. II. Development of entorhinal, commissural, and septal connections studied with the lipophilic tracer DiI. *j Comp Neurol* 344**,** 101-120 DOI: 10.1002/cne.903440108

Takacs, V. T., Freund, T. F., and Gulyas, A. I. (2008). Types and synaptic connections of hippocampal inhibitory neurons reciprocally connected with the medial septum. *Eur J Neurosci* 28**,** 148-164 DOI: 10.1111/j.1460-9568.2008.06319.x.

Takano, T., Kang, J., Jaiswal, J. K., Simon, S. M., Lin, J. H. C., Yu, Y., Li, Y., Yang, J., Dienel, G., Zielke, H. R., and Nedergaard, M. (2005). Receptor-mediated glutamate release from volume sensitive channels in astrocytes. *PNAS* 102**,** 16466-16471 DOI: 10.1073/pnas.0506382102

Taurin, S., Dulin, N. O., Pchejetski, D., Grygorczyk, R., Tremblay, J., Hamet, P., and Orlov, S. N. (2002). c-Fos expression in ouabain-treated vascular smooth muscle cells from rat aorta: evidence for an intracellular-sodium-mediated, calcium- independent mechanism. *J Physiol* 543**,** 835-847 DOI: 10.1113/jphysiol.2002.023259.

Theparambil, S. M., Naoshin, Z., Thyssen, A., and Deitmer, J. W. (2015). Reversed electrogenic sodium bicarbonate cotransporter 1 is the major acid loader during recovery from cytosolic alkalosis in mouse cortical astrocytes. *J Physiol* 593**,** 3533-3547 DOI: 10.1113/JP270086.

Tong, X. P., Li, X. Y., Zhou, B., Shen, W., Zhang, Z. J., Xu, T. L., and Duan, S. (2009). Ca^{2+} signaling evoked by activation of Na^+ channels and Na^+/Ca^{2+} exchangers is required for GABA-induced NG2 cell migration. *J Cell Biol* 186**,** 113-128 DOI: 10.1083/jcb.200811071.

Tritsch, N. X., Granger, A. J., and Sabatini, B. L. (2016). Mechanisms and functions of GABA co-release. *Nat Rev Neurosci* 17**,** 139-145 DOI: 10.1038/nrn.2015.21.

Tyzio, R., Allene, C., Nardou, R., Picardo, M. A., Yamamoto, S., Sivakumaran, S., Caiati, M. D., Rheims, S., Minlebaev, M., Milh, M., Ferre, P., Khazipov, R., Romette, J. L., Lorquin, J., Cossart, R., Khalilov, I., Nehlig, A., Cherubini, E., and Ben-Ari, Y. (2011). Depolarizing actions of GABA in immature neurons depend neither on ketone bodies nor on pyruvate. *J Neurosci* 31**,** 34-45 DOI: 10.1523/JNEUROSCI.3314-10.2011.

Tyzio, R., Minlebaev, M., Rheims, S., Ivanov, A., Jorquera, I., Holmes, G. L., Zilberter, Y., Ben-Ari, Y., and Khazipov, R. (2008). Postnatal changes in somatic gamma-aminobutyric acid signalling in the rat hippocampus. *Eur J Neurosci* 27**,** 2515-2528 DOI: 10.1111/j.1460-9568.2008.06234.x.

Tyzio, R., Represa, A., Jorquera, I., Ben-Ari, Y., Gozlan, H., and Aniksztejn, L. (1999). The Establishment of GABAergic and Glutamatergic Synapses on CA1 Pyramidal Neurons is Sequential and Correlates with the Development of the Apical Dendrite. *j Neurosci* 19**,** 1ß372-10382 DOI: 10.1523/JNEUROSCI.19-23-10372.1999.

Uhlen, P., Fritz, N., Smedler, E., Malmersjo, S., and Kanatani, S. (2015). Calcium signaling in neocortical development. *Dev Neurobiol* 75**,** 360-368 DOI: 10.1002/dneu.22273.

Unichenko, P., Dvorzhak, A., and Kirischuk, S. (2013). Transporter-mediated replacement of extracellular glutamate for GABA in the developing murine neocortex. *Eur J Neurosci* 38**,** 3580-3588 DOI: 10.1111/ejn.12380.

Unichenko, P., Kirischuk, S., and Luhmann, H. J. (2015). GABA transporters control GABAergic neurotransmission in the mouse subplate. *Neuroscience* 304**,** 217-227 DOI: 10.1016/j.neuroscience.2015.07.067.

Untiet, V., Kovermann, P., Gerkau, N. J., Gensch, T., Rose, C. R., and Fahlke, C. (2017). Glutamate transporter-associated anion channels adjust intracellular chloride concentrations during glial maturation. *Glia* 65**,** 388-400 DOI: 10.1002/glia.23098.

Valeeva, G., Abdullin, A., Tyzio, R., Skorinkin, A., Nikolski, E., Ben-Ari, Y., and Khazipov, R. (2010). Temporal coding at the immature depolarizing GABAergic synapse. *Front Cell Neurosci* 4 DOI: 10.3389/fncel.2010.00017.

Valeeva, G., Tressard, T., Mukhtarov, M., Baude, A., and Khazipov, R. (2016). An Optogenetic Approach for Investigation of Excitatory and Inhibitory Network GABA Actions in Mice Expressing Channelrhodopsin-2 in GABAergic Neurons. *J Neurosci* 36**,** 5961-5973 DOI: 10.1523/JNEUROSCI.3482-15.2016.

Van Damme, P., Van Den Bosch, L., Van Houtte, E., Eggermont, J., Callewaert, G., and Robberecht, W. (2002). Na^+ entry through AMPA receptors results in voltage-gated K^+ channel blockade in cultured rat spinal cord motoneurons. *J Neurophysiol* 88**,** 965-972 DOI: 10.1152/jn.2002.88.2.965.

Verkhratsky, A., Trebak, M., Perocchi, F., Khananshvili, D., and Sekler, I. (2018). Crosslink between calcium and sodium signalling. *Exp Physiol* 103**,** 157-169 DOI: 10.1113/EP086534.

Verkhratsky, A., Untiet, V., and Rose, C. R. (2019). Ionic signalling in astroglia beyond calcium. *J Physiol***,** 1655-1670 DOI: 10.1113/JP277478.

Wade, J. J., Breslin, K., Wong-Lin, K., Harkin, J., Flanagan, B., Van Zalinge, H., Hall, S., Dallas, M., Bithell, A., Verkhratsky, A., and Mcdaid, L. (2019). Calcium Microdomain Formation at the Perisynaptic Cradle Due to NCX Reversal: A Computational Study. *Front Cell Neurosci* 13**,** 185 DOI: 10.3389/fncel.2019.00185.

Wester, J. C., and Mcbain, C. J. (2016). Interneurons Differentially Contribute to Spontaneous Network Activity in the Developing Hippocampus Dependent on Their Embryonic Lineage. *J Neurosci* 36**,** 2646-2662 DOI: 10.1523/JNEUROSCI.4000-15.2016.

Wilson, C. S., and Mongin, A. A. (2018). Cell Volume Control in Healthy Brain and Neuropathologies. *Curr Top Membr* 81**,** 385-455 DOI: 10.1016/bs.ctm.2018.07.006.

Wu, Y., Wang, W., and Richerson, G. B. (2006). The transmembrane sodium gradient influences ambient GABA concentration by altering the equilibrium of GABA transporters. *J Neurophysiol* 96**,** 2425-2436 DOI: 10.1152/jn.00545.2006.

Yamada, J., Okabe, A., Toyoda, H., Kilb, W., Luhmann, H. J., and Fukuda, A. (2004). Cl- uptake promoting depolarizing GABA actions in immature rat neocortical neurones is mediated by NKCC1. *J Physiol* 557**,** 829-841 DOI: 10.1113/jphysiol.2004.062471.

Yamamoto, T., Vukelic, J., Hertzberg, E. L., and Nagy, J. I. (1992). Differential anatomical and cellular patterns of connexin43 expression during postnatal development of rat brain. *Brain Res Dev Brain Res* 66**,** 165-180 DOI: 10.1016/0165-3806(92)90077-a.

Yan, Y., Dempsy, R. J., and Sun, D. (2001). Expression of Na^+ -K^+ -Cl^- cotransporter in rat brain during development and its localization in mature astrocytes. *Brain Research* 911**,** 43-55 DOI: 10.1016/s0006-8993(01)02649-x.

Yang, J. W., Hanganu-Opatz, I. L., Sun, J. J., and Luhmann, H. J. (2009). Three patterns of oscillatory activity differentially synchronize developing neocortical networks in vivo. *J Neurosci* 29**,** 9011-9025 DOI: 10.1523/JNEUROSCI.5646-08.2009.

Yoon, B. E., Jo, S., Woo, J., Lee, J. H., Kim, T., Kim, D., and Lee, C. J. (2011). The amount of astrocytic GABA positively correlates with the degree of tonic inhibition in hippocampal CA1 and cerebellum. *Mol Brain* 4**,** 42 DOI: 10.1186/1756-6606-4-42.

Yoon, B. E., and Lee, C. J. (2014). GABA as a rising gliotransmitter. *Front Neural Circuits* 8**,** 141 DOI: 10.3389/fncir.2014.00141.

Yu, X. M., and Salter, M. W. (1999). Src, a molecular switch governing gain control of synaptic transmission mediated by N-methyl-D-aspartate receptors. *Proc Natl Acad Sci U S A* 96**,** 7697-7704 DOI: 10.1073/pnas.96.14.7697.

Yuan, X., Eisen, A. M., Mcbain, C. J., and Gallo, V. (1998). A role for glutamate and its receptors in the regulation of oligodendrocyte development in cerebellar tissue slices. *Development* 125**,** 2901-2914 DOI.

Yue, C., and Yaari, Y. (2004). KCNQ/M channels control spike afterdepolarization and burst generation in hippocampal neurons. *J Neurosci* 24**,** 4614-4624 DOI: 10.1523/JNEUROSCI.0765-04.2004.

Yuste, R., and Katz, L. C. (1991). Control of postsynaptic Ca^{2+} influx in dveeloping neocortex by excitatory and inhibitory neurotransmitters. *Neuron* 6**,** 333-344 DOI: 10.1016/0896-6273(91)90243-s

Zarzycka, B., Zaidi, S. A., Roth, B. L., and Katritch, V. (2019). Harnessing Ion-Binding Sites for GPCR Pharmacology. *Pharmacol Rev* 71**,** 571-595 DOI: 10.1124/pr.119.017863.

Ziemens, D., Oschmann, F., Gerkau, N. J., and Rose, C. R. (2019). Heterogeneity of Activity-Induced Sodium Transients between Astrocytes of the Mouse Hippocampus and Neocortex: Mechanisms and Consequences. *J Neurosci* 39**,** 2620-2634 DOI: 10.1523/JNEUROSCI.2029-18.2019.

Zilberter, M. (2016). Reality of Inhibitory GABA in Neonatal Brain: Time to Rewrite the Textbooks? *J Neurosci* 36**,** 10242-10244 DOI: 10.1523/JNEUROSCI.2270-16.2016.

Zur Nieden, R., and Deitmer, J. W. (2006). The role of metabotropic glutamate receptors for the generation of calcium oscillations in rat hippocampal astrocytes in situ. *Cereb Cortex* 16**,** 676-687 DOI: 10.1093/cercor/bhj013.

Spontaneous Ultraslow Na^+ Fluctuations in the Neonatal Mouse Brain.

***Felix, L.**, Ziemens, D., Seifert, G., and Rose, C. R.*

Cells 9, 102 DOI: 10.3390/cells9010102. (2020)

Impact factor 2020: 4.37

I performed

- All sodium, calcium and proton wide field experiments and analysis

I contributed to

- The experimental design
- Interpretation of data
- Drafting and revision of manuscript and figures

frontiers in Molecular Neuroscience

REVIEW
published: 17 January 2018
doi: 10.3389/fnmol.2017.00451

Astroglial Glutamate Signaling and Uptake in the Hippocampus

Christine R. Rose[1], Lisa Felix[1], Andre Zeug[2], Dirk Dietrich[3], Andreas Reiner[4] and Christian Henneberger[5,6,7]**

[1]*Institute of Neurobiology, Faculty of Mathematics and Natural Sciences, Heinrich Heine University Duesseldorf, Duesseldorf, Germany,* [2]*Cellular Neurophysiology, Hannover Medical School, Hannover, Germany,* [3]*Department of Neurosurgery, University of Bonn Medical School, Bonn, Germany,* [4]*Cellular Neurobiology, Faculty of Biology and Biotechnology, Ruhr University Bochum, Bochum, Germany,* [5]*Institute of Cellular Neurosciences, University of Bonn Medical School, Bonn, Germany,* [6]*German Center for Degenerative Diseases (DZNE), Bonn, Germany,* [7]*Institute of Neurology, University College London, London, United Kingdom*

Astrocytes have long been regarded as essentially unexcitable cells that do not contribute to active signaling and information processing in the brain. Contrary to this classical view, it is now firmly established that astrocytes can specifically respond to glutamate released from neurons. Astrocyte glutamate signaling is initiated upon binding of glutamate to ionotropic and/or metabotropic receptors, which can result in calcium signaling, a major form of glial excitability. Release of so-called gliotransmitters like glutamate, ATP and D-serine from astrocytes in response to activation of glutamate receptors has been demonstrated to modulate various aspects of neuronal function in the hippocampus. In addition to receptors, glutamate binds to high-affinity, sodium-dependent transporters, which results in rapid buffering of synaptically-released glutamate, followed by its removal from the synaptic cleft through uptake into astrocytes. The degree to which astrocytes modulate and control extracellular glutamate levels through glutamate transporters depends on their expression levels and on the ionic driving forces that decrease with ongoing activity. Another major determinant of astrocytic control of glutamate levels could be the precise morphological arrangement of fine perisynaptic processes close to synapses, defining the diffusional distance for glutamate, and the spatial proximity of transporters in relation to the synaptic cleft. In this review, we will present an overview of the mechanisms and physiological role of glutamate-induced ion signaling in astrocytes in the hippocampus as mediated by receptors and transporters. Moreover, we will discuss the relevance of astroglial glutamate uptake for extracellular glutamate homeostasis, focusing on how activity-induced dynamic changes of perisynaptic processes could shape synaptic transmission at glutamatergic synapses.

Keywords: astrocyte, glutamate receptor, glutamate transport, tripartite synapse, calcium, morphology

OPEN ACCESS

Edited by:
Andras Bilkei-Gorzo, University of Bonn, Germany

Reviewed by:
Chris Dulla, Tufts University School of Medicine, United States
Annalisa Scimemi, University at Albany (SUNY), United States

****Correspondence:***
Christine R. Rose
rose@hhu.de
Christian Henneberger
christian.henneberger@uni-bonn.de

Received: *20 November 2017*
Accepted: *22 December 2017*
Published: *17 January 2018*

Citation:
Rose CR, Felix L, Zeug A, Dietrich D, Reiner A and Henneberger C (2018) Astroglial Glutamate Signaling and Uptake in the Hippocampus. Front. Mol. Neurosci. 10:451. doi: 10.3389/fnmol.2017.00451

INTRODUCTION

Electrical activity of neurons is largely based on the diffusive movement of ions along their electrochemical gradient. This includes the diffusion of potassium ions (K^+) into the extracellular space (ECS) through K^+-permeable ion channels, resulting in a re- or hyperpolarization of the membrane potential. In addition, active neurons release chemical

transmitters such as glutamate from their presynaptic terminals into the ECS. As the volume of the brain is limited, mechanisms are needed which counteract the accumulation of these substances in the ECS. A major mechanism by which this is prevented is by the cellular (re-) uptake of neurotransmitters and ions. It is well established that astrocytes take over a large part of this housekeeping function and remove molecules released by neurons from the ECS (Kofuji and Newman, 2004; Marcaggi and Attwell, 2004). Once the molecules are in the astrocytic compartment, they are either degraded, recycled or shuttled out of the brain via transport routes such as the blood or the gliolymphatic system (Abbott et al., 2006; Thrane et al., 2015).

Glutamate is the major excitatory neurotransmitter released in the brain and well known for its potential to induce excitotoxicity. At the same time, glutamate also acts as an active signaling molecule for astrocytes. This review focuses on astroglial glutamate signaling in the hippocampus, highlighting the dual role glutamate plays in the function of astrocytes. Astrocytic glutamate signaling becomes particularly interesting as these cells not only express glutamate transporters, which transport glutamate molecules into the cell with the help of ion gradients, but also several types of glutamate receptors. The relevant functional domains of sub-micron-sized astrocyte processes controlling the spread of synaptically-released glutamate is difficult to assess with current optical or electrical recording techniques. We therefore start this review with an evaluation of available tools to analyze the distribution and function of astrocytic receptors and transporters for glutamate.

Glutamate receptors on astrocytes belong to the ionotropic and metabotropic classes and are activated by synaptically released glutamate, thereby allowing astrocytes to integrate ongoing neuronal activity within a time frame in the order of tens to hundreds of milliseconds (Verkhratsky and Kirchhoff, 2007a; Bindocci et al., 2017). High-affinity glutamate transporters on astrocytes, on the other hand, represent the major mechanism for removal of glutamate at synapses and protect the brain from glutamate-induced over-excitation of neurons and excitotoxicity (Parpura et al., 2012; Schousboe et al., 2014). Like for glutamate receptors, there exist several subtypes of glutamate transporters, also named excitatory amino acid transporters (EAATs), which are differentially expressed throughout the brain and during postnatal development (Danbolt, 2001). The different means by which astrocytes detect and remove synaptically-released glutamate are presented in section "Detection of Synaptically-released Glutamate by Astrocytes".

Transport of glutamate across the astrocytic cell membranes coincides with transmembrane flux of sodium, potassium, protons and chloride and a decrease in the membrane potential (Marcaggi and Attwell, 2004; Rose et al., 2016). The tiny processes and compartments of astrocytes may be sensitive to small ion fluxes associated with the release of individual synaptic vesicles, and high frequency or prolonged activity of neurons could alter intracellular ion concentrations and consequently transport capacity substantially. Metabotropic glutamate receptors activated by synaptic activity have been shown to cause global or local changes in intracellular calcium concentration. Such calcium transients can result in astrocytic gliotransmitter release which feeds back to neurons (Perea et al., 2009; Araque et al., 2014). Thus, the spatial and temporal patterns of intracellular ion concentration changes are important parameters for glutamate-related effects induced in and by astrocytes. The section "Role of Astrocytic Ion Signals for Glutamate Homeostasis" discusses such activity-dependent intracellular ion concentration changes in response to binding and transport of glutamate.

Astrocytes display especially delicate cellular processes, which, in contrast to other cells in the brain, are far beyond the resolution achievable using classical diffraction-limited microscopy (Ventura and Harris, 1999). There are several structural factors that could facilitate uptake by these astrocytic processes: a large surface area, close spatial association with synapses and axons, and strong coupling to neighboring astrocytes. Not only is the communication with the ECS critically shaped by the sub-micron structure of astrocytes: The very narrow diameter of their fine tube- and sheet-like processes likely has important implications for intracellular ion distribution and may create multiple functionally and diffusibly almost independent compartments. As a consequence, the finest morphological changes, invisible to conventional light microscopy, could significantly modify the essential functions of astrocytes. The role of sub-micron scale astrocytic structural changes and their dynamics are discussed in section "Regulation of Synaptic Transmission by Astroglial Glutamate Transporters and Perisynaptic Astrocyte Structure" with particular reference to the strategic positioning of glutamate transporters to perform glutamate uptake.

TOOLS TO INVESTIGATE ASTROCYTIC RESPONSES TO GLUTAMATE

Functional Analysis Using Electrophysiology and Optical Approaches

The impact of synaptically released glutamate on astrocytes and its functional consequences can be monitored by combining electrophysiology and pharmacological tools. While electrophysiological measurements represent a reliable and unambiguous method for functional detection of ion flux across the plasma membrane, it is worth keeping in mind that they are generally obtained from astrocyte somata and thus only provide a distant, filtered version of electrical signals generated in processes remote to the soma. This is especially critical when considering the low input resistance of astrocytes, resulting in a substantial loss of current with increasing distance from its site of generation, and in a poor control of the membrane potential in voltage-clamp experiments. In addition, astrocytes form electrically coupled networks via gap junctions, further complicating accurate measurement of individual cells (Giaume et al., 2010). Notwithstanding their very low input resistance, glutamate not only excites neurons but also depolarizes astrocytes as observed in early microelectrode

recordings (Bowman and Kimelberg, 1984; Kettenmann et al., 1984).

In functional experiments, astrocytes may be identified by their typical morphology, by staining with sulforhodamine (SR 101; Nimmerjahn et al., 2004; Kafitz et al., 2008) or by the expression of fluorescent marker proteins (e.g., GFP) under the control of an astrocyte-specific promoter such as glial fibrillary acidic protein (GFAP; Zhuo et al., 1997). Application of glutamate or agonists of subtypes of ionotropic glutamate receptors (iGluRs) such as N-methyl-D-aspartate (NMDA), cis-1-amino-1,3-dicarboxycyclopentane (cis-ACPD), α-amino-3-hydroxy-5-methyl-4-isoxazolepropionic acid (AMPA) or kainate, in combination with specific antagonists, among them (R)-3C4HPG for NMDA receptors, 6,7-dinitroquinoxaline-2,3-dione (DNQX) for AMPA/kainate receptors or GYKI53655 for AMPA receptors, allowed a more detailed functional investigation of astrocytes' electrophysiological responses to glutamate (Verkhratsky and Steinhäuser, 2000; Zhou and Kimelberg, 2001; Matthias et al., 2003; Zhou et al., 2006; Verkhratsky and Kirchhoff, 2007a). The specificity of such pharmacological manipulations, however, is not sufficient to further discriminate between the various iGluR subunit compositions, which could be addressed by using transgenic knockout animals.

High-affinity glutamate transporters are electrogenic and can thus also be analyzed using electrophysiological techniques such as whole-cell patch-clamp (**Figures 1A,B**). Electrophysiological approaches to study glutamate transporter currents in astrocytes and to simultaneously record neuronal and astrocytic activity are summarized in recent reviews (Dallérac et al., 2013; Cheung et al., 2015). Indeed, the inward current generated by activation of glutamate transporters upon agonist application or electrical stimulation of afferent fibers is a reliable, semi-quantitative measure for the functional expression of glutamate uptake in glial cells (Brew and Attwell, 1987; Barbour et al., 1988; Bergles and Jahr, 1997; Bergles et al., 1997; Diamond and Jahr, 1997). Expression of glutamate transporters can be down-regulated by inhibition of their synthesis using chronic antisense oligonucleotide administration (Rothstein et al., 1996). Several pharmacological agents, such as ceftriaxone, estrogen, tamoxifen and riluzole increase the expression of glial glutamate transporters at the transcriptional level via activation of nuclear factor κB (Karki et al., 2015). Acutely, different transporter subtypes can be specifically blocked by substances like UCPH101 (2-amino-5,6,7,8-tetrahydro-4-(4-methoxyphenyl)-7-(naphthalen-1-yl)-5-oxo-4*H*-chromene-3-carbonitrile) or dihydrokainic acid (DHK), whereas DL-threo-beta-benzyloxyaspartate (DL-TBOA) and its high-affinity analog TFB-TBOA are non-specific blockers which can be used to inhibit all known transporter isoforms (Shimamoto et al., 1998; Abrahamsen et al., 2013; Tse et al., 2014).

In addition to electrophysiology, imaging of intracellular ion transients can be employed for detecting the activation of glutamate receptors as well as transporters in astrocytes. This is especially relevant for metabotropic receptors for glutamate (mGluRs). For analysis of the latter, imaging of related intracellular signaling components, such as calcium or cyclic adenosine monophosphate (cAMP), combined with specific pharmacological tools, is usually employed (Pasti et al., 1995; Niswender and Conn, 2010; see also section "Metabotropic Receptors"). The glutamate-induced calcium signals can be monitored by either synthetic or genetically encoded fluorescence-based reporter molecules. A detailed description of these ratiometric and single-wavelength sensors is outside the scope of this review (for recent surveys see Khakh and McCarthy, 2015; Rusakov, 2015). A general advantage of imaging based methods is their spatial resolution, which provides further information on the site of origin and the propagation of intra- and intercellular signals.

Imaging can also reveal activation of glutamate transport, which is driven by cotransport of different ions, among them sodium (Marcaggi and Attwell, 2004; Rose et al., 2016; **Figure 1B**). Depending on the strength of stimulation, sodium signals induced by glutamatergic activity in astrocytes can be local or global (Rose and Verkhratsky, 2016), thus allowing functional activation of glutamate transport in astrocyte microdomains such as perisynaptic processes or endfeet (Langer and Rose, 2009; Langer et al., 2017). Genetically encoded voltage sensors could also be powerful tools for imaging local depolarizations in astrocytes, but currently used voltage sensors lack the sensitivity to quantify small voltage changes (Yang and St-Pierre, 2016).

Another important technical challenge is the specific activation of astrocytes (Li et al., 2013). Purely pharmacological approaches, such as the application of receptor agonists, do not provide sufficient specificity for studies *in situ* or *in vivo*, and even pharmaco-genetic approaches, which have excellent cell-type specificity (Fiacco et al., 2007), do not mimic the precise temporal and spatial aspects of astrocyte activation. Electrically evoking neuronal neurotransmitter release, e.g., via stimulation of afferent fibers can be used as an indirect, but more physiological means for astrocyte activation.

Temporally and spatially defined activation of astrocytes can also be obtained by optical techniques, such as photo-uncaging of glutamate. For instance, local photo-uncaging of 4-methoxy-7-nitroindolinyl- (MNI-) caged glutamate proved to be useful for mapping the distribution of glutamate transporters on individual astrocytes (Armbruster et al., 2014). Exclusive specificity for astrocytes can be achieved with optogenetic approaches, i.e., by using genetically encoded, light-sensitive tools that can be targeted to the desired cell types and brain regions. One example is the expression of channelrhodopsin, a light-gated ion channel isolated from green algae, which can be stimulated with blue light to achieve depolarization and to induce the influx of calcium. Channelrhodopsin has been successfully used in a number of studies addressing the physiological function of astrocyte signaling *in vivo* (Gradinaru et al., 2009; Gourine et al., 2010; Sasaki et al., 2012; Perea et al., 2014). Another optogenetic approach, which might be useful for controlling astrocyte signaling, is the use of light-gated glutamate receptors. In this approach, photo-switchable ligands are employed to control specific iGluRs or mGluRs

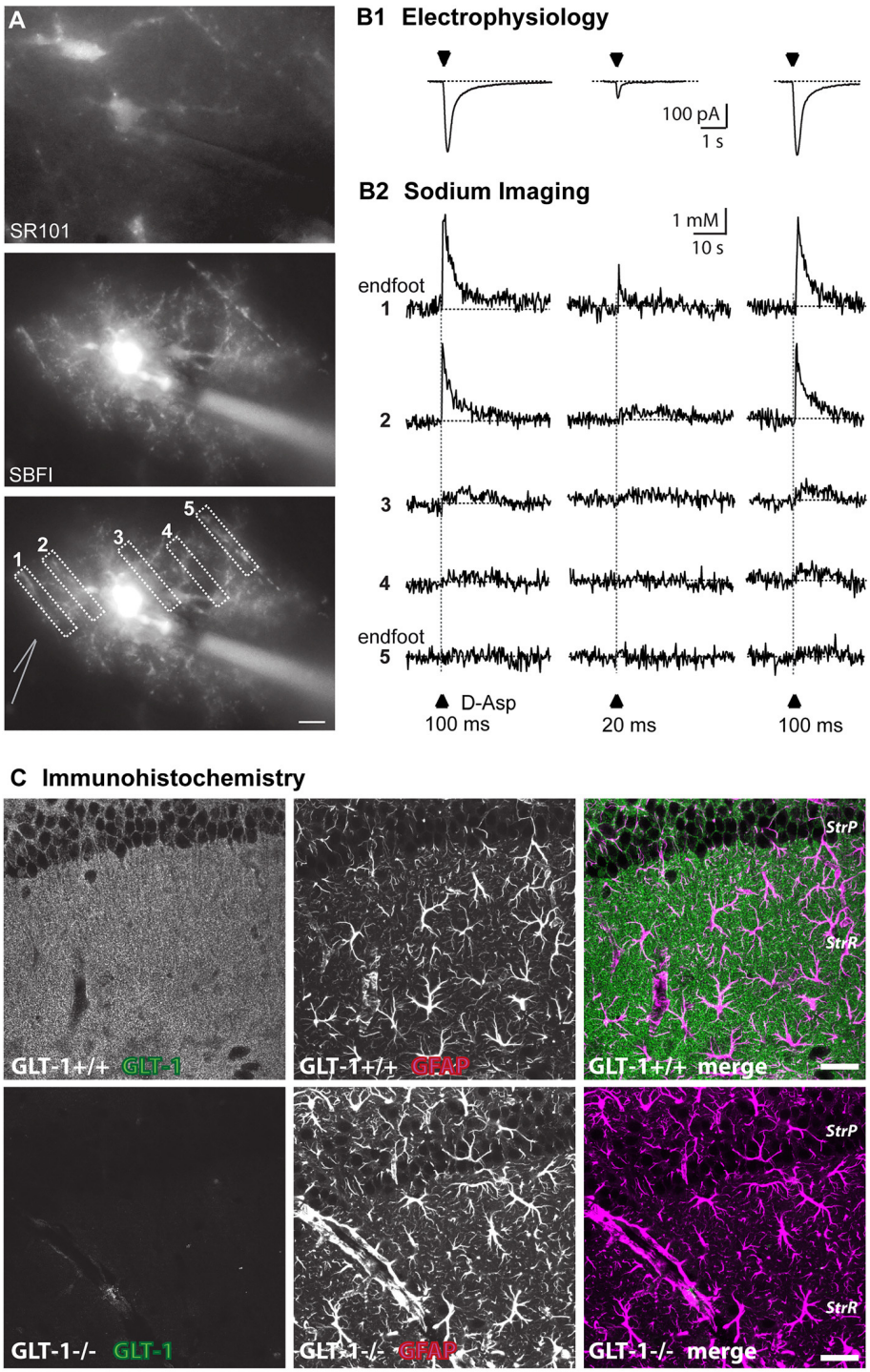

FIGURE 1 | Approaches to visualize astroglial glutamate signaling and uptake. **(A)** Top: image of SR101-staining of astrocytes in the stratum radiatum. Center: epifluorescence image of an astrocyte selectively loaded with SBFI via a patch pipette (visible on the right side). The astrocyte contacts blood vessels both at the left and the right side. Bottom: same image as above with ROIs indicated from which measurements shown in **(B)** were taken. The position of the D-aspartate application pipette is schematically indicated at the left side. Scale bar: 10 μm **(B)** somatic inward currents elicited by the glutamate transporter agonist D-aspartate (arrowheads) for 100 ms or 20 ms as indicated **(B1)**. Shown below **(B2)** are sodium signals from the different ROIs as denoted in **(A)** that accompanied the inward currents. Note that signals are largest in ROI1 which covers an endfoot. **(C)** Immunohistochemical labeling of glutamate transporter 1 (GLT-1; EAAT2) in wild-type (upper row) and GLT-1 k.o.-animals (bottom row). Images represent maximum projections of five consecutive optical CLSM sections (1 μm) of the hippocampal CA1-region of P22. In addition to GLT-1 (left images), glial fibrillary acidic protein (GFAP) was labeled (middle panel), the merge is shown on the right. Scale bar: 20 μm. StrP, *stratum pyramidale*; StrR, *stratum radiatum*. **(A,B)** taken from Langer et al. (2017); **(C)** taken from Schreiner et al. (2014).

with high precision (Levitz et al., 2013; Reiner et al., 2015; Berlin et al., 2016), mimicking their physiological activation as closely as possible. This technique has also been used in cultured astrocytes, where activation of a light-gated kainate receptor enabled induction of calcium signals, demonstrating astrocyte-to-astrocyte signaling (Li et al., 2012).

Immunocytochemistry to Study Protein Localization

During the last decades, confocal microscopy and multiphoton excitation microscopy, typically used for documentation of immunocytochemical and histochemical labeling, have been employed to directly visualize the distribution of glutamate receptors and transporters at the protein level. The utilization of antibodies against ionotropic and metabotropic glutamate receptors allowed analysis of their widespread distribution across neurons and glia (Martin et al., 1993; Petralia and Wenthold, 1998; Keifer and Carr, 2000; Aronica et al., 2001; Lee et al., 2010; Minbay et al., 2017). Today, a variety of antibodies directed against almost all known glutamate receptor subunits are available. The first antibodies against glutamate transporters became available in 1991 (Danbolt et al., 1992). Since that time, a substantial amount of knowledge has accumulated on the cellular localization and spatial and temporal distribution pattern of different subtypes of glutamate transporters (Rothstein et al., 1994; Furuta et al., 1997; Danbolt, 2001; Schreiner et al., 2014; Danbolt et al., 2016; **Figure 1C**).

Although these laser-scanning techniques are able to reveal not only laminar, but also cellular distribution patterns of receptor or transporter expression (see **Figure 1C**), they cannot provide information on the exact localization of antigens on fine astrocytic protrusions. The size of these structures (50–200 nm), which surround or approach excitatory synapses and are therefore often termed perisynaptic astrocytic processes (PAPs), is beyond resolution of conventional optical microscopy (200–300 nm; Derouiche and Frotscher, 1991; Witcher et al., 2007; Heller and Rusakov, 2015). The combination of optimized brain tissue clearing strategies like CLARITY (Chung et al., 2013) with super resolution confocal imaging using advanced Airy pattern reassignment strategies (first described by Sheppard (1988) and now implemented as Zeiss Airyscan (Huff, 2015)) improved the spatial resolution and enabled the counting and morphological reconstruction of astroglial processes in thick tissue (Chen et al., 2015; Miller and Rothstein, 2016).

In contrast to conventional light microscopy, electron microscopy (EM) provides sufficient resolution to identify and document the thinnest astroglial protrusions. Employing EM studies in combination with three-dimensional reconstruction techniques has allowed the identification of the fine structure of PAPs in various brain regions (Ventura and Harris, 1999; Grosche et al., 2002; Reichenbach et al., 2010; Heller and Rusakov, 2015). Pre- and post-embedding labeling of proteins of interest helped to further address the subcellular localization of glutamate receptors and transporters. The pre-immunoperoxidase labeling method, however, does not usually result in statistically reliable data and may not allow differentiation between proteins localized on the astrocytic membrane and neighboring neuronal membrane, since diffusion of the reaction product, diaminobenzidine, is a well-known technical limitation for precise localization (Ottersen and Landsend, 1997; Nusser, 2000). In contrast to this, post-embedding EM studies using the immunogold technique enables an estimation of various parameters e.g., the number, density and variability of receptors as well as transporters for glutamate at synapses (Chaudhry et al., 1995; He et al., 2000; Furness et al., 2008; Zhang et al., 2016).

Super-resolution Microscopy and Protein Dynamics

EM with its superior spatial resolution, however, does not enable monitoring of live cells in real time, and thus provides only a static image of glutamate receptor and transporter distribution. The key to address this challenge lies in the utilization of super-resolution imaging techniques in live tissue that -under optimal conditions- overcome resolution limits of conventional light microscopy. Heller and Rusakov provide a detailed discussion of various super-resolution methods (i.e., stimulated-emission depletion (STED) microscopy, single-molecule localization imaging, such as photo-activated localization microscopy (PALM) or stochastic optical reconstruction microscopy (STORM), structured illumination microscopy (SIM)) relevant to study astrocytic glutamate transport (Heller and Rusakov, 2015). Stochastic super-resolution approaches like PALM/STORM build on the advantage that the specific labels emit light at separate time points and thereby become resolvable in time and thus diffraction limited imaging systems can be used.

Various approaches have been developed to follow membrane proteins through space and time (Kim et al., 2010; Rusakov et al., 2011). Single particle tracking microscopy employs a comparable strategy by tracking single structures rather than labeling a complete ensemble of proteins simultaneously (Saxton and Jacobson, 1997). This technique was successfully applied to study diffusion dynamics of neurotransmitter receptors and glutamate transporters, sparsely labeled with quantum dots, in subcellular domains of the astrocyte membrane (Arizono et al., 2012; Murphy-Royal et al., 2015; Al Awabdh et al., 2016). An alternative and less complex approach to study the kinetics of protein diffusion or transport is by fluorescence recovery after photobleaching (FRAP). For this approach, a protein label is bleached in a defined, restricted regions and the fluorescence recovery is monitored (Axelrod et al., 1976). Recovery times then yield information about the kinetics of protein diffusion or transport.

Diffusion of fluorescent proteins (FPs) can be further studied with fluorescence correlation spectroscopy (FCS; Magde et al., 1974), where the correlation in fluorescence fluctuation can be used to obtain both fluorophore concentration and diffusion characteristics. This allows accurate determination of the diffusion of plasma membrane proteins in defined compartments, for example spines, at diffraction-limited resolution. To date, however, only few studies have used FCS to monitor the diffusion properties of specific membrane

proteins (Kim et al., 2010). One reason may be that high-end instrumentation with excellent signal-to-noise ratio and low concentrations of highly fluorescent fluorophores are required for successful implementation of FCS. By combining the techniques of super-resolution microscopy, single molecule imaging and electrophysiological recordings, knowledge on the surface dynamics of neurotransmitter receptors, transporters and ion channels in astrocytes could be substantially expanded (Ciappelloni et al., 2017).

Monitoring Glutamate Levels and Dynamics

Recently, several concepts were developed to directly monitor glutamate levels both inside and at the surface of living cells. The periplasmic glutamate/aspartate-binding protein GltI from *Escherichia coli* provides an attractive scaffold, and forms the basis on which various sensors were constructed. The ligand-dependent conformational change in GltI has been used to create glutamate sensors from small molecule dyes coupled to single introduced cysteines (de Lorimier et al., 2002). Similarly, EOS (for E (glutamate) optical sensor (OS)), is a fluorescent sensor, which is based on the glutamate-binding domain of the AMPA receptor subunit GluR2 and a small fluorescent molecule conjugated near the glutamate-binding pocket. Thus EOS changes its fluorescence intensity (by maximally 37%) upon binding of glutamate, for which it has both high affinity (dissociation constant of 148 nM) and high selectivity (Namiki et al., 2007). With improved EOS variants, it was possible to detect extrasynaptic glutamate activities in acute slice preparations (Okubo et al., 2010). It must be noted that these kinds of sensors require chemical synthesis and cannot be endogenously expressed by the cell system.

GltI was further functionalized as an *in vitro* glutamate sensor, and was thus employed as a recognition element for developing a fluorescent indicator protein for glutamate (FLIPE; Okumoto et al., 2005). This biosensor is based on Förster resonance energy transfer (FRET), the radiationless energy transfer from a donor to acceptor fluorophore where its efficiency depends on distance, orientation and spectral properties of the fluorophores (Förster, 1948). In FLIPE the hinge-bending motion upon glutamate binding leads to a conformational change which is transduced into a glutamate-dependent change in FRET efficiency between the attached enhanced cyan fluorescent protein (CFP) and Venus, acting as donor and acceptor, respectively. The resulting acceptor/donor emission ratio change is inversely correlated to the change in glutamate concentration. The FLIPE sensor detects glutamate but also aspartate with 10-fold lower affinity and glutamine with 100-fold lower affinity. By creating FLIPE variants with different affinities, it is suitable for applications such as visualizing glial glutamate metabolism, transport and spill-over effects (Okumoto et al., 2005).

At the same time, Hires et al. (2008) created glutamate-sensitive fluorescent reporters (GluSnFRs) by using FRET between cyan and yellow fluorescent proteins bracketing the GltI protein (Tsien, 2005). This variant was later improved by systematic optimization of linker sequences and glutamate affinities and the resulting SuperGluSnFR exhibits a 6.2-fold increase in response magnitude over the original GluSnFR. Quantitative optical measurements revealed the time course of synaptic glutamate release, spill-over, and reuptake with sub second temporal and spine-sized spatial resolution (Hires et al., 2008). So far, however, these sensors were rarely used beyond initial proof-of-principle experiments. Moreover, the authors of the latter paper discussed the need to develop sensors that can be targeted to specific subcellular regions, e.g., the active zone, to enable a distinction between synaptic and extrasynaptic changes in glutamate.

Ratiometric FRET sensors provide several advantages and drawbacks compared to single-wavelength indicators. In theory, ratiometric sensors facilitate quantification of the ambient ligand concentration because the ratio of fluorescence intensities should be independent of sensor concentration and concentration changes. However, FRET sensors often have a low dynamic range and therefore display small ratio changes upon ligand binding. Also, ratiometric measurements consume greater spectral bandwidth and may require multiplexing (Piston and Kremers, 2007). Single-wavelength indicators, typically based on circularly permuted or split FPs, although not being ratiometric, are an appealing alternative to FRET sensors. iGluSnFR provides a strong fluorescence change upon glutamate binding with an affinity of about 5 μM when expressed on a neuronal membrane (although varying considerably depending the exact expression system and environment) and has been used in different experimental settings. For instance, iGluSnFR enabled to monitor neuronal glutamate release at single spines (Marvin et al., 2013) and from single synapses (Jensen et al., 2017) and to reveal that glutamate released from mossy fibers reaches astrocytes in micromolar concentrations (Haustein et al., 2014). It has also been applied in *in vivo* experiments (Marvin et al., 2013; Hefendehl et al., 2016) and to investigate the mechanisms than control cortical glutamate uptake *in situ* (Armbruster et al., 2016). These recent experiments using iGluSnFR highlight its versatility.

DETECTION OF SYNAPTICALLY-RELEASED GLUTAMATE BY ASTROCYTES

Astrocytes detect synaptically-released glutamate by its binding to ionotropic and metabotropic glutamate receptors. Furthermore, astrocytes express high-affinity glutamate transporters, which represent the most important mechanism for removal of glutamate from the ECS. Both mechanisms result in the generation of intracellular signals, either by direct ion transport across the plasma membrane or by induction of store-mediated calcium release and/or other second messengers as discussed below.

Astrocyte Glutamate Receptors

Ionotropic Receptors

Expression of ionotropic glutamate receptors by astrocytes is astonishingly heterogeneous and differs between brain regions

(Verkhratsky and Kirchhoff, 2007b; Verkhratsky, 2010). There is clear evidence for functional expression of AMPA receptors on Bergmann glial cells of the cerebellar cortex, which are activated by ectopic release of glutamate at parallel fiber as well as climbing fiber synapses (Matsui et al., 2005). These have a relatively high calcium permeability and calcium signals resulting from AMPA receptor opening have been shown to control proper coverage of Purkinje cell synapses by Bergmann glia appendages (Iino et al., 2001). Retraction of Bergmann processes following deletion of AMPA receptors or their conversion to calcium-impermeable forms slowed the decay of excitatory postsynaptic potentials (EPSPs) in Purkinje cells by delaying the removal of glutamate at the synapse, resulting in an impairment of fine motor coordination (Iino et al., 2001; Saab et al., 2012). Therefore, it appears that AMPA receptors on Bergmann glial cells mediate an intricate interplay between glial calcium signaling, close ensheathment of synapses by perisynaptic glial processes and clearance of glutamate in the cerebellar cortex.

In the forebrain, AMPA receptor expression by astrocytes has been described in the neocortex (Lalo et al., 2006; Hadzic et al., 2017). They only mediate a small portion of the inward current induced by synaptic release of glutamate (the majority being carried by electrogenic glutamate uptake) and their functional relevance is as of yet unclear (Lalo et al., 2011). Moreover, there is clear evidence for AMPA receptors on processes, but not somata of radial-like glial cells in the subventricular zone of the dentate gyrus (Renzel et al., 2013). Astrocytes in the hippocampus apparently lack AMPA receptors, as opposed to NG2 cells, which were previously often classified as "immature", "complex" or "rectifying" astrocytes (Jabs et al., 1994; Latour et al., 2001; Zhou and Kimelberg, 2001; Matthias et al., 2003). A similar picture emerges for NMDA receptors. These have been identified on the mRNA, protein, and functional level in cortical astrocytes (Conti et al., 1996; Schipke et al., 2001; Lalo et al., 2006). While there are clear indications for the involvement of NMDA receptors in astroglial signaling in hippocampal astrocytes (Porter and McCarthy, 1995; Serrano et al., 2008; Letellier et al., 2016), there is still no unequivocal evidence for their expression in these cells, and their presence therefore remains subject to discussion (Matthias et al., 2003; Verkhratsky and Kirchhoff, 2007b; Lalo et al., 2011; Dzamba et al., 2013).

Suffice it to say, in contrast to Bergmann glial cells or NG2 cells, there is as yet no indication that AMPA or NMDA receptors might play any functional role in astrocytes in the hippocampus. Due to this, they will no longer be discussed in this review (see **Figure 2**). Why there is such heterogeneity in the expression profile of ionotropic glutamate receptors on different types of macroglial cells is unknown.

Metabotropic Receptors

In contrast to iGluRs, expression of metabotropic glutamate receptors (mGluRs) has been firmly established for astrocytes in the hippocampus (Schools and Kimelberg, 1999; Tamaru et al., 2001; Aronica et al., 2003). The most prominent role has long been attributed to mGluR5, a member of the group I mGluRs, which activates G_q and phospholipase C and has received particular attention as this results in the generation of calcium signaling by IP_3-mediated release from intracellular stores (**Figure 2**; Pasti et al., 1995; Porter and McCarthy, 1996; Latour et al., 2001; Zur Nieden and Deitmer, 2006; Panatier and Robitaille, 2016).

While this concept apparently holds true for the juvenile hippocampus, it was recently called into question for the adult brain, where application of mGluR5 agonists failed to induce calcium signaling in astrocyte somata (Sun et al., 2013). Moreover, in the mature hippocampal mossy fiber pathway, it was found that mGluR5 was only partially responsible for calcium signals induced by axonal glutamate release in astrocyte processes (Haustein et al., 2014). While differences may be related to different variations in experimental approaches (Panatier and Robitaille, 2016), these results clearly demonstrate that calcium signaling in astrocytes is still not completely understood. Employment of more advanced calcium imaging techniques like rapid 3D-scanning of astrocytes *in situ* and *in vivo* imaging approaches are needed to resolve this issue (Bazargani and Attwell, 2016; Shigetomi et al., 2016; Bindocci et al., 2017).

In addition, astrocytes express mGluR2/3, the activation of which is coupled to $G_{i/o}$ and results in inhibition of the adenylate cyclase (AC; **Figure 2**; Schools and Kimelberg, 1999; Tamaru et al., 2001; Aronica et al., 2003). This signaling pathway causes suppression of cAMP levels, and is generally not regarded as being directly involved in astrocyte calcium signaling (Sun et al., 2013). Notwithstanding this, activation of mGluR2/3 has recently been related to the generation of slow calcium transients in astrocytes in the mossy fiber pathway (Haustein et al., 2014). The mGluR2/3-induced calcium signaling was attributed to the action of G-protein β/γ subunits activating phospholipase C and interaction with IP_3 receptors (Haustein et al., 2014), in analogy to $GABA_B$ receptors.

High-affinity Glutamate Transporters

Although receptors allow cells to react to synaptically-released glutamate, arguably the biggest impact on extracellular glutamate itself is made by high-affinity glutamate transporters, the EAATs. Not only do these prevent excitotoxicity through the removal of glutamate from the cleft and the ECS, but in doing so they also act as a vital component of plasticity and synaptic function. A total of five different mammalian subtypes of EAAT have been identified (Danbolt, 2001), and these show distinctive expression patterns throughout the cortex (Arriza et al., 1994). The different isoforms all adhere to the same general glutamate uptake stoichiometry; importing one glutamate molecule into the astrocyte by using the energy gained from co-transporting three sodium ions and one proton down the electrochemical gradients, whilst also exporting one potassium ion (**Figure 2**; Nicholls and Attwell, 1990). While all of these subtypes thus couple cations to glutamate transport in the same ratios, they also exhibit and uncoupled anion conductance, and therefore act as chloride ion channels (Amara and Fontana, 2002; Fahlke and Nilius, 2016). Isoforms are functionally distinguished from each other via glutamate transport rates, substrate affinities and accompanying chloride conductance (Arriza et al., 1994; Maragakis and Rothstein, 2004; Rose et al., 2016).

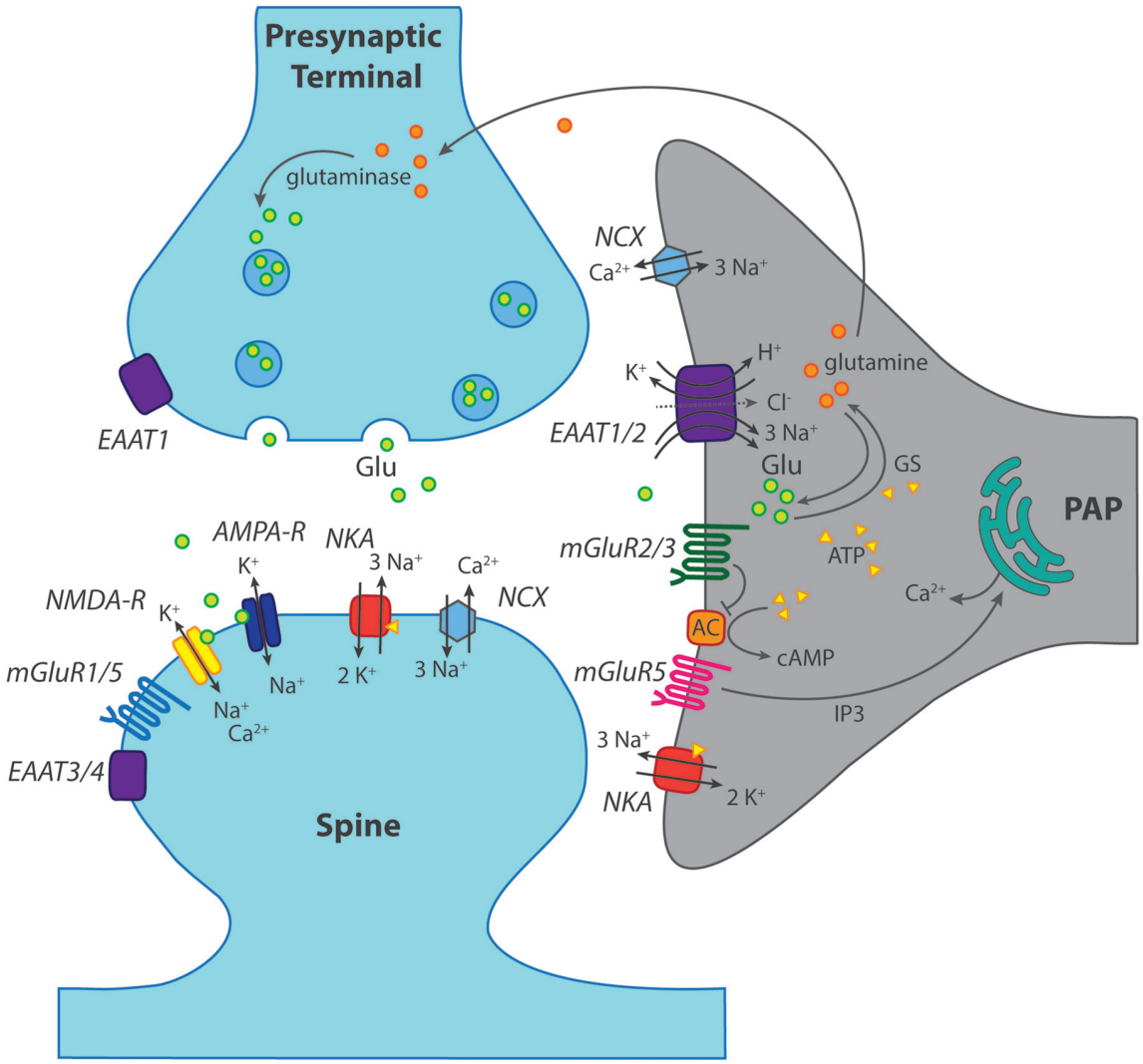

FIGURE 2 | Scheme of a "tripartite" glutamatergic synapse in the hippocampus. Shown is a presynaptic terminal and a postsynaptic spine as well as a perisynaptic astrocyte process (PAP) reaching close to the synaptic cleft. In addition to ionotropic (NMDA, AMPA) and metabotropic (mGluR) receptors for glutamate, glutamate transporters (EAAT1–4) are indicated. Moreover, main mechanisms of ion transport across the plasma membrane, such as the Na^+/K^+-ATPase (NKA) are schematically shown. GS, glutamine synthase; AC, adenylate cyclase; NCX, Na^+/Ca^{2+}-exchanger. For further explanations and abbreviations: see text.

The two predominant transporter isoforms present in the hippocampus are EAAT1 (rodent analog: GLAST; glutamate/aspartate-transporter) and EAAT2 (GLT-1; glutamate transporter 1). While various K_m (Michaelis-Menten constant, reflecting concentration of half-maximal occupancy) and V_{max} (maximal transport rate) values have been reported for these transporter species depending on the experimental system used, it is generally agreed on that EAAT2 is the more effective transporter with a higher turn-over rate than EAAT1 (Arriza et al., 1994). Additionally, EAAT3 (also known as EAAC1) can be found at post-synaptic neuronal membranes, albeit at a much lower density than astrocytic EAAT1 and 2 (Holmseth et al., 2012). Moreover, in the adult hippocampus, 10% of EAAT2 transporters are also expressed on neuronal axon terminals (Danbolt, 2001).

Transporter function is critical throughout brain development, and double knockout animals of EAAT 1 and 2 are not viable and display cortical abnormalities and disorganization (Matsugami et al., 2006). General ablation of only EAAT2 has severe effects as well and animals die soon after birth from major seizures (Rothstein et al., 1996; Tanaka et al., 1997). Importantly, knocking out EAAT2 specifically in astrocytes mimics these effects, demonstrating the vital relevance of glial glutamate uptake for glutamate homeostasis in the brain (Petr et al., 2015). Consistent with this view, knockout animals for the other transporters, including EAAT1, show only weak to moderate impairment (Watase et al., 1998).

In the neonatal hippocampus, astrocytes are still immature and developing their processes that will later define their distinct cellular domains (Bushong et al., 2004). The astrocytes in this

phase mainly rely on the subtype EAAT1 for glutamate transport and overall transport levels have been shown to be lower than in mature astrocytes (Diamond, 2005). Expression of this subtype increases over the first two postnatal weeks and then remains stable (Ullensvang et al., 1997; Schreiner et al., 2014). EAAT2 later takes over the bulk of hippocampal glutamate transport capacity, accounting for more than 90% of total uptake (Zhou et al., 2014). Its expression is delayed by around 10 days, starting to appear at p10–15 and increasing as cells mature until plateauing at p20–25 (Ullensvang et al., 1997; Schreiner et al., 2014). While this change in expression pattern has been shown to be regulated by neuronal activity (Swanson et al., 1997), the reason for the switch is unclear, especially as it is not universal across brain regions. For example, the same change happens in the cortex, but is delayed by around 2 weeks (Hanson et al., 2015), while Bergmann glia continue to primarily express EAAT1 into adulthood (Rothstein et al., 1994).

Influence of Glutamate Transporters on Extracellular Glutamate Homeostasis

Extracellular glutamate has a diffusion coefficient of ∼0.3–0.5 μm^2/ms (Zheng et al., 2008). While this suggests that glutamate will rapidly leave the synaptic cleft by diffusion after activity, it remains low at rest outside of the cleft, with a concentration of around 20–60 nM (Selkirk et al., 2005; Herman and Jahr, 2007; Yamashita et al., 2009). This is because astrocytes are very effective at clearing glutamate after activity. Indeed, in the rat hippocampus, glutamate transporters are not overwhelmed even during high frequency stimulation (Diamond and Jahr, 2000). However, in the mouse cortex, a considerable slowing of glutamate uptake following bursts of presynaptic action potentials was observed (Armbruster et al., 2016). The transport cycle, which exhibits turnover rates of 16 s^{-1} for EAAT1 (Wadiche and Kavanaugh, 1998) and ∼10–40 s^{-1} for EAAT2 (Wadiche et al., 1995; Bergles and Jahr, 1997; also see Danbolt, 2001), is relatively slow. This has lead to the idea that a major role of glutamate transporters is the fast buffering of synaptically released glutamate (Wadiche et al., 1995; Diamond and Jahr, 1997; Danbolt, 2001; Diamond, 2005). Given the high glutamate buffering and uptake capacity of transporters, the question arises how astroglial release of the gliotransmitter glutamate is coordinated with glutamate uptake, in other words if and how the immediate buffering/uptake of glutamate released by astrocytes is prevented. One potential scenario is the spatial segregation of astroglial glutamate uptake and glutamate release, which to our knowledge is not supported by any direct experimental data at the moment.

Extracellular glutamate concentrations outside of the synaptic cleft have been calculated to exceed 1 μM when 95% of astrocytes are no longer functional (Zheng et al., 2008). Failure to this extent can have critical consequences as it reduces signal-to-noise ratios at synapses and allows transmitter spill-over, which results in synaptic crosstalk (Asztely et al., 1997; Trabelsi et al., 2017). This effect can be mimicked through the deletion of astrocytic EAAT2, which produces epileptic activity (Petr et al., 2015) and subsequent excitotoxicity (Selkirk et al., 2005). Although neurons have some mechanisms to help them cope with higher glutamate levels, e.g., through the regulation of Kv2.1 channel clustering and phosphorylation after perisynaptic NMDA receptor activation (Mulholland et al., 2008), extended periods of elevated extracellular glutamate do cause irreversible damage to the surrounding cells.

While the most important determinant for sustained activation of NMDA receptors has been suggested to be release of glutamate upon presynaptic discharges (Zheng and Rusakov, 2015), transporters also have to be constantly active to counteract accumulation of tonically released glutamate (Jabaudon et al., 1999). This tonic release contributes to a constant stimulation of extrasynaptic NMDA receptors, which remains unaltered by additional saturation with glycine, therefore indicating that glutamate is the limiting factor of this activation (Le Meur et al., 2007). The glutamate release responsible for this was originally attributed to the action of the cysteine-glutamate exchanger, but it was later found that the blocking of its action hardly altered the resulting NMDA receptor activation (Cavelier and Attwell, 2005). It has now been shown that this tonic activation can be significantly reduced by inhibiting the glutamate-glutamine cycle in astrocytes, thereby identifying them as the primary source of the ambient synaptic glutamate levels (Cavelier and Attwell, 2005; Le Meur et al., 2007).

This glutamate-glutamine cycle is a critical component of hippocampal astrocyte function, wherein glutamate taken up by transporters is converted into non-toxic glutamine by glutamine synthase (GS) and ATP, before being transported back into neurons (**Figure 2**). Pharmacological inhibition of GS results in significantly larger and longer NMDA receptor currents in cortical pyramidal neurons upon high-frequency stimulation, indicating that suppression of enzyme activity elevates intracellular glutamate levels and impairs glutamate uptake (Trabelsi et al., 2017). Neurons recycle glutamine back into glutamate or GABA in order to replenish transmitter stores (Schousboe et al., 2014). This is an essential process as neurons are unable to produce these transmitters *de novo* (Bak et al., 2006). Interestingly, astrocytes also contain the enzyme glutaminase required to produce glutamate from glutamine (Cardona et al., 2015). Although the cycle has been proven critical to the glial release of transmitter, the exact release mechanisms remain unclear. However, this "gliotransmission" occurs independently of calcium, and it has been suggested that it may happen via a VAMP3 mechanism, regulated by cAMP (Li et al., 2015). Although the function of this release and uptake cycle remains unresolved at present, astrocytes seem to be the main mediator of both processes, which are important for the rapid turn-over rate of extracellular glutamate within the hippocampus (Jabaudon et al., 1999).

ROLE OF ASTROCYTIC ION SIGNALS FOR GLUTAMATE HOMEOSTASIS

As mentioned above, activation of astrocyte glutamate receptors as well as glutamate uptake through high-affinity transport leads to changes in intracellular ion concentrations. Such ion

concentration changes, in turn, may act as signals to trigger release of glutamate from astrocytes and/or modulate glutamate transport activity and thereby represent relevant mediators of astrocytes' control of extracellular glutamate homeostasis.

Ion Signaling Related to Glutamate Transport

Astrocytes experience major changes of their cytosolic ion concentrations in response to glutamate because of the activity of high-affinity and sodium-dependent glutamate uptake. These ions include primarily sodium and protons (Rose and Ransom, 1996; Kirischuk et al., 2016), which are transported together with glutamate. Moreover, depending on the EAAT isoform expressed, glutamate transporters mediate a detectable flux of chloride (Untiet et al., 2017). The resulting degradation of ion gradients reduces its driving force and exerts a negative feedback on transport capacity, which may in extreme cases, e.g., during additional disturbance in ion homeostasis, even result in reversal of glutamate uptake. Ion signaling related to glutamate transport thereby represents an important modulator of astroglial control of extracellular glutamate.

Under physiological conditions, glutamate transporters exhibit a reversal potential in the far positive range (>50 mV, Barbour et al., 1991; Bergles and Jahr, 1997). Changes in the plasma membrane gradients of the transported ions (Na^+, H^+, K^+) directly influence glutamate transport activity, and because of its transport stoichiometry, this is especially relevant for sodium ions (Szatkowski et al., 1990; Barbour et al., 1991; Zerangue and Kavanaugh, 1996; Levy et al., 1998). In addition, as glutamate uptake is electrogenic, the depolarization mediated by glutamate uptake, together with the depolarizing effect of activity-related increases in extracellular K^+, will cause a dampening of further transport activity (Barbour et al., 1988; Szatkowski et al., 1990).

During periods of metabolic inhibition, reverse operation of glutamate transport can serve as a source for glutamate and contribute to its accumulation in the ECS as described for neurons under severe ischemia (Rossi et al., 2000). The same is true for reverse glutamate uptake by glia, which in isolated Müller glial cells has been shown to be induced by (very) high external potassium (Szatkowski et al., 1990). It is important to emphasize, however, that as compared to uptake of other transmitters such as GABA, glutamate uptake is highly robust. Reverse glutamate uptake in brain tissue as a mechanism for glia-mediated release of glutamate is often proposed but only possible with excessive cellular sodium loading together with strong depolarization, conditions usually only found upon complete metabolic inhibition and failure of Na^+/K^+-ATPase activity in ischemic core regions (see Rossi et al., 2000; Gerkau et al., 2017).

While reverse glutamate uptake may occur only under severe ischemic conditions, less dramatic changes in astrocyte ion gradients may still directly feed back onto extracellular glutamate levels by reducing the driving force for transport. The relevance of ongoing glutamate uptake is evident from the fact that its pharmacological inhibition causes an immediate increase in extracellular glutamate accumulation, accompanied by activation of neuronal glutamate receptors (Rothstein et al., 1996; Jabaudon et al., 1999) and rapid, fatal sodium loading of both neurons and astrocytes (Langer and Rose, 2009; Karus et al., 2015). Moderately increasing the cytosolic sodium concentration in astrocytes (to ∼35–40 mM) is directly linked to a reduction of glial glutamate transport activity as demonstrated for astrocytes in hippocampal tissue slices exposed to elevated NH_4^+/NH_3 concentrations (Kelly et al., 2009). The same is true for a moderate depolarization (by ∼8–10 mV) of hippocampal astrocytes *in situ*, which—as expected based on the transport stoichiometry—significantly reduced the amplitude of glutamate uptake currents induced by application of the transporter agonist D-aspartate (Stephan et al., 2012).

These studies clearly show that if intracellular sodium rises in astrocytes, the reversal potential for glutamate transport is shifted in a negative direction, thereby reducing their glutamate uptake capacity. Notably, glutamate uptake simultaneously represents the most powerful pathway for the induction of sodium signals as demonstrated for astrocytes in the *stratum radiatum* of the hippocampal CA1 area (see **Figure 1B**; Langer and Rose, 2009; Karus et al., 2015; Langer et al., 2017), cerebellum (Kirischuk et al., 2007; Bennay et al., 2008), neocortex (Lamy and Chatton, 2011; Unichenko et al., 2013), and at the Calyx of Held (Uwechue et al., 2012). Activity-related sodium signals following activation of glutamate uptake are detectable in perisynaptic astrocyte processes, and their amplitudes have been shown to be related to the strength of synaptic stimulation over a wide range of stimulation intensities, reaching ∼6 mM with 10 pulses, (Langer and Rose, 2009). If such sodium elevations, and the accompanying reduction in transport capacity, result in a reduction of overall glutamate uptake by astrocytes and thereby in a modulation of extracellular glutamate concentrations and synaptic glutamate transients under physiological conditions, remains to be established.

Besides the direct negative feedback effect of sodium elevations on glutamate transport capacity, there is also accumulating evidence that sodium signals in response to transport activation might drive reversal of the sodium-calcium exchange (NCX) in astrocytes (**Figure 2**; Kirischuk et al., 2012; Boscia et al., 2016). The consequence of such a reversal is the generation of calcium influx into astrocytes (Kirischuk et al., 1997; Song et al., 2013; Gerkau et al., 2017). Calcium signals induced by sodium-driven NCX might then result in calcium-dependent release of glutamate, again linking astrocyte sodium signals to their regulation and modulation of extracellular glutamate concentrations.

Astrocyte Calcium Signaling

Astrocytes also detect synaptically-released glutamate by activation of glutamate receptors as described above. Their activation often leads to the generation of intracellular ion signals and/or second messengers (**Figure 2**). Transient astrocyte calcium elevations in response to glutamatergic activity were one of the first intracellular signals implicated in neuron-glia interaction at synapses

(Enkvist et al., 1989; Cornell-Bell et al., 1990; Kim et al., 1994; Hassinger et al., 1995). While initial experiments were performed in cell culture, it soon became clear that also astrocytes *in situ* also respond to neuronal release of transmitters with increases in calcium, as for example shown in acute hippocampal tissue slices (Dani et al., 1992; Porter and McCarthy, 1996; Pasti et al., 1997). Later on, this concept was shown to hold true within the intact brain by demonstrating that hippocampal astrocytes *in vivo* undergo calcium signaling in response to neuronal activity (Kuga et al., 2011; Takata et al., 2011; Navarrete et al., 2012). The exact astroglial mechanisms generating calcium transients and their spatial and temporal properties are still under debate despite the wealth of experimental evidence (Agulhon et al., 2010; Volterra et al., 2014; Bazargani and Attwell, 2016; Rungta et al., 2016; Shigetomi et al., 2016; Bindocci et al., 2017).

An important cellular response to these calcium transients includes calcium-dependent release of neurotransmitters from astrocytes targeting nearby neurons and their synapses. The considerable experimental evidence for the existence of such feedback signaling, the involved mechanisms, the current controversies and open questions have been discussed in detail recently by ourselves and others (Hamilton and Attwell, 2010; Araque et al., 2014; Rusakov et al., 2014; Verkhratsky et al., 2016; Bohmbach et al., 2017). The relevance of astroglial calcium signaling for neurotransmitter uptake is less explored. As discussed above, calcium and sodium signaling are linked via the NCX such that sodium elevations may trigger calcium-entry via the NCX. Whether the reverse, sodium-entry as a consequence of calcium export through NCX, can modify the driving force of astroglial glutamate uptake (and thus its efficiency) significantly, has not been explored to the best of our knowledge.

In addition, calcium increases could regulate insertion and internalization of glutamate transporters. Such a direct effect of astroglial calcium levels on neurotransmitter transport has been demonstrated for the GABA transporters GAT3 in the hippocampus. Chelation of intracellular calcium by infusing astroglia with the calcium buffer BAPTA via a patch pipette reduced the GAT3 levels and induced a tonic, GABA-receptor-mediated current recorded in interneurons, indicating that lowering astroglial calcium levels reduces GAT3-mediated GABA uptake (Shigetomi et al., 2011). Direct evidence for the calcium-dependence of glutamate transport in astrocytes *in situ* is currently not available but several experimental observations make the existence of such a mechanism plausible. First, an increase of glutamate uptake by cultured astrocytes can be induced by basic fibroblast growth factor on a time scale of hours via a partially calcium-dependent signal cascade (Suzuki et al., 2001). Second, the down-regulation of astroglial glutamate uptake currents in spinal cord slices by interleukin 1beta within minutes of its application is likely to involve astroglial calcium signaling (Yan et al., 2014). Finally, the manipulation of calcium levels in cultured astroglia affected the insertion and removal of eGFP-tagged GLT-1 into and out of the membrane (Stenovec et al., 2008). Together these studies demonstrate that changes of astroglial calcium levels could directly control glutamate uptake. Because astrocyte calcium signaling itself depends on neuronal activity (see above), glutamate uptake could be finely tuned by synaptic activity via astroglial calcium signaling.

REGULATION OF SYNAPTIC TRANSMISSION BY ASTROGLIAL GLUTAMATE TRANSPORTERS AND PERISYNAPTIC ASTROCYTE STRUCTURE

Astroglial Transporters Constrain the Spread of Synaptically Released Glutamate

As discussed above, astrocytes take up the vast majority of synaptically released glutamate (>90%). However, glutamate is released from the presynaptic terminal directly into the synaptic cleft, which is typically devoid of astrocyte processes and thus astroglial glutamate transporters. It is therefore thought that astrocytes do not control the initial spread of synaptically released glutamate inside the synaptic cleft under physiological conditions (see below) and that instead diffusion and dilution of glutamate primarily underlies the dissipation of the steep glutamate concentration gradients directly after release (Clements et al., 1992; Danbolt, 2001; Scimemi and Beato, 2009). At these nanometer and microsecond scales, intra-cleft glutamate concentration transients have escaped direct observation. Instead, numerical simulations have been employed to analyze the intra-cleft spread of glutamate and its escape into the perisynaptic space that contains perisynaptic astrocyte processes (Diamond, 2001; Zheng et al., 2008; Scimemi and Beato, 2009; Allam et al., 2012; see section "Influence of Glutamate Transporters on Extracellular Glutamate Homeostasis" for glutamate binding to astroglial transporters and uptake).

These simulations predicted that perisynaptic astrocyte branches and the glutamate transporters located on them reduce the probability of glutamate escaping into perisynaptic ECS and activating perisynaptic high-affinity receptors such as mGluRs or NMDA receptors (Zheng et al., 2008). Indeed, glutamate released at one synapse can activate high-affinity NMDA receptors at nearby synapses (a phenomenon called glutamate spill-over or synaptic crosstalk) and pharmacological blockade of glutamate transporters significantly exacerbates this process (Asztely et al., 1997; Diamond, 2001; Arnth-Jensen et al., 2002; Scimemi et al., 2004). Thus, astroglial glutamate transporters constrain but do not prevent synaptic crosstalk between hippocampal synapses via high-affinity NMDA receptors (**Figures 3A,B**).

Because astroglial glutamate transporters limit activation of NMDA receptors, it is likely that they also affect NMDA receptor-dependent synaptic plasticity. Indeed, the amplitude ratio of EPSCs mediated by NMDA and low-affinity AMPA receptors was increased in recordings from CA1 pyramidal cells in acute slices from GLT-1 knockout animals (Katagiri et al., 2001), suggesting a larger contribution of NMDA receptors. In the same preparation, long-term potentiation of CA3-CA1 synaptic transmission was impaired, which was attributed to excessive activation of NMDA receptors (Katagiri et al., 2001). In addition, up-regulation of GLT-1

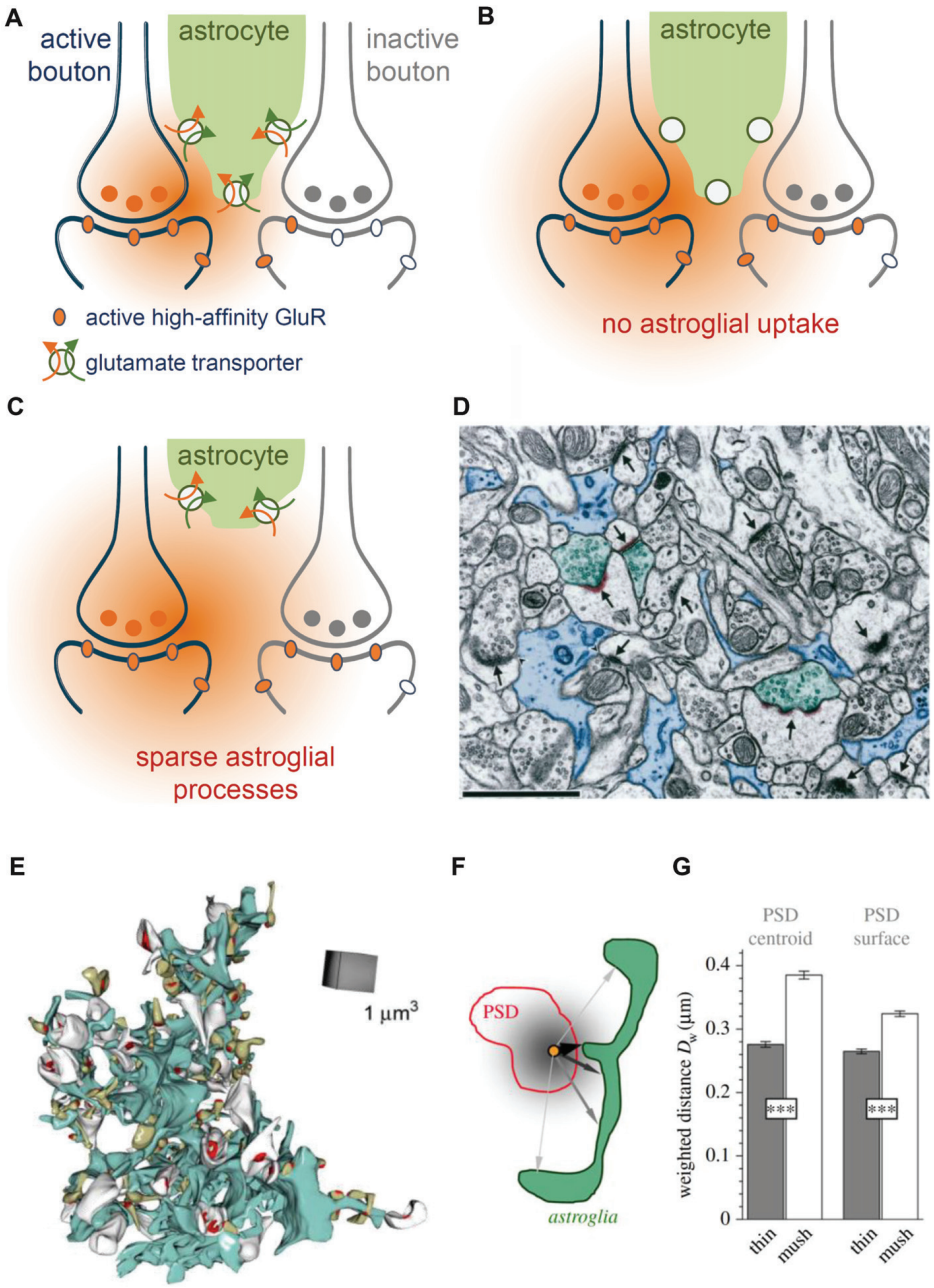

FIGURE 3 | Role of astroglial transporters and perisynaptic astroglial morphology. **(A)** Synaptically-released glutamate (orange) diffuses in extracellular space (ECS) before astroglial (green) clearance (orange arrow) along with uptake of sodium takes place (green arrow). Released glutamate will activate high-affinity glutamate receptors (orange oval) at active synapses (blue, left) but also some on neighboring, presynaptically-inactive synapses (gray, right, gray ovals represent inactive glutamate receptors), leading to "glutamate spill-over" or synaptic crosstalk. **(B)** When glutamate uptake is pharmacologically inhibited, glutamate spreads further into extrasynaptic space and is more likely to activate high-affinity glutamate receptors at nearby synapses. **(C)** Perisynaptic astroglial process structure is expected to affect the local efficiency of astroglial glutamate clearance. For example, an increased distance of astroglial processes from an active synapse is likely to reduce the efficiency of local clearance/uptake and to increase the probability of synaptic crosstalk via high affinity glutamate receptors. **(D)** Not all synapses are directly contacted by perisynaptic astroglial processes. Adopted with permission from Ventura and Harris (1999). Astroglial processes (blue, scale bar 1 μm) were visualized using electron microscopy (EM) and their spatial relationship to synapses (arrows) was studied. Note, that only three synapses (arrowheads) are directly contacted by astroglial processes (see Ventura and Harris, 1999 for quantification) suggesting a highly uneven coverage of synapses by astroglial glutamate transporters. **(E)** Example of an EM 3D-reconstruction of a single astroglial fragment (turquoise) with adjacent postsynaptic spines (white and greenish) with their postsynaptic densities (PSD) from the dentate gyrus (Medvedev et al., 2014). **(F)** The local abundance of astroglial processes around individual spines was determined by the average, diffusion-weighted distance from the PSD center or surface to perisynaptic astroglia. Analysis revealed (see Medvedev et al., 2014 for more details) that astroglial processes were on average closer to thin than to mushroom spines **(G)** suggesting that perisynaptic glutamate transients at thin spines are more tightly controlled by astroglial transporters.

expression by ceftriaxone impaired long-term depression and reduced long-term potentiation at mossy fiber-CA3 synapses (Omrani et al., 2009). A role of glutamate transporters for NMDA receptor-dependent synaptic plasticity has also been established outside of the hippocampus (Massey et al., 2004; Tsvetkov et al., 2004; Valtcheva and Venance, 2016), which indicates that the control of NMDA receptor-activation—and therefore NMDA receptor-dependent synaptic plasticity—by astroglial glutamate could be a ubiquitous phenomenon in the brain.

Glutamate transporters also control the activation of other high affinity glutamate receptors. For instance, mGluR activation of interneurons in response to synaptic glutamate release was strongly increased after pharmacological transporter blockade (Huang et al., 2004). To what extent synaptic crosstalk plays a role for low-affinity, post-synaptic AMPA receptor function is not fully explored. The net effect of the GLT-1 inhibitor DHK on AMPA receptor-mediated EPSCs varies between small decrease and no effect (Asztely et al., 1997 and references therein). Similarly, AMPA receptor-mediated EPSCs recorded from CA1 pyramidal cells were not affected by transporter blockade using TBOA, irrespective of whether these were action-potential independent EPSCs ("minis") or evoked by minimal-stimulation (Zheng et al., 2008). This effectively rules out a role of glutamate transporters in controlling AMPA receptor activation at the releasing synapse. However, it does not exclude that: (1) glutamate may reach AMPA receptors at nearby synapses of other neurons in the densely packed neuropil (not recorded from); and (2) that astroglial transporters control such AMPA receptor-dependent crosstalk. The latter scenario is hinted at by our previous experimental findings. The inhibition of astroglial metabolism using the gliotoxin fluoroacetate (FAC) is likely to impair astroglial glutamate uptake (Karus et al., 2015). At the same time, this treatment significantly increased the predominantly AMPA receptor-mediated field EPSP slope, a measurement reflecting all AMPA receptor-activity in the neuropil, by about 20% (Henneberger et al., 2010b). However, a direct measurement of the range of action of glutamate and its dependence on astroglial transporters is still missing.

It should be noted here that the often used broad-spectrum glutamate transporter inhibitors TBOA and TFB-TBOA (Shimamoto et al., 1998) do not selectively inhibit astroglial transporters but dose-dependently inhibit GLT-1 (expressed mostly but not exclusively by astrocytes in the hippocampus Mennerick et al., 1998; Danbolt, 2001), the astroglial GLAST and the neuronally-expressed EAAC1 (Shigeri et al., 2004). However, the volume density of EAAC1 (molecules/μm^3) is two orders of magnitude lower than GLT-1 in the CA1 *stratum radiatum*, which raises the question to what extent EAAC1 contributes specifically to glutamate clearance (Holmseth et al., 2012; but see Scimemi et al., 2009).

In summary, experimental evidence and modeling studies both support a role of astroglial glutamate uptake in constraining the invasion of extrasynaptic space by synaptically released glutamate and thereby the activation of high-affinity glutamate receptors beyond the active synapse.

The Role of Perisynaptic Astroglial Structure for Glutamate Clearance

It is intuitive that the positioning and density of astroglial glutamate transporters in the perisynaptic space determines how far glutamate diffuses into perisynaptic or extrasynaptic ECS before it binds to astrocytic glutamate transporters. Therefore, the spatial arrangement of PAPs relative to the synapse (for instance distance or astrocyte surface per volume) is expected to shape perisynaptic glutamate signaling as much as the transporter density in these PAPs.

Interestingly, PAPs are capable of local protein synthesis and both GLAST and GLT-1 transcripts are enriched in PAPs (Sakers et al., 2017). Insertion of these transporters into the astroglial cell membrane and their internalization are regulated processes, which can depend on astroglial calcium levels (see "Astrocyte Calcium Signaling" section for a discussion of experimental evidence). In addition, cell surface expression of GLT-1 is regulated by protein kinase C activity (Kalandadze et al., 2002), sumoylation (in cultured astrocytes; Foran et al., 2014) and ubiquitination (in HEK293 cells; Ibáñez et al., 2016). Once inserted in the membrane, glutamate transporters are mobile in the astroglial membrane as revealed by single molecule tracking techniques (Murphy-Royal et al., 2015). The mobility of GLT-1 on the astroglial cell membrane depends on neuronal activity and the transporter activity itself in dissociated and slice cultures (Murphy-Royal et al., 2015; Al Awabdh et al., 2016). Interestingly, diffusion of GLT-1 in membranes slows down near synapses and cross-linking of GLT-1, which reduced its mobility, was shown to affect synaptic transmission (Murphy-Royal et al., 2015). Together these studies indicate that the transporter density in astroglial membranes is tightly regulated and tuned by neuronal activity.

Together with the transporter density, the abundance of astroglial processes and membranes in the vicinity of a synapse (or in other words the exact arrangement and structure of PAPs) determines the total number of available transporters. As a consequence, changes of astrocytic morphology that modify the spatial relationship between synapses and PAPs will affect how efficiently or rapidly glutamate is captured by astrocytic transporters and how likely it is for glutamate to escape into the peri- and extrasynaptic space (**Figure 3C**). Pioneering work on this interplay between astrocyte morphology and synapse function was performed using the oxytocinergic system of the supraoptic nucleus as a model system. In this brain region, astrocyte processes less efficiently separate neurons during lactation, which leads to the increased occurrence of juxta-positioned neuronal membrane profiles (Theodosis and Poulain, 1993). Importantly, this reduction of astroglial coverage of neurons during lactation is associated with a reduced efficiency of glutamate clearance and changes in the control of synaptic transmission by presynaptic metabotropic glutamate receptors (Oliet et al., 2001). Thus, changes of astrocyte structure and therefore the spatial configuration of the ECS surrounding neurons and nearby astrocytes determines the extracellular dynamics of synaptically-released glutamate in the supraoptic nucleus. In the following, we discuss the

experimental evidence implying that glutamate clearance in the hippocampus could also depend on astroglial morphology and its changes.

Ventura and Harris reported in 1999 that only about half of the glutamatergic synapses in the CA1 *stratum radiatum* have astroglial processes directly apposed to them (**Figure 3D**), which in each case covered again only about half of the synaptic interface (Ventura and Harris, 1999). The efficiency of local glutamate clearance by astroglia is, therefore, expected to vary considerably from synapse to synapse. This observation raised the question, which synapses are particularly well-covered by astroglial transporters and what the functional relevance of the potential heterogeneity may be. Serial-section EM of astrocyte fragments in the dentate gyrus followed by their 3D-reconstruction along with nearby synapses provided some insights into this issue (Medvedev et al., 2014). It was found for instance that the diffusion-weighted average distance from the synapse to the surrounding astroglial processes was significantly smaller at thin synapses compared to larger, mushroom-type synapses (**Figures 3E–G**). This suggests that the size of the postsynaptic spine and therefore presumably synaptic strength (Schikorski and Stevens, 1997) are inversely correlated with local astroglial glutamate clearance. A testable hypothesis is therefore that larger synapses are associated with a lower efficiency of local astroglial glutamate clearance and that the glutamate escape into peri- and extrasynaptic space is more prominent. Such scenarios would be interesting to explore because spine size plasticity is tightly associated with synaptic plasticity (Bourne and Harris, 2007). It should be noted here that astrocyte morphologies also vary widely within and across brain regions (Matyash and Kettenmann, 2010; Anders et al., 2014) and therefore such relationships between astrocyte morphology and local abundance of astroglial glutamate transporters could be as heterogeneous.

Similar to the supraoptic nucleus, the morphology of astrocytes is not static in the hippocampus. Time lapse imaging of fluorescently-labeled astrocytes revealed a surprisingly high motility of astrocyte processes on a time scale of minutes in organotypic hippocampal slices cultures (Haber et al., 2006), which rapidly changed the relative positions to neuronal spines. A well-studied and potent trigger of PAP restructuring is the induction of synaptic plasticity (Wenzel et al., 1991; Lushnikova et al., 2009; Henneberger et al., 2010a; Bernardinelli et al., 2014; Perez-Alvarez et al., 2014). Plasticity-associated changes of PAP structure and motility have been shown to determine spine fate (Bernardinelli et al., 2014) and to affect astroglial control of presynaptic release (Perez-Alvarez et al., 2014). However, it is currently unclear if such rapid dynamic changes of PAP structure have an impact on astroglial glutamate uptake and synaptic crosstalk. Indirect supporting evidence is provided by elegant experiments using connexin 30 knockout mice in which PAPs invade the synaptic cleft and impair synaptic transmission and plasticity in a transporter-dependent manner (Pannasch et al., 2014). One potential experimental strategy to establish the effect of rapid changes of PAP/spine spatial relationships on glutamate clearance and synaptic crosstalk is to induce defined and isolated changes of PAP morphology. This could be done by targeting the signaling cascades that govern astrocyte morphology (Zeug et al., 2017) while monitoring glutamate signaling and crosstalk.

CONCLUSION

Excitatory glutamatergic transmission between neurons in the hippocampus cannot be separated functionally from the action of synaptically-released glutamate onto neighboring astrocytes. Recent advances in technical approaches such as genetically-targeted stimulation of specific cell types and single cells, genetically-encoded indicators and super-resolution imaging have shed more light on this intricate relationship. On the one hand side, astrocytes express glutamate receptors that can trigger intracellular signaling cascades. On the other hand, astrocytic transporters bind glutamate with high affinity, which rapidly buffers the glutamate released from presynaptic terminals thereby shaping extracellular glutamate concentrations transients and thus modifying the activation of receptors on postsynaptic neurons. Once taken up, astrocytes may use glutamate to fuel their own metabolite needs, but also convert it to glutamine and cycle it back to neurons. The exact temporal and spatial dynamics of this interplay between neurons and astrocytes are just starting to emerge. Recent studies suggest that astrocytes not only undergo slow changes in their shape and characteristics in response to pathological events. Moreover, there is evidence that astrocyte perisynaptic processes might undergo rapid activity-dependent structural changes at the sub-micron scale that will influence their glutamate clearance and thus, the functional properties of glutamatergic synapses. Future work will hopefully provide new and exciting insights into this dynamic aspect of neuron-glia interaction, which is needed to fully understand the function of glutamatergic synapses in the hippocampus and in other regions of the brain.

AUTHOR CONTRIBUTIONS

All authors contributed to the conception and drafting of the work, revised it critically for important intellectual content and approved the final version to be published.

FUNDING

CRR was supported by the Priority Program 1757 "Glial Heterogeneity" of the Deutsche Forschungsgemeinschaft (DFG) (German Research Foundation; Ro 2327/8-1, 2). Work in CH's laboratory was supported by the NRW-Rückkehrerprogramm, the DFG (SFB1089 B03, SPP1757 HE6949/1 and HE6949/3) and the European Union (EUGliaPhD). AR was supported by the NRW-Rückkehrerprogramm. AZ was supported by the German Research Foundation (ZE994/2) and the REBIRTH Excellence Cluster. DD received funding from the DFG (SPP 1757, SFB 1089, DI 853/3-2, DI 853/7-1, DI 853/5-1).

REFERENCES

Abbott, N. J., Rönnbäck, L., and Hansson, E. (2006). Astrocyte-endothelial interactions at the blood-brain barrier. *Nat. Rev. Neurosci.* 7, 41–53. doi: 10.1038/nrn1824

Abrahamsen, B., Schneider, N., Erichsen, M. N., Huynh, T. H., Fahlke, C., Bunch, L., et al. (2013). Allosteric modulation of an excitatory amino acid transporter: the subtype-selective inhibitor UCPH-101 exerts sustained inhibition of EAAT1 through an intramonomeric site in the trimerization domain. *J. Neurosci.* 33, 1068–1087. doi: 10.1523/JNEUROSCI.3396-12.2013

Agulhon, C., Fiacco, T. A., and McCarthy, K. D. (2010). Hippocampal short- and long-term plasticity are not modulated by astrocyte Ca^{2+} signaling. *Science* 327, 1250–1254. doi: 10.1126/science.1184821

Al Awabdh, S., Gupta-Agarwal, S., Sheehan, D. F., Muir, J., Norkett, R., Twelvetrees, A. E., et al. (2016). Neuronal activity mediated regulation of glutamate transporter GLT-1 surface diffusion in rat astrocytes in dissociated and slice cultures. *Glia* 64, 1252–1264. doi: 10.1002/glia.22997

Allam, S. L., Ghaderi, V. S., Bouteiller, J. M., Legendre, A., Ambert, N., Greget, R., et al. (2012). A computational model to investigate astrocytic glutamate uptake influence on synaptic transmission and neuronal spiking. *Front. Comput. Neurosci.* 6:70. doi: 10.3389/fncom.2012.00070

Amara, S. G., and Fontana, A. C. K. (2002). Excitatory amino acid transporters: keeping up with glutamate. *Neurochem. Int.* 41, 313–318. doi: 10.1016/s0197-0186(02)00018-9

Anders, S., Minge, D., Griemsmann, S., Herde, M. K., Steinhäuser, C., and Henneberger, C. (2014). Spatial properties of astrocyte gap junction coupling in the rat hippocampus. *Philos. Trans. R. Soc. Lond. B Biol. Sci.* 369:20130600. doi: 10.1098/rstb.2013.0600

Araque, A., Carmignoto, G., Haydon, P. G., Oliet, S. H., Robitaille, R., and Volterra, A. (2014). Gliotransmitters travel in time and space. *Neuron* 81, 728–739. doi: 10.1016/j.neuron.2014.02.007

Arizono, M., Bannai, H., Nakamura, K., Niwa, F., Enomoto, M., Matsu-Ura, T., et al. (2012). Receptor-selective diffusion barrier enhances sensitivity of astrocytic processes to metabotropic glutamate receptor stimulation. *Sci. Signal.* 5:ra27. doi: 10.1126/scisignal.2002498

Armbruster, M., Hampton, D., Yang, Y., and Dulla, C. G. (2014). Laser-scanning astrocyte mapping reveals increased glutamate-responsive domain size and disrupted maturation of glutamate uptake following neonatal cortical freeze-lesion. *Front. Cell. Neurosci.* 8:277. doi: 10.3389/fncel.2014.00277

Armbruster, M., Hanson, E., and Dulla, C. G. (2016). Glutamate clearance is locally modulated by presynaptic neuronal activity in the cerebral cortex. *J. Neurosci.* 36, 10404–10415. doi: 10.1523/jneurosci.2066-16.2016

Arnth-Jensen, N., Jabaudon, D., and Scanziani, M. (2002). Cooperation between independent hippocampal synapses is controlled by glutamate uptake. *Nat. Neurosci.* 5, 325–331. doi: 10.1038/nn825

Aronica, E., Catania, M. V., Geurts, J., Yankaya, B., and Troost, D. (2001). Immunohistochemical localization of group I and II metabotropic glutamate receptors in control and amyotrophic lateral sclerosis human spinal cord: upregulation in reactive astrocytes. *Neuroscience* 105, 509–520. doi: 10.1016/s0306-4522(01)00181-6

Aronica, E., Gorter, J. A., Ijlst-Keizers, H., Rozemuller, A. J., Yankaya, B., Leenstra, S., et al. (2003). Expression and functional role of mGluR3 and mGluR5 in human astrocytes and glioma cells: opposite regulation of glutamate transporter proteins. *Eur. J. Neurosci.* 17, 2106–2118. doi: 10.1046/j.1460-9568.2003.02657.x

Arriza, J. L., Fairman, W. A., Wadiche, J. I., Murdoch, G. H., Kavanaugh, M. P., and Amara, S. G. (1994). Functional comparisons of three glutamate transporter subtypes cloned from human motor cortex. *J. Neurosci.* 14, 5559–5569.

Asztely, F., Erdemli, G., and Kullmann, D. M. (1997). Extrasynaptic glutamate spillover in the hippocampus: dependence on temperature and the role of active glutamate uptake. *Neuron* 18, 281–293. doi: 10.1016/s0896-6273(00)80268-8

Axelrod, D., Koppel, D. E., Schlessinger, J., Elson, E., and Webb, W. W. (1976). Mobility measurement by analysis of fluorescence photobleaching recovery kinetics. *Biophys. J.* 16, 1055–1069. doi: 10.1016/s0006-3495(76)85755-4

Bak, L. K., Schousboe, A., and Waagepetersen, H. S. (2006). The glutamate/GABA-glutamine cycle: aspects of transport, neurotransmitter homeostasis and ammonia transfer. *J. Neurochem.* 98, 641–653. doi: 10.1111/j.1471-4159.2006.03913.x

Barbour, B., Brew, H., and Attwell, D. (1988). Electrogenic glutamate uptake in glial cells is activated by intracellular potassium. *Nature* 335, 433–435. doi: 10.1038/335433a0

Barbour, B., Brew, H., and Attwell, D. (1991). Electrogenic uptake of glutamate and aspartate into glial cells isolated from the salamander (Ambystoma) retina. *J. Physiol.* 436, 169–193. doi: 10.1113/jphysiol.1991.sp018545

Bazargani, N., and Attwell, D. (2016). Astrocyte calcium signaling: the third wave. *Nat. Neurosci.* 19, 182–189. doi: 10.1038/nn.4201

Bennay, M., Langer, J., Meier, S. D., Kafitz, K. W., and Rose, C. R. (2008). Sodium signals in cerebellar Purkinje neurons and Bergmann glial cells evoked by glutamatergic synaptic transmission. *Glia* 56, 1138–1149. doi: 10.1002/glia.20685

Bergles, D. E., Dzubay, J., and Jahr, C. (1997). Glutamate transporter currents in Bergmann glial cells follow the time course of extrasynaptic glutamate. *Proc. Natl. Acad. Sci. U S A* 94, 14821–14825. doi: 10.1073/pnas.94.26.14821

Bergles, D. E., and Jahr, C. (1997). Synaptic activation of glutamate transporters in hippocampal astrocytes. *Neuron* 19, 1297–1308. doi: 10.1016/s0896-6273(00)80420-1

Berlin, S., Szobota, S., Reiner, A., Carroll, E. C., Kienzler, M. A., Guyon, A., et al. (2016). A family of photoswitchable NMDA receptors. *Elife* 5:e12040. doi: 10.7554/eLife.12040

Bernardinelli, Y., Randall, J., Janett, E., Nikonenko, I., König, S., Jones, E. V., et al. (2014). Activity-dependent structural plasticity of perisynaptic astrocytic domains promotes excitatory synapse stability. *Curr. Biol.* 24, 1679–1688. doi: 10.1016/j.cub.2014.06.025

Bindocci, E., Savtchouk, I., Liaudet, N., Becker, D., Carriero, G., and Volterra, A. (2017). Three-dimensional Ca^{2+} imaging advances understanding of astrocyte biology. *Science* 356:eaai8185. doi: 10.1126/science.aai8185

Bohmbach, K., Schwarz, M. K., Schoch, S., and Henneberger, C. (2017). The structural and functional evidence for vesicular release from astrocytes *in situ*. *Brain Res. Bull.* doi: 10.1016/j.brainresbull.2017.01.015 [Epub ahead of print].

Boscia, F., Begum, G., Pignataro, G., Sirabella, R., Cuomo, O., Casamassa, A., et al. (2016). Glial Na(+) -dependent ion transporters in pathophysiological conditions. *Glia* 64, 1677–1697. doi: 10.1002/glia.23030

Bourne, J., and Harris, K. M. (2007). Do thin spines learn to be mushroom spines that remember? *Curr. Opin. Neurobiol.* 17, 381–386. doi: 10.1016/j.conb.2007.04.009

Bowman, C. L., and Kimelberg, H. K. (1984). Excitatory amino acids directly depolarize rat brain astrocytes in primary culture. *Nature* 311, 656–659. doi: 10.1038/311656a0

Brew, H., and Attwell, D. (1987). Electrogenic glutamate uptake is a major current carrier in the membrane of axolotl retinal glial cells. *Nature* 327, 707–709. doi: 10.1038/327707a0

Bushong, E. A., Martone, M. E., and Ellisman, M. H. (2004). Maturation of astrocyte morphology and the establishment of astrocyte domains during postnatal hippocampal development. *Int. J. Dev. Neurosci.* 22, 73–86. doi: 10.1016/j.ijdevneu.2003.12.008

Cardona, C., Sánchez-Mejías, E., Dávila, J. C., Martín-Rufián, M., Campos-Sandoval, J. A., Vitorica, J., et al. (2015). Expression of Gls and Gls2 glutaminase isoforms in astrocytes. *Glia* 63, 365–382. doi: 10.1002/glia.22758

Cavelier, P., and Attwell, D. (2005). Tonic release of glutamate by a DIDS-sensitive mechanism in rat hippocampal slices. *J. Physiol.* 564, 397–410. doi: 10.1113/jphysiol.2004.082131

Chaudhry, F. A., Lehre, K. P., van Lookeren Campagne, M., Ottersen, O. P., Danbolt, N. C., and Storm-Mathisen, J. (1995). Glutamate transporters in glial plasma membranes: highly differentiated localizations revealed by quantitative ultrastructural immunocytochemistry. *Neuron* 15, 711–720. doi: 10.1016/0896-6273(95)90158-2

Chen, F., Tillberg, P. W., and Boyden, E. S. (2015). Optical imaging. Expansion microscopy. *Science* 347, 543–548. doi: 10.1126/science.1260088

Cheung, G., Sibille, J., Zapata, J., and Rouach, N. (2015). Activity-dependent plasticity of astroglial potassium and glutamate clearance. *Neural Plast.* 2015:109106. doi: 10.1155/2015/109106

Chung, K., Wallace, J., Kim, S. Y., Kalyanasundaram, S., Andalman, A. S., Davidson, T. J., et al. (2013). Structural and molecular interrogation of intact biological systems. *Nature* 497, 332–337. doi: 10.1038/nature12107

Ciappelloni, S., Murphy-Royal, C., Dupuis, J. P., Oliet, S. H. R., and Groc, L. (2017). Dynamics of surface neurotransmitter receptors and transporters in glial cells: single molecule insights. *Cell Calcium* 67, 46–52. doi: 10.1016/j.ceca.2017.08.009

Clements, J. D., Lester, R. A., Tong, G., Jahr, C. E., and Westbrook, G. L. (1992). The time course of glutamate in the synaptic cleft. *Science* 258, 1498–1501. doi: 10.1126/science.1359647

Conti, F., DeBiasi, S., Minelli, A., and Melone, M. (1996). Expression of NR1 and NR2A/B subunits of the NMDA receptor in cortical astrocytes. *Glia* 17, 254–258. doi: 10.1002/(SICI)1098-1136(199607)17:3<254::AID-GLIA7>3.0.CO;2-0

Cornell-Bell, A. H., Finkbeiner, S. M., Cooper, M. S., and Smith, S. J. (1990). Glutamate induces calcium waves in cultured astrocytes: long-range glial signaling. *Science* 247, 470–473. doi: 10.1126/science.1967852

Dallérac, G., Chever, O., and Rouach, N. (2013). How do astrocytes shape synaptic transmission? Insights from electrophysiology. *Front. Cell. Neurosci.* 7:159. doi: 10.3389/fncel.2013.00159

Danbolt, N. C. (2001). Glutamate uptake. *Prog. Neurobiol.* 65, 1–105. doi: 10.1016/S0301-0082(00)00067-8

Danbolt, N. C., Storm-Mathisen, J., and Kanner, B. I. (1992). An $[Na^+ + K^+]$coupled L-glutamate transporter purified from rat brain is located in glial cell processes. *Neuroscience* 51, 295–310. doi: 10.1016/0306-4522(92)90316-t

Danbolt, N. C., Zhou, Y., Furness, D. N., and Holmseth, S. (2016). Strategies for immunohistochemical protein localization using antibodies: what did we learn from neurotransmitter transporters in glial cells and neurons. *Glia* 64, 2045–2064. doi: 10.1002/glia.23027

Dani, J. W., Chernjavsky, A., and Smith, S. J. (1992). Neuronal activity triggers calcium waves in hippocampal astrocyte networks. *Neuron* 8, 429–440. doi: 10.1016/0896-6273(92)90271-e

de Lorimier, R. M., Smith, J. J., Dwyer, M. A., Looger, L. L., Sali, K. M., Paavola, C. D., et al. (2002). Construction of a fluorescent biosensor family. *Protein Sci.* 11, 2655–2675. doi: 10.1110/ps.021860

Derouiche, A., and Frotscher, M. (1991). Astroglial processes around identified glutamatergic synapses contain glutamine synthetase: evidence for transmitter degradation. *Brain Res.* 552, 346–350. doi: 10.1016/0006-8993(91)90103-3

Diamond, J. S. (2001). Neuronal glutamate transporters limit activation of NMDA receptors by neurotransmitter spillover on CA1 pyramidal cells. *J. Neurosci.* 21, 8328–8338.

Diamond, J. S. (2005). Deriving the glutamate clearance time course from transporter currents in CA1 hippocampal astrocytes: transmitter uptake gets faster during development. *J. Neurosci.* 25, 2906–2916. doi: 10.1523/jneurosci.5125-04.2005

Diamond, J. S., and Jahr, C. E. (1997). Transporters buffer synaptically released glutamate on a submillisecond time scale. *J. Neurosci.* 17, 4672–4687.

Diamond, J. S., and Jahr, C. E. (2000). Synaptically released glutamate does not overwhelm transporters on hippocampal astrocytes during high-frequency stimulation. *J. Neurophysiol.* 83, 2835–2843. doi: 10.1152/jn.2000.83.5.2835

Dzamba, D., Honsa, P., and Anderova, M. (2013). NMDA receptors in glial cells: pending questions. *Curr. Neuropharmacol.* 11, 250–262. doi: 10.2174/1570159x11311030002

Enkvist, M. O., Holopainen, I., and Akerman, K. E. (1989). Glutamate receptor-linked changes in membrane potential and intracellular Ca^{2+} in primary rat astrocytes. *Glia* 2, 397–402. doi: 10.1002/glia.440020602

Fahlke, C., and Nilius, B. (2016). Molecular physiology of anion channels: dual function proteins and new structural motifs–a special issue. *Pflugers Arch.* 468, 369–370. doi: 10.1007/s00424-016-1791-z

Fiacco, T. A., Agulhon, C., Taves, S. R., Petravicz, J., Casper, K. B., Dong, X., et al. (2007). Selective stimulation of astrocyte calcium *in situ* does not affect neuronal excitatory synaptic activity. *Neuron* 54, 611–626. doi: 10.1016/j.neuron.2007.04.032

Foran, E., Rosenblum, L., Bogush, A., Pasinelli, P., and Trotti, D. (2014). Sumoylation of the astroglial glutamate transporter EAAT2 governs its intracellular compartmentalization. *Glia* 62, 1241–1253. doi: 10.1002/glia.22677

Förster, T. (1948). Zwischenmolekulare energiewanderung und fluoreszenz. *Ann. Phys.* 437, 55–75. doi: 10.1002/andp.19484370105

Furness, D. N., Dehnes, Y., Akhtar, A. Q., Rossi, D. J., Hamann, M., Grutle, N. J., et al. (2008). A quantitative assessment of glutamate uptake into hippocampal synaptic terminals and astrocytes: new insights into a neuronal role for excitatory amino acid transporter 2 (EAAT2). *Neuroscience* 157, 80–94. doi: 10.1016/j.neuroscience.2008.08.043

Furuta, A., Rothstein, J. D., and Martin, L. J. (1997). Glutamate transporter protein subtypes are expressed differentially during rat CNS development. *J. Neurosci.* 17, 8363–8375.

Gerkau, N. J., Rakers, C., Durry, S., Petzold, G., and Rose, C. R. (2017). Reverse NCX attenuates cellular sodium loading in metabolically compromised cortex. *Cereb. Cortex* doi: 10.1093/cercor/bhx280 [Epub ahead of print].

Giaume, C., Koulakoff, A., Roux, L., Holcman, D., and Rouach, N. (2010). Astroglial networks: a step further in neuroglial and gliovascular interactions. *Nat. Rev. Neurosci.* 11, 87–99. doi: 10.1038/nrn2757

Gourine, A. V., Kasymov, V., Marina, N., Tang, F., Figueiredo, M. F., Lane, S., et al. (2010). Astrocytes control breathing through pH-dependent release of ATP. *Science* 329, 571–575. doi: 10.1126/science.1190721

Gradinaru, V., Mogri, M., Thompson, K. R., Henderson, J. M., and Deisseroth, K. (2009). Optical deconstruction of parkinsonian neural circuitry. *Science* 324, 354–359. doi: 10.1126/science.1167093

Grosche, J., Kettenmann, H., and Reichenbach, A. (2002). Bergmann glial cells form distinct morphological structures to interact with cerebellar neurons. *J. Neurosci. Res.* 68, 138–149. doi: 10.1002/jnr.10197

Haber, M., Zhou, L., and Murai, K. K. (2006). Cooperative astrocyte and dendritic spine dynamics at hippocampal excitatory synapses. *J. Neurosci.* 26, 8881–8891. doi: 10.1523/JNEUROSCI.1302-06.2006

Hadzic, M., Jack, A., and Wahle, P. (2017). Ionotropic glutamate receptors: which ones, when, and where in the mammalian neocortex. *J. Comp. Neurol.* 525, 976–1033. doi: 10.1002/cne.24103

Hamilton, N. B., and Attwell, D. (2010). Do astrocytes really exocytose neurotransmitters? *Nat. Rev. Neurosci.* 11, 227–238. doi: 10.1038/nrn2803

Hanson, E., Armbruster, M., Cantu, D., Andresen, L., Taylor, A., Danbolt, N. C., et al. (2015). Astrocytic glutamate uptake is slow and does not limit neuronal NMDA receptor activation in the neonatal neocortex. *Glia* 63, 1784–1796. doi: 10.1002/glia.22844

Hassinger, T. D., Atkinson, P. B., Strecker, G. J., Whalen, L. R., Dudek, F. E., Kossel, A. H., et al. (1995). Evidence for glutamate-mediated activation of hippocampal neurons by glial calcium waves. *J. Neurobiol.* 28, 159–170. doi: 10.1002/neu.480280204

Haustein, M. D., Kracun, S., Lu, X. H., Shih, T., Jackson-Weaver, O., Tong, X., et al. (2014). Conditions and constraints for astrocyte calcium signaling in the hippocampal mossy fiber pathway. *Neuron* 82, 413–429. doi: 10.1016/j.neuron.2014.02.041

He, Y., Janssen, W. G., Rothstein, J. D., and Morrison, J. H. (2000). Differential synaptic localization of the glutamate transporter EAAC1 and glutamate receptor subunit GluR2 in the rat hippocampus. *J. Comp. Neurol.* 418, 255–269. doi: 10.1002/(sici)1096-9861(20000313)418:3<255::aid-cne2>3.3.co;2-y

Hefendehl, J. K., LeDue, J., Ko, R. W., Mahler, J., Murphy, T. H., and MacVicar, B. A. (2016). Mapping synaptic glutamate transporter dysfunction *in vivo* to regions surrounding Aβ plaques by iGluSnFR two-photon imaging. *Nat. Commun.* 7:13441. doi: 10.1038/ncomms13441

Heller, J. P., and Rusakov, D. A. (2015). Morphological plasticity of astroglia: understanding synaptic microenvironment. *Glia* 63, 2133–2151. doi: 10.1002/glia.22821

Henneberger, C., Medvedev, N. I., Papouin, T., Oliet, S. H. R., Stewart, M. G., and Rusakov, D. A. (2010a). "LTP at the CA3-CA1 synapse depends on D-serine release from astrocytes and involves changes in astrocyte morphology," in *Poster at the Neuroscience Meeting Planner. San Diego, CA: Society for Neuroscience*, 554.8/I29. Available online at: http://www.abstractsonline.com/Plan/ViewAbstract.aspx?mID=2554&sKey=1d482b45-4bf6-48aa-ad59-05ecd342c128&cKey=07ced13b-df86-466f-9f40-ca12b68725db&mKey=e5d5c83f-ce2d-4d71-9dd6-fc7231e090fb

Henneberger, C., Papouin, T., Oliet, S. H., and Rusakov, D. A. (2010b). Long-term potentiation depends on release of D-serine from astrocytes. *Nature* 463, 232–236. doi: 10.1038/nature08673

Herman, M. A., and Jahr, C. E. (2007). Extracellular glutamate concentration in hippocampal slice. *J. Neurosci.* 27, 9736–9741. doi: 10.1523/jneurosci.3009-07.2007

Hires, S. A., Zhu, Y., and Tsien, R. Y. (2008). Optical measurement of synaptic glutamate spillover and reuptake by linker optimized glutamate-sensitive fluorescent reporters. *Proc. Natl. Acad. Sci. U S A* 105, 4411–4416. doi: 10.1073/pnas.0712008105

Holmseth, S., Dehnes, Y., Huang, Y. H., Follin-Arbelet, V. V., Grutle, N. J., Mylonakou, M. N., et al. (2012). The density of EAAC1 (EAAT3) glutamate transporters expressed by neurons in the mammalian CNS. *J. Neurosci.* 32, 6000–6013. doi: 10.1523/jneurosci.5347-11.2012

Huang, Y. H., Sinha, S. R., Tanaka, K., Rothstein, J. D., and Bergles, D. E. (2004). Astrocyte glutamate transporters regulate metabotropic glutamate receptor-mediated excitation of hippocampal interneurons. *J. Neurosci.* 24, 4551–4559. doi: 10.1523/jneurosci.5217-03.2004

Huff, J. (2015). The Airyscan detector from ZEISS: confocal imaging with improved signal-to-noise ratio and super-resolution. *Nat. Methods* 12, i–ii. doi: 10.1038/nmeth.f.388

Ibáñez, I., Diez-Guerra, F. J., Giménez, C., and Zafra, F. (2016). Activity dependent internalization of the glutamate transporter GLT-1 mediated by β-arrestin 1 and ubiquitination. *Neuropharmacology* 107, 376–386. doi: 10.1016/j.neuropharm.2016.03.042

Iino, M., Goto, K., Kakegawa, W., Okado, H., Sudo, M., Ishiuchi, S., et al. (2001). Glia-synapse interaction through Ca^{2+}-permeable AMPA receptors in Bergmann glia. *Science* 292, 926–969. doi: 10.1126/science.1058827

Jabaudon, D., Shimamoto, K., Yasuda-Kamatani, Y., Scanziani, M., Gähwiler, B. H., and Gerber, U. (1999). Inhibition of uptake unmasks rapid extracellular turnover of glutamate of nonvesicular origin. *Proc. Natl. Acad. Sci. U S A* 96, 8733–8738. doi: 10.1073/pnas.96.15.8733

Jabs, R., Kirchhoff, F., Kettenmann, H., and Steinhäuser, C. (1994). Kainate activates Ca^{2+}-permeable glutamate receptors and blocks voltage-gated K^+ currents in glial cells of mouse hippocampal slices. *Pflugers Arch.* 426, 310–319. doi: 10.1007/bf00374787

Jensen, T. P., Zheng, K., Tyurikova, O., Reynolds, J. P., and Rusakov, D. A. (2017). Monitoring single-synapse glutamate release and presynaptic calcium concentration in organised brain tissue. *Cell Calcium* 64, 102–108. doi: 10.1016/j.ceca.2017.03.007

Kafitz, K. W., Meier, S. D., Stephan, J., and Rose, C. R. (2008). Developmental profile and properties of sulforhodamine 101–labeled glial cells in acute brain slices of rat hippocampus. *J. Neurosci. Methods* 169, 84–92. doi: 10.1016/j.jneumeth.2007.11.022

Kalandadze, A., Wu, Y., and Robinson, M. B. (2002). Protein kinase C activation decreases cell surface expression of the GLT-1 subtype of glutamate transporter. Requirement of a carboxyl-terminal domain and partial dependence on serine 486. *J. Biol. Chem.* 277, 45741–45750. doi: 10.1074/jbc.m203771200

Karki, P., Smith, K., Johnson, J. Jr., Aschner, M., and Lee, E. Y. (2015). Genetic dys-regulation of astrocytic glutamate transporter EAAT2 and its implications in neurological disorders and manganese toxicity. *Neurochem. Res.* 40, 380–388. doi: 10.1007/s11064-014-1391-2

Karus, C., Mondragão, M. A., Ziemens, D., and Rose, C. R. (2015). Astrocytes restrict discharge duration and neuronal sodium loads during recurrent network activity. *Glia* 63, 936–957. doi: 10.1002/glia.22793

Katagiri, H., Tanaka, K., and Manabe, T. (2001). Requirement of appropriate glutamate concentrations in the synaptic cleft for hippocampal LTP induction. *Eur. J. Neurosci.* 14, 547–553. doi: 10.1046/j.0953-816x.2001.01664.x

Keifer, J., and Carr, M. T. (2000). Immunocytochemical localization of glutamate receptor subunits in the brain stem and cerebellum of the turtle Chrysemys picta. *J. Comp. Neurol.* 427, 455–468. doi: 10.1002/1096-9861(20001120)427:3<455::aid-cne11>3.0.co;2-x

Kelly, T., Kafitz, K. W., Roderigo, C., and Rose, C. R. (2009). Ammonium-evoked alterations in intracellular sodium and pH reduce glial glutamate transport activity. *Glia* 57, 921–934. doi: 10.1002/glia.20817

Kettenmann, H., Backus, K. H., and Schachner, M. (1984). Aspartate, glutamate and gamma-aminobutyric acid depolarize cultured astrocytes. *Neurosci. Lett.* 52, 25–29. doi: 10.1016/0304-3940(84)90345-8

Khakh, B. S., and McCarthy, K. D. (2015). Astrocyte calcium signaling: from observations to functions and the challenges therein. *Cold Spring Harb. Perspect. Biol.* 7:a020404. doi: 10.1101/cshperspect.a020404

Kim, W. T., Rioult, M. G., and Cornell-Bell, A. H. (1994). Glutamate-induced calcium signaling in astrocytes. *Glia* 11, 173–184. doi: 10.1002/glia.440110211

Kim, S. A., Sanabria, H., Digman, M. A., Gratton, E., Schwille, P., Zipfel, W. R., et al. (2010). Quantifying translational mobility in neurons: comparison between current optical techniques. *J. Neurosci.* 30, 16409–16416. doi: 10.1523/jneurosci.3063-10.2010

Kirischuk, S., Héja, L., Kardos, J., and Billups, B. (2016). Astrocyte sodium signaling and the regulation of neurotransmission. *Glia* 64, 1655–1666. doi: 10.1002/glia.22943

Kirischuk, S., Kettenmann, H., and Verkhratsky, A. (1997). Na^+/Ca^{2+} exchanger modulates kainate-triggered Ca^{2+} signaling in Bergmann glial cells *in situ*. *FASEB J.* 11, 566–572.

Kirischuk, S., Kettenmann, H., and Verkhratsky, A. (2007). Membrane currents and cytoplasmic sodium transients generated by glutamate transport in Bergmann glial cells. *Pflugers Arch.* 454, 245–252. doi: 10.1007/s00424-007-0207-5

Kirischuk, S., Parpura, V., and Verkhratsky, A. (2012). Sodium dynamics: another key to astroglial excitability? *Trends Neurosci.* 35, 497–506. doi: 10.1016/j.tins.2012.04.003

Kofuji, P., and Newman, E. A. (2004). Potassium buffering in the central nervous system. *Neuroscience* 129, 1045–1056. doi: 10.1016/j.neuroscience.2004.06.008

Kuga, N., Sasaki, T., Takahara, Y., Matsuki, N., and Ikegaya, Y. (2011). Large-scale calcium waves traveling through astrocytic networks *in vivo*. *J. Neurosci.* 31, 2607–2614. doi: 10.1523/JNEUROSCI.5319-10.2011

Lalo, U., Pankratov, Y., Kirchhoff, F., North, R. A., and Verkhratsky, A. (2006). NMDA receptors mediate neuron-to-glia signaling in mouse cortical astrocytes. *J. Neurosci.* 26, 2673–2683. doi: 10.1523/jneurosci.4689-05.2006

Lalo, U., Pankratov, Y., Parpura, V., and Verkhratsky, A. (2011). Ionotropic receptors in neuronal-astroglial signalling: what is the role of "excitable" molecules in non-excitable cells. *Biochim. Biophys. Acta* 1813, 992–1002. doi: 10.1016/j.bbamcr.2010.09.007

Lamy, C. M., and Chatton, J. Y. (2011). Optical probing of sodium dynamics in neurons and astrocytes. *Neuroimage* 58, 572–578. doi: 10.1016/j.neuroimage.2011.06.074

Langer, J., Gerkau, N. J., Derouiche, A., Kleinhans, C., Moshrefi-Ravasdjani, B., Fredrich, M., et al. (2017). Rapid sodium signaling couples glutamate uptake to breakdown of ATP in perivascular astrocyte endfeet. *Glia* 65, 293–308. doi: 10.1002/glia.23092

Langer, J., and Rose, C. R. (2009). Synaptically induced sodium signals in hippocampal astrocytes *in situ*. *J. Physiol.* 587, 5859–5877. doi: 10.1113/jphysiol.2009.182279

Latour, I., Gee, C. E., Robitaille, R., and Lacaille, J. C. (2001). Differential mechanisms of Ca^{2+} responses in glial cells evoked by exogenous and endogenous glutamate in rat hippocampus. *Hippocampus* 11, 132–145. doi: 10.1002/hipo.1031

Lee, M. C., Ting, K. K., Adams, S., Brew, B. J., Chung, R., and Guillemin, G. J. (2010). Characterisation of the expression of NMDA receptors in human astrocytes. *PLoS One* 5:e14123. doi: 10.1371/journal.pone.0014123

Le Meur, K., Galante, M., Angulo, M. C., and Audinat, E. (2007). Tonic activation of NMDA receptors by ambient glutamate of non-synaptic origin in the rat hippocampus. *J. Physiol.* 580, 373–383. doi: 10.1113/jphysiol.2006.123570

Letellier, M., Park, Y. K., Chater, T. E., Chipman, P. H., Gautam, S. G., Oshima-Takago, T., et al. (2016). Astrocytes regulate heterogeneity of presynaptic strengths in hippocampal networks. *Proc. Natl. Acad. Sci. U S A* 113, E2685–E2694. doi: 10.1073/pnas.1523717113

Levitz, J., Pantoja, C., Gaub, B., Janovjak, H., Reiner, A., Hoagland, A., et al. (2013). Optical control of metabotropic glutamate receptors. *Nat. Neurosci.* 16, 507–516. doi: 10.1038/nn.3346

Levy, L. M., Warr, O., and Attwell, D. (1998). Stoichiometry of the glial glutamate transporter GLT-1 expressed inducibly in a Chinese hamster ovary cell line selected for low endogenous Na^+-dependent glutamate uptake. *J. Neurosci.* 18, 9620–9628.

Li, D., Agulhon, C., Schmidt, E., Oheim, M., and Ropert, N. (2013). New tools for investigating astrocyte-to-neuron communication. *Front. Cell. Neurosci.* 7:193. doi: 10.3389/fncel.2013.00193

Li, D., Hérault, K., Isacoff, E. Y., Oheim, M., and Ropert, N. (2012). Optogenetic activation of LiGluR-expressing astrocytes evokes anion channel-mediated glutamate release. *J. Physiol.* 590, 855–873. doi: 10.1113/jphysiol.2011.219345

Li, D., Hérault, K., Zylbersztejn, K., Lauterbach, M. A., Guillon, M., Oheim, M., et al. (2015). Astrocyte VAMP3 vesicles undergo Ca^{2+} -independent cycling and modulate glutamate transporter trafficking. *J. Physiol.* 593, 2807–2832. doi: 10.1113/jp270362

Lushnikova, I., Skibo, G., Muller, D., and Nikonenko, I. (2009). Synaptic potentiation induces increased glial coverage of excitatory synapses in CA1 hippocampus. *Hippocampus* 19, 753–762. doi: 10.1002/hipo.20551

Magde, D., Elson, E. L., and Webb, W. W. (1974). Fluorescence correlation spectroscopy. II. An experimental realization. *Biopolymers* 13, 29–61. doi: 10.1002/bip.1974.360130103

Maragakis, N. J., and Rothstein, J. D. (2004). Glutamate transporters: animal models to neurologic disease. *Neurobiol. Dis.* 15, 461–473. doi: 10.1016/j.nbd.2003.12.007

Marcaggi, P., and Attwell, D. (2004). Role of glial amino acid transporters in synaptic transmission and brain energetics. *Glia* 47, 217–225. doi: 10.1002/glia.20027

Martin, L. J., Blackstone, C. D., Levey, A. I., Huganir, R. L., and Price, D. L. (1993). AMPA glutamate receptor subunits are differentially distributed in rat brain. *Neuroscience* 53, 327–358. doi: 10.1016/0306-4522(93)90199-p

Marvin, J. S., Borghuis, B. G., Tian, L., Cichon, J., Harnett, M. T., Akerboom, J., et al. (2013). An optimized fluorescent probe for visualizing glutamate neurotransmission. *Nat. Methods* 10, 162–170. doi: 10.1038/nmeth.2333

Massey, P. V., Johnson, B. E., Moult, P. R., Auberson, Y. P., Brown, M. W., Molnar, E., et al. (2004). Differential roles of NR2A and NR2B-containing NMDA receptors in cortical long-term potentiation and long-term depression. *J. Neurosci.* 24, 7821–7828. doi: 10.1523/JNEUROSCI.1697-04.2004

Matsugami, T. R., Tanemura, K., Mieda, M., Nakatomi, R., Yamada, K., Kondo, T., et al. (2006). Indispensability of the glutamate transporters GLAST and GLT1 to brain development. *Proc. Natl. Acad. Sci. U S A* 103, 12161–12166. doi: 10.1073/pnas.0509144103

Matsui, K., Jahr, C. E., and Rubio, M. E. (2005). High-concentration rapid transients of glutamate mediate neural-glial communication via ectopic release. *J. Neurosci.* 25, 7538–7547. doi: 10.1523/jneurosci.1927-05.2005

Matthias, K., Kirchhoff, F., Seifert, G., Huttmann, K., Matyash, M., Kettenmann, H., et al. (2003). Segregated expression of AMPA-type glutamate receptors and glutamate transporters defines distinct astrocyte populations in the mouse hippocampus. *J. Neurosci.* 23, 1750–1758.

Matyash, V., and Kettenmann, H. (2010). Heterogeneity in astrocyte morphology and physiology. *Brain Res. Rev.* 63, 2–10. doi: 10.1016/j.brainresrev.2009.12.001

Medvedev, N., Popov, V., Henneberger, C., Kraev, I., Rusakov, D. A., and Stewart, M. G. (2014). Glia selectively approach synapses on thin dendritic spines. *Philos. Trans. R. Soc. Lond. B Biol. Sci.* 369:20140047. doi: 10.1098/rstb.2014.0047

Mennerick, S., Dhond, R. P., Benz, A., Xu, W., Rothstein, J. D., Danbolt, N. C., et al. (1998). Neuronal expression of the glutamate transporter GLT-1 in hippocampal microcultures. *J. Neurosci.* 18, 4490–4499.

Miller, S. J., and Rothstein, J. D. (2016). Astroglia in thick tissue with super resolution and cellular reconstruction. *PLoS One* 11:e0160391. doi: 10.1371/journal.pone.0160391

Minbay, Z., Serter Kocoglu, S., Gok Yurtseven, D., and Eyigor, O. (2017). Immunohistochemical localization of ionotropic glutamate receptors in the rat red nucleus. *Bosn. J. Basic Med. Sci.* 17, 29–37. doi: 10.17305/bjbms.2016.1629

Mulholland, P. J., Carpenter-Hyland, E. P., Hearing, M. C., Becker, H. C., Woodward, J. J., and Chandler, L. J. (2008). Glutamate transporters regulate extrasynaptic NMDA receptor modulation of Kv2.1 potassium channels. *J. Neurosci.* 28, 8801–8809. doi: 10.1523/jneurosci.2405-08.2008

Murphy-Royal, C., Dupuis, J. P., Varela, J. A., Panatier, A., Pinson, B., Baufreton, J., et al. (2015). Surface diffusion of astrocytic glutamate transporters shapes synaptic transmission. *Nat. Neurosci.* 18, 219–226. doi: 10.1038/nn.3901

Namiki, S., Sakamoto, H., Iinuma, S., Iino, M., and Hirose, K. (2007). Optical glutamate sensor for spatiotemporal analysis of synaptic transmission. *Eur. J. Neurosci.* 25, 2249–2259. doi: 10.1111/j.1460-9568.2007.05511.x

Navarrete, M., Perea, G., de Sevilla, D. F., Gómez-Gonzalo, M., Núñez, A., Martín, E. D., et al. (2012). Astrocytes mediate *in vivo* cholinergic-induced synaptic plasticity. *PLoS Biol.* 10:e1001259. doi: 10.1371/journal.pbio.1001259

Nicholls, D., and Attwell, D. (1990). The release and uptake of excitatory amino acids. *Trends Pharmacol. Sci.* 11, 462–468. doi: 10.1016/0165-6147(90)90129-v

Nimmerjahn, A., Kirchhoff, F., Kerr, J. N., and Helmchen, F. (2004). Sulforhodamine 101 as a specific marker of astroglia in the neocortex *in vivo*. *Nat. Methods* 1, 31–37. doi: 10.1038/nmeth706

Niswender, C. M., and Conn, P. J. (2010). Metabotropic glutamate receptors: physiology, pharmacology, and disease. *Annu. Rev. Pharmacol. Toxicol.* 50, 295–322. doi: 10.1146/annurev.pharmtox.011008.145533

Nusser, Z. (2000). AMPA and NMDA receptors: similarities and differences in their synaptic distribution. *Curr. Opin. Neurobiol.* 10, 337–341. doi: 10.1016/s0959-4388(00)00086-6

Okubo, Y., Sekiya, H., Namiki, S., Sakamoto, H., Iinuma, S., Yamasaki, M., et al. (2010). Imaging extrasynaptic glutamate dynamics in the brain. *Proc. Natl. Acad. Sci. U S A* 107, 6526–6531. doi: 10.1073/pnas.0913154107

Okumoto, S., Looger, L. L., Micheva, K. D., Reimer, R. J., Smith, S. J., and Frommer, W. B. (2005). Detection of glutamate release from neurons by genetically encoded surface-displayed FRET nanosensors. *Proc. Natl. Acad. Sci. U S A* 102, 8740–8745. doi: 10.1073/pnas.0503274102

Oliet, S. H., Piet, R., and Poulain, D. A. (2001). Control of glutamate clearance and synaptic efficacy by glial coverage of neurons. *Science* 292, 923–926. doi: 10.1126/science.1059162

Omrani, A., Melone, M., Bellesi, M., Safiulina, V., Aida, T., Tanaka, K., et al. (2009). Up-regulation of GLT-1 severely impairs LTD at mossy fibre—CA3 synapses. *J. Physiol.* 587, 4575–4588. doi: 10.1113/jphysiol.2009.177881

Ottersen, O. P., and Landsend, A. S. (1997). Organization of glutamate receptors at the synapse. *Eur. J. Neurosci.* 9, 2219–2224. doi: 10.1111/j.1460-9568.1997.tb01640.x

Panatier, A., and Robitaille, R. (2016). Astrocytic mGluR5 and the tripartite synapse. *Neuroscience* 323, 29–34. doi: 10.1016/j.neuroscience.2015.03.063

Pannasch, U., Freche, D., Dallérac, G., Ghézali, G., Escartin, C., Ezan, P., et al. (2014). Connexin 30 sets synaptic strength by controlling astroglial synapse invasion. *Nat. Neurosci.* 17, 549–558. doi: 10.1038/nn.3662

Parpura, V., Heneka, M. T., Montana, V., Oliet, S. H., Schousboe, A., Haydon, P. G., et al. (2012). Glial cells in (patho)physiology. *J. Neurochem.* 121, 4–27. doi: 10.1111/j.1471-4159.2012.07664.x

Pasti, L., Pozzan, T., and Carmignoto, G. (1995). Long-lasting changes of calcium oscillations in astrocytes. A new form of glutamate-mediated plasticity. *J. Biol. Chem.* 270, 15203–15210. doi: 10.1074/jbc.270.25.15203

Pasti, L., Volterra, A., Pozzan, T., and Carmignoto, G. (1997). Intracellular calcium oscillations in astrocytes: a highly plastic bidirectional form of communication between neurons and astrocytes *in situ*. *J. Neurosci.* 17, 7817–7830.

Perea, G., Navarrete, M., and Araque, A. (2009). Tripartite synapses: astrocytes process and control synaptic information. *Trends Neurosci.* 32, 421–431. doi: 10.1016/j.tins.2009.05.001

Perea, G., Yang, A., Boyden, E. S., and Sur, M. (2014). Optogenetic astrocyte activation modulates response selectivity of visual cortex neurons *in vivo*. *Nat. Commun.* 5:3262. doi: 10.1038/ncomms4262

Perez-Alvarez, A., Navarrete, M., Covelo, A., Martin, E. D., and Araque, A. (2014). Structural and functional plasticity of astrocyte processes and dendritic spine interactions. *J. Neurosci.* 34, 12738–12744. doi: 10.1523/JNEUROSCI.2401-14.2014

Petr, G. T., Sun, Y., Frederick, N. M., Zhou, Y., Dhamne, S. C., Hameed, M. Q., et al. (2015). Conditional deletion of the glutamate transporter GLT-1 reveals that astrocytic GLT-1 protects against fatal epilepsy while neuronal GLT-1 contributes significantly to glutamate uptake into synaptosomes. *J. Neurosci.* 35, 5187–5201. doi: 10.1523/jneurosci.4255-14.2015

Petralia, R. S., and Wenthold, R. J. (1998). "Glutamate receptor antibodies: production and immunocytochemistr," in *Receptor Localization: Laboratory Methods and Procedures*, ed. M. A. Ariano (New York, NY: Wiley), 46–74.

Piston, D. W., and Kremers, G. J. (2007). Fluorescent protein FRET: the good, the bad and the ugly. *Trends Biochem. Sci.* 32, 407–414. doi: 10.1016/j.tibs.2007.08.003

Porter, J. T., and McCarthy, K. D. (1995). GFAP-positive hippocampal astrocytes *in situ* respond to glutamatergic neuroligands with increases in $[Ca2+]_i$. *Glia* 13, 101–112. doi: 10.1002/glia.440130204

Porter, J. T., and McCarthy, K. D. (1996). Hippocampal astrocytes *in situ* respond to glutamate released from synaptic terminals. *J. Neurosci.* 16, 5073–5081.

Reichenbach, A., Derouiche, A., and Kirchhoff, F. (2010). Morphology and dynamics of perisynaptic glia. *Brain Res. Rev.* 63, 11–25. doi: 10.1016/j.brainresrev.2010.02.003

Reiner, A., Levitz, J., and Isacoff, E. Y. (2015). Controlling ionotropic and metabotropic glutamate receptors with light: principles and potential. *Curr. Opin. Pharmacol.* 20, 135–143. doi: 10.1016/j.coph.2014.12.008

Renzel, R., Sadek, A. R., Chang, C. H., Gray, W. P., Seifert, G., and Steinhäuser, C. (2013). Polarized distribution of AMPA, but not $GABA_A$, receptors in radial glia-like cells of the adult dentate gyrus. *Glia* 61, 1146–1154. doi: 10.1002/glia.22505

Rose, C. R., and Ransom, B. R. (1996). Mechanisms of H^+ and Na^+ changes induced by glutamate, kainate, and D-Aspartate in rat hippocampal astrocytes. *J. Neurosci.* 16, 5393–5404.

Rose, C. R., and Verkhratsky, A. (2016). Principles of sodium homeostasis and sodium signalling in astroglia. *Glia* 64, 1611–1627. doi: 10.1002/glia.22964

Rose, C. R., Ziemens, D., Untiet, V., and Fahlke, C. (2016). Molecular and cellular physiology of sodium-dependent glutamate transporters. *Brain Res. Bull.* doi: 10.1016/j.brainresbull.2016.12.013 [Epub ahead of print].

Rossi, D. J., Oshima, T., and Attwell, D. (2000). Glutamate release in severe brain ischaemia is mainly by reversed uptake. *Nature* 403, 316–321. doi: 10.1038/35002090

Rothstein, J. D., Dykes-Hoberg, M., Pardo, C. A., Bristol, L. A., Jin, L., Kuncl, R. W., et al. (1996). Knockout of glutamate transporters reveals a major role for astroglial transport in excitotoxicity and clearance of glutamate. *Neuron* 16, 675–686. doi: 10.1016/s0896-6273(00)80086-0

Rothstein, J. D., Martin, L., Levey, A. I., Dykes-Hoberg, M., Jin, L., Wu, D., et al. (1994). Localization of neuronal and glial glutamate transporters. *Neuron* 13, 713–725. doi: 10.1016/0896-6273(94)90038-8

Rungta, R. L., Bernier, L. P., Dissing-Olesen, L., Groten, C. J., LeDue, J. M., Ko, R., et al. (2016). Ca^{2+} transients in astrocyte fine processes occur via Ca^{2+} influx in the adult mouse hippocampus. *Glia* 64, 2093–2103. doi: 10.1002/glia.23042

Rusakov, D. A. (2015). Disentangling calcium-driven astrocyte physiology. *Nat. Rev. Neurosci.* 16, 226–233. doi: 10.1038/nrn3878

Rusakov, D. A., Bard, L., Stewart, M. G., and Henneberger, C. (2014). Diversity of astroglial functions alludes to subcellular specialisation. *Trends Neurosci.* 37, 228–242. doi: 10.1016/j.tins.2014.02.008

Rusakov, D. A., Savtchenko, L. P., Zheng, K., and Henley, J. M. (2011). Shaping the synaptic signal: molecular mobility inside and outside the cleft. *Trends Neurosci.* 34, 359–369. doi: 10.1016/j.tins.2011.03.002

Saab, A. S., Neumeyer, A., Jahn, H. M., Cupido, A., Šimek, A. A., Boele, H. J., et al. (2012). Bergmann glial AMPA receptors are required for fine motor coordination. *Science* 337, 749–753. doi: 10.1126/science.1221140

Sakers, K., Lake, A. M., Khazanchi, R., Ouwenga, R., Vasek, M. J., Dani, A., et al. (2017). Astrocytes locally translate transcripts in their peripheral processes. *Proc. Natl. Acad. Sci. U S A* 114, E3830–E3838. doi: 10.1073/pnas.1617782114

Sasaki, T., Beppu, K., Tanaka, K. F., Fukazawa, Y., Shigemoto, R., and Matsui, K. (2012). Application of an optogenetic byway for perturbing neuronal activity via glial photostimulation. *Proc. Natl. Acad. Sci. U S A* 109, 20720–20725. doi: 10.1073/pnas.1213458109

Saxton, M. J., and Jacobson, K. (1997). Single-particle tracking: applications to membrane dynamics. *Annu. Rev. Biophys. Biomol. Struct.* 26, 373–399. doi: 10.1146/annurev.biophys.26.1.373

Schikorski, T., and Stevens, C. F. (1997). Quantitative ultrastructural analysis of hippocampal excitatory synapses. *J. Neurosci.* 17, 5858–5867.

Schipke, C. G., Ohlemeyer, C., Matyash, M., Nolte, C., Kettenmann, H., and Kirchhoff, F. (2001). Astrocytes of the mouse neocortex express functional N-methyl-D-aspartate receptors. *FASEB J.* 15, 1270–1272. doi: 10.1096/fj.00-0439fje

Schools, G. P., and Kimelberg, H. K. (1999). mGluR3 and mGluR5 are the predominant metabotropic glutamate receptor mRNAs expressed in hippocampal astrocytes acutely isolated from young rats. *J. Neurosci. Res.* 58, 533–543. doi: 10.1002/(sici)1097-4547(19991115)58:4<533::aid-jnr6>3.0.co;2-g

Schousboe, A., Scafidi, S., Bak, L. K., Waagepetersen, H. S., and McKenna, M. C. (2014). Glutamate metabolism in the brain focusing on astrocytes. *Adv. Neurobiol.* 11, 13–30. doi: 10.1007/978-3-319-08894-5_2

Schreiner, A. E., Durry, S., Aida, T., Stock, M. C., Rüther, U., Tanaka, K., et al. (2014). Laminar and subcellular heterogeneity of GLAST and GLT-1 immunoreactivity in the developing postnatal mouse hippocampus. *J. Comp. Neurol.* 522, 204–224. doi: 10.1002/cne.23450

Scimemi, A., and Beato, M. (2009). Determining the neurotransmitter concentration profile at active synapses. *Mol. Neurobiol.* 40, 289–306. doi: 10.1007/s12035-009-8087-7

Scimemi, A., Fine, A., Kullmann, D. M., and Rusakov, D. A. (2004). NR2B-containing receptors mediate cross talk among hippocampal synapses. *J. Neurosci.* 24, 4767–4777. doi: 10.1523/jneurosci.0364-04.2004

Scimemi, A., Tian, H., and Diamond, J. S. (2009). Neuronal transporters regulate glutamate clearance, NMDA receptor activation, and synaptic plasticity in the hippocampus. *J. Neurosci.* 29, 14581–14595. doi: 10.1523/jneurosci.4845-09.2009

Selkirk, J. V., Nottebaum, L. M., Vana, A. M., Verge, G. M., Mackay, K. B., Stiefel, T. H., et al. (2005). Role of the GLT-1 subtype of glutamate transporter in glutamate homeostasis: the GLT-1-preferring inhibitor WAY-855 produces marginal neurotoxicity in the rat hippocampus. *Eur. J. Neurosci.* 21, 3217–3228. doi: 10.1111/j.1460-9568.2005.04162.x

Serrano, A., Robitaille, R., and Lacaille, J. C. (2008). Differential NMDA-dependent activation of glial cells in mouse hippocampus. *Glia* 56, 1648–1663. doi: 10.1002/glia.20717

Sheppard, C. J. R. (1988). Super-resolution in confocal imaging. *Optik* 80, 53–54.

Shigeri, Y., Seal, R. P., and Shimamoto, K. (2004). Molecular pharmacology of glutamate transporters, EAATs and VGLUTs. *Brain Res. Rev.* 45, 250–265. doi: 10.1016/j.brainresrev.2004.04.004

Shigetomi, E., Patel, S., and Khakh, B. S. (2016). Probing the complexities of astrocyte calcium signaling. *Trends Cell Biol.* 26, 300–312. doi: 10.1016/j.tcb.2016.01.003

Shigetomi, E., Tong, X., Kwan, K. Y., Corey, D. P., and Khakh, B. S. (2011). TRPA1 channels regulate astrocyte resting calcium and inhibitory synapse efficacy through GAT-3. *Nat. Neurosci.* 15, 70–80. doi: 10.1038/nn.3000

Shimamoto, K., Lebrun, B., Yasuda-Kamatani, Y., Sakaitani, M., Shigeri, Y., Yumoto, N., et al. (1998). DL-threo-beta-benzyloxyaspartate, a potent blocker of excitatory amino acid transporters. *Mol. Pharmacol.* 53, 195–201.

Song, H., Thompson, S. M., and Blaustein, M. P. (2013). Nanomolar ouabain augments Ca^{2+} signalling in rat hippocampal neurones and glia. *J. Physiol.* 591, 1671–1689. doi: 10.1113/jphysiol.2012.248336

Stenovec, M., Kreft, M., Grilc, S., Pangrsic, T., and Zorec, R. (2008). EAAT2 density at the astrocyte plasma membrane and Ca^{2+}-regulated exocytosis. *Mol. Membr. Biol.* 25, 203–215. doi: 10.1080/09687680701790925

Stephan, J., Haack, N., Kafitz, K. W., Durry, S., Koch, D., Hochstrate, P., et al. (2012). Kir4.1 channels mediate a depolarization of hippocampal astrocytes under hyperammonemic conditions *in situ*. *Glia* 60, 965–978. doi: 10.1002/glia.22328

Sun, W., McConnell, E., Pare, J. F., Xu, Q., Chen, M., Peng, W., et al. (2013). Glutamate-dependent neuroglial calcium signaling differs between young and adult brain. *Science* 339, 197–200. doi: 10.1126/science.1226740

Suzuki, K., Ikegaya, Y., Matsuura, S., Kanai, Y., Endou, H., and Matsuki, N. (2001). Transient upregulation of the glial glutamate transporter GLAST in response to fibroblast growth factor, insulin-like growth factor and epidermal growth factor in cultured astrocytes. *J. Cell Sci.* 114, 3717–3725.

Swanson, R. A., Liu, J., Miller, J. W., Rothstein, J. D., Farrell, K., Stein, B. A., et al. (1997). Neuronal regulation of glutamate transporter subtype expression in astrocytes. *J. Neurosci.* 17, 932–940.

Szatkowski, M., Barbour, B., and Attwell, D. (1990). Non-vesicular release of glutamate from glial cells by reversed electrogenic glutamate uptake. *Nature* 348, 443–446. doi: 10.1038/348443a0

Takata, N., Mishima, T., Hisatsune, C., Nagai, T., Ebisui, E., Mikoshib, K., et al. (2011). Astrocyte calcium signaling transforms cholinergic modulation to cortical plasticity *in vivo*. *J. Neurosci.* 31, 18155–18165. doi: 10.1523/JNEUROSCI.5289-11.2011

Tamaru, Y., Nomura, S., Mizuno, N., and Shigemoto, R. (2001). Distribution of metabotropic glutamate receptor mGluR3 in the mouse CNS: differential location relative to pre- and postsynaptic sites. *Neuroscience* 106, 481–503. doi: 10.1016/s0306-4522(01)00305-0

Tanaka, K., Watase, K., Manabe, T., Yamada, K., Watanabe, M., Takahashi, K., et al. (1997). Epilepsy and exacerbation of brain injury in mice lacking the glutamate transporter GLT-1. *Science* 276, 1699–1702. doi: 10.1126/science.276.5319.1699

Theodosis, D. T., and Poulain, D. A. (1993). Activity-dependent neuronal-glial and synaptic plasticity in the adult mammalian hypothalamus. *Neuroscience* 57, 501–535. doi: 10.1016/0306-4522(93)90002-w

Thrane, A. S., Rangroo Thrane, V., Plog, B. A., and Nedergaard, M. (2015). Filtering the muddied waters of brain edema. *Trends Neurosci.* 38, 333–335. doi: 10.1016/j.tins.2015.04.009

Trabelsi, Y., Amri, M., Becq, H., Molinari, F., and Aniksztejn, L. (2017). The conversion of glutamate by glutamine synthase in neocortical astrocytes from juvenile rat is important to limit glutamate spillover and peri/extrasynaptic activation of NMDA receptors. *Glia* 65, 401–415. doi: 10.1002/glia.23099

Tse, D. Y., Chung, I., and Wu, S. M. (2014). Pharmacological inhibitions of glutamate transporters EAAT1 and EAAT2 compromise glutamate transport in photoreceptor to ON-bipolar cell synapses. *Vision Res.* 103, 49–62. doi: 10.1016/j.visres.2014.07.020

Tsien, R. Y. (2005). Building and breeding molecules to spy on cells and tumors. *FEBS Lett.* 579, 927–932. doi: 10.1016/j.febslet.2004.11.025

Tsvetkov, E., Shin, R. M., and Bolshakov, V. Y. (2004). Glutamate uptake determines pathway specificity of long-term potentiation in the neural circuitry of fear conditioning. *Neuron* 41, 139–151. doi: 10.1016/s0896-6273(03)00800-6

Ullensvang, K., Lehre, K. P., Storm-Mathisen, J., and Danbolt, N. C. (1997). Differential developmental expression of the two rat brain glutamate transporter proteins GLAST and GLT. *Eur. J. Neurosci.* 9, 1646–1655. doi: 10.1111/j.1460-9568.1997.tb01522.x

Unichenko, P., Dvorzhak, A., and Kirischuk, S. (2013). Transporter-mediated replacement of extracellular glutamate for GABA in the developing murine neocortex. *Eur. J. Neurosci.* 38, 3580–3588. doi: 10.1111/ejn.12380

Untiet, V., Kovermann, P., Gerkau, N. J., Gensch, T., Rose, C. R., and Fahlke, C. (2017). Glutamate transporter-associated anion channels adjust intracellular chloride concentrations during glial maturation. *Glia* 65, 388–400. doi: 10.1002/glia.23098

Uwechue, N. M., Marx, M. C., Chevy, Q., and Billups, B. (2012). Activation of glutamate transport evokes rapid glutamine release from perisynaptic astrocytes. *J. Physiol.* 590, 2317–2331. doi: 10.1113/jphysiol.2011.226605

Valtcheva, S., and Venance, L. (2016). Astrocytes gate Hebbian synaptic plasticity in the striatum. *Nat. Commun.* 7:13845. doi: 10.1038/ncomms13845

Ventura, R., and Harris, K. M. (1999). Three-dimensional relationships between hippocampal synapses and astrocytes. *J. Neurosci.* 19, 6897–6906.

Verkhratsky, A. (2010). Physiology of neuronal-glial networking. *Neurochem. Int.* 57, 332–343. doi: 10.1016/j.neuint.2010.02.002

Verkhratsky, A., and Kirchhoff, F. (2007a). Glutamate-mediated neuronal-glial transmission. *J. Anat.* 210, 651–660. doi: 10.1111/j.1469-7580.2007.00734.x

Verkhratsky, A., and Kirchhoff, F. (2007b). NMDA receptors in glia. *Neuroscientist* 13, 28–37. doi: 10.1177/1073858406294270

Verkhratsky, A., Matteoli, M., Parpura, V., Mothet, J. P., and Zorec, R. (2016). Astrocytes as secretory cells of the central nervous system: idiosyncrasies of vesicular secretion. *EMBO J.* 35, 239–257. doi: 10.15252/embj.201592705

Verkhratsky, A., and Steinhäuser, C. (2000). Ion channels in glial cells. *Brain Res. Rev.* 32, 380–412. doi: 10.1016/s0165-0173(99)00093-4

Volterra, A., Liaudet, N., and Savtchouk, I. (2014). Astrocyte Ca^{2+} signalling: an unexpected complexity. *Nat. Rev. Neurosci.* 15, 327–335. doi: 10.1038/nrn3725

Wadiche, J. I., Amara, S. G., and Kavanaugh, M. P. (1995). Ion fluxes associated with excitatory amino acid transport. *Neuron* 15, 721–728. doi: 10.1016/0896-6273(95)90159-0

Wadiche, J. I., and Kavanaugh, M. P. (1998). Macroscopic and microscopic properties of a cloned glutamate transporter/chloride channel. *J. Neurosci.* 18, 7650–7661.

Watase, K., Hashimoto, K., Kano, M., Yamada, K., Watanabe, M., Inoue, Y., et al. (1998). Motor discoordination and increased susceptibility to cerebellar injury in GLAST mutant mice. *Eur. J. Neurosci.* 10, 976–988. doi: 10.1046/j.1460-9568.1998.00108.x

Wenzel, J., Lammert, G., Meyer, U., and Krug, M. (1991). The influence of long-term potentiation on the spatial relationship between astrocyte processes and potentiated synapses in the dentate gyrus neuropil of rat brain. *Brain Res.* 560, 122–131. doi: 10.1016/0006-8993(91)91222-m

Witcher, M. R., Kirov, S. A., and Harris, K. M. (2007). Plasticity of perisynaptic astroglia during synaptogenesis in the mature rat hippocampus. *Glia* 55, 13–23. doi: 10.1002/glia.20415

Yamashita, T., Kanda, T., Eguchi, K., and Takahashi, T. (2009). Vesicular glutamate filling and AMPA receptor occupancy at the calyx of Held synapse of immature rats. *J. Physiol.* 587, 2327–2339. doi: 10.1113/jphysiol.2008.167759

Yan, X., Yadav, R., Gao, M., and Weng, H. R. (2014). Interleukin-1 beta enhances endocytosis of glial glutamate transporters in the spinal dorsal horn through activating protein kinase C. *Glia* 62, 1093–1109. doi: 10.1002/glia.22665

Yang, H. H., and St-Pierre, F. (2016). Genetically encoded voltage indicators: opportunities and challenges. *J. Neurosci.* 36, 9977–9989. doi: 10.1523/jneurosci.1095-16.2016

Zerangue, N., and Kavanaugh, M. P. (1996). Flux coupling in a neuronal glutamate transporter. *Nature* 383, 634–637. doi: 10.1038/383634a0

Zeug, A., Müller, F. E., Anders, S., Herde, M. K., Minge, D., Ponimaskin, E., et al. (2017). Control of astrocyte morphology by Rho GTPases. *Brain Res. Bull.* doi: 10.1016/j.brainresbull.2017.05.003 [Epub ahead of print].

Zhang, J., Petralia, R. S., Wang, Y. X., and Diamond, J. S. (2016). High-resolution quantitative immunogold analysis of membrane receptors at retinal ribbon synapses. *J. Vis. Exp.* 108, 53547. doi: 10.3791/53547

Zheng, K., and Rusakov, D. A. (2015). Efficient integration of synaptic events by NMDA receptors in three-dimensional neuropil. *Biophys. J.* 108, 2457–2464. doi: 10.1016/j.bpj.2015.04.009

Zheng, K., Scimemi, A., and Rusakov, D. A. (2008). Receptor actions of synaptically released glutamate: the role of transporters on the scale from nanometers to microns. *Biophys. J.* 95, 4584–4596. doi: 10.1529/biophysj.108.129874

Zhou, M., and Kimelberg, H. K. (2001). Freshly isolated hippocampal CA1 astrocytes comprise two populations differing in glutamate transporter and AMPA receptor expression. *J. Neurosci.* 21, 7901–7908.

Zhou, M., Schools, G. P., and Kimelberg, H. K. (2006). Development of GLAST(+) astrocytes and NG2(+) glia in rat hippocampus CA1: mature astrocytes are electrophysiologically passive. *J. Neurophysiol.* 95, 134–143. doi: 10.1152/jn.00570.2005

Zhou, Y., Wang, X., Tzingounis, A. V., Danbolt, N. C., and Larsson, H. P. (2014). EAAT2 (GLT-1; slc1a2) glutamate transporters reconstituted in liposomes argues against heteroexchange being substantially faster than net uptake. *J. Neurosci.* 34, 13472–13485. doi: 10.1523/JNEUROSCI.2282-14.2014

Zhuo, L., Sun, B., Zhang, C. L., Fine, A., Chiu, S. Y., and Messing, A. (1997). Live astrocytes visualized by green fluorescent protein in transgenic mice. *Dev. Biol.* 187, 36–42. doi: 10.1006/dbio.1997.8601

Zur Nieden, R., and Deitmer, J. W. (2006). The role of metabotropic glutamate receptors for the generation of calcium oscillations in rat hippocampal astrocytes *in situ*. *Cereb. Cortex* 16, 676–687. doi: 10.1093/cercor/bhj013

Conflict of Interest Statement: The authors declare that the research was conducted in the absence of any commercial or financial relationships that could be construed as a potential conflict of interest.

Sodium Fluctuations in Astroglia and Their Potential Impact on Astrocyte Function.

***Felix, L**., Delekate, A., Petzold, G. C., and Rose, C. R.*

Frontiers in Physiology 11 DOI: 10.3389/fphys.2020.00871. (2020)

Impact factor 2020: 4.13

I contributed to

- Drafting and revision of manuscript and figures

cells

MDPI

Article

Spontaneous Ultraslow Na^+ Fluctuations in the Neonatal Mouse Brain

Lisa Felix [1], Daniel Ziemens [1], Gerald Seifert [2] and Christine R. Rose [1,*]

1. Institute of Neurobiology, Faculty of Mathematics and Natural Sciences, Heinrich Heine University Duesseldorf, 40225 Duesseldorf, Germany; Lisa.Felix@hhu.de (L.F.); Daniel.Ziemens@hhu.de (D.Z.)
2. Institute of Cellular Neurosciences, Medical Faculty, University of Bonn, D-53105 Bonn, Germany; Gerald.Seifert@ukbonn.de

* Correspondence: rose@uni-duesseldorf.de; Tel.: +49-211-8113416

Received: 25 November 2019; Accepted: 24 December 2019; Published: 31 December 2019

Abstract: In the neonate forebrain, network formation is driven by the spontaneous synchronized activity of pyramidal cells and interneurons, consisting of bursts of electrical activity and intracellular Ca^{2+} oscillations. By employing ratiometric Na^+ imaging in tissue slices obtained from animals at postnatal day 2–4 (P2–4), we found that 22% of pyramidal neurons and 43% of astrocytes in neonatal mouse hippocampus also exhibit transient fluctuations in intracellular Na^+. These occurred at very low frequencies (~2/h), were exceptionally long (~8 min), and strongly declined after the first postnatal week. Similar Na^+ fluctuations were also observed in the neonate neocortex. In the hippocampus, Na^+ elevations in both cell types were diminished when blocking action potential generation with tetrodotoxin. Neuronal Na^+ fluctuations were significantly reduced by bicuculline, suggesting the involvement of $GABA_A$-receptors in their generation. Astrocytic signals, by contrast, were neither blocked by inhibition of receptors and/or transporters for different transmitters including GABA and glutamate, nor of various Na^+-dependent transporters or Na^+-permeable channels. In summary, our results demonstrate for the first time that neonatal astrocytes and neurons display spontaneous ultraslow Na^+ fluctuations. While neuronal Na^+ signals apparently largely rely on suprathreshold GABAergic excitation, astrocytic Na^+ signals, albeit being dependent on neuronal action potentials, appear to have a separate trigger and mechanism, the source of which remains unclear at present.

Keywords: astrocytes; postnatal development; hippocampus; GABA; neuron-glia interaction

1. Introduction

The first week after birth constitutes a time of dynamic rearrangement within the mammalian CNS. In the mouse brain, this critical period sees shifts in cellular morphology, connectivity, and protein expression profiles as neurons and glia transform into their mature forms. Neurogenesis in rodents is mostly completed before birth and the neonatal period is characterized by synchronized, universal activity—which acts to guide the maturation of individual cells and their integration into the complex networks critical to the function of mature tissue [1–3]. This activity includes early network oscillations (ENOs) in intracellular calcium (Ca^{2+}) [4] and later, the related giant depolarizing potentials (GDPs) of neurons [5]. Excitatory activity in neonates' hippocampus and neocortex has mainly been attributed to GABAergic transmission from interneurons, with additionally modulatory roles for glutamate [6]. Glutamatergic excitation takes over at the end of the first postnatal week, and major synaptogenesis and synapse maturation start to surge in the 2nd and 3rd week after birth [7,8].

Gliogenesis is ongoing during this early stage [9,10] and newly formed astrocytes differ from their mature counterparts in several ways. The density of astrocytes strongly increases (e.g., [11]),

and gap junctional coupling between astrocytes develops during the first postnatal week [12]. Moreover, astrocytes undergo significant changes in the electrophysiological properties and alter their expression profile and repertoire of ion channels [13–17]. This process of differentiation and maturation during the first postnatal week produces a shift in GABA-induced intracellular Ca^{2+} signaling [18] and of the subcellular expression profile of Na^+-dependent GABA transporters [19]. For glutamate transport, the maturing cells initially express primarily glutamate-aspartate-transporter (GLAST) with glutamate transporter 1 (GLT-1) being barely detectable in neonates. GLT-1 levels then strongly increase after the first postnatal week and represents the major glutamate transporter in juveniles and adults [11,20].

While astrocytes are electrically non-excitable cells, a typical and prominent pattern of activity found in mature cells is intracellular Ca^{2+} signaling [21,22]. Pathways in the immature brain are less well reported on, but also involve the generation of spontaneous and evoked Ca^{2+} transients [23,24]. As mentioned above, immature astrocytes already express—albeit at low levels—transporters for GABA and glutamate and both are coupled to the influx of Na^+ [25–27]. Notably, our recent work has demonstrated that disinhibition induced by removal of external Mg^{2+} and application of the $GABA_A$-receptor antagonist bicuculline results in network Na^+ oscillations in the neonate hippocampus, encompassing both neurons as well as astrocytes [28]. Evoked network Na^+ oscillations required neuronal action potential generation as well as functional glutamate transport [28], demonstrating that neuronal activity and release of glutamate in the neonate brain can result in well-detectable elevations in both neuronal and astrocyte Na^+, even at this early stage of development.

In the present work, we studied if neurons and astrocytes in the neonate brain might also undergo spontaneous oscillations in intracellular Na^+. As Na^+ provides the driving force for a multitude of cellular processes, such Na^+ oscillations might play an important role in early network formation. To test this hypothesis, we used sodium-binding benzofuran isophthalate-acetoxymethyl ester (SBFI-AM), a ratiometric Na^+ indicator to monitor somatic Na^+ changes in astrocytes and neurons in acutely isolated tissue slices of the neonatal mouse hippocampus (P2–4). We found that 20% of neurons and 44% of astrocytes exhibit spontaneous, ultraslow Na^+ fluctuations that are largely restricted to the first postnatal week and greatly reduced in animals older than P14.

2. Materials and Methods

2.1. Preparation of Tissue Slices

This study was carried out in accordance with the institutional guidelines of the Heinrich Heine University Düsseldorf, as well as the European Community Council Directive (2010/63/EU). All experiments were communicated to and approved by the animal welfare office of the animal care and use facility of the Heinrich Heine University Düsseldorf (institutional act number: O52/05). In accordance with the German animal welfare act (Articles 4 and 7), no formal additional approval for the post-mortem removal of brain tissue was necessary. In accordance with the recommendations of the European Commission [29], animals up to 10 days old were killed by decapitation, while older mice were anaesthetized with CO_2 before the animals were quickly decapitated.

Acute slices of mouse hippocampus or neocortex (*mus musculus*, Balb/C; both sexes) of 250 μm thickness were generated using the methods previously published [30]. In addition, transgenic mice were used which displayed unrestricted deletion of connexin30, as well as Cre-recombinase-dependent deletion of connexin43 [31]. Cre-recombinase negative mice were used in control experiments for this section. For animals from postnatal days 10–17 (P10–P17), the dissection and slicing procedure were performed in cooled, modified artificial cerebrospinal fluid (mACSF), which contained a reduced $CaCl_2$ concentration (0.5 mM) and an increased $MgCl_2$ concentration (6 mM) as compared to standard ACSF (see below) to dampen synaptic release of transmitters and resulting excitotoxic effects during the cutting of the tissue. In addition, the mACSF contained (in mM): 125 NaCl, 2.5 KCl, 1.25 NaH_2PO_4, 26 $NaHCO_3$, and 20 glucose. This solution had an osmolality of 308–312 mOsm/L and was bubbled with 95% O_2/5% CO_2 to achieve a pH of ~7.4. For animals younger than P10 (which are less prone to excitotoxicity), standard ASCF (composition like mACSF apart from

2 mM $CaCl_2$ and 1 mM $MgCl_2$ in the solution) was used during all steps. For animals older than P18, a modified ACSF was used with (in mM); 60 NaCl, 2.5 KCl, 0.5 $CaCl_2$, 7 $MgCl_2$, 1.25 NaH_2PO_4, 1.3 ascorbic acid, 3 $C_3H_3NaO_3$, 26 $NaHCO_3$, 10 glucose, and 105 sucrose (sucrose added for neuroprotection; recipe modified from [32]). Directly after cutting, slices were incubated at 34 °C for 20 min with 0.5–1 μM sulforhodamine 101 (SR101) in order to stain astrocytes [17]. Following this, slices were transferred to standard ACSF for a further 10 min without SR101.

After this, slices were kept in ACSF at room temperature (20–22 °C) until used in experiments. Throughout experiments, slices were continuously perfused with standard ACSF at room temperature (unless otherwise specified). For experiments performed at near-physiological temperature (34 °C), an ACSF composed of (in mM): 131 NaCl, 2.5 KCl, 0.5 $CaCl_2$, 1.3 $MgSO_47H_20$, 1.25 NaH_2PO_4, 21 $NaHCO_3$, and 10 glucose and was used. Pharmacological substances were diluted in ACSF and bath applied to slices via the perfusion system for 15 min before the beginning of, and throughout the measurements. The different substances, the concentrations employed and manufacturers of the chemicals are detailed in Table 1.

Table 1. Blockers used.

Target Group	Blocker	Target	Solvent	Conc. (μM)	Manufacturer	Catalogue Number
Glutamatergic	MPEP	mGluR5	DMSO	25	Tocris	1212
	TFB-TBOA	EAATs	DMSO	1	Tocris	2532
	APV	NMDA	$NaHCO_3$	100	Cayman Chem.	14,540
	CNQX	AMPA	DMSO	25	Cayman Chem.	14,618
GABAergic/ Glycinergic	Bicuculline	$GABA_A$	σ H2O	10	Sigma-Aldrich	14,343
	CGP-55845	$GABA_B$	σ H2O	5	Sigma-Aldrich	SML0594
	NNC-711	GAT1	DMSO	100	Tocris	1779
	SNAP-5114	GAT2/3	DMSO	100	Sigma-Aldrich	S1069
	NPA	GAT1/2/3	σ H_2O	100	Tocris	0236
	Sarcosine	GlyTs	σ H_2O	500	Sigma-Aldrich	131,776
Cholinergic	α-Bungarotoxin	α7 nAChR	σ H_2O	0.1	Sigma-Aldrich	T0195
	Atropine	mAChR	σ H_2O	5	Sigma-Aldrich	A0132
Purinergic	PPADs	P2X/Y	σ H_2O	20	Sigma-Aldrich	P178
	Caffeine	P1	σ H_2O	100	Sigma-Aldrich	C0750
Adrenergic	Prazosin	α1 receptor	σ H_2O	0.2	Sigma-Aldrich	P7791
	Propranolol	β receptor	σ H_2O	10	Sigma-Aldrich	P0084
Na^+ dependant transporters	TTX	Na_v	σ H_2O	0.5	BioTrend	BN0518
	SEA0400	NCX	DMSO	10	MCE	HY15515
	Bumetanide	NKCC1	DMSO	40	BioTrend	BG0113
pH	Amiloride	NHE	σ H_2O	50	Sigma-Aldrich	BP008
Hemichannels	La^{3+}	TRP/Hemicha.	σ H_2O	50	Merck	203,521

Abbreviations are as follows: **MPEP** (2-Methyl-6-(phenylethynyl)pyridine), **TFB-TBOA** ((3*S*)-3-[[3-[[4-(Trifluoromethyl)benzoyl]amino]phenyl]methoxy]-L-aspartic acid), **APV** ((2*R*)-amino-5-phosphonovaleric acid; (2*R*)-amino-5-phosphonopentanoate), **CNQX** (6-cyano-7-nitroquinoxaline-2,3-dione), **CPG-55845** ((2S)-3-[[(1*S*)-1-(3,4-dichlorophenyl)ethyl]amino-2-hydro xypropyl] (phenylmethyl)phosphinic acid hydrochloride), **NNC-711** (1,2,5,6-tetrahydro-1-[2-[[(diphenylmethylene) amino]oxy]ethyl]-3-pyridinecarboxylic acid hydrochloride), **SNAP-5114** (1-[2-[tris(4-methoxyphenyl)methoxy]ethyl]-(*S*)-3-piperidinecarboxylic acid), **NPA** (nipecotic acid), **PPADs** (pyridoxalphosphate-6-azophenyl-2′,4′-disulfonic acid), **TTX** (tetrodotoxin), **SEA0400** (2-[4-[(2,5-difluorophenyl)methoxy]phenoxy]-5-ethoxyaniline), **mGluR5** (metabotropic glutamate receptor 5), **EAATs** (excitatory amino acid transporters), **NMDA** (*N*-methyl-D-aspartate receptors), **AMPA** (α-amino-3-hydroxy-5-methyl-4-isoxazolepropionic acid receptor), **GAT** (gamma-aminobutyric acid transporters), **GlyT** (glycine transporters), **nACh** (nicotinic acetylcholine receptors), **mACh** (muscarinic acetylcholine receptors), **Na_v** (voltage gated sodium channels), **NCX** (sodium calcium exchanger), **NKCC1** (sodium potassium chloride co-transporter), **NHE** (sodium proton exchanger), **TRP** (transient receptor potential channels). Manufacturers were located as follows (third party distributers are indicated in bold): Merck KGaA, Darmstadt, Germany; Biotrend, Köln, Germany; MCE, **Hycultec**, Beutelsbach, Germany; Tocris, **Bio-Techne GmbH**, Wiesbaden Germany; A.G.

Scientific, **Mobitec**, Göttingen Germany; Cayman chemical, **Biomol GmbH**, Hamburg Germany; Sigma-Aldrich Chemie GmbH, Munich, Germany.

2.2. Fluorescence-Based Ion Imaging

Slices were loaded via bolus injection (using a picospritzer 3, Parker, Cologne, Germany) with either SBFI-AM (sodium-binding benzofuran isophthalate-acetoxymethyl ester; Invitrogen, Schwerte, Germany) to measure $[Na^+]_i$, BCECF-AM (2′,7′-Bis-(2-Carboxyethyl)-5-(and-6)-Carboxyfluorescein, acetoxymethyl ester; A.G. Scientific, Göttingen, Germany) to measure pH, or OGB1-AM (Oregon Green BAPTA 1-acetoxymethyl ester; Invitrogen, Schwerte, Germany) to measure $[Ca^{2+}]_i$. The first two of these were used for wide-field ratiometric imaging as has been described previously [33–35], and were excited alternatingly by 340/380 nm and 440/490 nm, respectively. OGB1-AM was excited at 488 nm. Excitation light was produced by a PolychromeV monochromator (Thermo Fisher Scientific, Eindhoven, Netherlands). Imaging was performed using an upright microscope (Nikon Eclipse FN-1, Nikon, Düsseldorf, Germany) equipped with a Fluor 40×/0.8 W water immersion objective (Nikon). Emission was collected above 420 nm for SBFI-AM, above 505 nm for OGB1-AM, and between 511 nm and 563 nm for BCECF-AM. SR101 was excited at 575 nm and its emission collected above 590.

Images were generated with an ORCA FLASH 4.0LT camera (Hamamatsu Photonics Deutschland GmbH, Herrsching, Germany) controlled by the imaging software (Nikon NIS-Elements AR v4.5, Nikon, Düsseldorf, Germany). Emission/emission ratio was subsequently analyzed for each region of interest (ROI) using OriginPro 9.0 (OriginLab Corporation, Northampton, MA, USA) software. Changes in $[Na^+]_i$ were converted to mM on the basis of an in situ calibration performed as reported previously [33,34].

2.3. Determination of Baseline $[Na^+]_i$ and Electrophysiology

Baseline $[Na^+]_i$ was determined using a procedure as described in detail earlier [36]. To this end, cells were first loaded with SBFI-AM and the fluorescence ratio measured in cell bodies as described above. Subsequently, whole-cell patch-clamp recordings were performed on SR101-positive astrocytes employing an intracellular saline composed of (in mM): 114 (or 109) $KMeSO_3$, 32 KCl, 10 HEPES, 10 (or 15) NaCl, 4 Mg-ATP, and 0.4 Na_3GTP, pH adjusted to 7.3, to which 0.5 mM of the membrane-impermeable form of SBFI was added. Pipettes (2–3 MΩ) were pulled out from borosilicate glass capillaries (Hilgenberg, Malsfeld, Germany) using a vertical puller (PP-830, Narishige, Tokyo, Japan). Cells were held in voltage-clamp mode (holding potential −90 mV) using an EPC10 amplifier and PatchMaster software (HEKA Elektronik, Lambrecht, Germany).

2.4. Data Analysis and Statistics

Unless otherwise specified, data are illustrated in box plots indicating median (middle line), mean (red square), interquartile range (box), and standard deviation (whiskers). In addition, all individual data points are shown underneath the box plots.

Unless otherwise stated, each series of experiments was performed on at least four different animals; "n" represents the number of cells analyzed, "N" the number of individual experiments/slice preparations. Data were statistically analyzed by *t*-tests. *p*-values below 0.01 were considered to indicate a significant difference. The following symbols are used to illustrate the results of statistical tests in the figures: ** $0.001 \leq p < 0.01$; *** $p < 0.001$.

3. Results

3.1. Neonatal Cells Show Spontaneous Na^+ Fluctuations

To monitor Na^+ in astrocytes and neurons during early postnatal development, acutely isolated tissue slices of the neonatal mouse hippocampus (P2–4) were stained with SBFI-AM, a ratiometric Na^+ indicator. Under control conditions, during perfusion with standard ACSF, we detected

spontaneous fluctuations of somatic Na^+ in a subset of SR101-positive astrocytes in the CA1 stratum radiatum and in CA1 pyramidal neurons (Figure 1A). Within the observation period of 60 min (standard imaging frequency 0.2 Hz), fluctuations were present in 43% of recorded astrocytes (n = 92/213 cells; Table 2) and in 22% of recorded neurons (n = 89/412 cells; Table 2, Figure 1C). The frequency of these fluctuations was very low, with the active astrocytes averaging at 1.8 ± 1.2 fluctuations/hour and the active neurons exhibiting 1.9 ± 1.3 fluctuations/hour. Notably, apparent synchronicity of fluctuations between neurons and astrocytes or within each cell group was observed only rarely and only in small subsets of responding cells (see arrowheads in Figure 1A2,B2).

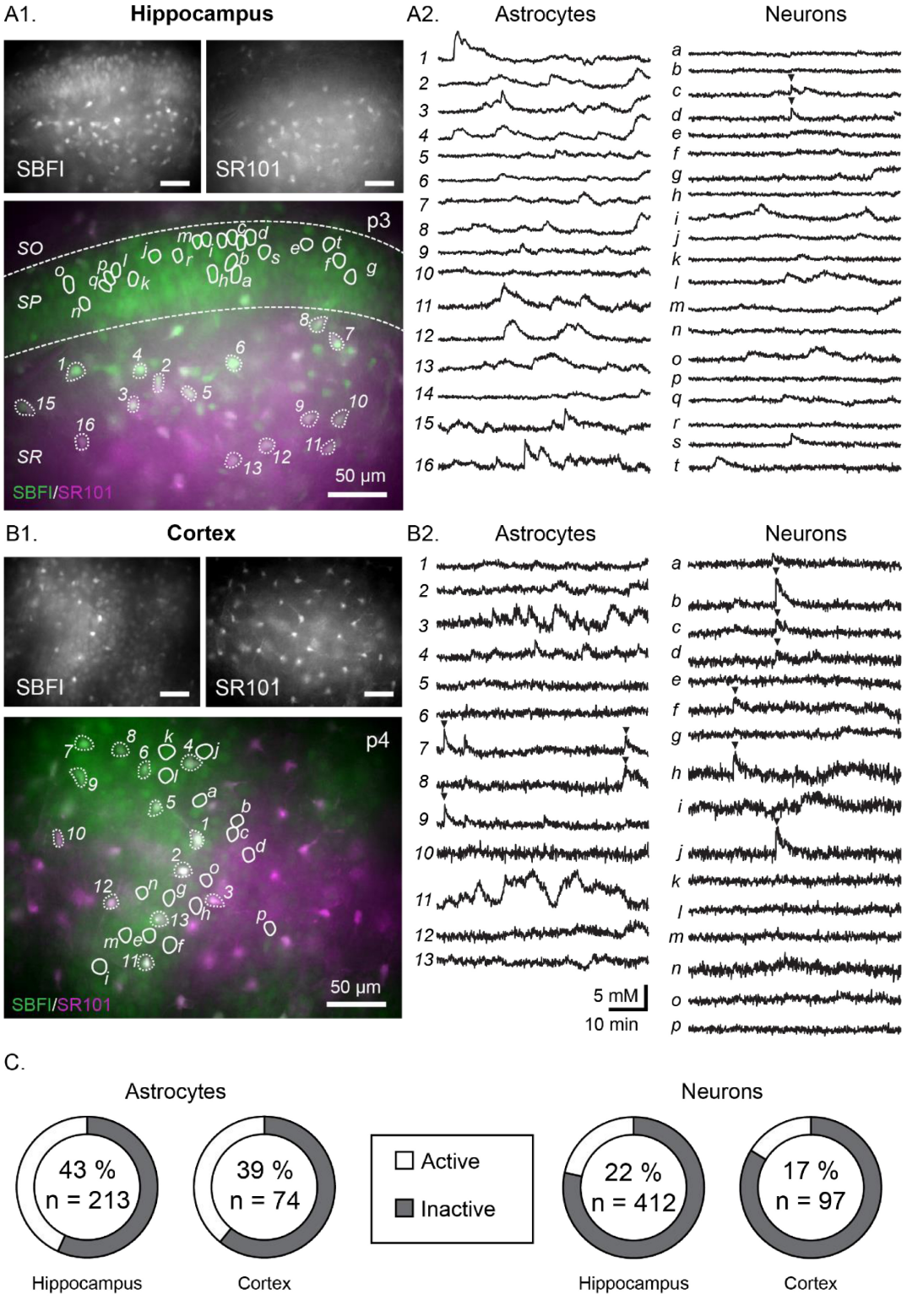

Figure 1. Example measurements showing spontaneous Na^+ fluctuations in the neonate hippocampus (**A1, A2**) and neocortex (**B1, B2**). (**A1**,**B1**) show SBFI (top left), SR101 (top right) and merge images (bottom) with all scale bars indicating 50 μm. Circled areas correspond to regions of interest (ROIs), the individual fluorescent measurement traces of which are illustrated in A2 and B2 (astrocytes on the left and numbered, neurons on the right and labelled with letters). Arrows indicate instances when cells appear to be synchronized. (**C**) Pie charts indicating the percentage of active astrocytes (left) and neurons (right) within each area (*n* = total number of cells measured). SBFI: sodium-binding benzofuran isophthalate-acetoxymethyl ester.

To test if fluctuations are restricted to the neonate hippocampus, we performed recordings in acute tissue slices of neonate neocortex (layer II/III). In the neocortex, similar Na^+ fluctuations were observed within both cell types (Figure 1B); the percentage of active cells was also comparable (39% astrocytes, *n* = 29/74; and 17% of neurons, *n* = 16/97, Figure 1C).

In order to further investigate the properties and origin of the spontaneous Na^+ transients, all following experiments and analysis were performed in the hippocampus CA1 region. The recorded fluctuations were long-lasting (Figure 2), with an average duration of 8.6 ± 3.2 min in astrocytes (*n* = 166 fluctuations; Table 2) and 9.2 ± 4.1 min in neurons (*n* = 166 fluctuations; Table 2). The mean amplitude for fluctuations was 2.1 ± 1.4 mM and 2.2 ± 1.2 mM for astrocytes and neurons respectively (Table 2). However, it must be noted there was a very high level of variation present within the properties (amplitude, and time course) of individual fluctuations for both cell types—as is illustrated in Figure 2.

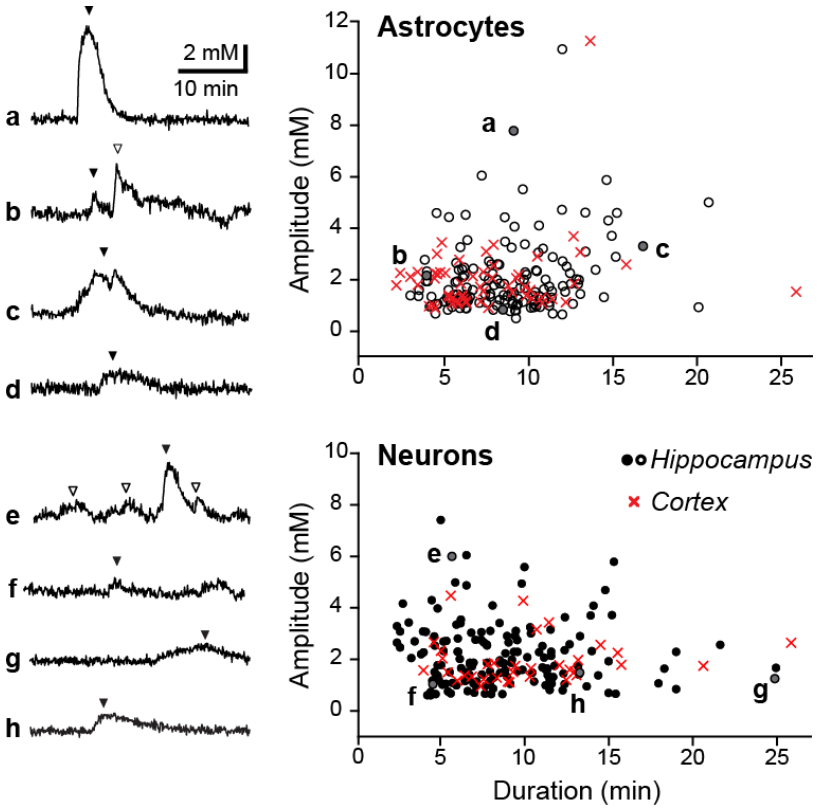

Figure 2. Properties of spontaneous Na^+ fluctuations. Left: Examples of individual Na^+ fluctuations in astrocytes (**a**–**d**) and neurons (**e**–**h**). Right: Scatter plot of all measured fluctuations in astrocytes (top) and neurons (bottom) with examples indicated by letters and shown by filled arrowheads on the left (hollow arrowheads are aditional fluctuations also analyzed).

Table 2. Number of neurons (left) and astrocytes (right) measured, the % of these showing activity, the total number of fluctuations analyzed under each condition and the mean and standard deviation for the amplitude (mM) and duration (minutes) for analyzed fluctuations.

	Neurons								Astrocytes							
	Cells (n)	% Cells (n) Active	Fluctuation (n)	mM Mean	mM SD	*p* Values	Min Mean	Min SD	Cells (n)	% Active	Fluctuation (n)	mM Mean	mM SD	*p* Values	Min Mean	Min SD
Control	**412**	**21.6**	**166**	**2.2**	**1.2**		**9.2**	**4.1**	**213**	**43**	**166**	**2.1**	**1.4**		**8.6**	**3.2**
TTX	**94**	7.4	7	**0.7**	**0.3**	**	8.2	3.7	**39**	35.9	23	**1**	**0.3**	***	8.7	4.1
BIC	**76**	19.7	32	**0.8**	**1**	***	6.6	2.3	**22**	59.1	20	2.7	1.9	0.06	8.1	2.3
CGP	**101**	12.9	20	2	0.6	0.48	10.9	3.5	**49**	44.9	42	2.1	1.2	0.78	9.6	4.6
SNAP/NNC	**53**	22.6	17	**1.1**	**0.2**	***	10.2	3.1	**86**	34.9	33	**3.2**	**2.0**	**	10.8	6.2
NPA	**70**	15.7	20	**1**	**0.3**	***	10.7	3.8	**43**	32.6	31	**1.3**	**0.6**	**	9.4	3.6
Sarcosine	**74**	20.3	20	1.5	0.5	0.02	11.3	3.7	**62**	21	25	2.6	1.7	0.06	8.5	3.5
TFB-TBOA									**36**	27.8	10	1.9	1.7	0.69	8.5	3.7
CNQX	**130**	6.2	9	2.6	1.3	0.29	9.6	4.1	**45**	37.8	25	2.1	1.1	0.86	8.9	3.1
APV	**156**	10.3	19	2.5	0.9	0.22	10.9	5.2	**52**	28.8	19	2.7	2.5	0.34	13.1	4.9
MPEP	**117**	16.2	30	1.9	0.7	0.28	9.5	3.8	**26**	46.2	53	3.9	2.2	0.36	9.1	6.2
α-BT	**118**	11.9	29	1.6	0.6	0.02	10.1	3.7	**43**	67.4	89	2	1.5	0.93	7.3	3.7
Atropine	**124**	16.1	28	2.6	1.3	0.14	8.5	2.9	**73**	49.3	74	2.5	1.2	0.02	7.7	2.9
PPADs	**70**	11.4	19	1.4	0.9	0.01	10.7	4.9	**57**	24.6	24	1.6	0.6	0.1	8	2.4
Caffeine	**142**	22.5	75	1.9	0.7	0.05	9.4	4.8	**32**	62.5	33	2	0.9	0.84	8.8	3.2
Prazosin	**111**	13.5	21	**1.3**	**0.4**	**	9.7	3.7	**81**	40.7	50	1.7	0.8	0.18	10.4	4.6
Propranolol	**123**	7.3	11	1.9	0.5	0.55	11.4	4.3	**59**	38.9	54	2.7	1.2	0.01	8.7	4.1
SEA0400	**85**	11.7	12	2	1.3	0.65	8.8	3.1	**18**	44.4	9	2.6	1	0.21	8	1.4
Bumet	**132**	6.1	8	1.8	0.5	0.44	11	3.1	**29**	37.9	15	1.6	1.3	0.28	8.5	3.5
Amiloride	**162**	11.1	31	1.8	0.6	0.11	8.7	2.7	**50**	28	20	1.7	0.5	0.34	8.8	3.5
La^{3+}	**144**	5.2	8	1.8	0.6	0.43	11.9	5.3	**84**	40.5	74	2.0	1.2	0.71	8.4	3.4
C57Bl/6 WT	**460**	11.1	66	1.5	0.8		10.8	4.9	**548**	51.1	620	2.1	1.5		8.7	4.0
Cx -/-	**77**	18.2	30	1.6	0.6	0.65	11.4	5.6	**46**	60.1	58	2.2	1.5	0.77	8.7	4.3

Abbreviations, see Table 1. Bumet: bumetanide; a-BT: a-bungarotoxin. Red color indicates statistically significant difference as compared to the control condition, *p*-values indicated apply to the amplitudes, ** $0.001 \leq p < 0.01$; *** $p < 0.001$.

3.2. *Fluctuations Are Developmentally Regulated*

To study the developmental profile of spontaneous Na^+ fluctuations, experiments were performed at different stages of postnatal development. Four age groups were compared for overall activity rates and for the individual fluctuation properties. These groups contained age ranges as follows: P2–4 (neonatal, example shown in Figure 3A1), P6–8, P10–12, and P14–32 (juvenile, example shown in Figure 3A2).

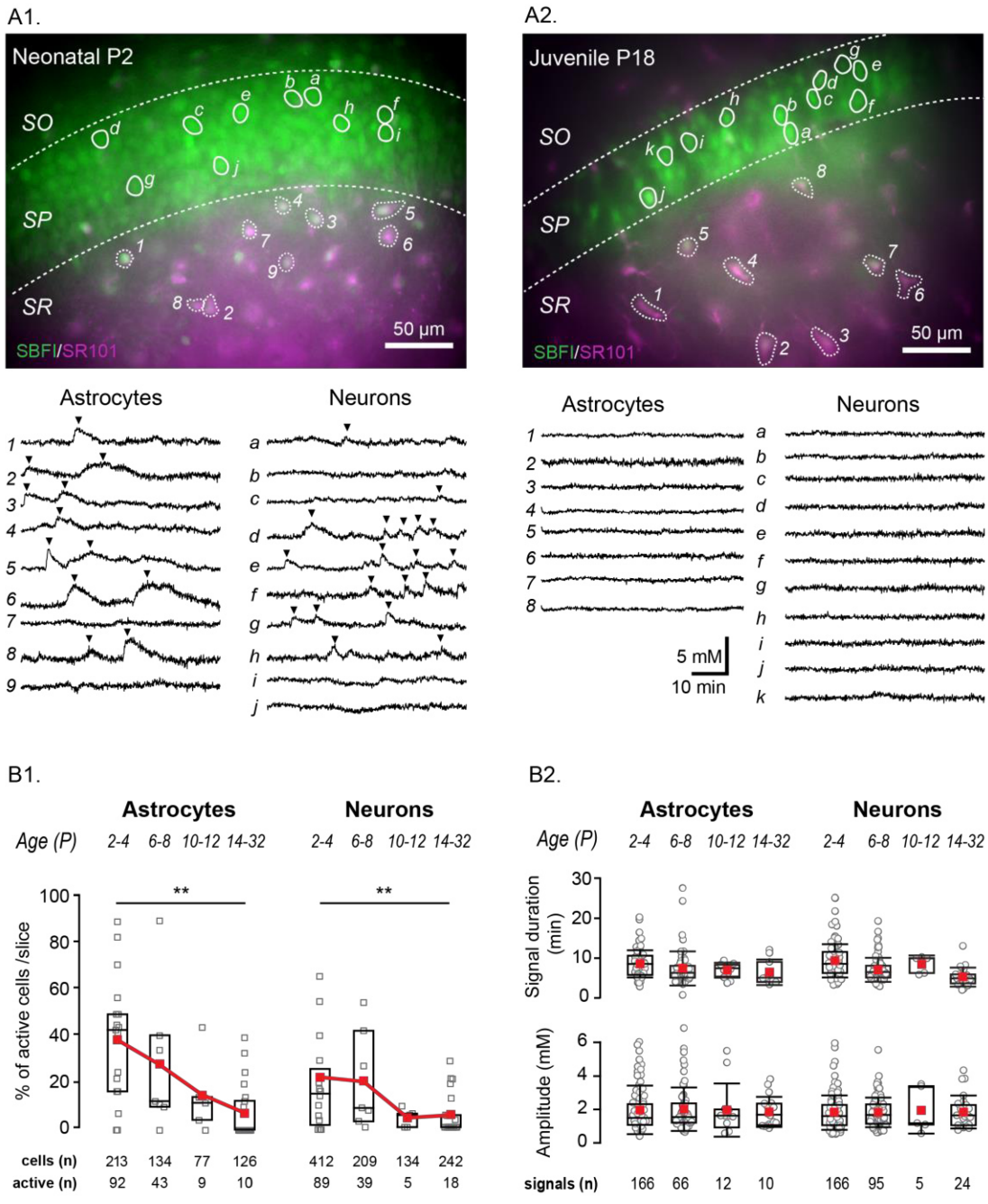

Figure 3. Age dependence of spontaneous Na^+ fluctuations. Example merged staining of a P2 (**A1**) and P18 (**A2**) hippocampal slice (SBFI in green, SR101 in magenta, overlapping regions in white) with example cells encircled and their individual fluorescent measurement traces shown below. Analyzed fluctuations are indicated by black arrows. Scale bars show 50 µm. SO, SP, SR: stratum oriens, pyramidale and radiatum, respectively. (**B1**) Box plots illustrating the decline in percentage of cells

showing activity per slice with increasing mouse age. (**B2**) Properties from fluctuations in different age groups as written above. Box-and-whisker plots indicating median (line), mean (red square), interquartile range (box) and standard deviation (whiskers). ** $0.001 \leq p < 0.01$.

Activity was reduced with ongoing postnatal development in both cell groups, dropping in astrocytes from 43% ($n = 213$) in neonatal animals to 32% in P6–8 ($n = 134$) to 11.7% in P10–12 ($n = 77$) and finally to 7.9% in juvenile animals ($n = 126$; $p = 0.001$) (Figure 3B1). While this reduction was fairly linear in astrocytes, neuronal transients remained high in the earliest two age groups, starting at 21.6% in neonates ($n = 412$) and staying at 18.7% in the P6–8 group ($n = 209$). However, after this they had a strong reduction to 3.7% ($n = 134$; $p = 0.028$) in the P10–12 group, and stayed low at 7.4% ($n = 242$; $p = 0.001$) in the juvenile group compared to neonates (Figure 3B1).

The frequency of fluctuation occurrence also trended to decrease with development, with the groups showing a mean frequency (signals/hour) of 1.8 ± 1.2, 1.7 ± 0.8, 1.4 ± 0.7, and 1.1 ± 0.3 for astrocytes and 1.9 ± 1.3, 2.6 ± 1.6, 1.0 ± 0, and 1.1 ± 0.4 for neurons (groups shown in order of ascending age). Notably, while the percentage of active cells was reduced with the progression of development, the properties of the fluctuation (duration and amplitude) themselves were not altered across the age groups for either cell type (Figure 3B2).

3.3. Fluctuations Are Not Causally Linked to Ca^{2+} Signalling

Neuronal Ca^{2+} based early network oscillations (ENOs) are strongly dampened at room temperature as compared to near physiological temperatures [37]. The opposite is true for astrocytic Ca^{2+} oscillations, which can occur at a lower frequency and have shorter durations when experimental temperatures are raised to physiological conditions [38].

We therefore investigated the effect of increasing the ACSF temperature from room temperature (20–22 °C) to 33–35 °C on spontaneous Na^+ fluctuations in neonates (P2–4). The increase in temperature had no effect on either the duration, amplitude or frequency of the fluctuations in astrocytes (cell $n = 86$, fluctuation n = 73), or neurons (cell $n = 43$, fluctuation $n = 38$, Figure 4A). While this does not rule out a shared origin for both spontaneous Ca^{2+} oscillations and Na^+ fluctuations, it does suggest that the signal types are not strictly mechanistically linked.

In order to further study a possible relation between spontaneous Na^+ fluctuations and intracellular Ca^{2+}-signaling, we performed measurements with the Ca^{2+} indicator dye OGB1-AM. Under control conditions, vivid spontaneous activity, encompassing essentially the entire populations of neurons and astrocytes was observed (100% active $n = 44/44$ astrocytes; and 98% active $n = 78/80$ neurons) (Figure 4B, left column). Slices were then perfused with a nominally Ca^{2+}-free saline that in addition contained 500 μM BAPTA-AM and 1 mM EGTA to chelate intra- and extracellular Ca^{2+}. Under these conditions, Ca^{2+}-signals were nearly completely absent (5% $n = 2/39$ astrocytes; and 3% $n = 1/35$ neurons) (Figure 4B, right column). When measuring intracellular Na^+ however, a large increase in spontaneous fluctuation amplitude ($p < 0.001$) and duration ($p < 0.001$) in astrocytes was observed (68% $n = 48/71$) (Figure 4C) in the chelated Ca^{2+} condition. Neurons under these conditions displayed repetitive, synchronous increases in $[Na^+]_i$ (cell $n = 52$) (Figure 4D).

Taken together, these result strongly suggest that spontaneous Na^+ fluctuations in astrocytes and neurons of the neonate brain are not causally linked to spontaneous Ca^{2+}-signals detected in this age group. They also hint at a correlation between neuronal activity and astrocytic fluctuations.

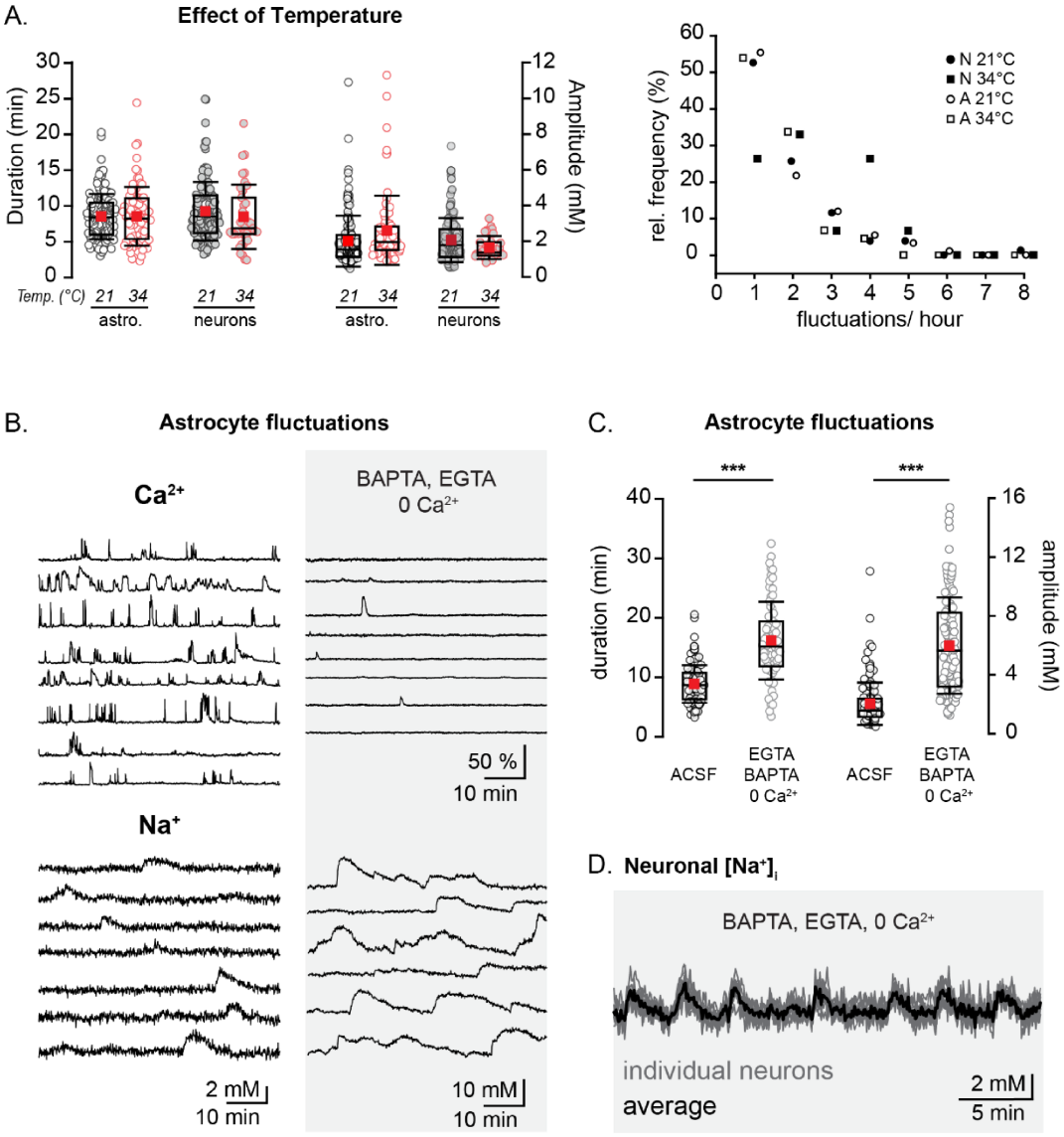

Figure 4. Temperature dependence and interrelation with spontaneous Ca^{2+}-signaling. (**A**) Left: duration and amplitude of neonatal astrocytic and neuronal Na^+ fluctuations at 21 °C (black) and 34 °C (red). Right: Relative frequency distribution plot of neonatal Na^+ fluctuations at 21 °C (neurons- black circles, astrocytes- white circles) and 34 °C (neurons- black squares, astrocytes- white squares). (**B**) Example traces from individual astrocytes in Ca^{2+} imaging experiments (top) and during Na^+ imaging (bottom), both in ACSF (left) and in the presence of a Ca^{2+} chelated solution (0 Ca^{2+}, ACSF containing 500 µM BAPTA-AM and 1 mM EGTA) (right). (**C**) Box plots illustrating the increase in astrocytic Na^+ fluctuation amplitudes after the chelation of Ca^{2+}. (**D**) Traces showing Na^+ fluctuations in several individual neurons (grey) and an averaged trace (black) in a Ca^{2+} chelated solution. *** $p < 0.001$.

3.4. Origin of Neuronal Na^+ Fluctuations

The mechanism behind the generation of the developmentally regulated Na^+ fluctuations was further studied using a broad pharmacological approach. To this end, we bath applied various blockers for ion channels, transmitter receptors, and transporters reported to be expressed by cells in this early developmental stage (summary of specific blockers used, their solvents and final concentrations can be found in Table 1). Experimental data from this pharmacological approach are illustrated in Figure 5 and detailed in Table 2.

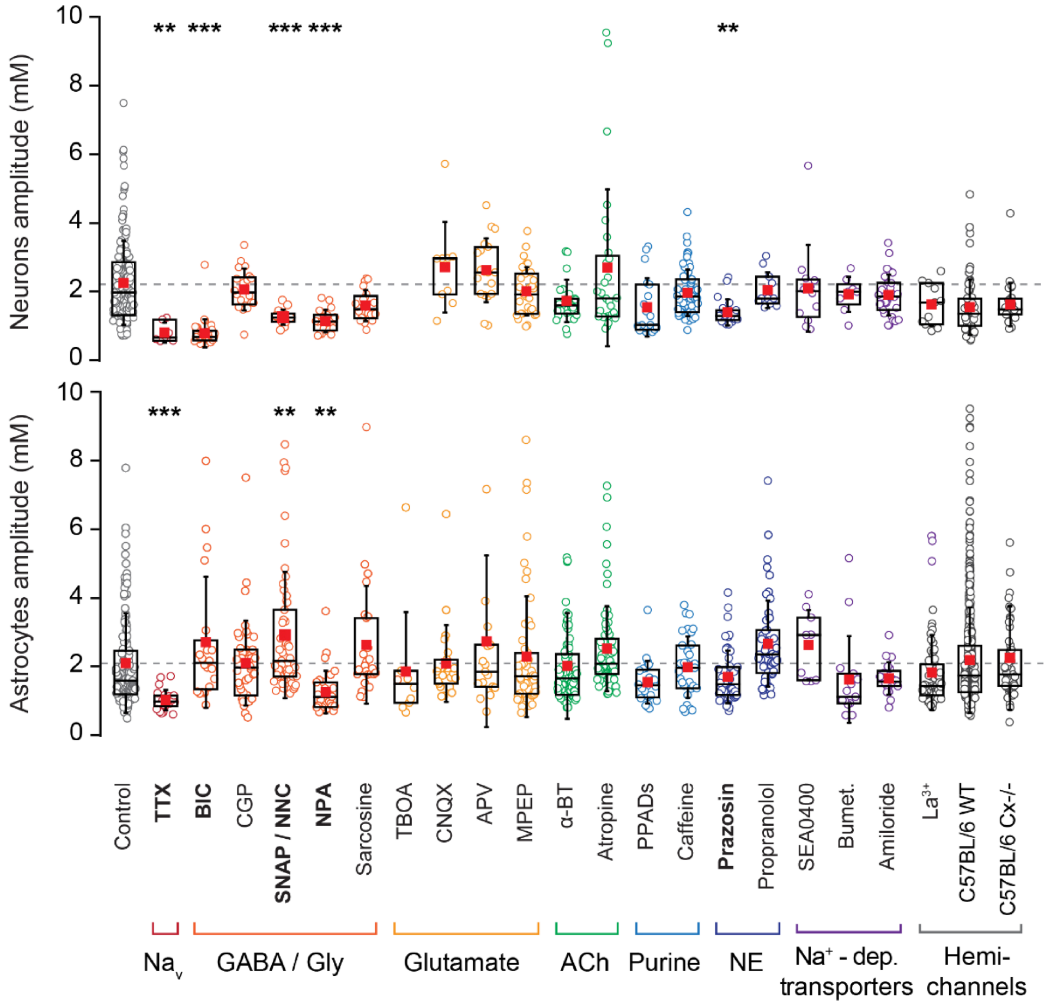

Figure 5. Pharmacological investigation. Comparison of fluctuation amplitudes in neurons and astrocytes in the presence of various pharmacological conditions as detailed in Tables 1 and 2. Blockers are arranged into color groups according to their target pathway as indicated below the plots. Abbreviations, see Table 1. Bumet: bumetanide; a-BT: a-bungarotoxin. One data point (10.95 mM) from the astrocytic control group is not shown here. ** $0.001 \leq p < 0.01$; *** $p < 0.001$.

Initially, tetrodotoxin (TTX) was introduced in order to block the activation of voltage gated Na^+ channels. Neuronal fluctuations under these conditions had strongly reduced amplitudes (0.7 ± 0.3 mM; $p = 0.002$), eluding to the fact that they are largely dependent on the generation of action potentials. We next looked at several different signaling pathways which could be activated by action potentials during this developmental phase. Neuronal Na^+ fluctuations and amplitudes were significantly reduced by an antagonist for $GABA_A$ receptors (bicuculline; 0.7 ± 0.4 mM, $p < 0.001$), while blocking $GABA_B$ receptors by CGP, had no effect. To further address the involvement of GABA in neuronal Na^+ fluctuations, we applied nipecotic acid (NPA), a competitive inhibitor of GABA transporters (GATs), which resulted in a significant reduction (1.0 ± 0.3 mM; $p < 0.001$). The same result was obtained when introducing SNAP, a blocker for the GABA-transporter GAT3 (mainly expressed by astrocytes) together with NNC, which blocks GAT1 (that is mainly expressed by neurons) [19] (1.1 ± 0.2 mM; $p = 0.003$).

In contrast to this, pharmacological inhibition of ionotropic and metabotropic glutamate receptors and of glutamate transporters (as listed in Table 2), did not significantly influence neuronal Na^+ fluctuations (Figure 5). The same was true for different other pathways tested, including cholinergic and purinergic receptors as well as various secondary-active, Na^+-dependent transporters. Interestingly, inhibition of α1-noradrenergic receptors with prazosin dampened Na^+

fluctuations in neurons (1.3 ± 0.4 mM, $p = 0.002$), while blocking ß2-receptors was without effect (Table 2, Figure 5).

These data strongly suggest that neuronal Na^+ fluctuations in neonate hippocampus are induced by suprathreshold activity, involve the action of GABA on $GABA_A$ receptors and an activation of α1-noradrenergic receptors, whereas glutamate-related pathways apparently do not play a role.

3.5. Pharmacology of Astrocytic Na^+ Fluctuations

Similar to what was observed in neurons (see above), the amplitudes of astrocyte Na^+ fluctuations were significantly reduced in the presence of TTX compared to control conditions (1.0 ± 0.3 mM; $p < 0.001$) (see Table 2 and Figure 5). In contrast to neurons, blocking of $GABA_A$ receptors had no effect on astrocytic fluctuations. However, nipecotic acid resulted in a significant reduction in the amplitudes of astrocyte Na^+ fluctuations (1.3 ± 0.6 mM; $p = 0.003$). Surprisingly, after blocking GABA transporters with SNAP and NNC, which had dampened neuronal fluctuations, we observed an increase in astrocyte amplitudes (2.9 ± 1.8 mM; $p < 0.002$).

In order to further explore the pathways for cellular generation of neonate astrocyte Na^+ fluctuations, we first determined the baseline Na^+ concentration in astrocyte somata of two different age groups, following a procedure as previously reported for neurons [36]. Experiments revealed a comparable baseline Na^+ concentration of astrocytes in neonatal animals (P2–4) (12.2 ± 2.6 mM; n = 15) and in juvenile animals (P14–16) (11.5 ± 3.0 mM; $n = 8$). The latter values are consistent with earlier reports [27]. Next, we pharmacologically inhibited a number of ion channels, transmitter receptors and transporters, which might be linked to their generation as listed in Table 2 and depicted in Figure 5.

Blocking of neither glutamate receptors nor excitatory amino acid transporters had any effect on the fluctuations in astrocytes. We then tested the possible involvement of glycinergic transporters and cholinergic receptors. However, application of antagonists for these components also had no effect on the astrocytic fluctuations observed here. Moreover, antagonists for different purinergic receptors (P2X, P2Y, and P1 receptors) were applied, but did not alter the observed Na^+ fluctuations in astrocytes. Furthermore, we analyzed the involvement of adrenergic signaling, but astrocyte fluctuations were not significantly altered neither by the α1 receptor antagonist prazosin (which dampened neuronal fluctuations), not by the non-selective ß-antagonist propranolol.

Next, a number of antagonists for Na^+ dependent transporters were implemented, including antagonists for the NCX (sodium/calcium exchanger), NKCC1 (sodium/potassium/chloride co-transporter 1) and NHE (sodium/proton exchanger). The blocking of these transporters also showed no significant effect on either fluctuation properties or prevalence (Figure 5).

Finally, we bath applied lanthanum (La^{3+}) which acts as a hemichannel antagonist, as well as blocking stretch-activated TRP channels and leak channels. However, this had no impact on Na^+ fluctuation prevalence or amplitude in astrocytes ($n = 84$, $N = 4$) nor in neurons ($n = 44$, $N = 4$) (Figure 5). Albeit weak as compared to more mature tissue, there is still a well detectable degree of gap junctional coupling between astrocytes in the first postnatal week [39]. In order to test for an involvement of gap junctions, we also used mice deficient for Cx30 and 43 (experiments performed in three slices from 2 animals). The Na^+ fluctuations in these were also found to be unaltered in astrocytes ($n = 46$) as well as in neurons ($n = 77$) of Cx-deficient mice in comparison to the respective controls (20 animals; astrocytes: $n = 548$, $N = 38$; neurons: $n = 460$, $N = 14$) (Figure 5, Table 2).

In summary, these results demonstrate that Na^+ fluctuations in neonate astrocytes are strongly dependent on the generation of action potentials and significantly affected upon increasing the concentration of GABA in the extracellular space. Moreover, our data suggest that they are apparently not primarily mediated by activation of $GABA_A$ receptors on astrocytes. Nipecotic acid, a competitive inhibitor of GABA uptake, reduced Na^+ fluctuations to a similar degree as TTX. This effect was, however, seemingly not directly related to its blocking of GABA transporters, because application of SNAP together with NNC, which target GAT1 and GAT3, had the opposite effect. None of the many other pathways tested significantly reduced astrocyte Na^+ fluctuations, so that their genesis remained unclear.

3.6. Astrocyte Fluctuations Are Not Bound to pH Regulation

Na^+ homeostasis is bound to the regulation of pH via sodium-dependent transporters such as the NHE and the NBC (sodium-bicarbonate co-transporter) [40]. In order to determine whether the spontaneous astrocytic Na^+ transients could be linked to changes in pH we measured $[Na^+]_i$ in astrocytes for 20 min, before washing in a HEPES-buffered ACSF. The removal of CO_2 and HCO_3- from the solution has been shown to reverse the NBC to transiently operate in its 'outward' mode, exporting Na^+. After a few minutes, HCO_3- is depleted from the cells, and NBC activity greatly reduced [41,42]. Evidence for this was also seen here, as switching to HEPES-buffered ACSF induced a fast, but transient drop in $[Na^+]_i$ when the solution was introduced (n = 62 astrocytes, Figure 6A).

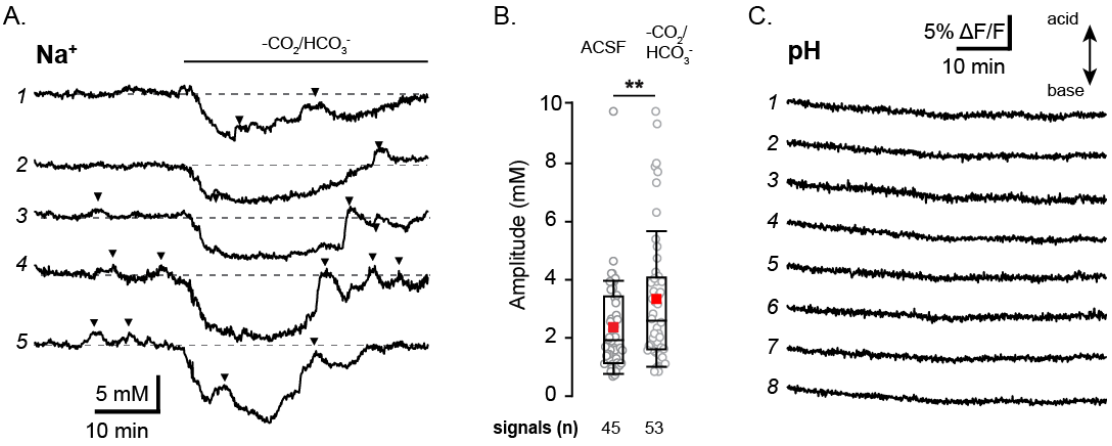

Figure 6. The influence of pH on astrocytic Na^+ fluctuations. (**A**) Shows five example astrocytes traces from a single SBFI experiment wherein HEPES buffered ACSF was washed in after 20 min of baseline measurement. Analyzed fluctuations are identified by black arrows. (**B**) Box plots comparing control condition fluctuation amplitudes to those measured in the HEPES buffered ACSF. (**C**) BCECF fluorescence traces from 8 individual astrocytes in a single experiment. ** $0.001 \leq p < 0.01$.

Spontaneous astrocyte Na^+ fluctuations were seen at similar levels both before and after the removal of CO_2 and HCO_3- (in 45% and 47% of measured astrocytes for each condition respectively). Interestingly, the fluctuations measured in HEPES-buffered ACSF were significantly longer (p = 0.002) and had a higher amplitude (p = 0.012) than those measured in standard ACSF (Figure 6B). This observation makes it unlikely that the NBC—which is likely reversed during this period—is a major driving factor in their generation.

To further address a possible involvement of pH in the spontaneous astrocyte Na^+ fluctuations, we performed measurements using the pH-sensitive indicator dye BCECF-AM. As illustrated in Figure 6C, 60 min measurements revealed no visible fluctuations in astrocyte pH (n = 97), further supporting that the spontaneous Na^+ fluctuations are not tied to pH regulation.

4. Discussion

The present study demonstrates for the first time that astrocytes and neurons in neonatal mouse hippocampus and cortex undergo slow, long-lasting fluctuations in their intracellular Na^+ concentration, which gradually decline during the first two weeks of postnatal development. Neuronal Na^+ fluctuations in neonates are dampened upon inhibition of action potentials and seemingly related to the activation of $GABA_A$ receptors. While Na^+ fluctuations in astrocytes are strongly dependent on the generation of action potentials as well, activation of $GABA_A$ did not play a role. Moreover, none of the many other pathways addressed was able to unambiguously reduce the astrocyte Na^+ fluctuations.

4.1. Neuronal Na^+ Fluctuations

As mentioned above, spontaneous Na^+ transients have never been reported before in any cell group—therefore the first but by no means least significant result is that these were indeed recorded in the neonatal mouse hippocampus and cortex. Significant reductions in neuronal fluctuation amplitudes were seen after the application of TTX and bicuculline, linking the changes in $[Na^+]_i$ to action potential firing and the activation of $GABA_A$ receptors respectively.

This suggests that GABA (likely released by interneurons) activates $GABA_A$ receptors on pyramidal cells causing their depolarization, which then drives the generation of neuronal Na^+ fluctuations, presumably via the opening of TTX-sensitive voltage gated Na^+ channels. Additionally, the blocking of GABA uptake by both NPA and SNAP/NNC dampened neuronal fluctuation amplitudes, an effect that could be explained by reduced neuronal activity caused by the build-up of extracellular GABA. Notably, spontaneous Na^+ fluctuations were primarily present during the first week after birth and were strongly diminished thereafter. The developmental regulation of the fluctuations along with their apparent mechanism, is similar to that which has been demonstrated to be responsible for GDPs and ENOs [37,43]. In these models the excitatory action of GABA is accounted for by high early expression of NKCC1 (sodium potassium chloride co-transporter) compared to KCC2 (potassium chloride co-transporter) which does not reach adult levels of expression until the third postnatal week [44]. This results in elevated intracellular Cl^- [45], reversing the Cl^--gradient and leading to an efflux upon $GABA_A$ opening—thus depolarizing the neuron [44,46,47]. In vivo experiments have recently called the principle of excitatory GABA back into question [48,49]. Notwithstanding, our experiments clearly link $GABA_A$ receptor activation and neuronal action potential generation to the slow Na^+ fluctuations observed in the neonate brain.

Although there are similarities between the previously described phenomena and Na^+ fluctuations found here, the link between them is not absolute. Along with the extended duration of each fluctuation, there appears to be very little synchronicity between neurons—a feature prominent among neurons for both ENOs and GDPs [7,50]. Additionally, it has been well established that neuronal Ca^{2+} based early network oscillations are almost completely blocked at room temperature [37], and the fluctuations here were unaffected in either propensity or property by alterations in experimental temperature. While these results do not rule out a shared origin for both spontaneous Ca^{2+} oscillations and Na^+ fluctuations, it does suggest that the signal types are not directly mechanistically linked e.g., via the Na^+/Ca^{2+} exchanger (NCX). This was again confirmed pharmacologically as the application of the NCX antagonist SEA0400 had no significant impact on fluctuation properties. Surprisingly, the pharmacological evidence shows that Na^+ fluctuation properties remained unchanged in the presence of bumetanide—a blocker for the NKCC1 which has been shown to reduce GDP frequency in neurons [51]. NMDA signaling too—made possible by the release of the Mg^{2+} block by GABA-induced depolarization [6]—has been implicated as assisting GDP propagation [5]. However, antagonists for this, along with other glutamatergic signaling components had no effect on the Na^+ fluctuations in this study.

Other signaling pathways were examined pharmacologically and were found to have no detectable influence on fluctuation properties, with the exception of the noradrenaline $\alpha 1$ receptor blocker prazosin which reduced fluctuation amplitude. While expression of $\alpha 1$ is low at early neonatal stages [52], activation has been shown to increase interneuron GABAergic output in the hippocampus [53] and may be upregulating activity even at this early stage.

These results suggest that the ultraslow Na^+ fluctuations in pyramidal cells are dependent on action potential firing, GABA release by interneurons and subsequent depolarization via $GABA_A$ receptors. Although this is a mechanism shared with GDPs, they appear not to be directly connected. GDPs generally constitute trains of neuronal bursts that last for hundreds of milliseconds and occur at a rate of around 0.1/s [7]. However, other patterns of electrical activity are also present in the developing brain. Along with shorter patterns like spindle bursts and gamma oscillations, long oscillations which last several minutes and have a frequency of around 3/h have been recorded (but their properties and origin not further investigated) [54]. The ultra-slow fluctuations seen in neuronal

$[Na^+]_i$ here may therefore represent a gradual accumulation and decline, caused by variations in the frequency of bursting within individual cells or populations, or by energy substrate availability.

4.2. Astrocytic Na^+ Fluctuations

Intriguingly, astrocytes of both the hippocampus and cortex were twice as likely to show $[Na^+]_i$ fluctuations as neurons. However, the properties of individual fluctuations did not differ significantly from their neuronal counterparts: they were unusually long (duration ~8 min) and had a very low occurrence rate (~2/h).

Unlike neuronal ENOs, synchronous, spontaneous Ca^{2+} signaling as detected in astrocyte somata first appears across several brain regions in early development and remains present (although at much lower levels) into adulthood [23,55]. While the trigger for these astrocytic Ca^{2+} signals often remained unclear, several studies have demonstrated an independence from neuronal activity and linked these signals to release of Ca^{2+} from intracellular stores [56–58]. However, a modulatory role for neurotransmitters (especially glutamate) has been reported [23,57]. In addition to somatic Ca^{2+} elevations, recent imaging studies uncovered the presence of highly localized, rapid Ca^{2+} signals in astrocyte processes that are apparently independent from IP_3-mediated Ca^{2+} release [21,59–62]. Notably, while these localized Ca^{2+}-signals in some cases do invade the soma, both the occurrence and temporal properties of somatic Ca^{2+}-signals reported earlier are still very much different from the Na^+ fluctuations observed here.

Aside from the obvious discrepancy in duration, frequency and synchronicity, several of the results here further strengthen the apparent independence of Na^+ fluctuations from astrocytic Ca^{2+} signals. While the chelation of intra and extracellular Ca^{2+} almost completely eradicated spontaneous Ca^{2+} activity, it did not reduce astrocytic Na^+ fluctuations. Indeed, Ca^{2+} chelation increased Na^+ fluctuation amplitudes, and produced repetitive, synchronous Na^+ transients in neurons, an effect which can be explained by a likely depolarization of neurons under these conditions [63,64].

The increase in astrocyte activity seen here along with the reduction of fluctuations by TTX suggests a strong link between astrocytic fluctuations and neuronal action potential firing. This is again confirmed by the increase in astrocyte fluctuation amplitude after the removal of CO_2 and HCO_3– from the ACSF, which has been shown to alkalinize neurons [42], in turn increasing excitability [40,65].

The results in the previous section show that the primary drive for neuronal Na^+ is GABAergic signaling. While this can be significantly reduced by the inhibition of $GABA_A$ receptors, doing so had no effect on astrocytic fluctuations. Inhibition of GABA uptake by NPA on the other hand resulted in a significant reduction in the amplitudes of astrocyte Na^+ fluctuations. In contrast, application of SNAP and NNC, which had dampened neuronal fluctuations, increased astrocyte fluctuation amplitudes. As both of these blockers target GABA transporters, this result may first seem counterintuitive, however, it may be related to their different modes of function. Both NPA and SNAP/NNC prevent the reuptake of GABA into cells- thereby resulting in a buildup of GABA in the extracellular space [66,67]. The opposite outcome of the two approaches, however, suggests that this buildup is probably not directly responsible for the observed actions.

Notably, substances were applied for rather long periods, that is for 15 min prior to and for 60 min during the measurements. A likely scenario is, therefore, that blocking GABA uptake resulted in a significant depletion of interneurons' GABA stores [68], thereby reducing its release in response to action potentials. NPA does this by acting as a competitive agonist, and is taken up into cells via GABA transporters [69]. As NPA has been reported to have a half-life of several hours inside cells [70], there would likely be considerable build-up of the acid inside cells. This acidification would reduce excitability [40,65], and thereby generally reduce interneuron activity (and release of any other transmitter or substance related to this). On the other hand, SNAP/NNC are not taken up directly [71] and also do not cause an intracellular acidification. While GABA builds up in the extracellular space, interneurons may still continue to fire action potentials—and may continue to release transmitters or substances besides GABA.

In addition, while astrocyte Na^+ fluctuations do seem to depend on neuronal activity, the differences in reaction to bicuculline and SNAP/NNC point to an independence from pyramidal cell firing. Interneurons have been widely reported to display co-transmission, especially in developing tissue [72,73]. Together, these findings suggest that interneurons could be co-releasing GABA (driving pyramidal activity) along with another transmitter or substance which interacts with astrocytes.

Transmitters reported to be co-released in this manner include glutamate, acetylcholine, and glycine [74,75]. Components from these signaling pathways were inhibited, but these experiments showed no significant difference compared to control experiments and these pathways were thus excluded from playing a role in the astrocytic fluctuations. The lack of input from glutamatergic signaling in particular was somewhat unexpected, as glutamate has been shown to elicit Na^+ transients in neonatal hippocampal astrocytes, mainly via EAAT based uptake [27,28]. Purinergic and adrenergic signaling pathways were also investigated, along with other Na^+ dependent membrane transporters including the NKCC1, NHE, NBC, and NCX. However, blocking of these components did not significantly impact astrocytic fluctuations and are therefore unlikely to be involved in their generation or propagation.

There are still a number of other pathways or signals which could be responsible for the changes in $[Na^+]_i$ seen here. A possible source for Na^+ influx might e.g., be mechanosensitive channels, and more specifically Piezo1, which was recently identified to be expressed in astrocytes [76,77]. Moreover, neuropeptides, growth factors, dopaminergic signaling, and nitric oxide are just some of the factors which have been shown to influence development and cellular physiology during development and might be linked to Na^+ influx. Additionally, because of the low expression levels of Kir4.1 channels in newborn animals, fluctuations in the membrane potential could contribute to the slow Na^+ fluctuations [15]. Alternatively, it is possible that what are perceived here as elevations are in fact due to the down-regulation of Na^+ extrusion, e.g., due to a transient inhibition of the NKA activity via cellular signaling pathways and/or metabolism.

Another point which remains to be clarified is which interneurons are specifically responsible for neuronal and astrocytic fluctuations and whether one group is simultaneously innervating both cell types or two separate subpopulations are interacting with one cell type each. The former system could offer an explanation for the lack of synchronicity and different levels of activation seen in astrocytes and neurons.

Of note, it cannot be entirely excluded that the slow Na^+ fluctuations are an artefact produced by preparation of brain slices, which still does not resolve the question of their origin. Testing for the presence of the fluctuations in the mouse brain in vivo, however, will be challenging as any anesthetics applied to the animal during the measurements could also have effects on signaling, as has been shown to be the case for Ca^{2+} signals (e.g., [78]). Neonatally restricted electrical activity first measured in acute tissue slices has now also been shown both in vivo (mouse) and in utero human EEG recordings [54,79]. The time frame for these patterns is very similar to the Na^+ fluctuations seen here, suggesting that they too are not merely the result of the preparation method.

5. Conclusions

Taken together our results reveal for the first time that there exists spontaneous Na^+ fluctuations in both neurons and astrocytes of the hippocampus and cortex within the early postnatal brain. They show that these fluctuations are developmentally regulated, but do not appear to be directly linked to Ca^{2+} signaling, which has previously been reported within the same age range. Both astrocytic and pyramidal cell fluctuations usually last several minutes, and are thus termed "ultraslow Na^+ fluctuations". Both appear to be driven by action potential activity in interneurons. In the model suggested by Figure 7, GABA released by this activity goes on to depolarize pyramidal cells via $GABA_A$ receptors, which in turn depolarizes the cells and opens voltage gated Na^+ channels, leading to bursts of action potentials underlying the neuronal Na^+ fluctuations. Astrocytic Na^+ fluctuations also appear to rely on interneuron firing, but their exact signaling mechanism excludes all indicated signaling pathways and remains to be determined.

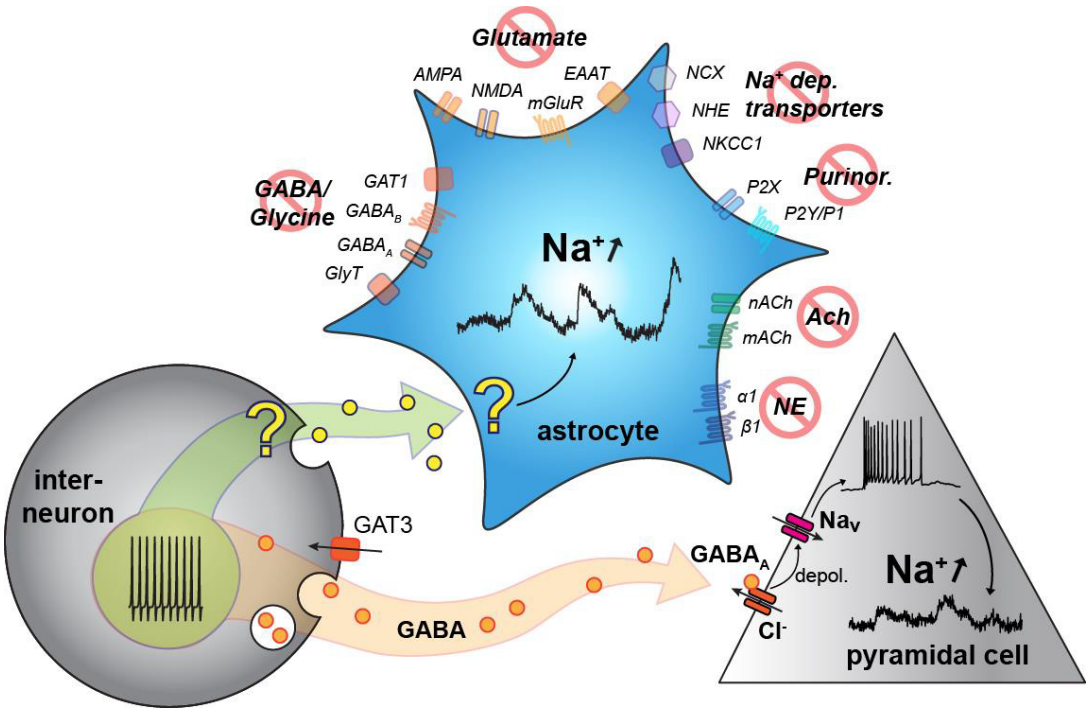

Figure 7. Summary of results. Interneuron firing (bottom left) stimulated release of GABA, which depolarises pyramidal cells (bottom right) via $GABA_A$ activation and subsequent Cl- efflux. This opens voltage gated Na^+ channels which produces neuronal Na^+ fluctuations. Interneuron activty also appears to be responsible for astrocytic fluctuations. These appear to have a separate trigger and mechanism, the source of which remains unclear at present. Abbreviations, see Table 1. NE: norepinephrine; Ach: acetylcholine; depol: depolarization; Na_V: TTX-sensitive voltage-gated Na^+ channel.

Author Contributions: Conceptualization, L.F. and C.R.R.; methodology, L.F., D.Z., and G.S.; validation, L.F., D.Z., G.S., and C.R.R.; formal analysis, L.F., D.Z., and G.S.; investigation, L.F., D.Z., and G.S.; data curation, L.F., D.Z., G.S., and C.R.R.; writing—original draft preparation, L.F. and C.R.R.; writing—review and editing, L.F., D.Z., G.S., and C.R.R.; visualization, L.F. and C.R.R; supervision, C.R.R.; project administration, C.R.R.; funding acquisition, C.R.R.

Funding: This research was funded by the Deutsche Forschungsgemeinschaft (SPP1757: Ro2327/8-2 and SE774/6-2).

Acknowledgments: We thank Claudia Roderigo and Simone Durry (Institute of Neurobiology; Heinrich Heine University Düsseldorf) for expert technical assistance.

Conflicts of Interest: The authors declare no conflict of interest.

References

1. Spitzer, N.C. Electrical activity in early neuronal development. *Nature* **2006**, *444*, 707–712, doi:10.1038/nature05300.
2. Luhmann, H.J.; Sinning, A.; Yang, J.W.; Reyes-Puerta, V.; Stuttgen, M.C.; Kirischuk, S.; Kilb, W. Spontaneous neuronal activity in developing neocortical networks: From single cells to large-scale interactions. *Front. Neural Circuits* **2016**, *10*, 40, doi:10.3389/fncir.2016.00040.
3. Griguoli, M.; Cherubini, E. Early correlated network activity in the hippocampus: Its putative role in shaping neuronal circuits. *Front. Cell. Neurosci.* **2017**, *11*, 255, doi:10.3389/fncel.2017.00255.
4. Garaschuk, O.; Linn, J.; Eilers, J.; Konnerth, A. Large-scale oscillatory calcium waves in the immature cortex. *Nat. Neurosci.* **2000**, *3*, 452–459, doi:10.1038/74823.
5. Ben-Ari, Y.; Cherubini, E.; Corradetti, R.; Gaiarsa, J.L. Giant synaptic potentials in immature rat CA3 hippocampal neurones. *J. Physiol.* **1989**, *416*, 303–325, doi:10.1113/jphysiol.1989.sp017762.
6. Ben-Ari, Y.; Khazipov, R.; Leinekugel, X.; Caillard, O.; Gaiarsa, J.L. GABAa, NMDA and AMPA receptors: A developmentally regulated 'menage a trois'. *Trends Neurosci.* **1997**, *20*, 523–529, doi:10.1016/s0166-2236(97)01147-8.

7. Ben-Ari, Y. Developing networks play a similar melody. *Trends Neurosci.* **2001**, *24*, 353–360, doi:10.1016/s0166-2236(00)01813-0.
8. Rivera, C.; Voipio, J.; Kaila, K. Two developmental switches in GABAergic signalling: The K^+-Cl- cotransporter KCC2 and carbonic anhydrase cavii. *J. Physiol.* **2005**, *562*, 27–36, doi:10.1113/jphysiol.2004.077495.
9. Kriegstein, A.; Alvarez-Buylla, A. The glial nature of embryonic and adult neural stem cells. *Annu. Rev. Neurosci.* **2009**, *32*, 149–184, doi:10.1146/annurev.neuro.051508.135600.
10. Wang, D.D.; Bordey, A. The astrocyte odyssey. *Prog. Neurobiol.* **2008**, *86*, 342–367, doi:10.1016/j.pneurobio.2008.09.015.
11. Schreiner, A.E.; Durry, S.; Aida, T.; Stock, M.C.; Rüther, U.; Tanaka, K.; Rose, C.R.; Kafitz, K.W. Laminar and subcellular heterogeneity of GLAST and GLT-1 immunoreactivity in the developing postnatal mouse hippocampus. *J. Comp. Neurol.* **2014**, *522*, 204–224, doi:10.1002/cne.23450.
12. Giaume, C.; Koulakoff, A.; Roux, L.; Holcman, D.; Rouach, N. Astroglial networks: A step further in neuroglial and gliovascular interactions. *Nat. Rev. Neurosci.* **2010**, *11*, 87–99, doi:10.1038/nrn2757.
13. Kressin, K.; Kuprijanova, E.; Jabs, R.; Seifert, G.; Steinhauser, C. Developmental regulation of Na^+ and K^+ conductances in glial cells of mouse hippocampal brain slices. *Glia* **1995**, *15*, 173–187, doi:10.1002/glia.440150210.
14. Bordey, A.; Sontheimer, H. Postnatal development of ionic currents in rat hippocampal astrocytes in situ. *J. Neurophysiol.* **1997**, *78*, 461–477, doi:10.1152/jn.1997.78.1.461.
15. Seifert, G.; Huttmann, K.; Binder, D.K.; Hartmann, C.; Wyczynski, A.; Neusch, C.; Steinhauser, C. Analysis of astroglial K^+ channel expression in the developing hippocampus reveals a predominant role of the Kir4.1 subunit. *J. Neurosci.* **2009**, *29*, 7474–7488, doi:10.1523/JNEUROSCI.3790-08.2009.
16. Zhou, M.; Schools, G.P.; Kimelberg, H.K. Development of GLAST(+) astrocytes and NG2(+) glia in rat hippocampus CA1: Mature astrocytes are electrophysiologically passive. *J. Neurophysiol.* **2006**, *95*, 134–143, doi:10.1152/jn.00570.2005.
17. Kafitz, K.W.; Meier, S.D.; Stephan, J.; Rose, C.R. Developmental profile and properties of sulforhodamine 101-labeled glial cells in acute brain slices of rat hippocampus. *J. Neurosci. Methods* **2008**, *169*, 84–92, doi:10.1016/j.jneumeth.2007.11.022.
18. Meier, S.D.; Kafitz, K.W.; Rose, C.R. Developmental profile and mechanisms of GABA-induced calcium signaling in hippocampal astrocytes. *Glia* **2008**, *56*, 1127–1137, doi:10.1002/glia.20684.
19. Scimemi, A. Structure, function, and plasticity of GABA transporters. *Front. Cell. Neurosci.* **2014**, *8*, 161, doi:10.3389/fncel.2014.00161.
20. Danbolt, N.C. Glutamate uptake. *Prog. Neurobiol.* **2001**, *65*, 1–105, doi:10.1016/s0301-0082(00)00067-8.
21. Volterra, A.; Liaudet, N.; Savtchouk, I. Astrocyte Ca(2+) signalling: An unexpected complexity. *Nat. Rev. Neurosci.* **2014**, *15*, 327–335, doi:10.1038/nrn3725.
22. Rusakov, D.A. Disentangling calcium-driven astrocyte physiology. *Nat. Rev. Neurosci.* **2015**, *16*, 226–233, doi:10.1038/nrn3878.
23. Aguado, F.; Espinosa-Parilla, J.; Carmona, M.; Soriano, E. Neuronal activity regulates correlated network properties of spontaneous calcium transients in astrocytes in situ. *J. Neurosci.* **2002**, *22*, 9430–9444, doi:10.1523/JNEUROSCI.22-21-09430.2002.
24. Lacar, B.; Young, S.Z.; Platel, J.C.; Bordey, A. Gap junction-mediated calcium waves define communication networks among murine postnatal neural progenitor cells. *Eur. J. Neurosci.* **2011**, *34*, 1895–1905, doi:10.1111/j.1460-9568.2011.07901.x.
25. Schousboe, A.; Sarup, A.; Bak, L.K.; Waagepetersen, H.S.; Larsson, O.M. Role of astrocytic transport processes in glutamatergic and GABAergic neurotransmission. *Neurochem. Int.* **2004**, *45*, 521–527, doi:10.1016/j.neuint.2003.11.001.
26. Chatton, J.Y.; Pellerin, L.; Magistretti, P.J. GABA uptake into astrocytes is not associated with significant metabolic cost: Implications for brain imaging of inhibitory transmission. *Proc. Natl. Acad. Sci. USA* **2003**, *100*, 12456–12461, doi:10.1073/pnas.2132096100.
27. Ziemens, D.; Oschmann, F.; Gerkau, N.J.; Rose, C.R. Heterogeneity of activity-induced sodium transients between astrocytes of the mouse hippocampus and neocortex: Mechanisms and consequences. *J. Neurosci.* **2019**, *39*, 2620–2634, doi:10.1523/JNEUROSCI.2029-18.2019.

28. Karus, C.; Gerkau, N.J.; Rose, C.R. Differential contribution of GLAST and GLT-1 to network sodium signaling in the early postnatal hippocampus *Opera Medica et Physiologica* **2017**, *3*, 71–83, doi:10.20388/omp2017.003.0048.
29. Close, B.; Banister, K.; Baumans, V.; Bernoth, E.M.; Bromage, N.; Bunyan, J.; Erhardt, W.; Flecknell, P.; Gregory, N.; Hackbarth, H.; et al. Recommendations for euthanasia of experimental animals: Part 2. Dgxt of the european commission. *Lab. Anim.* **1997**, *31*, 1–32, doi:10.1258/002367797780600297.
30. Gerkau, N.J.; Lerchundi, R.; Nelson, J.S.E.; Lantermann, M.; Meyer, J.; Hirrlinger, J.; Rose, C.R. Relation between activity-induced intracellular sodium transients and ATP dynamics in mouse hippocampal neurons. *J. Physiol.* **2019**, *597*, 5687–5705, doi:10.1113/jp278658.
31. Wallraff, A.; Kohling, R.; Heinemann, U.; Theis, M.; Willecke, K.; Steinhauser, C. The impact of astrocytic gap junctional coupling on potassium buffering in the hippocampus. *J. Neurosci.* **2006**, *26*, 5438–5447, doi:10.1523/JNEUROSCI.0037-06.2006.
32. Henneberger, C.; Rusakov, D.A. Monitoring local synaptic activity with astrocytic patch pipettes. *Nat. Protoc.* **2012**, *7*, 2171–2179, doi:10.1038/nprot.2012.140.
33. Langer, J.; Rose, C.R. Synaptically induced sodium signals in hippocampal astrocytes in situ. *J. Physiol.* **2009**, *587*, 5859–5877, doi:10.1113/jphysiol.2009.182279.
34. Langer, J.; Gerkau, N.J.; Derouiche, A.; Kleinhans, C.; Moshrefi-Ravasdjani, B.; Fredrich, M.; Kafitz, K.W.; Seifert, G.; Steinhauser, C.; Rose, C.R. Rapid sodium signaling couples glutamate uptake to breakdown of atp in perivascular astrocyte endfeet. *Glia* **2017**, *65*, 293–308, doi:10.1002/glia.23092.
35. Gerkau, N.J.; Rakers, C.; Durry, S.; Petzold, G.; Rose, C.R. Reverse NCX attenuates cellular sodium loading in metabolically compromised cortex. *Cereb. Cortex* **2018**, *28*, 4264–4280, doi:10.1093/cercor/bhx280.
36. Mondragao, M.A.; Schmidt, H.; Kleinhans, C.; Langer, J.; Kafitz, K.W.; Rose, C.R. Extrusion versus diffusion: Mechanisms for recovery from sodium loads in mouse CA1 pyramidal neurons. *J. Physiol.* **2016**, *594*, 5507–5527, doi:10.1113/JP272431.
37. Garaschuk, O.; Hanse, E.; Konnerth, A. Developmental profile and synaptic origin of early network oscillations in the CA1 region of rat neonatal hippocampus. *J. Physiol.* **1998**, *507 Pt 1*, 219–236, doi:10.1111/j.1469-7793.1998.219bu.x.
38. Schipke, C.G.; Heidemann, A.; Skupin, A.; Peters, O.; Falcke, M.; Kettenmann, H. Temperature and nitric oxide control spontaneous calcium transients in astrocytes. *Cell Calcium* **2008**, *43*, 285–295, doi:10.1016/j.ceca.2007.06.002.
39. Schools, G.P.; Zhou, M.; Kimelberg, H.K. Development of gap junctions in hippocampal astrocytes: Evidence that whole cell electrophysiological phenotype is an intrinsic property of the individual cell. *J. Neurophysiol.* **2006**, *96*, 1383–1392, doi:10.1152/jn.00449.2006.
40. Rose, C.R.; Ransom, B.R. *pH Regulation in Mammalian Glia*; Wiley-Liss, Inc.: New York, NY, USA, 1998; pp. 253–275.
41. Rose, C.R.; Ransom, B.R. Intracellular sodium homeostasis in rat hippocampal astrocytes. *J. Physiol.* **1996**, *491*, 291–305, doi:10.1113/jphysiol.1996.sp021216.
42. Theparambil, S.M.; Naoshin, Z.; Thyssen, A.; Deitmer, J.W. Reversed electrogenic sodium bicarbonate cotransporter 1 is the major acid loader during recovery from cytosolic alkalosis in mouse cortical astrocytes. *J. Physiol.* **2015**, *593*, 3533–3547, doi:10.1113/JP270086.
43. Leinekugel, X.; Khalilov, I.; McLean, H.; Caillard, O.; Gaiarsa, J.L.; Ben-Ari, Y.; Khazipov, R. GABA is the principal fast-acting excitatory transmitter in the neonatal brain. *Adv. Neurol.* **1999**, *79*, 189–201, doi:10.1016/j.neuroscience.2014.08.001.
44. Rivera, C.; Voipio, J.; Payne, J.A.; Ruusuvuori, E.; Lahtinen, H.; Lamsa, K.; Pirvola, U.; Saarma, M.; Kaila, K. The K^+/Cl- co-transporter KCC2 renders GABA hyperpolarizing during neuronal maturation. *Nature* **1999**, *397*, 251–255, doi:10.1038/16697.
45. Achilles, K.; Okabe, A.; Ikeda, M.; Shimizu-Okabe, C.; Yamada, J.; Fukuda, A.; Luhmann, H.J.; Kilb, W. Kinetic properties of Cl uptake mediated by Na^+-dependent K^+-2Cl cotransport in immature rat neocortical neurons. *J. Neurosci.* **2007**, *27*, 8616–8627, doi:10.1523/JNEUROSCI.5041-06.2007.
46. Brumback, A.C.; Staley, K.J. Thermodynamic regulation of NKCC1-mediated Cl-cotransport underlies plasticity of GABA(a) signaling in neonatal neurons. *J. Neurosci.* **2008**, *28*, 1301–1312, doi:10.1523/JNEUROSCI.3378-07.2008.

47. Sipila, S.T.; Huttu, K.; Yamada, J.; Afzalov, R.; Voipio, J.; Blaesse, P.; Kaila, K. Compensatory enhancement of intrinsic spiking upon NKCC1 disruption in neonatal hippocampus. *J. Neurosci.* **2009**, *29*, 6982–6988, doi:10.1523/JNEUROSCI.0443-09.2009.
48. Kirmse, K.; Kummer, M.; Kovalchuk, Y.; Witte, O.W.; Garaschuk, O.; Holthoff, K. GABA depolarizes immature neurons and inhibits network activity in the neonatal neocortex in vivo. *Nat. Commun.* **2015**, *6*, 7750, doi:10.1038/ncomms8750.
49. Zilberter, M. Reality of inhibitory GABA in neonatal brain: Time to rewrite the textbooks? *J. Neurosci.* **2016**, *36*, 10242–10244, doi:10.1523/JNEUROSCI.2270-16.2016.
50. Adelsberger, H.; Garaschuk, O.; Konnerth, A. Cortical calcium waves in resting newborn mice. *Nat. Neurosci.* **2005**, *8*, 988–990, doi:10.1038/nn1502.
51. Vargas, E.; Petrou, S.; Reid, C.A. Genetic and pharmacological modulation of giant depolarizing potentials in the neonatal hippocampus associates with increased seizure susceptibility. *J. Physiol.* **2013**, *591*, 57–65, doi:10.1113/jphysiol.2012.234674.
52. Hartley, E.J.; Seeman, P. Development of receptors for dopamine and noradrenaline in rat brain. *Eur. J. Pharmacol.* **1983**, *91*, 391–397, doi:10.1016/0014-2999(83)90163-2.
53. Hillman, K.L.; Lei, S.; Doze, V.A.; Porter, J.E. Alpha-1a adrenergic receptor activation increases inhibitory tone in CA1 hippocampus. *Epilepsy Res.* **2009**, *84*, 97–109, doi:10.1016/j.eplepsyres.2008.12.007.
54. Yang, J.W.; Hanganu-Opatz, I.L.; Sun, J.J.; Luhmann, H.J. Three patterns of oscillatory activity differentially synchronize developing neocortical networks in vivo. *J. Neurosci.* **2009**, *29*, 9011–9025, doi:10.1523/JNEUROSCI.5646-08.2009.
55. Parri, H.R.; Gould, T.M.; Crunelli, V. Spontaneous astrocytic Ca^{2+} oscillations in situ drive nmdar-mediated neuronal excitation. *Nat. Neurosci.* **2001**, *4*, 803–812, doi:10.1038/90507.
56. Nett, W.J.; Oloff, S.H.; McCarthy, K.D. Hippocampal astrocytes in situ exhibit calcium oscillations that occur independent of neuronal activity. *J. Neurophysiol.* **2002**, *87*, 528–537, doi:10.1152/jn.00268.2001.
57. Zur Nieden, R.; Deitmer, J.W. The role of metabotropic glutamate receptors for the generation of calcium oscillations in rat hippocampal astrocytes in situ. *Cereb. Cortex* **2006**, *16*, 676–687, doi:10.1093/cercor/bhj013.
58. Wang, T.F.; Zhou, C.; Tang, A.H.; Wang, S.Q.; Chai, Z. Cellular mechanism for spontaneous calcium oscillations in astrocytes. *Acta Pharmacol. Sin.* **2006**, *27*, 861–868, doi:10.1111/j.1745-7254.2006.00397.x.
59. Bindocci, E.; Savtchouk, I.; Liaudet, N.; Becker, D.; Carriero, G.; Volterra, A. Three-dimensional Ca^{2+} imaging advances understanding of astrocyte biology. *Science* **2017**, *356*, eaai8185, doi:10.1126/science.aai8185.
60. Shigetomi, E.; Bushong, E.A.; Haustein, M.D.; Tong, X.; Jackson-Weaver, O.; Kracun, S.; Xu, J.; Sofroniew, M.V.; Ellisman, M.H.; Khakh, B.S. Imaging calcium microdomains within entire astrocyte territories and endfeet with gcamps expressed using adeno-associated viruses. *J. Gen. Physiol.* **2013**, *141*, 633–647, doi:10.1085/jgp.201210949.
61. Srinivasan, R.; Huang, B.S.; Venugopal, S.; Johnston, A.D.; Chai, H.; Zeng, H.; Golshani, P.; Khakh, B.S. Ca(2+) signaling in astrocytes from IP3r2(-/-) mice in brain slices and during startle responses in vivo. *Nat. Neurosci.* **2015**, *18*, 708–717, doi:10.1038/nn.4001.
62. Khakh, B.S.; McCarthy, K.D. Astrocyte calcium signaling: From observations to functions and the challenges therein. *Cold Spring Harb. Perspect. Biol.* **2015**, *7*, a020404, doi:10.1101/cshperspect.a020404.
63. Frankenhaeuser, B.; Hodgkin, A.L. The action of calcium on the electrical properties of squid axons. *J. Physiol.* **1957**, *137*, 218–244, doi:10.1113/jphysiol.1957.sp005808.
64. Armstrong, C.M. Distinguishing surface effects of calcium ion from pore-occupancy effects in Na^{+} channels. *Proc. Natl. Acad. Sci. USA* **1999**, *96*, 4158–4163, doi:10.1073/pnas.96.7.4158.
65. Chesler, M. Regulation and modulation of pH in the brain. *Physiol. Rev.* **2003**, *83*, 1183–1221, doi:10.1152/physrev.00010.2003.
66. Lerma, J.; Herreras, O.; Herranz, A.S.; Munoz, D.; del Rio, R.M. In vivo effects of nipecotic acid on levels of extracellular gaba and taurine, and hippocampal excitability. *Neuropharmacology* **1984**, *23*, 595–598, doi:10.1016/0028-3908(84)90036-4.
67. Kersante, F.; Rowley, S.C.; Pavlov, I.; Gutierrez-Mecinas, M.; Semyanov, A.; Reul, J.M.; Walker, M.C.; Linthorst, A.C. A functional role for both-aminobutyric acid (GABA) transporter-1 and GABA transporter-3 in the modulation of extracellular GABA and GABAergic tonic conductances in the rat hippocampus. *J. Physiol.* **2013**, *591*, 2429–2441, doi:10.1113/jphysiol.2012.246298.

68. Wang, L.; Tu, P.; Bonet, L.; Aubrey, K.R.; Supplisson, S. Cytosolic transmitter concentration regulates vesicle cycling at hippocampal GABAergic terminals. *Neuron* **2013**, *80*, 143–158, doi:10.1016/j.neuron.2013.07.021.
69. Takahashi, K.; Miyoshi, S.; Kaneko, A.; Copenhagen, D.R. Actions of nipecotic acid and skf89976a on GABA transporter in cone-driven horizontal cells dissociated from the catfish retina. *Jpn. J. Physiol.* **1995**, *45*, 457–473, doi:10.2170/jjphysiol.45.457.
70. Madtes, P., Jr.; Redburn, D. Metabolism of [3 h] nipecotic acid in the rabbit retina. *J. Neurochem.* **1985**, *44*, 1520–1523, doi:10.1111/j.1471-4159.1985.tb08790.x.
71. Borden, L.A. GABA transporter heterogeneity: Pharmacology and cellular localization. *Neurochem. Int.* **1996**, *29*, 335–356, doi:10.1016/0197-0186(95)00158-1.
72. Tritsch, N.X.; Granger, A.J.; Sabatini, B.L. Mechanisms and functions of GABA co-release. *Nat. Rev. Neurosci.* **2016**, *17*, 139–145, doi:10.1038/nrn.2015.21.
73. Nusbaum, M.P.; Blitz, D.M.; Swensen, A.M.; Wood, D.; Marder, E. The roles of co-transmission in neural network modulation. *Trends Neurosci.* **2001**, *24*, 146–154, doi:10.1016/s0166-2236(00)01723-9.
74. Jonas, P.; Bischofberger, J.; Sandkuhler, J. Corelease of two fast neurotransmitters at a central synapse. *Science* **1998**, *281*, 419–424, doi:10.1126/science.281.5375.419.
75. Cattaneo, S.; Ripamonti, M.; Bedogni, F.; Sessa, A.; Taverna, S. Somatostatin-expressing interneurons co-release GABA and glutamate onto different postsynaptic targets in the striatum. *BioRxiv* **2019**, 566984, doi:10.1101/566984. T.
76. Choi, H.J.; Sun, D.; Jakobs, T.C. Astrocytes in the optic nerve head express putative mechanosensitive channels. *Mol. Vis.* **2015**, *21*, 749–766.
77. Velasco-Estevez, M.; Mampay, M.; Boutin, H.; Chaney, A.; Warn, P.; Sharp, A.; Burgess, E.; Moeendarbary, E.; Dev, K.K.; Sheridan, G.K. Infection augments expression of mechanosensing piezo1 channels in amyloid plaque-reactive astrocytes. *Front. Aging Neurosci.* **2018**, *10*, 332, doi:10.3389/fnagi.2018.00332.
78. Thrane, A.S.; Thrane, V.R.; Zeppenfeld, D.; Lou, N.; Xu, Q.; Nagelhus, E.A.; Nedergaard, M. General anesthesia selectively disrupts astrocyte calcium signaling in the awake mouse cortex. *Proc. Natl. Acad. Sci. USA* **2012**, *109*, 18974–18979, doi:10.1073/pnas.1209448109.
79. Khazipov, R.; Luhmann, H.J. Early patterns of electrical activity in the developing cerebral cortex of humans and rodents. *Trends Neurosci.* **2006**, *29*, 414–418, doi:10.1016/j.tins.2006.05.007.

Astrocytes of the early postnatal brain.

Felix, L*., Stephan, J., and Rose, C. R.*

Eur J Neurosci DOI: 10.1111/ejn.14780. (2020)

Impact factor 2020: 2.77

I contributed to

- Drafting and revision of manuscript and figures

frontiers in Physiology

REVIEW
published: 12 August 2020
doi: 10.3389/fphys.2020.00871

Sodium Fluctuations in Astroglia and Their Potential Impact on Astrocyte Function

Lisa Felix[1†], Andrea Delekate[2†], Gabor C. Petzold[2,3] and Christine R. Rose[1*]*

[1]Institute of Neurobiology, Heinrich Heine University Duesseldorf, Duesseldorf, Germany, [2]German Center for Neurodegenerative Diseases (DZNE), Bonn, Germany, [3]Division of Vascular Neurology, Department of Neurology, University Hospital Bonn, Bonn, Germany

Astrocytes are the main cell type responsible for the regulation of brain homeostasis, including the maintenance of ion gradients and neurotransmitter clearance. These processes are tightly coupled to changes in the intracellular sodium (Na^+) concentration. While activation of the sodium-potassium-ATPase (NKA) in response to an elevation of extracellular K^+ may decrease intracellular Na^+, the cotransport of transmitters, such as glutamate, together with Na^+ results in an increase in astrocytic Na^+. This increase in intracellular Na^+ can modulate, for instance, metabolic downstream pathways. Thereby, astrocytes are capable to react on a fast time scale to surrounding neuronal activity *via* intracellular Na^+ fluctuations and adjust energy production to the demand of their environment. Beside the well-documented conventional roles of Na^+ signaling mainly mediated through changes in its electrochemical gradient, several recent studies have identified more atypical roles for Na^+, including protein interactions leading to changes in their biochemical activity or Na^+-dependent regulation of gene expression. In this review, we will address both the conventional as well as the atypical functions of astrocytic Na^+ signaling, presenting the role of transporters and channels involved and their implications for physiological processes in the central nervous system (CNS). We will also discuss how these important functions are affected under pathological conditions, including stroke and migraine. We postulate that Na^+ is an essential player not only in the maintenance of homeostatic processes but also as a messenger for the fast communication between neurons and astrocytes, adjusting the functional properties of various cellular interaction partners to the needs of the surrounding network.

Keywords: astrocyte, brain, sodium/potassium-ATPase, sodium imaging, sodium signaling, glutamate, gamma-aminobutyric acid, ischemia

OPEN ACCESS

Edited by:
Alexander A. Mongin, Albany Medical College, United States

Reviewed by:
Miroslava Anderova, Institute of Experimental Medicine (ASCR), Czechia
Min Zhou, The Ohio State University, United States

***Correspondence:**
Gabor C. Petzold
gabor.petzold@dzne.de
Christine R. Rose
rose@uni-duesseldorf.de

[†]These authors share first authorship

Specialty section:
This article was submitted to Membrane Physiology and Membrane Biophysics, a section of the journal Frontiers in Physiology

Received: *25 May 2020*
Accepted: *29 June 2020*
Published: *12 August 2020*

Citation:
Felix L, Delekate A, Petzold GC and Rose CR (2020) Sodium Fluctuations in Astroglia and Their Potential Impact on Astrocyte Function. Front. Physiol. 11:871. doi: 10.3389/fphys.2020.00871

INTRODUCTION

The maintenance of ion gradients between the cytoplasm and the extracellular space (ECS) is one of the most important functions in living cells ensuring cell survival and the execution of physiological processes. Disruptions of this homeostasis can lead to cell damage or death. Beside its importance for homeostatic processes, the transport of ions across the plasma membrane

may change the membrane potential, thereby affecting cellular excitability. Changes in the ionic concentration can also modulate cellular responses, and ions themselves can act as a second messenger (Orlov and Hamet, 2006). Astrocytes, which essentially lack electrical excitability, use such ionic signaling as a main means for intracellular and intercellular communication (Verkhratsky and Nedergaard, 2018). So far, most of the studies on ionic signaling in astrocytes have focused on the role of Ca^{2+}, which is nowadays widely accepted to be a critical second messenger in astroglia (Petzold and Murthy, 2011; Volterra et al., 2014; Rusakov, 2015; Verkhratsky et al., 2019).

It has become clear, however, that astrocytic ionic signaling also involves monovalent cations, among them protons, which modulate a multitude of intracellular processes (Chesler, 2003). In addition, recent work has shown that a signaling role can also be assigned to sodium ions (Na^+), underlining the idea that Na^+ transients may represent a new form of astrocyte excitability (Rose and Verkhratsky, 2016a). In astrocytes, changes in the intracellular Na^+ concentration ($[Na^+]_i$) arise, e.g., in response to release of neuronal transmitters such as glutamate and gamma-aminobutyric acid (GABA; Rose and Ransom, 1996b; Chatton et al., 2000; Kirischuk et al., 2007). Astrocytic Na^+ signaling, thereby, couples neuronal activity to fast local astrocytic responses, which, among others, include an activation of astrocytic metabolism and lactate production (Rose and Verkhratsky, 2016a; Verkhratsky et al., 2019). Spatio-temporally organized fluctuations in cytosolic Na^+ concentration may, thus, represent a Na^+ signaling system that coordinates astrocyte physiology, as well as glial homeostatic support, to neuronal needs. Furthermore, emerging studies in the field identified more "atypical" roles for Na^+. These arise upon direct binding of Na^+ to different proteins, including plasma membrane receptors and ion channels, thereby influencing a variety of cellular functions.

With this review, we aim to give an overview on the conventional Na^+ signaling pathways in astrocytes, as well as newly identified atypical roles of Na^+. We will start by explaining how astrocytes regulate their Na^+ levels and then highlight the most important mechanisms involved in the generation of Na^+ signals in astrocytes. In the following two sections, different consequences of Na^+ signaling will be presented and their likely role in normal brain function will be discussed. The last part summarizes findings from studies that investigated how pathological changes in different diseases of the central nervous system (CNS) can affect Na^+ signaling pathways and vice versa.

Na^+ REGULATION IN ASTROCYTES

Efflux Pathways for Na^+

Astrocytes rely on a steeply inwardly directed Na^+ gradient to drive a multitude of membrane transport processes. The gradient is based on their low $[Na^+]_i$ reported values, for which vary between 10 and 17 mM (Kirischuk et al., 2012; Rose and Karus, 2013; Felix et al., 2020), coupled with an extracellular Na^+ concentration ($[Na^+]_o$) of 140–150 mM (Rose and Karus, 2013). The primary mechanism for its installation is the sodium-potassium-ATPase (NKA), which uses energy obtained *via* ATP breakdown in order to transport 3 Na^+ and 2 K^+ ions against their concentration gradients (out of and into the cell respectively; Jorgensen et al., 2003; Aperia, 2007; Hertz et al., 2015; **Figure 1**). The expression of the NKA is among the highest of all proteins in astrocytes, with around 90% of the isoforms being α2β2 and the final 10% being α2β1 (Stoica et al., 2017). NKA activity can be dampened by ouabain-like molecules, which exist endogenously within the brain and primarily target the α subunit (Song and Du, 2014). This effect is mimicked by the external application of ouabain, which – when applied at fully-blocking concentrations – causes a massive increase in $[Na^+]_i$ (Kimelberg et al., 1979; Rose and Ransom, 1996a; Chatton et al., 2000).

While NKA constitutes the major pathway for Na^+ efflux, it is not the only way to export Na^+. A number of transporters, for which the "forward" mode involves Na^+ influx, have reversal potentials (E_{rev}) that lie close to the highly negative resting membrane potential of astrocytes. Depending on the ion gradients and membrane potential, they may reverse and, therefore, offer alternative pathways for Na^+ removal. The membrane potential of astrocytes is mainly set by expression of different K^+ channels, among them Kir4.1 and K_2P, that allow the efflux of K^+ (Verkhratsky and Nedergaard, 2018). Notably, the values established for astrocytes' resting membrane potential differ between different conditions and preparations. While initial studies reported membrane potentials of around −70 to −80 mV (e. g., Wallraff et al., 2006; Zhou et al., 2006), other studies determined even higher values (e.g., −83 mV: Amzica et al., 2002; −85 mV: Kafitz et al., 2008; or −87 mV: Mishima and Hirase, 2010). A correct prediction of the transport direction of "readily-reversible" transporters, thus, requires not only knowledge of the ion gradients of the transported ions but also of the exact membrane potential of the astrocyte studied. Individual astrocytes in the intact tissue, however, seem to be protected from large changes in their membrane potential because the electrical coupling provided by gap junctions rapidly equalizes membrane potentials in the syncytium (Ma et al., 2016).

Among the transporters known to reverse under physiological conditions is the Na^+/Ca^{2+} exchanger (NCX; **Figure 1**), of which three subtypes t (1, 2, 3) have been reported in astrocytes (Rose et al., 2020). NCX exchanges 3 Na^+ for 1 Ca^{2+} and its E_{rev} lies between −90 and −60 mV; it can therefore operate either in forward (Na^+ in) or reverse (Na^+ out) mode (Verkhratsky et al., 2018; Rose et al., 2020). The latter is also true for the Na^+-HCO_3^- cotransporter (NBC; **Figure 1**), which serves to regulate HCO_3^- (and pH) in astrocytes (Chesler, 2003). Gray matter astrocytic NBCe1 transport 2 HCO_3^- for every Na^+, resulting in an E_{rev} of about −80 mV (Chesler, 2003). This makes the cotransporter easily reversible, offering a further mechanism to export Na^+ (Theparambil et al., 2014).

Transport reversal, involving the efflux of Na^+ under close-to-physiological conditions, was also demonstrated for several transporters for uptake of transmitters. These include gamma-aminobutyric acid transporters (GATs) and glycine transporters (GlyTs), which both transport 2 Na^+ and 1 Cl^- along with one GABA or glycine molecule, respectively (Eulenburg and Gomeza, 2010; Zhou and Danbolt, 2013; **Figure 1**). These electrogenic systems reverse at around −80 to −70 mV.

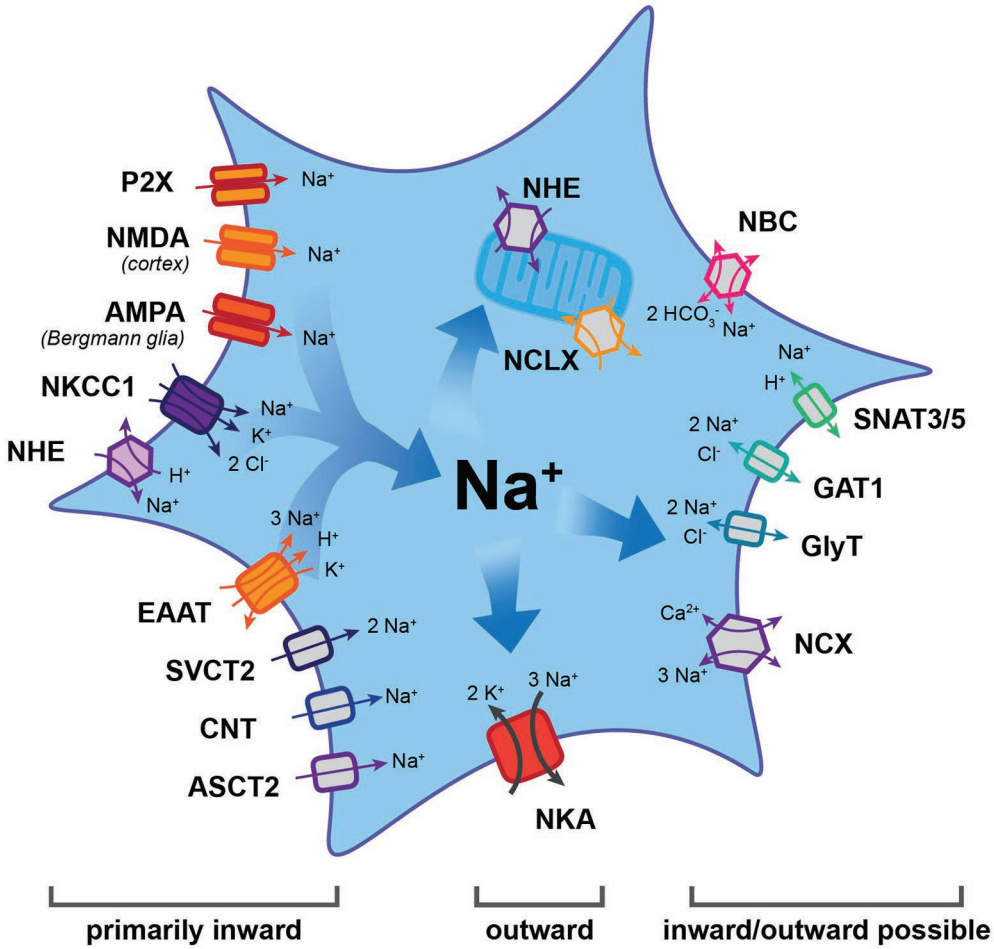

FIGURE 1 | Main efflux and influx pathways for Na^+ in astrocytes. Note that the Na^+/K^+-ATPase (NKA) is the major mechanism for Na^+ export. Other transporters may function in the inward or outward mode, thereby generating influx or efflux of Na^+. Most other carriers and all ion channels mediate Na^+ influx into astrocytes. AMPA, α-amino-3-hydroxy-5-methyl-4-isoxazolepropionic acid receptor; ASCT2, alanine, serine, cysteine transporter 2; CNT, concentrative nucleoside transporter; EAAT, excitatory amino acid transporter; GAT, gamma-aminobutyric acid transporter; GlyT, glycine transporter; NBC, Na^+-HCO_3^- cotransporter; NCX, Na^+/Ca^{2+} exchanger; NCLX, mitochondrial $Na^+/Ca^{2+}/Li^+$ exchanger; NHE, Na^+/H^+ exchanger; NKA, Na^+/K^+-ATPase; NKCC1, Na^+-K^+-2 Cl^- co-transporter 1; NMDA, N-methyl-d-aspartate receptor; SNAT3/5, sodium-coupled neutral amino acid transporter; and SVCT2, sodium-dependent vitamin C transporter 2.

In addition to depolarization, reversal can be triggered by increases in $[Na^+]_i$, e.g., following activation of glutamate uptake by excitatory amino acid transporters (EAATs; Huang and Bergles, 2004; Shibasaki et al., 2017). Astrocytic transport of glutamine across the membrane is mediated by sodium-coupled neutral amino acid transporters 3 and 5, SNAT3/5 (**Figure 1**), cotransporting 1 Na^+ and countertransporting a proton (Deitmer et al., 2003; Uwechue et al., 2012). Glutamine export is realized in the "outward" mode – which means exporting Na^+ – and constitutes a critical component of the glutamate-glutamine cycle (Danbolt, 2001).

Localized export of Na^+ from the cytosol can additionally be managed *via* its uptake into mitochondria by $Na^+/Ca^{2+}/Li^+$ exchangers (NCLX; **Figure 1**; Palty et al., 2010; Verkhratsky et al., 2018). These take in 3 Na^+ while releasing 1 Ca^{2+} from the organelle and their activity is highly sensitive to activity-induced $[Na^+]_i$ changes (Maack et al., 2006; Parnis et al., 2013). NCLX action has important implications, as it alters available Ca^{2+} in the mitochondria and the cytosol, while allowing mitochondria to act as a kind of Na^+ store (Ben-Kasus Nissim et al., 2017). In line with this view, mitochondrial $[Na^+]$ in astrocytes has been shown to be higher than the surrounding cytosol (Bernardinelli et al., 2006; Meyer et al., 2019). The release of Na^+ from these stores appears to be primarily mediated by the mitochondrial Na^+/H^+ exchanger (NHE; Bernardinelli et al., 2006).

Na^+ Influx Pathways

One of the best-described functions of astrocytes is their uptake of transmitters from the extracellular space. They carry this task out *via* transporters, which typically bring Na^+ into the cell, and use the energy gained to take in specific signaling molecules. Among these is glutamate, which is taken up by the EAATs glutamate-aspartate transporter (GLAST) and glutamate transporter 1 (GLT-1; Rothstein et al., 1996; Danbolt, 2001; **Figure 1**).

EAATs bring in one glutamate along with a proton using the energy gained from importing 3 Na^+, while simultaneously exporting 1 K^+. Their E_{rev} lies at around +50 mV, making reversal extremely unlikely (Eulenburg and Gomeza, 2010; Zhou and Danbolt, 2013). Similarly, transporters for ascorbic acid (sodium-dependent vitamin C transporter 2, SVCT2), adenosine (concentrative nucleoside transporter, CNT), and D-serine (alanine, serine, cysteine transporter 2, ASCT2) all have an E_{rev} of around +60 mV (**Figure 1**). While CNT2 and ASCT2 have a stoichiometry of 1 Na^+: one substrate, the SVCT2 brings in 2 Na^+ for every ascorbic acid molecule (Siushansian et al., 1997; Acuna et al., 2013; Maucler et al., 2013; Martineau et al., 2014; Rose and Verkhratsky, 2016b).

In addition, astrocytes heterogeneously express ionotropic transmitter receptors, which can trigger influx of Na^+. For example, cortical but not hippocampal, astrocytes express N-methyl-D-aspartate (NMDA) receptors (Schipke et al., 2001; Lalo et al., 2006) and Bergmann glial cells express α-amino-3-hydroxy-5-methyl-4-isoxazolepropionic acid (AMPA) receptors (Matsui, 2005). Furthermore, there is evidence for astrocytic expression of purinergic P2X receptors (**Figure 1**), which – depending on their subunit composition – may produce and inward Na^+ current (Lalo et al., 2008; Verkhratsky et al., 2012).

Prominent influx of Na^+ into astrocytes is provided by the Na^+/H^+ exchanger NHE1 (**Figure 1**), which plays a central role in their pH regulation (Chesler, 2003). It has a very positive E_{rev} (60–70 mV) and permanently functions in the forward mode under physiological conditions – taking in 1 Na^+ and extruding 1 proton (Chesler, 2003; Rose and Verkhratsky, 2016b). Like NHE1, the Na^+-K^+-2 Cl^- (NKCC1) cotransporter (**Figure 1**) is electro-neutral, importing 1 Na^+ along with 1 K^+ and 2 Cl^-. The result of that is that its operation at rest is inward under physiological conditions, with reversal only possible after extensive increases in $[Na^+]_i$ during pathological conditions (Su et al., 2002; MacAulay and Zeuthen, 2012).

Many more proteins do mediate Na^+ import into astrocytes and the reader is referred to several recent reviews presenting these in detail (e.g., Verkhratsky et al., 2019). What is clear is that inward transport of Na^+ along its electrochemical gradient offers a reliable mechanism for the regulation of other ions and diverse substances. Furthermore, the resulting changes in astrocytic $[Na^+]_i$ can themselves allow astrocytes to respond to changes in their environment by triggering other pathways as detailed in section "Functional Consequences of Astrocytic Na^+ Signaling in the Healthy Brain."

Na^+ SIGNALING IN ASTROCYTES

Spontaneous Na^+ Fluctuations

In addition to responding to neuronal activity, astrocytes are capable of communication within their own network, also independently from neurons. This had long been described in terms of spontaneous Ca^{2+} signals, which are present in astrocytes across several brain regions and developmental stages (Aguado et al., 2002). Seemingly spontaneous ion signaling in astrocytes, is, however, not restricted to Ca^{2+}. In addition, spontaneous Na^+ transients were reported from mitochondria of cultured astrocytes. These were around 10 s long and ~35 mM in amplitude and could be inhibited by NHE antagonists (Azarias and Chatton, 2011).

A recent study showed that neonatal astrocytes of mouse hippocampus and cortex display extremely long (~8 min), asynchronous and irregular changes in their somatic $[Na^+]$, termed "ultraslow Na^+ fluctuations" (Felix et al., 2020; **Figure 2**). These events had amplitudes of ~2 mM and were largely limited to the first 2 postnatal weeks. Comparable Na^+ fluctuations were measured in neurons of the same developmental stage, and these could be attributed to GABAergic signaling. However, antagonists for GABAergic components had no effect on the astrocytic signals – as was the case with several other major pathways (glutamate, acetylcholine, nor-adrenaline, and glycine). Astrocytic signals were dampened by the application of tetrodotoxin to block voltage-gated Na^+ channels. While this linked them to neuronal activity, it remained unclear which pathways are involved in their generation (Felix et al., 2020). Independent of the – as yet – unknown origin of the neonate ultraslow Na^+ fluctuations, the timing of their appearance makes it tempting to assign them a developmental function, as has been shown to be the case for other spontaneous activity patterns in the young brain (Ben-Ari, 2001).

Na^+ Transients Evoked by Neuronal Activity

Na^+ Transients in Cultured Cells

The first Na^+ signals measured in astrocytes were recorded in cell culture. Here, neuronal activity can be mimicked and Na^+ transients evoked by direct application of transmitters. Under these conditions, glutamate or its agonists evoke $[Na^+]_i$ increases of up to 20–30 mM in hippocampal astrocytes (Rose and Ransom, 1996a). The transients take up to a minute to reach their peak and typically return to their baseline levels within several minutes. Antagonist applications revealed these elevations to be primarily caused by EAAT-mediated glutamate uptake, with minor roles for ionotropic receptors (Rose and Ransom, 1996a; Chatton et al., 2000). Application of GABA under comparable conditions produces Na^+ transients with a similar time scale, albeit with a smaller amplitude of ~7 mM (Chatton et al., 2003; Unichenko et al., 2012).

Na^+ Transients in Astrocytes *in situ*

Astrocytic Na^+ responses occur in brain tissue slices as well. Notably, the properties of these responses and the mechanisms underlying them are heterogeneous across brain regions. In cerebellar Bergman glial cells, application of glutamate induced $[Na^+]_i$ increases in the range from 2 to 20 mM (Kirischuk et al., 1997, 2007; Bennay et al., 2008). These transients are faster than those reported from cell culture, with a rise time of several seconds and a mono-exponential decay time constant of ~25 s at room temperature. Transients recovered twice as fast at 32–34°C, indicating a major role of NKA in Na^+ export (Bennay et al., 2008). Pharmacological blockers confirmed that most of the response could be replicated by activation of EAATs alone. However, smaller transients could be induced both by applications

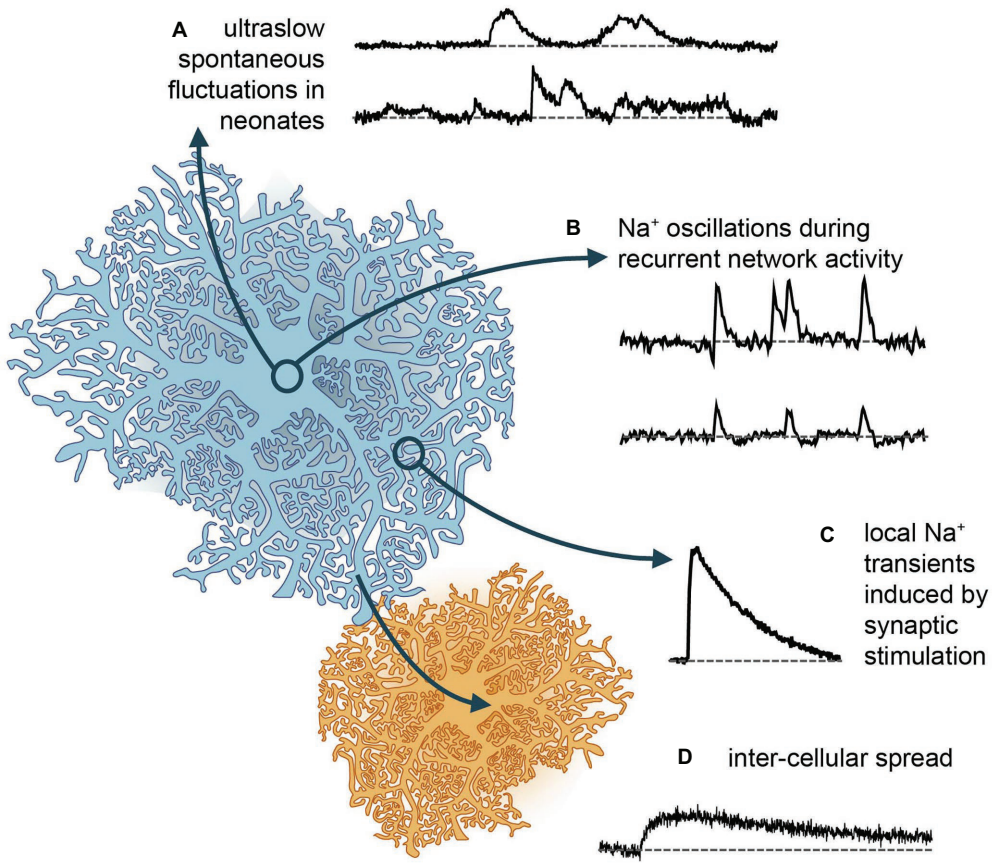

FIGURE 2 | Different forms of Na^+ signaling in astrocytes. **(A)** Spontaneous Na^+ fluctuations as recently reported from neonate hippocampus and cortex (Felix et al., 2020). **(B)** More rapid, global Na^+ oscillations, which are synchronized between cells and accompany recurrent network activity in mouse hippocampus (Karus et al., 2015, 2017). **(C)** Local Na^+ transients induced in different types of astrocytes and brain regions upon afferent synaptic stimulation of glutamatergic fibers (e.g., Kirischuk et al., 2007; Langer and Rose, 2009). **(D)** Gap junction mediated rapid spread of Na^+ signals in the astrocytic syncytium to neighboring cells, which then depict slower kinetics and reduced amplitudes (Langer et al., 2012, 2017).

of AMPA or kainate (but not NMDA), confirming functional AMPA receptor expression in Bergmann glia (Kirischuk et al., 2007; Bennay et al., 2008). Stimulation of either parallel and climbing fibers produced $[Na^+]_i$ increases with rise and decay times of 5 and 90 s respectively, and amplitudes of ~9 mM (Bennay et al., 2008; **Figure 2**). While climbing fiber stimulation resulted in global $[Na^+]_i$ increases, with a similar amplitude and time course across all processes, parallel fiber stimulation induced large Na^+ transients near the point of stimulation, which declined with increasing distance, indicative of the pattern of activated synapses (Bennay et al., 2008).

In contrast to Bergmann glia, the ionotropic receptor component of Na^+ transients in astrocytes within the hippocampus and Calyx of Held is minimal. These both react to puff application of D-aspartate (which activates EAATs) with $[Na^+]_i$ increases of around 5 mM (Langer and Rose, 2009; Uwechue et al., 2012). Comparable transients are induced in hippocampal astrocyte processes by Schaffer collateral stimulation (Langer and Rose, 2009). Stimulation with high intensity, presumably activating many afferent fibers, create large increases in $[Na^+]_i$, which can spread throughout the whole cell and further to adjacent cells (**Figure 2**). Stimulation with low intensity, in contrast, creates localized rises in $[Na^+]_i$ in individual processes, presumably nearest the synaptic release sites (Langer and Rose, 2009; Langer et al., 2017). Global, network-wide Na^+ oscillations are induced by hippocampal network activity during neuronal "disinhibition" (Karus et al., 2015; **Figure 2**). Herein, blocking (inhibitory) $GABA_A$-receptor activation and omission of Mg^{2+} in the perfusate produce epileptiform bursting. Under these conditions, hippocampal astrocytes undergo repetitive, synchronized increases in their $[Na^+]_i$, with amplitudes as large as 8–9 mM, followed by a brief undershoot in a subset of cells (Karus et al., 2015; **Figure 2**).

It is again worth to note that neocortical astrocyte Na^+ transients have properties which distinguish them from astrocytes of the hippocampus proper, as cortical cells express functional NMDA receptors (Schipke et al., 2001; Lalo et al., 2006). In layer 2/3 astrocytes, application of glutamate or synaptic stimulation produces Na^+ transients with an amplitude twice as large as those induced by the same protocol in hippocampal astrocytes (Ziemens et al., 2019). Large $[Na^+]_i$ increases of ~13 mM were induced specifically in processes and were

found to pass to the soma. Application of AP5 (an NMDA receptor antagonist) reduces these signals by 50%, and further addition of TFB-TBOA (to block EAAT responses) eliminates the transients completely. AMPA receptors appear not to contribute to astrocyte Na^+ signals in the neocortex (Ziemens et al., 2019).

Na^+ transients are not limited to gray matter. Astrocytes in the corpus callosum respond to glutamate application and electric stimulation with increases of around 2–5 mM and 1–2 mM, respectively. As is the case for protoplasmic astrocytes of the hippocampus – the majority of the measured Na^+ transients are removed by the application of EAAT blockers, suggesting that here too, glutamate uptake is the primary pathway for Na^+ influx (Moshrefi-Ravasdjani et al., 2017, 2018).

Na^+ Microdomains and Diffusion

A special compartment allowing localized increases in astrocytic $[Na^+]_i$ was postulated by Blaustein et al. (2002). In analogy to work by the Lederer et al. (1990), they proposed that the presence of the endoplasmic reticulum (ER) very close to the membrane creates a confined area, wherein Na^+ elevations could reach concentrations high enough to reverse the NCX – and thereby induce further Ca^{2+} release from intracellular stores. Immunohistochemical work indeed provided evidence that both the NCX and the α2β2 form of NKA are clustered around areas where the ER lies near the plasma membrane in astrocytes (Blaustein et al., 2002; Lee et al., 2006). Conversely, other work showed no evidence for such Na^+ domains at the ER adjacent sites, and the concept remains controversial (Lu and Hilgemann, 2017; Sachse et al., 2017).

Notably, the idea of ionic signaling microdomains to be present in astrocytes was again promoted by recent modeling work. Here, the authors proposed that the flow of cations in small perisynaptic processes enwrapping synapses like a "cradle" is strongly restricted, giving rise to astrocytic K^+ and Na^+ microdomains close to synapses (Breslin et al., 2018). In a follow-up paper, this conception was explored further to demonstrate that local increases in $[Na^+]_i$ promote a local reversal of the NCX (Wade et al., 2019). Very small compartments may, thus, form subcellular Na^+ domains, also with different resting concentrations to the rest of the cell, which could in turn impact the direction of the transporter function in these areas.

The extent to which Na^+ transients can spread throughout astrocytes is critical also because changes in $[Na^+]_i$ can directly pass on to mitochondria. *In vitro* applications of agonists including glutamate, kainate, D-aspartate, or AMPA, all showed mitochondrial $[Na^+]$ rises to a similar extent as their surroundings, for the duration of application (Bernardinelli et al., 2006). Although the function of this increase remains unclear, its recruitment of the NCLX and NHE is likely to impact respiratory pathways by altering the availability of both Ca^{2+} and protons (Azarias and Chatton, 2011).

While local microdomains established by fine perisynaptic processes may strongly restrict the diffusion of Na^+ in astrocytes, Na^+ diffusion along larger processes (large meaning microscopic scale) is very rapid in astrocytes, reaching velocities of >100 µm/s (Langer et al., 2012, 2017). Na^+ can moreover rapidly pass through gap junctions into neighboring cells – across the astrocytic syncytium (Langer et al., 2012, 2017; **Figure 2**). This spread has been shown to extend to other cell types with astrocytes, oligodendrocytes, and NG2 glia being connected into a panglial network in both gray, and white matter (Griemsmann et al., 2015; Augustin et al., 2016; Moshrefi-Ravasdjani et al., 2017, 2018). The spreading of Na^+ in this manner may help to maintain the low $[Na^+]_i$ critical for driving uptake at/near the site of its influx.

Spread of Na^+ from cells with locally elevated $[Na^+]_i$ toward cells with a lower $[Na^+]_i$ will not only be driven by the concentration gradient but also be dependent on the membrane potential of the involved cells. While the isopotentiality of the gap-junction-coupled astrocyte network might be initially be disturbed at the site of Na^+ influx, it will effectively dampen resulting changes in the membrane potential and thereby also facilitate the intercellular spread of Na^+, as has been shown for redistribution of K^+ (Ma et al., 2016).

FUNCTIONAL CONSEQUENCES OF ASTROCYTIC Na^+ SIGNALING IN THE HEALTHY BRAIN

So far, most studies addressed the possible consequences of changes in astrocytic Na^+ in the context of altered driving force for Na^+ dependent transporters. The latter couple Na^+ homeostasis to the regulation of other ions, neurotransmitters, and diverse substrates processes not only highly relevant for astrocytic function but also for their communication with neurons (Kirischuk et al., 2012; Rose and Karus, 2013; Verkhratsky et al., 2019). Increases in $[Na^+]_i$ moreover involve its re-export through the NKA, thereby coupling Na^+ signaling to astrocyte metabolism (Pellerin and Magistretti, 2012). In addition, Na^+ also exerts "atypical" roles (**Figure 3**), which are not related to changes in driving forces nor directly change the cellular energy status. Instead, a binding of Na^+ from either the intracellular or extracellular side, directly effects the functionality of discrete proteins as discussed below.

"Conventional" Roles

Na^+ and Regulation/Signaling of Other Ions

NKA and K^+ Clearance

It has long been established that the pump cycle of the NKA is dependent on binding of Na^+; once all three binding sites for Na^+ are occupied, the transporter undergoes conformational changes that regulate the cleavage of ATP (Clausen et al., 2017). In addition, mainly based on work on cardiac myocytes, a secondary activation of NKA by Na^+ was proposed, complemented by a so-called "Na^+-deficiency inactivation" that may serve to maintain the pumps in a "reserve state" when not needed (Hilgemann, 2020).

Astrocytic NKA plays an important role in the regulation of extracellular K^+ concentration ($[K^+]_o$) (**Figure 3**). Owing to its predominant subunit composition (α2/β2), it is selectively stimulated by increases in $[K^+]_o$, which triggers K^+ uptake into astrocytes (Karus et al., 2015; Larsen et al., 2016). K^+-induced

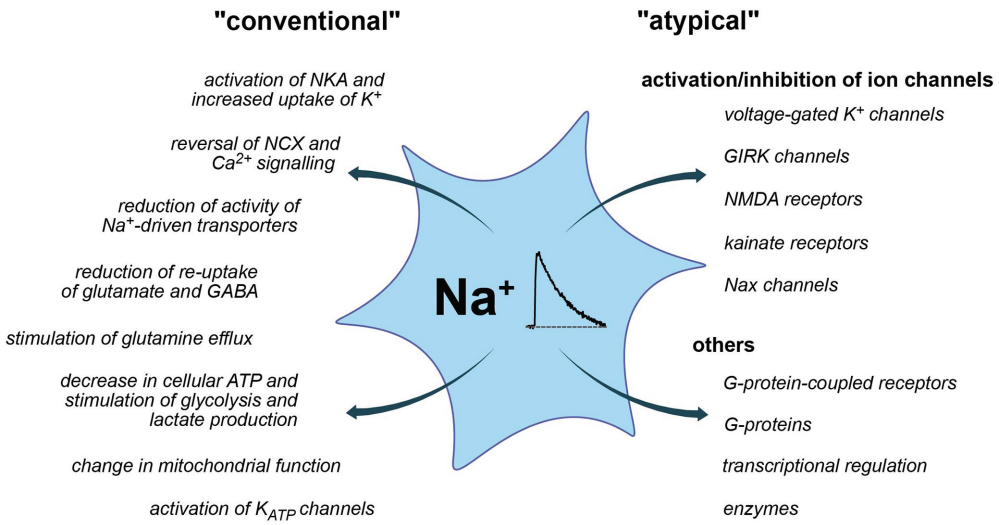

FIGURE 3 | Conventional and more "atypical" consequences of Na^+ and Na^+ signaling. **Left**: conventional roles, largely established and accepted to be relevant for astrocytes. **Right**: atypical roles, partly hypothetic and based on insights from other systems.

activation of astrocytic NKA can in fact result in a decrease in $[Na^+]_i$ below baseline (Rose and Ransom, 1996a; Karus et al., 2015). The minority isoform α2β1 is insensitive to changes in $[K^+]_o$ and its activity can instead be increased by elevations in astrocytic $[Na^+]_i$ (Larsen et al., 2016). In neurons, NKA is mainly activated by increases in $[Na^+]_i$, which contributes to their repolarization following high-frequency bursts of action potentials and may induce a long-lasting post-tetanic hyperpolarization (e.g., Gulledge et al., 2013). In *Drosophila* motor neurons, the NKA-mediated afterhyperpolarisation was suggested to serve as a specific form of long-term memory of recent activity (Glanzman, 2010; Pulver and Griffith, 2010). In astrocytes, where changes in the membrane potential play a less prominent role, such effects were not yet described. Notably, the K^+-induced activation of NKA and accompanying decrease in astrocytic $[Na^+]_i$, as well as efflux of positive charge are often counteracted or completely masked by Na^+ import *via* glutamate transporters (Langer and Rose, 2009; Karus et al., 2015) and/or by GABA uptake (Chatton et al., 2003; Unichenko et al., 2013). The resulting increases in astrocytic $[Na^+]_i$ then again will further promote NKA activity (and K^+ uptake).

NKCC1 and Cl^- Homeostasis

Another Na^+-dependent transporter for uptake of K^+ into astrocytes is the NKCC1. In cultured astrocytes and Bergmann glial cells in brain slices, NKCC1 is constitutively active, providing constant influx of all three ions (Rose and Ransom, 1996a; Untiet et al., 2017; Noor et al., 2018). Owing to its apparent low affinity for K^+, NKCC1 only effectively contributes to clearance of extracellular K^+ with increases above the ceiling level of 10–12 mM (Lenart et al., 2004; Hertz et al., 2015; Larsen et al., 2016). In addition, NKCC1 plays a major role in Cl^--homeostasis of astrocytes. In Bergmann glial cells, NKCC1 is responsible for its active accumulation, generating an outwardly-directed Cl^- gradient (Untiet et al., 2017). This in turn mediates the depolarizing effect of $GABA_A$ receptor activation on astrocytes (Kettenmann et al., 1984; MacVicar et al., 1989). Increases in astrocytic $[Na^+]_i$, reducing the driving force for NKCC1, might therefore, lower astrocyte Cl^- concentrations. This will reduce the "excitatory" effect of GABA on astrocytes, also dampening associated Ca^{2+} transients (Fraser et al., 1995; Meier et al., 2008).

pH Homeostasis

pH regulation in astrocytes by NHE and NBCe1 is intimately related to their Na^+ homeostasis (Deitmer and Rose, 1996; Chesler, 2003). Given, the very positive E_{rev} of the NHE (> +60 mV), proton export will not be significantly hampered unless $[Na^+]_i$ is elevated strongly. This is in stark contrast to NBCe1. Owing to its reversal potential of approximately −80 mV, a rise in astrocytic $[Na^+]_i$, together with an intracellular alkalosis, will dampen inward NBC activity and with strong Na^+ loading and/or alkalosis, NBC may even reverse (Theparambil et al., 2015). In the brain stem, Na^+ uptake by astrocytes is central for CO_2/H^+-sensing (Turovsky et al., 2016): a physiological increase in P_{CO2} activates inwardly-directed NBCe1, increasing astrocytic $[Na^+]_i$. This triggers reversal of the NCX, astrocytic Ca^{2+}-signaling, release of ATP, and adaptive responses in neighboring neurons of the respiratory network (Turovsky et al., 2016).

NCX and Ca^{2+}-Signaling

Na^+ elevations in astrocytes that are large enough to trigger secondary Ca^{2+} signaling through NCX can arise after influx through Na^+-permeable ion channels (Pappalardo et al., 2016; Verkhratsky et al., 2018; Rose et al., 2020). This was shown, e.g., for neocortical astrocytes upon activation of NMDA receptors (Ziemens et al., 2019). The resulting NCX-related Ca^{2+} import added to the influx through the receptor itself and significantly prolonged the duration of Ca^{2+} signals.

In neural (radial glia like) stem cells of the subependymal zone, Na^+ influx through epithelial sodium channels (ENaC) stimulated Ca^{2+} signaling, presumably through reverse NCX, contributing to the regulation of their proliferation (Petrik et al., 2018). Of note, and similar to Na^+-dependent regulation of NKA activity described above, NCX was proposed to be subject to a secondary Na^+-dependent inactivation following Na^+ binding to its inward facing transport sites in cardiac myocytes (Hilgemann, 2020). Such Na^+-dependent inactivation of NCX in astrocytes could reduce Ca^{2+} influx upon its reversal, a process which might be relevant to dampen Ca^{2+} overload under pathological conditions.

In addition to be aforementioned studies, there is an overwhelming number of other reports demonstrating Na^+-driven reversal of astrocytic NCX. By coupling Na^+ transients to Ca^{2+}-signaling, NCX represents a direct link between those two ions and forms of astrocytic excitability. Experimental evidence supporting the existence of this important link was reviewed recently and we kindly refer the reader to this earlier work (Kirischuk et al., 2012; Verkhratsky et al., 2019; Rose et al., 2020).

Na^+-Dependent Regulation of Transmitter Levels

The Na^+ gradient of astrocytes is intimately linked to their uptake of transmitters and regulation of extracellular transmitter levels (Verkhratsky et al., 2019). Again, there are relevant conceptual differences in the biophysical properties of the transporters involved. The stoichiometry of some transporters enables reversal under severe pathological conditions only, that is, with very strong increases in $[Na^+]_i$. Among those are GLAST and GLT-1, which operate as importers for glutamate over a wide range of physiological states but can release it in the core region of an ischemic stroke where $[Na^+]_i$ may rise to >50 mM (Friedman and Haddad, 1994; Rossi et al., 2000). Other transmitter transporters (e.g., those for GABA) operate close to their reversal potential, apparently enabling both uptake and release of their substrate, depending on the conditions (see section "Efflux Pathways for Na^+").

Glutamate uptake is one of the major pathways for generation of astrocytic Na^+ signaling (Rose and Verkhratsky, 2016b). Related $[Na^+]_i$ increases in the bulk cytosol are, however, apparently dampened by co-localization of GLAST and GLT-1 with α2-containing NKA (Cholet et al., 2002; Rose et al., 2009; Bauer et al., 2012; Illarionava et al., 2014; Melone et al., 2019). At the same time, even moderate glutamate-induced Na^+ signaling can cause reversal of the NCX and thereby induce Ca^{2+} signals (Rojas et al., 2007; Rose et al., 2020). Na^+-triggered, NCX-mediated Ca^{2+}-signaling has been implemented in the mobility of mitochondria, coupling neuronal activity to astrocyte metabolism (Jackson and Robinson, 2018). Since both GLAST and GLT-1 activity are mainly energized by the Na^+ gradient, increases in $[Na^+]_i$ reduce their driving force and may exert a negative feedback on extracellular glutamate clearance (Barbour et al., 1991; Bergles et al., 2002; Kelly et al., 2009; Unichenko et al., 2012). Notably, $[Na^+]_i$ elevations in astrocytes also drive the efflux of glutamine through Na^+-dependent system N transporters (Broer and Brookes, 2001; Todd et al., 2017), thereby enabling its direct re-supply to neurons (Uwechue et al., 2012). Na^+ signals thus directly link extracellular glutamate clearance to the re-cycling of its precursor glutamine to neurons.

As opposed to GLAST and GLT-1, the transporters for uptake of GABA and glycine can reverse much more easily (Eulenburg and Gomeza, 2010). Astrocytes may, therefore, not only serve to clear the extracellular space (ECS) from these inhibitory transmitters but also function as their source, depending on the prevailing driving forces (Kirischuk et al., 2016). While GABA uptake is linked with the uptake of 2 Na^+ only, its application still results in well-detectable Na^+ signals in astrocytes (Chatton et al., 2003; Doengi et al., 2009; Unichenko et al., 2012; Boddum et al., 2016). A reversal of astrocytic GABA transporters, presumably triggered by the related increase in $[Na^+]_i$, was demonstrated upon stimulation with glutamate (Heja et al., 2009; Unichenko et al., 2013). In hippocampal astrocytes, GAT-induced increases in $[Na^+]_i$ caused reversal of NCX, Ca^{2+} signaling, and release of ATP/adenosine, which inhibited presynaptic release of glutamate from neighboring neurons (Boddum et al., 2016). This again exemplifies the tight coupling of astrocyte $[Na^+]_i$ increases with functionally relevant Ca^{2+}-signaling.

Na^+-Dependent Regulation of Cellular Metabolism

Influx of Na^+ into astrocytes necessitates its export through the NKA, increasing ATP consumption and resulting in a decrease in ATP levels (Chatton et al., 2000; Langer et al., 2017; Winkler et al., 2017; Lerchundi et al., 2019). These triggers increased uptake of glucose, enhances the breakdown of glycogen, and stimulates glycolysis, as well as the production of lactate (Brown and Ransom, 2007; Pellerin and Magistretti, 2012). The latter is assumed to play a key role in the neuro-metabolic coupling between neurons and astrocytes (Chatton et al., 2016; Magistretti and Allaman, 2018).

As mentioned above, cytosolic Na^+ transients can be transmitted to mitochondria (Bernardinelli et al., 2006). Moreover, mitochondria may also generate seemingly spontaneous transient elevation in their $[Na^+]_i$ (Azarias and Chatton, 2011). While the functional consequences of such mitochondrial Na^+ signaling in astrocytes are not understood yet, they might change the driving force of the mitochondrial Na^+/Ca^{2+} exchanger NLCX, influencing mitochondrial Ca^{2+} regulation, signaling, and ATP production (Nita et al., 2015; Ben-Kasus Nissim et al., 2017).

Na^+ signaling might also feed back onto astrocyte metabolism and function through a secondary regulation of ATP-sensitive K^+-channels (K_{ATP}). These channels open, promoting efflux of K^+, when intracellular ATP concentrations decrease – as is the case following increases in $[Na^+]_i$ as described above. K_{ATP} channel expression in astrocytes is well documented (Verkhratsky and Nedergaard, 2018), where they apparently play a protective role in neurodegenerative diseases and in ischemia (Sun et al., 2008; Griffith et al., 2016; Zhong et al., 2019).

"Atypical" Roles

While Na^+ transients in astrocytes have abundant functional consequences due to the central role of the inward Na^+ gradient, there are also direct effects of Na^+ binding to diverse proteins (**Figure 3**). In contrast to the two prototypical ions involved in cellular signaling, Ca^{2+} and protons, endogenous buffer

systems for Na^+ are apparently absent and $[Na^+]_i$ is kept in the mM (not nM) range. Nonetheless, specific Na^+-binding to different proteins was reported that renders their function sensitive to changes in extracellular and/or intracellular $[Na^+]$. Moreover, the existence of Na^+-responsive elements regulating an entire battery of early genes was postulated. Many of these atypical actions of Na^+ were not yet described in astrocytes, but, in the context of this review, will be at least briefly mentioned.

Na^+-Regulated Ion Channels

Voltage-Dependent K^+-Channels

Na^+ has been reported to inhibit voltage-gated K^+ currents in various neuronal preparations, as well as in several types of glial cells (e. g., Van Damme et al., 2002). The amplitude of single-channel currents of two types of delayed rectifier outward K^+ channels was reduced by 30 mM internal $[Na^+]$ in cultured Schwann cells, suggesting a channel block from the intracellular side (Howe et al., 1992). In 1994, it was shown that activation of AMPA/kainate receptors in "complex glial cells" of mouse CA1 area (according to today's nomenclature presumably to be classified as NG2 cells) resulted in a Ca^{2+}-independent inhibition of the transient component of the outwardly rectifying K^+ current (Jabs et al., 1994). In oligodendrocyte precursor cells from embryonic cortex, Na^+ influx through AMPA/kainate receptors blocked delayed outwardly rectifying K^+ currents at concentrations >30 mM (Borges and Kettenmann, 1995). A similar phenomenon was described from stellate cortical astrocytes in culture. Here, opening of AMPA receptors resulted in a Na^+-dependent block of two types of outwardly rectifying K^+ currents that occurred at $[Na^+]_i$ between 20 and 40 mM (Robert and Magistretti, 1997).

The functional relevance and consequences of a Na^+-dependent block of outward K^+ currents in glial cells is only partly clear. It might prevent the release of K^+ during periods of strong neuronal activity (and neuronal glutamate release; Robert and Magistretti, 1997). At the same time, the K^+-current inhibition by Na^+ will promote glutamate-induced depolarizations, an effect which will reduce glial glutamate uptake, likely aggravating excitotoxic damage under ischemic conditions. In oligodendrocyte precursor cells, there is clear evidence for an anti-proliferative role. In O-2A cells cultured from rat cortex, activation of ionotropic glutamate receptors inhibited cell proliferation. This was mediated by an increase in $[Na^+]_i$ and an ensuing block of outward K^+ currents (Gallo et al., 1996; Knutson et al., 1997). Later, a specific role for glutamate-receptor induced inhibition of voltage-gated K^+ channels in oligodendrocyte (but not astrocyte) development was demonstrated in organotypic cerebellar slice cultures (Yuan et al., 1998).

In addition to inhibition of outward rectifier K^+ channels by internal Na^+, a block of inwardly rectifying K^+ channels (Kir) by extracellular Na^+ was reported in cultured astrocytes (Ransom et al., 1996). Moreover, a block of Kir-channels (mainly composed of Kir2.x subtypes) by Na^+ influx through AMPA receptors in complex glial cells was demonstrated (Schroder et al., 2002). Again, the functional significance of this is still largely unclear. Under conditions of enhanced glutamate release and accumulation in the ECS, an increase in $[Na^+]_i$ and a Na^+-dependent reduction in glial Kir conductance might decrease their contribution to the clearance of extracellular K^+ and thereby most likely aggravate excitotoxic conditions.

GIRK Channels

G-protein-gated inward rectifier K^+ channels (GIRK) are activated by Na^+ binding at their cytoplasmic side (Sui et al., 1996; Ho and Murrell-Lagnado, 1999). The binding of Na^+ appears to foster the interaction of GIRK channels with phosphatidylinositol 4,5bisphosphate (PIP_2), which is required for channel activation (Ho and Murrell-Lagnado, 1999; Yakubovich et al., 2005). The EC_{50} values reported for different GIRK channel compositions are between 27 and 44 mM Na^+ (Ho and Murrell-Lagnado, 1999). The latter suggests their modulation by intracellular Na^+ signaling under physiological, as well as pathophysiological conditions. Such an effect was proposed to support the inhibitory effect of vagus nerve stimulation on the heat rate following an acetylcholine-induced activation of GIRK channels in atrial pacemaker cells (Wang et al., 2014). GIRK channels are also highly expressed in the brain, where they, e. g., mediate the inhibitory action of $GABA_B$ receptors in neurons (Lesage et al., 1994; Lujan and Aguado, 2015). Evidence for expression of GIRK channels (Kir3.1/Kir3.2) in astrocytes is, however, weak (Verkhratsky and Nedergaard, 2018). In retinal Müller glia cells, mRNA for both Kir3.1 and Kir3.2 was detected (Raap et al., 2002) and immunoreactivity for Kir3.1 was found in cultured astrocytes from rat cortex and spinal cord, as well as in glioma cells (Olsen and Sontheimer, 2004). The latter work thus indicates that GIRK channels – and their Na^+-dependent regulation – might play a functional role at least in some subtypes of glial cells.

Na^+-Dependent K^+ Channels

Expression of this class of channels has to our knowledge so far not been described in astrocytes, but they shall nonetheless at least be mentioned here because of their relevance in neurons (Egan et al., 1992; Dryer, 1994). K_{Na} channels are most often composed of two subunits, called slack (or $K_{Na}1.1$) and slick (or $K_{Na}1.2$; Bhattacharjee and Kaczmarek, 2005). Their apparent function is to detect activity-related increases in $[Na^+]_i$, e.g., during action potential firing, upon which they open, thereby contributing to adaptation of the firing rate and to afterhyperpolarisations following bursts (Bhattacharjee and Kaczmarek, 2005).

Ionotropic Glutamate Receptors

Native and recombinant kainate receptors are gated by external Na^+ (Paternain et al., 2003). In astrocytes, kainate receptors were so far only demonstrated based on mRNA and protein expression studies (Verkhratsky and Nedergaard, 2018).

NMDA receptors are expressed by neocortical (but not hippocampal) astrocytes (Schipke et al., 2001; Zhou and Kimelberg, 2001; Matthias et al., 2003; Lalo et al., 2006; Dzamba et al., 2013), and their activation results in considerable Na^+ influx into these cells, promoting a reversal of the NCX and prolonging Ca^{2+} signals (Ziemens et al., 2019). In mammalian neurons,

moderate elevation of $[Na^+]_i$ to 30–40 mM increases the open probability of NMDA receptors through a channel-associated Src kinase (Yu and Salter, 1998, 1999). The latter plays a role in the induction of long-term potentiation (LTP) at CA3-CA1 synapses of the hippocampus (Lu et al., 1998). A Na^+-dependent regulation of NMDA receptor activity through Src kinases was also demonstrated in mouse cerebrocortical neurons. The resulting enhancement of NMDA receptor function promoted neurite outgrowth and synaptogenesis (George et al., 2012). So far, a possible role of a Na^+-dependent regulation of NMDA receptor current in astrocytes is unexplored.

Volume-Regulated Anion Channels

Depending on the osmolarity of the surrounding extracellular fluids, astrocytes show adaptive regulation in the form of a regulatory volume increase (RVI) or a regulatory volume decrease (RVD; Wilson and Mongin, 2018). In the latter, volume-regulated anion channels (VRACs) are thought to play a prominent role (Kimelberg et al., 2006). In cultured rat cortical astrocytes, VRAC conductance is negatively regulated by an increase in $[Na^+]_i$ to 50 mM (Minieri et al., 2014). Based on these observations, the authors suggested that a dampening of astrocytic Na^+ loading in ischemic conditions could present a new therapeutic target to reduce the development of brain edema.

Na^+_x Channels

These special channels are expressed by astrocytes in the subfornical organ (SFO), which is part of the circumventricular organs and is involved in regulation of salt levels (Iadecola, 2007; Noda and Hiyama, 2015). Na_x channels on astrocytes are activated by an increase in extracellular $[Na^+]$ above 140 mM (Noda and Hiyama, 2015). This mediates a direct, Na^+-triggered influx of Na^+, which activates the NKA, stimulates glycolysis, and results in an extensive production of lactate (Shimizu et al., 2007). Lactate is then released by the astrocytes and taken up by neighboring GABAergic neurons, where it is used for the generation of ATP. The resulting increase in neuronal ATP levels acts on K_{ATP} channels, thereby causing an increase in their firing rate. This regulates other efferent neurons of the SFO that are involved in the behavioral control of salt intake, promoting salt aversive behavior and Na^+ secretion (Noda and Hiyama, 2015).

Na^+-Dependent Regulation of Transcription, G-Protein Signaling and Enzymes

Transcriptional Regulation

The group of S. Orlov was instrumental in providing evidence for an involvement of Na^+ in gene expression (Klimanova et al., 2019). Most experiments were performed in rat smooth muscle cells, showing that an increase in $[Na^+]_i$, as, e.g., induced by application of ouabain, results in increased RNA synthesis and protein synthesis (Orlov et al., 2001). These effects were explained to result from a Na^+-dependent activation of early response genes such as c-Fos and c-Jun, and most likely based on dedicated Na^+-dependent response elements in those genes (Taurin et al., 2002; Haloui et al., 2007; Klimanova et al., 2019). Notably, a significant number of Na^+/K^+-dependent gene transcripts were also found in several other cell types, including rat brain neurons (Koltsova et al., 2012; Klimanova et al., 2019; Smolyaninova et al., 2019). The latter suggests that such regulation of gene transcription by intracellular Na^+ might also be effective in astrocytes.

G-Protein-Coupled Receptors

Many class A G-protein-coupled receptors (GPCRs), including A_1/A_{2A} adenosine and β-adrenergic receptors, as well as dopaminergic and histaminergic or mu-opioid GPCRs, show a negative modulation by Na^+ in the physiological range (Katritch et al., 2014). Na^+, binding to a highly conserved allosteric binding site, acts as a universal inverse agonist in these receptors; it reduces both their constitutive activity and decreases their agonist binding (Strasser et al., 2015; Zarzycka et al., 2019). Most work based on crystal structures and molecular simulations indicates that Na^+ accesses this site from the extracellular space (Strasser et al., 2015), but for there are also simulations predicting that it can bind from the intracellular side (Selvam et al., 2018). Reported binding affinities vary widely between different receptor subtypes, but many receptors are <50 mM, suggesting a saturation with Na^+ at a typical extracellular $[Na^+]$ of 145–150 mM. However, some receptors like the D4 or D2 dopamine or H1 histamine receptors show a rather low Na^+ affinity (K_B >100 mM), and might, therefore, be functionally altered by physiological or pathophysiological fluctuations in extracellular $[Na^+]$ (Zarzycka et al., 2019).

Despite manifold evidence for Na^+-dependent modulation of GPCRs also in the nervous system (e.g., Makman et al., 1982; Livingston and Traynor, 2014), its relevance for brain function is far from understood. In many studies, the Na^+-binding site of GPCRs is studied in the context of serving as a possible therapeutic target (Livingston and Traynor, 2014). Mutations in the allosteric Na^+ binding site of the orphan GPCR3, which promotes the processing of amyloid precursor protein to Aß peptides in neurons, resulted in a significant decline in Aß production, indicating that it may serve to counteract Aß accumulation in Alzheimer's disease (Capaldi et al., 2018). Because of the widespread expression of GCPRs in glial cells (Verkhratsky and Nedergaard, 2018), it is likely that such Na^+-dependent modulation is also relevant for astrocyte function.

G-Proteins

Na^+ also affects trimeric G-proteins. In *Xenopus* oocytes, internal Na^+ promotes the dissociation of heterotrimeric G-proteins to Gα and Gβγ (Rishal et al., 2003). This was dose-dependent with a half-maximal effect at 14 mM Na^+ and was directly affected the Gβγ-mediated activation of GIRK channels, suggesting that Na^+ may serve a signaling purpose (Rishal et al., 2003). In hippocampal neurons, the dissociation of Gβγ was enhanced by NMDA-receptor-mediated Na^+ influx and resulted in the inhibition of voltage-gated Ca^{2+}-channels (Blumenstein et al., 2004), again assigning Na^+ the role of a second messenger.

Furthermore, a separate sub-class of cation-dependent G-proteins does exist, which are either K^+-selective or activated by both K^+ and Na^+. The latter include different GTPases of the dynamin family which are involved in remodeling of membranes (Ash et al., 2012). The relevance of these Na^+-dependent proteins for astrocyte function remains so far essentially unexplored.

Enzymes

Several enzymes are directly regulated by Na^+. Among those are serine proteases involved in blood coagulation and complement like thrombin, which exhibits an allosteric enhancement by extracellular binding of Na^+ that strongly enhances its catalytic properties (Dang and Di Cera, 1996; Silva et al., 2006). A recent example of an enzyme directly regulated by intracellular Na^+ was found in skeletal muscle. Here, a member of the superfamily of calpains, namely p94/calpain3, was shown to be activated by Na^+ at physiological concentrations, suggesting that changes in $[Na^+]_i$ during muscle contractions might be involved in the regulation of this and also other Ca^{2+}-dependent enzymes (Ono et al., 2010).

Glutamine synthase is exclusively expressed by astrocytes and a key enzyme of the glutamate-glutamine cycle (Martinez-Hernandez et al., 1977; Danbolt, 2001). Moreover, it is essential in the detoxification of ammonium (NH_4^+), thereby protecting the brain from a harmful elevation of NH_3/NH_4^+ (Albrecht et al., 2010). In 1987, Benjamin showed that several manipulations to increase $[Na^+]_i$ in rat brain tissue slices resulted in an inhibition of glutamine formation (Benjamin, 1987). He speculated that this was either related *via* a direct effect on the enzyme itself or to an accompanying decrease of ATP levels in astrocytes.

FUNCTIONAL CONSEQUENCES OF Na^+ SIGNALING IN THE DISEASED BRAIN

In the previous sections, we discussed the implications of physiological Na^+ signaling. The subsequent part will address how these functions are disrupted in response to different pathologies and what future research questions may arise from these findings. The field is only slowly moving forward in realizing the importance of Na^+ signaling and its downstream effects, and most of the discussed work in the following sections addresses the more conventional functions of Na^+-dependent processes in the diseased brain. Here, we mainly focus on ischemia, migraine, aging, and neurodegenerative diseases, as most studies investigating Na^+ changes have been performed in these disease models.

Ischemia

Stroke represents one of the leading causes of death and disability (Nedergaard and Dirnagl, 2005). As the brain is in constant need of steady oxygen and glucose supply, the abrupt reduction of cerebral blood flow (CBF) during a stroke results in the fast consumption of the remaining energy sources, pushing the regions that are particularly affected into severe energy deficits. In the core, these disruptions in the core region of ischemic stroke cause a breakdown of ionic gradients that eventually lead to cell death if not reversed (Dirnagl et al., 1999; Moskowitz et al., 2010). In the penumbra, i.e., the tissue surrounding the core, a basal level of perfusion is maintained through vascular collaterals, enhancing the chances for neuronal survival (Dirnagl et al., 1999, Moskowitz et al., 2010).

Two factors can negatively affect the outcome of survival in the penumbra: (1) the available energy is too low for glutamate transporters to efficiently clear glutamate from the synaptic cleft, resulting in excess extracellular glutamate and intracellular Ca^{2+} leading to excitotoxicity (Rakers and Petzold, 2017) and (2) peri-infarct depolarizations (PID), i.e., repeated waves of spreading depolarizations traveling through the penumbra that lead to more glutamate release and an even higher energy consumption (Hossmann, 1996; Lauritzen et al., 2011; Rakers and Petzold, 2017). Astrocytes play an important role in the reduction of PID-induced excitotoxic mechanisms, owing to their ability to remove glutamate from the synaptic cleft (Nedergaard and Dirnagl, 2005). This uptake of glutamate during PIDs into astrocytes by EAATs produces an increase in their $[Na^+]_i$, a process aggravated by reduced NKA activity due to energy shortage in the hypoxic tissue (Rose and Karus, 2013).

The resulting strong elevation of $[Na^+]_i$ in neurons and astrocytes has several important consequences for cell function and survival in the ischemic brain. First, the scarce ATP resources that are left in the penumbra are further reduced by cells attempting to normalize Na^+ and K^+ homoeostasis through the NKA. Second, the failure to fully reconstitute Na^+/K^+ homoeostasis further aggravates extracellular K^+ accumulation, promoting depolarization and thus the initiation of more PIDs. Third, the $[Na^+]_i$ increase reduces the driving force for glutamate uptake, further increasing extracellular glutamate half-life and thereby excitoxicity (Rossi et al., 2000). Finally, Na^+ accumulation in neurons and astrocytes leads to a cellular overload with Ca^{2+} through reverse action of the NCX. This is because, as intracellular Na^+ levels become exceedingly high in the ischemic penumbra due to the abovementioned mechanisms, NCX reverses its action to shuttle excess Na^+ out of the cells in exchange for more Ca^{2+}, contributing to Ca^{2+} overload.

In a recent study, we addressed these mechanisms experimentally during PIDs *in vivo* and *in vitro* (Gerkau et al., 2018). We used multiphoton and wide-field Na^+ and Ca^{2+} imaging in the *in vivo* rodent stroke model of middle cerebral artery occlusion (MCAO) and in tissue slices (Gerkau et al., 2018). As expected, we found an association between PIDs and propagating Na^+ elevations in neurons and astrocytes *in vivo*, as well as in tissue slices that underwent brief chemical ischemia (**Figure 4**). The blockade of NMDA-receptors reduced PID-related Na^+ and Ca^{2+} elevations in both cell types. The pharmacological inhibition of NCX revealed a strong reduction in ischemia-induced intracellular Ca^{2+} signaling in neurons and astrocytes and led to an increase in $[Na^+]_i$ in both cell types (Gerkau et al., 2018). Thus, these results provided direct experimental evidence that the reversal of NCX during metabolic

failure is a major source of cellular Ca^{2+} increases in neurons and astrocytes while dampening their Na^+ overload.

The role of NCX in ischemic damage was also investigated by other studies that used knockout strategies to target different NCX isoforms. The first study used two lines of complete knockout animals deficient for NCX2 and NCX3, respectively, and evaluated the effect of the deletion after inducing an ischemic stroke by MCAO (Molinaro et al., 2013). Both KO lines showed increased neuronal vulnerability and increased infarct sizes. In the second study, the authors conditionally overexpressed or deleted the NCX1 isoform in cortical and hippocampal neurons and investigated its influence on stroke outcome (Molinaro et al., 2016). The conditional deletion of neuronal NCX1 led to increased brain damage and neurological deficits, while the overexpression of NCX1 resulted in reduced ischemic volume and an amelioration of neuronal deficits. These findings are surprising, given that, presuming a reverse mode of NCX, a neuron-specific deletion of NCX1 should lead to a lower calcium concentration and less neurotoxicity in the penumbra in neurons. In line with this notion, pharmacological inhibition of NCX revealed a strong reduction in ischemia-induced intracellular Ca^{2+} levels in neurons during ischemia, and PIDs, in particular, and should therefore lead to a better outcome (Gerkau et al., 2018). On the other hand, a neuron-specific deletion of NCX (as used in Molinaro et al., 2016) should also lead to increased intracellular and decreased extracellular Na^+ levels under reverse-mode conditions, perhaps further decreasing the driving force for glutamate uptake into astrocytes. Therefore, it will be important to also directly measure membrane potentials, as well as glutamate, Na^+, and Ca^{2+} levels in neurons and astrocytes *in vivo* during different levels of ischemia to address these open questions (Rakers and Petzold, 2017). Likewise, the cell-specific role of NCX remains to be established. For example, a deletion of NCX in astrocytes should result in lower astroglial Ca^{2+} levels during ischemia, and this may lead to a decreased accumulation of glutamate due to less Ca^{2+}-dependent glutamate release by astrocytes. On the other hand, it may also decrease the driving force for Na^+-glutamate-cotransport during PIDs, so the net effect on glutamate is unclear.

Migraine

Familial hemiplegic migraine 2 (FHM2), which is a rare autosomal-dominant subtype of migraine with aura, is linked to a loss-of-function mutation in the α2 subunit of NKA (De Fusco et al., 2003). Migraine aura is induced by cortical spreading depressions (CSD), and accordingly, CSD induction is facilitated in heterozygous FHM2 knock-in animals carrying this mutation. Capuani et al. (2016) showed 50% less NKA expression and a reduction of GLT-1a in astrocytic processes at cortical glutamatergic synapses in the dentate gyrus (DG) of these mice. This caused a reduced glutamate and K^+ clearance by astrocytes in cortical acute slices (Capuani et al., 2016), indicating

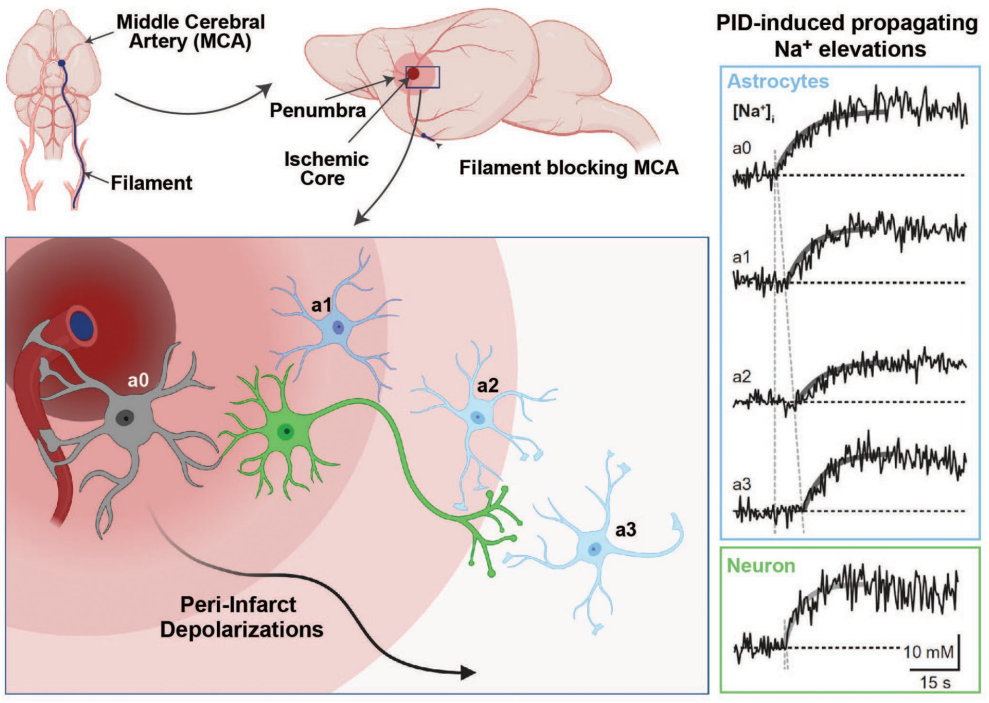

FIGURE 4 | Na^+ signaling in the experimental middle cerebral artery occlusion (MCAO) stroke model. Induction of an ischemic stroke by insertion of a filament into the internal carotid artery until the MCA is blocked **(upper panel).** In the ischemic core, dying cells initiate peri-infarct depolarizations (PIDs), which travel through the penumbra and lead to excess glutamate release and higher energy consumption **(bottom left panel)**. Glutamate uptake by astrocytes is accompanied by Na^+ cotransport through glutamate transporters, which results in detectable intracellular Na^+ elevations in response to PIDs (**right panel**; Na^+ traces adapted with permission from Gerkau et al. 2018; images created with BioRender.com).

that impaired glutamate clearance mechanisms may lead to the facilitation of CSDs. A recent study using the same model investigated synaptic plasticity processes in the hippocampus and found an abnormally increased long-term potentiation (LTP) in the dentate gyrus (DG), while CA1 LTP was not changed compared to wild type (WT) animals (Iure et al., 2019). Interestingly, basal synaptic transmission in these animals was unaltered in all investigated regions, pointing to an activity-dependent effect on synaptic plasticity processes. The previously described reduction in GLT-1a expression that is correlated to the reduced NKA α2-subunit expression may, thus, result in decreased glutamate clearance leading to the abnormally high LTP.

Of particular interest in this context is the finding that GLT-1 is not ubiquitously expressed at the same level within the hippocampus, but shows higher levels in the CA3 and DG, while in CA1 its expression is lower (Furuta et al., 1997), correlating with the electrophysiological LTP data. Another study investigated the impact of the heterozygous deletion of the NKA α2-subunit on behavior and reported increased anxiety-related behavior, reduced locomotor activity, and impaired spatial learning in the Morris water maze in these mice (Moseley et al., 2007). Thus, the reduction in α2 NKA activity either in the FHM2 loss-of-function mutation or heterozygous deletion of that subunit could play a crucial role in the observed memory deficits in patients with this type of migraine (Karner et al., 2012). Thus, the reduced NKA activity leads to dysregulated glutamate clearance, resulting in abnormally increased long-term synaptic plasticity, which may impact memory functions in patients (Dilekoz et al., 2015).

Aging

During aging, NKA activity declines in the CNS, but protein levels stay unchanged, pointing to an age-dependent downregulation of its activity (Scavone et al., 2000; Kawamoto et al., 2008; Vasconcelos et al., 2015). The decrease in NKA activity can lead to an increase in intracellular Ca^{2+}, most likely by the abovementioned downstream activation of reverse-mode NCX, which in turn may elicit excitotoxicity (Mattson and Liu, 2002). Kawamoto et al. (2008) found that the decreased NKA activity is also linked to changes in glutamate transport pathways, which again may lead to disturbances in the ionic homeostasis that may, if chronically perturbed, predispose to the development of neurodegenerative diseases (Kinoshita et al., 2016).

Mitochondria represent another important factor that can become compromised during aging and thereby increase the likelihood to develop a neurodegenerative disorder (Yankner et al., 2008). Impaired mitochondrial energy supply can directly affect NKA activity by producing less ATP, but also by production of more free radicals (Nathanson et al., 1995). Several studies showed that the NKA α subunit is sensitive to oxidative stress by free radicals, showing a degradation of the subunit (for review see Kinoshita et al., 2016).

A reduction of NKA activity by these different age-dependent mechanisms may result in a reduction in the Na^+ gradient that is crucial for the proper functioning of glutamate clearance mechanism after neuronal firing under healthy conditions. In this context, it has been shown that NKA impairment leads to a downregulation of synaptic AMPA receptors, which results in defective synaptic transmission and cognitive decline as a consequence (Zhang et al., 2009).

In addition to changes in glutamate receptor expression, the levels of EAAT glutamate transporters have been described to decrease in the cause of many neurodegenerative diseases (Sheldon and Robinson, 2007). As discussed above for the FHM2 model, the reduced capacity to remove glutamate out of the synaptic cleft after neuronal activity will lead to excitotoxicity, which will lead to further disruptions in NKA activity, thereby initiating a vicious circle.

Neurodegenerative Diseases

Alzheimer's disease (AD) is the most prevalent form of dementia and is characterized by memory loss and cognitive impairment. Its two pathological hallmarks are the extracellular deposition of amyloid-β peptide in senile plaques and the intracellular aggregation of hyperphosphorylated tau fibrils in neurofibrillary tangles (Hardy, 2006). Several studies have revealed that these proteopathic changes are also accompanied by altered NKA activity and a disturbed Na^+ homeostasis. An *in vitro* study showed that the acute application of Aβ oligomers to rat hippocampal neurons reduced NKA activity (Mark et al., 1995). This impairment resulted in an accumulation of intracellular Na^+ and successive influx of Ca^{2+}, pointing to an important role of the NKA in pathological dysregulation in AD (Mark et al., 1995). More recently, a decrease in hippocampal NKA activity, as well as a reduction in overall protein levels, was demonstrated in an AD mouse model (Dickey et al., 2005). The latter studies did not further differentiate between neuronal or glial NKA levels or activity. Others, however, found that the *in vitro* treatment of primary astrocytes with Aβ oligomers resulted in a downregulation of NKA and an imbalance of Na^+ and K^+ concentrations, an effect replicated in postmortem tissue from AD patients (Vitvitsky et al., 2012; Graham et al., 2015). As the NKA maintains the electrochemical Na^+ gradient that provides the main driving force for glutamate uptake by EAATs, this may in part explain changes observed in extracellular glutamate half-life in the vicinity of amyloid plaques (Hefendehl et al., 2016).

About 20% of familial forms of amyotrophic lateral sclerosis (ALS) are characterized by mutations in the superoxide dismutase 1 (SOD1) gene. One study found an enrichment of a protein complex consisting of α2-NKA and α-adducin in astrocytes of $SOD1^{G93A}$ model mice. The knockdown of both proteins in astrocytes or the pharmacological blockade of the NKA with digoxin prevented motor neuron degeneration (Gallardo et al., 2014). Interestingly, the same study also reported an upregulation of both proteins in spinal cord lysates of ALS patients. This suggested that chronic activation of the α2-NKA/α-adducin complex might represent a critical pathological mechanism for motor neuron degeneration that could serve as a potential target in this disease. Of note, mechanisms independent of NKA leading to ion disequilibrium in ALS have been described as well (Almad et al., 2016). Future studies will be necessary to reveal the impact of these changes on Na^+ homeostasis and regulation and glutamate levels.

CONCLUSIONS

Astrocytes are the main supportive cells of the CNS playing important homeostatic roles. Many of the astroglial regulatory processes that are initiated in response to neuronal activity are directly correlated to transient changes in their $[Na^+]_i$, which were demonstrated to occur in various preparations and brain regions. While it is widely accepted that astrocyte $[Na^+]_i$ indeed changes with different forms of neuronal activity, many highly relevant questions as to the functional consequences of such fluctuations in Na^+ still remain unanswered.

Of foremost importance is to further differentiate and thereby clarify the specific physiological functions of astrocytic Na^+-dependent signaling pathways and to separate them from neuronal ones. The central player mediating Na^+ efflux and controlling the distribution of all major ions in both cell types is the NKA, both by directly controlling the levels of Na^+ and K^+ and indirectly by affecting the transport of Ca^{2+} (*via* NCX), Cl^- (*via* NKCC1), and protons (*via* NHE or NBC). In addition, alteration of astrocytic Na^+ levels can have direct effects on glial signaling, as well as on neuronal properties, by changing the driving force for transmitter transporters. However, more studies addressing glia-specific NKA regulation, its relation to astroglial $[Na^+]_i$ and Na^+ signals, and the functional consequences of the latter, are needed. The same is true for most, if not all, other processes involving Na^+ transport across the plasma membrane and generating $[Na^+]_i$ changes in astrocytes.

Besides the direct effect of $[Na^+]_i$ on transporters and channels, there is increasing evidence that Na^+ can interact with several other binding partners. The latter include ion channels, GPCRs, trimeric G-proteins, or enzymes. By modulating the functions of these interacting proteins, changes in $[Na^+]_i$ can alter the physiological state of the cells. Furthermore, there is evidence that Na^+ is directly involved in gene regulation through Na^+-responsive elements, affecting the expression of early response genes. These atypical modulatory functions of Na^+ have mainly been investigated in cell types other than astrocytes; therefore, more experimental work needs to be performed to study their role in astrocytes. Such work could significantly impact our understanding of various CNS pathologies, where changes in several of the atypical Na^+-interacting partners have been described, but a possible direct link to Na^+ signals and especially Na^+ signals in astrocytes has not yet not been addressed.

Due to the technical progress in the field, our knowledge of astrocyte physiology and Na^+ signaling in particular has increased tremendously within the last 2 decades. These advances have revealed a role for Na^+ far more active than only offering a convenient, transporter-driving gradient. However, our understanding of its putative role as an intracellular messenger system and the extent to which it interacts with partners in astrocytes is far from complete. Until now, tools to study Na^+ within cells have been very limited in comparison to those available for Ca^{2+}. However, the development of techniques such as fluorescent lifetime imaging and genetic reporter animals could help elucidate the true importance of astrocytic Na^+ homeostasis under physiological as well as pathological conditions.

AUTHOR CONTRIBUTIONS

All authors contributed to the design, concept, and writing of this review. All authors contributed to the article and approved the submitted version.

FUNDING

This work was supported by grants to CR from the Deutsche Forschungsgemeinschaft DFG (SPP1757: Ro2327/8-2 and FOR2795: Ro2327/13-1). LF obtained a start-up grant from the SPP1757. GP is supported by the DFG (FOR 2795/PE1193/6-1), the European Union (EU) Joint Program Neurodegenerative Disease Research (JPND; Horizon 2020 Framework Programme, grant agreement 643417/DACAPO-AD), and the German Center for Neurodegenerative Diseases (DZNE).

REFERENCES

Acuna, A. I., Esparza, M., Kramm, C., Beltran, F. A., Parra, A. V., Cepeda, C., et al. (2013). A failure in energy metabolism and antioxidant uptake precede symptoms of Huntington's disease in mice. *Nat. Commun.* 4:2917. doi: 10.1038/ncomms3917

Aguado, F., Espinosa-Parrilla, J. F., Carmona, M. A., and Soriano, E. (2002). Neuronal activity regulates correlated network properties of spontaneous calcium transients in astrocytes in situ. *J. Neurosci.* 22, 9430–9444. doi: 10.1523/JNEUROSCI.22-21-09430.2002

Albrecht, J., Zielinska, M., and Norenberg, M. D. (2010). Glutamine as a mediator of ammonia neurotoxicity: a critical appraisal. *Biochem. Pharmacol.* 80, 1303–1308. doi: 10.1016/j.bcp.2010.07.024

Almad, A. A., Doreswamy, A., Gross, S. K., Richard, J. P., Huo, Y., Haughey, N., et al. (2016). Connexin 43 in astrocytes contributes to motor neuron toxicity in amyotrophic lateral sclerosis. *Glia* 64, 1154–1169. doi: 10.1002/glia.22989

Amzica, F., Massimini, M., and Manfridi, A. (2002). Spatial buffering during slow and paroxysmal sleep oscillations in cortical networks of glial cells *in vivo*. *J. Neurosci.* 22, 1042–1053. doi: 10.1523/JNEUROSCI.22-03-01042.2002

Aperia, A. (2007). New roles for an old enzyme: Na,K-ATPase emerges as an interesting drug target. *J. Intern. Med.* 261, 44–52. doi: 10.1111/j.1365-2796.2006.01745.x

Ash, M. R., Maher, M. J., Mitchell Guss, J., and Jormakka, M. (2012). The cation-dependent G-proteins: in a class of their own. *FEBS Lett.* 586, 2218–2224. doi: 10.1016/j.febslet.2012.06.030

Augustin, V., Bold, C., Wadle, S. L., Langer, J., Jabs, R., Philippot, C., et al. (2016). Functional anisotropic panglial networks in the lateral superior olive. *Glia* 64, 1892–1911. doi: 10.1002/glia.23031

Azarias, G., and Chatton, J. Y. (2011). Selective ion changes during spontaneous mitochondrial transients in intact astrocytes. *PLoS One* 6:e28505. doi: 10.1371/journal.pone.0028505

Barbour, B., Brew, H., and Attwell, D. (1991). Electrogenic uptake of glutamate and aspartate into glial cells isolated from the salamander (Ambystoma) retina. *J. Physiol.* 436, 169–193. doi: 10.1113/jphysiol.1991.sp018545

Bauer, D. E., Jackson, J. G., Genda, E. N., Montoya, M. M., Yudkoff, M., and Robinson, M. B. (2012). The glutamate transporter, GLAST, participates in a macromolecular complex that supports glutamate metabolism. *Neurochem. Int.* 61, 566–574. doi: 10.1016/j.neuint.2012.01.013

Ben-Ari, Y. (2001). Developing networks play a similar melody. *Trends Neurosci.* 24, 353–360. doi: 10.1016/S0166-2236(00)01813-0

Benjamin, A. M. (1987). Influence of Na^+, K^+, and Ca^{2+} on glutamine synthesis and distribution in rat brain cortex slices: a possible linkage of glutamine synthetase with cerebral transport processes and energetics in the astrocytes. *J. Neurochem.* 48, 1157–1164. doi: 10.1111/j.1471-4159.1987.tb05641.x

Ben-Kasus Nissim, T., Zhang, X., Elazar, A., Roy, S., Stolwijk, J. A., Zhou, Y., et al. (2017). Mitochondria control store-operated $Ca2^+$ entry through Na^+ and redox signals. *EMBO J.* 36, 797–815. doi: 10.15252/embj.201592481

Bennay, M., Langer, J., Meier, S. D., Kafitz, K. W., and Rose, C. R. (2008). Sodium signals in cerebellar purkinje neurons and Bergmann glial cells evoked by glutamatergic synaptic transmission. *Glia* 56, 1138–1149. doi: 10.1002/glia.20685

Bergles, D. E., Tzingounis, A. V., and Jahr, C. E. (2002). Comparison of coupled and uncoupled currents during glutamate uptake by GLT-1 transporters. *J. Neurosci.* 22, 10153–10162. doi: 10.1523/JNEUROSCI.22-23-10153.2002

Bernardinelli, Y., Azarias, G., and Chatton, J. Y. (2006). In situ fluorescence imaging of glutamate-evoked mitochondrial Na^+ responses in astrocytes. *Glia* 54, 460–470. doi: 10.1002/glia.20387

Bhattacharjee, A., and Kaczmarek, L. K. (2005). For K^+ channels, Na^+ is the new Ca^{2+}. *Trends Neurosci.* 28, 422–428. doi: 10.1016/j.tins.2005.06.003

Blaustein, M. P., Juhaszova, M., Golovina, V. A., Church, P. J., and Stanley, E. F. (2002). Na/Ca exchanger and PMCA localization in neurons and astrocytes. *Ann. N. Y. Acad. Sci.* 976, 356–366. doi: 10.1111/j.1749-6632.2002.tb04762.x

Blumenstein, Y., Maximyuk, O. P., Lozovaya, N., Yatsenko, N. M., Kanevsky, N., Krishtal, O., et al. (2004). Intracellular Na^+ inhibits voltage-dependent N-type Ca^{2+} channels by a G protein betagamma subunit-dependent mechanism. *J. Physiol.* 556, 121–134. doi: 10.1113/jphysiol.2003.056168

Boddum, K., Jensen, T. P., Magloire, V., Kristiansen, U., Rusakov, D. A., Pavlov, I., et al. (2016). Astrocytic GABA transporter activity modulates excitatory neurotransmission. *Nat. Commun.* 7:13572. doi: 10.1038/ncomms13572

Borges, K., and Kettenmann, H. (1995). Blockade of K^+ channels induced by AMPA/kainate receptor activation in mouse oligodendrocyte precursor cells is mediated by Na^+ entry. *J. Neurosci. Res.* 42, 579–593. doi: 10.1002/jnr.490420416

Breslin, K., Wade, J. J., Kongfatt, W., Harkin, J., Flanagan, B., Zalinge, H. V., et al. (2018). Potassium and sodium microdomains in thin astroglial processes: a computational model study. *PLoS Comput. Biol.* 14:e1006151. doi: 10.1371/journal.pcbi.1006151

Broer, S., and Brookes, N. (2001). Transfer of glutamine between astrocytes and neurons. *J. Neurochem.* 77, 705–719. doi: 10.1046/j.1471-4159.2001.00322.x

Brown, A. M., and Ransom, B. R. (2007). Astrocyte glycogen and brain energy metabolism. *Glia* 55, 1263–1271. doi: 10.1002/glia.20557

Capaldi, S., Suku, E., Antolini, M., Di Giacobbe, M., Giorgetti, A., and Buffelli, M. (2018). Allosteric sodium binding cavity in GPR3: a novel player in modulation of abeta production. *Sci. Rep.* 8:11102. doi: 10.1038/s41598-018-29475-7

Capuani, C., Melone, M., Tottene, A., Bragina, L., Crivellaro, G., Santello, M., et al. (2016). Defective glutamate and K^+ clearance by cortical astrocytes in familial hemiplegic migraine type 2. *EMBO Mol. Med.* 8, 967–986. doi: 10.15252/emmm.201505944

Chatton, J. Y., Magistretti, P. J., and Barros, L. F. (2016). Sodium signaling and astrocyte energy metabolism. *Glia* 64, 1667–1676. doi: 10.1002/glia.22971

Chatton, J. Y., Marquet, P., and Magistretti, P. J. (2000). A quantitative analysis of L-glutamate-regulated Na^+ dynamics in mouse cortical astrocytes: implications for cellular bioenergetics. *Eur. J. Neurosci.* 12, 3843–3853. doi: 10.1046/j.1460-9568.2000.00269.x

Chatton, J. Y., Pellerin, L., and Magistretti, P. J. (2003). GABA uptake into astrocytes is not associated with significant metabolic cost: implications for brain imaging of inhibitory transmission. *Proc. Natl. Acad. Sci. U. S. A.* 100, 12456–12461. doi: 10.1073/pnas.2132096100

Chesler, M. (2003). Regulation and modulation of pH in the brain. *Physiol. Rev.* 83, 1183–1221. doi: 10.1152/physrev.00010.2003

Cholet, N., Pellerin, L., Magistretti, P. J., and Hamel, E. (2002). Similar perisynaptic glial localization for the Na^+,K^+-ATPase α^2 subunit and the glutamate transporters GLAST and GLT-1 in the rat somatosensory cortex. *Cereb. Cortex* 12, 515–525. doi: 10.1093/cercor/12.5.515

Clausen, M. V., Hilbers, F., and Poulsen, H. (2017). The structure and function of the Na,K-ATPase isoforms in health and disease. *Front. Physiol.* 8:371. doi: 10.3389/fphys.2017.00371

Danbolt, N. C. (2001). Glutamate uptake. *Prog. Neurobiol.* 65, 1–105. doi: 10.1016/S0301-0082(00)00067-8

Dang, Q. D., and Di Cera, E. (1996). Residue 225 determines the Na^+-induced allosteric regulation of catalytic activity in serine proteases. *Proc. Natl. Acad. Sci. U. S. A.* 93, 10653–10656. doi: 10.1073/pnas.93.20.10653

De Fusco, M., Marconi, R., Silvestri, L., Atorino, L., Rampoldi, L., Morgante, L., et al. (2003). Haploinsufficiency of ATP1A2 encoding the Na^+/K^+ pump α^2 subunit associated with familial hemiplegic migraine type 2. *Nat. Genet.* 33, 192–196. doi: 10.1038/ng1081

Deitmer, J. W., Bröer, A., and Bröer, S. (2003). Glutamine efflux from astrocytes is mediated by multiple pathways. *J. Neurochem.* 87, 127–135. doi: 10.1046/j.1471-4159.2003.01981.x

Deitmer, J. W., and Rose, C. R. (1996). pH regulation and proton signalling by glial cells. *Prog. Neurobiol.* 48, 73–103. doi: 10.1016/0301-0082(95)00039-9

Dickey, C. A., Gordon, M. N., Wilcock, D. M., Herber, D. L., Freeman, M. J., and Morgan, D. (2005). Dysregulation of Na^+/K^+ ATPase by amyloid in APP+PS1 transgenic mice. *BMC Neurosci.* 6:7. doi: 10.1186/1471-2202-6-7

Dilekoz, E., Houben, T., Eikermann-Haerter, K., Balkaya, M., Lenselink, A. M., Whalen, M. J., et al. (2015). Migraine mutations impair hippocampal learning despite enhanced long-term potentiation. *J. Neurosci.* 35, 3397–3402. doi: 10.1523/JNEUROSCI.2630-14.2015

Dirnagl, U., Iadecola, C., and Moskowitz, M. A. (1999). Pathobiology of ischaemic stroke: an integrated view. *J. Neurosci.* 22, 391–397. doi: 10.1016/S0166-2236(99)01401-0

Doengi, M., Hirnet, D., Coulon, P., Pape, H. C., Deitmer, J. W., and Lohr, C. (2009). GABA uptake-dependent Ca^{2+} signaling in developing olfactory bulb astrocytes. *Proc. Natl. Acad. Sci. U. S. A.* 106, 17570–17575. doi: 10.1073/pnas.0809513106

Dryer, S. E. (1994). Na^+-activated K^+ channels: a new family of large-conductance ion channels. *Trends Neurosci.* 17, 155–160. doi: 10.1016/0166-2236(94)90093-0

Dzamba, D., Honsa, P., and Anderova, M. (2013). NMDA receptors in glial cells: pending questions. *Curr. Neuropharmacol.* 11, 250–262. doi: 10.2174/1570159X11311030002

Egan, T. M., Dagan, D., Kupper, J., and Levitan, I. B. (1992). Na^+-activated K^+ channels are widely distributed in rat CNS and in *Xenopus* oocytes. *Brain Res.* 584, 319–321. doi: 10.1016/0006-8993(92)90913-T

Eulenburg, V., and Gomeza, J. (2010). Neurotransmitter transporters expressed in glial cells as regulators of synapse function. *Brain Res. Rev.* 63, 103–112. doi: 10.1016/j.brainresrev.2010.01.003

Felix, L., Ziemens, D., Seifert, G., and Rose, C. R. (2020). Spontaneous ultraslow Na^+ fluctuations in the neonatal mouse brain. *Cell* 9:102. doi: 10.3390/cells9010102

Fraser, D. D., Duffy, S., Angelides, K. J., Perez-Velazquez, J. L., Kettenmann, H., and Macvicar, B. A. (1995). GABAA/benzodiazepine receptors in acutely isolated hippocampal astrocytes. *J. Neurosci.* 15, 2720–2732. doi: 10.1523/JNEUROSCI.15-04-02720.1995

Friedman, J. E., and Haddad, G. G. (1994). Anoxia induces an increase in intracellular sodium in rat central neurons in vitro. *Brain Res.* 663, 329–334. doi: 10.1016/0006-8993(94)91281-5

Furuta, A., Rothstein, J. D., and Martin, L. J. (1997). Glutamate transporter protein subtypes are expressed differentially during rat CNS development. *J. Neurosci.* 17, 8363–8375. doi: 10.1523/JNEUROSCI.17-21-08363.1997

Gallardo, G., Barowski, J., Ravits, J., Siddique, T., Lingrel, J. B., Robertson, J., et al. (2014). An α^2-Na/K ATPase/alpha-adducin complex in astrocytes triggers non-cell autonomous neurodegeneration. *Nat. Neurosci.* 17, 1710–1719. doi: 10.1038/nn.3853

Gallo, V., Zhou, J. M., Mcbain, C. J., Wright, P., Knutson, P. L., and Armstrong, R. C. (1996). Oligodendrocyte progenitor cell proliferation and lineage progression are regulated by glutamate receptor-mediated K^+ channel block. *J. Neurosci.* 16, 2659–2670. doi: 10.1523/JNEUROSCI.16-08-02659.1996

George, J., Baden, D. G., Gerwick, W. H., and Murray, T. F. (2012). Bidirectional influence of sodium channel activation on NMDA receptor-dependent cerebrocortical neuron structural plasticity. *Proc. Natl. Acad. Sci. U. S. A.* 109, 19840–19845. doi: 10.1073/pnas.1212584109

Gerkau, N. J., Rakers, C., Durry, S., Petzold, G. C., and Rose, C. R. (2018). Reverse NCX attenuates cellular sodium loading in metabolically compromised cortex. *Cereb. Cortex* 28, 4264–4280. doi: 10.1093/cercor/bhx280

Glanzman, D. L. (2010). Ion pumps get more glamorous. *Nat. Neurosci.* 13, 4–5. doi: 10.1038/nn0110-4

Graham, S. F., Nasarauddin, M. B., Carey, M., Mcguinness, B., Holscher, C., Kehoe, P. G., et al. (2015). Quantitative measurement of $[Na^+]$ and $[K^+]$

in postmortem human brain tissue indicates disturbances in subjects with Alzheimer's disease and dementia with Lewy bodies. *J. Alzheimers Dis.* 44, 851–857. doi: 10.3233/JAD-141869

Griemsmann, S., Hoft, S. P., Bedner, P., Zhang, J., Von Staden, E., Beinhauer, A., et al. (2015). Characterization of panglial gap junction networks in the thalamus, neocortex, and hippocampus reveals a unique population of glial cells. *Cereb. Cortex* 25, 3420–3433. doi: 10.1093/cercor/bhu157

Griffith, C. M., Xie, M. X., Qiu, W. Y., Sharp, A. A., Ma, C., Pan, A., et al. (2016). Aberrant expression of the pore-forming K_{ATP} channel subunit Kir6.2 in hippocampal reactive astrocytes in the 3xTg-AD mouse model and human Alzheimer's disease. *Neuroscience* 336, 81–101. doi: 10.1016/j.neuroscience.2016.08.034

Gulledge, A. T., Dasari, S., Onoue, K., Stephens, E. K., Hasse, J. M., and Avesar, D. (2013). A sodium-pump-mediated afterhyperpolarization in pyramidal neurons. *J. Neurosci.* 33, 13025–13041. doi: 10.1523/JNEUROSCI.0220-13.2013

Haloui, M., Taurin, S., Akimova, O. A., Guo, D. F., Tremblay, J., Dulin, N. O., et al. (2007). [Na]i-induced c-Fos expression is not mediated by activation of the 5'-promoter containing known transcriptional elements. *FEBS J.* 274, 3557–3567. doi: 10.1111/j.1742-4658.2007.05885.x

Hardy, J. (2006). A hundred years of Alzheimer's disease research. *Neuron* 52, 3–13. doi: 10.1016/j.neuron.2006.09.016

Hefendehl, J. K., Ledue, J., Ko, R. W., Mahler, J., Murphy, T. H., and Macvicar, B. A. (2016). Mapping synaptic glutamate transporter dysfunction *in vivo* to regions surrounding Aβ plaques by iGluSnFR two-photon imaging. *Nat. Commun.* 7:13441. doi: 10.1038/ncomms13441

Heja, L., Barabas, P., Nyitrai, G., Kekesi, K. A., Lasztoczi, B., Toke, O., et al. (2009). Glutamate uptake triggers transporter-mediated GABA release from astrocytes. *PLoS One* 4:e7153. doi: 10.1371/journal.pone.0007153

Hertz, L., Song, D., Xu, J., Peng, L., and Gibbs, M. E. (2015). Role of the astrocytic Na, K-ATPase in K homeostasis in brain: K uptake, signaling pathways and substrate utilization. *Neurochem. Res.* 40, 2506–2516. doi: 10.1007/s11064-014-1505-x

Hilgemann, D. W. (2020). Regulation of ion transport from within ion transit pathways. *J. Gen. Physiol.* 152:e201912455. doi: 10.1085/jgp.201912455

Ho, I. H., and Murrell-Lagnado, R. D. (1999). Molecular determinants for sodium-dependent activation of G protein-gated K^+ channels. *J. Biol. Chem.* 274, 8639–8648. doi: 10.1074/jbc.274.13.8639

Hossmann, K. A. (1996). Periinfarct depolarizations. *Cerebrovasc. Brain Metab. Rev.* 8, 195–208.

Howe, J. R., Baker, M., and Ritchie, J. M. (1992). On the block of outward potassium current in rabbit Schwann cells by internal sodium ions. *Proc. Biol. Sci.* 249, 309–316. doi: 10.1098/rspb.1992.0120

Huang, Y. H., and Bergles, D. E. (2004). Glutamate transporters bring competition to the synapse. *Curr. Opin. Neurobiol.* 14, 346–352. doi: 10.1016/j.conb.2004.05.007

Iadecola, C. (2007). Astrocytes take center stage in salt sensing. *Neuron* 54, 3–5. doi: 10.1016/j.neuron.2007.03.013

Illarionava, N. B., Brismar, H., Aperia, A., and Gunnarson, E. (2014). Role of Na,K-ATPase alpha1 and alpha2 isoforms in the support of astrocyte glutamate uptake. *PLoS One* 9:e98469. doi: 10.1371/journal.pone.0098469

Iure, A., Mazzocchetti, P., Bastioli, G., Picconi, B., Costa, C., Marchionni, I., et al. (2019). Differential effect of FHM2 mutation on synaptic plasticity in distinct hippocampal regions. *Cephalalgia* 39, 1333–1338. doi: 10.1177/0333102419839967

Jabs, R., Kirchhoff, F., Kettenmann, H., and Steinhauser, C. (1994). Kainate activates Ca^{2+}-permeable glutamate receptors and blocks voltage-gated K^+ currents in glial cells of mouse hippocampal slices. *Pflugers Arch.* 426, 310–319. doi: 10.1007/BF00374787

Jackson, J. G., and Robinson, M. B. (2018). Regulation of mitochondrial dynamics in astrocytes: mechanisms, consequences, and unknowns. *Glia* 66, 1213–1234. doi: 10.1002/glia.23252

Jorgensen, P. L., Håkansson, K. O., and Karlish, S. J. D. (2003). Structure and mechanism of Na,K-ATPase: functional sites and their interactions. *Annu. Rev. Physiol.* 65, 817–849. doi: 10.1146/annurev.physiol.65.092101.142558

Kafitz, K. W., Meier, S. D., Stephan, J., and Rose, C. R. (2008). Developmental profile and properties of sulforhodamine 101-labeled glial cells in acute brain slices of rat hippocampus. *J. Neurosci. Methods* 169, 84–92. doi: 10.1016/j.jneumeth.2007.11.022

Karner, E., Nachbauer, W., Bodner, T., Benke, T., Boesch, S., and Delazer, M. (2012). Long-term outcome of cognitive functions, emotional behavior, and quality of life in a family with familial hemiplegic migraine. *Cogn. Behav. Neurol.* 25, 85–92. doi: 10.1097/WNN.0b013e318259cb36

Karus, C., Gerkau, N. J., and Rose, C. R. (2017). Differential contribution of GLAST and GLT-1 to network sodium signaling in the early postnatal hippocampus. *Opera Med. Physiol.* 3, 71–83. doi: 10.20388/omp2017.003.0048

Karus, C., Mondragao, M. A., Ziemens, D., and Rose, C. R. (2015). Astrocytes restrict discharge duration and neuronal sodium loads during recurrent network activity. *Glia* 63, 936–957. doi: 10.1002/glia.22793

Katritch, V., Fenalti, G., Abola, E. E., Roth, B. L., Cherezov, V., and Stevens, R. C. (2014). Allosteric sodium in class A GPCR signaling. *Trends Biochem. Sci.* 39, 233–244. doi: 10.1016/j.tibs.2014.03.002

Kawamoto, E. M., Munhoz, C. D., Lepsch, L. B., De Sá Lima, L., Glezer, I., Markus, R. P., et al. (2008). Age-related changes in cerebellar phosphatase-1 reduce Na,K-ATPase activity. *Neurobiol. Aging* 29, 1712–1720. doi: 10.1016/j.neurobiolaging.2007.04.008

Kelly, T., Kafitz, K. W., Roderigo, C., and Rose, C. R. (2009). Ammonium-evoked alterations in intracellular sodium and pH reduce glial glutamate transport activity. *Glia* 57, 921–934. doi: 10.1002/glia.20817

Kettenmann, H., Backus, K. H., and Schachner, M. (1984). Aspartate, glutamate and gamma-aminobutyric acid depolarize cultured astrocytes. *Neurosci. Lett.* 52, 25–29. doi: 10.1016/0304-3940(84)90345-8

Kimelberg, H. K., Bowman, C., Biddlecome, S., and Bourke, R. S. (1979). Cation transport and membrane potential properties of primary astroglial cultures from neonatal rat brains. *Brain Res.* 177, 533–550. doi: 10.1016/0006-8993(79)90470-0

Kimelberg, H. K., Macvicar, B. A., and Sontheimer, H. (2006). Anion channels in astrocytes: biophysics, pharmacology, and function. *Glia* 54, 747–757. doi: 10.1002/glia.20423

Kinoshita, P. F., Leite, J. A., Orellana, A. M., Vasconcelos, A. R., Quintas, L. E. M., Kawamoto, E. M., et al. (2016). The influence of Na^+, K^+-ATPase on glutamate signaling in neurodegenerative diseases and senescence. *Front. Physiol.* 7:195. doi: 10.3389/fphys.2016.00195

Kirischuk, S., Heja, L., Kardos, J., and Billups, B. (2016). Astrocyte sodium signaling and the regulation of neurotransmission. *Glia* 64, 1655–1666. doi: 10.1002/glia.22943

Kirischuk, S., Kettenmann, H., and Verkhratsky, A. (1997). Na^+/Ca^{2+} exchanger modulates kainate-triggered Ca^{2+} signaling in Bergmann glial cells in situ. *FASEB J.* 11, 566–572. doi: 10.1096/fasebj.11.7.9212080

Kirischuk, S., Kettenmann, H., and Verkhratsky, A. (2007). Membrane currents and cytoplasmic sodium transients generated by glutamate transport in Bergmann glial cells. *Pflugers Arch.* 454, 245–252. doi: 10.1007/s00424-007-0207-5

Kirischuk, S., Parpura, V., and Verkhratsky, A. (2012). Sodium dynamics: another key to astroglial excitability? *Trends Neurosci.* 35, 497–506. doi: 10.1016/j.tins.2012.04.003

Klimanova, E. A., Sidorenko, S. V., Smolyaninova, L. V., Kapilevich, L. V., Gusakova, S. V., Lopina, O. D., et al. (2019). Ubiquitous and cell type-specific transcriptomic changes triggered by dissipation of monovalent cation gradients in rodent cells: physiological and pathophysiological implications. *Curr. Top. Membr.* 83, 107–149. doi: 10.1016/bs.ctm.2019.01.006

Knutson, P., Ghiani, C. A., Zhou, J. M., Gallo, V., and Mcbain, C. J. (1997). K^+ channel expression and cell proliferation are regulated by intracellular sodium and membrane depolarization in oligodendrocyte progenitor cells. *J. Neurosci.* 17, 2669–2682. doi: 10.1523/JNEUROSCI.17-08-02669.1997

Koltsova, S. V., Trushina, Y., Haloui, M., Akimova, O. A., Tremblay, J., Hamet, P., et al. (2012). Ubiquitous $[Na^+]_i/[K^+]_i$-sensitive transcriptome in mammalian cells: evidence for Ca^{2+}_i-independent excitation-transcription coupling. *PLoS One* 7:e38032. doi: 10.1371/journal.pone.0038032

Lalo, U., Pankratov, Y., Kirchhoff, F., North, R. A., and Verkhratsky, A. (2006). NMDA receptors mediate neuron-to-glia signaling in mouse cortical astrocytes. *J. Neurosci.* 26, 2673–2683. doi: 10.1523/JNEUROSCI.4689-05.2006

Lalo, U., Pankratov, Y., Wichert, S. P., Rossner, M. J., North, R. A., Kirchhoff, F., et al. (2008). $P2X_1$ and $P2X_5$ subunit form the functional P2X receptor in mouse cortical astrocytes. *J. Neurosci.* 28, 5473–5480. doi: 10.1523/JNEUROSCI.1149-08.2008

Langer, J., Gerkau, N. J., Derouiche, A., Kleinhans, C., Moshrefi-Ravasdjani, B., Fredrich, M., et al. (2017). Rapid sodium signaling couples glutamate uptake

to breakdown of ATP in perivascular astrocyte endfeet. *Glia* 65, 293–308. doi: 10.1002/glia.23092

Langer, J., and Rose, C. R. (2009). Synaptically induced sodium signals in hippocampal astrocytes in situ. *J. Physiol.* 587, 5859–5877. doi: 10.1113/jphysiol.2009.182279

Langer, J., Stephan, J., Theis, M., and Rose, C. R. (2012). Gap junctions mediate intercellular spread of sodium between hippocampal astrocytes in situ. *Glia* 60, 239–252. doi: 10.1002/glia.21259

Larsen, B. R., Stoica, A., and Macaulay, N. (2016). Managing brain extracellular K^+ during neuronal activity: the physiological role of the Na^+/K^+-ATPase subunit isoforms. *Front. Physiol.* 7:141. doi: 10.3389/fphys.2016.00141

Lauritzen, M., Dreier, J. P., Fabricius, M., Hartings, J. A., Graf, R., and Strong, A. J. (2011). Clinical relevance of cortical spreading depression in neurological disorders: migraine, malignant stroke, subarachnoid and intracranial hemorrhage, and traumatic brain injury. *J. Cereb. Blood Flow Metab.* 31, 17–35. doi: 10.1038/jcbfm.2010.191

Lederer, W. J., Niggli, E., and Hadley, R. W. (1990). Sodium-calcium exchange in excitable cells: fuzzy space. *Science* 248, 283–283. doi: 10.1126/science.2326638

Lee, M. Y., Song, H., Nakai, J., Ohkura, M., Kotlikoff, M. I., Kinsey, S. P., et al. (2006). Local subplasma membrane Ca^{2+} signals detected by a tethered Ca^{2+} sensor. *PNAS* 103, 13232–13237. doi: 10.1073/pnas.0605757103

Lenart, B., Kintner, D. B., Shull, G. E., and Sun, D. (2004). Na-K-Cl cotransporter-mediated intracellular Na^+ accumulation affects Ca^{2+} signaling in astrocytes in an in vitro ischemic model. *J. Neurosci.* 24, 9585–9597. doi: 10.1523/JNEUROSCI.2569-04.2004

Lerchundi, R., Kafitz, K. W., Winkler, U., Farfers, M., Hirrlinger, J., and Rose, C. R. (2019). FRET-based imaging of intracellular ATP in organotypic brain slices. *J. Neurosci. Res.* 97, 933–945. doi: 10.1002/jnr.24361

Lesage, F., Duprat, F., Fink, M., Guillemare, E., Coppola, T., Lazdunski, M., et al. (1994). Cloning provides evidence for a family of inward rectifier and G-protein coupled K^+ channels in the brain. *FEBS Lett.* 353, 37–42. doi: 10.1016/0014-5793(94)01007-2

Livingston, K. E., and Traynor, J. R. (2014). Disruption of the Na^+ ion binding site as a mechanism for positive allosteric modulation of the mu-opioid receptor. *Proc. Natl. Acad. Sci. U. S. A.* 111, 18369–18374. doi: 10.1073/pnas.1415013111

Lu, F. M., and Hilgemann, D. W. (2017). Na/K pump inactivation, subsarcolemmal Na measurements, and cytoplasmic ion turnover kinetics contradict restricted Na spaces in murine cardiac myocytes. *J. Gen. Physiol.* 149, 727–749. doi: 10.1085/jgp.201711780

Lu, Y. M., Roder, J. C., Davidow, J., and Salter, M. W. (1998). Src activation in the induction of long-term potentiation in CA1 hippocampal neurons. *Science* 279, 1363–1367. doi: 10.1126/science.279.5355.1363

Lujan, R., and Aguado, C. (2015). Localization and targeting of GIRK channels in mammalian central neurons. *Int. Rev. Neurobiol.* 123, 161–200. doi: 10.1016/bs.irn.2015.05.009

Ma, B., Buckalew, R., Du, Y., Kiyoshi, C. M., Alford, C. C., Wang, W., et al. (2016). Gap junction coupling confers isopotentiality on astrocyte syncytium. *Glia* 64, 214–226. doi: 10.1002/glia.22924

Maack, C., Cortassa, S., Aon, M. A., Ganesan, A. N., Liu, T., and O'rourke, B. (2006). Elevated cytosolic Na^+ decreases mitochondrial Ca^{2+} uptake during excitation-contraction coupling and impairs energetic adaptation in cardiac myocytes. *Circ. Res.* 99, 172–182. doi: 10.1161/01.RES.0000232546.92777.05

Macaulay, N., and Zeuthen, T. (2012). Glial K^+ clearance and cell swelling: key roles for cotransporters and pumps. *Neurochem. Res.* 37, 2299–2309. doi: 10.1007/s11064-012-0731-3

Macvicar, B. A., Tse, F. W., Crichton, S. A., and Kettenmann, H. (1989). GABA-activated Cl-channels in astrocytes of hippocampal slices. *J. Neurosci.* 9, 3577–3583. doi: 10.1523/JNEUROSCI.09-10-03577.1989

Magistretti, P. J., and Allaman, I. (2018). Lactate in the brain: from metabolic end-product to signalling molecule. *Nat. Rev. Neurosci.* 19, 235–249. doi: 10.1038/nrn.2018.19

Makman, M. H., Dvorkin, B., and Klein, P. N. (1982). Sodium ion modulates D2 receptor characteristics of dopamine agonist and antagonist binding sites in striatum and retina. *Proc. Natl. Acad. Sci. U. S. A.* 79, 4212–4216. doi: 10.1073/pnas.79.13.4212

Mark, R. J., Hensley, K., Butterfield, D. A., and Mattson, M. P. (1995). Amyloid beta-peptide impairs ion-motive ATPase activities: evidence for a role in loss of neuronal Ca^{2+} homeostasis and cell death. *J. Neurosci.* 15, 6239–6249. doi: 10.1523/JNEUROSCI.15-09-06239.1995

Martineau, M., Parpura, V., and Mothet, J. P. (2014). Cell-type specific mechanisms of D-serine uptake and release in the brain. *Front. Synaptic Neurosci.* 6:12. doi: 10.3389/fnsyn.2014.00012

Martinez-Hernandez, A., Bell, K. P., and Norenberg, M. D. (1977). Glutamine synthetase: glial localization in brain. *Science* 195, 1356–1358. doi: 10.1126/science.14400

Matsui, K. (2005). High-concentration rapid transients of glutamate mediate neural-glial communication via ectopic release. *J. Neurosci.* 25, 7538–7547. doi: 10.1523/JNEUROSCI.1927-05.2005

Matthias, K., Kirchhoff, F., Seifert, G., Hüttmann, K., Matyash, M., Kettenmann, H., et al. (2003). Segregated expression of AMPA-type glutamate receptors and glutamate transporters defines distinct astrocyte populations in the mouse hippocampus. *J. Neurosci.* 23, 1750–1758. doi: 10.1523/JNEUROSCI.23-05-01750.2003

Mattson, M. P., and Liu, D. (2002). Energetics and oxidative stress in synaptic plasticity and neurodegenerative disorders. *NeuroMolecular Med.* 2, 215–231. doi: 10.1385/NMM:2:2:215

Maucler, C., Pernot, P., Vasylieva, N., Pollegioni, L., and Marinesco, S. (2013). In vivo D-serine hetero-exchange through alanine-serine-cysteine (ASC) transporters detected by microelectrode biosensors. *ACS Chem. Neurosci.* 4, 772–781. doi: 10.1021/cn4000549

Meier, S. D., Kafitz, K. W., and Rose, C. R. (2008). Developmental profile and mechanisms of GABA-induced calcium signaling in hippocampal astrocytes. *Glia* 56, 1127–1137. doi: 10.1002/glia.20684

Melone, M., Ciriachi, C., Pietrobon, D., and Conti, F. (2019). Heterogeneity of astrocytic and neuronal GLT-1 at cortical excitatory synapses, as revealed by its colocalization with Na^+/K^+-ATPase α isoforms. *Cereb. Cortex* 29, 3331–3350. doi: 10.1093/cercor/bhy203

Meyer, J., Untiet, V., Fahlke, C., Gensch, T., and Rose, C. R. (2019). Quantitative determination of cellular $[Na^+]$ by fluorescence lifetime imaging with CoroNaGreen. *J. Gen. Physiol.* 151, 1319–1331. doi: 10.1085/jgp.201912404

Minieri, L., Pivonkova, H., Harantova, L., Anderova, M., and Ferroni, S. (2014). Intracellular Na^+ inhibits volume-regulated anion channel in rat cortical astrocytes. *J. Neurochem.* 132, 286–300. doi: 10.1111/jnc.12962

Mishima, T., and Hirase, H. (2010). In vivo intracellular recording suggests that gray matter astrocytes in mature cerebral cortex and hippocampus are electrophysiologically homogeneous. *J. Neurosci.* 30, 3093–3100. doi: 10.1523/JNEUROSCI.5065-09.2010

Molinaro, P., Cataldi, M., Cuomo, O., Viggiano, D., Pignataro, G., Sirabella, R., et al. (2013). "Genetically modified mice as a strategy to unravel the role played by the Na^+/Ca^{2+} exchanger in brain ischemia and in spatial learning and memory deficits" in *Sodium calcium exchange: A growing spectrum of pathophysiological implications. Advances in experimental medicine and biology. Vol. 961*. ed. L. Annunziato (Boston, MA: Springer US).

Molinaro, P., Sirabella, R., Pignataro, G., Petrozziello, T., Secondo, A., Boscia, F., et al. (2016). Neuronal NCX1 overexpression induces stroke resistance while knockout induces vulnerability via Akt. *J. Cereb. Blood Flow Metab.* 36, 1790–1803. doi: 10.1177/0271678X15611913

Moseley, A. E., Williams, M. T., Schaefer, T. L., Bohanan, C. S., Neumann, J. C., Behbehani, M. M., et al. (2007). Deficiency in Na,K-ATPase α isoform genes alters spatial learning, motor activity, and anxiety in mice. *J. Neurosci.* 27, 616–626. doi: 10.1523/JNEUROSCI.4464-06.2007

Moshrefi-Ravasdjani, B., Hammel, E. L., Kafitz, K. W., and Rose, C. R. (2017). Astrocyte sodium signalling and panglial spread of sodium signals in brain white matter. *Neurochem. Res.* 42, 2505–2518. doi: 10.1007/s11064-017-2197-9

Moshrefi-Ravasdjani, B., Ziemens, D., Pape, N., Färfers, M., and Rose, C. R. (2018). Action potential firing induces sodium transients in macroglial cells of the mouse corpus callosum. *Neuroglia* 1, 106–125. doi: 10.3390/neuroglia1010009

Moskowitz, M. A., Lo, E. H., and Iadecola, C. (2010). The science of stroke: mechanisms in search of treatments. *Neuron* 67, 181–198. doi: 10.1016/j.neuron.2010.07.002

Nathanson, J. A., Scavone, C., Scanlon, C., and Mckee, M. (1995). The cellular Na^+ pump as a site of action for carbon monoxide and glutamate: a mechanism for long-term modulation of cellular activity. *Neuron* 14, 781–794. doi: 10.1016/0896-6273(95)90222-8

Nedergaard, M., and Dirnagl, U. (2005). Role of glial cells in cerebral ischemia. *Glia* 50, 281–286. doi: 10.1002/glia.20205

Nita, I. I., Hershfinkel, M., Lewis, E. C., and Sekler, I. (2015). A crosstalk between Na^+ channels, Na^+/K^+ pump and mitochondrial Na^+ transporters controls glucose-dependent cytosolic and mitochondrial Na^+ signals. *Cell Calcium* 57, 69–75. doi: 10.1016/j.ceca.2014.12.007

Noda, M., and Hiyama, T. Y. (2015). Sodium sensing in the brain. *Pflugers Arch.* 467, 465–474. doi: 10.1007/s00424-014-1662-4

Noor, Z. N., Deitmer, J. W., and Theparambil, S. M. (2018). Cytosolic sodium regulation in mouse cortical astrocytes and its dependence on potassium and bicarbonate. *J. Cell. Physiol.* 234, 89–99. doi: 10.1002/jcp.26824

Olsen, M. L., and Sontheimer, H. (2004). Mislocalization of K_{ir} channels in malignant glia. *Glia* 46, 63–73. doi: 10.1002/glia.10346

Ono, Y., Ojima, K., Torii, F., Takaya, E., Doi, N., Nakagawa, K., et al. (2010). Skeletal muscle-specific calpain is an intracellular Na^+-dependent protease. *J. Biol. Chem.* 285, 22986–22998. doi: 10.1074/jbc.M110.126946

Orlov, S. N., and Hamet, P. (2006). Intracellular monovalent ions as second messengers. *J. Membr. Biol.* 210, 161–172. doi: 10.1007/s00232-006-0857-9

Orlov, S. N., Taurin, S., Tremblay, J., and Hamet, P. (2001). Inhibition of Na^+,K^+ pump affects nucleic acid synthesis and smooth muscle cell proliferation via elevation of the $[Na^+]_i/[K^+]_i$ ratio: possible implication in vascular remodelling. *J. Hypertens.* 19, 1559–1565. doi: 10.1097/00004872-200109000-00007

Palty, R., Silverman, W. F., Hershfunkel, M., Caporale, T., Sensi, S. L., Parnis, J., et al. (2010). NCLX is an essential component of mitochondrial Na^+/Ca^{2+} exchange. *PNAS* 107, 436–441. doi: 10.1073/pnas.0908099107

Pappalardo, L. W., Black, J. A., and Waxman, S. G. (2016). Sodium channels in astroglia and microglia. *Glia* 64, 1628–1645. doi: 10.1002/glia.22967

Parnis, J., Montana, V., Delgado-Martinez, I., Matyash, V., Parpura, V., Kettenmann, H., et al. (2013). Mitochondrial exchanger NCLX plays a major role in the intracellular Ca^{2+} signaling, gliotransmission, and proliferation of astrocytes. *J. Neurosci.* 33, 7206–7219. doi: 10.1523/JNEUROSCI.5721-12.2013

Paternain, A. V., Cohen, A., Stern-Bach, Y., and Lerma, J. (2003). A role for extracellular Na^+ in the channel gating of native and recombinant kainate receptors. *J. Neurosci.* 23, 8641–8648. doi: 10.1523/JNEUROSCI.23-25-08641.2003

Pellerin, L., and Magistretti, P. J. (2012). Sweet sixteen for ANLS. *J. Cereb. Blood Flow Metab.* 32, 1152–1166. doi: 10.1038/jcbfm.2011.149

Petrik, D., Myoga, M. H., Grade, S., Gerkau, N. J., Pusch, M., Rose, C. R., et al. (2018). Epithelial sodium channel regulates adult neural stem cell proliferation in a flow-dependent manner. *Cell Stem Cell* 22, 865–878.e8. doi: 10.1016/j.stem.2018.04.016

Petzold, G. C., and Murthy, V. N. (2011). Role of astrocytes in neurovascular coupling. *Neuron* 71, 782–797. doi: 10.1016/j.neuron.2011.08.009

Pulver, S. R., and Griffith, L. C. (2010). Spike integration and cellular memory in a rhythmic network from Na^+/K^+ pump current dynamics. *Nat. Neurosci.* 13, 53–59. doi: 10.1038/nn.2444

Raap, M., Biedermann, B., Braun, P., Milenkovic, I., Skatchkov, S. N., Bringmann, A., et al. (2002). Diversity of K_{ir} channel subunit mRNA expressed by retinal glial cells of the guinea-pig. *Neuroreport* 13, 1037–1040. doi: 10.1097/00001756-200206120-00012

Rakers, C., and Petzold, G. C. (2017). Astrocytic calcium release mediates peri-infarct depolarizations in a rodent stroke model. *J. Clin. Invest.* 127, 511–516. doi: 10.1172/JCI89354

Ransom, C. B., Sontheimer, H., and Janigro, D. (1996). Astrocytic inwardly rectifying potassium currents are dependent on external sodium ions. *J. Neurophysiol.* 76, 626–630. doi: 10.1152/jn.1996.76.1.626

Rishal, I., Keren-Raifman, T., Yakubovich, D., Ivanina, T., Dessauer, C. W., Slepak, V. Z., et al. (2003). Na^+ promotes the dissociation between galpha GDP and Gbeta gamma, activating G protein-gated K^+ channels. *J. Biol. Chem.* 278, 3840–3845. doi: 10.1074/jbc.C200605200

Robert, A., and Magistretti, P. J. (1997). AMPA/kainate receptor activation blocks K^+ currents via internal Na^+ increase in mouse cultured stellate astrocytes. *Glia* 20, 38–50. doi: 10.1002/(SICI)1098-1136(199705)20:1<38::AID-GLIA4>3.0.CO;2-1

Rojas, H., Colina, C., Ramos, M., Benaim, G., Jaffe, E. H., Caputo, C., et al. (2007). Na^+ entry via glutamate transporter activates the reverse Na^+/Ca^{2+} exchange and triggers $Ca(i)^{2+}$-induced Ca^{2+} release in rat cerebellar Type-1 astrocytes. *J. Neurochem.* 100, 1188–1202. doi: 10.1111/j.1471-4159.2006.04303.x

Rose, C. R., and Karus, C. (2013). Two sides of the same coin: sodium homeostasis and signaling in astrocytes under physiological and pathophysiological conditions. *Glia* 61, 1191–1205. doi: 10.1002/glia.22492

Rose, E. M., Koo, J. C., Antflick, J. E., Ahmed, S. M., Angers, S., and Hampson, D. R. (2009). Glutamate transporter coupling to Na,K-ATPase. *J. Neurosci.* 29, 8143–8155. doi: 10.1523/JNEUROSCI.1081-09.2009

Rose, C. R., and Ransom, B. R. (1996a). Intracellular sodium homeostasis in rat hippocampal astrocytes. *J. Physiol.* 491, 291–305. doi: 10.1113/jphysiol.1996.sp021216

Rose, C. R., and Ransom, B. R. (1996b). Mechanisms of H^+ and Na^+ changes induced by glutamate, kainate, and D-aspartate in rat hippocampal astrocytes. *J. Neurosci.* 16, 5393–5404. doi: 10.1523/JNEUROSCI.16-17-05393.1996

Rose, C. R., and Verkhratsky, A. (2016a). Glial ionic excitability: the role for sodium. *Glia* 64, 1609–1610. doi: 10.1002/glia.23012

Rose, C. R., and Verkhratsky, A. (2016b). Principles of sodium homeostasis and sodium signalling in astroglia. *Glia* 64, 1611–1627. doi: 10.1002/glia.22964

Rose, C. R., Ziemens, D., and Verkhratsky, A. (2020). On the special role of NCX in astrocytes: translating Na^+-transients into intracellular Ca^{2+} signals. *Cell Calcium* 86:102154. doi: 10.1016/j.ceca.2019.102154

Rossi, D. J., Oshima, T., and Attwell, D. (2000). Glutamate release in severe brain ischaemia is mainly by reversed uptake. *Nature* 403, 316–321. doi: 10.1038/35002090

Rothstein, J. D., Dykes-Hoberg, M., Pardo, C. A., Bristol, L. A., Jin, L., Kuncl, R. W., et al. (1996). Knockout of glutamate transporters reveals a major role for astroglial transport in excitotoxicity and clearance of glutamate. *Neuron* 16, 675–686. doi: 10.1016/S0896-6273(00)80086-0

Rusakov, D. A. (2015). Disentangling calcium-driven astrocyte physiology. *Nat. Rev. Neurosci.* 16, 226–233. doi: 10.1038/nrn3878

Sachse, F. B., Clarke, R., and Giles, W. R. (2017). No fuzzy space for intracellular Na^+ in healthy ventricular myocytes. *J. Gen. Physiol.* 149, 683–687. doi: 10.1085/jgp.201711826

Scavone, C., Glezer, I., Munhoz, C. D., De Sena Bernardes, C., and Markus, R. P. (2000). Influence of age on nitric oxide modulatory action on Na^+, K^+-ATPase activity through cyclic GMP pathway in proximal rat trachea. *Eur. J. Pharmacol.* 388, 1–7. doi: 10.1016/S0014-2999(99)00850-X

Schipke, C. G., Ohlemeyer, C., Matyash, M., Nolte, C., Kettenmann, H., and Kirchhoff, F. (2001). Astrocytes of the mouse neocortex express functional N-methyl-D-aspartate receptors. *FASEB J.* 15, 1270–1272. doi: 10.1096/fj.00-0439fje

Schroder, W., Seifert, G., Huttmann, K., Hinterkeuser, S., and Steinhauser, C. (2002). AMPA receptor-mediated modulation of inward rectifier K^+ channels in astrocytes of mouse hippocampus. *Mol. Cell. Neurosci.* 19, 447–458. doi: 10.1006/mcne.2001.1080

Selvam, B., Shamsi, Z., and Shukla, D. (2018). Universality of the sodium ion binding mechanism in class A G-protein-coupled receptors. *Angew. Chem. Int. Ed. Eng.* 57, 3048–3053. doi: 10.1002/anie.201708889

Sheldon, A. L., and Robinson, M. B. (2007). The role of glutamate transporters in neurodegenerative diseases and potential opportunities for intervention. *Neurochem. Int.* 51, 6–7. doi: 10.1016/j.neuint.2007.03.012

Shibasaki, K., Hosoi, N., Kaneko, R., Tominaga, M., and Yamada, K. (2017). Glycine release from astrocytes via functional reverse of GlyT1. *J. Neurochem.* 140, 395–403. doi: 10.1111/jnc.13741

Shimizu, H., Watanabe, E., Hiyama, T. Y., Nagakura, A., Fujikawa, A., Okado, H., et al. (2007). Glial Na_x channels control lactate signaling to neurons for brain $[Na^+]$ sensing. *Neuron* 54, 59–72. doi: 10.1016/j.neuron.2007.03.014

Silva, F. P. Jr., Antunes, O. A., De Alencastro, R. B., and De Simone, S. G. (2006). The Na^+ binding channel of human coagulation proteases: novel insights on the structure and allosteric modulation revealed by molecular surface analysis. *Biophys. Chem.* 119, 282–294. doi: 10.1016/j.bpc.2005.10.001

Siushansian, R., Tao, L., Dixon, S. D., and Wilson, J. X. (1997). Cerebral astrocytes transport ascorbic acid and dehydroascorbic acid through distinct mechanisms regulated by cyclic AMP. *J. Neurochem.* 68, 2378–2385. doi: 10.1046/j.1471-4159.1997.68062378.x

Smolyaninova, L. V., Shiyan, A. A., Kapilevich, L. V., Lopachev, A. V., Fedorova, T. N., Klementieva, T. S., et al. (2019). Transcriptomic changes triggered by ouabain in rat cerebellum granule cells: role of alpha3- and alpha1-Na^+,K^+-ATPase-mediated signaling. *PLoS One* 14:e0222767. doi: 10.1371/journal.pone.0222767

Song, D., and Du, T. (2014). Ammonium activates ouabain-activated signalling pathways in astrocytes: therapeutic potential of ouabain antagonist. *Curr. Neuropharmacol.* 12, 334–341. doi: 10.2174/1570159X12666140828222115

Stoica, A., Larsen, B. R., Assentoft, M., Holm, R., Holt, M. G., Vilhardt, F., et al. (2017). The α2β2 isoform combination dominates the astrocytic Na^+/K^+-ATPase activity and is rendered nonfunctional by the α2.G301R famial

hemiplegic migraine type 2-associated mutation. *Glia* 65, 1777–1793. doi: 10.1002/glia.23194

Strasser, A., Wittmann, H. J., Schneider, E. H., and Seifert, R. (2015). Modulation of GPCRs by monovalent cations and anions. *Naunyn Schmiedeberg's Arch. Pharmacol.* 388, 363–380. doi: 10.1007/s00210-014-1073-2

Su, G., Kintner, D. B., and Sun, D. (2002). Contribution of Na^+-K^+-Cl^- cotransporter to high-$[K^+]_o$-induced swelling and EAA release in astrocytes. *Am. J. Phys. Cell Phys.* 282, 1136–1146. doi: 10.1152/ajpcell.00478.2001

Sui, J. L., Chan, K. W., and Logothetis, D. E. (1996). Na^+ activation of the muscarinic K^+ channel by a G-protein-independent mechanism. *J. Gen. Physiol.* 108, 381–391. doi: 10.1085/jgp.108.5.381

Sun, X. L., Zeng, X. N., Zhou, F., Dai, C. P., Ding, J. H., and Hu, G. (2008). KATP channel openers facilitate glutamate uptake by GluTs in rat primary cultured astrocytes. *Neuropsychopharmacology* 33, 1336–1342. doi: 10.1038/sj.npp.1301501

Taurin, S., Dulin, N. O., Pchejetski, D., Grygorczyk, R., Tremblay, J., Hamet, P., et al. (2002). C-Fos expression in ouabain-treated vascular smooth muscle cells from rat aorta: evidence for an intracellular-sodium-mediated, calcium-independent mechanism. *J. Physiol.* 543, 835–847. doi: 10.1113/jphysiol.2002.023259

Theparambil, S. M., Naoshin, Z., Thyssen, A., and Deitmer, J. W. (2015). Reversed electrogenic sodium bicarbonate cotransporter 1 is the major acid loader during recovery from cytosolic alkalosis in mouse cortical astrocytes. *J. Physiol.* 593, 3533–3547. doi: 10.1113/JP270086

Theparambil, S. M., Ruminot, I., Schneider, H. P., Shull, G. E., and Deitmer, J. W. (2014). The electrogenic sodium bricarbonate cotransporter NBCe1 is a high-affinity bicarbonate carrier in cortical astrocytes. *J. Neurosci.* 34, 1148–1157. doi: 10.1523/JNEUROSCI.2377-13.2014

Todd, A. C., Marx, M. C., Hulme, S. R., Broer, S., and Billups, B. (2017). SNAT3-mediated glutamine transport in perisynaptic astrocytes in situ is regulated by intracellular sodium. *Glia* 65, 900–916. doi: 10.1002/glia.23133

Turovsky, E., Theparambil, S. M., Kasymov, V., Deitmer, J. W., Del Arroyo, A. G., Ackland, G. L., et al. (2016). Mechanisms of CO2/H^+ sensitivity of astrocytes. *J. Neurosci.* 36, 10750–10758. doi: 10.1523/JNEUROSCI.1281-16.2016

Unichenko, P., Dvorzhak, A., and Kirischuk, S. (2013). Transporter-mediated replacement of extracellular glutamate for GABA in the developing murine neocortex. *Eur. J. Neurosci.* 38, 3580–3588. doi: 10.1111/ejn.12380

Unichenko, P., Myakhar, O., and Kirischuk, S. (2012). Intracellular Na^+ concentration influences short-term plasticity of glutamate transporter-mediated currents in neocortical astrocytes. *Glia* 60, 605–614. doi: 10.1002/glia.22294

Untiet, V., Kovermann, P., Gerkau, N. J., Gensch, T., Rose, C. R., and Fahlke, C. (2017). Glutamate transporter-associated anion channels adjust intracellular chloride concentrations during glial maturation. *Glia* 65, 388–400. doi: 10.1002/glia.23098

Uwechue, N. M., Marx, M., Chevy, Q., and Billups, B. (2012). Activation of glutamate transport evokes rapid glutamine release from perisynaptic astrocytes. *J. Physiol.* 590, 2317–2331. doi: 10.1113/jphysiol.2011.226605

Van Damme, P., Van Den Bosch, L., Van Houtte, E., Eggermont, J., Callewaert, G., and Robberecht, W. (2002). Na^+ entry through AMPA receptors results in voltage-gated k^+ channel blockade in cultured rat spinal cord motoneurons. *J. Neurophysiol.* 88, 965–972. doi: 10.1152/jn.2002.88.2.965

Vasconcelos, A. R., Kinoshita, P. F., Yshii, L. M., Marques Orellana, A., Böhmer, A. E., De Sá Lima, L., et al. (2015). Effects of intermittent fasting on age-related changes on Na,K-ATPase activity and oxidative status induced by lipopolysaccharide in rat hippocampus. *Neurobiol. Aging* 36, 1914–1923. doi: 10.1016/j.neurobiolaging.2015.02.020

Verkhratsky, A., and Nedergaard, M. (2018). Physiology of astroglia. *Physiol. Rev.* 98, 239–389. doi: 10.1152/physrev.00042.2016

Verkhratsky, A., Pankratov, Y., Lalo, U., and Nedergaard, M. (2012). P2X receptors in neuroglia. *Wiley Interdiscip. Rev. Membr. Transp. Signal* 1. doi: 10.1002/wmts.12

Verkhratsky, A., Trebak, M., Perocchi, F., Khananshvili, D., and Sekler, I. (2018). Crosslink between calcium and sodium signalling. *Exp. Physiol.* 103, 157–169. doi: 10.1113/EP086534

Verkhratsky, A., Untiet, V., and Rose, C. R. (2019). Ionic signalling in astroglia beyond calcium. *J. Physiol.* 598, 1655–1670. doi: 10.1113/JP277478

Vitvitsky, V. M., Garg, S. K., Keep, R. F., Albin, R. L., and Banerjee, R. (2012). Na^+ and K^+ ion imbalances in Alzheimer's disease. *Biochim. Biophys. Acta* 1822, 1671–1681. doi: 10.1016/j.bbadis.2012.07.004

Volterra, A., Liaudet, N., and Savtchouk, I. (2014). Astrocyte Ca^{2+} signalling: an unexpected complexity. *Nat. Rev. Neurosci.* 15, 327–335. doi: 10.1038/nrn3725

Wade, J. J., Breslin, K., Wong-Lin, K., Harkin, J., Flanagan, B., Van Zalinge, H., et al. (2019). Calcium microdomain formation at the perisynaptic cradle due to NCX reversal: a computational study. *Front. Cell. Neurosci.* 13:185. doi: 10.3389/fncel.2019.00185

Wallraff, A., Kohling, R., Heinemann, U., Theis, M., Willecke, K., and Steinhauser, C. (2006). The impact of astrocytic gap junctional coupling on potassium buffering in the hippocampus. *J. Neurosci.* 26, 5438–5447. doi: 10.1523/JNEUROSCI.0037-06.2006

Wang, W., Whorton, M. R., and Mackinnon, R. (2014). Quantitative analysis of mammalian GIRK2 channel regulation by G proteins, the signaling lipid PIP2 and Na^+ in a reconstituted system. *Elife* 3:e03671. doi: 10.7554/eLife.03671

Wilson, C. S., and Mongin, A. A. (2018). Cell volume control in healthy brain and neuropathologies. *Curr. Top. Membr.* 81, 385–455. doi: 10.1016/bs.ctm.2018.07.006

Winkler, U., Seim, P., Enzbrenner, Y., Kohler, S., Sicker, M., and Hirrlinger, J. (2017). Activity-dependent modulation of intracellular ATP in cultured cortical astrocytes. *J. Neurosci. Res.* 95, 2172–2181. doi: 10.1002/jnr.24020

Yakubovich, D., Rishal, I., and Dascal, N. (2005). Kinetic modeling of Na^+-induced, Gbetagamma-dependent activation of G protein-gated K^+ channels. *J. Mol. Neurosci.* 25, 7–19. doi: 10.1385/JMN:25:1:007

Yankner, B. A., Lu, T., and Loerch, P. (2008). The aging brain. *Annu. Rev. Pathol.* 3, 41–66. doi: 10.1146/annurev.pathmechdis.2.010506.092044

Yu, X. M., and Salter, M. W. (1998). Gain control of NMDA-receptor currents by intracellular sodium. *Nature* 396, 469–474. doi: 10.1038/24877

Yu, X. M., and Salter, M. W. (1999). Src, a molecular switch governing gain control of synaptic transmission mediated by N-methyl-D-aspartate receptors. *Proc. Natl. Acad. Sci. U. S. A.* 96, 7697–7704. doi: 10.1073/pnas.96.14.7697

Yuan, X., Eisen, A. M., Mcbain, C. J., and Gallo, V. (1998). A role for glutamate and its receptors in the regulation of oligodendrocyte development in cerebellar tissue slices. *Development* 125, 2901–2914.

Zarzycka, B., Zaidi, S. A., Roth, B. L., and Katritch, V. (2019). Harnessing ion-binding sites for GPCR pharmacology. *Pharmacol. Rev.* 71, 571–595. doi: 10.1124/pr.119.017863

Zhang, D., Hou, Q., Wang, M., Lin, A., Jarzylo, L., Navis, A., et al. (2009). Na,K-ATPase activity regulates AMPA receptor turnover through proteasome-mediated proteolysis. *J. Neurosci.* 29, 4498–4511. doi: 10.1523/JNEUROSCI.6094-08.2009

Zhong, C. J., Chen, M. M., Lu, M., Ding, J. H., Du, R. H., and Hu, G. (2019). Astrocyte-specific deletion of Kir6.1/K-ATP channel aggravates cerebral ischemia/reperfusion injury through endoplasmic reticulum stress in mice. *Exp. Neurol.* 311, 225–233. doi: 10.1016/j.expneurol.2018.10.005

Zhou, Y., and Danbolt, N. C. (2013). GABA and glutamate transporters in the brain. *Front. Endocrinol.* 4:165. doi: 10.3389/fendo.2013.00165

Zhou, M., and Kimelberg, H. K. (2001). Freshly isolated hippocampal CA1 astrocytes comprise two populations differing in glutamate transporter and AMPA receptor expression. *J. Neurosci.* 21, 7901–7908. doi: 10.1523/JNEUROSCI.21-20-07901.2001

Zhou, M., Schools, G. P., and Kimelberg, H. K. (2006). Development of $GLAST^+$ astrocytes and $NG2^+$ glia in rat hippocampus CA1: mature astrocytes are electrophysiologically passive. *J. Neurophysiol.* 95, 134–143. doi: 10.1152/jn.00570.2005

Ziemens, D., Oschmann, F., Gerkau, N. J., and Rose, C. R. (2019). Heterogeneity of activity-induced sodium transients between astrocytes of the mouse hippocampus and neocortex: mechanisms and consequences. *J. Neurosci.* 39, 2620–2634. doi: 10.1523/JNEUROSCI.2029-18.2019

Conflict of Interest: The authors declare that the research was conducted in the absence of any commercial or financial relationships that could be construed as a potential conflict of interest.

On the Origin of Ultraslow Spontaneous Na^+ Fluctuations in Neurons of the Neonatal Forebrain.

Perez, C., ***Felix, L****., Rose, C. R., Ullah, G.*

J Neurophysiology DOI: 10.1101/2020.05.29.123026 (2020)

Impact factor 2020: 2.66

I performed

- All sodium, calcium wide field experiments and analysis

I contributed to

- The experimental design
- Interpretation of data
- Drafting and revision of manuscript and figures

Received: 13 March 2020 | Revised: 30 April 2020 | Accepted: 6 May 2020

DOI: 10.1111/ejn.14780

SPECIAL ISSUE REVIEW

Molecular and Synaptic Mechanisms

EJN European Journal of Neuroscience FENS WILEY

Astrocytes of the early postnatal brain

Lisa Felix | **Jonathan Stephan** | **Christine R. Rose**

Institute of Neurobiology, Faculty of Mathematics and Natural Sciences, Heinrich Heine University Duesseldorf, Duesseldorf, Germany

Correspondence
Christine R. Rose, Institute of Neurobiology, Faculty of Mathematics and Natural Sciences, Heinrich Heine University Duesseldorf, Universitaetsstrasse 1, D-40225 Duesseldorf, Germany.
Email: rose@hhu.de

Funding information
Deutsche Forschungsgemeinschaft, Grant/Award Number: Ro2327/8-2

Abstract

In the rodent forebrain, the majority of astrocytes are generated during the early postnatal phase. Following differentiation, astrocytes undergo maturation which accompanies the development of the neuronal network. Neonate astrocytes exhibit a distinct morphology and domain size which differs to their mature counterparts. Moreover, many of the plasma membrane proteins prototypical for fully developed astrocytes are only expressed at low levels at neonatal stages. These include connexins and Kir4.1, which define the low membrane resistance and highly negative membrane potential of mature astrocytes. Newborn astrocytes moreover express only low amounts of GLT-1, a glutamate transporter critical later in development. Furthermore, they show specific differences in the properties and spatio-temporal pattern of intracellular calcium signals, resulting from differences in their repertoire of receptors and signalling pathways. Therefore, roles fulfilled by mature astrocytes, including ion and transmitter homeostasis, are underdeveloped in the young brain. Similarly, astrocytic ion signalling in response to neuronal activity, a process central to neuron–glia interaction, differs between the neonate and mature brain. This review describes the unique functional properties of astrocytes in the first weeks after birth and compares them to later stages of development. We conclude that with an immature neuronal network and wider extracellular space, astrocytic support might not be as demanding and critical compared to the mature brain. The delayed differentiation and maturation of astrocytes in the first postnatal weeks might thus reflect a reduced need for active, energy-consuming regulation of the extracellular space and a less tight control of glial feedback onto synaptic transmission.

Abbreviations: AMPA, α-amino-3-hydroxy-5-methyl-4-isoxazolepropionic acid receptor; ATP, Adenosine triphosphate; cAMP, Cyclic adenosine monophosphate; C_M, Membrane Capacitance; Cx, Connexin; EAAT1/2, Excitatory amino acid transporter 1/2; ECS, Extracellular space; E_M, Membrane potential; ENO, Early network oscillation; GABA, γ-aminobutyric acid; GAT, GABA transporter; GDP, Giant depolarizing potential; GFAP, Glial fibrillary acidic protein; GLAST, Glutamate/aspartate transporter; GLT-1, Glutamate transporter 1; GlyT, Glycine transporter; K_2P, Two-pore domain K^+ channel; KCC2, Potassium Chloride co-transporter 2; Kir, Inwardly rectifying K^+ channel; K_V, Voltage-activated K^+ channel; mGluR, Metabotropic glutamate receptor; nAChR, Nicotinic acetylcholine receptor; NCX, Sodium potassium exchanger; NKA, Sodium potassium ATPase; NKCC1, Sodium potassium 2 chloride co-transporter 1; NMDA, N-methyl-D-aspartate receptor; PAP, Peripheral astrocytic processes; R_M, Membrane resistance; SR101, Sulforhodamine 101; TRP, Transient receptor potential channel; TTX, Tetrodotoxin.

Edited by Alexej Verkhratsky

[Correction added on 25 June 2020, after first online publication: URL for peer review history has been corrected.]
The peer review history for this article is available at https://publons.com/publon/10.1111/EJN.14780

KEYWORDS
calcium, extracellular potassium, forebrain, glutamate transport, mouse

1 | INTRODUCTION

In the forebrain of rodents, the majority of astrocytes are generated postnatally, at a time point when neuronal differentiation is already largely terminated (Freeman, 2010; Kriegstein & Alvarez-Buylla, 2009). The early postnatal differentiation of astrocytes accompanies the development of the neuronal network, and both processes interact and influence each other. While cells of the astrocytic lineage themselves are key players in the regulation of both neuro- and gliogenesis (Abbott, Ronnback, & Hansson, 2006; Campbell & Götz, 2002; Heins et al., 2002; Kriegstein & Alvarez-Buylla, 2009), astrocytic input in particular has also been shown to be critical for proper synapse and circuit formation in the postnatal brain (Allen & Eroglu, 2017; Clarke & Barres, 2013). The ability of astrocytes to promote neuronal network formation is undoubtedly underpinned by their special properties which change along with their maturation. On the other hand side, astrocytes themselves are too subjected to constant modulation and fine-tuning via a variety of pathways (Freeman, 2010). Not surprisingly then, recent analysis has revealed significant changes in the transcriptome of astrocytes during the first weeks after birth (Cahoy et al., 2008). In addition to this developmental heterogeneity, there is a notable regional heterogeneity. This encompasses morphology, protein expression and signalling pathways, resulting in a substantial diversity of astrocytes that reflects their functional adaptations to the given local neural networks (Zhang & Barres, 2010; Khakh & Sofroniev, 2015). Notably, such heterogeneity is not only observed between different brain regions, such as the hippocampus and cortex, but also within the latter (Seifert & Steinhäuser, 2018; Miller et al., 2019).

In this review, we will give an overview on the properties of astrocytes of the neonate rodent brain, which are indeed very different from mature astrocytes found at later stages of postnatal development. Special focus will be put onto aspects relevant for the specific functions of astrocytes at synapses: the formation of perisynaptic processes and gap junctional coupling, regulation of extracellular K^+ homeostasis and uptake of neurotransmitters, as well as intracellular calcium signalling. For astrocytes' involvement in the formation of blood vessels and their functional roles at the blood–brain barrier during postnatal development, we refer the reader to excellent recent reviews covering this subject (e.g. Abbott et al., 2006; Iadecola, 2017).

2 | GENESIS AND MORPHOLOGICAL CHARACTERISTICS OF ASTROCYTES IN THE NEONATE FOREBRAIN

The genesis of astrocytes is a complex multiphase process, which occurs in several waves, and is only completed after birth in the forebrain of rodents (Molofsky & Deneen, 2015). In the developing cortex of vertebrates, astrocytes begin life as neural stem cells in the subventricular zone which undergo the "gliogenic switch" at around E16-18 in order to form astrocyte precursor cells (Ge, Miyawaki, Gage, Jan, & Jan, 2013). These newly formed astrocytes (much like newly formed neurons) reach their final destinations within the cortex by migrating along radial glia. However, migration is not yet complete during early postnatal development, when radial glia are in the process of losing their guiding processes before differentiating themselves (Kriegstein & Alvarez-Buylla, 2009).

While this "second wave" of astrocytes is travelling through the tissue (albeit not reaching quite as far as their "first wave" predecessors), proliferation is also underway throughout the cortex, with astrocytic numbers increasing strongly between birth and the end of the third postnatal week (Kriegstein & Alvarez-Buylla, 2009). During this stage, new astrocytes are formed from differentiating radial glia, subventricular zone progenitors and division of local immature astrocytes and go on to make up around 50% of all astrocytes in the mature cortex (Ge et al., 2013; Molofsky & Deneen, 2015). This time frame, covering the first postnatal weeks in rodents, is also the time period in which the growth of neuronal dendrites and synapses surges and in which mature neuronal communication and networks properties develop (Freeman, 2010; Semple, Blomgren, Gimlin, Ferriero, & Noble-Haeusslein, 2013; Wang & Bordey, 2008).

It is well established that astrocytes—like neurons—are a heterogeneous cell type (Khakh & Sofroniew, 2015; Rusakov, Bard, Stewart, & Henneberger, 2014; Wang & Bordey, 2008; Zhang & Barres, 2010), and several strategies are commonly used for their identification in brain tissue. Besides immunohistochemistry, an approach often employed is the use of transgenic mice, in which a fluorescent protein is expressed under the control of a promotor predominately/specifically active in astrocytes, such as for glial fibrillary acidic protein (GFAP) (Hirrlinger, Scheller, Braun, Hirrlinger, & Kirchhoff, 2006; Nolte et al., 2001; Zhuo et al., 1997),

glutamate transporters GLAST or GLT-1 (glutamate/aspartate transporter and glutamate transporter-1, respectively) (Mori et al., 2006; Yang et al., 2011) or Aldh1/L1 (Morel et al., 2019; Yang et al., 2011). Alternatively, the vital fluorescent marker sulforhodamine 101 (SR101), which specifically stains astrocytes in the healthy forebrain (Kafitz, Meier, Stephan, & Rose, 2008; Nimmerjahn & Helmchen, 2012; Schnell et al., 2015), may be used in living tissue.

The use of such approaches has revealed that astrocytes undergo substantial changes in their density and cellular morphology during early postnatal development of the forebrain. Studies employing GFAP as a marker have found that the density of astrocytes in the first postnatal week after birth is significantly lower than that in the juvenile and adult brain (Kimoto, Eto, Abe, Kato, & Araki, 2009; Nixdorf-Bergweiler, Albrecht, & Heinemann, 1994; Schreiner et al., 2014) (Figure 1a,b). The increase in astrocyte density is accompanied by an increase in GFAP levels (Kim et al., 2011; Schreiner et al., 2014) (Figure 1a,b). GFAP not only serves as an important structural component of the cytoskeleton, but is also involved in the anchoring and trafficking of different proteins to the membrane (including GLAST and GLT-1 (Middeldorp & Hol, 2011; Sullivan et al., 2007)), thereby promoting the postnatal maturation of astrocytes.

While growing in number and overall density, astrocytes also rearrange their morphology. During the first two postnatal weeks, astrocytes in grey matter exhibit a less delicate and complex architecture of their fine processes (Figure 1d) (Bushong, Martone, & Ellisman, 2004; Morel, Higashimori, Tolman, & Yang, 2014). Mature astrocytes, in contrast, are characterized by numerous very thin processes, called PAPs (peripheral astrocytic processes) (Derouiche & Frotscher, 2001) that reach out to contact many thousands of synapses (Reichenbach, Derouiche, & Kirchhoff, 2010; Ventura & Harris, 1999).

Furthermore, at early postnatal stages, astrocytes do not display the discrete tiling characteristic of mature brains, in which they occupy non-overlapping individual domains (Bushong, Martone, Jones, & Ellisman, 2002; Halassa, Fellin, Takano, Dong, & Haydon, 2007; Nedergaard, Ransom, & Goldman, 2003). Instead, neonate astrocytes exhibit long processes reaching beyond the borders of their main territory, invading the domains of neighbouring astrocytes (Bushong et al., 2004) (Figure 1d). Notably, in the mature brain, astrocyte tiling may be lost again in response to disease (Oberheim et al., 2008). Formation of discrete astrocytic domains from postnatal day (P) 7 to P26 is accompanied by an approximately fourfold increase in the number of glutamatergic synapses present in the domain of an individual astrocyte (Morel et al., 2014). Silencing glutamatergic synapses during this period results in a reduced domain size, a reduced number of synapses contacted by each astrocyte and a reduced expression of GLT-1 at P26. This growth-promoting effect of glutamatergic transmission on maturing astrocytes has been reported to be related to activation of mGluR5 (metabotropic glutamate receptor 5) and astrocytic calcium signalling (Morel et al., 2014).

3 | CONNEXINS AND ASTROCYTE COUPLING

Astrocytes in the mature mouse hippocampus express connexins (Cx) 30 and 43, which form gap junctions that allow the passage of ions and small molecules between cells (Dermietzel et al., 1989; Giaume, Koulakoff, Roux, Holcman, & Rouach, 2010; Nagy & Rash, 2000; Ransom & Ye, 2005). Moreover, Cx can exist as uncoupled hemichannels serving as gated and selective pores in the cell membrane (Nielsen, Hansen, Ransom, Nielsen, & MacAulay, 2017). Recent work has provided evidence that Cx43 hemichannels are involved in the regulation of basal synaptic transmission at glutamatergic synapses (Chever, Lee, & Rouach, 2014).

The fully developed astrocytic gap junction network in the rodent forebrain is extensive, encompassing many dozens of cells (e.g. Rouach, Koulakoff, Abudara, Willecke, & Giaume, 2008; Wallraff, Odermatt, Willecke, & Steinhauser, 2004) (Figure 1c). Importantly, gap junctions also mediate the spread of glucose and its metabolites through the astrocytic network to regions of increased neuronal activity (Clasadonte, Scemes, Wang, Boison, & Haydon, 2017; Rouach et al., 2008), indicating that they play an important role in neuro-metabolic coupling in the mature network (Belanger, Allaman, & Magistretti, 2011; Escartin & Rouach, 2013). Another consequence of gap junctional coupling is that it results in isopotentiality of the astrocytes involved, reducing local depolarizations induced, for example, by elevation of extracellular K^+ (Kiyoshi et al., 2018; Ma et al., 2016).

While Cx play an important role in embryonic development and development of the cerebral cortex in rodents (Elias & Kriegstein, 2008), astrocytes in the neonate brain show low expression levels of Cx and, therefore, only weak gap junctional coupling as compared to later stages (Houades, Koulakoff, Ezan, Seif, & Giaume, 2008; Schools, Zhou, & Kimelberg, 2006; Yamamoto, Vukelic, Hertzberg, & Nagy, 1992) (Figure 1c). As a consequence, the different physiological functions attributed to a mature astrocytic syncytium, such as an efficient intercellular spread of ions and metabolites, will be less strongly expressed in neonates. This was, for example, shown for the intercellular spread of Na^+ between astrocytes in the hippocampus, which is considerably reduced at P4 as compared to P16-21 (Langer, Stephan, Theis, & Rose, 2012). The same is likely to hold true for intercellular diffusion of K^+, which has been implicated to contribute to the regulation of extracellular K^+ by astrocytes in older animals (Pannasch et al., 2011; Wallraff et al., 2006).

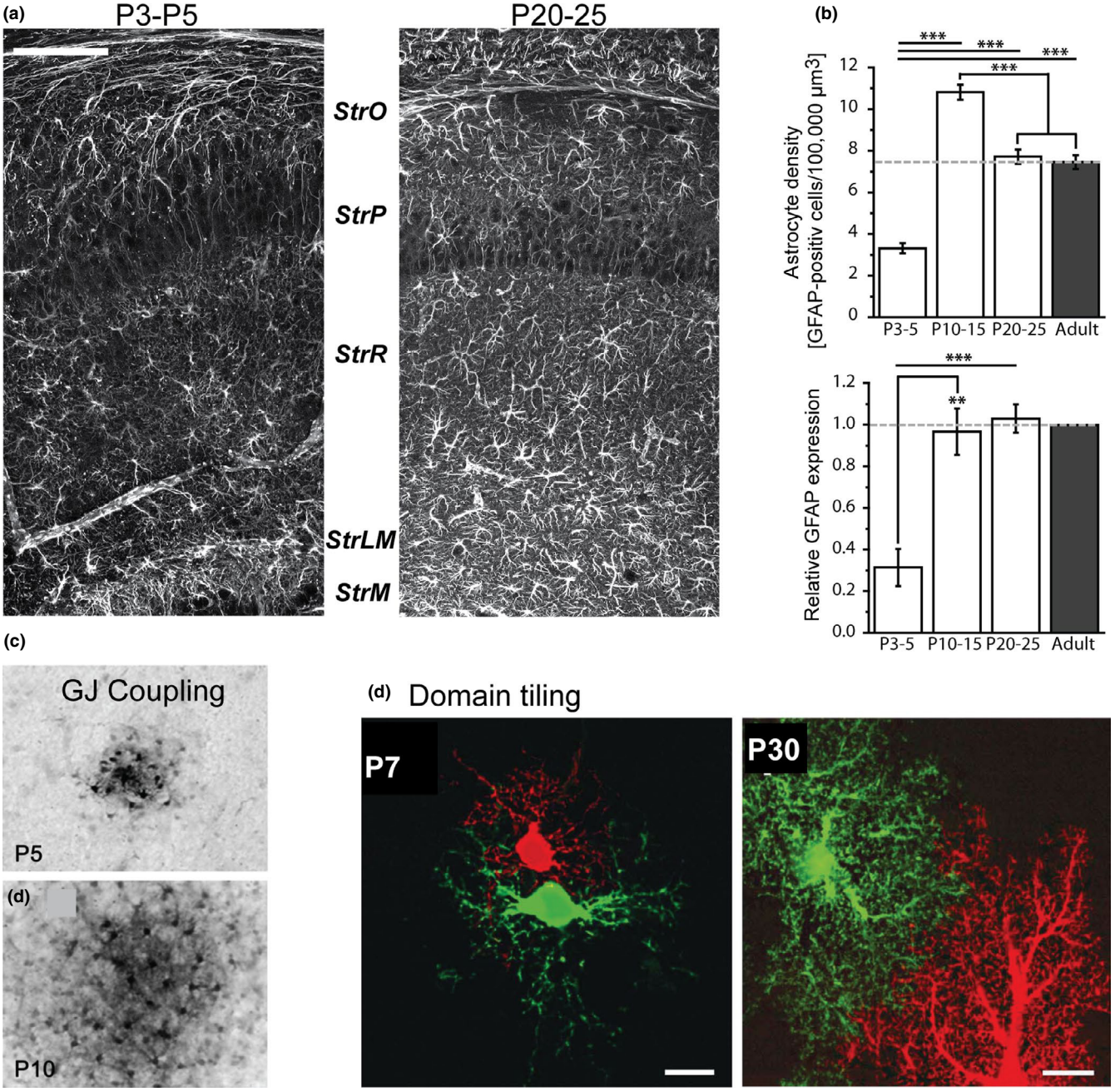

FIGURE 1 Astrocyte morphology and dye coupling in early postnatal development. (a) Expression of GFAP in neonate and juvenile mouse hippocampus. Immunohistochemical staining for GFAP at postnatal days (P) 3-5 and P20-25. (b) Density of GFAP-positive cells (top) and relative GFAP protein expression levels (bottom) in the mouse hippocampus at the indicated developmental stages. (c) Dye coupling among astrocytes in the somatosensory cortex at P5 (top) and P10 (bottom). GJ: "gap junctional" (d) Morphology and domain formation of two neighbouring astrocytes in the rat hippocampus at P7 (left) and P30 (right). Data taken from: (a, b) Schreiner et al. (2014), modified; (c) Houades et al. (2008) Copyright [2008] Society for Neuroscience; (d) Bushong et al. (2004)

Similarly, one could speculate that the reduced gap junctional coupling of neonate astrocytes reduces metabolite trafficking, thereby resulting in a reduced delivery of metabolites from astrocytes to active synapses compared to more developed brains. Interestingly, it also appears that Cx, namely Cx30, can regulate the spatial proximity of PAPs with glutamatergic synapses and thereby the efficacy of glutamate uptake by astrocytes (Pannasch et al., 2014). On the other hand side, it was shown that neurons themselves control the expression of Cx (Koulakoff, Ezan, & Giaume, 2008). The functional relevance of the morphological arrangement of PAPs at tripartite synapses has been exemplified in the hypothalamus of adult rodents, in which changes in the astrocytic coverage directly modify extracellular ion homeostasis and neuronal synaptic transmission (Theodosis, Poulain, & Oliet, 2008). Astrocyte

morphology, domain formation and gap junctional coupling are thus tightly connected to major physiological roles of astrocytes at glutamatergic synapses, namely the clearance of the synaptic cleft from K^+ and glutamate (Pannasch & Rouach, 2013).

4 | K^+ CHANNELS, ELECTROPHYSIOLOGICAL PROPERTIES AND EXTRACELLULAR K^+ HOMEOSTASIS

The first electrophysiological studies performed on brain tissue slices did not differentiate between *bona fide* astrocytes and NG2 glia. Originally, the latter cells were instead classified as "complex" cells/astrocytes, "GluR" cells or "outwardly rectifying" glia/astrocytes by the different authors (Bordey & Sontheimer, 2000; Matthias et al., 2003; Zhou, Schools, & Kimelberg, 2006). For the last 20 years, however, NG2 glia have been recognized as a separate type of macroglial cell (Dimou & Gallo, 2015; Nishiyama, 2001).

Classical astrocytes express a variety of different K^+ channels, that is inwardly rectifying (Kir), two-pore domain (K_2P) and voltage-activated (K_V) channels (for review see e.g. Verkhratsky & Nedergaard, 2018; Verkhratsky & Steinhauser, 2000). Among those, Kir4.1 is of particular interest as it is the predominant K^+ channel in fully developed astrocytes, massively influencing their physiology and behaviour.

Neonatal and mature astrocytes show prominent differences in their expression of different K^+ channels and can thus be distinguished electrophysiologically. Immature neonatal astrocytes exhibit a non-linear current–voltage relationship due to high expression levels of time- and voltage-dependent K^+ currents (Bordey & Sontheimer, 1997; Kafitz et al., 2008) (Figure 2a). In contrast, matured astrocytes display a linear current–voltage relationship due to the predominant expression of ohmic currents originating from Kir and K_2P channels (Bordey & Sontheimer, 2000; D'Ambrosio, Wenzel, Schwartzkroin, McKhann, & Janigro, 1998; Kafitz et al., 2008; Seifert et al., 2009; Zhou et al., 2006) (Figure 2a). During early postnatal development, there is a shift from non-linear to linear current–voltage relationship (Kafitz et al., 2008; Zhong et al., 2016; Zhou et al., 2006) which is in large part due to a strong upregulation of Kir4.1 during this period (Lunde et al., 2015; Moroni, Inverardi, Regondi, Pennacchio, & Frassoni, 2015; Nwaobi, Lin, Peramsetty, & Olsen, 2014; Olsen et al., 2015; Seifert et al., 2009) (Figure 2b). Moreover, localization of Kir4.1 shifts from a predominantly somatic towards a mainly distal expression in perisynaptic processes and perivascular endfeet (Moroni et al., 2015).

Astrocytes exhibit a highly negative resting membrane potential (E_M) independent from the developmental stage (Kafitz et al., 2008; Zhong et al., 2016; Zhou et al., 2006). It is largely defined by the efflux of K^+ through Kir4.1 and K_2P channels, and therefore, inactivation of Kir4.1 causes strong depolarization of astrocytes (Djukic, Casper, Philpot, Chin, & McCarthy, 2007; Kofuji et al., 2000; Seifert et al., 2009; Stephan et al., 2012). A smaller fraction of the E_M is set by the hyperpolarizing activity of the sodium/potassium ATPase (NKA) (Verkhratsky & Nedergaard, 2018). The negative E_M provides the driving force for electrogenic transport of glutamate, GABA (γ-aminobutyric acid) and glycine via GLAST/GLT-1, GAT and GlyT (glycine transporter), respectively. Transport direction and strength of these carriers depend on the electrochemical gradients of the ions and molecules involved. Thus, depolarization reduces or may even reverse transmitter uptake in astrocytes (Barakat & Bordey, 2002; Djukic et al., 2007; Huang, Barakat, Wang, & Bordey, 2004; Stephan et al., 2012) as discussed below.

During neonatal stages, astrocytes exhibit a relatively high membrane resistance (R_M). However, there is a developmental decrease in R_M (Bordey & Sontheimer, 1997; Kafitz et al., 2008; Stephan et al., 2012; Zhong et al., 2016; Zhou et al., 2006) due to increased K^+ channel expression and consequent increase in K^+ permeability (Seifert et al., 2009). The membrane capacitance (C_M) of neonatal astrocytes is relatively low (Kafitz et al., 2008; Zhou et al., 2006). C_M is a measure of the membrane surface, and neonatal astrocytes exhibit a low degree of branching (Bushong et al., 2004; Morel et al., 2014). In contrast, mature astrocytes have many finer processes and display much stronger gap junctional coupling as delineated above. Together, the elaborate branching of astrocyte processes and the formation of a large syncytium of electrically coupled cells increase the total surface area, which results in basically immeasurable high C_M (Kafitz et al., 2008; Zhou et al., 2006).

Kir and K_2P channels are open under resting conditions causing a high K^+ permeability (Stephan et al., 2012; Zhou et al., 2009). In turn, astrocytes are strongly susceptible to changes in $[K^+]_o$, representing near-perfect "K^+-electrodes" (Kimelberg, Bowman, Biddlecome, & Bourke, 1979; Ransom & Goldring, 1973; Stephan et al., 2012) (Figure 2c). There is evidence that Kir4.1 mediates temporary local buffering of K^+ that is released from neurons upon activation (Bay & Butt, 2012; Chever, Djukic, McCarthy, & Amzica, 2010; D'Ambrosio, Gordon, & Winn, 2002; Larsen et al., 2014; Sibille, Pannasch, & Rouach, 2014). Neonatal astrocytes exhibit a restricted K^+ buffering capacity through Kir4.1, which then becomes more effective during development and increased expression of Kir4.1 (Larsen, Stoica, & MacAulay, 2019; Zhong et al., 2016).

Regulation of $[K^+]_o$ by astrocytes is not only mediated through K^+ channels. In addition, uptake of K^+ into

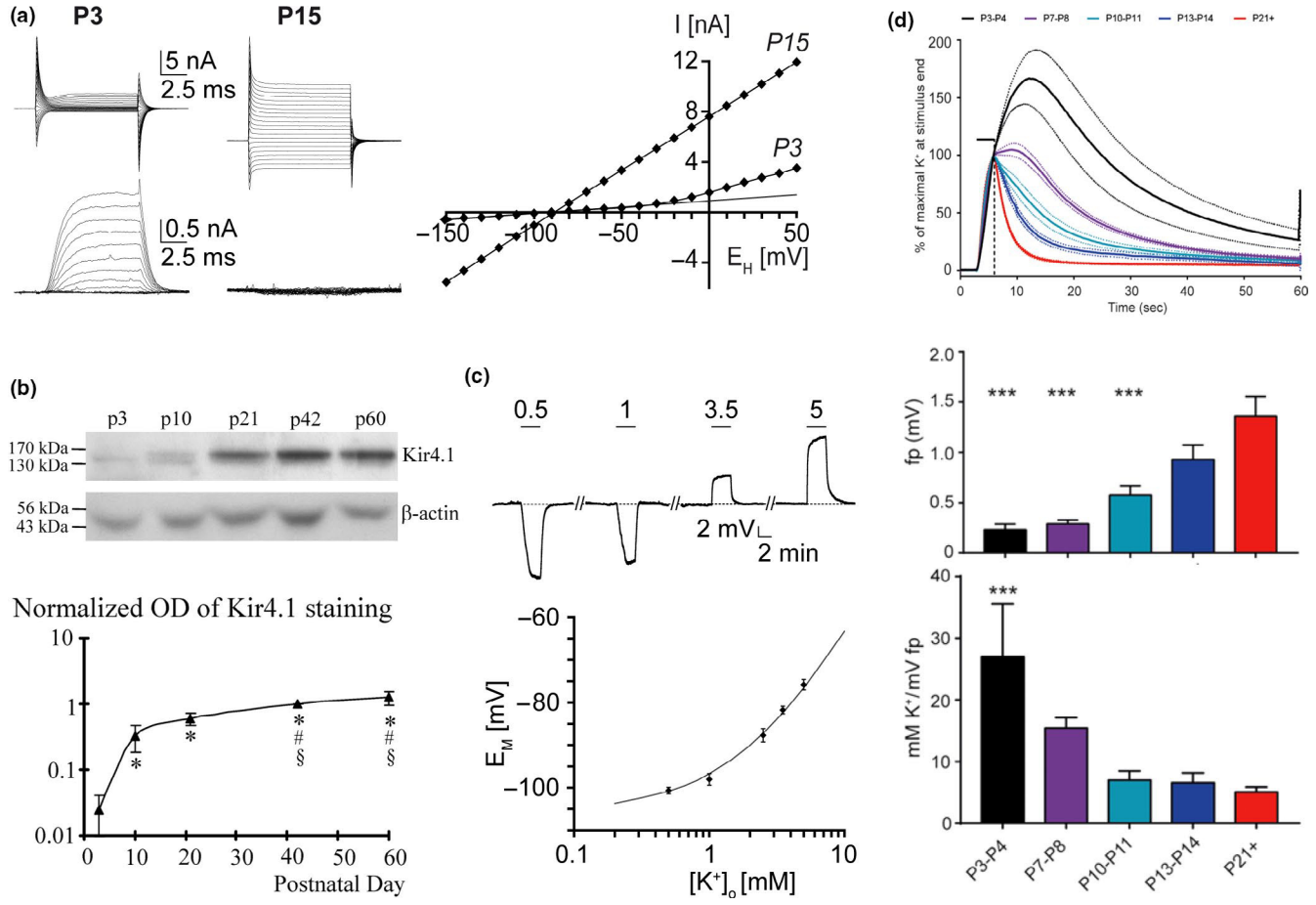

FIGURE 2 Astrocyte K^+ channels and extracellular K^+ homeostasis. (a) Current–voltage relationships in neonate and juvenile mouse hippocampus. At P3, time- and voltage-dependent outward currents are strongly expressed, resulting in a non-linear current–voltage relationship. At P15, ohmic currents dominate, and current–voltage relationship is linear. Upper and lower current traces represent recordings before and after leak subtraction, respectively. (b) Kir4.1 protein levels in the hippocampus increase during the first postnatal weeks. (c) Dependence of astrocytic membrane potentials on $[K^+]_o$. Reduction and increase of baseline $[K^+]_o$ (2.5 mM) results in hyper- and depolarization, respectively (top; numbers depict $[K^+]_o$ in mM). Bottom: Plot showing dependence of astrocytic membrane potentials on $[K^+]_o$. The line represents a fit of the data using the Goldman–Hodgkin–Katz equation and a relative Na^+ permeability of 0.015. (d) Activity-related $[K^+]_o$ transients in the rat hippocampus during early postnatal development. Top: normalized changes in $[K^+]_o$ evoked by synaptic stimulation at the different postnatal stages indicated. Middle: field potential amplitudes in response to synaptic stimulation. Bottom: $[K^+]_o$ amplitudes, normalized to the corresponding field potential. Data taken from: (a) Kafitz et al. (2008), modified; (B) Seifert et al. (2009), modified, Copyright [2009] Society for Neuroscience; (c) Stephan et al. (2012), modified; (d) Larsen et al. (2019)

astrocytes by the sodium/potassium ATPase (NKA) plays a prominent role (Hertz et al., 2015; Karus, Mondragao, Ziemens, & Rose, 2015; Larsen, Stoica, & MacAulay, 2016). A recent study performed on rat hippocampus revealed that all three isoforms of the α subunit of the NKA are up-regulated during the first three postnatal weeks (Larsen et al., 2019). Similarly, expression levels of the sodium-potassium-2 chloride co-transporter 1 (NKCC1), another transporter likely involved in the regulation of extracellular K^+ (MacVicar, Feighan, Brown, & Ransom, 2002; Su, Kintner, & Sun, 2002), increase strongly from P0 to adulthood (Yan, Dempsy, & Sun, 2001).

The capacity for both channels—as well as transporter-mediated astrocytic uptake of K^+ from the extracellular space (ECS), is thus relatively weak in the neonate brain. Indeed, the activity-induced extracellular changes in K^+ are much larger and longer-lasting in neonate animals and may even exceed the so-called ceiling level of 10–12 mM (Connors, Ransom, Kunis, & Gutnick, 1982; Heinemann & Lux, 1977; Jendelova & Sykova, 1991; Larsen et al., 2019) (Figure 2d). Within the first three postnatal weeks, the number of synapses increases strongly, resulting in a greater activity-related release of K^+. At the same time, however, the increase in capacity for astrocytic K^+ uptake is even stronger, resulting in smaller and briefer increases in K^+ for a given intensity of neuronal activity (Larsen et al., 2019) (Figure 2d).

Of note, the first postnatal weeks also experience significant changes in the brain's ECS, including a decrease in the extracellular volume fraction of about 37% at P4-6 to 24% at P12 to about 15% in adults (Nicholson & Hrabetova, 2017;

Sykova & Nicholson, 2008). Diffusion in the neonate ECS, therefore, plays a much more prominent functional role as compared to later stages of development, where the ECS is narrow and does not enable efficient passive clearance. The apparent weakness of astrocytic K^+ uptake ability in neonate brain seems thus be compensated for by the increased volume fraction of the ECS (Larsen et al., 2019). *Vice versa*, astrocytes adapt to the requirements of the growing network and neuronal activity by increasing their ability to buffer elevations in $[K^+]_o$.

5 | GLUTAMATE TRANSPORTERS

Glutamate uptake by astrocytes is vital to protect the brain from excitotoxic cell damage and related cell death (Maragakis & Rothstein, 2004; Parpura et al., 2012; Schousboe, Scafidi, Bak, Waagepetersen, & McKenna, 2014). By removing synaptically released glutamate from near the synaptic cleft, astrocytes also control its diffusion to peri- and extrasynaptic receptors (Huang & Bergles, 2004; Zheng, Scimemi, & Rusakov, 2008). In the adult neocortex and hippocampus, astrocytes mainly express two isoforms of high-affinity glutamate transporters, namely GLT-1 (glutamate transporter 1; human analogue: EAAT2 (excitatory amino acid transporter 2)) and GLAST (glutamate/aspartate transporter; human analogue: EAAT1 (excitatory amino acid transporter 1)) (Danbolt, 2001). The two transporters share the same stoichiometry, with 3 Na^+ taken up together with 1 H^+ and 1 glutamate in exchange for a K^+, but exhibit differences in their associated anion conductance (Marcaggi & Attwell, 2004; Rose, Ziemens, Untiet, & Fahlke, 2018).

The activity of glutamate transporters is critical for adult brains, but also for brain development and maturation. Double knockout mice for GLAST and GLT-1 suffer from perinatal mortality and show multiple brain defects (Matsugami et al., 2006). GLAST knockout mice develop normally, but display moderate motor discoordination and increased vulnerability to excitotoxic damage (Watase et al., 1998). Animals devoid of GLT-1 exhibit a much more severe phenotype, including neurodegeneration and premature death from spontaneous seizures (Rothstein et al., 1996; Tanaka et al., 1997).

Notably, while these results point to an essential role of GLT-1 during embryonic and postnatal development, it is GLAST (and not GLT-1) which is mainly expressed by radial glial cells and by astrocytes of the neonate brain (Regan et al., 2007; Shibata et al., 1997). In the mouse hippocampus, GLAST is well detectable at birth and its expression increases during the first three weeks, after which it remains at a relatively stable level until adulthood (Schreiner et al., 2014; Ullensvang, Lehre, Storm-Mathisen, & Danbolt, 1997) (Figure 3a). Expression of GLT-1 starts to appear only after the first postnatal week and then increases to reach near-adult levels at about three weeks after birth (Cahoy et al., 2008; Schreiner et al., 2014; Ullensvang et al., 1997) (Figure 3a). In the neocortex, the strong upregulation of GLT-1 happens even later, suggesting that GLAST is indeed the predominant glutamate transporter of immature astrocytes, while GLT-1 is the major isoform in adult brain (Furuta, Rothstein, & Martin, 1997; Hanson et al., 2015). The upregulation of GLT-1 is regulated by neuronal activity (Ghosh, Yang, Rothstein, & Robinson, 2011; Morel et al., 2014; Swanson et al., 1997), but GLT-1 itself is also necessary for the establishment of synapses (Verbich, Prenosil, Chang, Murai, & McKinney, 2012), again illustrating the tight interrelationship of astrocyte maturation and formation of the neuronal network (Benediktsson et al., 2012).

Interestingly, the switch in glutamate transporter expression is not seen in cerebellar Bergmann glial cells and Müller glial cells of the retina, which continue to express high levels of GLAST throughout postnatal development (Rose et al., 2018). The postnatal upregulation of glutamate transporters in Bergmann glial cells was shown to be accompanied by a significant drop in their $[Cl^-]_i$ (Untiet et al., 2017), most likely due to the transporter-associated anion conductance of GLAST/GLT-1 (Rose et al., 2018). Based on these results, it was speculated that the high $[Cl^-]$ of neonatal glial cells might result in a higher ambient GABA concentration in the extracellular space as compared to adulthood (Untiet et al., 2017). In addition, the high astrocytic $[Cl^-]$ sets the Cl^--reversal potential to values more positive than the E_M of astrocytes, resulting in the efflux of Cl^- upon the opening of GABA receptors, thereby depolarizing the cells (see below) (Kettenmann, Backus, & Schachner, 1984; Meier, Kafitz, & Rose, 2008).

The relatively low glutamate transporter expression in the first week after birth coincides with a period in which GABA acts as an important depolarizung drive in the rodent forebrain (Ben-Ari, 2001). Despite the low density of functional glutamatergic synapses, however, many neurons express NMDA (N-methyl-D-aspartate receptor) receptors and blocking glutamate uptake results in seizure-like activity in the neuronal network (Demarque et al., 2004). Functional glutamate transport, predominantly through GLAST, is also essential for the maintenance of neuronal Na^+ homeostasis and integrity during recurrent activity in neonates (Karus, Gerkau, & Rose, 2017).

Using the glutamate transporter current in astrocytes as a readout (Bergles & Jahr, 1997), it was shown that the overall increase in transporter expression during the first three postnatal weeks is accompanied by a significant increase in the cellular clearance rate for glutamate (Diamond, 2005) (Figure 3b). While it was first speculated that in young brains, this lower level of active clearance could result in an increased activation of extrasynaptic glutamate receptors, a

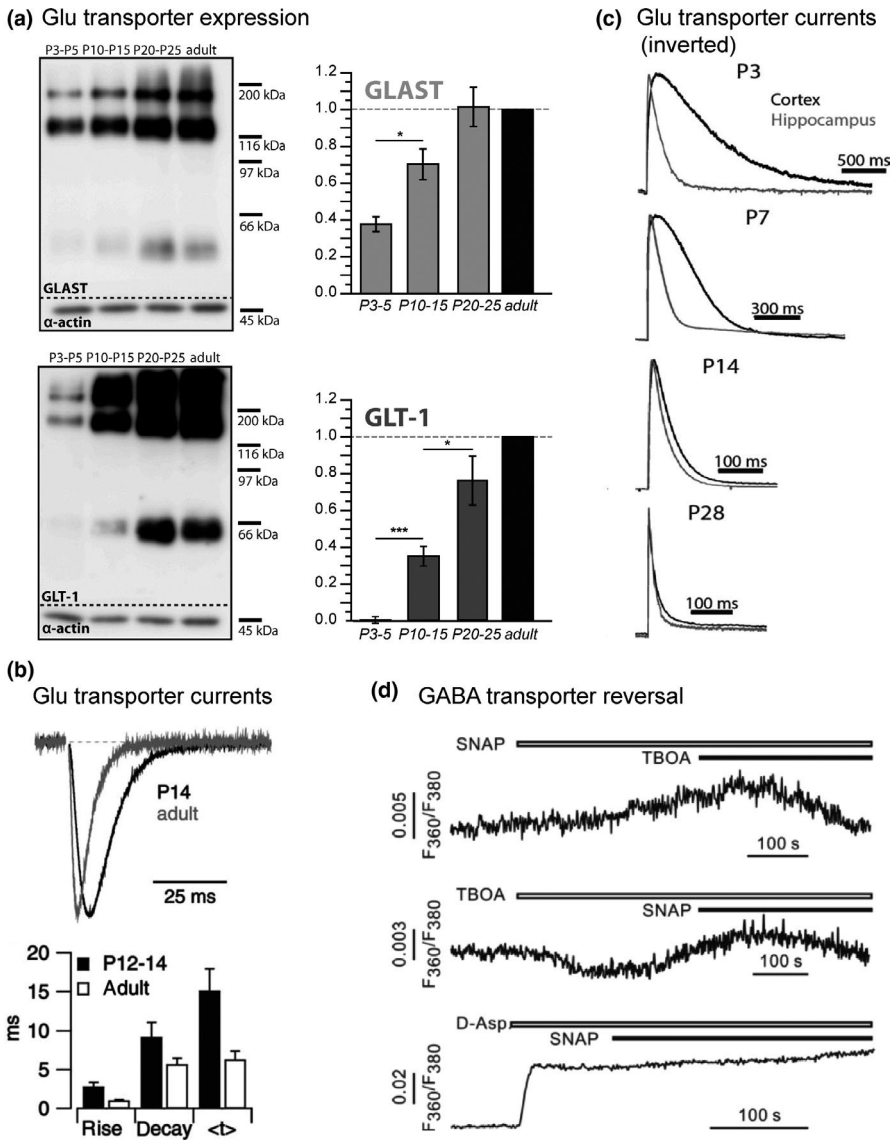

FIGURE 3 Properties of astrocytic glutamate and GABA transport. (a) Right: GLAST (top) and GLT-1 (bottom) protein content in the CA1 region of the mouse hippocampus. Left: relative protein expression levels of the transporters indicated. (b) Glutamate transport-induced synaptic current in a rat hippocampal astrocyte at P14 as compared to adult brain. (c) Peak-normalized, inverted glutamate transporter currents of astrocytes from rat cortex and hippocampus at the indicated age. (d) Top two traces: changes in $[Na^+]_i$ in SBFI-AM loaded cortical astrocytes (P5-7) after application of GAT and EAAT agonists (SNAP-5114 and DL-TBOA, respectively). Bottom trace: blocking GAT still elicits increases in $[Na^+]_i$ in the presence of D-aspartate. activity Data taken from: (a) Schreiner et al. (2014), modified; (b) Diamond (2005) Copyright [2005] Society for Neuroscience; (c) Hanson et al. (2015); (d) Unichenko et al. (2013)

later study provided evidence that the reduced glutamate uptake capacity of astrocytes is compensated for by the larger ECS of neonates (Thomas, Tian, & Diamond, 2011).

Interestingly, electrophysiological analysis during the first postnatal weeks also demonstrated that glutamate transport is substantially slower in the neocortex compared to the hippocampus of rats, most likely due to lower overall transporter expression levels on neocortical astrocytes throughout postnatal development (Hanson et al., 2015) (Figure 3c). The reduced capacity for uptake of glutamate by cortical astrocytes results in a less strict control of extracellular glutamate concentration and a stronger activation of neuronal NMDA receptors compared to the hippocampus (Hanson et al., 2015).

6 | GABA TRANSPORTERS

The three main GABA transporters of the rodent forebrain are (following rat nomenclature) GAT-1, GAT-2 and GAT-3 (Borden, 1996; Conti, Minelli, & Melone, 2004; Ghirardini et al., 2018; Stephan, 2015). Astrocytic expression of the different isoforms seems to be heterogeneous, depending on the subcellular compartment, brain region and developmental state (Scimemi, 2014b). GAT-1 is expressed in the cortex and hippocampus from P1 onwards, but does not appear in the cerebellum until the second postnatal week (Frahm & Draguhn, 2001; Rosina, Morara, & Provini, 1999). While astrocytic GAT-2 is strongly expressed around cortical blood vessels during the first postnatal week, it is downregulated shortly after this and levels in the mature cortex are very low. In contrast, GAT-3 is present at birth and then increases with ongoing development (particularly within the first postnatal week), until adult levels and patterns are reached at P20 (Minelli, Barbaresi, & Conti, 2003; Vitellaro-Zuccarello, Calvaresi, & De Biasi, 2003). GAT-3 is not restricted to astrocyte processes at synapses, but also found at extrasynaptic locations (Minelli, DeBiasi, Brecha, Zuccarello, & Conti, 1996).

Like other transporters, levels of GAT are dynamically regulated, which not only includes changes in gene expression, but also changes in the plasma membrane levels (Scimemi, 2014a). Interestingly, studies in the fruit fly Drosophila indicate that the recruitment of GATs into the astrocytic membrane is upregulated by GABAergic signalling—specifically via the activation of $GABA_B$ receptors (Muthukumar, Stork, & Freeman, 2014).

GABA uptake requires the co-transport of Na^+ and Cl^- (Barakat & Bordey, 2002; Stephan & Friauf, 2014)—with a stoichiometry of 2 Na^+: 1 Cl^-: 1 GABA (Eulenburg & Gomeza, 2010). This makes the action of GATs electrogenic, and therefore, their activity is dependent on the electrochemical gradients of the involved ions as well as on GABA concentrations. As these parameters are not fixed and can change with activity, GAT transport capacity and even the transport direction of GATs may change.

Dynamic control of extracellular GABA through GATs in fact seems to play a critical role during development. In the early postnatal brain, local increases in synaptic GABA concentrations during periods of high activity drive inward transport through subsynaptic GATs (Savtchenko, Megalogeni, Rusakov, Walker, & Pavlov, 2015), reducing the activation of $GABA_A$ receptors driving giant depolarizing potentials (GDPs) (Sipila, Huttu, Voipio, & Kaila, 2004). The latter arise as a consequence of the high intracellular Cl^- concentrations in neonate neurons which set their Cl^--reversal potential to values more positive than their E_M, resulting in Cl^- efflux upon the opening of $GABA_A$ receptors (Ben-Ari, 2001).

At the same time, the limited uptake capability of GATs expressed at extrasynaptic sites effectively clamps ambient GABA at a level high enough to tonically activate both $GABA_B$ and extrasynaptic $GABA_A$ receptors. These $GABA_A$ receptors have different subunit compositions to their subsynaptic counterparts, bestowing them with a higher sensitivity and reduced level of desensitization (Belelli et al., 2009). Their tonic activation has been implicated in processes such as the modulation of neuronal migration and differentiation. While they are persistently activated by ambient GABA, they are not saturated at resting levels and transient increases in extracellular GABA concentrations can therefore induce additional phasic depolarization (Luhmann, Fukuda, & Kilb, 2015; Song et al., 2013).

Activation of GABA uptake in neonate astrocytes may have functional consequences for astrocyte signalling itself. In the developing olfactory bulb, increases in Na^+ caused by astrocytic inward GAT activity can be sufficient to decrease the activity of the sodium/calcium exchanger (NCX), thereby increasing intracellular Ca^{2+} levels enough to trigger IP_3-mediated Ca^{2+} release from intracellular stores (Doengi et al., 2009). GAT-induced rise in intracellular Ca^{2+} signalling has also been shown to induce release of ATP (adenosine triphosphate) from astrocytes in juvenile animals, which heterosynaptically activates pre- and postsynaptic A1 receptors on hippocampal pyramidal neurons and exerts an inhibitory effect on the network (Boddum et al., 2016; Matos et al., 2018).

In addition to being dependent on GABA, transport activity through GATs is dependent on Na^+ and Cl^- concentrations which bring the reversal potential close to the resting membrane potential (Richerson & Wu, 2003). Increases in the intracellular Na^+ concentration occurring after glutamate uptake, depolarization via increased extracellular K^+ or an increase in intracellular GABA, are therefore all sufficient to reverse astrocytic GABA transport in a dose-dependent manner—thereby increasing extracellular GABA (Heja et al., 2012; Wu, Wang, Diez-Sampedro, & Richerson, 2007).

As mentioned above, astrocytes display a highly negative E_M already from birth on. Moreover, astrocyte Na^+ concentrations are apparently stable in this period (Felix, Ziemens, Seifert, & Rose, 2020), amounting to about 12-15 mM (Rose, Ziemens, & Verkhratsky, 2019). The situation is, however, less clear for Cl^-. Reported values for astrocytic Cl^- concentration have (independent from age) varied from 20 to 50 mM depending on the technique and preparation used (Wilson & Mongin, 2019). A recent study employing fluorescence lifetime microscopy has now shown neonate Bergmann glia to have a $[Cl^-]_i$ of around 52 mM, a value significantly higher than their mature counterparts, which sit at roughly 35 mM (Untiet et al., 2017). It should be noted that the high Cl^- content in young astrocytes is most likely not primarily due to influx via the NKCC1 (as is the case in neurons), as astrocytic expression of the transporter remains low during early development and only reaches maximal values after the third postnatal week (Yan et al., 2001).

The developmental change in glial Cl^- is of particular importance, as the higher $[Cl^-]_i$ in neonates as compared to the mature brain shift the reversal potential of GATs. Indeed, Unichenko, Dvorzhak, and Kirischuk (2013) showed that in the neonatal neocortex, Na^+ influx caused by glutamate uptake is sufficient to keep GATs functioning primarily in the outward mode, resulting in a higher ambient level of extracellular GABA (around 250 nM as opposed to 125 nM in older animals, Figure 3d) (Dvorzhak, Myakhar, Unichenko, Kirmse, & Kirischuk, 2010; Kirmse & Kirischuk, 2006; Untiet et al., 2017).

7 | ACTIVITY PATTERNS AND CALCIUM SIGNALLING IN THE NEONATE BRAIN

Patterns of synchronized, universal neuronal activity emerge at birth and characterize the neonatal stage. This early activity shapes local circuit creation in the developing

forebrain (Ben-Ari, 2001; Griguoli & Cherubini, 2017; Hanganu-Opatz, 2010; Khazipov & Luhmann, 2006; Kilb, Kirischuk, & Luhmann, 2011; Yang, Hanganu-Opatz, Sun, & Luhmann, 2009). These patterns include GDPs of the hippocampus (Ben-Ari, Cherubini, Corradetti, & Gaiarsa, 1989), which have been largely attributed to GABAergic excitation of neonate neurons (Ben-Ari, 2001; Canepari, Mammano, Kachalsky, Rahamimoff, & Cherubini, 2000; Garaschuk, Hanse, & Konnerth, 1998; Mohajerani & Cherubini, 2006). The excitatory action of GABA during early development is due to the well-documented "chloride switch"—the result of an early upregulation of the NKCC1 (Ben-Ari, 2014).

Another feature of the developing postnatal brain is the so-called early network oscillations (ENOs), which are bursts of synchronized Ca^{2+} elevations, moving in slow oscillatory waves throughout entire populations of neurons in the hippocampus and cortex (Garaschuk, Linn, Eilers, & Konnerth, 2000; Nakayama, Sasaki, Tanaka, & Ikegaya, 2016). Within the cortex, they appear to be generated by glutamatergic signals and are suspended by the end of the first postnatal week (Allene et al., 2008; Corlew, Bosma, & Moody, 2004; Garaschuk et al., 2000). In contrast, hippocampal ENOs are present to the end of the second postnatal week and are the products of $GABA_A$ activation and glutamatergic innervation (Barger, Easton, Neuzil, & Moody, 2016; Bolea, Sanchez-Andres, Huang, & Wu, 2006; Canepari et al., 2000; Garaschuk et al., 1998).

Strong hippocampal and cortical ENOs can also involve a delayed recruitment of astrocytic networks (Figure 4a) (Barger et al., 2016). While the functional consequences astrocytic contributions to ENOs have not been investigated in detail, local and global Ca^{2+} elevations and can lead to release of glio-transmitters feeding back onto neurons as formalized by the term "tripartite synapse" (Araque, Parpura, Sanzgiri, & Haydon, 1999). However, it is worth noting that recent studies have called the concept back into question (for a review of both arguments, see reviews from (Fiacco & McCarthy, 2018) and (Savtchouk & Volterra, 2018)). Although most evidence for glio-transmission has been gained in the juvenile and mature rodent brain, it cannot be excluded from also playing an important role in neonates.

While the exact contribution of astrocytes to GDPs and ENOs is not clear, developing astrocytes in the neonatal neocortex, hippocampus, ventral thalamus and several other brain regions have also been shown to have synchronous, seemingly spontaneous oscillations in somatic Ca^{2+} concentrations (Figure 4b) (Aguado, Espinosa-Parrilla, Carmona, & Soriano, 2002), and more recently, asynchronous slow fluctuations in somatic Na^+ (Felix et al., 2020). Spontaneous changes in both of these ions appear in a subset of measured astrocytes, with ~ 70% showing Ca^{2+} oscillations and ~ 40% Na^+ fluctuations in the hippocampus. Unlike Ca^{2+} waves seen in mature astrocytes, this early activity apparently occurs independently of neuronal transmission, as it was not reduced after inhibition of GABAergic, glutamatergic and purinergic receptors (Aguado et al., 2002; Felix et al., 2020; Parri, Gould, & Crunelli, 2001). In fact, it appears that astrocytic Ca^{2+} oscillations may trigger Ca^{2+} transients in neighbouring neurons, via the stimulation of NMDA receptors (Parri et al., 2001). The resulting transients can be eradicated in neurons by application of TTX (tetrodotoxin), but remain present in astrocytes—although the lack of neuronal input appears to reduce their network synchronicity (Aguado et al., 2002). Additionally, similar—purinergic transmission independent—waves have been shown to travel throughout neonatal populations of astrocyte-like "B cells" via gap junction coupling (Lacar, Young, Platel, & Bordey, 2011). The temporal regulation of such intrinsically triggered Ca^{2+} oscillations are heterogeneous, with neocortical astrocytes showing a reduction but not complete ablation with developmental progression, and hippocampal astrocytes displaying oscillating behaviour to a similar level in mature cells (Aguado et al., 2002; Nett, Oloff, & McCarthy, 2002).

While the preponderance of former studies have concentrated on detecting somatic Ca^{2+} oscillations in neonatal astrocyte networks, astrocytes also show subcellular Ca^{2+} elevations already during early development. The latter tend to be small in amplitude but grow as the cells reach morphological maturation (Nakayama et al., 2016). This temporal correlation may be related to the increase in the surface-to-volume ratio produced by the increasing arborization of processes, as morphology has been shown to influence the form and frequency of calcium transients (Wu et al., 2019). While the amplitude of subcellular Ca^{2+} events increases with age, the mechanism (which remains to be identified) could remain constant—as events in both P7 and P30 animals continue at a similar level after applications of antagonists for purinergic receptors and TRPA1 (transient receptor potential) channels (although mGluRs inhibitors have showed mixed results). Additionally, spontaneous subcellular events in neither young nor mature astrocytes appear to be connected to neuronal activity (Nakayama et al., 2016; Rungta et al., 2016; Zur Nieden & Deitmer, 2006). These subcellular signals constitute the majority of spontaneous Ca^{2+} signals in adult astrocytes and have been shown to be confined to and synchronized within individual cellular compartments (Bindocci et al., 2017; Rungta et al., 2016; Stobart et al., 2018).

In addition to spontaneous subcellular activity, both developing and mature astrocytes respond to and integrate a range of sensory signals with changes in their Ca^{2+} concentration (Slezak et al., 2019). In the last 10 years, a broad range of highly sensitive and selective tools has been developed to study these changes. These include the creation of astrocyte-specific transgenic mouse lines, the improvement of imaging to allow multiphoton 3D depiction of entire cells, and resolutions high enough to show interactions at individual

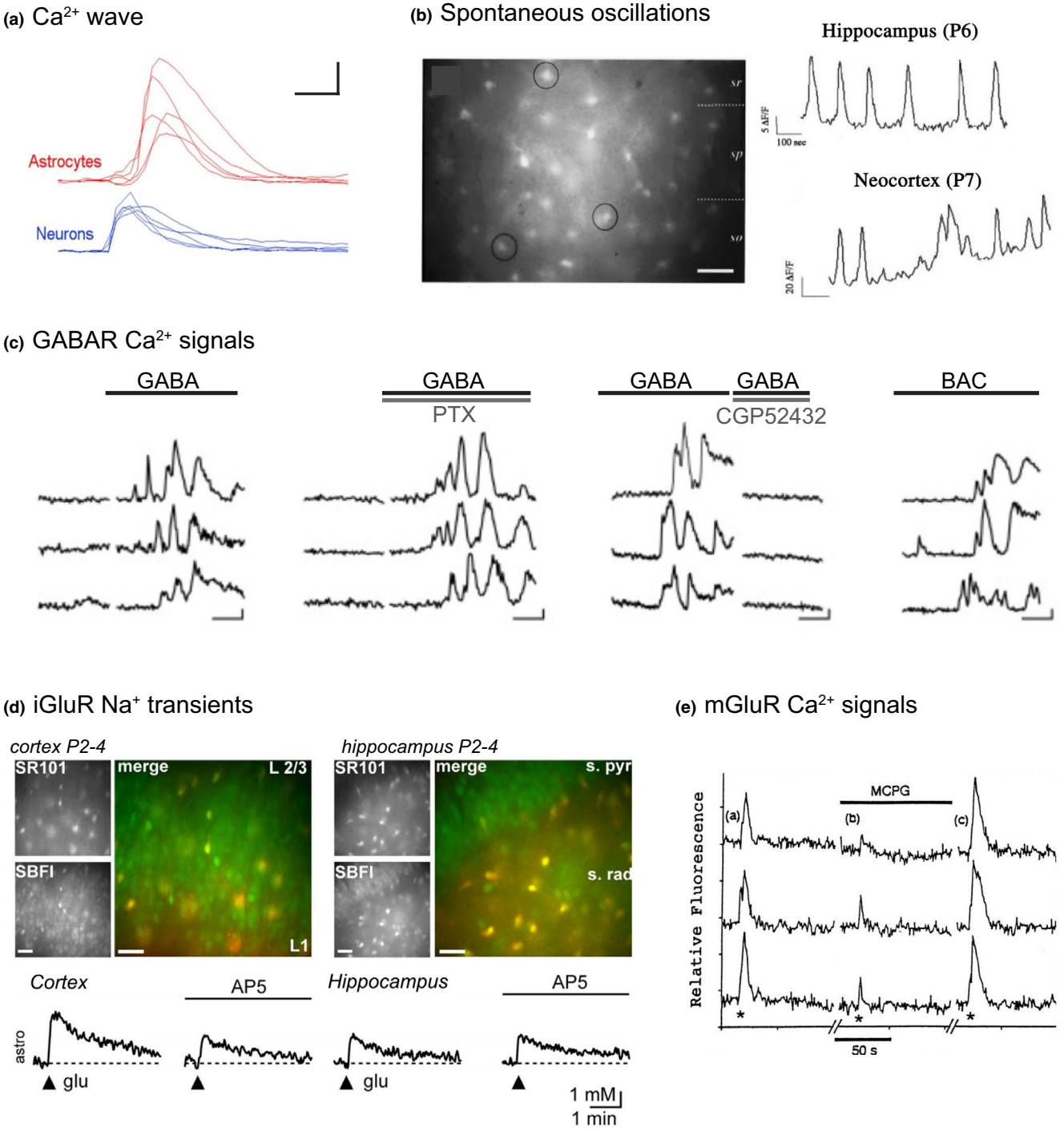

FIGURE 4 Ca^{2+} activity and transmitter receptors on astrocytes. (a) Propagation of a Ca^{2+} wave through the neocortex, with neurons reacting first, followed by astrocytes. Scale bar: 2 s, 10% ΔF/F. (b) (Left) Wide field microscope image of the stratum radiatum of the hippocampal CA1 region (P6) labelled with Fura-2. (Right) Example traces from individual astrocytes in the hippocampus (top) and cortex (bottom), showing spontaneous oscillations in intracellular Ca^{2+}. (c) GABA-induced Ca^{2+} signals in cortical astrocytes (P15-20) and effect of blockers for GABAA (PTX: picrotoxin) and GABAB (CGP52432) receptors. (d) Top: Wide field images of neonatal cortex (left) and hippocampus (right), co-stained with SBFI-AM and SR101 as indicated. Bottom: Astrocyte Na^{+} transients after puff applications of glutamate in both regions, both with and without the presence of the NMDA channel blocker APV. (e) Ca^{2+} signals measured in hippocampal astrocytes (P10-13) after Schaffer collateral stimulation and effect of the mGluR5 inhibitor MCPG (1 mM). Data taken from: (a) Barger et al. (2016), modified; (b) Aguado et al. (2002), modified, Copyright [2002] Society for Neuroscience; (c) Mariotti et al. (2016); (d) Ziemens et al. (2019); (e) Porter & McCarthy (1996) Copyright [1996] Society for Neuroscience

synapses, models which integrate the complex morphology of mature cells and fluorescence lifetime imaging to reveal absolute Ca^{2+} concentrations within cell subcompartments (Bindocci et al., 2017; Reynolds, Zheng, & Rusakov, 2019; Savtchenko et al., 2018; Srinivasan et al., 2016; Zheng & Rusakov, 2015). While these technical advances have until now been primarily used to investigate adult signalling, they will undoubtedly also further our understanding of the described "spontaneous" astrocytic Ca^{2+} signals in the neonatal brain in future studies.

8 | GABA RECEPTORS ON ASTROCYTES

As outlined above, GABA plays an important role in early postnatal development (Ben-Ari, 2001). In addition to binding and taking up GABA through GATs, astrocytes are capable of reacting to released GABA directly via both $GABA_A$ and $GABA_B$ receptors (Losi, Mariotti, & Carmignoto, 2014; Schousboe, 2000). These interactions have been shown to play a critical role in astrocytic maturation.

For example, in culture, the introduction of GABAergic neurons induced a shift in astrocyte morphology and produced a more complex shape in cells with neuronal contact (Matsutani & Yamamoto, 1997). This was confirmed in situ, wherein astrocytes from areas with higher levels of GABAergic terminals also display the highest degree of stellation. Furthermore, increasing GABA or activating $GABA_A$ receptors in vivo increases GFAP content and astrocytic branching across the forebrain (Runquist & Alonso, 2003). These results may be linked to steroid-induced differentiation, as astrocytic $GABA_A$ receptor activation has been shown to be a modulating factor here (Mong, Nunez, & McCarthy, 2002). In addition to branching, $GABA_A$ receptor activation appears to play a role in cell migration, as low concentration applications (levels which would stimulate tonic, but not phasic $GABA_A$ receptor activation) reduce migration distances, an effect which can be rescued by application of bicuculline (Bolteus & Bordey, 2004). The exact mechanisms of these effects are not yet fully understood; however, the two direct effects of GABA on astrocytes are depolarization, and Ca^{2+} elevations, the details of which will be discussed below.

In contrast to neurons, astrocytes retain their NKCC1 expression into adulthood and do not switch to KCC2 (potassium chloride co-transporter 2) (Losi et al., 2014). Taken together with an extracellular Cl^- concentration of around 120 mM, this produces an $[Cl^-]_e$ of roughly −25 to −30 mV (at intracellular $[Cl^-]$ of 40–50 mM, 37°C), resulting in $GABA_A$ receptor activation being depolarizing for astrocytes (Fraser, Mudrick-Donnon, & MacVicar, 1994). It has been suggested that GABA-induced Cl^- efflux from astrocytes could help to maintain high extracellular Cl^- content during high frequency interneuron firing (Bormann & Kettenmann, 1988; MacVicar, Tse, Crichton, & Kettenmann, 1989).

$GABA_A$ receptor-induced depolarization in astrocytes can be sufficient to open L-type voltage-gated Ca^{2+} channels, creating Ca^{2+} signals (Figure 4c) (Fraser et al., 1995; Nilsson, Eriksson, Ronnback, & Hansson, 1993). In the mouse hippocampus, $GABA_A$ receptor-mediated Ca^{2+} signals such as these are present from the first postnatal week and remain consistent throughout development (Meier et al., 2008). $GABA_B$ receptor activation too has been linked to intracellular oscillations in Ca^{2+}, which are mainly attributed to IP_3-related release from intracellular stores (Figure 4c) (Losi et al., 2014; Mariotti, Losi, Sessolo, Marcon, & Carmignoto, 2016; Meier et al., 2008). In hippocampal slices, this reaction was demonstrated using application of the $GABA_B$ agonist baclofen—and was shown to be greatest during the second postnatal week—wherein around 60% of cells respond, in contrast to around 10% in earlier and later stages (Meier et al., 2008). In contrast to this, cortical astrocytes display $GABA_B$ receptor-evoked, extended Ca^{2+} signals in both developing and mature mice (Mariotti et al., 2016). The functional importance of $GABA_B$ receptors on neonate as well as mature astrocytes is still not entirely clear. However, it has been shown that GABAergic stimulation of astrocytes increases their Ca^{2+} and can trigger release of other transmitters (such as glutamate or ATP) and thereby modulate activity of neighbouring cells (Kang et al., 2008; Mariotti et al., 2016; Serrano, Haddjeri, Lacaille, & Robitaille, 2006).

9 | GLUTAMATE RECEPTORS ON ASTROCYTES

Astrocytic glutamate receptors are heterogeneously expressed across the brain. One of the best described examples of this is the spatial patterning of AMPA (α-amino-3-hydroxy-5-methyl-4-isoxazolepropionic acid) receptors, which are present in cerebellar Bergmann glia, have low expression levels in the neocortex and are apparently largely absent in the hippocampus (Matthias et al., 2003; Molders, Koch, Menke, & Klocker, 2018; Verkhratsky & Nedergaard, 2018; Zhou & Kimelberg, 2001). Additionally, these receptors are temporally regulated, with expression in astrocytes sorted from whole brains highest in first postnatal week (Molders et al., 2018). Their presence in the cerebellum appears to be involved in the formation of Purkinje cell synapses, as deletion leads to a retraction of astrocytic processes from neuronal contacts and therefore a reduction in glutamate uptake and delayed synaptogenesis (Iino et al., 2001; Saab et al., 2012).

NMDA receptors have been shown to be expressed in astrocytes within the cortex throughout development (Verkhratsky & Kirchhoff, 2007). They account for around 50% of the

astrocytic Na^+ response to glutamate both in neonates (P2) and in adult mice (P90) (Ziemens, Oschmann, Gerkau, & Rose, 2019) (Figure 4d). This is in contrast to hippocampus, where astrocytic responses to NMDA are either very small or absent (Figure 4d) (Serrano, Robitaille, & Lacaille, 2008; Ziemens et al., 2019). NMDA receptors on astrocytes differ in properties to their neuronal counterparts, appearing to lack the Mg^{2+} block and displaying a lower permeability to Ca^{2+} (Palygin, Lalo, Verkhratsky, & Pankratov, 2010). Inhibition of NMDA receptors has developmental consequences and induced a prolonged proliferative phase, delaying neuronal maturation in the neocortex (Hirasawa, Wada, Kohsaka, & Uchino, 2003) and disrupting migration (Reiprich, Kilb, & Luhmann, 2005).

One of the most thoroughly studied mechanisms for astrocytic glutamate response is the developmental regulation of metabotropic glutamate receptors (mGluR). The majority of hippocampal astrocytes (82%) were shown to respond to the application of glutamate in the first postnatal week via mGluR5 (Figure 4e) (Cai, Schools, & Kimelberg, 2000; Porter & Mccarthy, 1996). mGluR5 mRNA levels are gradually downregulated over the first three postnatal weeks, at the end of which it is almost completely replaced with mGluR3 (Sun et al., 2013). It is important to note that although mRNA levels have been heavily reduced in adult animals, mGluR5 receptors may continue to be functional in subdomains, with expression being limited to PAPs at specific synapses (Panatier & Robitaille, 2016). The two receptor subtypes have contrasting consequences, with mGluR5 triggering Ca^{2+} increases through IP_3-mediated release from internal stores (Panatier & Robitaille, 2016) and mGluR3 decreasing cAMP (cyclic adenosine monophosphate) levels and thereby also transmitter release probabilities (Grosche & Reichenbach, 2013).

The mGluR5-induced Ca^{2+} elevations have been implicated in glio-transmission, such as the local release of purines by astrocytes after glutamatergic innervation, which can upregulate the activity of a single presynaptic terminal by binding A_{2A} receptors. However, if mGluR5 activation is sustained over a longer period, an extrasynaptic release of glutamate is triggered, acting to synchronize a wider network of neurons (Panatier & Robitaille, 2016). This flexibility in response makes mGluR5 ideally suited to striking balances in the dynamic postnatal brain environment, and it has been shown to be a key player in several specifically developmental processes such as astrocytic domain growth, GLT-1 induction and synaptic ensheathing (Morel et al., 2014). Additionally, there is evidence that mGluR5 mediates the spontaneous Ca^{2+} oscillations seen in hippocampal astrocytes (see Figure 4b) (Zur Nieden & Deitmer, 2006).

Of note, the importance of IP_3 receptors for astrocytic Ca^{2+} signals is a topic of debate. Several studies have shown that knocking out IP_3 has little effect on Ca^{2+} signalling within astrocytic distal processes, the location for the majority of Ca^{2+} events (Rungta et al., 2016; Srinivasan et al., 2016; Stobart et al., 2018). However, a recent study utilizing high resolution Ca^{2+} imaging has suggested that in these animals, IP_3 independent mechanisms may create Ca^{2+} "nanodomains" which could compensate the loss and prevent an effect from being seen (Okubo et al., 2019). This and other questions surrounding the receptor may be clarified, for example, using the recently developed photo-switchable mGluRs which can be expressed and measured in vivo (Acosta-Ruiz et al., 2020) and/or using advanced imaging techniques in astrocytic processes as outlined above (Bindocci et al., 2017; Reynolds et al., 2019; Savtchenko et al., 2018; Srinivasan et al., 2016; Zheng & Rusakov, 2015).

10 | PURINERGIC RECEPTORS ON ASTROCYTES

An established form of astrocytic communication is the triggering of Ca^{2+} waves by ATP (Kuga, Sasaki, Takahara, Matsuki, & Ikegaya, 2011). While these waves persist in adult tissue, they are more prominent in the developing brain, where their propagation through radial glia has been shown to modulate proliferation and migration of neurons and astrocytes, as well as DNA production and cellular differentiation (Weissman, Riquelme, Ivic, Flint, & Kriegstein, 2004). Transcriptional and immunohistochemical studies have shown that mammalian astrocytes express both ionic P2X (Palygin et al., 2010; Verkhratsky, Pankratov, Lalo, & Nedergaard, 2012) and metabotropic P2Y receptors (Cheung, Ryten, & Burnstock, 2003) from before birth and throughout development. However, the largest proportion of hippocampal astrocytes reacts to ATP application in the first postnatal week (Cai et al., 2000).

P2X receptors expressed in vitro appear to be functional—opening upon binding to allow an influx of Na^+ and Ca^{2+} and efflux of K^+ (Verkhratsky et al., 2012). However, their ion permeability, as well as their sensitivity and rate of desensitization, is determined by their subunit composition, which varies by region in situ. In slice preparations, ATP might undergo rapid extracellular break down into adenosine (Centemeri et al., 1997). Acutely isolated astrocytes from somatosensory cortex have P2X receptors with a higher sensitivity. While these showed a consistent Ca^{2+} response to ATP (via application and neuronal afferent stimulation) in adult astrocytes, the response in young brains was significantly smaller (Palygin et al., 2010).

Being metabotropic and therefore G protein-coupled, P2Y receptors are generally considered to have long-lasting and trophic actions. They are expressed by around 10% of freshly isolated rat cortical astrocytes from the first postnatal week and by 20%–40% of hippocampal astrocytes (Zhu &

Kimelberg, 2001). These receptors appear to be functional and induced Ca^{2+} elevations—albeit at low levels—in response to the application of ATP in young hippocampal cells. This response increases during the second and third postnatal weeks before dropping again as development continues (Cai et al., 2000). Interestingly, the intracellular signalling cascades triggered in neuronal precursor cells by P2Y activation are the same as those produced by epidermal growth factor (EGF)—suggesting a possible functional co-ordination (Grimm, Messemer, Stanke, Gachet, & Zimmermann, 2009). This is supported by studies wherein animals lacking P2Y1 receptors showed reduced proliferation despite no change in growth factor levels (Mishra et al., 2006).

11 | OTHER RECEPTORS AND CHANNELS ON NEONATE ASTROCYTES

Despite the fact that the majority of developmental astrocyte research has focused on the three transmitters detailed above, immature astrocytes are able to respond to a much broader range of signals. Here, we will briefly explore some of these mechanisms and their place in the context of development.

Glycine receptors have long been reported to be expressed across spinal cord astrocytes, where they are involved in interneuron differentiation and synaptogenesis (Pastor, Chvatal, Sykoca, & Kettenmann, 1995). More recently, however, the receptors have been shown to modulate ATP-induced Ca^{2+} signals in cultured cortical astrocytes (Morais, Coelho, Vaz, Sebastiao, & Valente, 2017). Furthermore, mRNA and protein analysis from the whole hippocampus show peak expression of GlyRs at P7, suggesting that the transmitter may also play a developmental role here (Aroeira, Ribeiro, Sebastiao, & Valente, 2011). In line with this, astrocytes in the juvenile hippocampus were shown to express GlyT1 (Ghirardini et al., 2018). Like GABA, the Cl^- switch renders the action of glycine excitatory during early development. A further similarity is that ambient levels within the extracellular space are controlled by the reversal of astrocytically expressed transporters (GlyT1). Their specific deletion from glia has no effects in adult animals; however, it causes severe neuromotor deficits if removed within the first postnatal week (Eulenburg, Retiounskaia, Papadopoulos, Gomeza, & Betz, 2010). While we do not yet have complete picture of glycinergic transmission in astrocytes, these findings point to a more prominent role in young animals than in the mature brain, wherein glycine is prevailingly utilized in the spinal cord and brain stem (Bowery & Smart, 2006; Friauf, Fischer, & Fuhr, 2015).

Cholinergic transmission is present in the young hippocampus, where astrocytes are known to express functional α7-nAChRs (nicotinic acetylcholine receptor) which elicit small Ca^{2+} elevations upon activation (Shen & Yakel, 2012). There is evidence that this activation can alter neuro-inflammation during early development and could therefore provide a neuroprotective mechanism (Cao et al., 2019). While mature hippocampal astrocytes also express cholinergic muscarinic receptors, expression has not been reported during the first postnatal week (Shelton & McCarthy, 2000).

Likewise, adrenergic α1/2 and β receptor expression is very low across the hippocampus, cortex and hypothalamus and does not mature until the end of the third and fourth postnatal week (Hartley & Seeman, 1983). The same is true of serotonin, for which no reaction by hippocampal astrocytes has been reported within the first two postnatal weeks (Cai et al., 2000).

Aside from transmitter receptors and transporters, astrocytic ion signalling can also be instigated by a variety of membrane proteins—most notably, mechanosensitive channels. As astrocytes mature, they stretch out new processes and begin arborization, the progression of which would continuously activate mechanical channels. Therefore, these seem ideally suited for signalling during the developmental process. These include Piezos, which are Ca^{2+}-permeable non-selective cation channels. While studies looking at their functions and roles are still limited, there is evidence that they are upregulated during development and that they play a role in cell fate determination (Sugimoto et al., 2017) and vascular development (Ranade et al., 2014).

Another class of mechanosensitive channel important for astroglial function is TRP channels. TRPV4, the channel responsible for sensing vasodilation/constriction at astrocytic endfeet in mature tissue, is downregulated during early development (Dunn, Hill-Eubanks, Liedtke, & Nelson, 2013). In contrast, TRPC1 channels are already present on around 50% of astrocytes freshly isolated from P1 animals and 100% of adult astrocytes (Malarkey & Parpura, 2008). These have been identified as the primary pathway for Ca^{2+} release from stores in astrocytes. In addition, they are permeable for Na^+, and studies have shown the regulation of both ion fluxes to be dynamic. This along with their co-localization with the NCX makes them ideal coordinators for Ca^{2+} and Na^+ signalling (Reyes, Verkhratsky, & Parpura, 2013; Verkhratsky, Trebak, Perocchi, Khananshvili, & Sekler, 2018).

12 | SYNOPSIS

The first postnatal weeks of the rodent brain constitute a period in which cellular networks undergo morphological and functional maturation. This not only relates to neuronal maturation, involving a surge in dendritic outgrowth and synapse formation, but also comprises the terminal differentiation and maturation of astrocytes and the astrocytic network (Figure 5). Generally, the neonate brain has a significantly lower functional expression of many plasma membrane

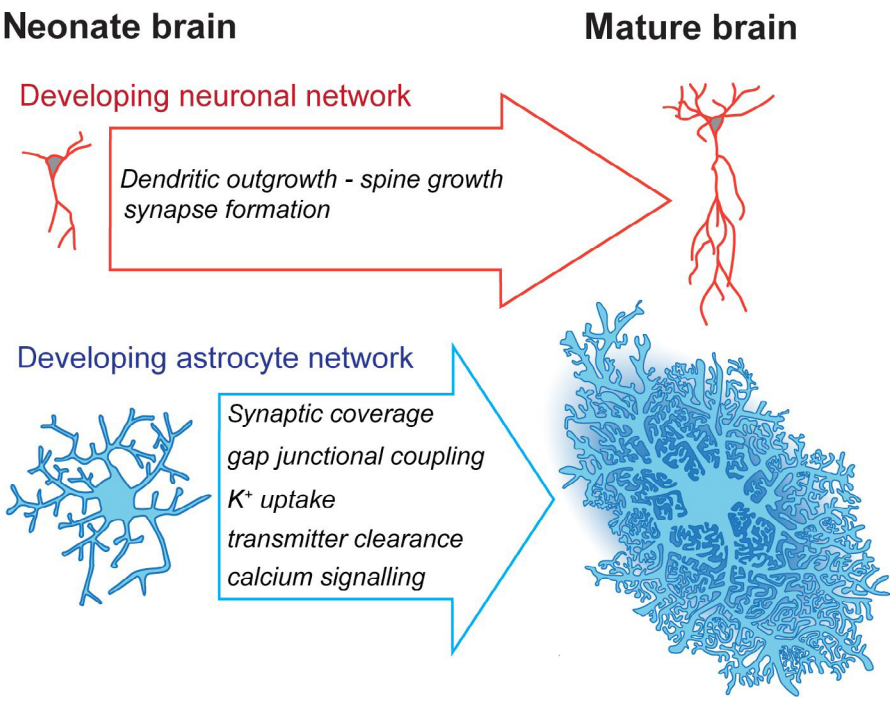

FIGURE 5 Graphic summarizing major developmental changes for neurons and astrocytic networks

proteins than the adult brain. These proteins form the basis of established astrocyte functions at active synapses, such as regulation of extracellular K^+ or uptake of transmitters (Figure 5). Astrocytes in the neonatal brain, therefore, appear to play a different role, with a reduced focus on the support of active neurons in terms of controlling the ionic composition of the ECS. On the other hand side, the clearance of substances released by active neurons in the neonate might not be as demanding as compared to the mature brain. First of all, the much lower density of synapses will result in a lower overall release of K^+ and transmitters. Moreover, the increased size of the ECS enables for a more efficient and rapid diffusion, counteracting a local accumulation of both. The delayed differentiation and functional maturation of astrocytes, compared to neurons in the first postnatal weeks, might thus reflect the reduced need for active (and energy-consuming) regulation of the ECS.

This is by no means to say that astrocytes within young brains are silent bystanders. In fact, multiple lines of evidence point to them as playing a formative role. They do this both by taking up and/or responding to ions and molecules released by other cells (Figure 5) and by actively releasing signalling compounds themselves. This is a tightly regulated process, which has to shift over time to suit the brain's needs as it matures. Dynamic control of astrocyte activity is governed primarily by Ca^{2+} signalling, which offers astrocytes an alternative to classical electrical excitability. Many studies have shown the broad patterns of activity that move across populations of both neurons and astrocytes during development, and the signalling systems involved have largely been described. Yet, the fine differences that distinguish one outcome from another in the wake of a Ca^{2+} influx have yet to be elucidated. The last decade has greatly expanded the toolbox available for Ca^{2+} studies and has undoubtedly furthered our understanding of astrocytic Ca^{2+} signals in the juvenile and mature brain. Implementing these techniques in the neonatal brain will provide valuable insight into the mechanisms fine-tuning Ca^{2+} signals in maturing astrocytes and determining their consequences. In turn, we may be able to better understand and treat the plethora of developmental disorders which impair the growth and development of the CNS.

ACKNOWLEDGEMENTS

Authors' work is supported by funds from the Deutsche Forschungsgemeinschaft (SPP1757 “Glial heterogeneity“) to CRR (Ro2727/8-2) and a Start-up Grant of the SPP1757 to LF.

CONFLICT OF INTERESTS

The authors are not aware of any potential sources of conflict of interest.

AUTHOR CONTRIBUTIONS

All authors contributed to the conceptualization and writing of this manuscript.

ORCID

Jonathan Stephan http://orcid.org/0000-0003-4869-8092
Christine R. Rose https://orcid.org/0000-0002-9684-3592

REFERENCES

Abbott, N. J., Ronnback, L., & Hansson, E. (2006). Astrocyte-endothelial interactions at the blood-brain barrier. *Nature Reviews Neuroscience*, *7*, 41–53. https://doi.org/10.1038/nrn1824

Acosta-Ruiz, A., Gutzeit, V. A., Skelly, M. J., Meadows, S., Lee, J., Parekh, P., … Levitz, J. (2020). Branched photoswitchable tethered ligands enable ultra-efficient optical control and detection of g protein-coupled receptors in vivo. *Neuron*, *105*, 446–463.

Aguado, F., Espinosa-Parrilla, J. F., Carmona, M. A., & Soriano, E. (2002). Neuronal activity regulates correlated network properties of spontaneous calcium transients in astrocytes in situ. *Journal of Neuroscience*, *22*, 9430–9444.

Allen, N. J., & Eroglu, C. (2017). Cell biology of astrocyte-synapse interactions. *Neuron*, *96*, 697–708. https://doi.org/10.1016/j.neuron.2017.09.056

Allene, C., Cattani, A., Ackman, J. B., Bonifazi, P., Aniksztejn, L., Ben-Ari, Y., & Cossart, R. (2008). Sequential generation of two distinct synapse-driven network patterns in developing neocortex. *Journal of Neuroscience*, *28*, 12851–12863. https://doi.org/10.1523/JNEUROSCI.3733-08.2008

Araque, A., Parpura, V., Sanzgiri, R. P., & Haydon, P. G. (1999). Tripartite synapses: Glia, the unacknowledged partner. *Trends in Neurosciences*, *22*, 208–215. https://doi.org/10.1016/S0166-2236(98)01349-6

Aroeira, R. I., Ribeiro, J. A., Sebastiao, A. M., & Valente, C. A. (2011). Age-related changes of glycine receptor at the rat hippocampus: From the embryo to the adult. *Journal of Neurochemistry*, *118*, 339–353. https://doi.org/10.1111/j.1471-4159.2011.07197.x

Barakat, L., & Bordey, A. (2002). GAT-1 and reversible GABA transport in Bergmann glia in slices. *Journal of Neurophysiology*, *88*, 1407–1419. https://doi.org/10.1152/jn.2002.88.3.1407

Barger, Z., Easton, C. R., Neuzil, K. E., & Moody, W. J. (2016). Early network activity propagates bidirectionally between hippocampus and cortex. *Developmental Neurobiology*, *76*, 661–672. https://doi.org/10.1002/dneu.22351

Bay, V., & Butt, A. M. (2012). Relationship between glial potassium regulation and axon excitability: A role for glial Kir4.1 channels. *Glia*, *60*, 651–660. https://doi.org/10.1002/glia.22299

Belanger, M., Allaman, I., & Magistretti, P. J. (2011). Brain energy metabolism: Focus on astrocyte-neuron metabolic cooperation. *Cell Metabolism*, *14*, 724–738. https://doi.org/10.1016/j.cmet.2011.08.016

Belelli, D., Harrison, N. L., Maguire, J., Macdonald, R. L., Walker, M. C., & Cope, D. W. (2009). Extrasynaptic GABAA receptors: Form, pharmacology, and function. *Journal of Neuroscience*, *29*, 12757–12763. https://doi.org/10.1523/JNEUROSCI.3340-09.2009

Ben-Ari, Y. (2001). Developing networks play a similar melody. *Trends in Neurosciences*, *24*, 353–360. https://doi.org/10.1016/S0166-2236(00)01813-0

Ben-Ari, Y. (2014). The GABA excitatory/inhibitory developmental sequence: A personal journey. *Neuroscience*, *279*, 187–219. https://doi.org/10.1016/j.neuroscience.2014.08.001

Ben-Ari, Y., Cherubini, E., Corradetti, R., & Gaiarsa, J. L. (1989). Giant synaptic potentials in immature rat CA3 hippocampal neurones. *Journal of Physiology*, *416*, 303–325. https://doi.org/10.1113/jphysiol.1989.sp017762

Benediktsson, A. M., Marrs, G. S., Tu, J. C., Worley, P. F., Rothstein, J. D., Bergles, D. E., & Dailey, M. E. (2012). Neuronal activity regulates glutamate transporter dynamics in developing astrocytes. *Glia*, *60*, 175–188. https://doi.org/10.1002/glia.21249

Bergles, D., & Jahr, C. (1997). Synaptic activation of glutamate transporters in hippocampal astrocytes. *Neuron*, *19*, 1297–1308. https://doi.org/10.1016/S0896-6273(00)80420-1

Bindocci, E., Savtchouk, I., Liaudet, N., Becker, D., Carriero, G., & Volterra, A. (2017). Three-dimensional Ca^{2+} imaging advances understanding of astrocyte biology. *Science*, *356*, eaai8185.

Boddum, K., Jensen, T. P., Magloire, V., Kristiansen, U., Rusakov, D. A., Pavlov, I., & Walker, M. C. (2016). Astrocytic GABA transporter activity modulates excitatory neurotransmission. *Nature Communications*, *7*, 13572. https://doi.org/10.1038/ncomms13572

Bolea, S., Sanchez-Andres, J. V., Huang, X., & Wu, J. Y. (2006). Initiation and propagation of neuronal coactivation in the developing hippocampus. *Journal of Neurophysiology*, *95*, 552–561. https://doi.org/10.1152/jn.00321.2005

Bolteus, A. J., & Bordey, A. (2004). GABA release and uptake regulate neuronal precursor migration in the postnatal subventricular zone. *Journal of Neuroscience*, *24*, 7623–7631. https://doi.org/10.1523/JNEUROSCI.1999-04.2004

Borden, L. A. (1996). GABA transporter heterogeneity: Pharmacology and cellular localization. *Neurochemistry International*, *29*, 335–356. https://doi.org/10.1016/0197-0186(95)00158-1

Bordey, A., & Sontheimer, H. (1997). Postnatal development of ionic currents in rat hippocampal astrocytes in situ. *Journal of Neurophysiology*, *78*, 461–477. https://doi.org/10.1152/jn.1997.78.1.461

Bordey, A., & Sontheimer, H. (2000). Ion channel expression by astrocytes in situ: Comparison of different CNS regions. *Glia*, *30*, 27–38. https://doi.org/10.1002/(SICI)1098-1136(200003)30:1<27:AID-GLIA4>3.0.CO;2-#

Bormann, J., & Kettenmann, H. (1988). Patch-clamp study of gamma-aminobutyric acid receptor Cl^- channels in cultured astrocytes. *Neurobiology*, *85*, 9336–9340.

Bowery, N. G., & Smart, T. G. (2006). GABA and glycine as neurotransmitters: A brief history. *British Journal of Pharmacology*, *147*(Suppl 1), S109–S119. https://doi.org/10.1038/sj.bjp.0706443

Bushong, E. A., Martone, M. E., & Ellisman, M. H. (2004). Maturation of astrocyte morphology and the establishment of astrocyte domains during postnatal hippocampal development. *International Journal of Developmental Neuroscience*, *22*, 73–86. https://doi.org/10.1016/j.ijdevneu.2003.12.008

Bushong, E. A., Martone, M. E., Jones, Y. Z., & Ellisman, M. H. (2002). Protoplasmic astrocytes in CA1 stratum radiatum occupy separate anatomical domains. *Journal of Neuroscience*, *22*, 183–192. https://doi.org/10.1523/JNEUROSCI.22-01-00183.2002

Cahoy, J. D., Emery, B., Kaushal, A., Foo, L. C., Zamanian, J. L., Christopherson, K. S., … Barres, B. A. (2008). A transcriptome database for astrocytes, neurons, and oligodendrocytes: A new resource for understanding brain development and function. *Journal of Neuroscience*, *28*, 264–278. https://doi.org/10.1523/JNEUROSCI.4178-07.2008

Cai, Z., Schools, G. P., & Kimelberg, H. K. (2000). Metabotropic glutamate receptors in acutely isolated hippocampal astrocytes: Developmental changes of mGluR5 mRNA and functional expression. *Glia*, *29*, 70–80. https://doi.org/10.1002/(SICI)1098-1136(20000101)29:1<70:AID-GLIA7>3.0.CO;2-V

Campbell, K., & Götz, M. (2002). Radial glia: Multi-purpose cells for vertebrate brain development. *Trends in Neuroscience*, *25*, 235–238. https://doi.org/10.1016/S0166-2236(02)02156-2

Canepari, M., Mammano, F., Kachalsky, S. G., Rahamimoff, R., & Cherubini, E. (2000). GABA- and glutamate-mediated network activity in the hippocampus of neonatal and juvenile rats revealed by fast calcium imaging. *Cell Calcium*, *27*, 25–33. https://doi.org/10.1054/ceca.1999.0086

Cao, M., MacDonald, J. W., Liu, H. L., Weaver, M., Cortes, M., Durosier, L. D., … Frasch, M. G. (2019). α7 Nicotinic acetylcholine receptor signaling modulates ovine fetal brain astrocytes transcriptome in

response to endotoxin. *Frontiers in Immunology*, *10*, 1–13. https://doi.org/10.3389/fimmu.2019.01063

Centemeri, A., Bolego, C., Abbracchio, M. P., Cattabeni, F., Puglisi, L., Burnstock, G., & Nicosia, S. (1997). Characterization of the Ca^{2+} responses evoked by ATP and other nucleotides in mammalian brain astrocytes. *British Journal of Pharmacology*, *121*, 1700–1706.

Cheung, K. K., Ryten, M., & Burnstock, G. (2003). Abundant and dynamic expression of G protein-coupled P2Y receptors in mammalian development. *Developmental Dynamics*, *228*, 254–266. https://doi.org/10.1002/dvdy.10378

Chever, O., Djukic, B., McCarthy, K. D., & Amzica, F. (2010). Implication of Kir4.1 channel in excess potassium clearance: An in vivo study on anesthetized glial-conditional Kir4.1 knock-out mice. *Journal of Neuroscience*, *30*, 15769–15777. https://doi.org/10.1523/JNEUROSCI.2078-10.2010

Chever, O., Lee, C. Y., & Rouach, N. (2014). Astroglial connexin43 hemichannels tune basal excitatory synaptic transmission. *Journal of Neuroscience*, *34*, 11228–11232. https://doi.org/10.1523/JNEUROSCI.0015-14.2014

Clarke, L. E., & Barres, B. A. (2013). Emerging roles of astrocytes in neural circuit development. *Nature Reviews Neuroscience*, *14*, 311–321. https://doi.org/10.1038/nrn3484

Clasadonte, J., Scemes, E., Wang, Z., Boison, D., & Haydon, P. G. (2017). Connexin 43-mediated astroglial metabolic networks contribute to the regulation of the sleep-wake cycle. *Neuron*, *95*, 1365–1380. https://doi.org/10.1016/j.neuron.2017.08.022

Connors, B. W., Ransom, B. R., Kunis, D. M., & Gutnick, M. J. (1982). Activity-dependent K^+ accumulation in the developing rat optic nerve. *Science*, *216*, 1341–1343. https://doi.org/10.1126/science.7079771

Conti, F., Minelli, A., & Melone, M. (2004). GABA transporters in the mammalian cerebral cortex: Localization, development and pathological implications. *Brain Research Reviews*, *45*, 196–212. https://doi.org/10.1016/j.brainresrev.2004.03.003

Corlew, R., Bosma, M. M., & Moody, W. J. (2004). Spontaneous, synchronous electrical activity in neonatal mouse cortical neurones. *Journal of Physiology*, *560*, 377–390. https://doi.org/10.1113/jphysiol.2004.071621

D'Ambrosio, R., Gordon, D. S., & Winn, H. R. (2002). Differential role of KIR channel and Na^+/K^+-pump in the regulation of extracellular K^+ in rat hippocampus. *Journal of Neurophysiology*, *87*, 87–102.

D'Ambrosio, R., Wenzel, J., Schwartzkroin, P. A., McKhann, G. M. 2nd, & Janigro, D. (1998). Functional specialization and topographic segregation of hippocampal astrocytes. *Journal of Neuroscience*, *18*, 4425–4438. https://doi.org/10.1523/JNEUROSCI.18-12-04425.1998

Danbolt, N. C. (2001). Glutamate uptake. *Progress in Neurobiology*, *65*, 1–105. https://doi.org/10.1016/S0301-0082(00)00067-8

Demarque, M., Villeneuve, N., Manent, J. B., Becq, H., Represa, A., Ben-Ari, Y., & Aniksztejn, L. (2004). Glutamate transporters prevent the generation of seizures in the developing rat neocortex. *Journal of Neuroscience*, *24*, 3289–3294. https://doi.org/10.1523/JNEUROSCI.5338-03.2004

Dermietzel, R., Traub, O., Hwang, T. K., Beyer, E., Bennett, M. V., Spray, D. C., & Willecke, K. (1989). Differential expression of three gap junction proteins in developing and mature brain tissues. *Proceedings of the National Academy of Sciences, USA*, *86*, 10148–10152. https://doi.org/10.1073/pnas.86.24.10148

Derouiche, A., & Frotscher, M. (2001). Peripheral astrocyte processes: Monitoring by selective immunostaining for the actin-binding ERM proteins. *Glia*, *36*, 330–341. https://doi.org/10.1002/glia.1120

Diamond, J. S. (2005). Deriving the glutamate clearance time course from transporter currents in CA1 hippocampal astrocytes: Transmitter uptake gets faster during development. *Journal of Neuroscience*, *25*, 2906–2916. https://doi.org/10.1523/JNEUROSCI.5125-04.2005

Dimou, L., & Gallo, V. (2015). NG2-glia and their functions in the central nervous system. *Glia*, *63*, 1429–1451.

Djukic, B., Casper, K. B., Philpot, B. D., Chin, L. S., & McCarthy, K. D. (2007). Conditional knock-out of Kir4.1 leads to glial membrane depolarization, inhibition of potassium and glutamate uptake, and enhanced short-term synaptic potentiation. *Journal of Neuroscience*, *27*, 11354–11365. https://doi.org/10.1523/JNEUROSCI.0723-07.2007

Doengi, M., Hirnet, D., Coulon, P., Pape, H. C., Deitmer, J. W., & Lohr, C. (2009). GABA uptake-dependent Ca^{2+} signaling in developing olfactory bulb astrocytes. *Proceedings of the National Academy of Sciences, USA*, *106*, 17570–17575. https://doi.org/10.1073/pnas.0809513106

Dunn, K. M., Hill-Eubanks, D. C., Liedtke, W. B., & Nelson, M. T. (2013). TRPV4 channels stimulate Ca^{2+}-induced Ca^{2+} release in astrocytic endfeet and amplify neurovascular coupling responses. *Proceedings of the National Academy of Sciences, USA*, *110*, 6157–6162. https://doi.org/10.1073/pnas.1216514110

Dvorzhak, A., Myakhar, O., Unichenko, P., Kirmse, K., & Kirischuk, S. (2010). Estimation of ambient GABA levels in layer I of the mouse neonatal cortex in brain slices. *Journal of Physiology*, *588*, 2351–2360. https://doi.org/10.1113/jphysiol.2010.187054

Elias, L. A., & Kriegstein, A. R. (2008). Gap junctions: Multifaceted regulators of embryonic cortical development. *Trends in Neurosciences*, *31*, 243–250. https://doi.org/10.1016/j.tins.2008.02.007

Escartin, C., & Rouach, N. (2013). Astroglial networking contributes to neurometabolic coupling. *Front Neuroenergetics*, *5*, 4. https://doi.org/10.3389/fnene.2013.00004

Eulenburg, V., & Gomeza, J. (2010). Neurotransmitter transporters expressed in glial cells as regulators of synapse function. *Brain Research Reviews*, *63*, 103–112. https://doi.org/10.1016/j.brainresrev.2010.01.003

Eulenburg, V., Retiounskaia, M., Papadopoulos, T., Gomeza, J., & Betz, H. (2010). Glial glycine transporter 1 function is essential for early postnatal survival but dispensable in adult mice. *Glia*, *58*, 1066–1073. https://doi.org/10.1002/glia.20987

Felix, L., Ziemens, D., Seifert, G., & Rose, C. R. (2020). Spontaneous ultraslow Na^+ fluctuations in the neonatal mouse brain. *Cells*, *9*(1), 102. https://doi.org/10.3390/cells9010102

Fiacco, T. A., & McCarthy, K. D. (2018). Multiple lines of evidence indicate that gliotransmission does not occur under physiological conditions. *Journal of Neuroscience*, *38*, 3–13. https://doi.org/10.1523/JNEUROSCI.0016-17.2017

Frahm, C., & Draguhn, A. (2001). GAD and GABA transporter (GAT-1) mRNA expression in the developing rat hippocampus. *Developmental Brain Research*, *132*, 1–13. https://doi.org/10.1016/S0165-3806(01)00288-7

Fraser, D. D., Duffy, S., Angelides, K. J., Perez-Velazquez, J. L., Kettenmann, H., & MacVicar, B. A. (1995). GABAA/benzodiazepine receptors in acutely isolated hippocampal astrocytes. *Journal of Neuroscience*, *15*, 2720–2732. https://doi.org/10.1523/JNEUROSCI.15-04-02720.1995

Fraser, D. D., Mudrick-Donnon, L. A., & MacVicar, B. A. (1994). Astrocytic GABA receptors. *Glia*, *11*, 83–93. https://doi.org/10.1002/glia.440110203

Freeman, M. R. (2010). Specification and morphogenesis of astrocytes. *Science*, *330*, 774–778. https://doi.org/10.1126/science.1190928

Friauf, E., Fischer, A. U., & Fuhr, A. F. (2015). Synaptic plasticity in the auditory system: A review. *Cell and Tissue Research*, *361*, 177–213. https://doi.org/10.1007/s00441-015-2176-x

Furuta, A., Rothstein, J. D., & Martin, L. J. (1997). Glutamate transporter protein subtypes are expressed differentially during rat CNS development. *Journal of Neuroscience*, *17*, 8363–8375. https://doi.org/10.1523/JNEUROSCI.17-21-08363.1997

Garaschuk, O., Hanse, E., & Konnerth, A. (1998). Developmental profile and synaptic origin of early network oscillations in the CA1 region of rat neonatal hippocampus. *Journal of Physiology*, *507*, 219–236. https://doi.org/10.1111/j.1469-7793.1998.219bu.x

Garaschuk, O., Linn, J., Eilers, J., & Konnerth, A. (2000). Large-scale oscillatory calcium waves in the immature cortex. *Nature Neuroscience*, *3*, 452–459. https://doi.org/10.1038/74823

Ge, W. P., Miyawaki, A., Gage, F. H., Jan, Y. N., & Jan, L. Y. (2013). Local generation of glia is a major astrocyte source in postnatal cortex. *Nature*, *484*, 376–380. https://doi.org/10.1038/nature10959

Ghirardini, E., Wadle, S. L., Augustin, V., Becker, J., Brill, S., Hammerich, J., … Stephan, J. (2018). Expression of functional inhibitory neurotransmitter transporters GlyT1, GAT-1, and GAT-3 by astrocytes of inferior colliculus and hippocampus. *Molecular Brain*, *11*, 4. https://doi.org/10.1186/s13041-018-0346-y

Ghosh, M., Yang, Y., Rothstein, J. D., & Robinson, M. B. (2011). Nuclear factor-kappaB contributes to neuron-dependent induction of glutamate transporter-1 expression in astrocytes. *Journal of Neuroscience*, *31*, 9159–9169.

Giaume, C., Koulakoff, A., Roux, L., Holcman, D., & Rouach, N. (2010). Astroglial networks: A step further in neuroglial and gliovascular interactions. *Nature Reviews Neuroscience*, *11*, 87–99. https://doi.org/10.1038/nrn2757

Griguoli, M., & Cherubini, E. (2017). Early correlated network activity in the hippocampus: its putative role in shaping neuronal circuits. *Frontiers in Cellular Neuroscience*, *11*, 1–11. https://doi.org/10.3389/fncel.2017.00255

Grimm, I., Messemer, N., Stanke, M., Gachet, C., & Zimmermann, H. (2009). Coordinate pathways for nucleotide and EGF signaling in cultured adult neural progenitor cells. *Journal of Cell Science*, *122*, 2524–2533. https://doi.org/10.1242/jcs.044891

Grosche, A., & Reichenbach, A. (2013). Developmental refining of neuroglial signaling? *Neuroscience*, *339*, 152–153. https://doi.org/10.1126/science.1233208

Halassa, M. M., Fellin, T., Takano, H., Dong, J. H., & Haydon, P. G. (2007). Synaptic islands defined by the territory of a single astrocyte. *Journal of Neuroscience*, *27*, 6473–6477. https://doi.org/10.1523/JNEUROSCI.1419-07.2007

Hanganu-Opatz, I. L. (2010). Between molecules and experience: Role of early patterns of coordinated activity for the development of cortical maps and sensory abilities. *Brain Research Reviews*, *64*, 160–176. https://doi.org/10.1016/j.brainresrev.2010.03.005

Hanson, E., Armbruster, M., Cantu, D., Andresen, L., Taylor, A., Danbolt, N. C., & Dulla, C. G. (2015). Astrocytic glutamate uptake is slow and does not limit neuronal NMDA receptor activation in the neonatal neocortex. *Glia*, *63*, 1784–1796. https://doi.org/10.1002/glia.22844

Hartley, E. J., & Seeman, P. (1983). Development of receptors for dopamine and noradrenaline in rat brain. *European Journal of Pharmacology*, *91*, 391–397. https://doi.org/10.1016/0014-2999(83)90163-2

Heinemann, U., & Lux, H. D. (1977). Ceiling of stimulus induced rises in extracellular potassium concentration in the cerebral cortex of cat. *Brain Research*, *120*, 231–249. https://doi.org/10.1016/0006-8993(77)90903-9

Heins, N., Malatesta, P., Cecconi, F., Nakafuku, M., Tucker, K. L., Hack, M. A., … Gotz, M. (2002). Glial cells generate neurons: The role of the transcription factor Pax6. *Nature Neuroscience*, *5*, 308–315. https://doi.org/10.1038/nn828

Heja, L., Nyitrai, G., Kekesi, O., Dobolyi, A., Szabo, P., Fiath, R., … Kardos, J. (2012). Astrocytes convert network excitation to tonic inhibition of neurons. *BMC Biology*, *10*, 1–21. https://doi.org/10.1186/1741-7007-10-26

Hertz, L., Gerkau, N. J., Xu, J., Durry, S., Song, D., Rose, C. R., & Peng, L. (2015). Roles of astrocytic Na^+, K^+ -ATPase and glycogenolysis for K^+ homeostasis in mammalian brain. *Journal of Neuroscience Research*, *93*, 1019–1030.

Hirasawa, T., Wada, H., Kohsaka, S., & Uchino, S. (2003). Inhibition of NMDA receptors induces delayed neuronal maturation and sustained proliferation of progenitor cells during neocortical development. *Journal of Neuroscience Research*, *74*, 676–687. https://doi.org/10.1002/jnr.10795

Hirrlinger, P. G., Scheller, A., Braun, C., Hirrlinger, J., & Kirchhoff, F. (2006). Temporal control of gene recombination in astrocytes by transgenic expression of the tamoxifen-inducible DNA recombinase variant CreERT2. *Glia*, *54*, 11–20. https://doi.org/10.1002/glia.20342

Houades, V., Koulakoff, A., Ezan, P., Seif, I., & Giaume, C. (2008). Gap junction-mediated astrocytic networks in the mouse barrel cortex. *Journal of Neuroscience*, *28*, 5207–5217. https://doi.org/10.1523/JNEUROSCI.5100-07.2008

Huang, H., Barakat, L., Wang, D., & Bordey, A. (2004). Bergmann glial GlyT1 mediates glycine uptake and release in mouse cerebellar slices. *Journal of Physiology*, *560*, 721–736. https://doi.org/10.1113/jphysiol.2004.067801

Huang, Y. H., & Bergles, D. E. (2004). Glutamate transporters bring competition to the synapse. *Current Opinion in Neurobiology*, *14*, 346–352. https://doi.org/10.1016/j.conb.2004.05.007

Iadecola, C. (2017). The neurovascular unit coming of age: a journey through neurovascular coupling in health and disease. *Neuron*, *96*, 17–42. https://doi.org/10.1016/j.neuron.2017.07.030

Iino, M., Goto, K., Kakegawa, W., Okado, H., Sudo, M., Ishiuchi, S., … Ozawa, S. (2001). Glia-synapse interaction through Ca^{2+} permiable AMPA receptors in Bergmann Glia. *Science*, *292*, 926–929.

Jendelova, P., & Sykova, E. (1991). Role of glia in K^+ and pH homeostasis in the neonatal rat spinal cord. *Glia*, *4*, 56–63.

Kafitz, K. W., Meier, S. D., Stephan, J., & Rose, C. R. (2008). Developmental profile and properties of sulforhodamine 101–Labeled glial cells in acute brain slices of rat hippocampus. *Journal of Neuroscience Methods*, *169*, 84–92. https://doi.org/10.1016/j.jneumeth.2007.11.022

Kang, J., Kang, N., Lovatt, D., Torres, A., Zhao, Z., Lin, J., & Nedergaard, M. (2008). Connexin 43 hemichannels are permeable to ATP. *Journal of Neuroscience*, *28*, 4702–4711. https://doi.org/10.1523/JNEUROSCI.5048-07.2008

Karus, C., Gerkau, N. J., & Rose, C. R. (2017). Differential contribution of GLAST and GLT-1 to network sodium signaling in the early postnatal hippocampus. *Opera Medica et Physiologica*, *3*, 71–83.

Karus, C., Mondragao, M. A., Ziemens, D., & Rose, C. R. (2015). Astrocytes restrict discharge duration and neuronal sodium loads

during recurrent network activity. *Glia*, *63*, 936–957. https://doi.org/10.1002/glia.22793

Kettenmann, H., Backus, K. H., & Schachner, M. (1984). Aspartate, glutamate and gamma-aminobutyric acid depolarize cultured astrocytes. *Neuroscience Letters*, *52*, 25–29.

Khakh, B. S., & Sofroniew, M. V. (2015). Diversity of astrocyte functions and phenotypes in neural circuits. *Nature Neuroscience*, *18*, 942–952. https://doi.org/10.1038/nn.4043

Khazipov, R., & Luhmann, H. J. (2006). Early patterns of electrical activity in the developing cerebral cortex of humans and rodents. *Trends in Neurosciences*, *29*, 414–418. https://doi.org/10.1016/j.tins.2006.05.007

Kilb, W., Kirischuk, S., & Luhmann, H. J. (2011). Electrical activity patterns and the functional maturation of the neocortex. *European Journal of Neuroscience*, *34*, 1677–1686. https://doi.org/10.1111/j.1460-9568.2011.07878.x

Kim, J. S., Kim, J., Kim, Y., Yang, M., Jang, H., Kang, S., … Moon, C. (2011). Differential patterns of nestin and glial fibrillary acidic protein expression in mouse hippocampus during postnatal development. *Journal of Veterinary Science*, *12*, 1–6. https://doi.org/10.4142/jvs.2011.12.1.1

Kimelberg, H. K., Bowman, C., Biddlecome, S., & Bourke, R. S. (1979). Cation transport and membrane potential properties of primary astroglial cultures from neonatal rat brains. *Brain Research*, *177*, 533–550. https://doi.org/10.1016/0006-8993(79)90470-0

Kimoto, H., Eto, R., Abe, M., Kato, H., & Araki, T. (2009). Alterations of glial cells in the mouse hippocampus during postnatal development. *Cellular and Molecular Neurobiology*, *29*, 1181–1189. https://doi.org/10.1007/s10571-009-9412-4

Kirmse, K., & Kirischuk, S. (2006). Ambient GABA constrains the strength of GABAergic synapses at Cajal-Retzius cells in the developing visual cortex. *Journal of Neuroscience*, *26*, 4216–4227. https://doi.org/10.1523/JNEUROSCI.0589-06.2006

Kiyoshi, C. M., Du, Y., Zhong, S., Wang, W., Taylor, A. T., Xiong, B., … Zhou, M. (2018). Syncytial isopotentiality: A system-wide electrical feature of astrocytic networks in the brain. *Glia*, *66*, 2756–2769. https://doi.org/10.1002/glia.23525

Kofuji, P., Ceelen, P., Zahs, K. R., Surbeck, L. W., Lester, H. A., & Newman, E. A. (2000). Genetic inactivation of an inwardly rectifying potassium channel (Kir4.1 subunit) in mice: Phenotypic impact in retina. *Journal of Neuroscience*, *20*, 5733–5740. https://doi.org/10.1523/JNEUROSCI.20-15-05733.2000

Koulakoff, A., Ezan, P., & Giaume, C. (2008). Neurons control the expression of connexin 30 and connexin 43 in mouse cortical astrocytes. *Glia*, *56*, 1299–1311. https://doi.org/10.1002/glia.20698

Kriegstein, A., & Alvarez-Buylla, A. (2009). The glial nature of embryonic and adult neural stem cells. *Annual Review of Neuroscience*, *32*, 149–184. https://doi.org/10.1146/annurev.neuro.051508.135600

Kuga, N., Sasaki, T., Takahara, Y., Matsuki, N., & Ikegaya, Y. (2011). Large-scale calcium waves traveling through astrocytic networks in vivo. *Journal of Neuroscience*, *31*, 2607–2614. https://doi.org/10.1523/JNEUROSCI.5319-10.2011

Lacar, B., Young, S. Z., Platel, J. C., & Bordey, A. (2011). Gap junction-mediated calcium waves define communication networks among murine postnatal neural progenitor cells. *European Journal of Neuroscience*, *34*, 1895–1905. https://doi.org/10.1111/j.1460-9568.2011.07901.x

Langer, J., Stephan, J., Theis, M., & Rose, C. R. (2012). Gap junctions mediate intercellular spread of sodium between hippocampal astrocytes in situ. *Glia*, *60*, 239–252. https://doi.org/10.1002/glia.21259

Larsen, B. R., Assentoft, M., Cotrina, M. L., Hua, S. Z., Nedergaard, M., Kaila, K., … MacAulay, N. (2014). Contributions of the Na^+/K^+-ATPase, NKCC1, and Kir4.1 to hippocampal K^+ clearance and volume responses. *Glia*, *62*, 608–622.

Larsen, B. R., Stoica, A., & MacAulay, N. (2016). Managing brain extracellular K^+ during neuronal activity: The physiological role of the Na^+/K^+-ATPase subunit isoforms. *Frontiers in Physiology*, *7*, 141. https://doi.org/10.3389/fphys.2016.00141

Larsen, B. R., Stoica, A., & MacAulay, N. (2019). Developmental maturation of activity-induced K^+ and pH transients and the associated extracellular space dynamics in the rat hippocampus. *Journal of Physiology*, *597*, 583–597.

Losi, G., Mariotti, L., & Carmignoto, G. (2014). GABAergic interneuron to astrocyte signalling: A neglected form of cell communication in the brain. *Philosophical Transactions of the Royal Society B: Biological Sciences*, *369*, 20130609.

Luhmann, H. J., Fukuda, A., & Kilb, W. (2015). Control of cortical neuronal migration by glutamate and GABA. *Frontiers in Cellular Neuroscience*, *9*, 4. https://doi.org/10.3389/fncel.2015.00004

Lunde, L. K., Camassa, L. M., Hoddevik, E. H., Khan, F. H., Ottersen, O. P., Boldt, H. B., & Amiry-Moghaddam, M. (2015). Postnatal development of the molecular complex underlying astrocyte polarization. *Brain Structure & Function*, *220*, 2087–2101. https://doi.org/10.1007/s00429-014-0775-z

Ma, B., Buckalew, R., Du, Y., Kiyoshi, C. M., Alford, C. C., Wang, W., … Zhou, M. (2016). Gap junction coupling confers isopotentiality on astrocyte syncytium. *Glia*, *64*, 214–226. https://doi.org/10.1002/glia.22924

MacVicar, B. A., Feighan, D., Brown, A., & Ransom, B. (2002). Intrinsic optical signals in the rat optic nerve: Role for K^+ uptake via NKCC1 and swelling of astrocytes. *Glia*, *37*, 114–123. https://doi.org/10.1002/glia.10023

MacVicar, B. A., Tse, F. W. Y., Crichton, S. A., & Kettenmann, H. (1989). GABA-activated Cl-channels in astrocytes of hippocampal slices. *The Journal of Neuroscience*, *9*, 3577–3583. https://doi.org/10.1523/JNEUROSCI.09-10-03577.1989

Malarkey, E. B., & Parpura, V. (2008). Mechanisms of glutamate release from astrocytes. *Neurochemistry International*, *52*, 142–154. https://doi.org/10.1016/j.neuint.2007.06.005

Maragakis, N. J., & Rothstein, J. D. (2004). Glutamate transporters: Animal models to neurologic disease. *Neurobiology of Diseases*, *15*, 461–473. https://doi.org/10.1016/j.nbd.2003.12.007

Marcaggi, P., & Attwell, D. (2004). Role of glial amino acid transporters in synaptic transmission and brain energetics. *Glia*, *47*, 217–225. https://doi.org/10.1002/glia.20027

Mariotti, L., Losi, G., Sessolo, M., Marcon, I., & Carmignoto, G. (2016). The inhibitory neurotransmitter GABA evokes long-lasting Ca^{2+} oscillations in cortical astrocytes. *Glia*, *64*, 363–373.

Matos, M., Bosson, A., Riebe, I., Reynell, C., Vallee, J., Laplante, I., … Lacaille, J. C. (2018). Astrocytes detect and upregulate transmission at inhibitory synapses of somatostatin interneurons onto pyramidal cells. *Nature Communications*, *9*, 4254. https://doi.org/10.1038/s41467-018-06731-y

Matsugami, T. R., Tanemura, K., Mieda, M., Nakatomi, R., Yamada, K., Kondo, T., … Tanaka, K. (2006). From the Cover: Indispensability of the glutamate transporters GLAST and GLT1 to brain development. *Proceedings of the National Academy of Sciences, USA*, *103*, 12161–12166. https://doi.org/10.1073/pnas.0509144103

Matsutani, S., & Yamamoto, N. (1997). Neuronal regulation of astrocyte morphology in vitro is mediated by GABAergic signalling. *Glia*, *20*, 1–9.

Matthias, K., Kirchhoff, F., Seifert, G., Huttmann, K., Matyash, M., Kettenmann, H., & Steinhauser, C. (2003). Segregated expression of AMPA-type glutamate receptors and glutamate transporters defines distinct astrocyte populations in the mouse hippocampus. *Journal of Neuroscience*, *23*, 1750–1758. https://doi.org/10.1523/JNEUROSCI.23-05-01750.2003

Meier, S. D., Kafitz, K. W., & Rose, C. R. (2008). Developmental profile and mechanisms of GABA-induced calcium signaling in hippocampal astrocytes. *Glia*, *56*, 1127–1137. https://doi.org/10.1002/glia.20684

Middeldorp, J., & Hol, E. M. (2011). GFAP in health and disease. *Progress in Neurobiology*, *93*, 421–443. https://doi.org/10.1016/j.pneurobio.2011.01.005

Miller, S. J., Philips, T., Kim, N., Dastgheyb, R., Chen, Z., Hsieh, Y. C., … Rothstein, J. D. (2019). Molecularly defined cortical astroglia subpopulation modulates neurons via secretion of Norrin. *Nature Neuroscience*, *22*, 741–752. https://doi.org/10.1038/s41593-019-0366-7

Minelli, A., Barbaresi, P., & Conti, F. (2003). Postnatal development of high-affinity plasma membrane GABA transporters GAT-2 and GAT-3 in the rat cerebral cortex. *Developmental Brain Research*, *142*, 7–18. https://doi.org/10.1016/S0165-3806(03)00007-5

Minelli, A., DeBiasi, S., Brecha, N. C., Zuccarello, L. V., & Conti, F. (1996). GAT-3, a high affinity GABA plasma membrane transporter, is localized to astrocytic processes, and it is not confined to the vicinity of GABAergic synapses in the cerebral cortex. *Journal of Neuroscience*, *16*, 6255–6264. https://doi.org/10.1523/JNEUROSCI.16-19-06255.1996

Mishra, S. K., Braun, N., Shukla, V., Fullgrabe, M., Schomerus, C., Korf, H. W., … Zimmermann, H. (2006). Extracellular nucleotide signaling in adult neural stem cells: Synergism with growth factor-mediated cellular proliferation. *Development*, *133*, 675–684. https://doi.org/10.1242/dev.02233

Mohajerani, M. H., & Cherubini, E. (2006). Role of giant depolarizing potentials in shaping synaptic currents in the developing hippocampus. *Critical Reviews™ in Neurobiology*, *18*, 13–23. https://doi.org/10.1615/CritRevNeurobiol.v18.i1-2.30

Molders, A., Koch, A., Menke, R., & Klocker, N. (2018). Heterogeneity of the astrocytic AMPA-receptor transcriptome. *Glia*, *66*, 2604–2616. https://doi.org/10.1002/glia.23514

Molofsky, A. V., & Deneen, B. (2015). Astrocyte development: A Guide for the Perplexed. *Glia*, *63*, 1320–1329.

Mong, J. A., Nunez, J. L., & McCarthy, M. M. (2002). GABA mediates steroid-induced astrocytes differentiation in the neonatal rat hippocampus. *Journal of Neuroendocrinology*, *14*, 45–55.

Morais, T. P., Coelho, D., Vaz, S. H., Sebastiao, A. M., & Valente, C. A. (2017). Glycine receptor activation impairs ATP-induced calcium transients in cultured cortical astrocytes. *Frontiers in Molecular Neuroscience*, *10*, 444. https://doi.org/10.3389/fnmol.2017.00444

Morel, L., Higashimori, H., Tolman, M., & Yang, Y. (2014). VGluT1+ neuronal glutamatergic signaling regulates postnatal developmental maturation of cortical protoplasmic astroglia. *Journal of Neuroscience*, *34*, 10950–10962. https://doi.org/10.1523/JNEUROSCI.1167-14.2014

Morel, L., Men, Y., Chiang, M. S. R., Tian, Y., Jin, S., Yelick, J., … Yang, Y. (2019). Intracortical astrocyte subpopulations defined by astrocyte reporter Mice in the adult brain. *Glia*, *67*, 171–181. https://doi.org/10.1002/glia.23545

Mori, T., Tanaka, K., Buffo, A., Wurst, W., Kuhn, R., & Gotz, M. (2006). Inducible gene deletion in astroglia and radial glia-A valuable tool for functional and lineage analysis. *Glia*, *54*, 21–34. https://doi.org/10.1002/glia.20350

Moroni, R. F., Inverardi, F., Regondi, M. C., Pennacchio, P., & Frassoni, C. (2015). Developmental expression of Kir4.1 in astrocytes and oligodendrocytes of rat somatosensory cortex and hippocampus. *International Journal of Developmental Neuroscience*, *47*, 198–205. https://doi.org/10.1016/j.ijdevneu.2015.09.004

Muthukumar, A. K., Stork, T., & Freeman, M. R. (2014). Activity-dependent regulation of astrocyte GAT levels during synaptogenesis. *Nature Neuroscience*, *17*, 1340–1350. https://doi.org/10.1038/nn.3791

Nagy, J. I., & Rash, J. E. (2000). Connexins and gap junctions of astrocytes and oligodendrocytes in the CNS. *Brain Research. Brain Research Reviews*, *32*, 29–44. https://doi.org/10.1016/S0165-0173(99)00066-1

Nakayama, R., Sasaki, T., Tanaka, K. F., & Ikegaya, Y. (2016). Subcellular calcium dynamics during juvenile development in mouse hippocampal astrocytes. *European Journal of Neuroscience*, *43*, 923–932. https://doi.org/10.1111/ejn.13188

Nedergaard, M., Ransom, B., & Goldman, S. A. (2003). New roles for astrocytes: Redefining the functional architecture of the brain. *Trends in Neurosciences*, *26*, 523–530. https://doi.org/10.1016/j.tins.2003.08.008

Nett, W. J., Oloff, S. H., & McCarthy, K. D. (2002). Hippocampal astrocytes in situ exhibit calcium oscillations that occur independent of neuronal activity. *Journal of Neurophysiology*, *87*, 528–537. https://doi.org/10.1152/jn.00268.2001

Nicholson, C., & Hrabetova, S. (2017). Brain extracellular space: the final frontier of neuroscience. *Biophysical Journal*, *113*, 2133–2142.

Nielsen, B. S., Hansen, D. B., Ransom, B. R., Nielsen, M. S., & MacAulay, N. (2017). Connexin hemichannels in astrocytes: an assessment of controversies regarding their functional characteristics. *Neurochemical Research*, *42*, 2537–2550. https://doi.org/10.1007/s11064-017-2243-7

Nilsson, M., Eriksson, P. S., Ronnback, L., & Hansson, E. (1993). GABA induces Ca^{2+} transients in astrocytes. *Neuroscience*, *54*, 605–614. https://doi.org/10.1016/0306-4522(93)90232-5

Nimmerjahn, A., & Helmchen, F. (2012). In vivo labeling of cortical astrocytes with sulforhodamine 101 (SR101). *Cold Spring Harbor Protocols*, *2012*, 326–334. https://doi.org/10.1101/pdb.prot068155

Nishiyama, A. (2001). NG2 cells in the brain: A novel glial cell population. *Human Cell*, *14*, 77–82.

Nixdorf-Bergweiler, B. E., Albrecht, D., & Heinemann, U. (1994). Developmental changes in the number, size, and orientation of GFAP-positive cells in the CA1 region of rat hippocampus. *Glia*, *12*, 180–195. https://doi.org/10.1002/glia.440120304

Nolte, C., Matyash, M., Pivneva, T., Schipke, C. G., Ohlemeyer, C., Hanisch, U. K., … Kettenmann, H. (2001). GFAP promoter-controlled EGFP-expressing transgenic mice: A tool to visualize astrocytes and astrogliosis in living brain tissue. *Glia*, *33*, 72–86. https://doi.org/10.1002/1098-1136(20010101)33:1<72:AID-GLIA1007>3.0.CO;2-A

Nwaobi, S. E., Lin, E., Peramsetty, S. R., & Olsen, M. L. (2014). DNA methylation functions as a critical regulator of Kir4.1 expression during CNS development. *Glia*, *62*, 411–427. https://doi.org/10.1002/glia.22613

Oberheim, N. A., Tian, G. F., Han, X., Peng, W., Takano, T., Ransom, B., & Nedergaard, M. (2008). Loss of astrocytic domain organization in the epileptic brain. *Journal of Neuroscience*, *28*, 3264–3276. https://doi.org/10.1523/JNEUROSCI.4980-07.2008

Okubo, Y., Kanemaru, K., Suzuki, J., Kobayashi, K., Hirose, K., & Iino, M. (2019). Inositol 1,4,5-trisphosphate receptor type 2-independent Ca^{2+} release from the endoplasmic reticulum in astrocytes. *Glia*, *67*, 113–124.

Olsen, M. L., Khakh, B. S., Skatchkov, S. N., Zhou, M., Lee, C. J., & Rouach, N. (2015). New insights on astrocyte ion channels: Critical for homeostasis and neuron-glia signaling. *Journal of Neuroscience*, *35*, 13827–13835. https://doi.org/10.1523/JNEUROSCI.2603-15.2015

Palygin, O., Lalo, U., Verkhratsky, A., & Pankratov, Y. (2010). Ionotropic NMDA and P2X1/5 receptors mediate synaptically induced Ca^{2+} signalling in cortical astrocytes. *Cell Calcium*, *48*, 225–231. https://doi.org/10.1016/j.ceca.2010.09.004

Panatier, A., & Robitaille, R. (2016). Astrocytic mGluR5 and the tripartite synapse. *Neuroscience*, *323*, 29–34. https://doi.org/10.1016/j.neuroscience.2015.03.063

Pannasch, U., Freche, D., Dallerac, G., Ghezali, G., Escartin, C., Ezan, P., … Rouach, N. (2014). Connexin 30 sets synaptic strength by controlling astroglial synapse invasion. *Nature Neuroscience*, *17*, 549–558. https://doi.org/10.1038/nn.3662

Pannasch, U., & Rouach, N. (2013). Emerging role for astroglial networks in information processing: From synapse to behavior. *Trends in Neurosciences*, *36*, 405–417. https://doi.org/10.1016/j.tins.2013.04.004

Pannasch, U., Vargova, L., Reingruber, J., Ezan, P., Holcman, D., Giaume, C., … Rouach, N. (2011). Astroglial networks scale synaptic activity and plasticity. *Proceedings of the National Academy of Sciences, USA*, *108*, 8467–8472. https://doi.org/10.1073/pnas.1016650108

Parpura, V., Heneka, M. T., Montana, V., Oliet, S. H., Schousboe, A., Haydon, P. G., … Verkhratsky, A. (2012). Glial cells in (patho) physiology. *Journal of Neurochemistry*, *121*, 4–27. https://doi.org/10.1111/j.1471-4159.2012.07664.x

Parri, R. H., Gould, T. M., & Crunelli, V. (2001). Spontaneous astrocytic Ca2] oscillations in situ drive NMDAR/mediated neuronal excitation. *Nature Neuroscience*, *4*(803), 812. https://doi.org/10.1038/90507

Pastor, A., Chvatal, A., Sykoca, E., & Kettenmann, H. (1995). Glycine- and GABA-activated currents in identified glial cells of the developing rat spinal cord slice. *European Journal of Neuroscience*, *7*, 1188–1198. https://doi.org/10.1111/j.1460-9568.1995.tb01109.x

Porter, J. T., & Mccarthy, K. D. (1996). Hippocampal astrocytes in situ respond to glutamate released from synaptic terminals. *Journal of Neuroscience*, *16*, 5073–5081.

Ranade, S. S., Qiu, Z., Woo, S. H., Hur, S. S., Murthy, S. E., Cahalan, S. M., … Patapoutian, A. (2014). Piezo1, a mechanically activated ion channel, is required for vascular development in mice. *Proceedings of the National Academy of Sciences, USA*, *111*, 10347–10352. https://doi.org/10.1073/pnas.1409233111

Ransom, B. R., & Goldring, S. (1973). Ionic determinants of membrane potential of cells presumed to be glia in cerebral cortex of cat. *Journal of Neurophysiology*, *36*, 855–868. https://doi.org/10.1152/jn.1973.36.5.855

Ransom, B. R., & Ye, Z.-C. (2005). *Gap junctions and hemichannels*. Oxford: Oxford University Press.

Regan, M. R., Huang, Y. H., Kim, Y. S., Dykes-Hoberg, M. I., Jin, L., Watkins, A. M., … Rothstein, J. D. (2007). Variations in promoter activity reveal a differential expression and physiology of glutamate transporters by glia in the developing and mature CNS. *Journal of Neuroscience*, *27*, 6607–6619. https://doi.org/10.1523/JNEUROSCI.0790-07.2007

Reichenbach, A., Derouiche, A., & Kirchhoff, F. (2010). Morphology and dynamics of perisynaptic glia. *Brain Research Reviews*, *63*, 11–25. https://doi.org/10.1016/j.brainresrev.2010.02.003

Reiprich, P., Kilb, W., & Luhmann, H. J. (2005). Neonatal NMDA receptor blockade disturbs neuronal migration in rat somatosensory cortex in vivo. *Cerebral Cortex*, *15*, 349–358. https://doi.org/10.1093/cercor/bhh137

Reyes, R. C., Verkhratsky, A., & Parpura, V. (2013). TRPC1-mediated Ca^{2+} and Na^{+} signalling in astroglia: Differential filtering of extracellular cations. *Cell Calcium*, *54*, 120–125. https://doi.org/10.1016/j.ceca.2013.05.005

Reynolds, J. P., Zheng, K., & Rusakov, D. A. (2019). Multiplexed calcium imaging of single-synapse activity and astroglial responses in the intact brain. *Neuroscience Letters*, *689*, 26–32. https://doi.org/10.1016/j.neulet.2018.06.024

Richerson, G. B., & Wu, Y. (2003). Dynamic equilibrium of neurotransmitter transporters: Not just for reuptake anymore. *Journal of Neurophysiology*, *90*, 1363–1374. https://doi.org/10.1152/jn.00317.2003

Rose, C. R., Ziemens, D., Untiet, V., & Fahlke, C. (2018). Molecular and cellular physiology of sodium-dependent glutamate transporters. *Brain Research Bulletin*, *136*, 13–16. https://doi.org/10.1016/j.brainresbull.2016.12.013

Rose, C. R., Ziemens, D., & Verkhratsky, A. (2019). On the special role of NCX in astrocytes: Translating Na^{+}-transients into intracellular Ca^{2+} signals. *Cell Calcium*, *86*, 102154. https://doi.org/10.1016/j.ceca.2019.102154

Rosina, A., Morara, S., & Provini, L. (1999). GAT-1 developmental expression in the rat cerebellar cortex: Basket and pinceau formation. *NeuroReport*, *10*, 1613–1618. https://doi.org/10.1097/00001756-199905140-00041

Rothstein, J. D., Dykes-Hoberg, M., Pardo, C. A., Bristol, L. A., Jin, L., Kuncl, R. W., … Welty, D. F. (1996). Knockout of glutamate transporters reveals a major role for astroglial transport in excitotoxicity and clearance of glutamate. *Neuron*, *16*, 675–686. https://doi.org/10.1016/S0896-6273(00)80086-0

Rouach, N., Koulakoff, A., Abudara, V., Willecke, K., & Giaume, C. (2008). Astroglial metabolic networks sustain hippocampal synaptic transmission. *Science*, *322*, 1551–1555. https://doi.org/10.1126/science.1164022

Rungta, R. L., Bernier, L. P., Dissing-Olesen, L., Groten, C. J., LeDue, J. M., Ko, R., … MacVicar, B. A. (2016). Ca^{2+} transients in astrocyte fine processes occur via Ca^{2+} influx in the adult mouse hippocampus. *Glia*, *64*, 2093–2103.

Runquist, M., & Alonso, G. (2003). Gabaergic signaling mediates the morphological organization of astrocytes in the adult rat forebrain. *Glia*, *41*, 137–151. https://doi.org/10.1002/glia.10166

Rusakov, D. A., Bard, L., Stewart, M. G., & Henneberger, C. (2014). Diversity of astroglial functions alludes to subcellular specialisation. *Trends in Neurosciences*, *37*, 228–242. https://doi.org/10.1016/j.tins.2014.02.008

Saab, A. S., Neumeyer, A., Jahn, H. M., Cupido, A., Simek, A. A. M., Boele, H. J., … Kirchhoff, F. (2012). Bergmann glial AMPA receptors are required for fine motor coordination. *Science*, *337*, 749–753. https://doi.org/10.1126/science.1221140

Savtchenko, L. P., Bard, L., Jensen, T. P., Reynolds, J. P., Kraev, I., Medvedev, N., … Rusakov, D. A. (2018). Disentangling astroglial physiology with a realistic cell model in silico. *Nature Communications*, *9*, 3554. https://doi.org/10.1038/s41467-018-05896-w

Savtchenko, L., Megalogeni, M., Rusakov, D. A., Walker, M. C., & Pavlov, I. (2015). Synaptic GABA release prevents GABA transporter type-1 reversal during excessive network activity. *Nature Communications*, *6*, 6597. https://doi.org/10.1038/ncomms7597

Savtchouk, I., & Volterra, A. (2018). Gliotransmission: Beyond black-and-white. *Journal of Neuroscience*, *38*, 14–25. https://doi.org/10.1523/JNEUROSCI.0017-17.2017

Schnell, C., Shahmoradi, A., Wichert, S. P., Mayerl, S., Hagos, Y., Heuer, H., … Hulsmann, S. (2015). The multispecific thyroid hormone transporter OATP1C1 mediates cell-specific sulforhodamine 101-labeling of hippocampal astrocytes. *Brain Structure & Function*, *220*, 193–203. https://doi.org/10.1007/s00429-013-0645-0

Schools, G. P., Zhou, M., & Kimelberg, H. K. (2006). Development of gap junctions in hippocampal astrocytes: Evidence that whole cell electrophysiological phenotype is an intrinsic property of the individual cell. *Journal of Neurophysiology*, *96*, 1383–1392. https://doi.org/10.1152/jn.00449.2006

Schousboe, A. (2000). Pharmacological and functional characterization of astrocytic GABA transport: A short review. *Neurochemical Research*, *25*, 1241–1244.

Schousboe, A., Scafidi, S., Bak, L. K., Waagepetersen, H. S., & McKenna, M. C. (2014). Glutamate metabolism in the brain focusing on astrocytes. *Advance Neurobiology*, *11*, 13–30.

Schreiner, A. E., Durry, S., Aida, T., Stock, M. C., Rüther, U., Tanaka, K., … Kafitz, K. W. (2014). Laminar and subcellular heterogeneity of GLAST and GLT-1 immunoreactivity in the developing postnatal mouse hippocampus. *Journal of Comparative Neurology*, *522*, 204–224. https://doi.org/10.1002/cne.23450

Scimemi, A. (2014a). Structure, function, and plasticity of GABA transporters. *Frontiers in Cellular Neuroscience*, *8*, 161. https://doi.org/10.3389/fncel.2014.00161

Seifert, G., Huttmann, K., Binder, D. K., Hartmann, C., Wyczynski, A., Neusch, C., & Steinhauser, C. (2009). Analysis of astroglial K^+ channel expression in the developing hippocampus reveals a predominant role of the Kir4.1 subunit. *Journal of Neuroscience*, *29*, 7474–7488. https://doi.org/10.1523/JNEUROSCI.3790-08.2009

Seifert, G., & Steinhauser, C. (2018). Heterogeneity and function of hippocampal macroglia. *Cell and Tissue Research*, *373*, 653–670. https://doi.org/10.1007/s00441-017-2746-1

Semple, B. D., Blomgren, K., Gimlin, K., Ferriero, D. M., & Noble-Haeusslein, L. J. (2013). Brain development in rodents and humans: Identifying benchmarks of maturation and vulnerability to injury across species. *Progress in Neurobiology*, *106–107*, 1–16. https://doi.org/10.1016/j.pneurobio.2013.04.001

Serrano, A., Haddjeri, N., Lacaille, J. C., & Robitaille, R. (2006). GABAergic network activation of glial cells underlies hippocampal heterosynaptic depression. *Journal of Neuroscience*, *26*, 5370–5382. https://doi.org/10.1523/JNEUROSCI.5255-05.2006

Serrano, A., Robitaille, R., & Lacaille, J. C. (2008). Differential NMDA-dependent activation of glial cells in mouse hippocampus. *Glia*, *56*, 1648–1663. https://doi.org/10.1002/glia.20717

Shelton, M. K., & McCarthy, K. D. (2000). Hippocampal astrocytes exhibit Ca^{2+}-elevating muscarinic cholinergic and histaminergic receptors in situ. *Journal of Neurochemistry*, 555–563. https://doi.org/10.1046/j.1471-4159.2000.740555.x

Shen, J. X., & Yakel, J. L. (2012). Functional alpha7 nicotinic ACh receptors on astrocytes in rat hippocampal CA1 slices. *Journal of Molecular Neuroscience*, *48*, 14–21.

Shibata, T., Yamada, K., Watanabe, M., Ikenaka, K., Wada, K., Tanaka, K., & Inoue, Y. (1997). Glutamate transporter GLAST is expressed in the radial glia-astrocyte lineage of developing mouse spinal cord. *Journal of Neuroscience*, *17*, 9212–9219. https://doi.org/10.1523/JNEUROSCI.17-23-09212.1997

Sibille, J., Pannasch, U., & Rouach, N. (2014). Astroglial potassium clearance contributes to short-term plasticity of synaptically evoked currents at the tripartite synapse. *Journal of Physiology*, *592*, 87–102. https://doi.org/10.1113/jphysiol.2013.261735

Sipila, S., Huttu, K., Voipio, J., & Kaila, K. (2004). GABA uptake via GABA transporter-1 modulates GABAergic transmission in the immature hippocampus. *Journal of Neuroscience*, *24*, 5877–5880. https://doi.org/10.1523/JNEUROSCI.1287-04.2004

Slezak, M., Kandler, S., Van Veldhoven, P. P., Van den Haute, C., Bonin, V., & Holt, M. G. (2019). Distinct mechanisms for visual and motor-related astrocyte responses in mouse visual cortex. *Current Biology*, *29*, 3120–3127. https://doi.org/10.1016/j.cub.2019.07.078

Song, I., Volynski, K., Brenner, T., Ushkaryov, Y., Walker, M., & Semyanov, A. (2013). Different transporter systems regulate extracellular GABA from vesicular and non-vesicular sources. *Frontiers in Cellular Neuroscience*, *7*, 23. https://doi.org/10.3389/fncel.2013.00023

Srinivasan, R., Lu, T. Y., Chai, H., Xu, J., Huang, B. S., Golshani, P., … Khakh, B. S. (2016). New transgenic mouse lines for selectively targeting astrocytes and studying calcium signals in astrocyte processes in situ and in vivo. *Neuron*, *92*, 1181–1195.

Stephan, J. (2015). Heterogeneous distribution and utilization of inhibitory neurotransmitter transporters. *Neurotransmitter*, *2*, 1–7.

Stephan, J., & Friauf, E. (2014). Functional analysis of the inhibitory neurotransmitter transporters GlyT1, GAT-1, and GAT-3 in astrocytes of the lateral superior olive. *Glia*, *62*, 1992–2003. https://doi.org/10.1002/glia.22720

Stephan, J., Haack, N., Kafitz, K. W., Durry, S., Koch, D., Hochstrate, P., … Rose, C. R. (2012). Kir4.1 channels mediate a depolarization of hippocampal astrocytes under hyperammonemic conditions in situ. *Glia*, *60*, 965–978. https://doi.org/10.1002/glia.22328

Stobart, J. L., Ferrari, K. D., Barrett, M. J. P., Stobart, M. J., Looser, Z. J., Saab, A. S., & Weber, B. (2018). Long-term in vivo calcium imaging of astrocytes reveals distinct cellular compartment responses to sensory stimulation. *Cerebral Cortex*, *28*, 184–198. https://doi.org/10.1093/cercor/bhw366

Su, G., Kintner, D. B., & Sun, D. (2002). Contribution of Na^+-K^+-Cl^- cotransporter to high-$[K^+]_o$- induced swelling and EAA release in astrocytes. *American Journal of Physiology. Cell Physiology*, *282*, 1136–1146.

Sugimoto, A., Miyazaki, A., Kawarabayashi, K., Shono, M., Akazawa, Y., Hasegawa, T., … Iwamoto, T. (2017). Piezo type mechanosensitive ion channel component 1 functions as a regulator of the cell fate determination of mesenchymal stem cells. *Scientific Reports*, *7*, 17696. https://doi.org/10.1038/s41598-017-18089-0

Sullivan, S. M., Lee, A., Bjorkman, S. T., Miller, S. M., Sullivan, R. K., Poronnik, P., … Pow, D. V. (2007). Cytoskeletal anchoring of GLAST determines susceptibility to brain damage: An identified role for GFAP. *Journal of Biological Chemistry*, *282*, 29414–29423. https://doi.org/10.1074/jbc.M704152200

Sun, W., McConnell, E., Pare, J.-F., Xu, Q., Chen, M., Peng, W., … Nedergaard, M. (2013). Glutamate-dependent neuroglial calcium signaling differs between young and adult brain. *Science*, *339*, 197–200. https://doi.org/10.1126/science.1226740

Swanson, R. A., Liu, J., Miller, J. W., Rothstein, J. D., Farrell, K., Stein, B. A., & Longuemare, M. C. (1997). Neuronal regulation of glutamate

transporter subtype expression in astrocytes. *Journal of Neuroscience*, *17*, 932–940. https://doi.org/10.1523/JNEUROSCI.17-03-00932.1997

Sykova, E., & Nicholson, C. (2008). Diffusion in brain extracellular space. *Physiological Reviews*, *88*, 1277–1340. https://doi.org/10.1152/physrev.00027.2007

Tanaka, K., Watase, K., Manabe, T., Yamada, K., Watanabe, M., Takahashi, K., … Wada, K. (1997). Epilepsy and exacerbation of brain injury in mice lacking the glutamate transporter GLT-1. *Science*, *276*, 1699–1702. https://doi.org/10.1126/science.276.5319.1699

Theodosis, D. T., Poulain, D. A., & Oliet, S. H. (2008). Activity-dependent structural and functional plasticity of astrocyte-neuron interactions. *Physiological Reviews*, *88*, 983–1008. https://doi.org/10.1152/physrev.00036.2007

Thomas, C. G., Tian, H., & Diamond, J. S. (2011). The relative roles of diffusion and uptake in clearing synaptically released glutamate change during early postnatal development. *Journal of Neuroscience*, *31*, 4743–4754. https://doi.org/10.1523/JNEUROSCI.5953-10.2011

Ullensvang, K., Lehre, K. P., Storm-Mathisen, J., & Danbolt, N. C. (1997). Differential developmental expression of the two rat brain glutamate transporter proteins GLAST and GLT. *European Journal of Neuroscience*, *9*, 1646–1655. https://doi.org/10.1111/j.1460-9568.1997.tb01522.x

Unichenko, P., Dvorzhak, A., & Kirischuk, S. (2013). Transporter-mediated replacement of extracellular glutamate for GABA in the developing murine neocortex. *European Journal of Neuroscience*, *38*, 3580–3588. https://doi.org/10.1111/ejn.12380

Untiet, V., Kovermann, P., Gerkau, N. J., Gensch, T., Rose, C. R., & Fahlke, C. (2017). Glutamate transporter-associated anion channels adjust intracellular chloride concentrations during glial maturation. *Glia*, *65*, 388–400. https://doi.org/10.1002/glia.23098

Ventura, R., & Harris, K. M. (1999). Three-dimensional relationships between hippocampal synapses and astrocytes. *Journal of Neuroscience*, *19*, 6897–6906. https://doi.org/10.1523/JNEUROSCI.19-16-06897.1999

Verbich, D., Prenosil, G. A., Chang, P. K., Murai, K. K., & McKinney, R. A. (2012). Glial glutamate transport modulates dendritic spine head protrusions in the hippocampus. *Glia*, *60*, 1067–1077. https://doi.org/10.1002/glia.22335

Verkhratsky, A., & Kirchhoff, F. (2007). NMDA receptors in glia. *The Neuroscientist*, *13*, 28–37. https://doi.org/10.1177/1073858406294270

Verkhratsky, A., & Nedergaard, M. (2018). Physiology of Astroglia. *Physiological Reviews*, *98*, 239–389. https://doi.org/10.1152/physrev.00042.2016

Verkhratsky, A., Pankratov, Y., Lalo, U., & Nedergaard, M. (2012). P2X receptors in neuroglia. *Wiley Interdisciplinary Reviews: Membrane Transport and Signaling*, *1*(2), 151–161. https://doi.org/10.1002/wmts.12

Verkhratsky, A., & Steinhauser, C. (2000). Ion channels in glial cells. *Brain Research. Brain Research Reviews*, *32*, 380–412. https://doi.org/10.1016/S0165-0173(99)00093-4

Verkhratsky, A., Trebak, M., Perocchi, F., Khananshvili, D., & Sekler, I. (2018). Crosslink between calcium and sodium signalling. *Experimental Physiology*, *103*, 157–169. https://doi.org/10.1113/EP086534

Vitellaro-Zuccarello, L., Calvaresi, N., & De Biasi, S. (2003). Expression of GABA transporters, GAT-1 and GAT-3, in the cerebral cortex and thalamus of the rat during postnatal development. *Cell and Tissue Research*, *313*, 245–257. https://doi.org/10.1007/s00441-003-0746-9

Wallraff, A., Kohling, R., Heinemann, U., Theis, M., Willecke, K., & Steinhauser, C. (2006). The impact of astrocytic gap junctional coupling on potassium buffering in the hippocampus. *Journal of Neuroscience*, *26*, 5438–5447. https://doi.org/10.1523/JNEUROSCI.0037-06.2006

Wallraff, A., Odermatt, B., Willecke, K., & Steinhauser, C. (2004). Distinct types of astroglial cells in the hippocampus differ in gap junction coupling. *Glia*, *48*, 36–43. https://doi.org/10.1002/glia.20040

Wang, D. D., & Bordey, A. (2008). The astrocyte odyssey. *Progress in Neurobiology*, *86*, 342–367. https://doi.org/10.1016/j.pneurobio.2008.09.015

Watase, K., Hashimoto, K., Kano, M., Yamada, K., Watanabe, M., Inoue, Y., … Tanaka, K. (1998). Motor discoordination and increased susceptibility to cerebellar injury in GLAST mutant mice. *European Journal of Neuroscience*, *10*, 976–988. https://doi.org/10.1046/j.1460-9568.1998.00108.x

Weissman, T. A., Riquelme, P. A., Ivic, L., Flint, A. C., & Kriegstein, A. R. (2004). Calcium waves propagate through radial glial cells and modulate proliferation in the developing neocortex. *Neuron*, *43*, 647–661. https://doi.org/10.1016/j.neuron.2004.08.015

Wilson, C. S., & Mongin, A. A. (2019). The signaling role for chloride in the bidirectional communication between neurons and astrocytes. *Neuroscience Letters*, *689*, 33–44. https://doi.org/10.1016/j.neulet.2018.01.012

Wu, Y. W., Gordleeva, S., Tang, X., Shih, P. Y., Dembitskaya, Y., & Semyanov, A. (2019). Morphological profile determines the frequency of spontaneous calcium events in astrocytic processes. *Glia*, *67*, 246–262. https://doi.org/10.1002/glia.23537

Wu, Y., Wang, W., Diez-Sampedro, A., & Richerson, G. B. (2007). Nonvesicular inhibitory neurotransmission via reversal of the GABA transporter GAT-1. *Neuron*, *56*, 851–865. https://doi.org/10.1016/j.neuron.2007.10.021

Yamamoto, T., Vukelic, J., Hertzberg, E. L., & Nagy, J. I. (1992). Differential anatomical and cellular patterns of connexin43 expression during postnatal development of rat brain. *Brain Research. Developmental Brain Research*, *66*, 165–180. https://doi.org/10.1016/0165-3806(92)90077-A

Yan, Y., Dempsy, R. J., & Sun, D. (2001). Expression of Na^+ -K^+ -Cl^- cotransporter in rat brain during development and its localization in mature astrocytes. *Brain Research*, *911*, 43–55. https://doi.org/10.1016/S0006-8993(01)02649-X

Yang, J. W., Hanganu-Opatz, I. L., Sun, J. J., & Luhmann, H. J. (2009). Three patterns of oscillatory activity differentially synchronize developing neocortical networks in vivo. *Journal of Neuroscience*, *29*, 9011–9025. https://doi.org/10.1523/JNEUROSCI.5646-08.2009

Yang, Y., Vidensky, S., Jin, L., Jie, C., Lorenzini, I., Frankl, M., & Rothstein, J. D. (2011). Molecular comparison of GLT1+ and ALDH1L1+ astrocytes in vivo in astroglial reporter mice. *Glia*, *59*, 200–207. https://doi.org/10.1002/glia.21089

Zhang, Y., & Barres, B. A. (2010). Astrocyte heterogeneity: An underappreciated topic in neurobiology. *Current Opinion in Neurobiology*, *20*, 588–594. https://doi.org/10.1016/j.conb.2010.06.005

Zheng, K., & Rusakov, D. A. (2015). Efficient integration of synaptic events by NMDA receptors in three-dimensional neuropil. *Biophysical Journal*, *108*, 2457–2464. https://doi.org/10.1016/j.bpj.2015.04.009

Zheng, K., Scimemi, A., & Rusakov, D. A. (2008). Receptor actions of synaptically released glutamate: The role of transporters on the scale from nanometers to microns. *Biophysical Journal*, *95*, 4584–4596. https://doi.org/10.1529/biophysj.108.129874

Zhong, S., Du, Y., Kiyoshi, C. M., Ma, B., Alford, C. C., Wang, Q., … Zhou, M. (2016). Electrophysiological behavior of neonatal astrocytes in hippocampal stratum radiatum. *Molecular Brain*, *9*, 34. https://doi.org/10.1186/s13041-016-0213-7

Zhou, M., & Kimelberg, H. K. (2001). Freshly isolated hippocampal CA1 astrocytes comprise two populations differing in glutamate transporter and AMPA receptor expression. *Journal of Neuroscience*, *21*, 7901–7908. https://doi.org/10.1523/JNEUROSCI.21-20-07901.2001

Zhou, M., Schools, G. P., & Kimelberg, H. K. (2006). Development of GLAST(+) astrocytes and NG2(+) glia in rat hippocampus CA1: Mature astrocytes are electrophysiologically passive. *Journal of Neurophysiology*, *95*, 134–143. https://doi.org/10.1152/jn.00570.2005

Zhou, M., Xu, G., Xie, M., Zhang, X., Schools, G. P., Ma, L., … Chen, H. (2009). TWIK-1 and TREK-1 are potassium channels contributing significantly to astrocyte passive conductance in rat hippocampal slices. *Journal of Neuroscience*, *29*, 8551–8564. https://doi.org/10.1523/JNEUROSCI.5784-08.2009

Zhu, Y., & Kimelberg, H. K. (2001). Developmental expression of metabotropic P2Y1 and P2Y2 receptors in freshly isolated astrocytes from rat hippocampus. *Journal of Neurochemistry*, *77*, 530–541. https://doi.org/10.1046/j.1471-4159.2001.00241.x

Zhuo, L., Sun, B., Zhang, C. L., Fine, A., Chiu, S. Y., & Messing, A. (1997). Live astrocytes visualized by green fluorescent protein in transgenic mice. *Developmental Biology*, *187*, 36–42. https://doi.org/10.1006/dbio.1997.8601

Ziemens, D., Oschmann, F., Gerkau, N. J., & Rose, C. R. (2019). Heterogeneity of activity-induced sodium transients between astrocytes of the mouse hippocampus and neocortex: mechanisms and consequences. *Journal of Neuroscience*, *39*, 2620–2634. https://doi.org/10.1523/JNEUROSCI.2029-18.2019

Zur Nieden, R., & Deitmer, J. W. (2006). The role of metabotropic glutamate receptors for the generation of calcium oscillations in rat hippocampal astrocytes in situ. *Cerebral Cortex*, *16*, 676–687. https://doi.org/10.1093/cercor/bhj013

How to cite this article: Felix L, Stephan J, Rose CR. Astrocytes of the early postnatal brain. *Eur J Neurosci*. 2020;00:1–24. https://doi.org/10.1111/ejn.14780

Astroglial Glutamate Signaling and Uptake in the Hippocampus.

Rose, C. R., ***Felix, L****., Zeug, A., Dietrich, D., Reiner, A., Henneberger, C.*

Frontiers in Molecular Neuroscience 10 DOI: 10.3389/fnmol.2017.00451 (2018)

Impact factor 2018: 3.82

I contributed to

- Drafting and revision of manuscript and figures

On the Origin of Ultraslow Spontaneous Na^+ Fluctuations in Neurons of the Neonatal Forebrain

Carlos Perez[1,$], Lisa Felix[2,$], Simone Durry[2], Christine R. Rose[2], and Ghanim Ullah[1,*]

[1] Department of Physics, University of South Florida, Tampa, FL 33620, USA

[2] Institute of Neurobiology, Faculty of Mathematics and Natural Sciences, Heinrich Heine University Düsseldorf, 40225 Düsseldorf, Germany

Short Title: Ultraslow Spontaneous Na^+ Fluctuations in the Neonatal Brain

[$] These two authors contributed equally to this manuscript

[*] Corresponding Author

4202 E Fowler Ave, ISA 2019

Tampa, FL 33620, USA

Email: gullah@usf.edu

Tel: 813-974-0698

Abstract

Spontaneous neuronal and astrocytic activity in the neonate forebrain is believed to drive the maturation of individual cells and their integration into complex brain-region-specific networks. The previously reported forms include bursts of electrical activity and oscillations in intracellular Ca^{2+} concentration. Here, we use ratiometric Na^+ imaging to demonstrate spontaneous fluctuations in the intracellular Na^+ concentration of CA1 pyramidal neurons and astrocytes in tissue slices obtained from the hippocampus of mice at postnatal days 2-4 (P2-4). These occur at very low frequency (~2/h), can last minutes with amplitudes up to several mM, and mostly disappear after the first postnatal week. To further investigate their mechanisms, we model a network consisting of pyramidal neurons and interneurons. Experimentally observed Na^+ fluctuations are mimicked when GABAergic inhibition in the simulated network is made depolarizing. Both our experiments and computational model show that blocking voltage-gated Na^+ channels or GABAergic signaling significantly diminish the neuronal Na^+ fluctuations. On the other hand, blocking a variety of other ion channels, receptors, or transporters including glutamatergic pathways, does not have significant effects. Our model also shows that the amplitude and duration of Na^+ fluctuations decrease as we increase the strength of glial K^+ uptake. Furthermore, neurons with smaller somatic volumes exhibit fluctuations with higher frequency and amplitude. As opposed to this, larger extracellular to intracellular volume ratio observed in neonatal brain exerts a dampening effect. Finally, our model predicts that these periods of spontaneous Na^+ influx leave neonatal neuronal networks more vulnerable to seizure-like states when compared to mature brain.

New and Noteworthy

Spontaneous activity in the neonate forebrain plays a key role in cell maturation and brain development. We report spontaneous, ultraslow, asynchronous fluctuations in the intracellular Na^+ concentration of neurons and astrocytes. We show that this activity is not correlated with the previously reported synchronous neuronal population bursting or Ca^{2+} oscillations, both of which occur at much faster timescales. Furthermore, extracellular K^+ concentration remains nearly constant. The spontaneous Na^+ fluctuations disappear after the first postnatal week.

Introduction

Spontaneous neuronal activity is a hallmark of the developing central nervous system (Spitzer 2006), and has been described in terms of intracellular Ca^{2+} oscillations both in neurons and astrocytes (Felix et al. 2020b; Garaschuk et al. 2000; Leinekugel et al. 1997; Spitzer 1994) and bursts of neuronal action potentials (Ben-Ari et al. 1989; Garaschuk et al. 1998b; Katz and Shatz 1996). This activity is believed to promote the maturation of individual cells and their integration into complex brain-region-specific networks (Griguoli and Cherubini 2017; Luhmann et al. 2016; Penn et al. 1998; Spitzer 2006). In the rodent hippocampus, early network activity and Ca^{2+} oscillations are mainly attributed to the excitatory role of GABAergic transmission originating from inhibitory neurons (Ben-Ari et al. 1997; Cherubini et al. 1991; Garaschuk et al. 1998b; Lohmann and Kessels 2014).

The excitatory action of GABAergic neurotransmission is one of the most notable characteristics that distinguish neonate brain from the mature brain, where GABA typically inhibits neuronal networks (Ben-Ari et al. 2007; Ben-Ari and Holmes 2005; Ben-Ari et al. 1997; Ben-Ari et al. 1989; Garaschuk et al. 1998b; Griguoli and Cherubini 2017; Luhmann et al. 2016; Rivera et al. 2005; Spitzer 2006). While recent work has also called the inhibitory action of GABA on cortical networks into question (Kirmse et al. 2015), there are many other pathways that could play a significant role in the observed spontaneous activity in neonate brain (discussed below). Additional key features of the early network oscillations in the hippocampus include their synchronous behavior across most of the neuronal network, modulation by glutamate, recurrence with regular frequency, and a limitation to early post-natal development (Ben-Ari et al. 1997; Garaschuk et al. 1998b; Garaschuk et al. 2000).

More recently, Felix and co-workers (Felix et al. 2020b) reported a new form of seemingly spontaneous activity in acutely isolated tissue slices of hippocampus and cortex of neonatal mice. It consists of spontaneous fluctuations in intracellular Na^+, which occur to similar degrees at room temperature and physiological temperature both in astrocytes and neurons and were observed in ~21% of pyramidal neurons and ~32% of astrocytes tested. Na^+ fluctuations are ultraslow in nature, averaging ~2 fluctuations/hour, are not synchronized between cells, and are not significantly affected by an array of pharmacological blockers for various channels, receptors, and transporters. Only using the voltage-gated Na^+ channel (VGSC) blocker tetrodotoxin (TTX) diminished the Na^+ fluctuations in neurons and astrocytes, indicating that they are driven by the generation of neuronal action potentials. In addition, neuronal fluctuations were significantly reduced by the application of the $GABA_A$ receptor antagonist bicuculline, suggesting the involvement of GABAergic neurotransmission (Felix et al. 2020b).

This paper follows up on the latter study (Felix et al. 2020b), and uses dual experiment-theory approach to systematically confirm, and further investigate the properties of neuronal Na^+ fluctuations in the neonate hippocampal CA1 area and to identify the pathways that generate and shape them. Notably, a range of factors that play a key role in controlling the dynamics of extra- and intracellular ion concentrations, are not fully developed in the neonate forebrain (Felix et al. 2020a; Larsen et al. 2019; Lohmann and Kessels 2014; MacAulay 2020; Safiulina et al. 2008). These factors, such as the cellular uptake capacity of K^+ from the extracellular space (ECS), the expression levels of the three isoforms ($\alpha1$, $\alpha2$, and $\alpha3$) of the Na^+/K^+ pump that restore resting Na^+ and K^+ concentrations, the ratio of intra- to extracellular volumes, and the magnitude of relative shrinkage of the ECS in response to neuronal stimulus, all increase with age and cannot be easily manipulated experimentally (Larsen et al. 2019). The gap-junctional network between

98 astrocytes is also less developed in neonates and therefore has a lower capacity for the spatial
99 buffering of ions, neurotransmitters released by neurons, and metabolites (Felix et al. 2020a;
100 Larsen et al. 2019). At the same time, the synaptic density and expression levels of most
101 isoforms of AMPA and NMDA receptors are very low in neonates and only begin to increase
102 rapidly during the second week (Lohmann and Kessels 2014). Additionally, while GABAergic
103 synapses develop earlier than their glutamatergic counterparts, synaptogenesis is incomplete and
104 ongoing. Therefore, synapses of varying strengths exist across the network. Each of these aspects
105 impacts the others and their individual specific roles in the early spontaneous activity is
106 consequently difficult to test experimentally. Their involvement in neonatal Na^+ fluctuations will
107 therefore be addressed for the first time by the data-driven modelling approach here.
108 We employ ratiometric Na^+ imaging in tissue slices of the hippocampal CA1 region
109 obtained from neonate animals at postnatal days 2-4 (P2-4) and juveniles at P14-21 to record
110 intracellular Na^+ fluctuations in both age groups. We begin by reporting the key statistics about
111 spontaneous Na^+ fluctuations observed in neonates and juveniles. Next, we develop a detailed
112 network model, consisting of pyramidal cells and inhibitory neurons, which also incorporates the
113 exchange of K^+ in the ECS with astrocytes and perfusion solution *in vitro* (or vasculature in
114 intact brain). Individual neurons are modeled by Hodgkin-Huxley type formalism for membrane
115 potential and rate equations for intra- and extracellular ion concentrations. In addition to closely
116 reproducing our experimental results, the model provides new key insights into the origin of
117 spontaneous slow Na^+ oscillations in neonates. Furthermore, our model also predicts that the
118 network representing a developing brain is more prone to seizure-like excitability when
119 compared to mature brain.
120

Materials and Methods

Experimental Methods

Relevant abbreviations and source of chemicals

MPEP (2-Methyl-6-(phenylethynyl)pyridine) from Tocris

APV ((2*R*)-amino-5-phosphonovaleric acid; (2*R*)-amino-5-phosphonopentanoate) from Cayman Chemical

NBQX (2,3-Dioxo-6-nitro-1,2,3,4-tetrahydrobenzo[f]quinoxaline-7-sulfonamide) from Tocris

CGP-55845 ((2S)-3-[[(1S)-1-(3,4-Dichlorophenyl)ethyl]amino-2-hydro xypropyl](phenylmethyl)phosphinic acid hydrochloride) from Sigma-Aldrich

NNC-711 (1,2,5,6-Tetrahydro-1-[2-[[(diphenylmethylene)amino]oxy]ethyl]-3-pyridinecarboxylic acid hydrochloride) from Tocris

SNAP-5114 (1-[2-[tris(4-methoxyphenyl)methoxy]ethyl]-(S)-3-piperidinecarboxylic acid) from Sigma-Aldrich

Preparation of tissue slices

This study was carried out in accordance with the institutional guidelines of the Heinrich Heine University Düsseldorf, as well as the European Community Council Directive (2010/63/EU). All experiments were communicated to and approved by the animal welfare office of the animal care and use facility of the Heinrich Heine University Düsseldorf (institutional act number: O52/05). In accordance with the German animal welfare act (Articles 4 and 7), no formal additional approval for the post-mortem removal of brain tissue was necessary. In accordance with the recommendations of the European Commission (Close et al. 1997), juvenile mice were first anaesthetized with CO_2 before the animals were quickly decapitated, while animals younger than P10 received no anesthetics.

Acute brain slices with a thickness of 250 µm were generated from mice (*mus musculus*, Balb/C; both sexes) using methods previously published (Gerkau et al. 2019). An artificial cerebro-spinal fluid (ACSF) containing (in mM): 2 $CaCl_2$, 1 $MgCl_2$ 125 NaCl, 2.5 KCl, 1.25 NaH_2PO_4, 26 $NaHCO_3$, and 20 glucose was used throughout all experiments and preparation of animals younger than P10. For animals at P10 or older, a modified ACSF (mACSF) was used during preparation, containing a lower $CaCl_2$ concentration (0.5 mM), and a higher $MgCl_2$ concentration (6 mM) but being otherwise identical to the normal ACSF. Both solutions were bubbled with 95% O_2/5% CO_2 to produce a pH of ~7.4 throughout experiments, and each had an osmolarity of 308-312 mOsm/l. Immediately after slicing, the slices were transferred to a water bath and incubated at 34°C with 0.5-1 µM sulforhodamine 101 (SR101) for 20 minutes, followed by 10 minutes in 34°C ACSF without SR101. During experiments, slices were continuously perfused with ACSF at room temperature. For experiments utilizing antagonists, these were dissolved in ASCF and bath applied for 15 minutes before the beginning, and subsequently throughout the measurements.

Sodium Imaging

Slices were dye-loaded using the bolus injection technique (via use of a picospritzer 3, Parker, Cologne, Germany) and cells were imaged at a depth of 30-60 µm under the slice surface. The sodium-sensitive ratiometric dye SBFI-AM (sodium-binding benzofuran isophthalate-acetoxymethyl ester; Invitrogen, Schwerte, Germany) was used for detection of Na^+. SBFI was excited alternatingly at 340 nm (Na^+-insensitive wavelength) and 380 nm (Na^+-sensitive wavelength) by a PolychromeV monochromator (Thermo Fisher Scientific, Eindhoven, Netherlands). Emission was collected above 420 nm from defined regions of interest (ROIs) drawn around cell somata using an upright microscope (Nikon Eclipse FN-1, Nikon, Düsseldorf,

Germany) equipped with a Fluor 40x/0.8W immersion objective (Nikon), and attached to an ORCA FLASH 4.0 LT camera (Hamamatsu Photonics Deutschland GmbH, Herrsching, Germany). The imaging software used was NIS-elements AR v4.5 (Nikon, Düsseldorf, Germany). For the identification of astrocytes (Kafitz et al. 2008), SR101 was excited at 575 nm and its emission collected above 590 nm.

Dual Imaging of Na^+ and Ca^{2+}

Slices were simultaneously bolus-loaded with the Na^+ sensitive dye, SBFI-AM and with the Ca^{2+}-indicator OGB1-AM (Oregon Green BAPTA 1-acetoxymethyl ester; Invitrogen, Schwerte, Germany). SBFI was imaged as stated above, OGB1 was excited at 488 nm with emission collected above 505 nm. Ca^{2+}-imaging experiments with OGB1 were performed at 32 ± 1°C, for which an ACSF containing (in mM): 2 $CaCl_2$, 1 $MgCl_2$, 136.5 NaCl, 4 KCl, 1.3 NaH_2PO_4, 18 $NaHCO_3$, and 10 glucose, titrated to pH 7.4, was used.

K^+-Sensitive Microelectrodes

Changes in $[K^+]_e$ were detected using ion-selective microelectrodes, with tops placed 50 µm below the surface of the slice. These were built as described previously (Gerkau et al. 2018; Haack et al. 2015) using borosilicate glass capillaries with filament. Tips were silanized via exposure to vaporized hexamethyldisilazane (Fluka, Buchs, Switzerland), before being filled with valinomycin (Ionophore I, Cocktail B, Fluka). Capillaries were then backfilled with 100 mM KCl, while reference electrodes were filled with 150 mM NaCl/1 mM HEPES (titrated to pH 7.0 with NaOH). The electrodes were calibrated immediately before and directly after experiments using solutions with defined K^+ concentrations.

Data analysis and statistics

For each ROI, a ratio of the sensitive and insensitive emissions was calculated and analyzed using OriginPro 9.0 software (OriginLab Corporation, Northampton, MA, USA).

Changes in fluorescence ratio were converted to mM Na^+ on the basis of an *in situ* calibration performed as reported previously (Langer et al. 2017; Langer and Rose 2009). A signal was defined as being any change from the baseline, if Na^+ levels exceeded 3 standard deviations of the baseline noise. Each series of experiments was performed on at least four different animals, with 'n' reflecting the total number of individual cells analyzed. Values from experiments mentioned in the text are presented as mean ± standard error, while values taken from models are presented as mean ± standard deviation.

Computational Methods

The basic equations for the membrane potential of individual neurons, various ion channels, and synaptic currents used in our model are adopted from (Kopell et al. 2010). The network topology follows the scheme for hippocampus from the same work. As shown in Figure 1, the network consists of pyramidal cells and fast-spiking interneurons with five to one ratio. The results reported in this paper are from a network with 100 excitatory and 20 inhibitory neurons. Astrocytes are not explicitly illustrated as cellular entities in Figure 1, but included in the model through their ability to take up K^+. Of note, increasing or decreasing the network size does not change the conclusions from the model. We tested a network with 25 excitatory and 5 inhibitory neurons and found similar results. Each inhibitory neuron makes synaptic connections with 5 adjacent postsynaptic pyramidal neurons (I-to-E synapses). Thus five excitatory and one inhibitory neurons constitute one "domain". As shown in the "Results" section, we observed significant variability in the neuronal behavior. Approximately 21% of neurons tested exhibited Na^+ fluctuations. Furthermore, the amplitude, duration, and frequency of the fluctuations varied over a wide range, pointing towards a heterogeneity in the network topology. To incorporate the

observed variability in the neuronal behavior, the synaptic strengths vary randomly from one domain to another. For inhibitory-to-inhibitory (I-to-I), excitatory-to-excitatory (E-to-E), and excitatory-to-inhibitory (E-to-I) synapses, we consider all-to-all connections. However, restricting these synapses spatially does not change the conclusions in the paper. We remark that if one wishes to use a network of a different size with all-to-all connections, the maximum strength of these three types of synaptic inputs will need to be scaled according to the network size.

The equations for individual cells are modified and extended to incorporate the dynamics of various ion species in the intra- and extracellular spaces of the neurons using the formalism previously developed in (Cressman et al. 2009; Hübel et al. 2017; Huebel and Ullah 2016; Krishnan et al. 2018; Somjen et al. 2008; Ullah and Schiff 2010; Ullah et al. 2015). The change in the membrane potential, V_m, for both excitatory and inhibitory neurons in the network is controlled by various Na^+ (I_{Na}), K^+ (I_K), and Cl^- (I_{Cl}) currents, current due to Na^+/K^+-ATPase (I_{pump}), and random inputs from neurons that are not a part of the network (I_{stoch}^{Ex}), and is given as

$$C\frac{dV_m^{Ex,In}}{dt} = I_{Na}^{Ex,In} + I_K^{Ex,In} + I_{Cl}^{Ex,In} + I_{pump}^{Ex,In} + I_{stoch}^{Ex/In}. \qquad (1)$$

The superscripts *Ex* and *In* correspond to excitatory and inhibitory neurons respectively. The Na^+ and K^+ currents consist of active currents corresponding to fast sodium and delayed rectifier potassium channels (I_{Na}^F & I_K^{DR}), passive leak currents (I_{Na}^{leak} & I_K^{leak}), and excitatory synaptic currents (I_{Na}^{syn} & I_K^{syn}). The chloride currents consist of contributions from passive leak current (I_{Cl}^{leak}) and inhibitory synaptic currents (I_{Cl}^{syn}). In this paper, we use positive and negative conventions for all inward (causing positive change in V_m) and outward currents, respectively.

$$I_{Na}^{Ex,In} = I_{Na}^F + I_{Na}^{leak} + I_{Na}^{syn},$$

$$I_K^{Ex,In} = I_K^{DR} + I_K^{leak} + I_K^{syn},$$

$$I_{Cl}^{Ex,In} = I_{Cl}^{leak} + I_{Cl}^{syn}.$$

The equations for active neuronal currents are given by the following equations,

$$I_{Na}^{F} = g_{Na} m_{\infty}^{3} h (V_{Na} - V_m),$$

$$I_{K}^{DR} = g_{k} n^{4} (V_K - V_m),$$

where g_{Na}, g_k, m_∞, h, and n represent the maximum conductance of fast Na^+ channels, maximum conductance of delayed rectifier K^+, steady state gating variable for fast Na^+ activation, fast Na^+ inactivation variable, and delayed rectifier K^+ activation variable. As in (Kopell et al. 2010), the gating variables and peak conductances for I_{Na}^{F}, I_{K}^{DR}, and leak currents for the pyramidal neurons in this study are based on the model of Ermentrout and Kopell (Ermentrout and Kopell 1998), which is a reduction of a model due to Traub and Miles (Traub and Miles 1991). The equations for fast-spiking inhibitory neurons are taken from the model in (Tort et al. 2007) and (Wang and Buzsáki 1996), which is a reduction of the multi-compartmental model described in Ref. (Saraga et al. 2003). These equations were originally chosen such that the model would result in the intrinsic frequency as a function of stimulus strength observed in pyramidal cells and fast-spiking inhibitory neurons respectively. The gating variables obey the following equations,

$$x_\infty = \frac{\alpha_x}{\alpha_x + \beta_x},\ \tau_x = \frac{1}{5(\alpha_x + \beta_x)}\ , For\ x = m, n, h.$$

Here x_∞ and τ_x represent the steady state and time constant of the gating variable respectively. The factor 5 in τ_x results from the fact that the Hodgkin and Huxley original formalism was based on electrophysiological data scaled at 6.3° C (Hodgkin and Huxley 1952). They suggested multiplying the forward and reverse rates (α_x and β_x) by a factor of 5 if the model is supposed to represent experiments at room temperature. The rates α_x and β_x for the channel activation and inactivation are calculated using the equations below.

$$\alpha_n = \frac{-0.01(V_m+34)}{\exp(-0.1(V_m+34))-1},$$

$$\beta_n = 0.125\exp(-\frac{V_m+44}{80}),$$

$$\alpha_h = 0.07\exp(-\frac{V_m+58}{20}),$$

$$\beta_h = \frac{1}{\exp(-0.1(V_m+28))+1},$$

$$\alpha_m = \frac{0.1(V_m+35)}{1-\exp(-\frac{V_m+35}{10})},$$

$$\beta_m = 4\exp(-\frac{V_m+60}{10}).$$

The leak currents are given by

$$I_{Na}^{leak} = g_{Na}^{leak}(V_{Na} - V_m),$$

$$I_{K}^{leak} = g_{K}^{leak}(V_{K} - V_m),$$

$$I_{Cl}^{leak} = g_{Cl}^{leak}(V_{Cl} - V_m),$$

where V_{Na}, V_K, and V_{Cl} are the reversal potentials for Na^+, K^+, and Cl^- currents respectively and are updated according to the instantaneous values of respective ion concentrations.

The functional form of stochastic current ($I_{stoch}^{Ex/In}$) received by each neuron is also based on (Kopell et al. 2010) and is given as

$$I_{stoch} = -g_{stoch}s_{stoch}V_m.$$

Where g_{stoch}represents the maximal conductance associated with the stochastic synaptic input and is set to 1 for both cell types. The gating variable s_{stoch} decays exponentially with time constant τ_{stoch}= 100 ms during each time step Δt, that is

$$s_{stoch} = s_{stoch}\exp\left(-\frac{\Delta t}{2\times\tau_{stoch}}\right).$$

At the end of each time step, s_{stoch} jumps to 1 with probability $\Delta t \times f_{stoch}/1000$, where f_{stoch} is the mean frequency of the stochastic inputs. These equations simulate the arrival of external synaptic input pulses from the neurons that are not included in the network (Kopell et al. 2010).

The excitatory and inhibitory synaptic currents corresponding to AMPA, NMDA, and GABA receptors are given by the equations below,

$$I_{Na}^{syn} = G_{AMPA/NMDA} S_{AMPA/NMDA} (V_{Na} - V_m),$$

$$I_{K}^{syn} = G_{AMPA/NMDA} S_{AMPA/NMDA} (V_{K} - V_m),$$

$$I_{Cl}^{syn} = G_{GABA} S_{GABA} (V_{Cl} - V_m).$$

$G_{AMPA/NMDA}$, G_{GABA}, $S_{AMPA/NMDA}$, and S_{GABA} represent the synaptic conductance and gating variables for AMPA and NMDA (represented by a single excitatory current) and GABA receptors. To incorporate the observed variability in neuronal behavior, we randomly select the maximal conductance value for I-to-E synapses inside a single domain from a Gaussian distribution between 0.1 and 3.0 mS/cm^2. In order to model the excitatory role of GABAergic neurotransmission observed in neonate brain, we change the sign of G_{GABA} from positive to negative.

The change in synaptic gating variables for both excitatory and inhibitory neurons is modeled as in (Kopell et al. 2010). That is

$$\frac{dS}{dt} = \frac{1}{2}\left(1 + \tanh\left(\frac{V_m}{4}\right)\right)\frac{1-S}{\tau_R} - \frac{S}{\tau_D}, \qquad (2)$$

where τ_R and τ_D represent the rise and decay time constants for synaptic signals. The reversal potentials used in the above equations are calculated using the Nernst equilibrium potential equations, i.e.

$$V_K = 26.64 \ln\left(\frac{[K^+]_o}{[K^+]_i}\right),$$

300 $$V_{Na} = 26.64 \ln\left(\frac{[Na^+]_o}{[Na^+]_i}\right),$$

301 $$V_{Cl} = 26.64 \ln\left(\frac{[Cl^+]_i}{[Cl^+]_o}\right).$$

302 Where $[K^+]_{o/i}$, $[Na^+]_{o/i}$, and $[Cl^-]_{o/i}$ represent the concentration of Na^+, K^+, and Cl^- outside
303 and inside the neuron respectively. We consider the ECS as a separate compartment surrounding
304 each cell, having a volume of approximately 15% of the intracellular space (ICS) in the
305 hippocampus of adult brain (McBain et al. 1990; Zuzana and Syková 1998) and ~40% of the ICS
306 in neonates (Lehmenkühler et al. 1993; Nicholson and Hrabětová 2017). Each neuron exchanges
307 ions with its ECS compartment through active and passive currents, and the Na^+/K^+-ATPase. The
308 ECS compartment can also exchange K^+ with the glial compartment, perfusion solution (or
309 vasculature in intact brain), and the ECS compartments of the nearby neurons (Fröhlich et al.
310 2008; Krishnan and Bazhenov 2011; Ullah et al. 2009).

311 The change in $[K^+]_o$ is a function of I_K, I_{pump}, uptake by glia surrounding the neuron (I_{glia}),
312 diffusion between the neuron and bath perfusate (I_{diff1}), and lateral diffusion between adjacent
313 neurons (I_{diff2}).

314 $$\frac{d[K^+]_o}{dt} = -\gamma\beta I_K + 2\gamma\beta I_{pump} + I_{glia} - I_{diff1} + I_{diff2}. \qquad (3)$$

315 Where β is the ratio of ICS to ECS. We set β = 7 in adult and 2.5 in neonates to
316 incorporate the larger ECS (~15% and ~40% of the ICS in adults and neonates respectively)
317 observed in neonates (Lehmenkühler et al. 1993; Nicholson and Hrabětová 2017). To see how
318 the relative volume of ECS affects the behavior of spontaneous Na^+ fluctuations, we vary β over
319 a wide range in some simulations of neonate network. We remark that using β = 2.5 in the
320 network representing the adult brain (mature inhibition) didn't cause spontaneous Na^+
321 fluctuations (not shown). $\gamma = 3 \times 10^4/(F \times r_{in})$ is the conversion factor from current units to flux

units, where F and r_{in} are the Faraday's constant and radius of the neuron, respectively. The factor 2 in front of I_{pump} is due to the fact that the Na^+/K^+ pump extrudes two K^+ in exchange for three Na^+.

The rate of change of $[Na^+]_i$ is controlled by I_{Na} and I_{pump} (Cressman et al. 2009), that is

$$\frac{d[Na^+]_i}{dt} = \gamma I_{Na} + 3\gamma I_{pump}. \qquad (4)$$

The equations modeling I_{pump}, I_{glia}, and I_{diff1} are given as

$$I_{pump} = -\frac{\rho}{1+\exp((25-[Na^+]_i)/3)} \frac{1}{1.0+exp(5.5-[K^+]_o)}.$$

$$I_{diff1} = \epsilon_K([K^+]_o - [K^+]_{bath}),$$

$$I_{glia} = \frac{G_{glia}}{1+\exp(10(3-[K^+]_o))}.$$

Where ρ is the pump strength and is a function of available oxygen concentration in the tissue ($[O_2]$) or perfusion solution (Wei et al. 2014a), that is

$$\rho = \frac{\rho_{max}}{1+\exp(\frac{20-[O_2]}{3})}.$$

and ρ_{max}, G_{glia}, ϵ_k, and $[K^+]_{bath}$ represent the maximum Na^+/K^+ pump strength, maximum glial K^+ uptake, constant for K^+ diffusion to vasculature or bath solution, and K^+ concentration in the perfusion solution respectively. The change in oxygen concentration is given by the following rate equation (Wei et al. 2014a).

$$\frac{d[O_2]_o}{dt} = \alpha I_{pump} + \epsilon_0([O_2]_{bath} - [O_2]_o). \qquad (5)$$

Where $[O_2]_{bath}$ is the bath oxygen concentration in the perfusion solution, α converts flux through Na^+/K^+ pumps (mM/sec) to the rate of oxygen concentration change (mg/(L×sec)), and ε_O is the diffusion rate constant for oxygen from bath solution to the neuron. We also incorporate lateral diffusion of K^+ (I_{diff2}) between adjacent neurons where the extracellular K^+ of each neuron

in the excitatory layer diffuses to/from the nearest neighbors in the same layer and one nearest neuron in the inhibitory layer. That is,

$$I_{diff2} = \frac{D_k}{dx^2}([K^+]^{Ex}_{o,i+1} + [K^+]^{Ex}_{o,i-1} + [K^+]^{In}_{o,i} - 3[K^+]^{Ex}_{o,i}),$$

where the subscript *i* indicates the index of the neuron with which the exchange occurs, D_k is the diffusion coefficient of K^+, and *dx* represents the separation between neighboring cells. The diffusion of K^+ in the inhibitory layer is modified so that each inhibitory neuron exchanges K^+ with the two nearest neighbors in the same layer and five nearest neighbors in the excitatory layer. The separation between neighboring neurons in the inhibitory layer is five times that of neighboring neurons in the excitatory layer.

To simplify the formalism, $[K^+]_i$ and $[Na^+]_o$ are linked to $[Na^+]_i$ as previously described (Cressman et al. 2009; Hübel et al. 2016; Ullah and Schiff 2010; Ullah et al. 2015; Wei et al. 2014b).

$$[K^+]_i = 140 + (18 - [Na^+]_i),$$

$$[Na^+]_o = 144 + \beta([Na^+]_i - 18).$$

$[Cl^-]_i$ and $[Cl^-]_o$ are given by the conservation of charge inside and outside the cell respectively.

$$[Cl^-]_i = [Na^+]_i + [K^+]_i - 150,$$

$$[Cl^-]_o = [Na^+]_o + [K^+]_o.$$

The number 150 in the above equation represents the concentration of impermeable anions. The values of various parameters used in the model are given in Table 1.

Numerical Methods

The rate equations were solved in Fortran 90 using the midpoint method, with a time step of 0.02 ms. The statistical analysis of the data obtained from simulations is performed in Matlab.

Codes reproducing key results are available upon request from authors. Significance was determined using students t-tests ($p<0.001$: ***).

Results

Pyramidal neurons in neonate hippocampus exhibit spontaneous ultraslow Na^+ fluctuations.

Acutely isolated parasagittal slices from hippocampi of neonatal mice (P2-4) were bolus-stained with the sodium-sensitive ratiometric dye SBFI-AM along the CA1 region (Figure 2A1). Experimental measurements lasted for 60 minutes, with an imaging frequency of 0.2 Hz. Astrocytes were identified via SR101 staining (Figure 2A1), and were analyzed separately to the neurons in the pyramidal layer. Out of the measured cells, 21% of neurons (n=73/350) and 32% of astrocytes (n=57/179) showed detectable fluctuations in their intracellular Na^+ concentrations (Figure 2A2, 1B). Detection threshold was calculated individually for each cell, and was defined as being 3 times the standard deviation of the baseline noise of each ROI analyzed (this ranged from 0.57 to 2.2 mM). Astrocyte Na^+ fluctuations were 11.3 ± 1.95 minutes long, at a frequency of 2.0 ± 0.2 signals/hour and with average amplitudes of 2.7 ± 0.1 mM. Neuronal Na^+ fluctuations had an average duration of 11.5 ± 0.6 minutes. They occurred at a frequency of 1.52 ± 0.1 fluctuations/hour with average amplitudes of 1.9 ± 0.05 mM. The high variability in the shapes of fluctuations is demonstrated in Figure 2A2. Apparent synchronicity between cells of the same or different classes was only observed rarely, confirming the observations reported in our earlier study (Felix et al. 2020b).

In addition, SBFI-loaded cells in the stratum radiatum, but not stained by SR101, were analyzed as a separate group. Of these SR101-negative cells, 28% showed Na^+ fluctuations (n=33/118; not shown). The properties of these fluctuations were comparable to those seen in the

two other cell types (pyramidal neurons and SR101-positive astrocytes), with an average amplitude of 2.17 ± 0.17 mM, duration of 9.3 ± 0.47 minutes and frequency of 1.81 ± 0.15 fluctuations per hour. It should be noted that although the SR101-negative group is likely to contain some interneurons, the identity of these cannot be conclusively determined. The group may also encompass immature astrocytes which do not yet take up the SR101 marker (see (Kafitz et al. 2008)).

To investigate the developmental profile of the fluctuations, the same protocol was repeated in hippocampal tissue from juvenile (P14-20) mice. Here, only 5.3% of all measured neurons (n=7/132) and 4.3% of all measured astrocytes (n=1/23) showed fluctuations in their intracellular Na^+ concentrations (Figure 2B). This strong reduction confirmed the significant down-regulation of spontaneous Na^+ oscillations from neonatal to juvenile animals reported recently (Felix et al. 2020b). However, the properties of the neuronal fluctuations themselves remained unchanged during postnatal development, with the average amplitude, frequency, and duration being 1.9 ± 0.13 mM, 2 ± 0.3 fluctuations/hour, and 6.5 ± 0.9 minutes in juvenile tissue (Figure 2C).

Spontaneous Na^+ fluctuations are reproduced by a computational model with excitatory GABAergic neurotransmission.

To explore the properties and mechanisms of neonate neuronal Na^+ fluctuations, we developed a computational model consisting of CA1 pyramidal cells and inhibitory neurons as detailed in the Methods section. Resulting typical time traces of intracellular Na^+ from four randomly selected excitatory neurons in a network representative of the juvenile hippocampus (where GABAergic neurotransmission is inhibitory) are shown in the right panel of Figure 3A.

412 Na^+ in individual neurons shows minor irregular fluctuations of less than 0.05 mM around the
413 resting values mostly because of the random synaptic inputs from the network. However, no
414 clear large-amplitude fluctuations can be seen in the network. To mimic neonates, we invert the
415 sign of I-to-E and I-to-I synaptic inputs, making the GABAergic neurotransmission excitatory.
416 The depolarizing inhibition results in the occurrence of spontaneous Na^+ fluctuations in the low
417 mM range in individual neurons that persist for several minutes (Figure 3A, left column). In
418 some cases, the peak amplitude of oscillations reached values of more than 5 mM.

419 The simulated data shows a comparable pattern of irregular fluctuations to the
420 experimental results (Figure 3B). The properties of these events are very similar—with peak
421 amplitudes mostly in the 1-3 mM range and durations spanning over several minutes. However,
422 the simulated data also appears to show a high rate of low amplitude spiking, apparently absent
423 from the experimental traces. As mentioned above, the detection threshold for experimental data
424 ranged from 0.57-2.2 mM (see also Figure 3B), and the imaging frequency was kept at 0.2 Hz in
425 order to prevent phototoxic effects during the long-lasting continuous recordings. Fast, low
426 amplitude transients as revealed in simulated experiments are thus below the experimental
427 detection threshold- as indicated in Figure 3.

428

429 *Neonate network does not exhibit spontaneous fluctuations in $[K^+]_o$.*

430 Since the dynamics of Na^+ and K^+ are generally coupled in mature brain, we next look at
431 K^+ concentration in the ECS of individual neurons ($[K^+]_o$) in the network to see if it exhibits
432 similar spontaneous fluctuations. A sample trace for a randomly selected neuron is shown in
433 Figure 4A (gray). As clear from the figure, there are only minimal fluctuations in $[K^+]_o$ (peak
434 amplitudes of residual changes are < 0.05 mM) with respect to the resting state when compared

435 to the much larger $[Na^+]_i$ fluctuations in the same cell (gray line in Figure 4A). Next, we
436 recorded $[K^+]_o$ traces for all pyramidal neurons in the network and calculated the mean $[K^+]_o$
437 (averaged over all excitatory neurons). The mean $[K^+]_o$ as a function of time shows that all
438 excitatory neurons in the network exhibit very small changes in the $[K^+]_o$, which are essentially
439 canceled out at the network level (Figure 4A, black line). These small fluctuations diminish
440 further when I-to-I and I-to-E synaptic inputs are blocked, mimicking the effect of bicuculline
441 (not shown).

442 These results obtained in our simulations are in agreement with experiments in neonatal
443 brain slices utilizing ion-sensitive microelectrodes, which were used to measure changes in $[K^+]_e$.
444 During these measurements, the average $[K^+]_e$ in the slices was found to be 2.66 ± 0.005 mM
445 (N=9 slices) (Figure 4B). Comparing the average noise level before impalement of the slices with
446 that after impalement, revealed that the threshold for detection of changes in $[K^+]_e$ was 0.09 ± 0.03
447 mM. This would make the small peaks predicted by the model (~0.05 mM, Figure 4A) unlikely to
448 be resolvable by this method. In line with this, no spontaneous changes in $[K^+]_e$ were detected in
449 neonatal slices (Figure 4B).

450 The mean intracellular Na^+ fluctuates slightly more than the mean $[K^+]_o$ (Figure 4C,
451 black line). However, a comparison between the traces showing the average Na^+ over all
452 excitatory neurons in the network and that from the single neuron indicates that the amplitude of
453 Na^+ fluctuations varies from cell to cell and that they are not necessarily phase-locked.

454

455 *The model replicates the observed effects of TTX and other blockers*

456 We next performed imaging experiments in which various blockers were applied.
457 Addition of 0.5 μM TTX reduced the number of neurons showing fluctuations to 4 % (n=7/167),

458 suggesting a dependence on action potential generation via the opening of voltage-gated Na^+
459 channels (Figure 5A). However, blocking of glutamatergic receptors with a cocktail containing
460 APV (100 μM), NBQX (25 μM), and MPEP (25 μM) (targeting NMDA, AMPA/kainate, and
461 mGluR5 receptors, respectively) had no effect on the number of neurons showing fluctuations
462 (21% active, n=33/155) (Figure 5A). Additionally, the role of GABAergic signaling was tested
463 via combined application of bicuculline (10 μM), CGP-55845 (5 μM), NNC-711 (100 μM), and
464 SNAP-5114 (100 μM) (antagonists for $GABA_A$ receptors, $GABA_B$ receptors, GABA transporters
465 GAT1, and GAT2/3, respectively). This combination of antagonists reduced the number of
466 active neurons to a similar degree as TTX (3% active, n=5/158) (Figure 5A). These data are
467 concordant with the results previously published (Felix et al. 2020b), and suggest that the slow
468 fluctuations in intracellular Na^+ are produced by the accumulation of Na^+ during trains of action
469 potentials, triggered by GABAergic transmission.

470 The pharmacological profile of the experimentally observed Na^+ fluctuations in the
471 neonatal brain summarized above strongly suggests that the excitatory effect of GABAergic
472 neurotransmission plays a key role in their generation, whereas glutamatergic activity contributes
473 very little. Before making model-based predictions, we first confirm that our model reproduces
474 these key observations in our experiments. We first incorporate the effect of TTX in the model
475 by setting the peak conductance of voltage-gated Na^+ channels to zero. We also mimic the effect
476 of blocking ionotropic glutamate receptors with CNQX and APV by setting E-to-E and E-to-I
477 synaptic conductances to zero. Finally, we mimic the effect of blocking GABAergic transmission
478 on the activity of the network, and set the I-to-I and I-to-E synaptic currents to zero, thereby
479 removing all $GABA_A$-receptor-related effects. The model results are largely in line with
480 observations, where we see that inhibiting GABA-related currents and voltage-gated Na^+

channels mostly eliminate Na^+ fluctuations and blocking NMDA and AMPA synaptic inputs has little effect on the observed spontaneous activity (Figure 5B).

Spontaneous Na^+ fluctuations are shaped by neuronal morphology and glial K^+ uptake capacity.

As pointed out above, significant changes occur in the physical and functional properties of the neurons during postnatal maturation at the synaptic, single cell, and network levels (Larsen et al. 2019; Lohmann and Kessels 2014). Therefore, we use the model to examine if changes in some key physical and functional characteristics of the network such as the neuronal radius (r_{in}), the ratio of ICS to ECS (β), and glial K^+ uptake rate play any role in the observed Na^+ fluctuations. In the following, we show Na^+ time traces for four randomly selected excitatory neurons. We observe that smaller neurons in general exhibit larger Na^+ fluctuations ($p>0.001$, Figure 6A, left panels). Both the amplitude and frequency of fluctuations decrease as we increase r_{in} (Figure 6A, center panels). The panel on the right in Figure 6A (and Figure 6B, C) shows the average amplitude of Na^+ fluctuations as we change the parameter of interest.

The observed fraction of ECS with respect to ICS in neonates is approximately 40% ($\beta = 2.5$) (Lehmenkühler et al. 1993; Nicholson and Hrabětová 2017), compared to adult animals where ECS is about 15% of the ICS ($\beta \sim 7$) (McBain et al. 1990; Zuzana and Syková 1998). We vary β from 1 to 10 to see how it affects Na^+ fluctuations. An opposite trend as compared to neuronal radius can be seen when we change β, where larger β results in Na^+ fluctuations that are larger in amplitude and have longer duration (Figure 6B, center panels) compared to those in neurons with smaller β values ($p>0.001$, Figure 6B, left panels). Thus the relative larger ECS in neonates does not favor the generation of large Na^+ fluctuations, but on the contrary dampens ion changes. We remark that with the exception of Figure 6B, all simulations in this paper are

504 performed at $\beta = 2.5$. In Figure 6B, we report results at the smallest and largest values tested to
505 show how drastic changes in this parameter can affect the behavior of slow Na^+ fluctuations.

506 The expression levels of astrocytic channels and transporters involved in K^+ uptake
507 (Na^+/K^+ ATPase, Kir4.1 channels, and $Na^+/K^+/Cl^-$ co-transporter 1 (NKCC1)) and connexins
508 forming gap junctions are low in neonates (Felix et al. 2020a; Giaume et al. 2010; MacAulay
509 2020). Astrocytes in the neonate brain, therefore, have a lower capacity for uptake of
510 extracellular K^+ released by neurons (Larsen et al. 2019; Zhong et al. 2016). To analyze the
511 influence of glial K^+ uptake, we varied the maximum glial K^+ uptake strength in the model from
512 12 mM/sec (significantly lower than 66 mM/sec - the value used for mature neurons in
513 (Cressman et al. 2009)) to 96 mM/sec to see how it affects Na^+ fluctuations. We observed a
514 strong effect of varying peak glial K^+ uptake on the amplitude and frequency of Na^+ fluctuations
515 ($p>0.001$). Overall, the amplitude and frequency of Na^+ fluctuations decrease as we increase
516 peak glial K^+ uptake (Figure 6C). This occurs because a stronger glial K^+ uptake leads to
517 decreased excitability of neurons, and consequently weaker $[Na^+]_i$ fluctuations.

518 As pointed out above, Na^+/K^+ ATPase changes significantly with age. For example, the
519 expression levels of all three isoforms ($\alpha1$, $\alpha2$, and $\alpha3$) of the Na^+/K^+ pump that restore resting
520 Na^+ and K^+ concentrations in rats increase stepwise by more than fourfold from P3-4 to P21-22
521 (Larsen et al. 2019). To mimic the changes in the expression level of Na^+/K^+ ATPase and how it
522 affects slow Na^+ fluctuations, we change the maximum strength of the Na^+/K^+ pump (ρ_{max}) in the
523 model. While increasing the pump strength beyond the value given in Table 1 (we increased ρ_{max}
524 by up to a factor of 3) did not significantly affect Na^+ fluctuations, decreasing ρ_{max} by 40%
525 increases their mean amplitude (Figure 7). Furthermore, the frequency of Na^+ fluctuations

526 decreases from 3.17/hr to 2.54/hr as we decrease ρ_{max} by 40%, whereas the average duration does
527 not change significantly.
528
529 *Link to synchronous neonatal network activity*
530 The pharmacological properties of the Na^+ fluctuations share similarities with other
531 spontaneous developmental activity patterns, including the well-described giant depolarizing
532 potentials (GDPs) (Ben-Ari et al. 1989). These GDPs are associated with transient elevations in
533 $[Ca^{2+}]_i$, termed early network oscillations (ENOs) (Garaschuk et al. 1998a), which require near-
534 physiological temperatures. In our earlier study (Felix et al., Cells, 2020), increasing the ACSF
535 temperature from room temperature to 33–35 °C, had no effect on either the duration, amplitude
536 or frequency of the Na^+ fluctuations in neurons, suggesting that these signals are not strictly
537 linked to each other.
538 To further experimentally investigate possible links between the two phenomena, we
539 used a dual staining approach in order to be able to monitor Na^+ and Ca^{2+} signaling sequentially
540 in the same set of cells. To this end, neonatal slices (number of slices N=4; number of neurons
541 analyzed n=202) were loaded with both SBFI and OGB (Figure 8A). To reduce damage and
542 phototoxic effects during the long-lasting Na^+ recordings, slices were first measured using the
543 excitation wavelength specific for the Na^+ sensitive SBFI for an hour, at room temperature, with
544 a frequency of 0.2 Hz. Thereafter, the temperature of the perfusion saline was gradually raised to
545 32 ±1 °C, at which point Ca^{2+} imaging was performed for a further 20 minutes at 4 Hz (Figure
546 8B).
547 The level of Ca^{2+} activity was analyzed both by counting the number of events which
548 exhibited peaks reflecting a change in fluorescence emission by at least of 2% relative to the

549 baseline as well as by integrating the area over the curve for the entire recording of an individual
550 cell. As expected, we found synchronized, repetitive Ca^{2+} signaling in the neuronal cell
551 population (Figure 8B) at near physiological temperature, confirming the occurrence of
552 synchronous neonatal network activity under these conditions. Comparing those cells which had
553 displayed Na^{+} fluctuations against those which had not, revealed no distinction in their level of
554 Ca^{2+} activity (Figure 8C). These results demonstrate that there is no clear correlation between
555 cells undergoing slow spontaneous Na^{+} fluctuations and their ability to contribute to
556 synchronized Ca^{2+} oscillations.
557
558 *The model shows synchronized bursting in populations of neurons*
559 The network representing the neonatal brain shows clear synchronous bursting activity in
560 sub-populations of neurons without making any changes to the parameters (Figure 9A). In line
561 with previous observations, the time scale of these events is shorter (~150 ms) as compared to
562 Na^{+} fluctuations (Ben-Ari 2001; Ben-Ari et al. 1989; Garaschuk et al. 1998a; Katz and Shatz
563 1996) (Figure 9A1). While our model does not incorporate intracellular Ca^{2+} dynamics, which
564 precludes computational investigation of the synchronous Ca^{2+} fluctuations observed in our
565 experiments and elsewhere (Felix et al. 2020b; Garaschuk et al. 2000; Leinekugel et al. 1997;
566 Spitzer 1994), we believe that the synchronous bursting activity shown here would lead to the
567 observed synchronous intracellular Ca^{2+} fluctuations. In its current form, the model is also not
568 equipped to properly investigate the correlation between slow Na^{+} fluctuations and GDPs.
569 Incorporating such details is beyond the scope of this study and is the subject of our future
570 research (see "Discussion" section). The number of cells exhibiting synchronous bursting

571 increases as we increase the connectivity among cells or consider a common input from a source
572 outside the network, for example, one representing the input from CA3 to CA1 region.

573 To see if any correlation between the bursting behavior and Na^+ fluctuations exists in the
574 model, we identified two neurons in the network that show similar pattern of intermittent
575 bursting activity and plot $[Na^+]_i$ for both neurons (black and red traces in Figure 9A2) with their
576 firing patterns (black and red dots in Figure 9A2). Despite having similar bursting behavior, both
577 cells exhibit $[Na^+]_i$ with different amplitudes. The duration of both events is also different as
578 $[Na^+]_i$ of the cell indicated by the red line will go above the threshold for the event detection later
579 and drop below sooner. Another example neuron exhibit longer bursts (Figure 9A2, inset) but
580 $[Na^+]_i$ peaks with even smaller amplitude and shorter duration (blue line and dots in Figure 9A2).
581 We also identified neurons with sporadic and synchronized bursting activity but no detectable
582 $[Na^+]_i$ fluctuations (that is, the change in $[Na^+]_i$ failed to go above the event detection threshold)
583 and vice versa (not shown). This result shows that while short-lived synchronous bursts can
584 occur on top of long-lived $[Na^+]_i$ events, they do not control the characteristics of the slow $[Na^+]_i$
585 fluctuations. Both can also occur independent of each other.

586 Blocking GABA synaptic currents, mimicking the effect of bicuculline prevents the
587 synchronous bursting events from occurring (Figure 9B). Upon closer inspection, we noticed that
588 blocking I-to-E synaptic inputs are more effective in disrupting these events whereas I-to-I
589 connections only play a minor role (not shown). Similarly, blocking E-to-E and E-to-I
590 connections affect these events moderately (not shown). The synchronous activity is also
591 disrupted by partially blocking VGSCs, mimicking the effect of TTX (G_{Na}^F was decreased by
592 50%, not shown). Decreasing the K^+ buffering capacity of glia and strength of Na^+/K^+-ATPase
593 or increasing the radius of individual cells and ratio of intracellular to extracellular volume (β)

do not affect such events significantly (not shown). This points to another difference between the short-lived synchronous bursting activing and long-lived Na^+ fluctuations where these microenvironmental variables play a significant role.

Next, we test the effect of temperature on the synchronous bursting activity in the model. Note that the model presented above is valid at room temperature only. Thus, we incorporate the effect of raising temperature to physiological values by following the approach proposed by Hodgkin and Huxley (Hodgkin and Huxley 1952), where the forward and reverse rates for the channels activation and inactivation (α_x, β_x in "Computational Methods" section) and peak conductance of the channels are multiplied by a factor $Q_{10} = a^{(T-T0)/10}$. Here $a = 3$, T is the temperature that the model is supposed to represent in ^{o} C (here T = 35^{o} C), and $T0$ = 6.3^{o} C. In our formalism, temperature also appears in the Nernst equilibrium potentials (V_K, V_{Na}, and V_{Cl} in "Computational Methods"). Simulating the model after this change shows that the frequency of synchronous bursts increases at physiological temperature (Figure 9C) and mostly disappear as the temperature drops below the room temperature. Moreover, the Na^+ fluctuations persist at physiological temperature (not shown).

The model predicts that neonatal brain is more excitable in response to external stimuli.

Significant evidence shows that the neonatal brain is more excitable in response to external stimuli or insults as compared to adult brain (Bender and Baram 2007; Panayiotopoulos 2005; Van Zundert et al. 2008; Zanelli et al. 2015). For example, the frequency of seizure incidences is highest in the immature human brain (Ben-Ari et al. 2007; Hauser 1994; 1992). Critical periods where the animal brain is prone to seizures have also been well-documented (Ben-Ari et al. 2007). Various epileptogenic agents and conditions, including an increase in

617 $[K^+]_o$, result in sigmoid-shaped age-dependence of seizure susceptibility in postnatal
618 hippocampus (Ben-Ari et al. 2007; Dzhala and Staley 2003; Isaev et al. 2005; Khazipov et al.
619 2004). The developmental changes in GABAergic function are suspected to play a key role in the
620 change in seizure threshold and the higher incidences of seizures in neonates (Ben-Ari and
621 Holmes 2006; 2005).

622 To test this hypothesis, we next investigate how excitatory GABAergic
623 neurotransmission affects the excitability of the network in response to different levels of $[K^+]_o$.
624 In the model, we take the average frequency of action potential (AP) generation (average number
625 of spikes per minute per neuron) of all excitatory neurons as a measure of the susceptibility of
626 the network to excited states such as seizures. As illustrated in Figure 10, the overall AP
627 frequency is significantly larger in the network with depolarizing inhibition (representing the
628 neonatal brain) than the network with mature inhibition (representing a mature network). For all
629 $[K^+]_o$ values tested, the average AP frequency in the neonatal network is doubled that of mature
630 network. Thus, our simulation predicts that depolarizing inhibition strongly increases the
631 excitability of the network, indicating a significantly lower threshold for highly excited states
632 such as seizure in neonates (Figure 10). Our simulations also show that decreasing the radius of
633 neurons or the K^+ uptake capacity of astrocytes further increases the vulnerability of neonate
634 brain to highly excited states (not shown).

635

636 ## Discussion

637 Spontaneous neuronal and astrocytic activity is the hallmark of the developing brain and
638 drives cell differentiation, maturation, and network formation (Ben-Ari et al. 1989; Felix et al.
639 2020b; Garaschuk et al. 1998b; Garaschuk et al. 2000; Griguoli and Cherubini 2017; Katz and

Shatz 1996; Leinekugel et al. 1997; Luhmann et al. 2016; Penn et al. 1998; Spitzer 2006; 1994). In the neonate hippocampus, this activity is mostly attributed to the excitatory effect of GABAergic neurotransmission (Cherubini et al. 1991). While spontaneous activity has also been shown in cortical neuronal networks, these appear to originate primarily from pace-maker cells in the piriform cortex, and are driven by a separate mechanism involving both glutamate and GABA (Barger et al. 2016). In contrast, hippocampal early network oscillations stem solely from GABA released by interneurons. Hippocampal interneurons constitute a diverse group of cells, including the fast-spiking inhibitory neurons simulated in this study. These cells have previously been implicated in the generation of early network activity in the hippocampus and cortex as the timing of their synapse formation around pyramidal cells closely match that of the appearance of giant depolarizing potentials in the neonatal brain. Additionally, the optogenetic blocking of their activity was shown to halt spontaneous giant depolarizing potentials almost entirely (Pelkey et al. 2017).

The excitatory effect of GABA on neurons is related to the higher expression of the $Na^+/K^+/Cl^-$ cotransporter (NKCC) as compared to the K^+/Cl^- cotransporter (KCC) in the first week after birth. This results in elevated intracellular Cl^-, leading to an outwardly directed Cl^- gradient (Achilles et al. 2007; Kaila et al. 2014; Rivera et al. 1999), and in an efflux of Cl^- when $GABA_A$ receptor channels open, causing the post-synaptic neuron to depolarize (Kirmse et al. 2015). Notably, and as opposed to neurons, astrocytes do not show a developmental switch to KCC2, but maintain high expression levels of NKCC1 expression into adulthood (Losi et al. 2014). $[Cl^-]_i$ thus continues to be relatively high, and the resulting depolarization upon activation of $GABA_A$ receptors can induce opening of voltage-gated Ca^{2+} channels (Fraser et al. 1995;

662 Nilsson et al. 1993). In the hippocampus of mice, $GABA_A$ receptor-mediated astrocytic Ca^{2+}
663 signaling is thus present throughout development (Felix et al. 2020a; Meier et al. 2008).

664 In this study, we report spontaneous, ultraslow fluctuations in the intracellular Na^+
665 concentration of CA1 pyramidal neurons and astrocytes in tissue slices from mouse
666 hippocampus, recorded using ratiometric Na^+ imaging, thereby confirming our recent
667 observations (Felix et al. 2020b). As reported in the latter study, these spontaneous fluctuations
668 are primarily present during the first postnatal week and rapidly diminish afterwards. Unlike the
669 giant depolarizing potentials (GDPs) and early network Ca^{2+} oscillations observed in the
670 hippocampus previously (Ben-Ari et al. 1997; Garaschuk et al. 1998b; Garaschuk et al. 2000),
671 the Na^+ fluctuations reported here are not synchronous, involve only about a quarter of all
672 pyramidal cells recorded, are not significantly modulated by glutamatergic neurotransmission,
673 and do not occur with regular frequency. Furthermore, these fluctuations are extremely rare
674 (~2/hour), long-lasting (each fluctuation lasting up to several minutes), and strongly attenuated
675 by the application of TTX to block VGSCs and application of inhibitors of GABAergic
676 neurotransmission. A range of other pharmacological blockers targeting various channels,
677 receptors, co-transporters, or transporters did not significantly affect these fluctuations (Figure 5
678 and (Felix et al. 2020b)).

679 To investigate the origin of the spontaneous neuronal Na^+ fluctuations further, we
680 developed a detailed computational model that represents a hippocampal network, incorporating
681 the three main cell types (pyramidal cells, inhibitory neurons, and astrocytes) and ion
682 concentration dynamics in principal neurons and the extracellular space. In agreement with
683 observations from our experimental data presented here and the earlier experimental study (Felix
684 et al. 2020b), the computational results suggest that voltage-gated Na^+ channels and the

685 excitatory effect of GABAergic neurotransmission play key roles in the generation of the
686 ultraslow Na^+ fluctuations. Our simulation results also show that these fluctuations occur at the
687 individual neuronal level, are not phase-locked, and are not strictly a network phenomenon,
688 thereby confirming experimental results. Moreover, the fluctuations are confined to intracellular
689 Na^+ and are not observed in extracellular K^+, further supporting the conclusion that these
690 fluctuations are a local phenomenon.

691 Because synaptogenesis is ongoing during the first postnatal week, synapses across the
692 neuronal network display varying strengths. This means that while activity such as GDPs can
693 happen synchronously across populations, individual synapses will experience different levels of
694 Na^+ influx in response to action potentials. A neuron with a large number of strong synapses
695 from an interneuron would therefore have a larger influx of Na^+ (considering the depolarizing
696 inhibition in the neonate brain) than neurons with fewer, weaker connections. The pattern of
697 connectivity and variations in GABA release between several interneurons could therefore
698 explain the unusually long, irregular, asynchronous fluctuations seen in individual neurons here,
699 as they might arise from the summation of inputs. This mechanism is also compatible with the
700 results gained from the dual staining experiments (Figure 8), which showed no correlation
701 between levels of synchronized Ca^{2+} activity, and the presence or lack of Na^+ fluctuations in
702 individual cells. These results suggest that the two activity patterns are not present sequentially
703 during development, but are rather two different patterns generated in the same population of
704 cells.

705 In addition to the outwardly directed Cl^- gradient and the excitatory action of GABA, the
706 neonate forebrain in the first week after birth is in a constant state of flux where many functional
707 and morphological changes occur along with the differentiation and maturation of cells and the

cellular network (Ben-Ari et al. 1997; Bordey and Sontheimer 1997; Garaschuk et al. 1998b; Larsen et al. 2019; Lohmann and Kessels 2014). Two of the most significant changes include the still ongoing gliogenesis and astrocyte maturation (Kriegstein and Alvarez-Buylla 2009; Privat 1975; Wang and Bordey 2008). Immature astrocytes have a reduced glial uptake capacity for K^+ as well as for glutamate compared to the mature brain (Felix et al. 2020a; Larsen et al. 2019; Schreiner et al. 2014). Furthermore, the neonate brain exhibits an increased volume fraction of the ECS (Lehmenkühler et al. 1993; Nicholson and Hrabětová 2017; Syková and Nicholson 2008). These factors along with the morphological properties of cells, play key roles in ion concentration dynamics. Indeed, we found the behavior of intracellular Na^+ fluctuations to be strongly reliant on neuronal radius. However, the larger extra- to intracellular volume ratio appears to suppress Na^+ fluctuations, suggesting that the larger relative ECS observed in neonates does not play a significant mechanistic role in the generation of spontaneous activity. Our model also suggests that increasing glial K^+ uptake capacity results in decreasing the amplitude and frequency of Na^+ fluctuations in the individual neurons and thus may play a role in their suppression at later stages of postnatal development.

Convincing evidence shows that the developing brain is more excitable as compared to adult brain. This is supported by the significantly higher frequency of seizures in the neonatal brain (Ben-Ari et al. 2007; Hauser 1994; 1992). The higher occurrence of seizures is primarily attributed to the excitatory effect of GABA (Khalilov et al. 2005). Based on the above analysis, we believe that the inability of astrocytes to effectively take up extracellular K^+ and morphological changes together with the inverted Cl^- gradients leave the developing brain more susceptible to highly excited states such as seizures. As a proof of concept, we exposed our model network to increasing concentrations of K^+ in the bath solution, similar to experimental

731 protocols used to generate epileptiform activity in brain slices. Indeed, we found that the network
732 representing the neonate brain is unable to cope with the elevated extracellular K^+ concentration
733 efficiently and exhibits higher excitability as we increase bath K^+. Decreasing the radius of
734 neurons or the K^+ uptake capacity of astrocytes further increases the vulnerability of neonate
735 brain to higher excitability (not shown).

736 To summarize, our dual experiment-theory approach asserts that the ultraslow, long-
737 lasting, spontaneous intracellular Na^+ fluctuations observed in neonate brain are non-
738 synchronous, not coupled with fluctuations in extracellular K^+, and only occur in a fraction of
739 neurons (and astrocytes, see Figure 2 and (Felix et al. 2020b)). These fluctuations are most likely
740 due to a combination of factors with the excitatory GABAergic neurotransmission and action
741 potential generation playing dominant roles. In addition, other conditions in the neonate brain
742 such as decreased K^+ uptake capacity of astrocytes and morphological properties of neurons also
743 play key roles. Furthermore, glutamatergic and other pathways do not seem to make notable
744 contributions to the Na^+ fluctuations. The combination of factors described above also provides
745 an environment in the neonate brain that is conducive to seizure-like states. Thus, the
746 experimental and computational work presented here provides deep insights into this newly
747 observed phenomena and its possible link with seizure-like states in the developing brain.

748 Finally, we remark that our model is a simpler representation of a very complex reality,
749 and involves several simplifying assumptions. Specifically, Ca^{2+} signaling in both neurons and
750 astrocytes and neurotransmitter uptake through transporters is not taken into account.
751 Furthermore, gap junctional coupling between astrocytes develops during the first postnatal week
752 (Giaume et al. 2010), and is not explicitly incorporated in the model. Instead, the effect of
753 change in astrocytic coupling is approximated by changing their K^+ buffering capacity. Neonatal

754 astrocytes differ from mature astrocytes in other significant ways as well. They exhibit a more
755 negative membrane potential as compared to mature astrocytes, and express a variety of
756 rectifying K^+ conductances. In addition to deficient K^+ homeostatic capacity, the nonlinear
757 interaction between these channels (with expression levels different than mature astrocytes) may
758 result in the function of neonatal astrocytes that is significantly different than their mature
759 counterparts (Ma et al. 2016; Zhong et al. 2016). Moreover, strong evidence supports the
760 existence of $GABA_A$ currents in astrocytes that would affect the function of neonatal astrocytes
761 differently than the mature astrocytes (Ballanyi et al. 1987; Fraser et al. 1994; Ma et al. 2012;
762 Nilsson et al. 1993). Additionally, the model only approximates CA1 region, ignoring the CA3-
763 CA1 connectivity and the properties of CA3 neurons, which are crucial for the origination of
764 GDPs and their propagation to CA1 region (Ben-Ari 2001; Ben-Ari et al. 1989; Sipilä et al.
765 2005; Sipilä et al. 2006). Thus, in its current form, the model is not equipped to properly
766 investigate the correlation between slow Na^+ fluctuations and GDPs. Incorporating these key
767 factors in the model and addressing several remaining questions about this exciting topic is the
768 subject of our future research.
769

770 ## Acknowledgements

771 This works was supported by NIH through grant number R01AG053988 (GU), the Deutsche
772 Forschungsgemeinschaft through grant number SPP1757:Ro2327/8-2 (CRR), and a start-up fund
773 of the SPP1757 (LF).
774

References

Achilles K, Okabe A, Ikeda M, Shimizu-Okabe C, Yamada J, Fukuda A, Luhmann HJ, and Kilb W. Kinetic properties of Cl− uptake mediated by Na+-dependent K+-2Cl− cotransport in immature rat neocortical neurons. *Journal of Neuroscience* 27: 8616-8627, 2007.

Ballanyi K, Grafe P, and Ten Bruggencate G. Ion activities and potassium uptake mechanisms of glial cells in guinea-pig olfactory cortex slices. *The Journal of physiology* 382: 159-174, 1987.

Barger Z, Easton CR, Neuzil KE, and Moody WJ. Early network activity propagates bidirectionally between hippocampus and cortex. *Developmental neurobiology* 76: 661-672, 2016.

Ben-Ari Y. Developing networks play a similar melody. *Trends in neurosciences* 24: 353-360, 2001.

Ben-Ari Y, Gaiarsa J-L, Tyzio R, and Khazipov R. GABA: a pioneer transmitter that excites immature neurons and generates primitive oscillations. *Physiological reviews* 87: 1215-1284, 2007.

Ben-Ari Y, and Holmes GL. Effects of seizures on developmental processes in the immature brain. *The Lancet Neurology* 5: 1055-1063, 2006.

Ben-Ari Y, and Holmes GL. The multiple facets of γ-aminobutyric acid dysfunction in epilepsy. *Current opinion in neurology* 18: 141-145, 2005.

Ben-Ari Y, Khazipov R, Leinekugel X, Caillard O, and Gaiarsa J-L. GABAA, NMDA and AMPA receptors: a developmentally regulatedmenage a trois'. *Trends in neurosciences* 20: 523-529, 1997.

Ben-Ari Y, Cherubini E, Corradetti R, and Gaiarsa J. Giant synaptic potentials in immature rat CA3 hippocampal neurones. *The Journal of physiology* 416: 303-325, 1989.

798 **Bender RA, and Baram TZ**. Epileptogenesis in the developing brain: what can we learn from
799 animal models? *Epilepsia* 48: 2-6, 2007.
800 **Bordey A, and Sontheimer H**. Postnatal development of ionic currents in rat hippocampal
801 astrocytes in situ. *Journal of Neurophysiology* 78: 461-477, 1997.
802 **Cherubini E, Gaiarsa JL, and Ben-Ari Y**. GABA: an excitatory transmitter in early postnatal
803 life. *Trends in neurosciences* 14: 515-519, 1991.
804 **Close B, Banister K, Baumans V, Bernoth EM, Bromage N, Bunyan J, Erhardt W,**
805 **Flecknell P, Gregory N, Hackbarth H, Morton D, and Warwick C**. Recommendations for
806 euthanasia of experimental animals: Part 2. DGXT of the European Commission. *Laboratory*
807 *animals* 31: 1-32, 1997.
808 **Cressman JR, Ullah G, Ziburkus J, Schiff SJ, and Barreto E**. The influence of sodium and
809 potassium dynamics on excitability, seizures, and the stability of persistent states: I. Single
810 neuron dynamics. *Journal of computational neuroscience* 26: 159-170, 2009.
811 **Dzhala VI, and Staley KJ**. Excitatory actions of endogenously released GABA contribute to
812 initiation of ictal epileptiform activity in the developing hippocampus. *Journal of Neuroscience*
813 23: 1840-1846, 2003.
814 **Ermentrout GB, and Kopell N**. Fine structure of neural spiking and synchronization in the
815 presence of conduction delays. *Proceedings of the National Academy of Sciences* 95: 1259-1264,
816 1998.
817 **Felix L, Stephan J, and Rose CR**. Astrocytes of the early postnatal brain. *European Journal of*
818 *Neuroscience* 2020a.
819 **Felix L, Ziemens D, Seifert G, and Rose CR**. Spontaneous Ultraslow Na+ Fluctuations in the
820 Neonatal Mouse Brain. *Cells* 9: 102, 2020b.

Fraser DD, Duffy S, Angelides KJ, Perez-Velazquez JL, Kettenmann H, and MacVicar BA. GABAA/benzodiazepine receptors in acutely isolated hippocampal astrocytes. *Journal of Neuroscience* 15: 2720-2732, 1995.

Fraser DD, Mudrick-Donnon LA, and Macvicar BA. Astrocytic GABA receptors. *Glia* 11: 83-93, 1994.

Fröhlich F, Bazhenov M, Iragui-Madoz V, and Sejnowski TJ. Potassium dynamics in the epileptic cortex: new insights on an old topic. *The Neuroscientist* 14: 422-433, 2008.

Garaschuk O, Hanse E, and Konnerth A. Developmental profile and synaptic origin of early network oscillations in the CA1 region of rat neonatal hippocampus. *The Journal of physiology* 507: 219-236, 1998a.

Garaschuk O, Hanse E, and Konnerth A. Developmental profile and synaptic origin of early network oscillations in the CA1 region of rat neonatal hippocampus. *J Physiol* 507 (Pt 1): 219-236, 1998b.

Garaschuk O, Linn J, Eilers J, and Konnerth A. Large-scale oscillatory calcium waves in the immature cortex. *Nature neuroscience* 3: 452-459, 2000.

Gerkau NJ, Lerchundi R, Nelson JS, Lantermann M, Meyer J, Hirrlinger J, and Rose CR. Relation between activity-induced intracellular sodium transients and ATP dynamics in mouse hippocampal neurons. *The Journal of physiology* 597: 5687-5705, 2019.

Gerkau NJ, Rakers C, Durry S, Petzold GC, and Rose CR. Reverse NCX attenuates cellular sodium loading in metabolically compromised cortex. *Cerebral Cortex* 28: 4264-4280, 2018.

Giaume C, Koulakoff A, Roux L, Holcman D, and Rouach N. Astroglial networks: a step further in neuroglial and gliovascular interactions. *Nature Reviews Neuroscience* 11: 87-99, 2010.

844 **Griguoli M, and Cherubini E**. Early correlated network activity in the hippocampus: its
845 putative role in shaping neuronal circuits. *Frontiers in cellular neuroscience* 11: 255, 2017.
846 **Haack N, Durry S, Kafitz KW, Chesler M, and Rose CR**. Double-barreled and concentric
847 microelectrodes for measurement of extracellular ion signals in brain tissue. *JoVE (Journal of*
848 *Visualized Experiments)* e53058, 2015.
849 **Hauser WA**. The prevalence and incidence of convulsive disorders in children. *Epilepsia* 35:
850 S1-S6, 1994.
851 **Hauser WA**. Seizure disorders: the changes with age. *Epilepsia* 33: 6-14, 1992.
852 **Hodgkin AL, and Huxley AF**. A quantitative description of membrane current and its
853 application to conduction and excitation in nerve. *The Journal of physiology* 117: 500, 1952.
854 **Hübel N, Andrew RD, and Ullah G**. Large extracellular space leads to neuronal susceptibility
855 to ischemic injury in a Na+/K+ pumps–dependent manner. *Journal of computational*
856 *neuroscience* 40: 177-192, 2016.
857 **Hübel N, Hosseini-Zare MS, Žiburkus J, and Ullah G**. The role of glutamate in neuronal ion
858 homeostasis: A case study of spreading depolarization. *PLoS computational biology* 13:
859 e1005804, 2017.
860 **Huebel N, and Ullah G**. Anions govern cell volume: a case study of relative astrocytic and
861 neuronal swelling in spreading depolarization. *PloS one* 11: 2016.
862 **Isaev D, Isaeva E, Khazipov R, and Holmes GL**. Anticonvulsant action of GABA in the high
863 potassium–low magnesium model of ictogenesis in the neonatal rat hippocampus in vivo and in
864 vitro. *Journal of neurophysiology* 94: 2987-2992, 2005.

865 **Kafitz KW, Meier SD, Stephan J, and Rose CR**. Developmental profile and properties of
866 sulforhodamine 101—Labeled glial cells in acute brain slices of rat hippocampus. *Journal of*
867 *neuroscience methods* 169: 84-92, 2008.
868 **Kaila K, Price TJ, Payne JA, Puskarjov M, and Voipio J**. Cation-chloride cotransporters in
869 neuronal development, plasticity and disease. *Nature Reviews Neuroscience* 15: 637, 2014.
870 **Katz LC, and Shatz CJ**. Synaptic activity and the construction of cortical circuits. *Science* 274:
871 1133-1138, 1996.
872 **Khalilov I, Le Van Quyen M, Gozlan H, and Ben-Ari Y**. Epileptogenic actions of GABA and
873 fast oscillations in the developing hippocampus. *Neuron* 48: 787-796, 2005.
874 **Khazipov R, Khalilov I, Tyzio R, Morozova E, Ben-Ari Y, and Holmes GL**. Developmental
875 changes in GABAergic actions and seizure susceptibility in the rat hippocampus. *European*
876 *Journal of Neuroscience* 19: 590-600, 2004.
877 **Kirmse K, Kummer M, Kovalchuk Y, Witte OW, Garaschuk O, and Holthoff K**. GABA
878 depolarizes immature neurons and inhibits network activity in the neonatal neocortex in vivo.
879 *Nature communications* 6: 1-13, 2015.
880 **Kopell N, Börgers C, Pervouchine D, Malerba P, and Tort A**. Gamma and theta rhythms in
881 biophysical models of hippocampal circuits. In: *Hippocampal microcircuits*Springer, 2010, p.
882 423-457.
883 **Kriegstein A, and Alvarez-Buylla A**. The glial nature of embryonic and adult neural stem cells.
884 *Annual review of neuroscience* 32: 149-184, 2009.
885 **Krishnan GP, and Bazhenov M**. Ionic dynamics mediate spontaneous termination of seizures
886 and postictal depression state. *Journal of Neuroscience* 31: 8870-8882, 2011.

887 **Krishnan GP, González OC, and Bazhenov M**. Origin of slow spontaneous resting-state
888 neuronal fluctuations in brain networks. *Proceedings of the National Academy of Sciences* 115:
889 6858-6863, 2018.
890 **Langer J, Gerkau NJ, Derouiche A, Kleinhans C, Moshrefi-Ravasdjani B, Fredrich M,**
891 **Kafitz KW, Seifert G, Steinhäuser C, and Rose CR**. Rapid sodium signaling couples
892 glutamate uptake to breakdown of ATP in perivascular astrocyte endfeet. *Glia* 65: 293-308,
893 2017.
894 **Langer J, and Rose CR**. Synaptically induced sodium signals in hippocampal astrocytes in situ.
895 *The Journal of physiology* 587: 5859-5877, 2009.
896 **Larsen BR, Stoica A, and MacAulay N**. Developmental maturation of activity-induced K+ and
897 pH transients and the associated extracellular space dynamics in the rat hippocampus. *The*
898 *Journal of Physiology* 597: 583-597, 2019.
899 **Lehmenkühler A, Syková E, Svoboda J, Zilles K, and Nicholson C**. Extracellular space
900 parameters in the rat neocortex and subcortical white matter during postnatal development
901 determined by diffusion analysis. *Neuroscience* 55: 339-351, 1993.
902 **Leinekugel X, Medina I, Khalilov I, Ben-Ari Y, and Khazipov R**. Ca2+ oscillations mediated
903 by the synergistic excitatory actions of GABAA and NMDA receptors in the neonatal
904 hippocampus. *Neuron* 18: 243-255, 1997.
905 **Lohmann C, and Kessels HW**. The developmental stages of synaptic plasticity. *The Journal of*
906 *physiology* 592: 13-31, 2014.
907 **Losi G, Mariotti L, and Carmignoto G**. GABAergic interneuron to astrocyte signalling: a
908 neglected form of cell communication in the brain. *Philosophical Transactions of the Royal*
909 *Society B: Biological Sciences* 369: 20130609, 2014.

Luhmann HJ, Sinning A, Yang J-W, Reyes-Puerta V, Stüttgen MC, Kirischuk S, and Kilb W. Spontaneous neuronal activity in developing neocortical networks: from single cells to large-scale interactions. *Frontiers in neural circuits* 10: 40, 2016.

Ma B, Buckalew R, Du Y, Kiyoshi CM, Alford CC, Wang W, McTigue DM, Enyeart JJ, Terman D, and Zhou M. Gap junction coupling confers isopotentiality on astrocyte syncytium. *Glia* 64: 214-226, 2016.

Ma BF, Xie MJ, and Zhou M. Bicarbonate efflux via GABAA receptors depolarizes membrane potential and inhibits two-pore domain potassium channels of astrocytes in rat hippocampal slices. *Glia* 60: 1761-1772, 2012.

MacAulay N. Molecular mechanisms of K+ clearance and extracellular space shrinkage—Glia cells as the stars. *Glia* 2020.

McBain CJ, Traynelis SF, and Dingledine R. Regional variation of extracellular space in the hippocampus. *Science* 249: 674-677, 1990.

Meier SD, Kafitz KW, and Rose CR. Developmental profile and mechanisms of GABA-induced calcium signaling in hippocampal astrocytes. *Glia* 56: 1127-1137, 2008.

Nicholson C, and Hrabětová S. Brain extracellular space: the final frontier of neuroscience. *Biophysical journal* 113: 2133-2142, 2017.

Nilsson M, Eriksson P, Rönnbäck L, and Hansson E. GABA induces Ca2+ transients in astrocytes. *Neuroscience* 54: 605-614, 1993.

Panayiotopoulos C. Neonatal seizures and neonatal syndromes. In: *The Epilepsies: Seizures, Syndromes and Management*Bladon Medical Publishing, 2005.

Pelkey KA, Chittajallu R, Craig MT, Tricoire L, Wester JC, and McBain CJ. Hippocampal GABAergic inhibitory interneurons. *Physiological reviews* 97: 1619-1747, 2017.

Penn AA, Riquelme PA, Feller MB, and Shatz CJ. Competition in retinogeniculate patterning driven by spontaneous activity. *Science* 279: 2108-2112, 1998.

Privat A. Postnatal gliogenesis in the mammalian brain. *Int Rev Cytol* 40: l-323, 1975.

Rivera C, Voipio J, and Kaila K. Two developmental switches in GABAergic signalling: the K+–Cl− cotransporter KCC2 and carbonic anhydrase CAVII. *The Journal of physiology* 562: 27-36, 2005.

Rivera C, Voipio J, Payne JA, Ruusuvuori E, Lahtinen H, Lamsa K, Pirvola U, Saarma M, and Kaila K. The K+/Cl− co-transporter KCC2 renders GABA hyperpolarizing during neuronal maturation. *Nature* 397: 251-255, 1999.

Safiulina VF, Zacchi P, Taglialatela M, Yaari Y, and Cherubini E. Low expression of Kv7/M channels facilitates intrinsic and network bursting in the developing rat hippocampus. *The Journal of physiology* 586: 5437-5453, 2008.

Saraga F, Wu C, Zhang L, and Skinner F. Active dendrites and spike propagation in multicompartment models of oriens-lacunosum/moleculare hippocampal interneurons. *The Journal of physiology* 552: 673-689, 2003.

Schreiner AE, Durry S, Aida T, Stock MC, Rüther U, Tanaka K, Rose CR, and Kafitz KW. Laminar and subcellular heterogeneity of GLAST and GLT-1 immunoreactivity in the developing postnatal mouse hippocampus. *Journal of Comparative Neurology* 522: 204-224, 2014.

Sipilä ST, Huttu K, Soltesz I, Voipio J, and Kaila K. Depolarizing GABA acts on intrinsically bursting pyramidal neurons to drive giant depolarizing potentials in the immature hippocampus. *Journal of Neuroscience* 25: 5280-5289, 2005.

Sipilä ST, Huttu K, Voipio J, and Kaila K. Intrinsic bursting of immature CA3 pyramidal neurons and consequent giant depolarizing potentials are driven by a persistent Na+ current and terminated by a slow Ca2+-activated K+ current. *European Journal of Neuroscience* 23: 2330-2338, 2006.

Somjen G, Kager H, and Wadman W. Computer simulations of neuron-glia interactions mediated by ion flux. *Journal of computational neuroscience* 25: 349-365, 2008.

Spitzer NC. Electrical activity in early neuronal development. *Nature* 444: 707-712, 2006.

Spitzer NC. Spontaneous Ca2+ spikes and waves in embryonic neurons: signaling systems for differentiation. *Trends in neurosciences* 17: 115-118, 1994.

Syková E, and Nicholson C. Diffusion in brain extracellular space. *Physiological reviews* 88: 1277-1340, 2008.

Tort AB, Rotstein HG, Dugladze T, Gloveli T, and Kopell NJ. On the formation of gamma-coherent cell assemblies by oriens lacunosum-moleculare interneurons in the hippocampus. *Proceedings of the National Academy of Sciences* 104: 13490-13495, 2007.

Traub RD, and Miles R. *Neuronal networks of the hippocampus*. Cambridge University Press, 1991.

Ullah G, Cressman Jr JR, Barreto E, and Schiff SJ. The influence of sodium and potassium dynamics on excitability, seizures, and the stability of persistent states: II. Network and glial dynamics. *Journal of computational neuroscience* 26: 171-183, 2009.

Ullah G, and Schiff SJ. Assimilating seizure dynamics. *PLoS computational biology* 6: e1000776, 2010.

Ullah G, Wei Y, Dahlem MA, Wechselberger M, and Schiff SJ. The role of cell volume in the dynamics of seizure, spreading depression, and anoxic depolarization. *PLoS computational biology* 11: e1004414, 2015.

Van Zundert B, Peuscher MH, Hynynen M, Chen A, Neve RL, Brown RH, Constantine-Paton M, and Bellingham MC. Neonatal neuronal circuitry shows hyperexcitable disturbance in a mouse model of the adult-onset neurodegenerative disease amyotrophic lateral sclerosis. *Journal of Neuroscience* 28: 10864-10874, 2008.

Wang DD, and Bordey A. The astrocyte odyssey. *Progress in neurobiology* 86: 342-367, 2008.

Wang X-J, and Buzsáki G. Gamma oscillation by synaptic inhibition in a hippocampal interneuronal network model. *Journal of neuroscience* 16: 6402-6413, 1996.

Wei Y, Ullah G, Ingram J, and Schiff SJ. Oxygen and seizure dynamics: II. Computational modeling. *Journal of neurophysiology* 112: 213-223, 2014a.

Wei Y, Ullah G, and Schiff SJ. Unification of neuronal spikes, seizures, and spreading depression. *Journal of Neuroscience* 34: 11733-11743, 2014b.

Zanelli S, Rajasekaran K, Grosenbaugh D, and Kapur J. Increased excitability and excitatory synaptic transmission during in vitro ischemia in the neonatal mouse hippocampus. *Neuroscience* 310: 279-289, 2015.

Zhong S, Du Y, Kiyoshi CM, Ma B, Alford CC, Wang Q, Yang Y, Liu X, and Zhou M. Electrophysiological behavior of neonatal astrocytes in hippocampal stratum radiatum. *Molecular brain* 9: 1-16, 2016.

Zuzana S, and Syková E. Diffusion heterogeneity and anisotropy in rat hippocampus. *Neuroreport* 9: 1299-1304, 1998.

Figures Legends

Figure 1: Network schematic showing connections between adjacent neurons within the two neuronal layers. The network consists of pyramidal (E) and inhibitory (I) neurons at five to one ratio, where five excitatory and one inhibitory neurons make one domain. In addition to synaptic inputs, we also consider the diffusion of extracellular K^+ between neighboring cells and incorporate the effect of glial K^+ uptake. Incorporating Na^+ and Cl^- diffusion in the extracellular space does not change our conclusions (not shown) and is therefore not included in the model.

Figure 2. In situ experiments. (A1) Images showing representative stainings in the CA1 region of the neonatal (P4; upper images) and juvenile (P18; lower images) hippocampus. In the merge, SBFI is shown in green and SR101 in magenta. ROIs representing cell bodies of neurons and astrocytes are labeled with numbers and letters, respectively. Scale bars: 50 μm. (A2) Na^+ fluctuations in the ROIs as depicted in (A1). (B) The percentage of pyramidal neurons and astrocytes showing activity for each age group and the total number of cells measured. (C) Scatter plot showing the peak amplitude and duration of neuronal fluctuations within the two indicated age groups.

Figure 3: Simulated spontaneous activity in 4 example neurons with excitatory GABAergic neurotransmission representing neonatal hippocampus (A, left) and mature inhibition representing juvenile hippocampus (A, right). Grey bar indicates three times the average standard deviation in experimental traces upwards of the mean. (B) Experimental data, showing excerpts from example measurements shown in Figure 2, both from neonatal neurons (P2-4, left; cell 3- upper; cell 5- lower), and juvenile neurons (P14-21, right; cell 1- upper; cell 2- lower). Traces

show changes in intracellular Na^+ concentration over 17 minutes, a time course directly comparable to (A).

Figure 4: Simulated spontaneous fluctuations in intracellular Na^+ ($[Na^+]_i$) are not coupled with significant fluctuations in extracellular K^+ ($[K^+]_o$). $[K^+]_o$ (A) and $[Na^+]_i$ (C) time traces from a randomly selected excitatory neuron (gray) and averaged over the entire excitatory network (black). (B) Ion sensitive electrode experiments showed no detectable spontaneous changes in extracellular K^+ in neonatal tissue. Note the artifact occurring when the electrode touches the slice surface.

Figure 5: Inhibiting $GABA_A$ receptors or voltage-gated Na^+ channels eliminates $[Na^+]_i$ fluctuations, whereas blocking glutamatergic synaptic inputs has little effect. (A) Bar plot showing the percentage of neurons exhibiting Na^+ fluctuations as determined in experiments under the four conditions simulated in (B). That is, the percentage of neurons exhibiting Na^+ fluctuations in slices from juveniles under control conditions (black) and in the presence of 0.5 μM TTX to block voltage gated Na^+ channels (gray), a cocktail containing APV (100 μM), NBQX (25 μM), and MPEP (25 μM) to block glutamatergic receptors (purple), and a combined application of bicuculline (10 μM), CGP-55845 (5 μM), NNC-711 (100 μM), and SNAP-5114 (100 μM) to block GABAergic signaling (cyan). (B) Time trace of $[Na^+]_i$ from a randomly selected excitatory neuron in the network in control conditions (depolarizing inhibition, representing neonatal brain) (black, top panel), with voltage-gated Na^+ channels blocked (gray, top panel), glutamatergic synapses blocked (purple, bottom panel), and GABAergic synapses blocked (cyan, bottom panel).

Figure 6: The neuronal radius, ratio of ECS to ICS (β), and K^+ uptake capacity of glia affect spontaneous Na^+ fluctuations in the model. (A) Time traces of $[Na^+]_i$ for five excitatory neurons from a network representing neonatal brain with a neuronal radius of 3 μm (left panels) and 9 μm (center panels). The panel on the right shows the mean amplitude of Na^+ fluctuations (averaged over all pyramidal neurons in the network) under the two conditions. The error bars indicate the standard deviation of the mean. β was fixed at 2.5. (B) Same as (A) at β = 1 (left panels) and 10 (center panels). (C) Same as (A) with maximum glial K^+ buffering strength G_{glia}=12 mM/s (left panels) and G_{glia}=96 mM/s (right panels). The radius of individual neurons is set at 6 μm in both (B) and (C). ***: $p<0.001$.

Figure 7: A significant decrease in the strength of Na^+/K^+ pump increases the amplitude of Na^+ fluctuations in the simulations. Average amplitude of spontaneous Na^+ fluctuations (averaged over all pyramidal neurons in the network) as a function of maximum pump strength (normalized with respect to the control value given in Table 1). ***: $p < 0.001$.

Figure 8: Dual imaging experiments. (A) Images show a section of the CA1 region of a P4 hippocampal slice stain with both OGB-1 and SBFI (individual stainings shown below). Scale bars indicate 20 μm. (B) Traces from individual cells as shown in (A). Room temperature Na^+ measurements (left) were followed by an increase to 32°C at which point Ca^{2+} measurements were conducted (right). (C) Lack of correlation between levels of Ca^{2+} activity as measured by area under the trace and number of Ca^{2+} at least 2% over the baseline value, and the presence or lack of Na^+ fluctuations in the same cell.

Figure 9: Sub-populations of neurons in the model network representing neonatal brain exhibit synchronized bursting behavior. (A) Raster plot showing the spiking activity of all excitatory neurons as a function of time. Each dot represents a spike by the neuron number indicated along vertical axis at a given time (horizontal axis). An example of synchronized burst is shown in (A1). (A2) The spiking activity of three neurons (dots on the top) in the network with the $[Na^+]_i$ (lines). Black, red, and blue color each correspond to one neuron. The inset shows an expanded view of a sample burst by each neuron. The synchronous bursting disappears by fully blocking GABA synaptic currents (B), and gets more prevalent after raising temperature to a physiological value of 35^o C.

Figure 10: Depolarizing inhibition leaves the model network more prone to excited states such as seizures. (A) Bar plot showing the number of spikes per minute averaged over all excitatory neurons as we systematically increase K^+ concentration in the bath. The black and gray bars correspond to neural network with normal and depolarizing inhibition respectively. The error bars indicate the standard deviation of the mean. ***: $p < 0.001$

Parameter	**Value and Unit** (Excitatory, Inhibitory neuron)	**Description**
C	1.0 μF/cm^2	Membrane capacitance
γ	$3 \times 10^4/(F \times r_{in})$ mM/(cm•μA)	Current to concentration conversion factor
r_{in}	6 μm	Radius of the neuron
β	2.5	Ratio of ICS to ECS
G_{Cl}^L	0.001 mS/cm^2	Conductance of Cl^- leak channels
G_{Na}^F	165 mS/cm^2, 35 mS/cm^2	Maximal conductance of fast Na^+ channels
G_K^{DR}	80 mS/cm^2, 9 mS/cm^2	Maximal conductance of delayed rectified K^+ channels
G_K^L	0.02 mS/cm^2	Conductance of K^+ leak channels
G_{Na}^L	7.6 μS/cm^2, 8.55 μS/cm^2	Conductance of Na^+ channels
$G_{AMPA/NMDA}$	1 μS/cm^2	Maximal conductance of E-to-E and E-to-I synapses
G_{GABA}^{ii}	10 μS/cm^2	Maximal conductance of I-to-I synapses
G_{GABA}^{ie}	0.1 - 3.0 mS/cm^2	Maximal conductance of I-to-E synapses
τ_R	0.1 ms	Rise constant for synaptic gating
τ_D	4.0 ms, 30.0 ms	Decay constant for synaptic gating
f_{stoch}	1 Hz, 0.1 Hz	Mean arrival frequency of stochastic input
ρ_{max}	29 mM/s	Maximum Na^+ /K^+ pump strength
$[O_2]_{bath}$	32 mg/l	Oxygen concentration in the bath solution
α	5.3 g/mol	Conversion factor from Na^+/K^+-ATPase current to oxygen consumption rate
ϵ_o	0.17 s^{-1}	Oxygen diffusion constant
G_{glia}	60 mM/s	Maximum glia K^+ uptake
ϵ_K	3 s^{-1}	Constant for K^+ diffusion between ECS and bath solution (blood vassals *in vivo*)
$[K^+]_{bath}$	3.0 mM	K^+ concentration in the bath solution *in vitro* or in vasculature *in vivo*
D_K	2.5 x 10^{-5} cm^2/s	Diffusion coefficient of K^+ in the ECS
dx	200 μm	Distance between adjacent neurons

1085 **Table 1:** Values and meanings of various parameters used in the model.

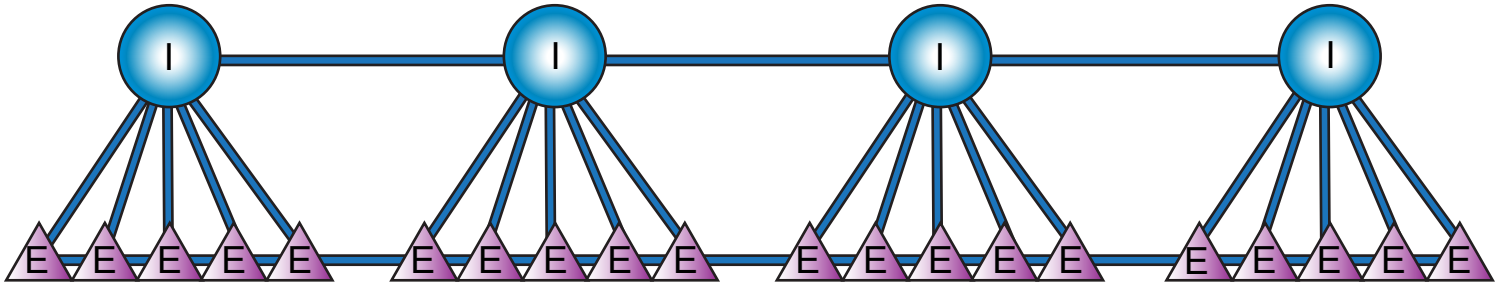

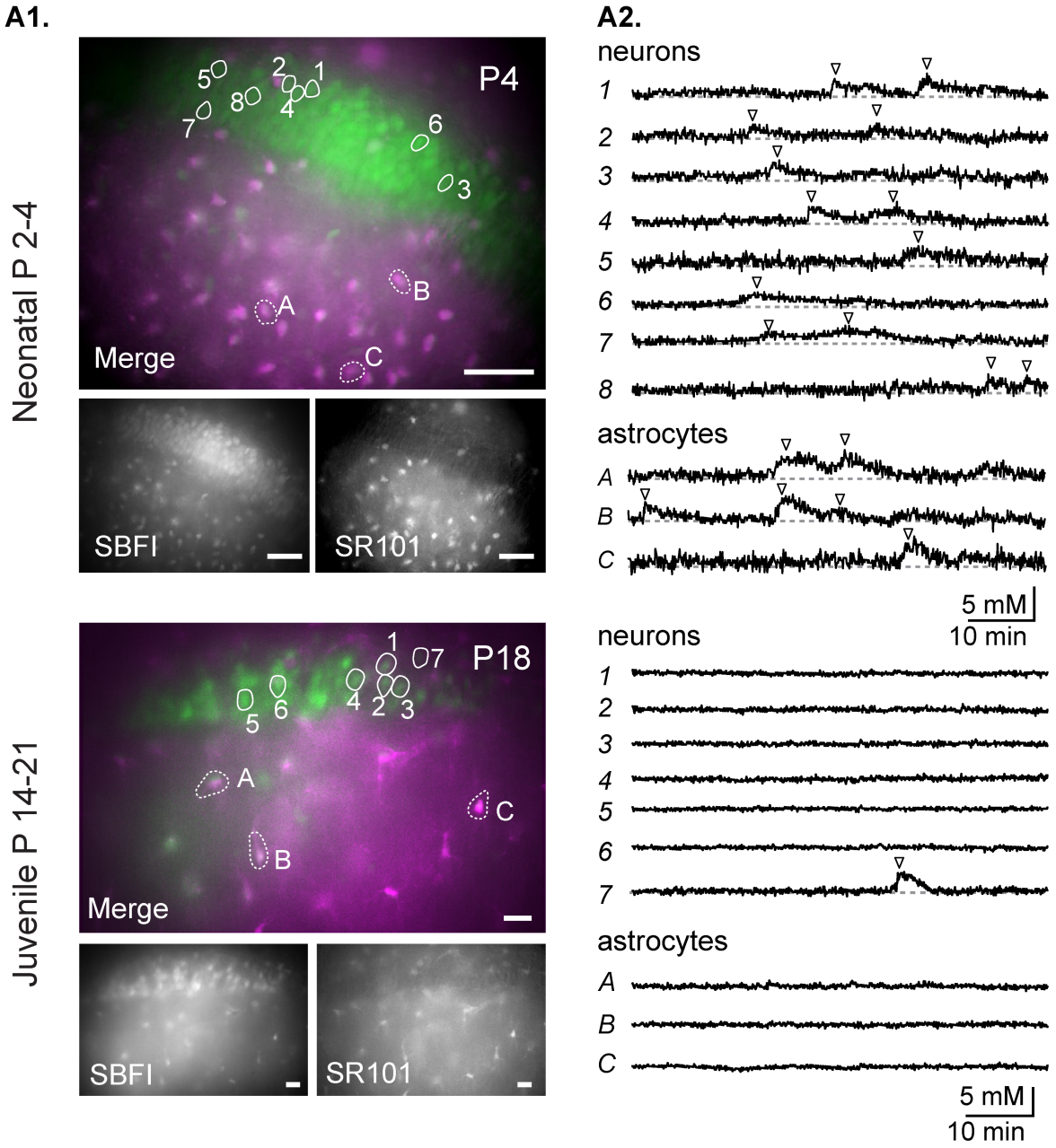

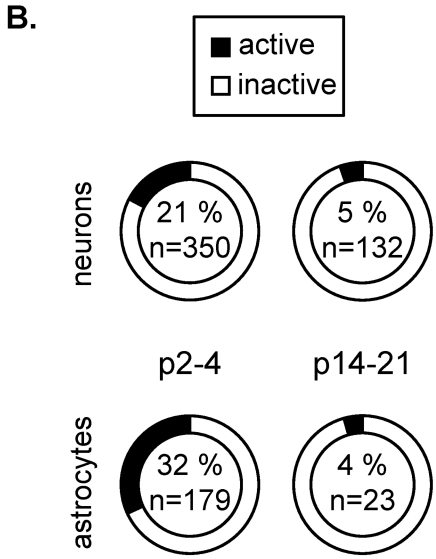

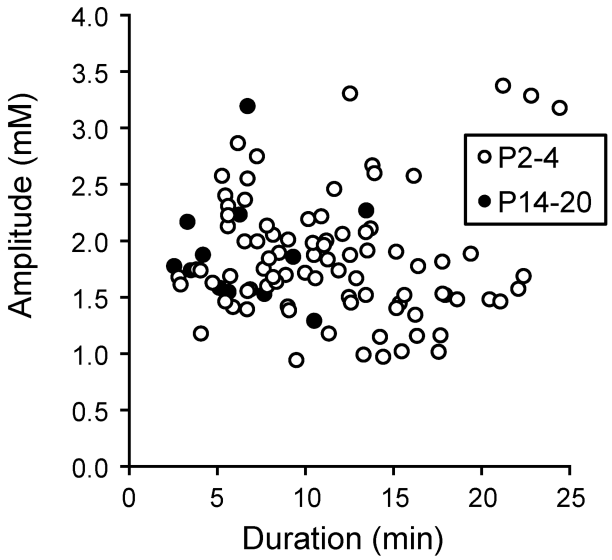

A. Simulation

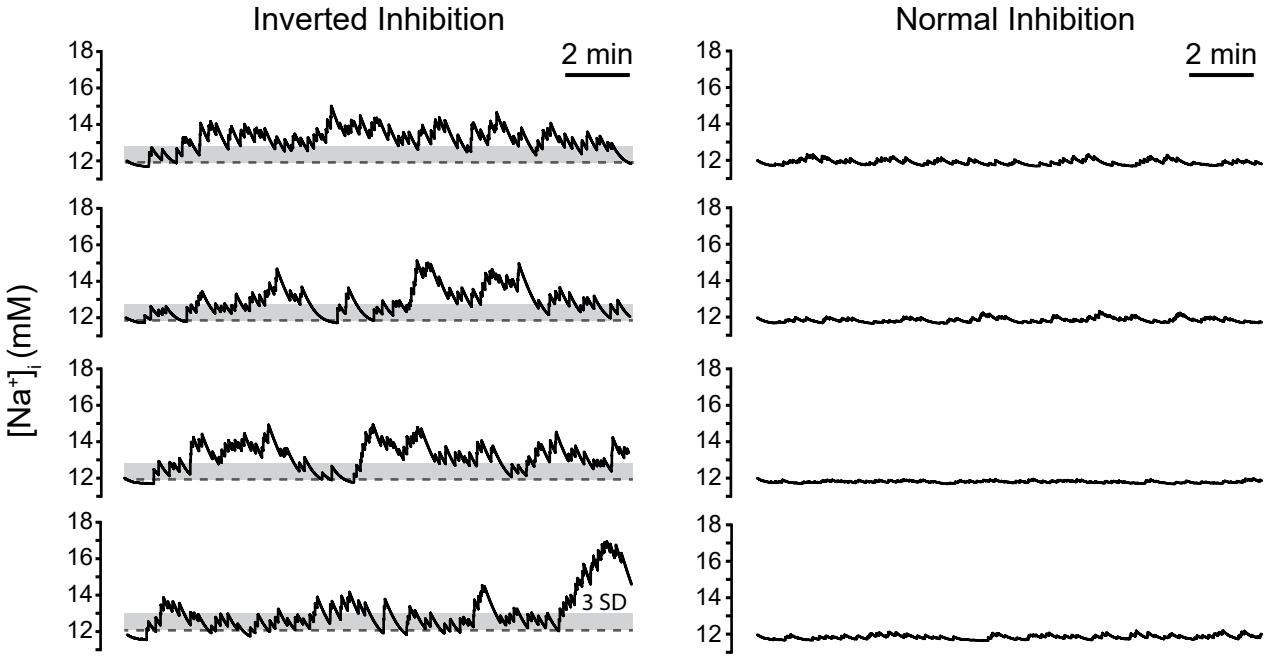

B. Experiment

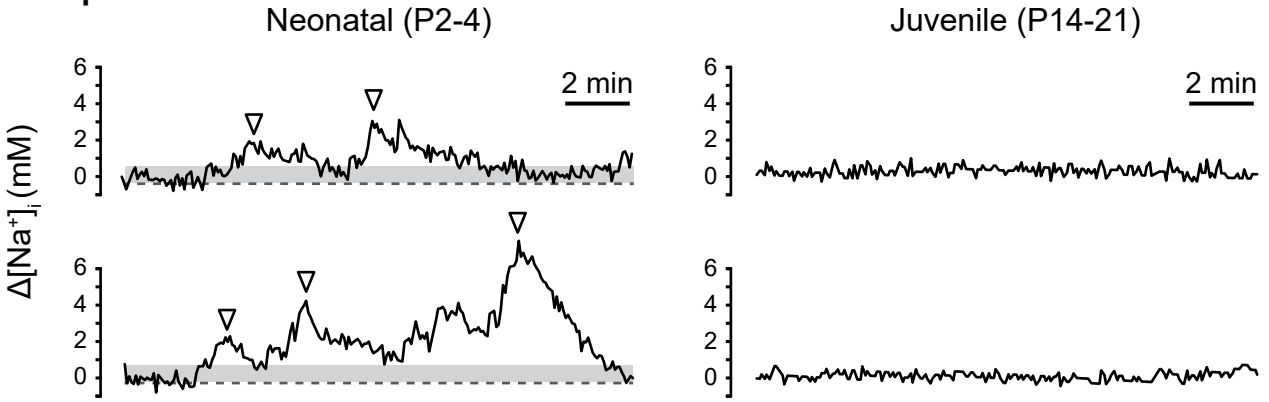

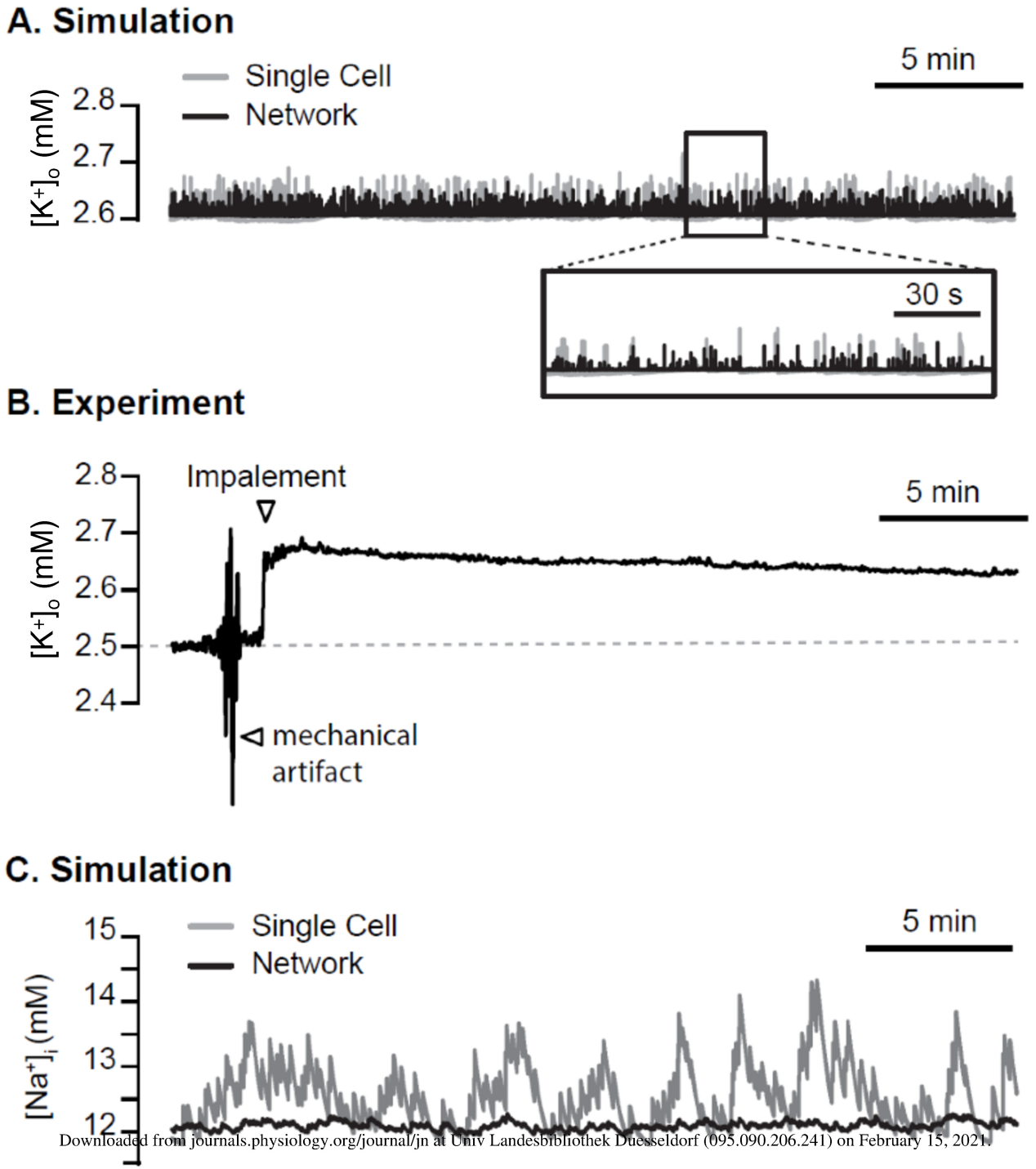

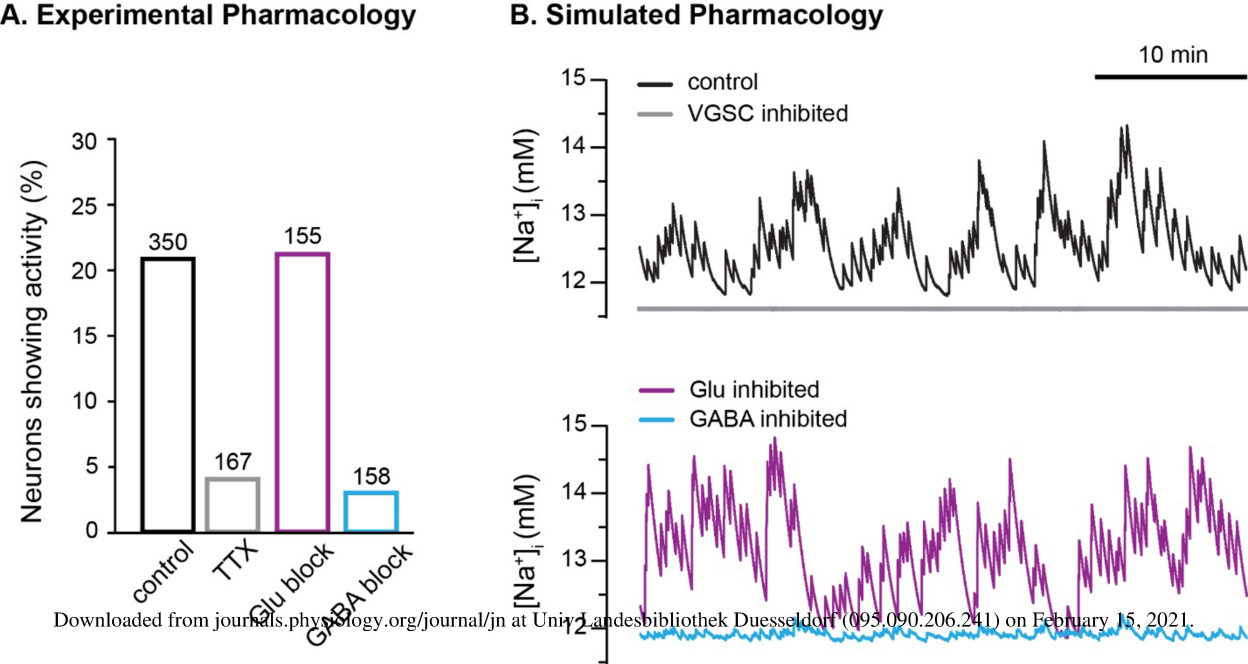

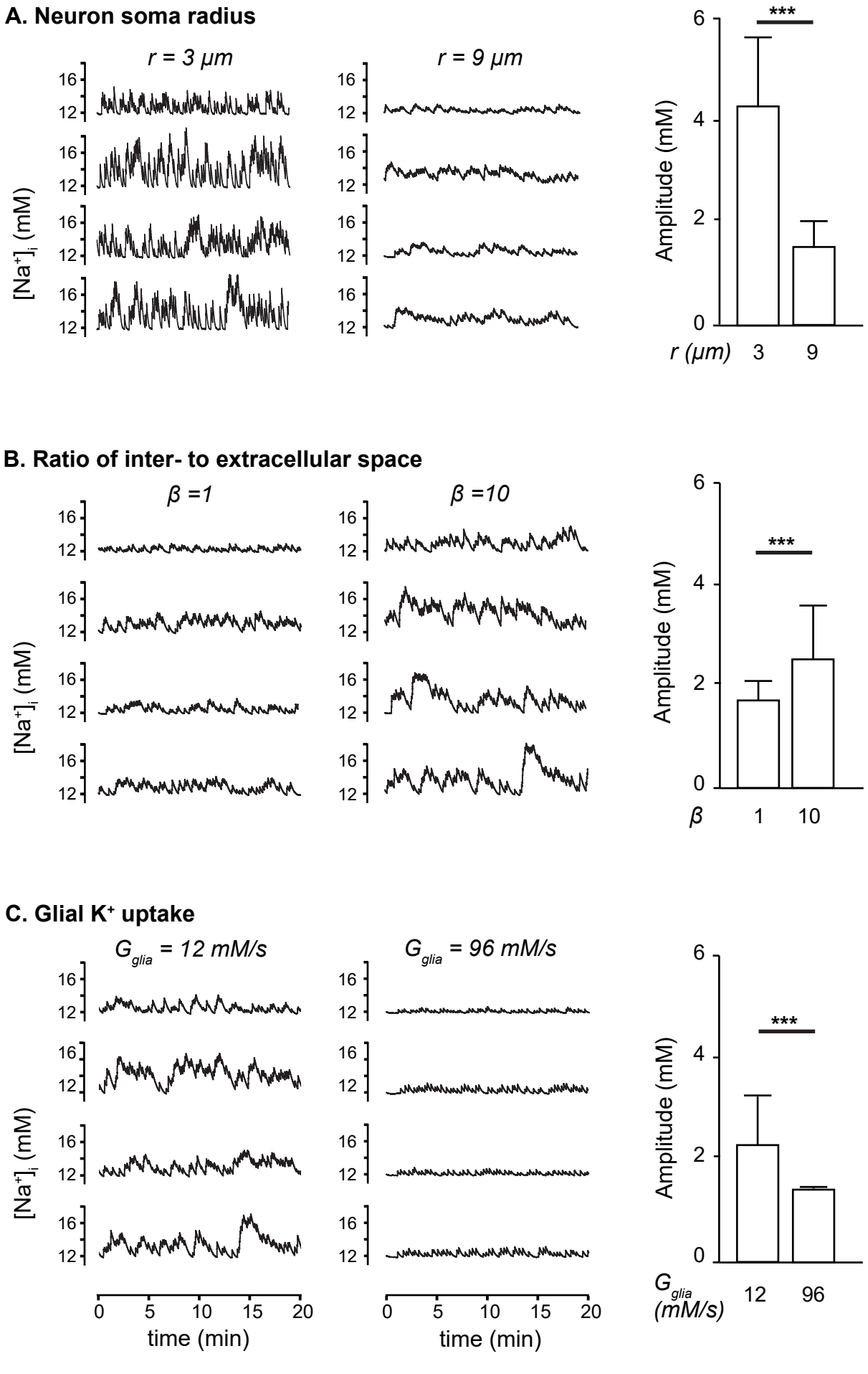

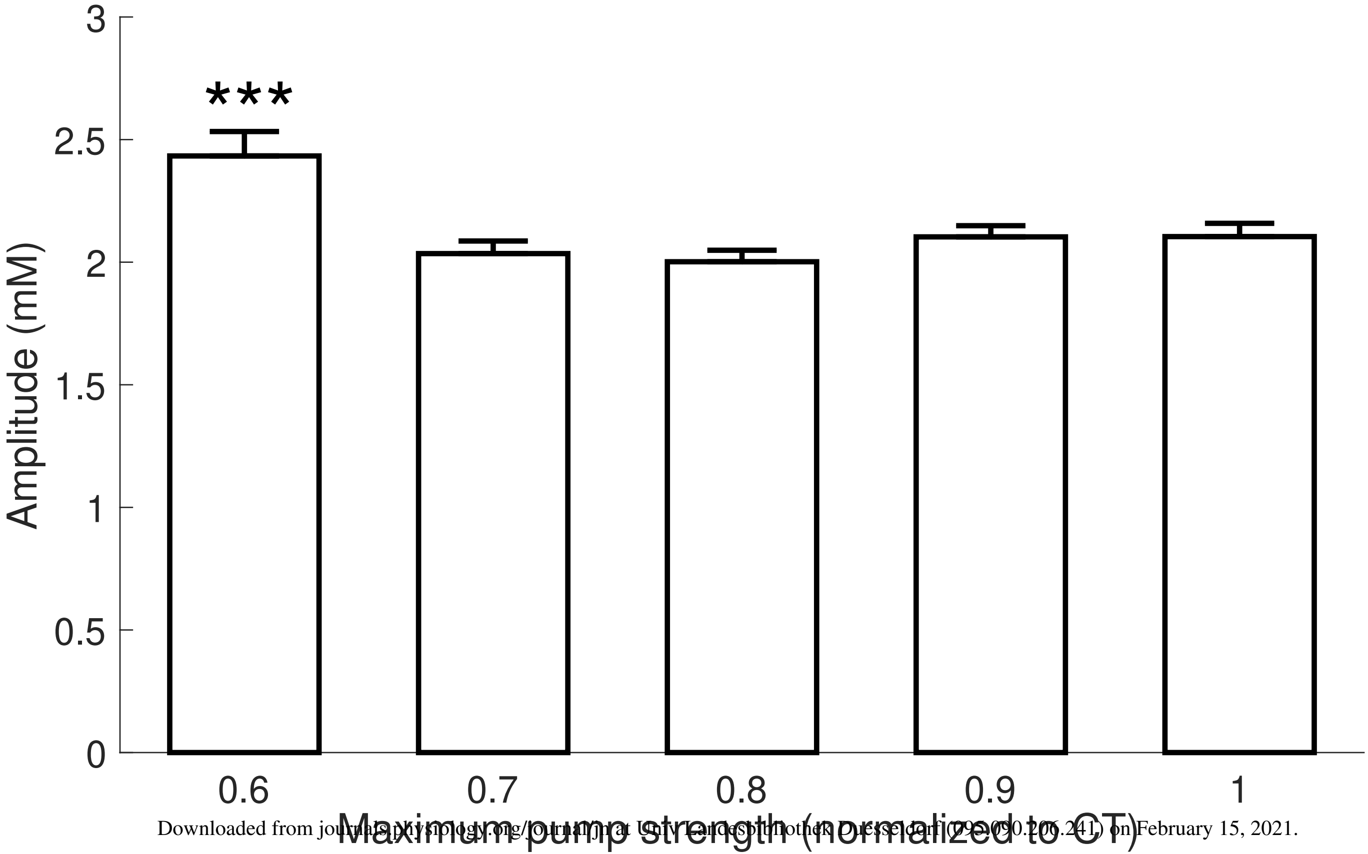

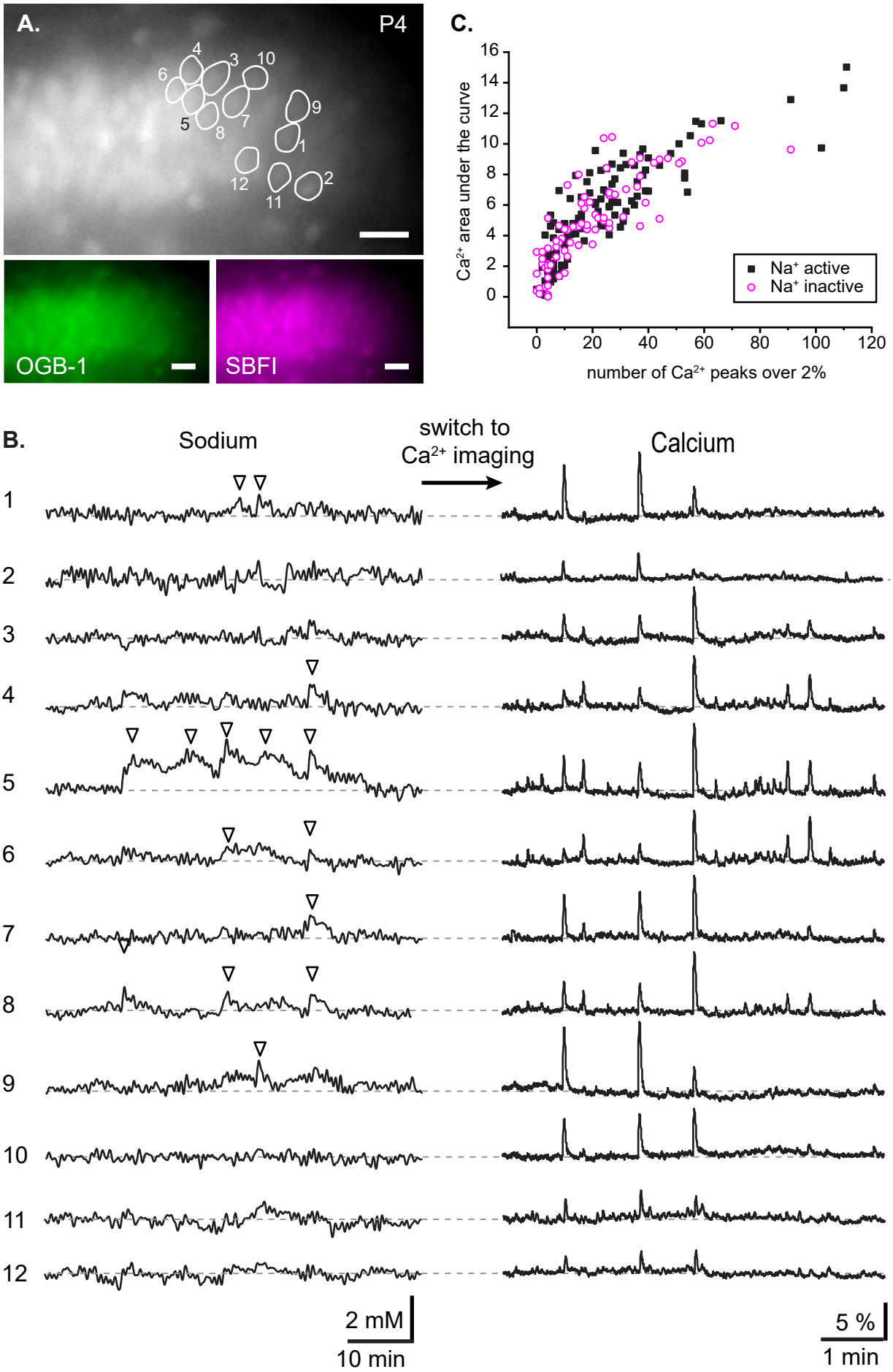

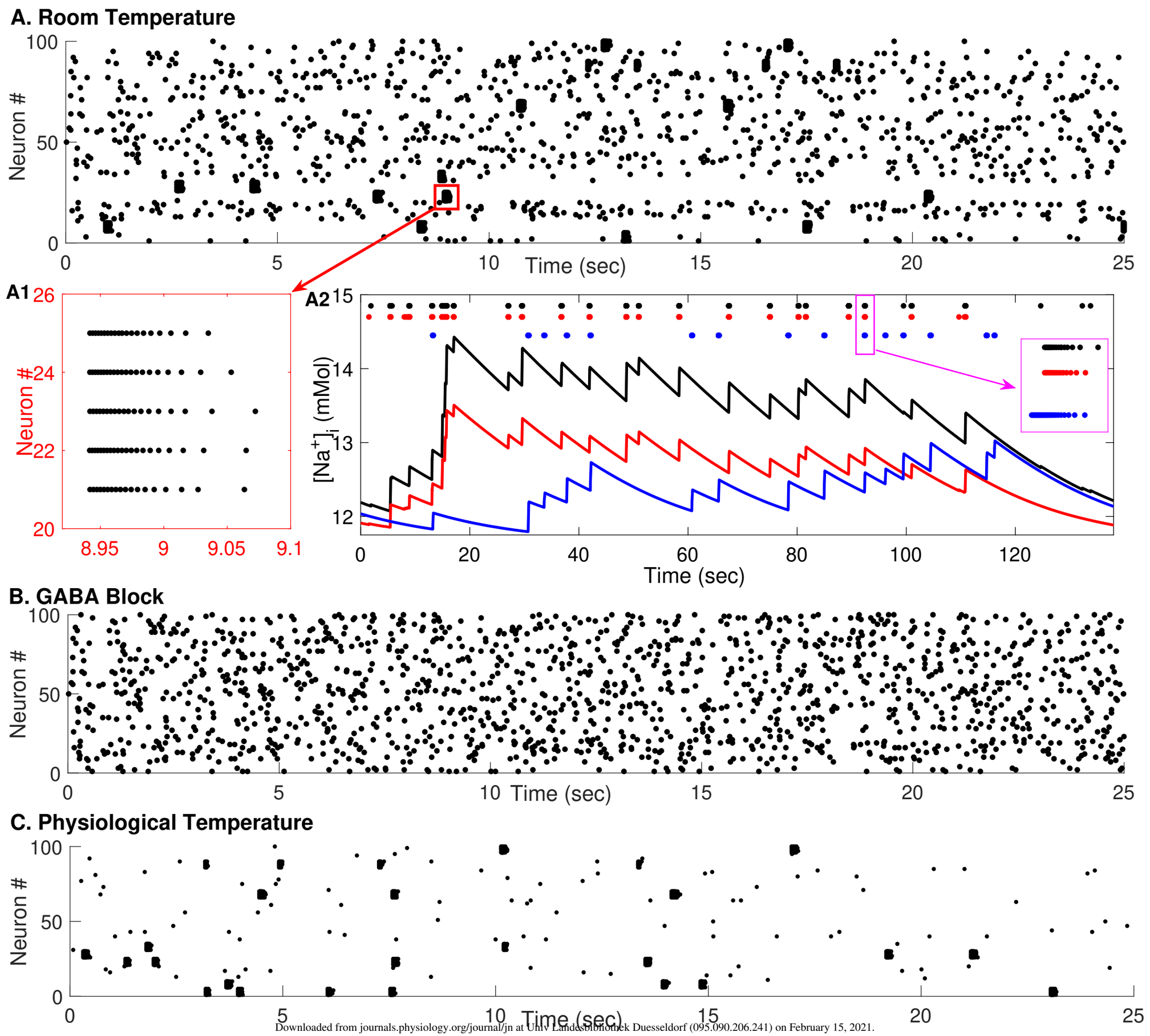

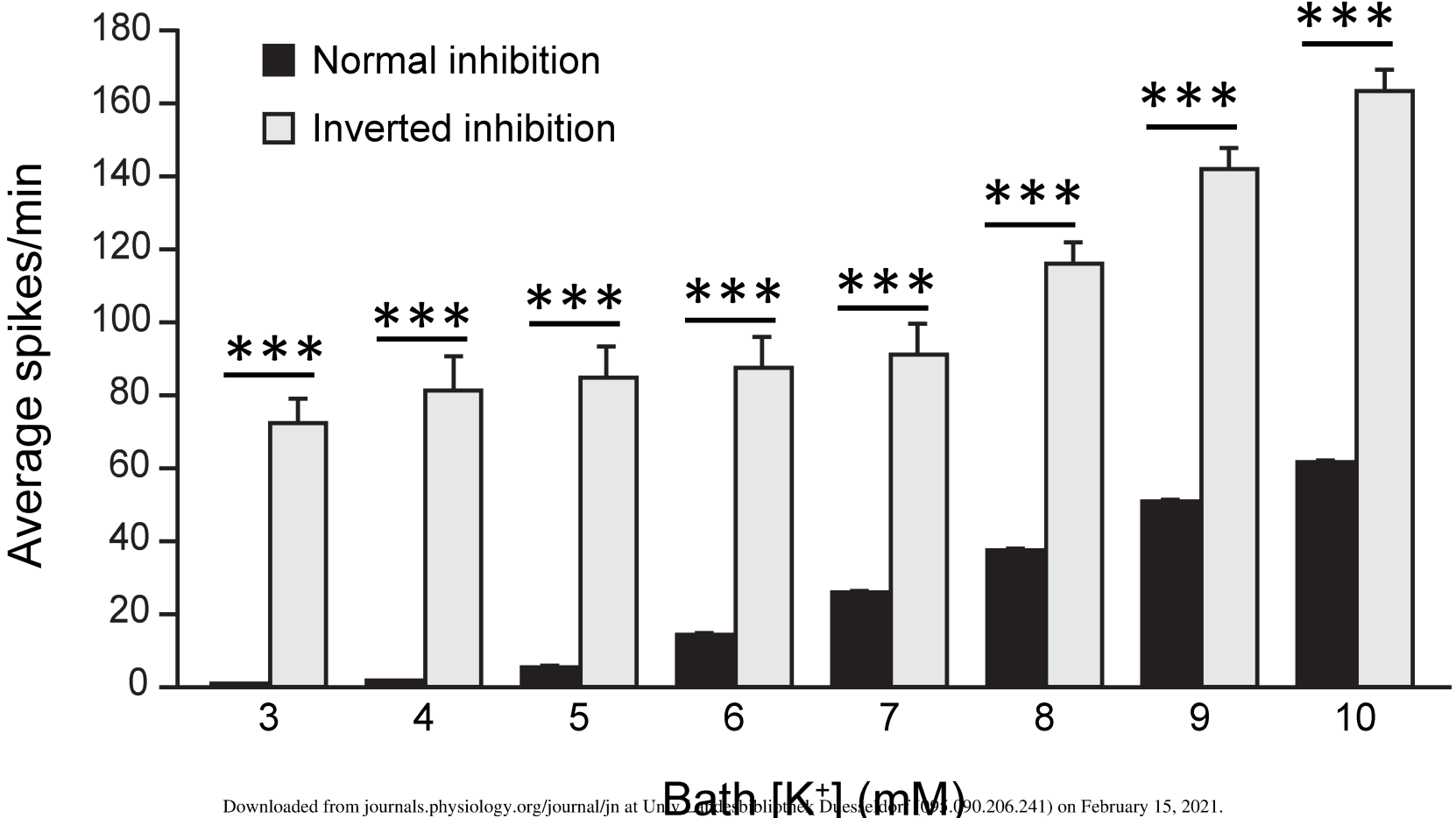

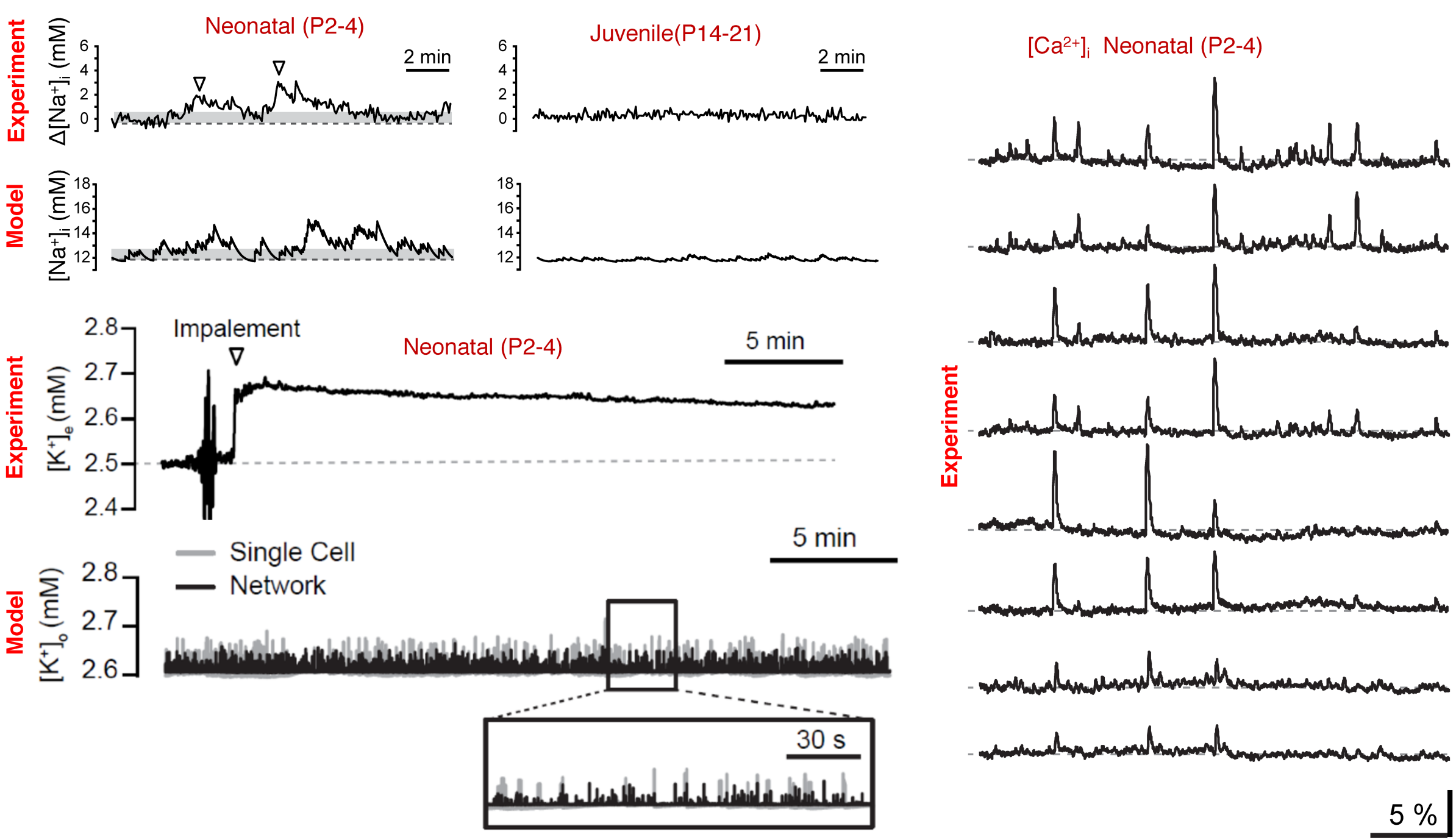

from the institute for Neurobiology
at the Heinrich Heine University Düsseldorf

Published by permission of the
Faculty of Mathematics and Natural Sciences at
Heinrich Heine University Düsseldorf

Supervisor: Prof. Dr. rer. nat. Christine R. Rose
Co-supervisor: Prof. Dr. rer. nat. Kurt Gottmann

Date of the oral examination: 26/02/2021